CORA Cork Open Research Archive
Cartlann Taighde Oscailte Chorcaí

Title	Development and application of synthetic methodologies based on organosulfur and organophosphorus chemistry
Authors	Flynn, Aaran J.
Publication date	2020-05-22
Original Citation	Flynn, A. J. 2020. Development and application of synthetic methodologies based on organosulfur and organophosphorus chemistry. PhD Thesis, University College Cork.
Type of publication	Doctoral thesis
Rights	© 2020, Aaran J. Flynn. - https://creativecommons.org/licenses/by-nc-nd/4.0/
Download date	2026-08-12 18:40:37
Item downloaded from	https://hdl.handle.net/10468/11355

UCC
University College Cork, Ireland
Coláiste na hOllscoile Corcaigh

Development and Application of Synthetic Methodologies based on Organosulfur and Organophosphorus Chemistry

Aaran J. Flynn, B.Sc.

A Thesis Presented for the Degree of

Doctor of Philosophy

to

THE NATIONAL UNIVERSITY OF IRELAND, CORK

School of Chemistry

University College Cork

Supervisor: Prof. Anita R. Maguire

Head of School: Dr. Humphrey Moynihan

May: 2020

Acknowledgements

I would like to express my sincere gratitude to my supervisor, Prof. Anita Maguire, for her guidance, support and enthusiasm throughout the course of this research and in particular during the preparation of this thesis. Most importantly, thank you for affording me the opportunity to pursue a PhD in your group, and in doing so, allowing me to develop my interest in organic chemistry. I'd like to think that I learned a thing or two along the way.

To Debbie Curran, thank you for always finding the time to arrange meetings for me despite the inevitable shuffling no doubt required, but more importantly for being a friendly face over the years. The group is exceptionally fortunate to have you in our corner. I hope my Jazz weekend shenanigans haven't left you too scarred for life!

I would like to extend my appreciation to Dr. Dan McCarthy, Dr. Lorraine Bateman and Dr. Denis Lynch for NMR services, to Dr. Florence McCarthy, Dr. Denis Lynch and Mick O' Shea for mass spectrometry, to Dr. Nuala Maguire for HPLC, to Barry O' Mahony, John Meehan and Noel Browne for microanalysis, to Derry Kearney for glass-blowing services and to Dr. Simon Lawrence and Dr. Udaya Khandavilli for X-ray crystallography data. I would like to extend my gratitude to the technical staff at UCC for their help throughout the duration of these studies, in particular Tina Kent, Noel Browne, Dr. Matthias Jauch, Dr. Michael Cronin, Dr. Tom O'Mahony, Dr. Aoife O'Sullivan, Dr. Ian O'Connor, Dr. Trevor Carey and Dr. Francis Harrington. Of course, this research would not have been possible without financial support from the SSPC and SFI, for which I am very grateful.

Ultimately, a PhD is a story, but as any master storyteller would claim, you cannot tell a good story without the inclusion of a few interesting characters along the way. In this regard, I consider myself very fortunate to have crossed paths with a few 'jokers' along the way, and it would be a terrible injustice not to give them a deserved mention. While starting anything new in life can be daunting, every beginning has a silver lining, and the silver lining in this instance were the two fresh faced boyos who had the distinct pleasure of starting their PhDs with me, Thomas and Dan. Thomas, or Tom, in respect of his preference, and 'old man' Crowley, who may in fact be from a past generation, both suffer from a lack of redeemable qualities, but have made up for it throughout the years by being good craic. Against my better judgement I find myself having to admit that ye are…… alright! It's safe to say that with the two of ye, and Denis and Davy of course, plenty of fun was had along the way. Despite the inevitability of us all going our separate ways I'm sure we'll find a reason to frequent our second home, the Abbey, in the years ahead. Not that we ever needed a reason.

To all the members of the ARM/SGC research team, past and present, that I've had the pleasure of meeting, ye are a great bunch and I hope to see you around in the future. I'm sure we'll have plenty more stories to tell. Massive thank you to Declan Gavin and Denis Lynch for answering the numerous silly but necessary questions when I first started, and continued to answer long long after. Denis you deserve a second mention for the inspired decision that was introducing me to Guinness – what a game changer! I'd like to further extend my gratitude to Alan Ford, Nuala Maguire, Niki Mullins, Francis Harrington, Maria Schwarz, Aoife Buckley, Amy Shiely, Aoife Foley, Thomas 'Tom' Brouder, Dan 'old man' Crowley, Chloe Murphy, Patrick McCaw, Valérie Cacheux, Rosella O' Mahony, Laura McCarthy, Edel Murphy, Aoife Kearney, Eilís Ní Thuama, Michelle Ryan, Amy O'Donoghue, Ciara Tyner, Katie O'Callaghan and Orla Lynch. Hopefully we'll have a few group brunches to look forward to in the not so distant future, or better yet Dingle 2.0!

To those who occupied the 'most sought after real-estate' in the Kane write up area, more fondly known as 'the Corner' thank you for all the craic down through the years. So many different

personalities graced this spot over the years, and we definitely had many an unproductive day, but I wouldn't change a thing. This journey was all the richer for it. Keep up the chats and shenanigans in the years ahead! Thank you Thomas Brouder, Edel Murphy, Lorraine Crowley, Leti Pardo, Aisling Prendergast, Rachel Shanahan, Aobha Hickey, Emma Alcock, Eoin Ó Muimhneacháin, Katrina Mackey, Pamela Mackey, and Amy Lowry.

Thank you also to the extended community of those I've had the pleasure of meeting and getting to know throughout these studies. They are Ryan Kruschel, Kevin O' Shea, Hannah Winfield, Mary McKee, Louise Cooney, Robyn Keogh, Kevin Sheehy, Josh O'Donnell, David Ryan, Olga Dennehy, Mark Lynch, Will Daly, Eimear Courtney, Vera Foley, Louise Shanahan, Danielle Dineen, Udaya Khandavilli, Claire O' Brien, Patricia Hanlon, Katie O'Connor, Mick McGrath, Fiona O' Donovan, Ryan Alam, Conor Horgan, Mary Hennessy, Therese Lyons, Roisín Jones and Kevin Daly.

To Aidan Cregan and Mark Power please remove me from the 'Reaction of the Week' mailing list. Other than that, ye are alright. I have high hopes that ye will become the future leaders of the Christmas 'Stout crawl.' No pressure!!

I'd like to especially thank Dr. Alan Ford for all your input over the years, your massive involvement in our publications, and especially for proof-reading this thesis and everything you do for the group. Your eye for detail and chemistry knowledge is something I aspire to. I really wouldn't be here without you.

To all those who have worked on the nucleoside project, both past and present, I express my sincerest gratitude. I would like to extend this gratitude to Prof. Dr. Christa Müller, Prof. Jan Balzarini and their respective research teams for collaborating on this project. Alan and Nuala thank you for all your help on this project. It was definitely the one I enjoyed the most, and your input and advice played a massive role in that.

To Mom and Dad, this thesis would not have been possible without your unconditional love, support and patience throughout the duration of these studies. My great learning from this experience is that the pursuit of a PhD is not, and never was, an individual effort; it requires a team, and from day one I've always had the best team. Let it be known that every home-cooked meal and late-night lift amongst all the other little things you do for me has not gone unnoticed. This accomplishment is most certainly more yours than mine, and now it is my turn to start paying you back.

To Nana, the most influential woman in my life, you are the person in my life who gave me the confidence to be who I am, and to be unapologetically so. You'll be pleased to know that I did it my way while not forgetting to live a little along the way. If there was anyone who backed my education it was Grandad, and it brings me tremendous joy to know that this thesis would have made him extremely proud.

Finally, to Clodagh, the most important woman in my life, there are not enough pages here to describe how much I love you, and hopefully now after years of sacrifice we can have the life together that we have dreamed of. No achievement in my life comes close to getting you to agree to give an immature Cork lad a chance. I promise that I'll spend the rest of my life proving to you that it was worth it. Love always, Aaran.

Abstract

This thesis describes the development and application of synthetic methodologies based on various aspects of organosulfur and organophosphorus chemistry with a focus on understanding the underlying features and synthetic application.

The first chapter systematically compiles and reviews, for the first time, the synthetic and mechanistic aspects of sulfonyl migrations over the last twenty years. Notably, the fact that these reactions are frequently described as 'unusual', 'unprecedented', 'unexpected', 'serendipitous' and 'novel' by authors, highlights that these potentially synthetically powerful transformations remain only partially understood. This introductory chapter explores the synthetic utility of sulfonyl migrations, while significant attention is afforded to the efforts made to elucidate their underlying mechanisms. This literature review was inspired by the observation of an 'unprecedented' carbon–carbon 1,2-sulfonyl migration in our work, which is discussed in detail in Chapter 2.

The second chapter describes the use of α-thio-β-chloroacrylamides, a series of highly functionalised sulfur containing compounds pioneered in our group, as versatile dipolarophiles in [3+2] dipolar cycloaddition reactions. The [3+2] dipolar cycloaddition of highly reactive α-diazoalkanes with a range of dipolarophiles is well explored in the synthesis of pyrazolines and pyrazoles, however, analogous cycloadditions of electron deficient terminal diazo compounds such as α-diazoacetates, α-diazosulfones and α-diazoacetamides remains significantly less studied despite the synthetic and biological importance of ester, sulfone and amide moieties.

The reactivity of these α-thio-β-chloroacrylamides at each of the sulfide, sulfoxide and sulfone oxidation levels with electron deficient α-diazoacetates, and related derivatives, is explored in the formation of densely functionalised pyrazole derivatives that would otherwise be difficult to obtain via traditional methods. Observation of an unprecedented 1,2-carbon to carbon sulfonyl migration is of particular interest. Significant attention is afforded to the elucidation of the tautomeric composition of the 3,4,5-substituted pyrazole products, while the synthetic versatility of these products is demonstrated via a series of derivatisations.

Chapter three details the design and preparation of a series of acyclic α-carboxy nucleoside phosphonate derivatives envisaged to possess anti-viral and/or anti-cancer properties. This chapter details the use of Mitsunobu coupling and transition metal catalysed O–H insertion methodology as key synthetic steps in the formation of these biological targets. This work was conducted in collaboration with Prof. Dr. Christa Müller and Prof. Jan Balzarini.

The fourth chapter explores in detail synthetic challenges in the copper-catalysed asymmetric sulfur oxidation of aryl benzyl sulfides. Significant attention is afforded to the concept of self-disproportionation of enantiomers (SDE), an underappreciated phenomenon despite being known in the literature, but also to the observation of *localised partitioning of enantiomers in the solid state* even in the absence of SDE, which can lead to erroneous determination of enantiopurity.

Each of chapters 2–4 is concluded with the associated experimental details, including spectroscopic and analytical data, for compounds synthesised during this work.

Declaration

I hereby confirm that the body of work described within this thesis for the degree of Doctor of Philosophy, is my own research, and has not been submitted for any other degree, either in University College Cork or elsewhere.

_____ _____

Aaran J. Flynn Date

To Mom, Dad, Nana and Grandad

Contents

Chapter 1

Introduction 1

Chapter 2

[3+2] Dipolar Cycloadditions of α-Thio-β-Chloroacrylamides 115

Chapter 3

Design, Synthesis and Evaluation of Acyclic α-Carboxyl Phosphononucleosides 250

Chapter 4

Asymmetric Copper-Catalysed Oxidation of Sulfides to Sulfoxides 329

Appendices

- *i) Crystallographic data*
- *ii) ^{1}H and ^{13}C NMR spectra for Weinreb amide **226***
- *iii) HPLC conditions for determination of enantiopurity (% ee) of sulfoxides*
- *iv) Representative examples of HPLC chromatograms for enantioenriched sulfoxides*
- *v) Abbreviations*

Publications

Chapter 1

Introduction

Contents

1.1. Introduction to Sulfonyl Migrations 3
1.2. Nitrogen to Carbon Sulfonyl Migration 3
1.2.1. Transition Metal-Catalysed Reactions 3
1.2.1.1. Gold-Catalysed Sulfonyl Migration 3
1.2.1.2. Silver-Catalysed Sulfonyl Migration 12
1.2.1.3. Transition Metal-Catalysed Sulfonyl Migrations using *N*-Sulfonylhydrazones 15
1.2.1.3.1. Copper-Catalysed Sulfonyl Migration using *N*-Sulfonylhydrazones 15
1.2.1.3.2. Palladium-Catalysed Sulfonyl Migration using *N*-Sulfonylhydrazones 22
1.2.1.4. Miscellaneous Metal-Catalysed Sulfonyl Migration 23
1.2.2. Single-Electron-Mediated Sulfonyl Migration 26
1.2.2.1. Radical-Mediated Sulfonyl Migration 26
1.2.2.2. Photoinduced Sulfonyl Migration 29
1.2.2.3. Non-Metal-Catalysed Radical-Mediated Sulfonyl Migration of *N*-Sulfonylhydrazones 34
1.2.3. Non-Metal-Catalysed Sulfonyl Migration 37
1.3. Nitrogen to Nitrogen Sulfonyl migration 56
1.4. Nitrogen to Oxygen sulfonyl migration 62
1.4.1. Transition-Metal Catalysed Migration 62
1.4.2. Non-Metal-Catalysed Sulfonyl Migration 65
1.5. Oxygen to Carbon Sulfonyl Migration 69
1.5.1. Photoinduced Sulfonyl Migration 69
1.5.2. Thia-Fries Rearrangement 72
1.5.2.1. Anionic Thia-Fries Rearrangement 73
1.5.2.2. Remote Anionic Thia-Fries Rearrangement 80
1.5.2.3. Anionic Thia-Fries Rearrangement of Organometallic Complexes 83
1.5.2.4. Non-Anionic Thia-Fries Rearrangement 87
1.6. Oxygen to Oxygen Sulfonyl Migration 89
1.7. Carbon to Carbon Sulfonyl Migration 90
1.7.1. *N*-Heterocyclic Carbene-Catalysed Sulfonyl Migration 90
1.7.2. Triphenylphosphine-Catalysed Sulfonyl Migration 92
1.7.3. Miscellaneous Sulfonyl Migration 95
1.8. Summary and Outlook 109
Bibliography 111

Note: This introductory chapter, written by the PhD candidate, was published as a review article in *Organic and Biomolecular Chemistry* on the 3rd of February 2020. The article entitled 'Synthetic and Mechanistic Aspects of Sulfonyl Migrations' was conceptualised by Aaran J. Flynn and Prof. Anita R. Maguire. The PhD candidate Aaran J. Flynn undertook the literature search, compilation of reports and the writing of the article in its entirety. Dr. Alan Ford and Prof. Anita R. Maguire were involved in the proof-reading and editing of the original and revised manuscripts, as well as advising throughout. For clarity, the elements of the introduction herein discussed excludes results obtained in the PhD candidate's research work that were subsequently reported and included in the final accepted review manuscript.

Reference to published review article: A. J. Flynn, A. Ford, A. R. Maguire, *Org. Biomol. Chem*., **2020**, 18, 2549-2610. **DOI:** 10.1039/C9OB02587A.

1.1. Introduction to Sulfonyl Migrations

Retrosynthetic analysis, formalised by E. J. Corey in the 1989 book *The Logic of Chemical Synthesis* revolutionised the art of total synthesis of complex organic molecules,[1] and coupled with an ever increasing number of efficient and selective synthetic methodologies with predictable outcomes across a diverse substrate range, has delivered elegant total syntheses. Critical to success is the ability to accurately anticipate the reactivity of molecules under different conditions, which requires an excellent understanding of functional group chemistry including identification of trends in reactivity that are both predictable and readily rationalisable.

Numerous reports observing 'unusual', 'unprecedented', 'unexpected' and 'novel' sulfonyl migrations attracted our attention, following observation of an unanticipated sulfonyl migration in our work (see **Chapter 2** for details).[2] What became clear from a survey of the literature is that sulfonyl migrations remain only partially understood despite their potential synthetic utility. Sulfones[3-14] and related species[15-17] are widely used as activating groups and / or protecting groups and offer substantial synthetic versatility. Accordingly, sulfonyl migrations are potentially valuable from a synthetic perspective, provided they are sufficiently understood to enable their use in a predictive manner.

While most sulfonyl migrations prior to the beginning of the 21st century were originally discovered as side reactions, and regularly as isolated cases, the last 20 years has seen a significant increase in the number of reports focusing on the utility of incorporating a sulfonyl molecular handle capable of migration. As such, attempts to understand the mechanisms of these often 'unexpected' reactions have garnered significant recent attention; however, the ability to observe formal 1,2-, 1,3-, 1,4-, 1,5-, 1,6- or 1,7-sulfonyl migrations, in an inter- or intramolecular fashion, occurring through either radical or polar processes, highlights the difficulty in accurately predicting the outcome of such reactions. Bearing this complexity in mind, it is not surprising that the current knowledge in this field is not sufficiently developed to enable incorporation of sulfonyl migration into a retrosynthetic plan.

In this chapter, sulfonyl migrations reported over the last two decades (up to early 2019) are compiled, and their synthetic and mechanistic development is described; the sulfonyl migrations are classified based on the migration type, namely nitrogen-carbon, nitrogen-oxygen, nitrogen-nitrogen, oxygen-carbon (including anionic and non-anionic thia-Fries rearrangements), oxygen-oxygen and carbon-carbon. Particular emphasis is afforded to the efforts made to elucidate the mechanistic pathway for the migrations.

1.2. Nitrogen to Carbon Sulfonyl Migration

1.2.1. Transition-metal catalysed reactions

1.2.1.1. Gold-catalysed sulfonyl migration

Nakamura *et al*. reported the gold- and indium-catalysed synthesis of 3- and 6-sulfonylindoles from *ortho*-alkynyl-*N*-sulfonylanilines **1 (Scheme 1.1)**.[18-19] In the presence of catalytic $AuBr_3$, a 1,3-sulfonyl migration was observed, to afford 3-sulfonylindoles **2** in good to high yields (up to 95%), with minor amounts of the regioisomers **3** and **4** also observed. Interestingly, using $InBr_3$ as catalyst the major products are 6-sulfonylindoles **5** which were isolated in up to 99% yield, indicating that an unprecedented 1,7-sulfonyl migration has occurred. The presence of a methoxy group at the 6-position of the *ortho*-alkynyl-*N*-sulfonylanilines proved crucial in yielding the 1,7-sulfonyl migration products.

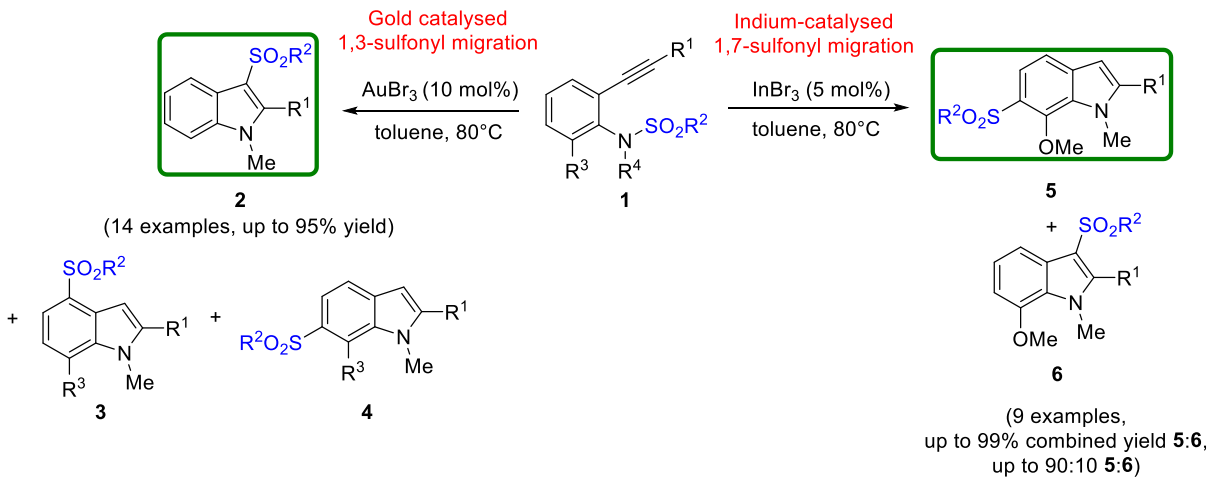

Scheme 1.1: Gold- and indium-catalysed synthesis of 3- and 6-sulfonylindoles from *ortho*-alkynyl-*N*-sulfonylanilines, via 1,3- and 1,7-sulfonyl migration

In order to probe the mechanism of the sulfonyl migration, crossover experiments were performed which determined that both the gold- and indium-catalysed reactions were intramolecular processes. Interconversion of the reaction products was eliminated as a possibility by stirring a mixture of the 3-, 4- and 6-sulfonylindole products in the presence of catalyst for a further two hours – no change in product distribution was observed.

The following mechanism was postulated in accordance with the observed results **(Scheme 1.2)**. Coordination of the Lewis-acidic transition metal to the alkyne of **1** forms the intermediate π-complex **7**. Nucleophilic addition of the nitrogen to the electron-deficient alkynyl moiety leads to the cyclised intermediate **8**, which can undergo two diverging pathways depending on the metal catalyst employed. For the gold-catalysed process, intramolecular 1,3-sulfonyl migration occurs followed by elimination of $AuBr_3$ to afford the 3-sulfonylindole products **2**. Alternatively, for the indium-catalysed process, a consecutive 1,7-sulfonyl migration and 1,5-proton shift occurs. Elimination of $InBr_3$ yields the 6-sulfonylindole products **5**. Notably, the formation of indole **2** is the first example of sulfodemetalation, in which the vinyl–Au intermediate is captured intramolecularly by the sulfonyl group (**Scheme 1.2**, **8** to **2**).

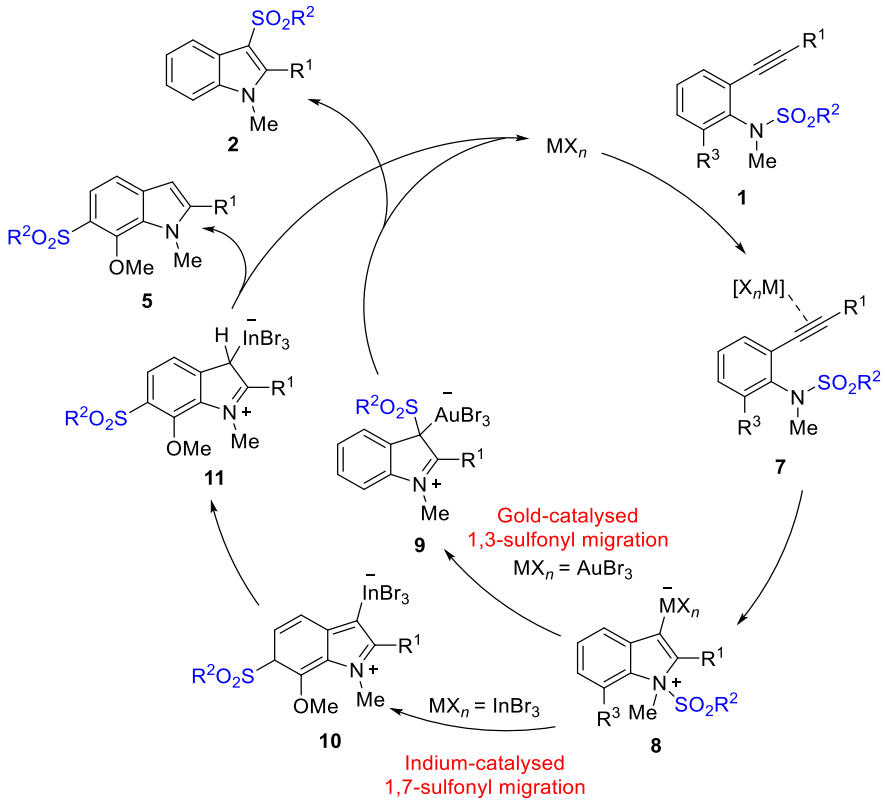

Scheme 1.2: Proposed mechanistic cycle for the gold- and indium-catalysed synthesis of 3- and 6-sulfonylindoles

In an earlier communication the authors described the reaction of *N*-methoxymethyl-2-(1-pentynyl)-*N*-tosylaniline **12** in the presence of catalytic $PdBr_2$, to give the indole **13** in 33% yield, with only trace amounts of the tosyl migration product **14** observed **(Scheme 1.3)**.[20] Interestingly, repeating this reaction using the optimised $AuBr_3$ catalyst afforded exclusively **13** albeit in 10% yield.[19] Therefore, regardless of the catalyst species, the migratory aptitude of the migrating group appears to be crucial to the outcome. Specifically, in this instance, the methoxymethyl group has a greater ability to migrate than the tosyl group. Similarly, in a separate report, Fürstner and Davies observed that an allyl group preferentially migrated in the presence of a mesyl group for the platinum-catalysed transformation of **15** to **16 (Scheme 1.3)**.[21]

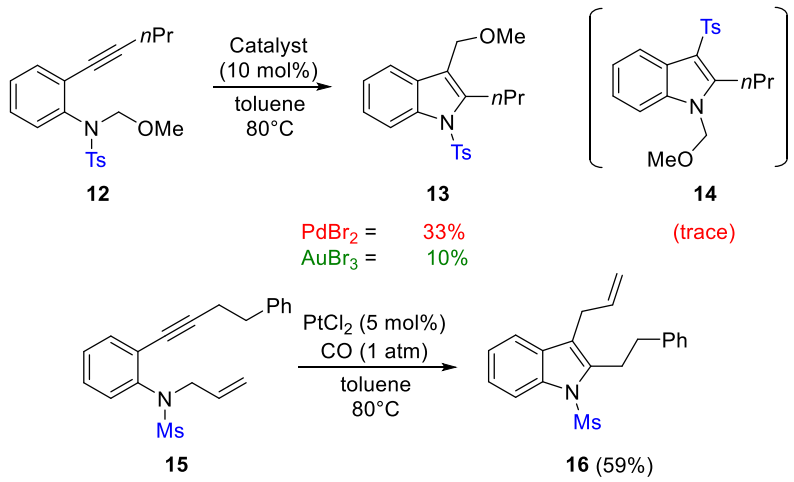

Scheme 1.3: Migratory aptitude of tosyl and mesyl groups relative to methoxymethyl and allyl groups respectively.

In 2011, the Chan group described the gold-catalysed tandem 1,3-migration/[2+2]-cycloaddition of 1,7-enyne benzoates **19** to azabicyclo[4.2.0]oct-5-enes **20 (Scheme 1.4**, **Catalyst 17)**.[22] Interestingly, during optimisation studies, the gold(I) carbene complex **18** catalysed the cycloisomerisation of 1,7-enyne ester **19** to afford the 3-sulfonyl-1*H*-pyrrole **22** in 20% yield **(Scheme 1.4, Catalyst 18)**. Inspired by this fortuitous result, and recognising that the reaction pathway may have involved a deaurative 1,3-sulfonyl migration, the authors set out to investigate the rearrangement process.

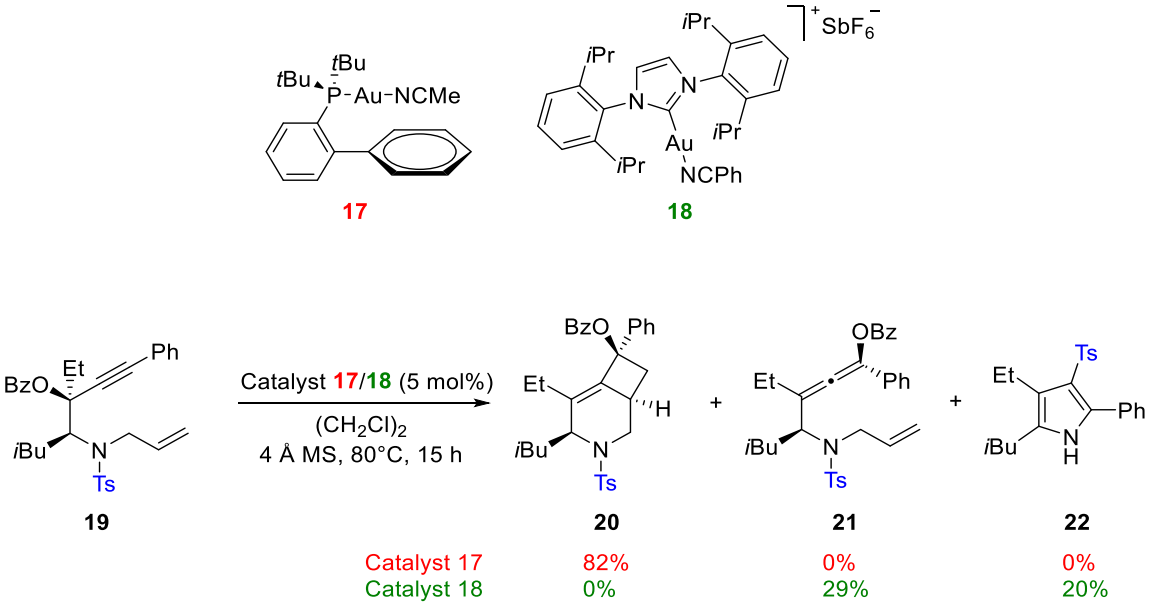

Scheme 1.4: Gold-catalysed tandem 1,3-migration/[2+2]-cycloaddition of 1,7-enyne benzoates to azabicyclo[4.2.0]oct-5-enes; observation of a potential deaurative 1,3-sulfonyl migration

In their continuation of these studies, the authors reasoned that the chemical yield of the process could be enhanced by use of the corresponding 1,7-enyne alcohols **23** as substrates **(Scheme 1.5)**, presumably due to ease of water elimination. The NHC–gold(I) complex **18** was determined to be the optimal catalyst, with moderate to excellent yields of the rearranged pyrroles **24** obtained.[23] An

intramolecular 1,3-sulfonyl migration was postulated based on the results of crossover experiments, and the fact that pyrrole **25** was recovered unchanged after exposure to *p*-toluenesulfonyl chloride under the optimised reaction conditions. The reaction mechanism was postulated to proceed via activation of the propargylic alcohol **23** through coordination of the gold catalyst with the alkyne moiety to give the Au(I)-intermediate **26**. An intramolecular aminocyclisation is triggered involving *anti* addition of the *N*,*N*-disubstituted amino moiety to the triple bond affording the vinyl gold complex **27**. Dehydration of this species leads to the formation of the cationic pyrrole–gold adduct **28**, which subsequently undergoes an intramolecular 1,3-sulfonyl migration resulting in deauration and generation of the pyrrole product **24 (Scheme 1.5**, **path A)**. Alternatively, the vinyl gold complex **27** undergoes the deaurative 1,3-sulfonyl migration first to afford the 2,3-dihydro-1*H*-pyrrol-3-ol adduct **29** that upon dehydrative aromatisation affords the pyrrole **24 (Scheme 1.5**, **path B)**.

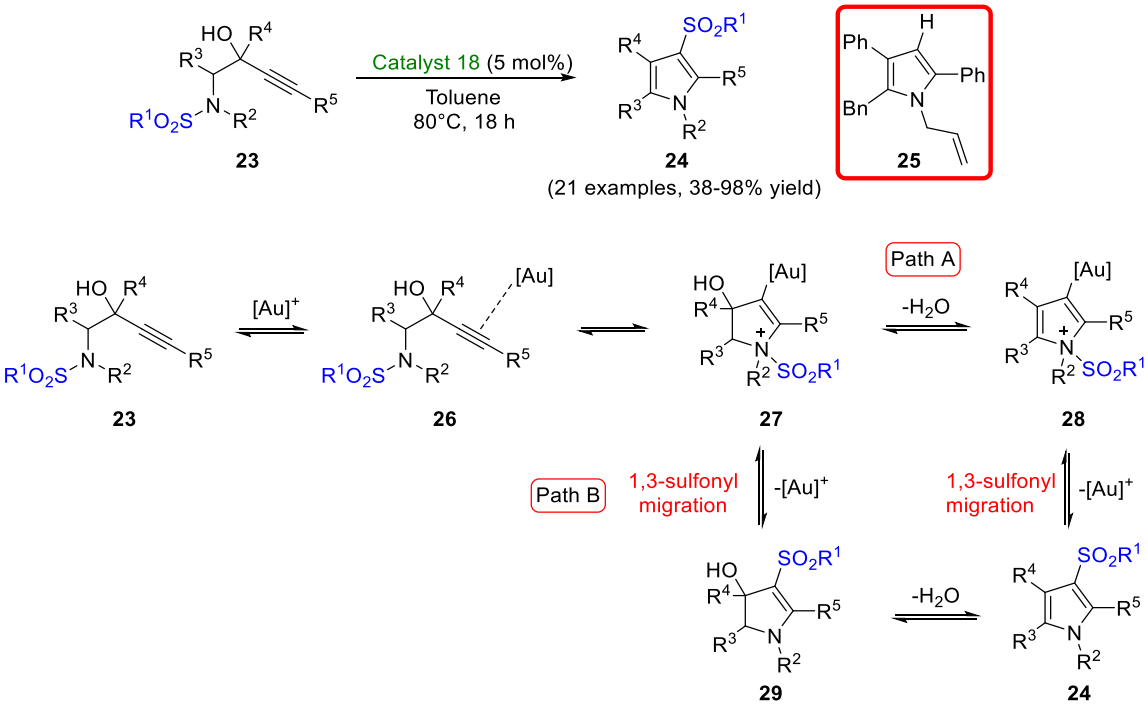

Scheme 1.5: Gold-catalysed domino aminocyclisation/1,3-sulfonyl migration of *N*-substituted *N*-sulfonyl-aminobut-3-yn-2-ols to 1-substituted 3-sulfonyl-1*H*-pyrroles

The Shin group reported the gold-catalysed synthesis of 3-pyrrolidinones **31** and nitrones **32** from *N*-sulfonyl hydroxylamines **30** via oxygen-transfer redox and 1,3-sulfonyl migration **(Scheme 1.6)**.[24] In the case of terminal alkynes, a gold-catalysed 5-*exo*-dig addition of the hydroxylamine moiety to the alkyne occurs through the oxygen **(Scheme 1.6)**. Cleavage of the N–O bond is rate limiting, and the presence of the electron-withdrawing sulfonyl moiety facilitates the overall reaction process to afford 3-pyrolidinones **31** in moderate to good yields.

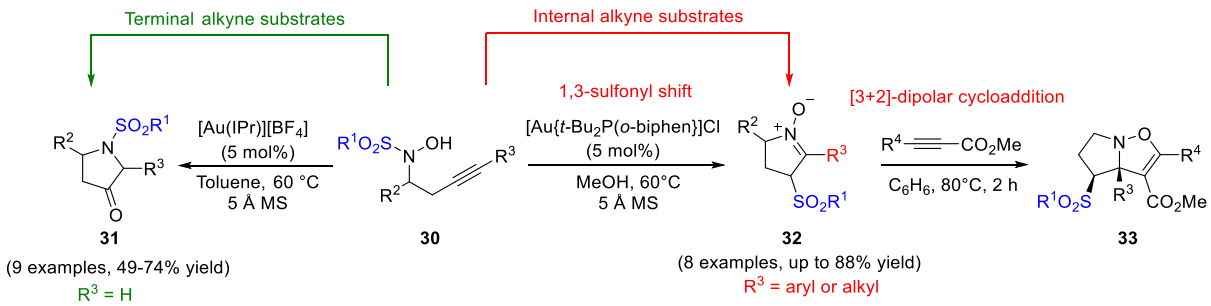

Scheme 1.6: Gold-catalysed synthesis of 3-pyrrolidinones and nitrones from *N*-sulfonyl hydroxylamines via oxygen-transfer redox and 1,3-sulfonyl migration

However, to the surprise of the authors, when internal alkynes are utilised a different mechanistic pathway occurs, resulting in the formation of 3-sulfonylnitrones **32**. In this instance, the nitrogen of the hydroxylamine moiety is the preferred nucleophile, which allows for a 5-*endo*-dig cyclisation to occur giving **36 (Scheme 1.7)**. Subsequent 1,3-sulfonyl migration leads to **37**. Loss of the gold catalyst and tautomerisation of the resulting vinyl hydroxylamine leads to the nitrone **32**. The identity of the nitrone products **32** were confirmed by trapping with dipolarophiles via [3+2]-dipolar cycloaddition **(Scheme 1.6)**.

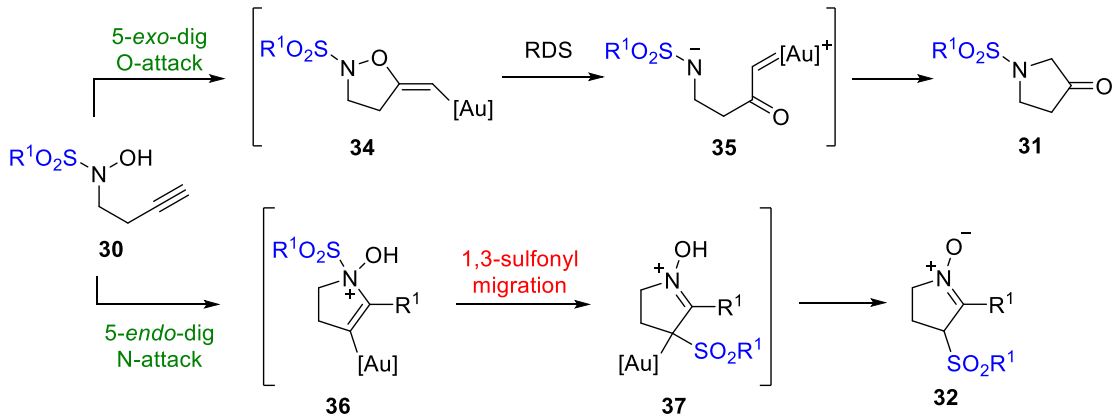

Scheme 1.7: Access to 3-pyrrolidinones and nitrones via *N*-sulfonylhydroxylamines

Liu *et al*. recently developed a gold-catalysed cascade reaction of diynamides **38** to generate a series of sulfone containing pyrrolo[2,l-*a*]isoquinolines **39** featuring the core structural motif of the lemellarin alkaloids **(Scheme 1.8)**.[25] Notably, all three functional moieties on the nitrogen of the ynamide participate in the cascade transformation, with a formal 1,4-sulfonyl migration a key mechanistic step. A crossover experiment, with two different sulfonyl diynamides, did not lead to crossover products, indicating that the migration of the sulfonyl group occurs in an intramolecular fashion. DFT studies suggested that the formal 1,4-sulfonyl migration is in fact two sequential 1,2-sulfonyl shifts **(Scheme 1.8)**. The alternative 1,3-sulfonyl shift was considered to be an unlikely mechanistic route as the transition states for both the suprafacial and antarafacial 1,3-sulfonyl shifts are 24.0 and 22.6 kcal/mol higher in energy than that for **TS6 (Scheme 1.8)**.

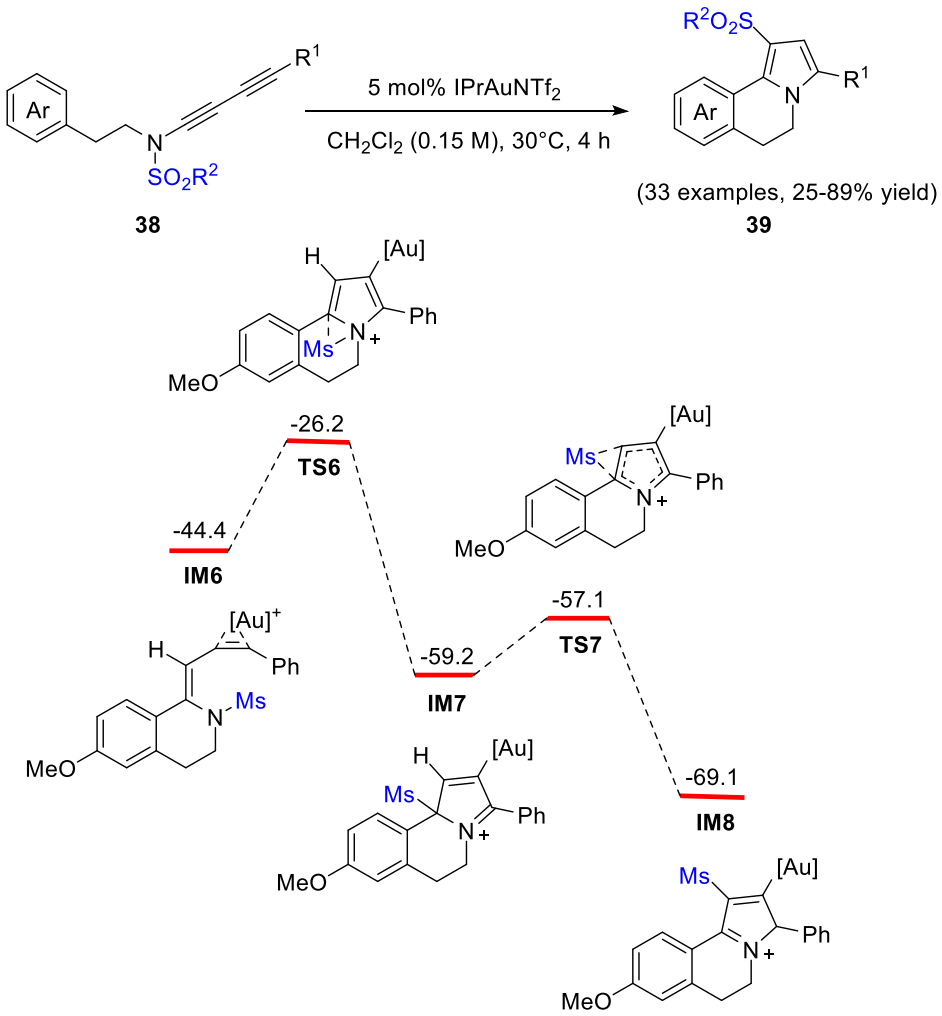

Scheme 1.8: Cascade reaction of diynamides and relevant section of the DFT reaction coordinate for sulfonyl migration

The Sahoo group recently developed a regioselective sulfonyl/sulfinyl migration cycloisomerisation cascade of alkyne-tethered ynamides **40** in the presence of XPhosgold catalyst to afford a series of novel 4-sulfinylated pyrroles **41** in yields up to 85% **(Scheme 1.9)**.[26] Notably, this reaction process is the first example of a general [1,3]-sulfonyl migration from the nitrogen centre to the β-carbon of ynamides, followed by umpolung 5-*endo*-dig cyclisation of the ynamide α-carbon atom to the gold-activated alkyne, and final deaurative [1,5]-sulfinylation. Control experiments in conjunction with DFT calculations were used to deduce an operative reaction pathway.

The de-sulfinylated pyrroles **45** and **46** were generated from *N*-mesyl protected yne-ynamides **42** and **43** respectively under the optimised conditions **(Scheme 1.9, a)**, highlighting the role of adventitious water in the protodeauration of the organo-Au intermediate **44**. Furthermore, the transformation of **43** in the presence of D_2O afforded [D]**47** indicating that a deuterium quench of **44** is preferred to the consecutive migration of the methyl sulfinyl cation motif in the pyrrole ring. A crossover experiment between **42** and **48** (1:1) generated **49** and **50** exclusively, indicating that both the [1,3]-sulfonyl and [1,5]-sulfinyl migration are intramolecular processes **(Scheme 1.9, b)**. No sulfinylated pyrrole **53** was observed when the pyrrole **45** was reacted in the presence of **51**, highlighting that intermolecular deaurative sulfinylation is unlikely **(Scheme 1.9, c)**. The reaction of **54** in the presence of [^{18}O]-labelled

H_2O under the optimised conditions did not yield the [^{18}O]-labelled **56**, with **55** instead exclusively formed, indicating that an intramolecular oxygen transfer could be utilised in the mechanistic pathway **(Scheme 1.9, d)**.

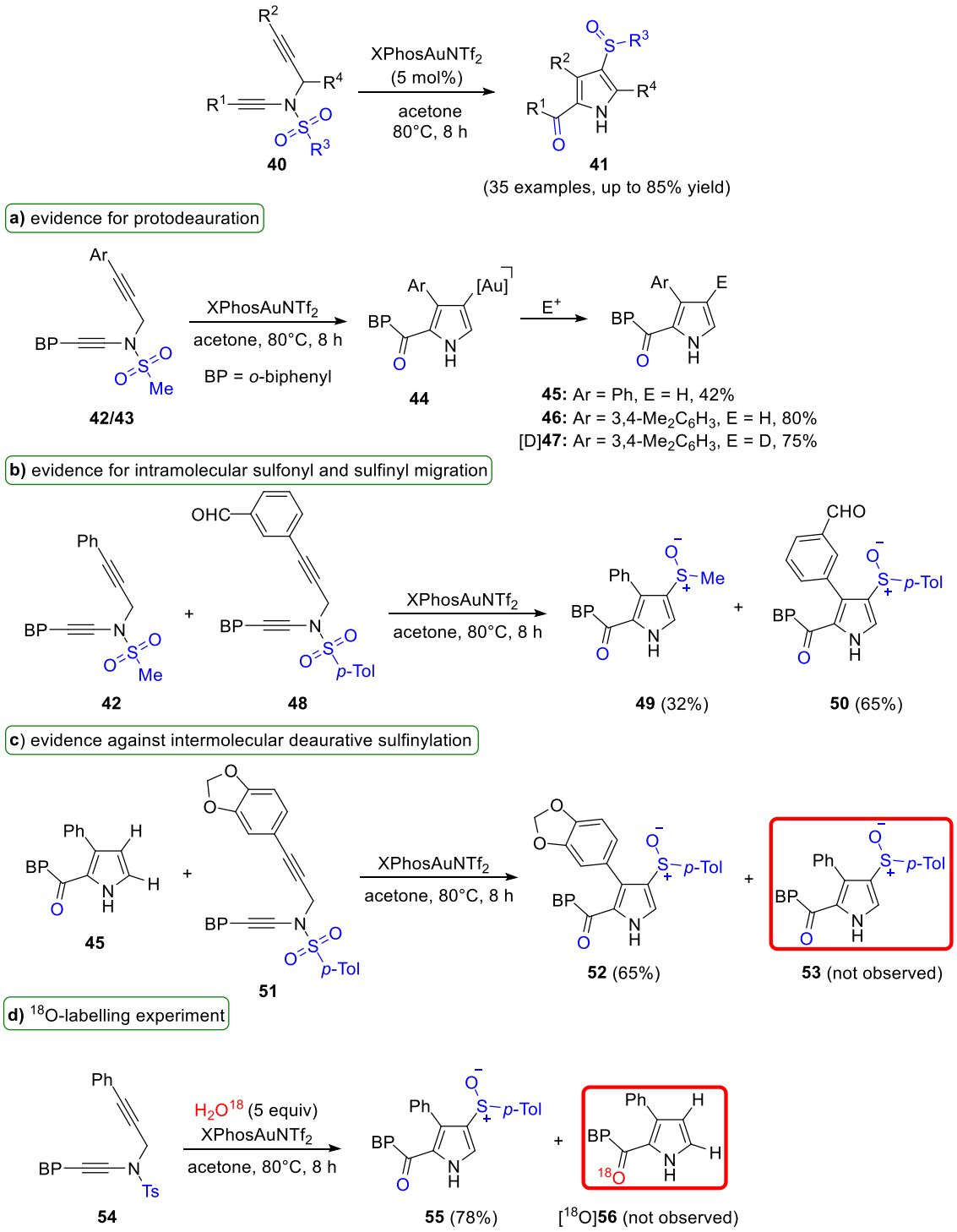

Scheme 1.9: Control experiments for mechanism elucidation

DFT calculations proved useful in further understanding the mechanistic features of the cascade process **(Scheme 1.10)**. The gold complex **(IM1)** was chosen as reference for the free energy, while coordination of the gold catalyst to the ynamide affords the isomerised allene-type complex **(IM2)**.

Attack of the sulfonyl oxygen onto the ynamide β-carbon yields the cyclic sulfoniminium **(IM3)**, while extrusion of the sulfinylium ion $PhSO^+$ affords the heterodiene complex **(IM4).** Migration of AuL^+ to the propargyl triple bond generates a 1,2-azadiene (ketinimine) core **(IM5)**, while subsequent 5-*endo*-dig cyclisation generates the 2*H*-pyrrole complex **(IM6)**, which is is strongly exergonic by 27.0 kcal mol^{-1}. Migration of the $PhSO^+$ to the nitrogen atom of the pyyrole ring affords **IM7**, which lies very low on the potential energy surface (-53.3 kcal mol^{-1}). The sulfoxide oxygen is utilised as a base to shuttle one of the hydrogen atoms of the CH_2 group to the nitrogen atom of the pyrrole ring to afford **IM10**, despite being energetically unfavourable. The sulfonimidate-oxygen assisted 1,4-H shift via $\mathbf{TS_{7-8}}$ at − 25.2 kcal mol^{-1} was found to be feasible affording **IM8**. Subsequent [1,2]-migration of the $[PhSOH]^+$ moiety, followed by [1,5]-H shift generates **IM10**, while antarafacial [1,4]-S shift of the $PhSO^+$ to afford **IM11** was observed to be favourable requiring 9.8 kcal mol^{-1} of free energy. To complete the transformation, a suprafacial [1,2]-S shift affords the **IM12** located at − 76.6 kcal mol^{-1} on the PES.

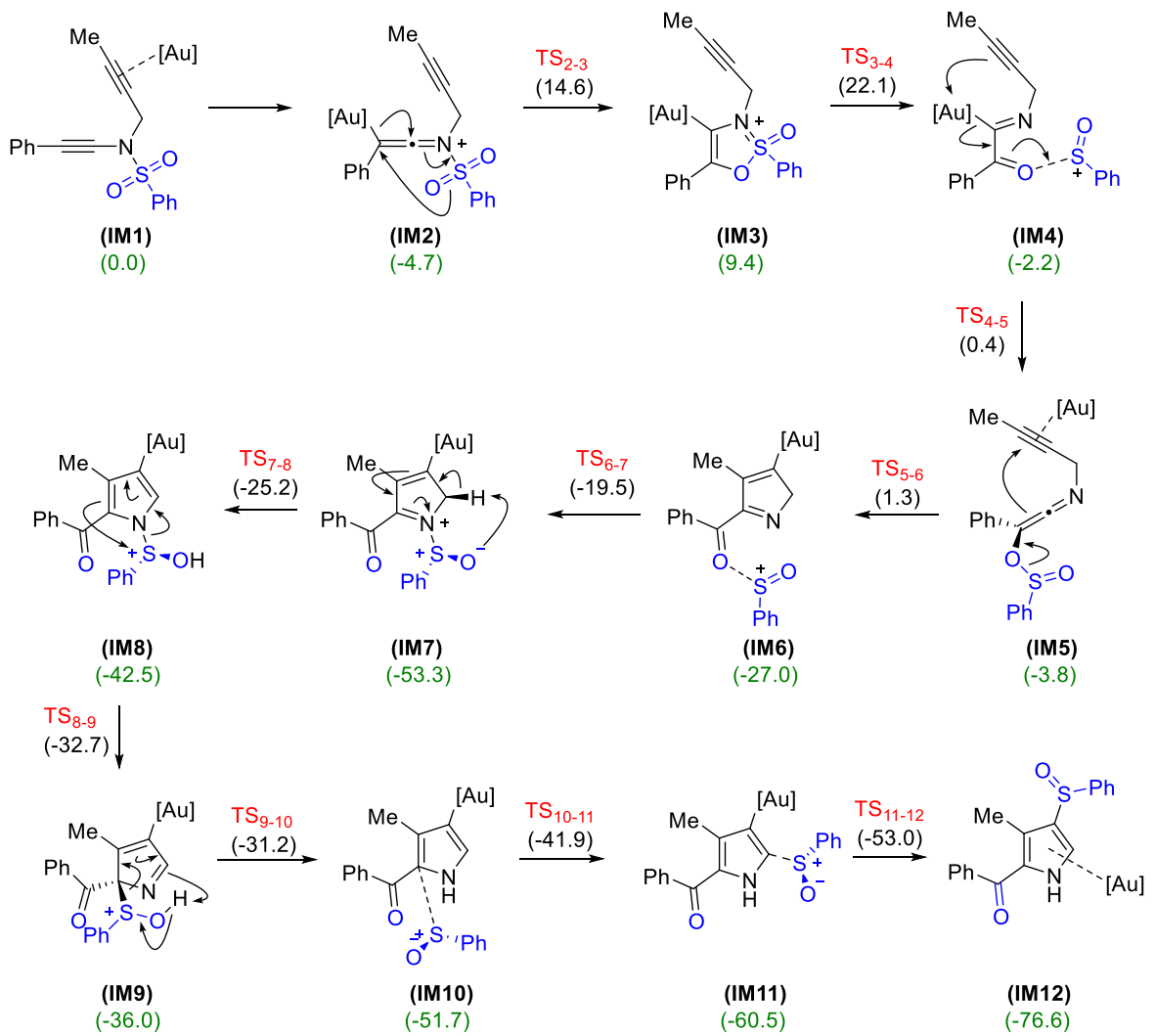

Scheme 1.10: Calculated energy profile of the umpolung cycloisomerisation migration cascade process (ΔG_{298}, kcal mol^{-1})

1.2.1.2 Silver-catalysed sulfonyl migration

The synthesis of pyrazoles **58**/**59** via the silver(I)-catalysed rearrangement of propargyl *N*-sulfonylhydrazones **57**, involving a 1,3- or 1,5-sulfonyl migration, was described by the Chung group.[27] Using this methodology efficient and regioselective synthesis of 1,3- and 1,5-disubstituted, and 1,3,5-trisubstituted pyrazoles can be achieved in moderate to excellent yields **(Scheme 1.11)**. Notably, in the absence of a sulfonyl moiety no pyrazole formation is observed. An intermolecular sulfonyl migration was elucidated by means of crossover experiments. Interestingly, deuterium incorporation studies highlighted an unexpected scrambling of deuterium at the C(4) and C(5) positions in the pyrazole product **61**; this was rationalised through the silver(I) allene intermediate **63 (Scheme 1.11)**. Loss of a deuterium ion causes the π-intermediate **62** to rearrange to a silver-substituted allene intermediate **63**. Subsequently, recombination with **63** affords intermediate **64**, which can isomerise to regenerate the π-intermediate **65,** which when cyclised gives pyrazole derivatives with deuterium incorporated at both the C(4) and C(5) positions in addition to C(3).

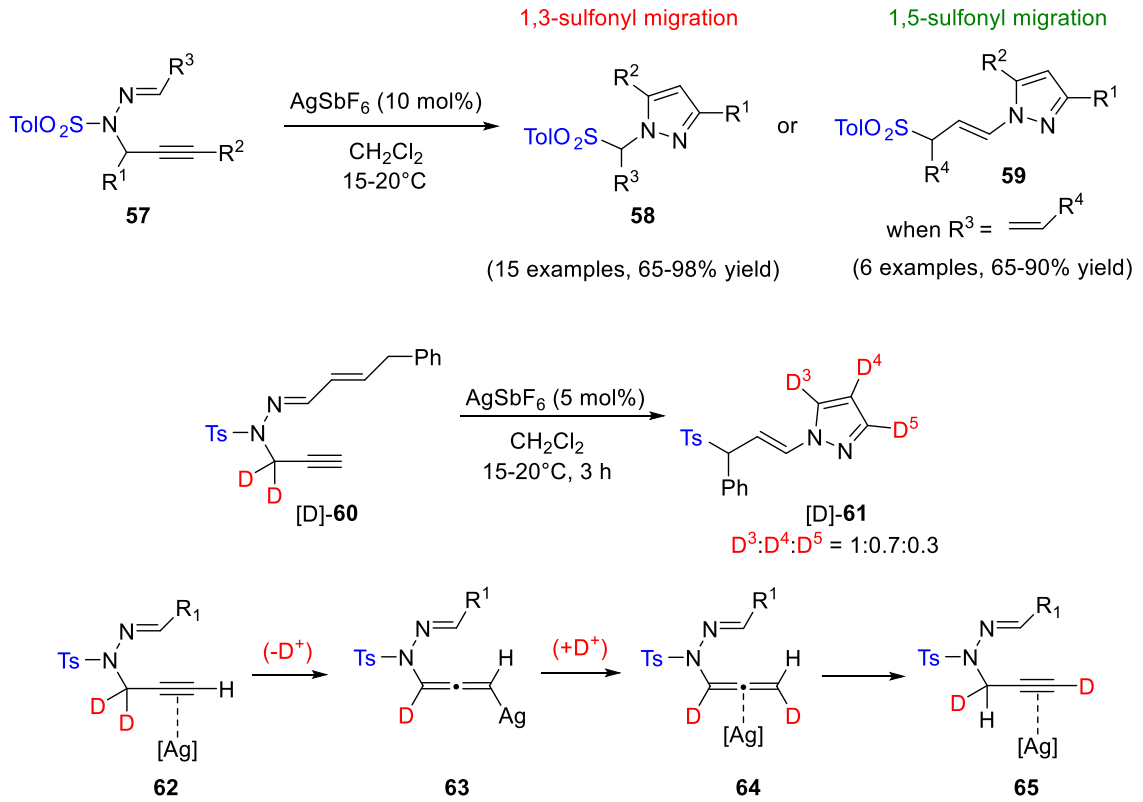

Scheme 1.11: Silver(I)-catalysed synthesis of pyrazoles from propargyl *N*-sulfonylhydrazones via 1,3- or 1,5-sulfonyl migration; Proposition of a silver(I)-substituted allene intermediate

Taking the above into account the following mechanism was postulated **(Scheme 1.12)**. Upon coordination of the electrophilic silver source to the alkyne moiety of **57**, nucleophilic cyclisation occurs yielding the silver(I) intermediate **67**. Deprotonation leads to elimination of the sulfonyl moiety affording the ion pairs **68**. The sulfinate anion attacks the electrophilic iminium carbon completing the 1,3-sulfonyl migration. In instances in which the imine substituent is extended by conjugation, the sulfonate anion attacks the β-carbon leading to 1,5-sulfonyl migration being preferred. Finally, protodemetallation of **69** regenerates the catalytic silver species and gives the pyrazole products **58**.

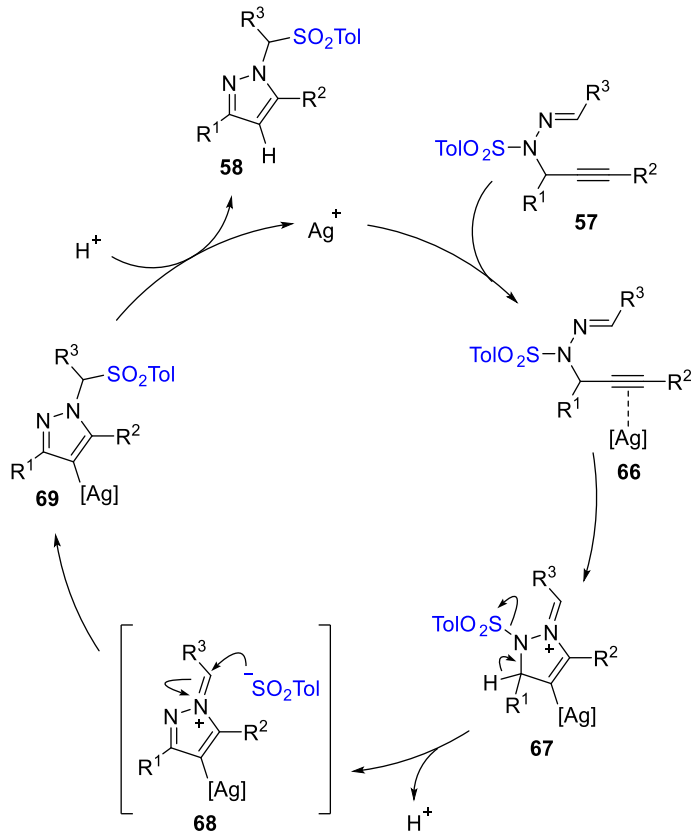

Scheme 1.12: Postulated mechanism for the silver(I)-catalysed synthesis of pyrazoles from propargyl *N*-sulfonylhydrazones via 1,3- or 1,5-sulfonyl migration

The Wan group subsequently reported the silver(I)-catalysed cyclisation of *N*-sulfonyl propargylamides **70** for the synthesis of 4-(sulfonylmethyl)oxazoles **71** in moderate to good yields **(Scheme 1.13)**.[28] The introduction of an aryl acyloxy directing group proved critical in realising the key silver-mediated [3,3]-rearrangement. Crossover experiments indicated that the sulfonyl migration may occur in both an intra- and intermolecular manner. The following plausible mechanism was presented **(Scheme 1.13)**. Coordination of the silver(I) cation to the alkyne moiety of the propargylamide **70** as well as the acyloxy directing group generates the π-complex **72**. Due to the increased electrophilicity of the alkyne moiety an intramolecular nucleophilic attack of the amide oxygen occurs via a 6-*endo*-dig cyclisation giving the intermediate **73**. Subsequent collapse of the cyclic intermediate **73** affords the allene intermediate **74**. Nucleophilic attack of the nitrogen atom on the allene affords the 5-membered cyclic zwitterionic intermediate **75**. It is envisaged that the 1,3-sulfonyl migration occurs at this point in both an intra- and intermolecular manner, to give the rearranged 4-(sulfonylmethyl)oxazole **71**.

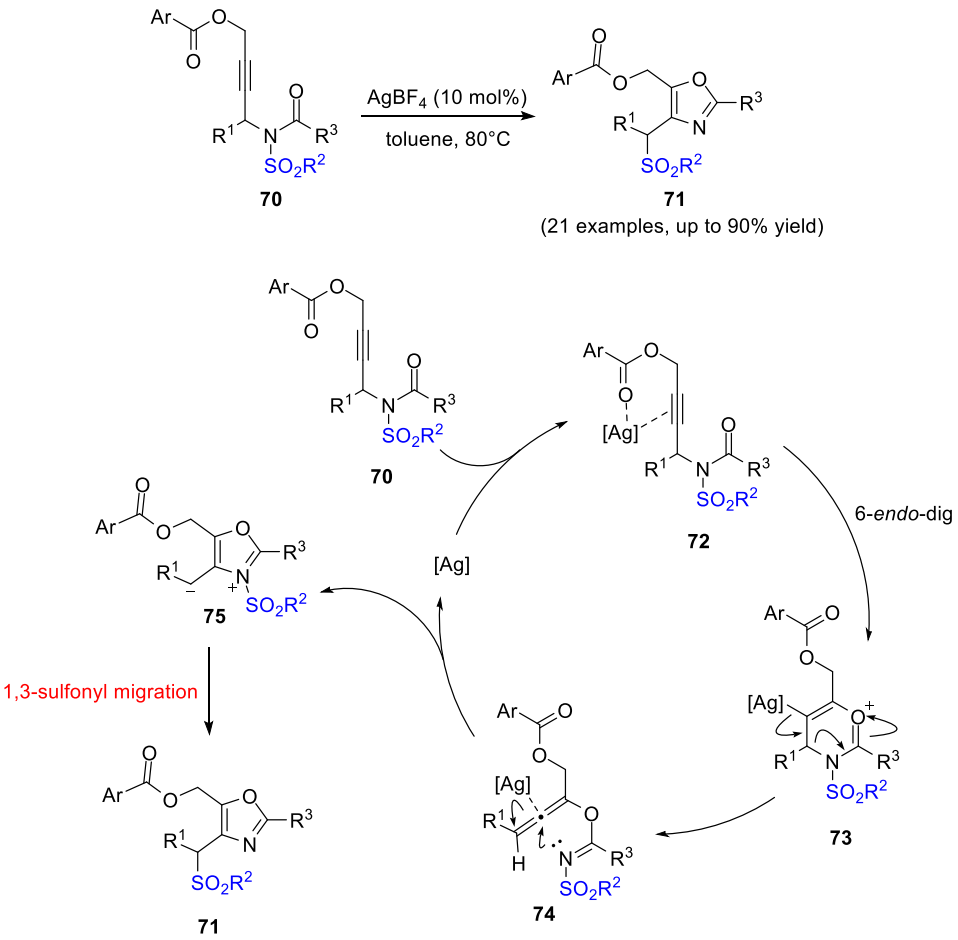

Scheme 1.13: Silver-catalysed cyclisation of propargylamides in the generation of functionalised oxazoles via 1,3-sulfonyl migration

The Wan group further demonstrated that silver catalysis can be used in conjunction with trifluoromethyl-substituted 3-aza-1,5-enynes **76** to generate highly functionalised pyrroles **77** containing a trifluoromethyl group at the 2-position in a selective manner **(Scheme 1.14)**.[29] Analogous to the group's previously mentioned report, a 1,3-sulfonyl migration again occurs. Both electron-rich and electron-deficient aryl moieties were well tolerated at R^1, however, the reaction does not work with alkyl substituents at this position. The alkynyl substituent could be readily diversified, with both alkyl and aryl groups tolerated. Crossover experiments indicated an intermolecular process for the sulfonyl migration, while a deuterium incorporation experiment was consistent with the absence of C–H bond cleavage at the C-4 position. As a result, the following mechanism was proposed **(Scheme 1.14)**. Initial aza-Claisen rearrangement of **76** affords the intermediate **78**, which upon isomerisation gives the allene **79**. Coordination of the silver(I) catalyst with the allene intermediate **79** leads to cyclisation of the silver complex **80**, affording the cationic pyrrole **81**. Cleavage of the N–S bond ensues affording the intermediate **82** and the sulfinate anion. Regioselective recombination displaces the silver(I) cation in an intermolecular manner and in doing so generates the rearranged pyrrole **77**.

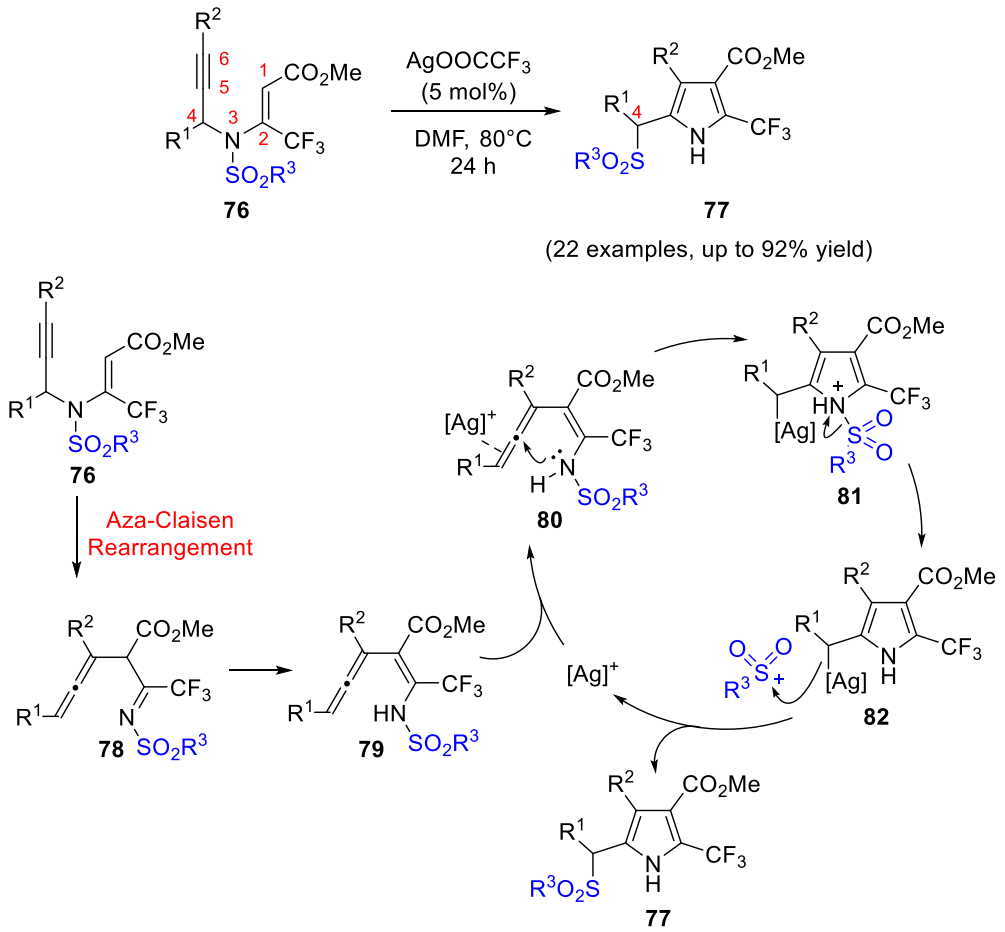

Scheme 1.14: Generation of 2-trifluoromethyl-5-(arylsulfonyl)methyl pyrroles via silver-catalysed 1,3-sulfonyl migration

1.2.1.3. Transition metal-catalysed sulfonyl migration using *N*-sulfonylhydrazones

N-Sulfonylhydrazones undergo a range of transition-metal-catalysed and transition-metal-free transformations. The breadth of reactivity and synthetic application of this family of compounds has been reviewed extensively in recent years,[30-32] however, the overwhelming majority of reports involve either retention of the sulfonyl moiety at nitrogen or decomposition with elimination of the sulfonyl moiety. Notwithstanding, *N*-sulfonylhydrazones have recently been observed to be synthetically useful precursors to both allyl and vinyl sulfones, utilising sulfonyl migration in atom-economical syntheses. In this section, recent advances in the reactivity of these compounds utilising transition-metal catalysis, incorporating sulfonyl migration, will be considered.

1.2.1.3.1. Copper-catalysed sulfonyl migration using *N*-sulfonylhydrazones

Mao *et al*. developed a high-yielding stereoselective synthesis of terminal and α,β-unsaturated (*E*)-vinyl sulfones **84** from *N*-sulfonylhydrazones **83** via a radical pathway **(Scheme 1.15)**.[33] The radical pathway was confirmed by the addition of TEMPO to the standard reaction conditions, which completely inhibited the formation of the sulfonyl migration product. The role of the sulfonyl free radical was further confirmed by the addition of 1,1-diphenylethylene (DPE), an alternative radical scavenger, with **85** isolated as the major product in 72% yield completely replacing formation of **84**.

A small amount of water was required for an efficient transformation to occur; when anhydrous $Cu(OAc)_2$ was used a 35% reduction in yield was observed for **84** (R^1 = R^2 = Ph) when compared to when one drop of water was added. The mechanism is postulated to proceed via isomerisation of the *N*-tosylhydrazone **83** to **86**. Coordination of the copper catalyst to the alkene promotes the decomposition of **87**, with concomitant extrusion of diazene and the free tosyl radical affording the complex **88**. Recombination of **88** and the tosyl radical affords the carbenoid **89**, which undergoes O–H insertion with water to afford the alcohol **90**. *Trans*-elimination of water stereoselectively affords the desired *(E)*-vinyl sulfone.

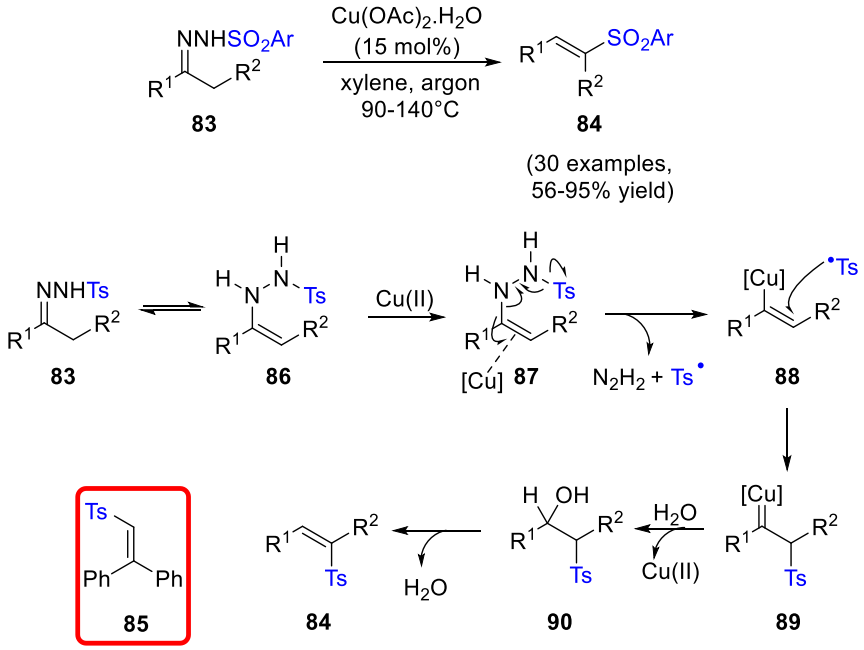

Scheme 1.15: Copper-catalysed stereoselective synthesis of (*E*)-vinyl sulfones via the radical reaction of *N*-tosylhydrazones

The Zhang group reported the one-pot generation of 2-sulfonylmethyl 1*H*-indenes **93** in moderate yields via a copper-mediated sulfonyl radical-enabled cyclisation of *N*-arylsulfonyl hydrazones **(Scheme 1.16)**.[34] A radical process was confirmed through the suppression of the reaction pathway on the addition of the radical scavengers TEMPO or 1,4-benzoquinone (BQ). Starting with the benzaldehyde **94**, in the absence of either CuBr or DTBP, the major product isolated was the *N*-sulfonylhydrazone **95**, highlighting the key role of the copper salt and oxidant in the reaction process. Stopping the reaction after 5 minutes afforded exclusively **95**, with complete consumption of starting material. The *N*-tosylhydrazone **95** was demonstrated to afford the indene **100** on treatment with $TsNHNH_2$ under the standard conditions. In the absence of a second equivalent of $TsNHNH_2$ the desired product was afforded in 10% yield, highlighting that efficient sulfonyl radical attack at the terminal vinyl carbon requires the second equivalent of $TsNHNH_2$.

Considering this the following mechanism was proposed. Condensation of $TsNHNH_2$ with the aldehyde **94** affords the *N*-tosylhydrazone **95**. A tosyl radical is generated in situ via the DTBP and copper-mediated oxidative decomposition of the second equivalent of $TsNHNH_2$. Subsequent addition of the sulfonyl radical to the terminal alkenyl carbon of **95** affords the intermediate radical **96**. Intramolecular 5-*exo*-trig cyclisation and hydrogen abstraction affords **98**, which loses dinitrogen and a tosyl radical

to give **99**. Finally, a copper-mediated single electron transfer oxidation, and subsequent elimination via β-H abstraction by *tert*-butoxide affords the indene product **100**.

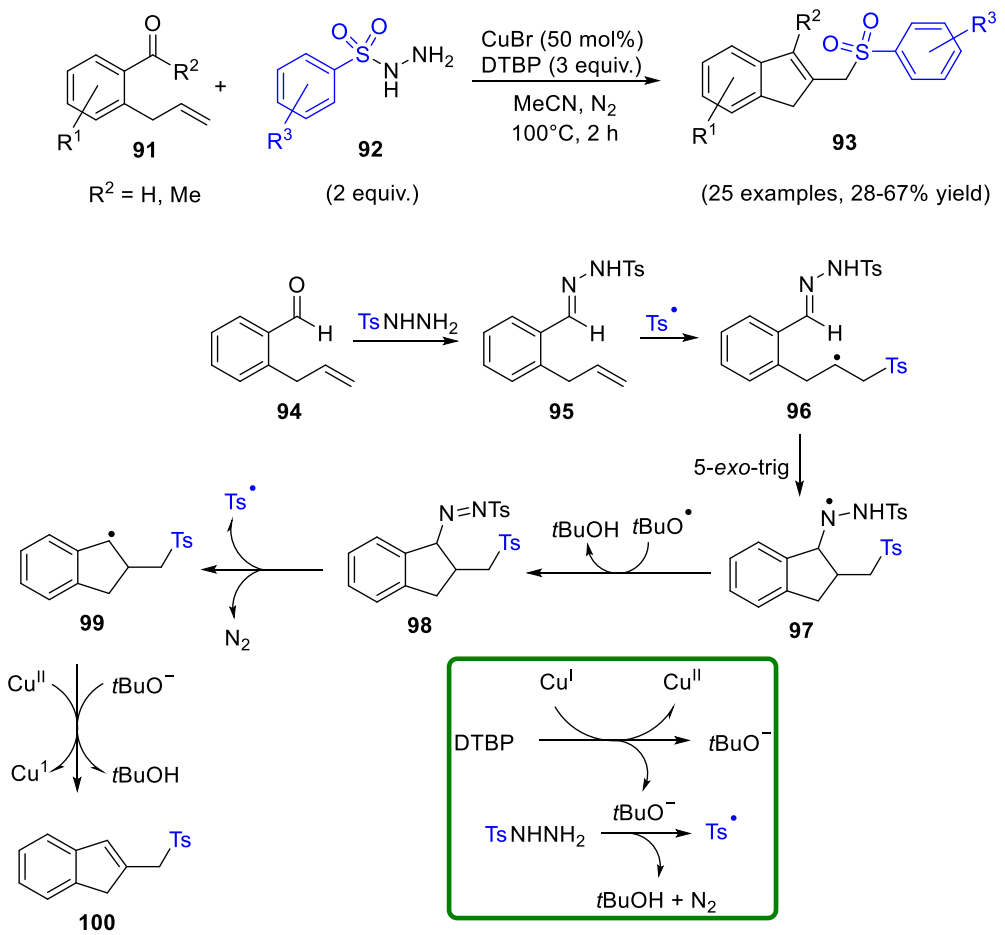

Scheme 1.16: Access to sulfonylmethyl 1*H*-indenes via copper-mediated sulfonyl radical-enabled 5-*exo*-trig cyclisation of alkenyl aldehydes

The Wang group described the copper(I)-catalysed one-step cross-coupling of terminal alkynes **101** with *N*-sulfonylhydrazones **102** to afford α,β-disubstituted vinyl sulfones **103** in moderate to excellent yields **(Scheme 1.17)**.[35] Notably, the reaction proceeds readily for various *N*-tosylhydrazones with both electron-donating and electron-withdrawing groups tolerated on the aryl ring, albeit in lower yield when electron-withdrawing groups are present. Both naphthyl- and alkysulfonyl derivatives are also well tolerated, while both the ester substituent and the electronics of the aryl ring of the terminal alkyne can readily be altered with no deleterious effect. A radical-mediated transformation was excluded based on the absence of inhibition of the reaction on addition of TEMPO or BHT to the optimised reaction medium. Both the alkyne **110** and allene **111** afforded the desired product **112** when treated with *p*-toluenesulfinate in the presence of triethylamine. Notably, the alkyne **110** did not furnish any product in the absence of base, confirming the role of the allene intermediate **111** in the reaction cascade.

In light of these findings and previous reports the authors postulated the following mechanism **(Scheme 1.17)**. Base-mediated decomposition of the *N*-tosylhydrazone **104** affords the tosylate anion and diazo compound **105**. Subsequent reaction of **105** with the copper acetylide **107** affords the carbenoid **108** which undergoes migratory insertion of the alkynyl moiety to the α-carbon to give the

intermediate **109**. Protonation of **109** releases the copper cation which becomes available for the next catalytic cycle and generates the internal alkyne **110**. Deprotonation with triethylamine affords the allene intermediate **111** which reacts with the tosyl anion in a regioselective manner, completing the sulfonyl migration, and affording the product **112**. The stereoselectivity of the reaction can be explained by the steric hindrance between the tosyl and phenyl moieties that inhibits the formation of the *Z*-isomer **113**.

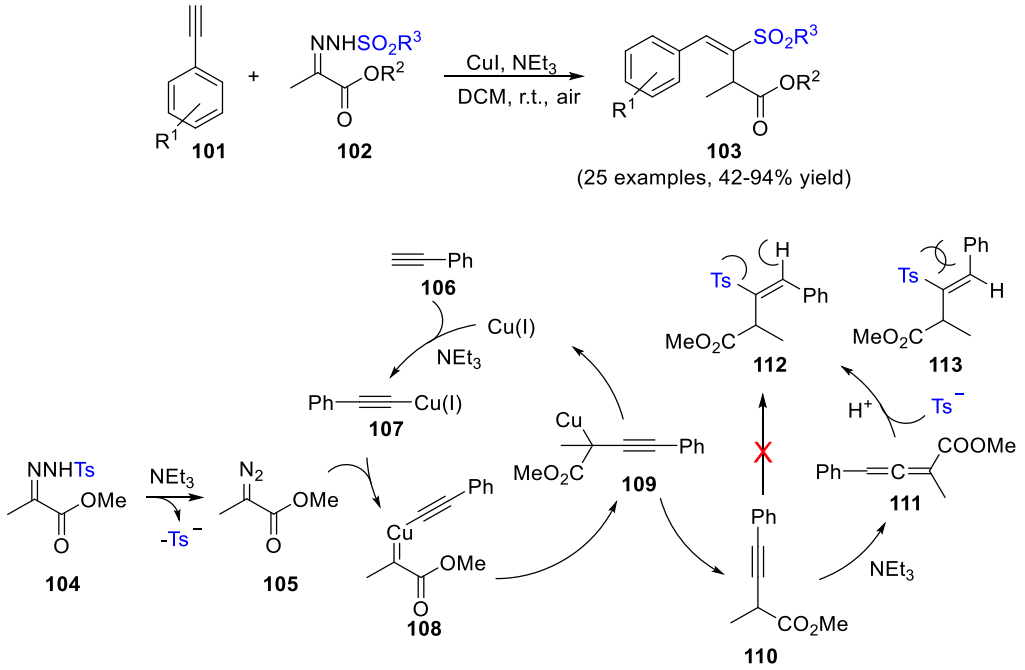

Scheme 1.17: One-step copper(I)-catalysed cross-coupling of terminal alkynes with *N*-sulfonylhydrazones affording α,β-disubstituted vinyl sulfones

The Ji group described a copper(II)/silver(I)-catalysed domino reaction of anthranils **114** with *N*-sulfonylhydrazones **115** to afford a series of 2-aryl-3-sulfonyl disubstituted quinoline derivatives **116** in moderate yields (**Scheme 1.18**).[36] To elucidate a mechanism the authors carried out a series of control experiments. The presence of TEMPO suppressed the reaction of **114** and **117** affording the desired product **118** in only 16% yield, while also forming the decomposition product **119** and the quinoline **120**. Additionally, in the presence of the alternative radical scavenger DPE, the trapped vinyl sulfone product **85** was observed by LC-MS confirming the presence of a sulfonyl radical in the mechanistic pathway. When **114** and **122** were reacted in the presence of the quinoline **123** no formation of **118** was observed highlighting that the sulfonyl migration occurs prior to the formation of the quinoline skeleton.

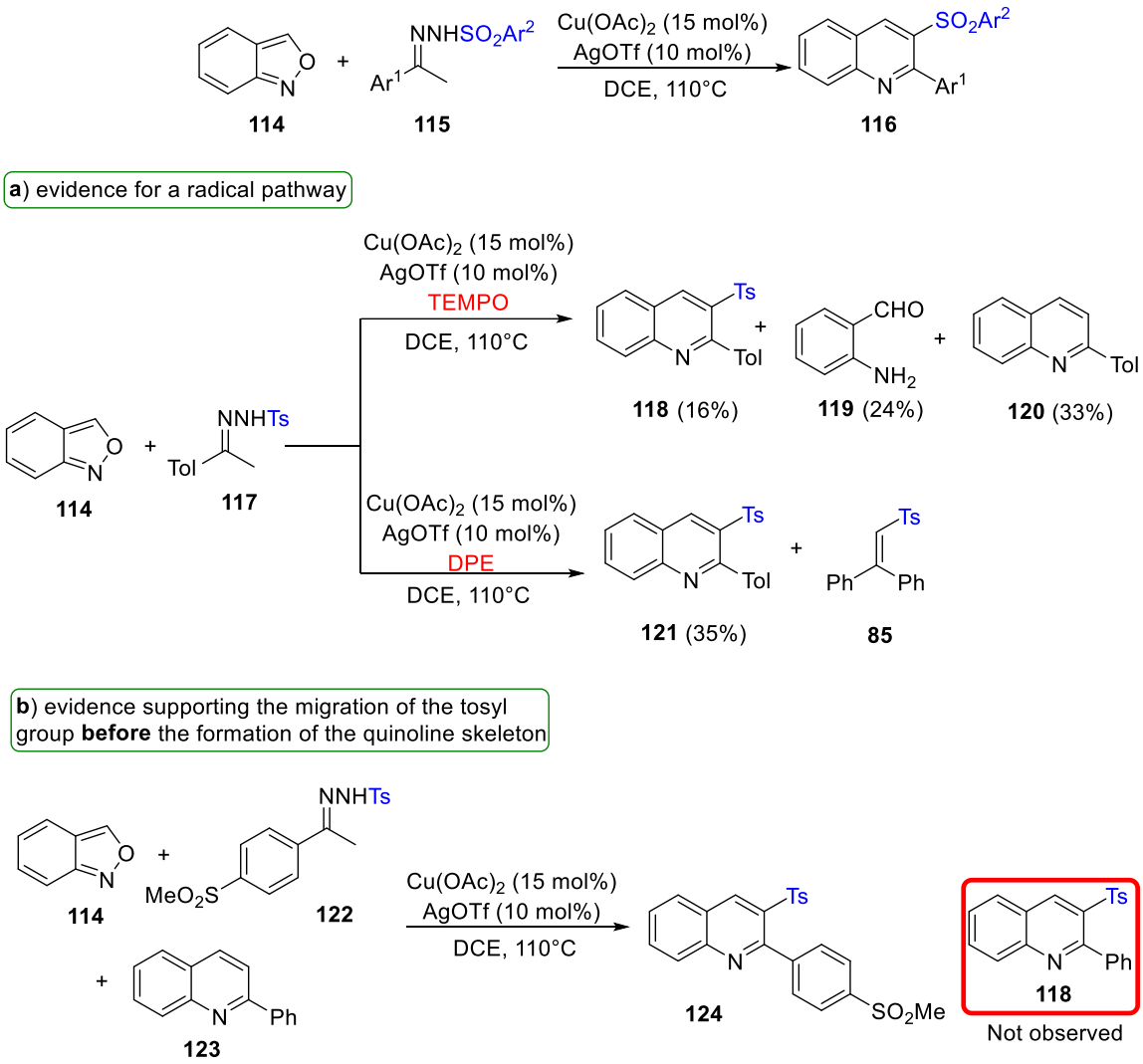

Scheme 1.18: Copper(II)/silver(I)-catalysed formation of 2-aryl 3-sulfonyl disubstituted quinoline derivatives via the reaction of *N*-sulfonylhydrazones and anthranils

In light of the above the authors proposed that the zwitterion **114** reacts with the *N*-tosylhydrazone **126** under thermal conditions to afford the diazo intermediate **127** with expulsion of a tosyl radical **(Scheme 1.19)**. Loss of nitrogen from the diazo compound **127** effected by the copper catalyst gives the carbenoid **128**, which subsequently coordinates with the anthranil **114** to give **129**. Carbene migratory insertion ensues to form **130**, while the following N–O bond cleavage affords the tautomer pair **131** and **132**. Addition of the tosyl radical to the terminal alkenyl carbon of **132** leads to the intermediate **133**, which cyclises in the presence of the AgOTf catalyst to yield the rearranged quinoline **125**.

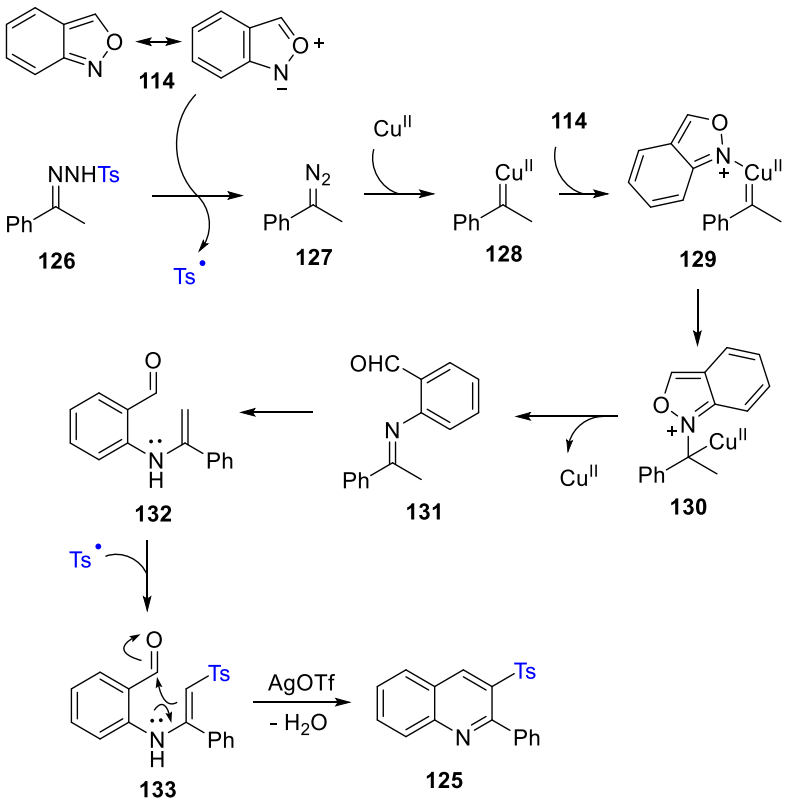

Scheme 1.19: Proposed mechanism for the copper(II)/silver(I)-catalysed formation of 2-aryl-3-sulfonyl quinolines

Xu and co-workers recently reported the synthesis of 4-methyl 2*H*-chromene derivatives **135** from alkyne tethered *N*-sulfonyl hydrazones **134** using copper catalysis **(Scheme 1.20)**.[37] Notably, in the absence of copper spiro-4*H*-pyrazoles (e.g. **139)** are instead the major products. Monitoring of the reaction progress by ^{1}H NMR allowed the identification of the 3*H*-pyrazole **137**, which was isolable. Furthermore, reacting **137** with one equivalent of CuI under thermal conditions gave **138** and **139** in 44% and 55% conversion respectively, highlighting that the 3*H*-pyrazole **137** is a key intermediate in both potential transformations. The formation of **138** in this instance, which does not require a catalyst, suggested that dintrogen extrusion could be preceded by anion exchange (Ts^{-}/I^{-}) and/or coordination of the copper catalyst with **137**. As such, using CuOTf as catalyst, both the copper complex **140** and the triflyl addition product **141** were observed by ESI-MS. Crossover experiments indicated not only that the sulfonyl migration is an intermolecular process but also that it is likely that the counter ion is either in close proximity or associated to the intermediate during the transformation, and that the catalytic rate of reaction is faster than the counter ion exchange; this is as a result of observing that the less nucleophilic nosyl anion afforded a significantly higher combined yield than that of the tosyl anion **(Scheme 1.20)**. Isolation of the deuterated product [D]-**138** rationalised the protonation after recombination with the tosyl anion. Further evidence for the reaction pathway was obtained via the identification of the intermediates **145** and **146** by ^{1}H NMR and HRMS (see **Scheme 1.21**).

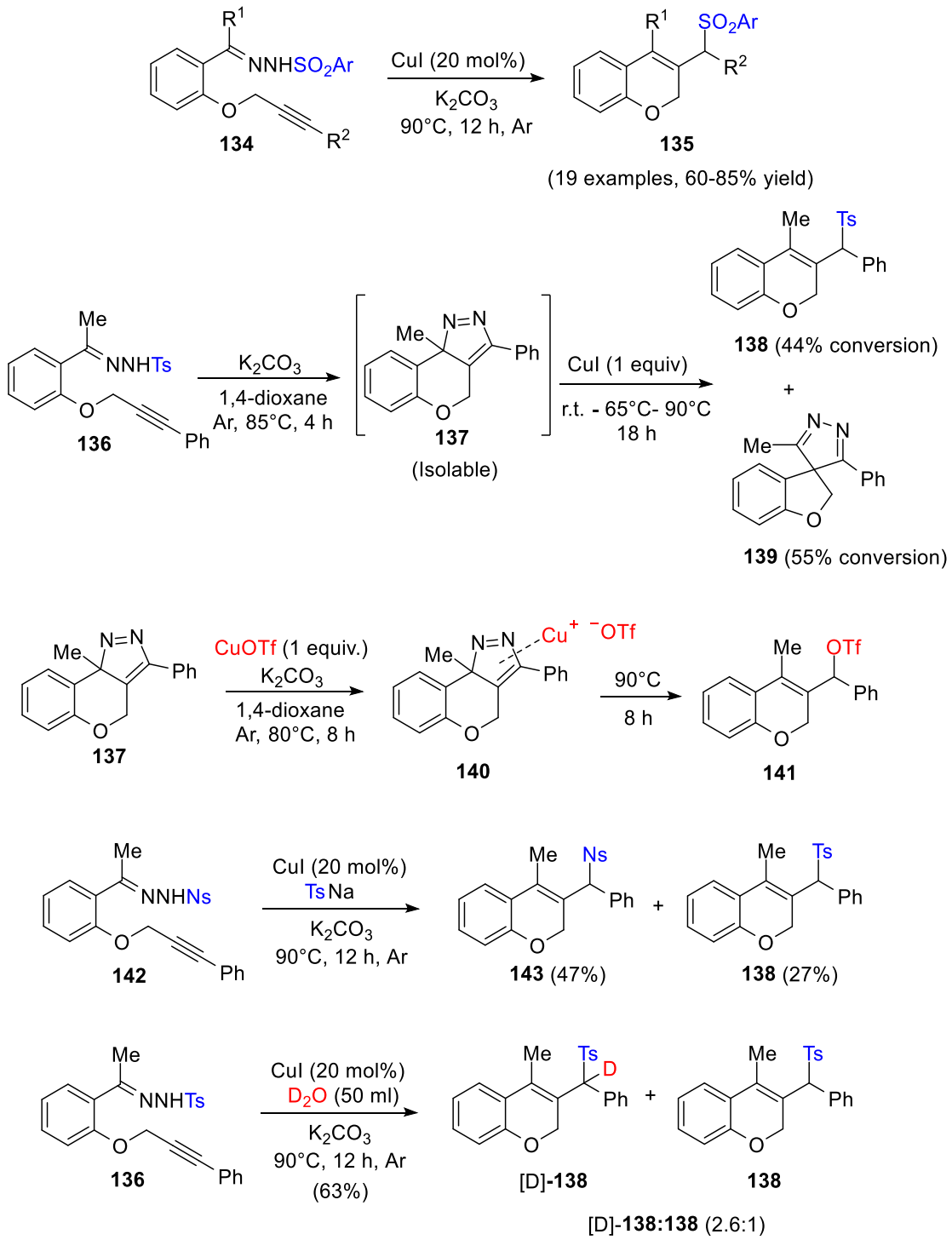

Scheme 1.20: Copper-catalysed synthesis of 4-methyl 2*H*-chromenes alkyne tethered *N*-sulfonyl hydrazones

Considering this the following mechanism was proposed **(Scheme 1.21)**. K_2CO_3-mediated deprotonation of the *N*-sulfonyl hydrazone **144** affords the potassium salt **145**. Subsequent ion exchange affords the copper complex **146**, which undergoes a [3+2] cycloaddition/dinitrogen extrusion/sulfonyl anion recombination to give the desired product **148** via **147**. Alternatively, dissociation of the copper catalyst could occur leading to the rearranged spiro-product **150** via van Alphen-Hüttel rearrangement of **149**.

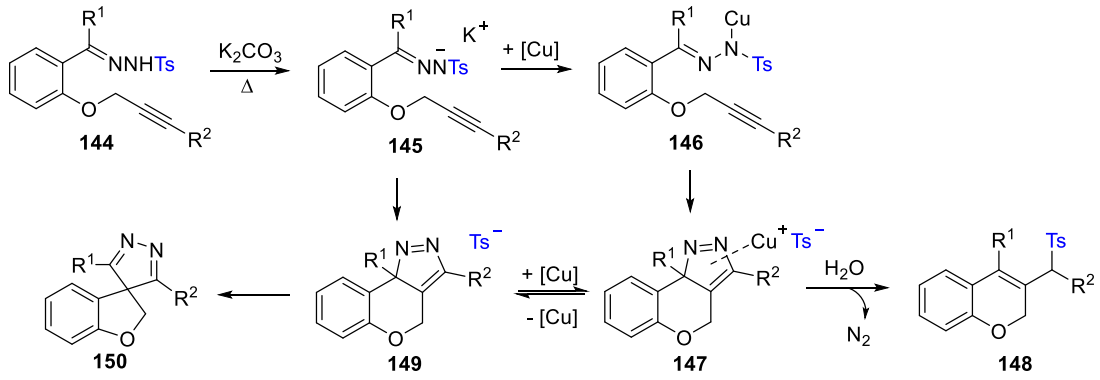

Scheme 1.21: Proposed mechanism for the copper-catalysed transformation of alkyne tethered *N*-sulfonyl hydrazones to 4-methyl 2*H*-chromene derivatives

1.2.1.3.2. Palladium-catalysed sulfonyl migration using *N*-sulfonylhydrazones

Allylic sulfones are accessible via palladium-catalysed cross-coupling of aryl and vinyl iodides **151** and **154** with *N*-sulfonylhydrazones **152** and **155**, involving carbene migratory insertion and regioselective addition of the released sulfonyl anion **(Scheme 1.22)**.[38-39] For example, using $Pd(OAc)_2$ and triphenylphosphine as catalyst, and BTAC as phase-transfer additive, a series of allylic sulfones **156** were generated in moderate to high yields, with electron-deficient and electron-rich aryl rings all well tolerated, as well as a range of sulfonyl moieties. The reactions are believed to proceed via initial base-mediated decomposition of the *N*-tosylhydrazone **159** to afford the diazo **160** with concomitant release of the tosylate salt. The diazo **160** reacts with the vinylpalladium iodide complex **158** to form the carbenoid **161**, which undergoes migratory insertion to afford the η^1-allylpalladium intermediate **162**. Isomerisation to the η^3-allylpalladium complex **163** is followed by selective nucleophilic addition of the tosylate anion to give **164** as the exclusive product.

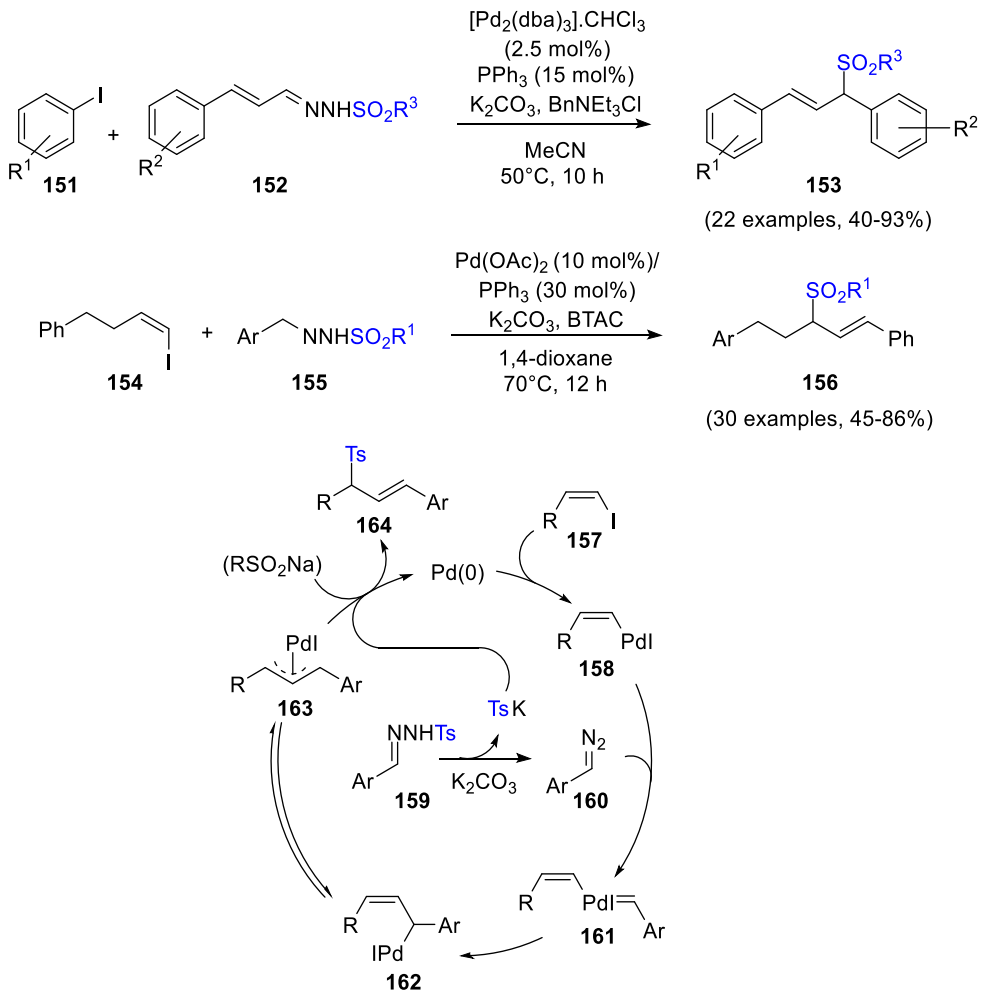

Scheme 1.22: Generation of allylic sulfones via palladium-catalysed cross-coupling of aryl iodides and *N*-tosylhydrazones

1.2.1.4. Miscellaneous metal-catalysed sulfonyl migration

The introduction of a sulfonyl group to the C-7 position of indoles can be achieved in moderate to good yields through the aluminium trichloride-mediated regioselective 1,3-sulfonyl migration of *N*-sulfonyl indoles **165 (Scheme 1.23)**.[40] The sulfonyl migration was found to proceed smoothly when an electron-donating group was present at the C-5 position of **165**, however the regioselectivity of the transformation was attenuated by the presence of electron-withdrawing groups with some formation of the 3-sulfonyl indole observed. The presence of the bulky *tert*-butyl group at the C2 position appears to assist the cleavage of the N–S bond allowing the sulfonyl migration to occur; when a *n*-butyl substituent was present at C2 no migration was observed, despite the acylation readily occurring. In the absence of acyl chloride the sulfonyl migration still readily occurred, highlighting the key role of $AlCl_3$ in the reaction. The mechanism was proposed to involve a non-concerted, intermolecular sulfonyl migration based on the outcome of crossover experiments. Thus, the reaction seems to proceed via $AlCl_3$-assisted activation of the indolyl double bond followed by cleavage of the N–S bond to give **168** which subsequently undergoes sulfonylation at the C7 position to give **171** via **170**, completing the sulfonyl migration.

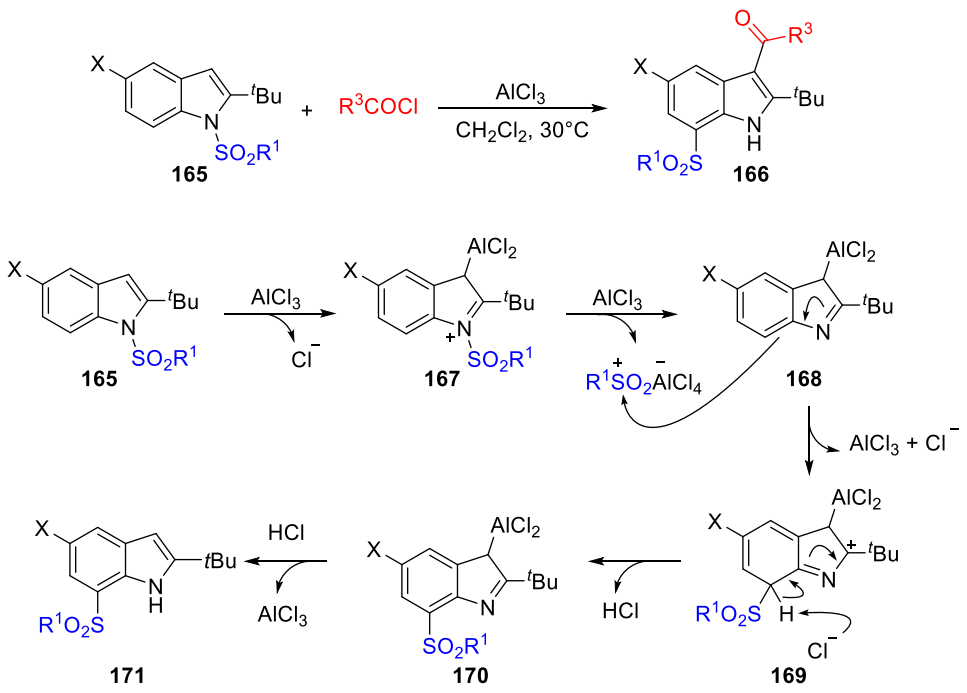

Scheme 1.23: $AlCl_3$-mediated 1,3-sulfonyl migration of *N*-sulfonyl indoles; access to 7-sulfonyl indoles

The Zhan group reported the copper(I)-catalysed stereoselective synthesis of (1*E*,3*E*)-2-sulfonyl-1,3-dienes **173** from *N*-propargylic sulfonylhydrazones **172** involving a stereoselective sulfonyl migration **(Scheme 1.24)**.[41] When employing catalytic $[Cu(PPh)_3I]_4$ in refluxing toluene yields of 51–92% were achieved, with electron-poor sulfonylhydrazones leading to higher yields than electron-rich analogues. Aryl groups at both R^2 and R^4 bearing electron-withdrawing and electron-donating substituents were also well tolerated.

Crossover experiments indicated that the migration of the sulfonyl group is an intermolecular process. Based on these observations the authors hypothesised that the mechanism involves initial 6-*endo-dig* addition of the sulfonylhydrazone onto the copper(I)-alkyne complex **174** to generate the intermediate **175** which collapses to the allenic intermediate **176**, completing the initial [3,3]-rearrangement. Intermediate **176** is unstable and readily loses dinitrogen, leaving ion pair **177**. Finally, the tosyl anion regioselectively and stereoselectively attacks the central *sp* carbon atom of the allenic moiety, with subsequent electon transfer affording the (1*E*,3*E*)-2-sulfonyl-1,3-diene **173 (Scheme 1.24)**. The release of nitrogen is most likely the trigger for the sulfonyl migration.

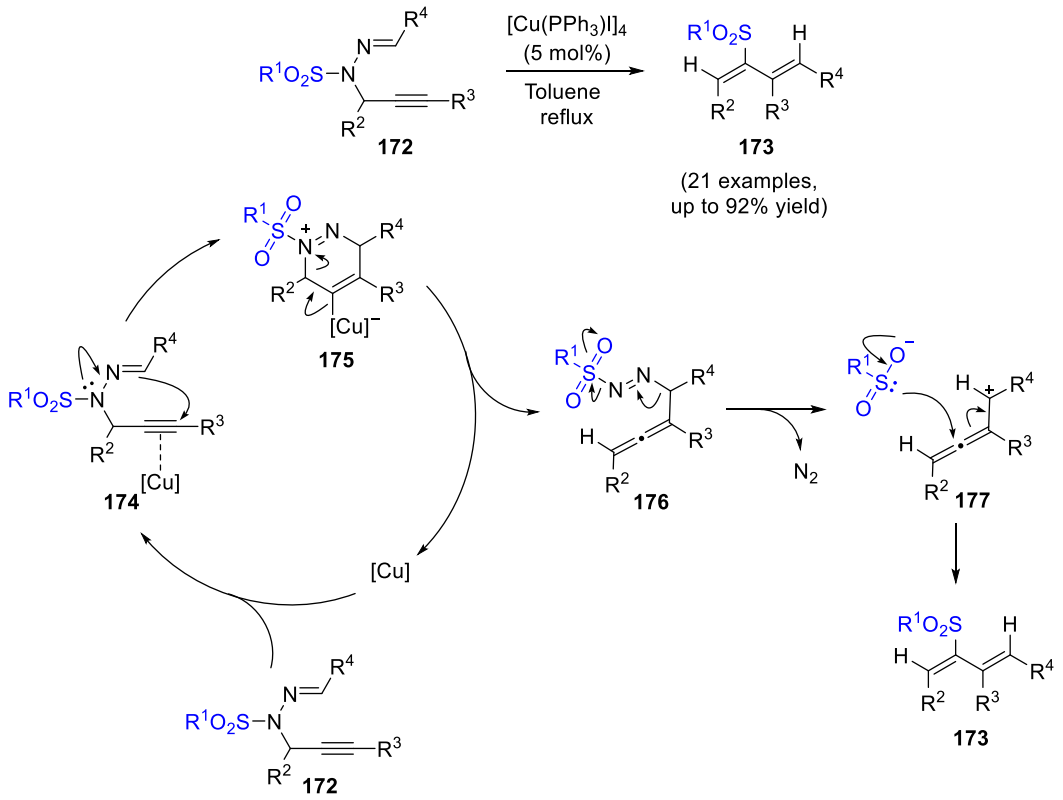

Scheme 1.24: Copper(I)-catalysed stereoselective synthesis of (1*E*,3*E*)-2-sulfonyl-1,3-dienes utilising migration of the sulfonyl group

Zhan and co-workers reported the zinc chloride mediated synthesis of 4-(sulfonyl)-methyl-1*H*-pyrazoles **179** in excellent yields from *N*-allenic sulfonylhydrazones **178** via a formal 1,4-nitrogen to carbon sulfonyl migration **(Scheme 1.25)**.[42] Crossover experiments utilising two different *N*-allenic sulfonylhydrazones highlighted an intermolecular process for the sulfonyl migration. Mesyl, tosyl and benzenesulfonyl substituents were tolerated. The authors postulated that coordination of $ZnBr_2$ to the azomethine nitrogen atom of **178** induces a nucleophilic addition of the central allenyl carbon to the azomethine carbon to give exclusively (*E*)-**182**. Formation of (*Z*)-**181** is inhibited due to steric hindrance between the R^3 and R^4 substituents. Bromide assists the N–S bond scission to generate the intermediate **183** and tosyl bromide, which then reacts with the exocyclic alkene moiety to complete the formal 1,4-tosyl migration, and in doing so generates **184**. Tautomerisation affords the rearranged aromatic pyrazole **179**.

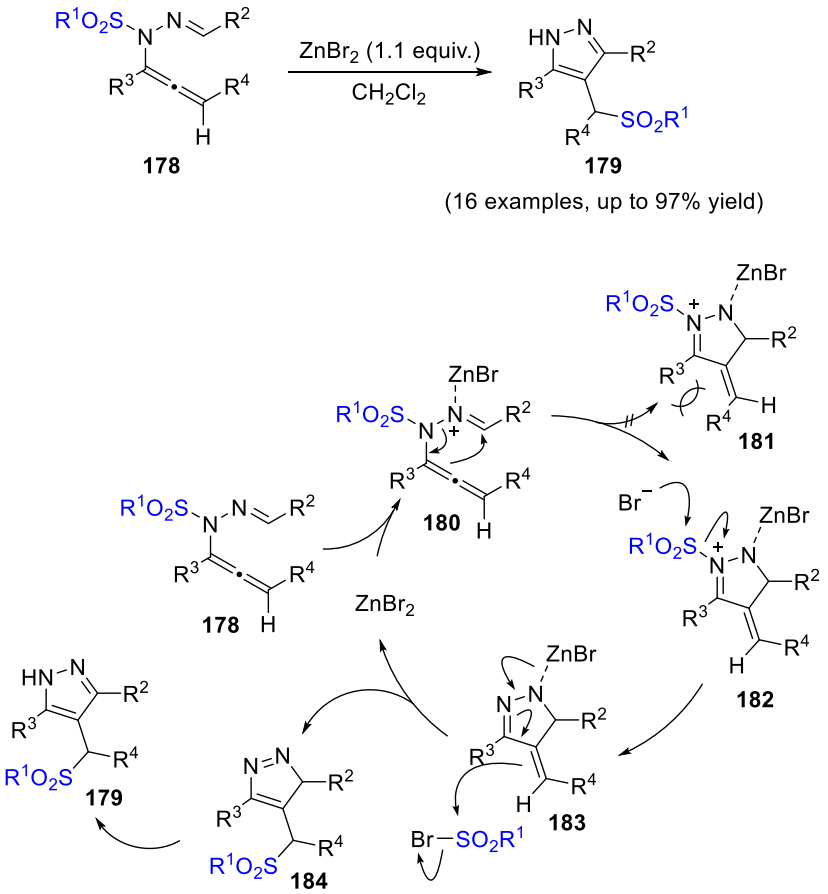

Scheme 1.25: Selective synthesis of 4-(sulfonyl)-methyl-1*H*-pyrazoles from *N*-allenic sulfonylhydrazones via 1,4-nitrogen to carbon sulfonyl migration (see also **Scheme 1.66**)

1.2.2. Single electron-mediated sulfonyl migration

1.2.2.1. Radical-mediated sulfonyl migration

The Maulide group observed an unexpected nitrogen to carbon 1,3-sulfonyl migration of a tosyl group when attempting to expand the scope of electrophilic Claisen rearrangements to aza-derivatives. While alkyl and alkenyl oxygen-based substrates underwent straightforward Claisen rearrangement to afford a series of hydrocoumarins, aza-derivatives **185–187** did not afford the expected α-substituted lactams **191**, but instead the amidinium derivatives **188–190 (Scheme 1.26)**.[43] Both the allyl and benzyl derivatives **185** and **186** underwent tosyl migration, while the propargyl derivative **187** underwent an additional cyclisation with concurrent tosyl migration. It was postulated that the tosyl migration occurs as a result of a radical pathway, with homolytic cleavage of N–S bond in the intermediate **193**. It was suggested that recombination of the radical pair **194** to afford **188** may be faster than diffusion, and that this process is more favourable energetically than migration of the allyl group.

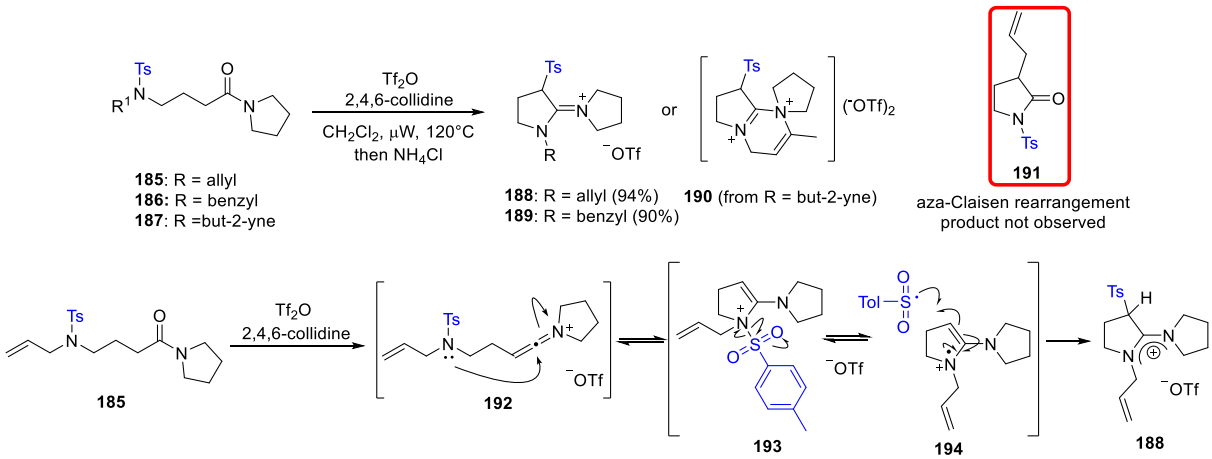

Scheme 1.26: Generation of amidinium derivatives via 1,3-tosyl migration

The thermal 1,3- and 1,5-sulfonyl migrations of *N*-arenesulfonylphenothiazines **195** and *N*-arenesulfonylphenoxazines **196** were realised by the Xu group **(Scheme 1.27)**.[44] Under neutral, thermal conditions a series of sulfonyl substituted phenothiazine **197**/**199** or phenoxazine derivatives **198**/**200** are afforded with moderate yields and regioselectivities. Crossover experiments indicated that the sulfonyl migration was an intermolecular process while a radical-radical coupling reaction mechanism was proposed based on competitive trapping experiments using electron-rich 1,4-dimethoxybenzene, which ultimately allowed the ruling out of a possible ion-pair mechanism. As such, homolytic cleavage of the N–S bond affords the free radical **203** and a sulfonyl radical. The radical intermediate **203** can readily interconvert between the resonance structures **204** and **205** through electron delocalisation. Recombination of the sulfonyl radical with **204** or **205**, leads to formal 1,3- and 1,5-sulfonyl migrations to give intermediates **206** and **207**. Finally, isomerisation of these intermediates affords the rearranged phenothiazine or phenoxazine products **197**–**200**. The formation of the dissociation products **201**/**202**, via abstraction of a hydrogen atom from a neighbouring molecule, such as solvent, provides further supportive evidence for the radical mechanism.

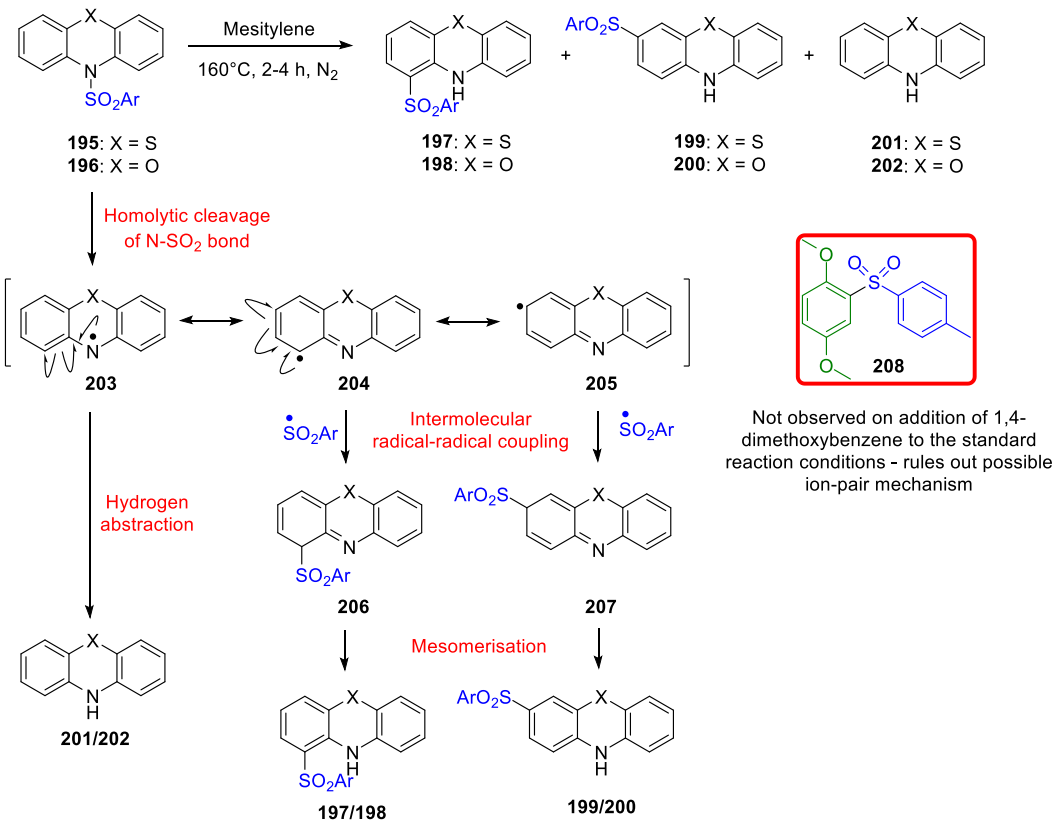

Scheme 1.27: Radical-radical coupling reaction mechanism for the 1,3- and 1,5-sulfonyl migrations of *N*-arenesulfonyl-phenothiazines and phenoxazines

The She group developed a sequential catalysed cycloaddition of *N*-heterocyclic carbene (NHC) activated 1,3-dioxoisoindolin-2-yl 2-phenyl acetate **210** and α,β-unsaturated imines **209** in which the *N*-hydroxyphthalimide (NHPI) by-product **212** of the first reaction catalysed a further nitrogen to carbon 1,3-sulfonyl migration of the tosyl group **(Scheme 1.28)**.[45] Notably, the enantiomeric composition of the major product **211** from the cycloaddition step was retained through the subsequent sulfonyl migration to afford the desired product **213** in moderate yields and high enantioselectivities. The efficiency of the NHC/NHPI catalytic cascade process was found to be strongly dependant on the electronic nature of the R^2 substituent, with electron donating groups on the aromatic ring affording final products in significantly higher yields after 2 steps. While the mechanism of the sulfonyl migration is not fully understood, a radical mechanism was deemed most likely, as the addition of the radical scavenger TEMPO completely inhibited the migration.

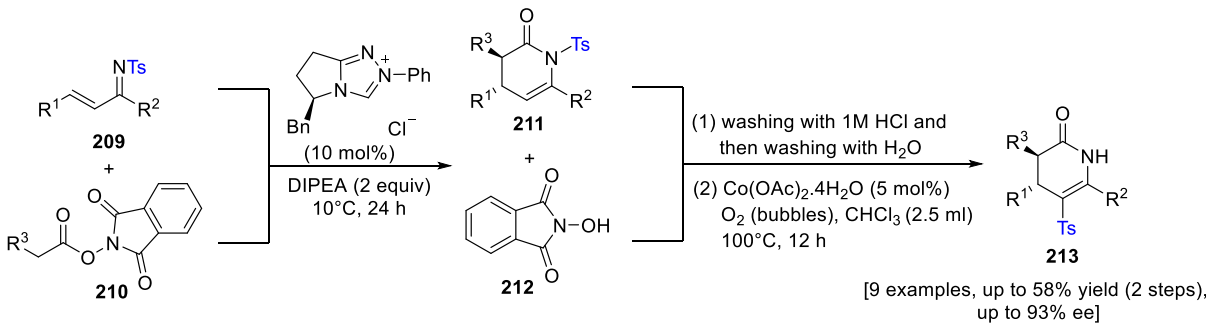

Scheme 1.28: Application of upstream by-product NHPI as catalyst for sequential 1,3-sulfonyl migration

Wang *et al*. reported the di-*tert*-butyl peroxide-mediated radical rearrangement of *N*-sulfonyl-*N*-aryl propynamides **214** to afford 3-sulfonyl-2-(1*H*)-quinolinones **215** in moderate to good yields with good functional group compatibilities, with a 1,3-sulfonyl migration from nitrogen to carbon a key step **(Scheme 1.29)**.[46] Crossover experiments indicated the involvement of an intermolecular process, while a radical pathway was postulated based on the inhibition of the reaction cycle upon the addition of the radical scavengers TEMPO, BHT or galvinoxyl. The intramolecular and intermolecular kinetic isotope effect (KIE) was determined to be 1.08 and 1.04 respectively, indicating that the rate determining step was unlikely to involve the cleavage of the aromatic C–H bond, while also suggesting that either a radical or electrophilic aromatic substitution pathway was involved. Considering this the authors proposed that homolytic scission of the N–SO_2 bond leads to the radical **216** and a sulfonyl radical. Addition of the sulfonyl radical to the alkyne group of radical **216** generates the diradical **217**, which abstracts a hydrogen atom from the solvent, to give the radical **218**. A 6-*endo-dig* cyclisation affords the cyclised radical **219**, which on abstraction of a hydrogen by a *tert*-butoxyl radical affords the 3-sulfonyl-2-(1*H*)-quinolinone **215**.

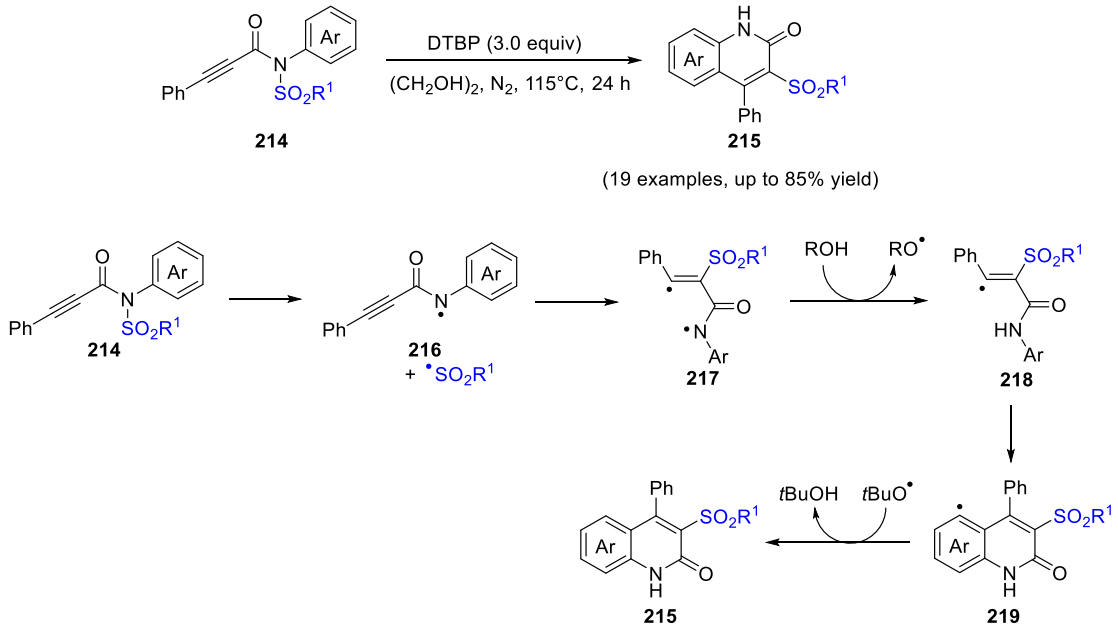

Scheme 1.29: Di-*tert*-butyl peroxide mediated radical rearrangement of *N*-sulfonyl-*N*-aryl propynamides; observation of a formal 1,3-sulfonyl migration

1.2.2.2. Photoinduced sulfonyl migration

Photochemical irradiation of *N*-sulfonyl anilines **220** was found to promote thia-Fries-type rearrangements to afford mixtures of regioisomeric *ortho*- and *para*-aminophenyl sulfone derivatives **221** and **222** in moderate yields, via nitrogen to carbon 1,3- or 1,5-sulfonyl migration **(Scheme 1.30)**.[47] *N*-Alkylation of the sulfonanilides **220** increased the yield of the rearranged products, while the presence of electron-withdrawing groups on the aromatic ring did not greatly lower the yields.

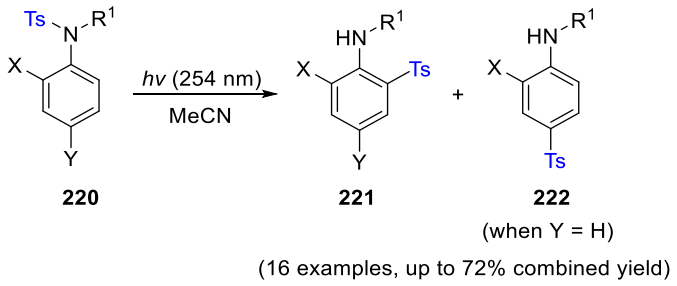

Scheme 1.30: Photochemical thia-Fries-type rearrangement of *N*-sulfonyl anilines

In their efforts to establish a total synthesis of the kopsifoline alkaloid framework **225**, Padwa and co-workers observed an unanticipated desulfonylation of **223**, while attempting to carry out a photochemical rearrangement. The desulfonylation proceeded efficiently, affording **224** in 90% yield **(Scheme 1.31)**.[48-49]

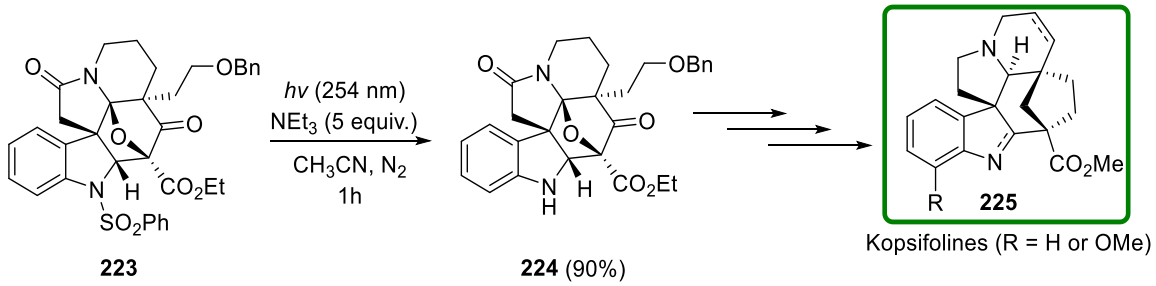

Scheme 1.31: Photoinduced desulfonylation strategy toward the synthesis of the kopsifoline alkaloid framework

Due to the efficiency of this reaction, and the mild conditions required, the authors sought to extend the scope of the reaction to a series of related indoles **226**, however a significant reduction in yield was observed for this class of compound due to the competing formation of both *ortho*- and *para*-photo Fries rearrangement products **228** and **229 (Scheme 1.32)**. In most instances the *para*-rearrangement by-product **228**, the result of a formal 1,5-sulfonyl migration, was the major isomer formed. The reaction is likely initiated by single electron transfer from triethylamine to the electronically excited indole **226*** leading to the triethylamine radical cation and the indole radical anion **231** (via the indole radical **230**). Proton transfer from the radical cation of triethylamine affords the desired desulfonylated indole **227**. In competing processes, the phenylsulfonyl radical can also add to the aromatic framework of the radical anion **231** to afford the transient intermediates **232** or **233**. Subsequent electron transfer from **232** and **233** to the triethylamine radical cation affords the *ortho*- and *para*-sulfonylated indoles **228** and **229**. The competing thia-Fries pathway can be suppressed by addition of n-Bu_3SnH, which allows capture of the sulfonyl radical via hydrogen atom transfer.

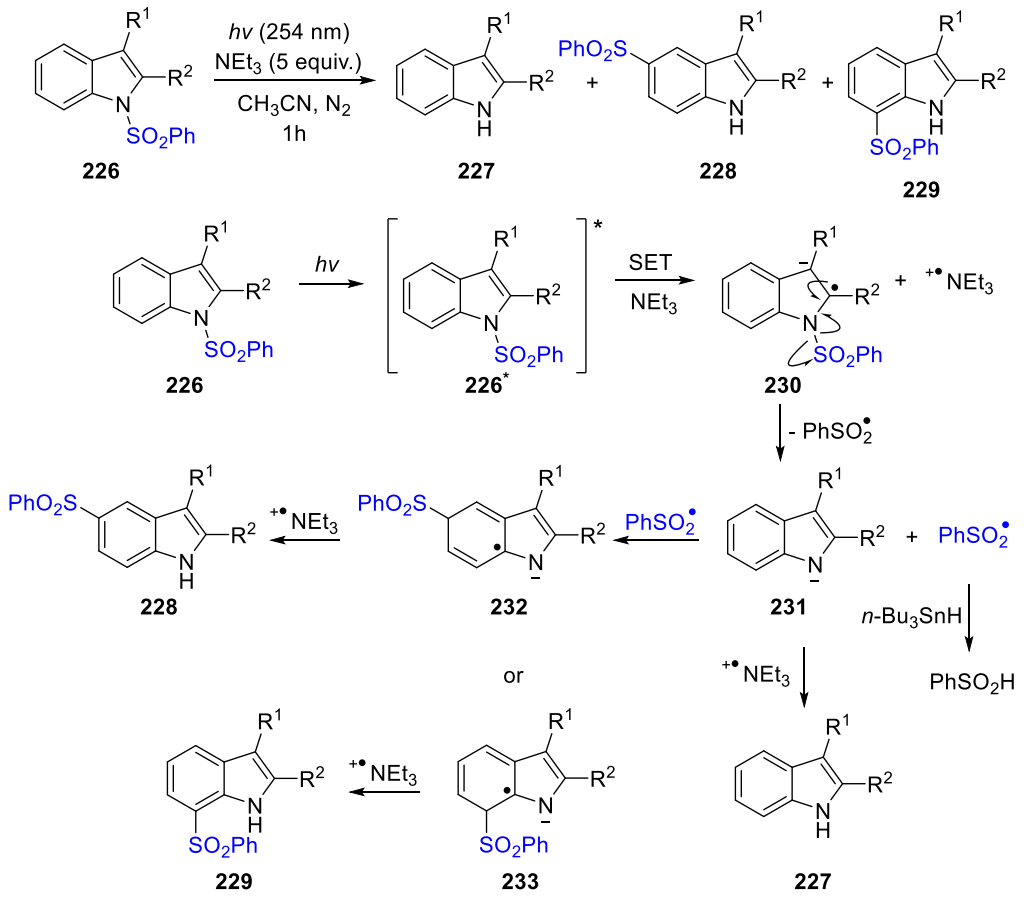

Scheme 1.32: Mechanism for the photoinduced thia-Fries type rearrangement of indoles

Smith and coworkers reported the first selective example of a nitrogen to carbon 1,3-sulfonyl migration of dihydropyridones **234** via prolonged storage and heating, however, most notable was the quantitative isomerisation observed under photochemical conditions **(Scheme 1.33)**.[50-51] Highlights of the methodology include a high degree of tolerance for both *N*- and *C*-substituent diversification around the dihydropyridinone ring, to afford the corresponding rearranged C-sulfonyl products **235** in moderate to high yields with no erosion of stereochemical integrity. Significant efforts to rationalise the mechanism of the sulfonyl migration were made by the authors. Crossover experiments elucidated an intermolecular event, while adding TEMPO under the standard conditions led to complete suppression of the sulfonyl transfer, indicating a radical mechanism. Rather than a straightforward homolytic N–S bond cleavage to give a sulfonyl radical and radical **236** followed by recombination at carbon to give the rearranged product **235**, electron paramagnetic resonance (EPR) spectroscopy indicated the presence of a larger radical that was assigned as the intermediate benzylic radical **237**. Therefore the authors proposed that after the homolytic cleavage, the sulfonyl radical adds to the dihydropyridinone **234** generating the benzylic radical **237** which can extrude a sulfone radical to generate the neutral imine **238**. Tautomerisation of **238** affords the rearranged dihydropyridinone **235**.

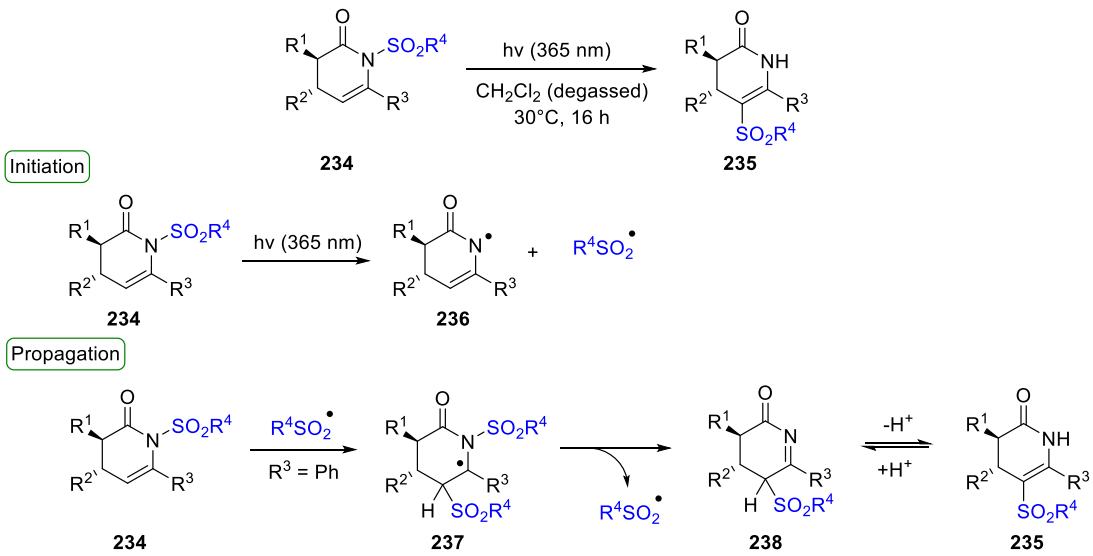

Scheme 1.33: Photoisomerisation of *N*-sulfonyldihydropyridinones; observation of a visible light induced 1,3-sulfonyl migration

The Rutjes group discovered the first example of a photoinduced rearrangement of 1,2-benzothiazole-1,1-diones **240** to form 3-amino-1-benzothiophene-1,1-dione derivatives **241** in excellent yields via a nitrogen to carbon 1,3-sulfonyl migration **(Scheme 1.34)**.[52] Based on literature precedent for the photoinduced cleavage of sulfonamides the authors postulated the following radical mechanism.[53-56] Irradiation of **240** induces homolytic cleavage of the N–S bond which generates the di-radical **242**. Recombination of the sulfinate radical with the C-terminus of the enaminyl radical generates the imine **243**, which subsequently tautomerises to generate the rearranged 3-amino-1-benzothiophene-1,1-dione **241**. The requisite substrates **240** for the photoinduced sulfonyl migration were demonstrated to be accessible through a palladium-catalysed regioselective and highly stereoselective intramolecular hydroarylation of sulfonyl ynamines **239**.

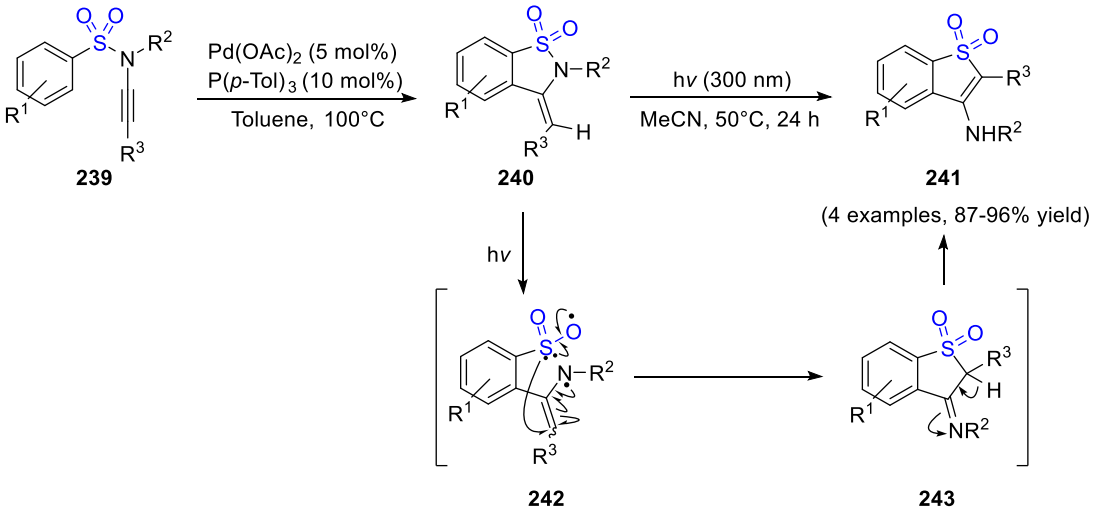

Scheme 1.34: Photochemical rearrangement of 1,2-benzothiazole-1,1-diones to 3-amino-1-benzothiophene-1,1-diones; observation of a nitrogen to carbon 1,3-sulfonyl migration

Torti *et al*. described the use of *N*-arylsulfonimides **244** as potential nonionic photoacid generators able to photorelease up to two equivalents of sulfonic acids for each mole of substrate under deaerated conditions in acetonitrile.[57-58] The product distribution of the reaction under deaerated conditions proved to be complex with all compounds formed arising from the cleavage of the S–N bond to afford both photo thia-Fries rearrangement products **246**, **247**, **249** or **250** and desulfonylated products **245** or **248 (Scheme 1.35)**.

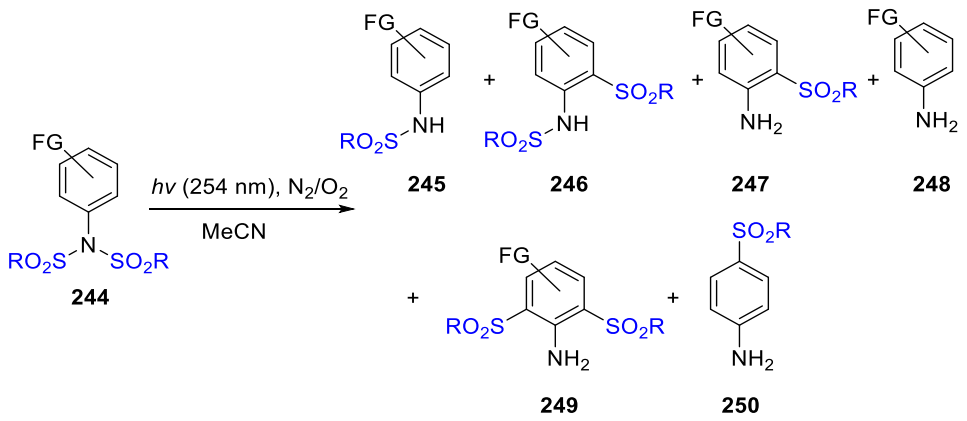

Scheme 1.35: Irradiation of *N*-aryl sulfonimides; observation of single and double photo thia-Fries rearrangement

In order to further understand the photoreactivity of the *N*-arylsulfonamides **244**, and to investigate secondary photochemical pathways, laser flash photolysis (LFP) and electron paramagnetic resonance (EPR) spectroscopy experiments were performed. Considering the supporting evidence of these studies the authors tentatively proposed the following mechanism **(Scheme 1.36)**. Initial irradiation of **244** causes excitation to the singlet state ^{1}**244**, which undergoes homolytic cleavage of the N–S bond to generate the sulfamido **251** and sulfonyl **252** radicals, the presence of which were confirmed by both time-resolved absorption and EPR spectroscopy **(path A)**. Once formed, the radicals **251** and **252** can undergo either thia-Fries rearrangement as a result of recombination **(path D)** to afford **246** via intermediate **253**, or escape from the solvent cage to release sulfonic acids. The photoreactive sulfonamide **246** can undergo a second thia-Fries rearrangement to generate the rearranged aniline **249 (path D")**, however desulfonylation appears to have no role **(path D')**. In contrast, hydrogen abstraction by the sulfamido radical **251** from the reaction medium affords the sulfonamide **245 (path C)**. The favoured pathway, between **path C** and **D**, is dependent on both the functional groups present on the aryl ring and the reaction medium. The single thia-Fries rearrangement product **246** is preferred in less polar solvents and in the presence of electron-donating groups (NMe_2, OMe) on the aromatic ring.

The *N*-arylsulfonamide **245** is also photoactive and can undergo both thia-Fries rearrangement to afford the rearranged aniline **247 (path C")**, or desulfonylation to give **248 (path C')**. The thia-Fries rearrangement is favoured for electron-rich sulfonamides, while for unsubstituted *N*-arylsulfonamides **245** (FG = H) both desulfonylation to generate aniline **248** or thia-Fries rearrangement to give the *para*-substituted aniline **250** can occur.

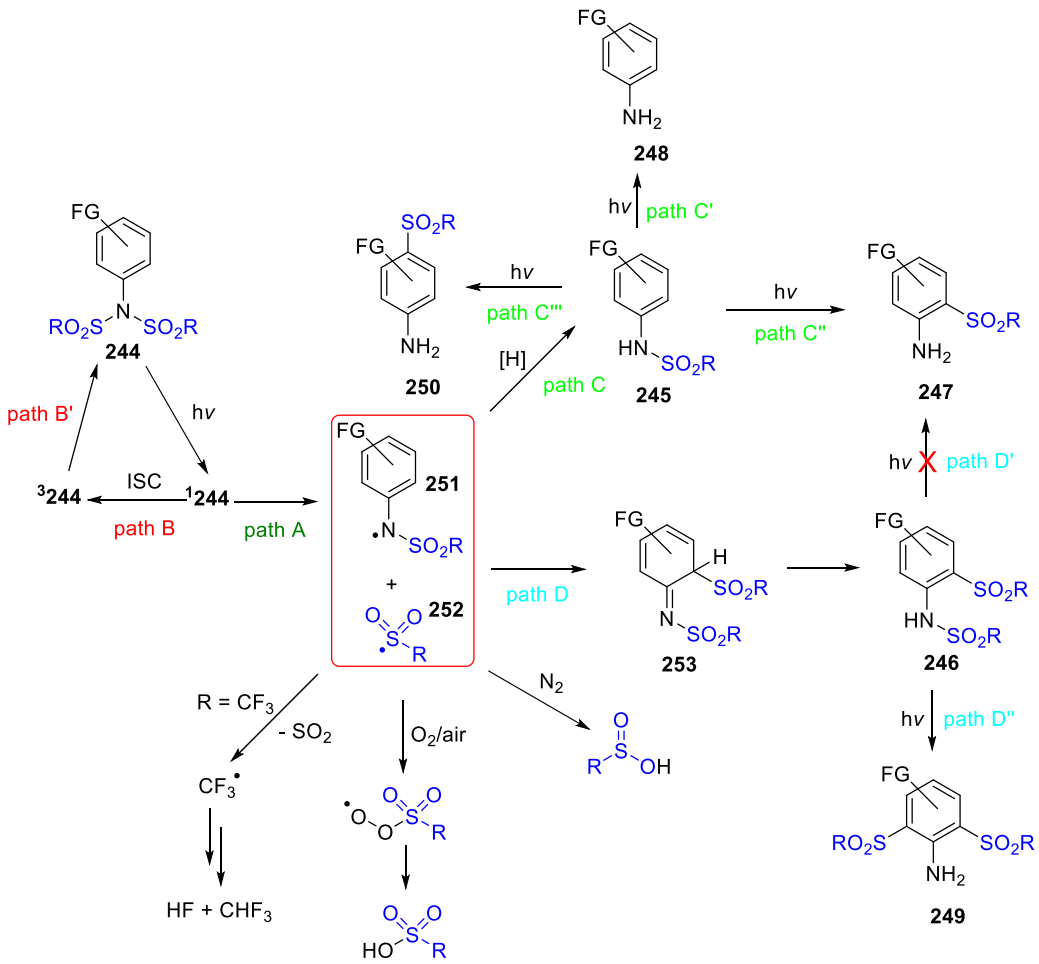

Scheme 1.36: Mechanism for the photochemical reactivity of *N*-arylsulfonimides under inert and aerated conditions

1.2.2.3. Non-metal-catalysed radical-mediated sulfonyl migration of *N*-sulfonylhydrazones

In 2014, the Prabhu group reported the generation of (*E*)-vinyl sulfones **255** from the reaction of *N*-tosylhydrazones **254** with cyanogen bromide and TBAB; involving 1,2-tosyl migration for derivatives bearing a methyl or aryl substituent at R^1 **(Scheme 1.37)**.[59] The reaction is thought to proceed via generation of a bromine radical from the reaction of CNBr–TBAB, which adds to **254** affording the bromo-azo-sulfone **256**, which releases dinitrogen and a tosyl radical to afford **257**. Recombination of the tosyl radical and **257** affords the isolable intermediate **258**, which undergoes either dehydrohalogenation to give the vinyl sulfone **259** when R^1 = H, or a 1,2-sulfone migration in addition to elimination of HBr to afford **255**. Crossover experiments were used to confirm an intermolecular tosyl migration.

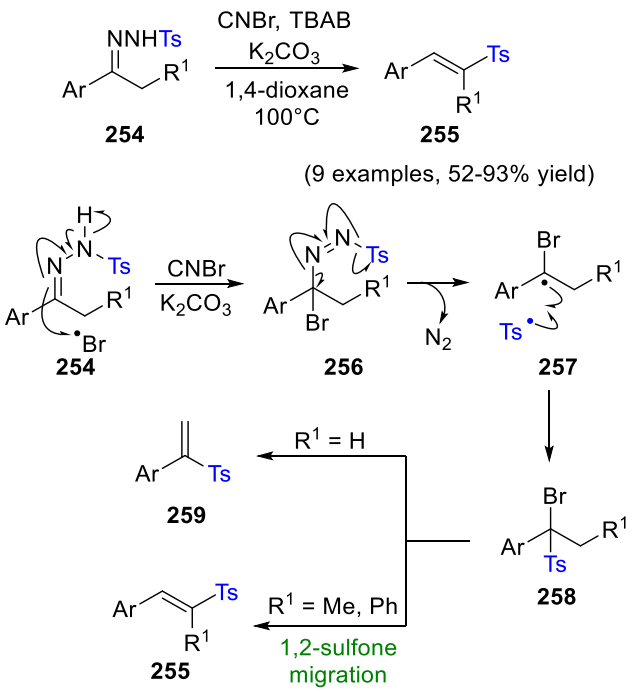

Scheme 1.37: Generation of vinyl sulfones via the reaction of *N*-tosylhydrazones with CNBr and aliphatic quaternary ammonium salts; observation of an intermolecular tosyl migration

Luo *et al*. described a $PhI(OAc)_2$-mediated stereoselective synthesis of (*E*)-vinyl sulfones **261** from aliphatic and aryl *N*-sulfonyl hydrazones **260** in moderate to high yields **(Scheme 1.38)**.[60] Both electron-withdrawing and electron-donating aryl moieties at R^1 were well tolerated, while the methodology was further applied to a range of aromatic heterocyclic derivatives. A radical mechanism was envisaged based on the inhibition of the reaction on the addition of the radical scavenger TEMPO. As such, the authors postulated that the hypervalent iodine intermediate **263** forms in the presence of $PhI(OAc)_2$, which undergoes homolytic N–S bond cleavage to afford a sulfonyl radical and **264**. Subsequent elimination of dinitrogen from **264** affords the radical intermediate **265**, which on recombination with the sulfonyl radical affords **268** (or **266** when R^2 = H). Base-mediated reductive elimination of **266/268** affords either the α- or β-substituted vinyl sulfones **267** or **269**.

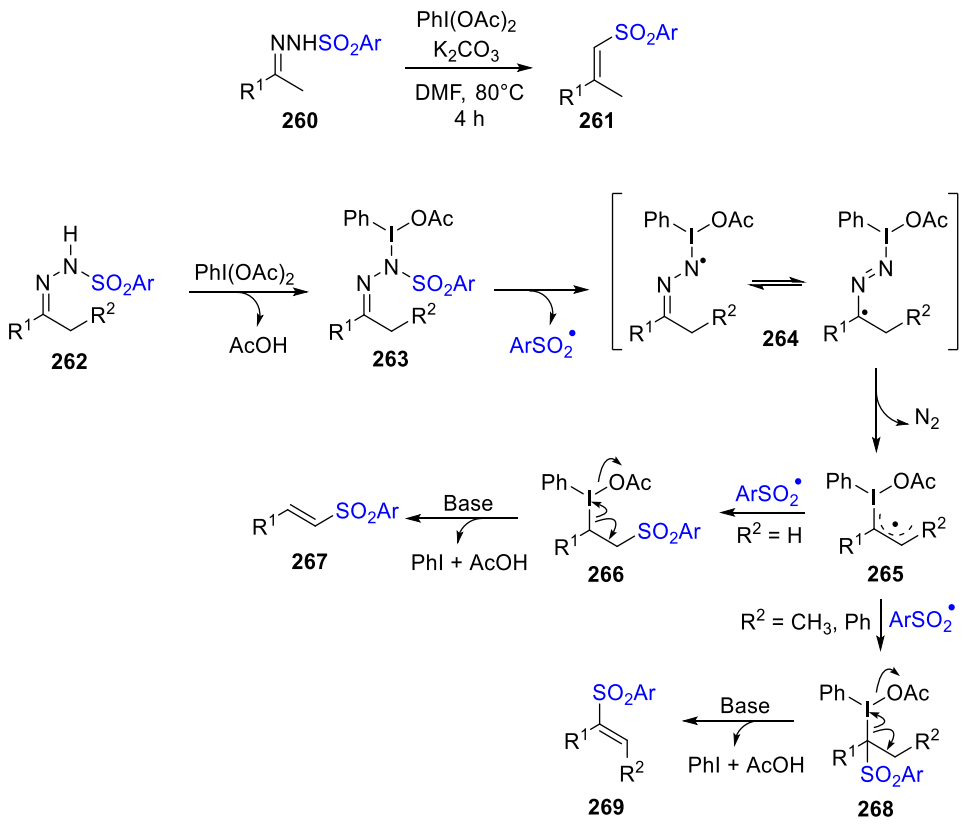

Scheme 1.38: $PhI(OAc)_2$-mediated synthesis of (*E*)-vinyl sulfones from aliphatic and aromatic *N*-sulfonyl hydrazones

Deagostino and co-workers described the first visible-light-mediated transformation of α,β-unsaturated-*N*-sulfonylhydrazones **270** to allylic sulfones **271** with optimal results achieved using $[Ru(bpy)_3]Cl_2 6H_2O$ as photocatalyst **(Scheme 1.39)**.[61] Tosyl, mesyl, and triflyl moieties were well tolerated. Interestingly, on addition of TEMPO, to the standard reaction conditions, **272** was isolated confirming that the process involves a vinyl radical intermediate. A radical chain mechanism was excluded based on observation that no reaction occurs in the presence of AIBN, while the use of the more reactive benzoyl peroxide produced a complex mixture of products. In light of these results the authors postulated the following mechanism. Treatment of the *N*-tosylhydrazone **272** with base affords the anion **273**. Visible-light promotes the excitation of the photocatalyst, and it is the excited state $^*[Ru(bpy)_3]^{2+}$ that induces the single electron oxidation of **273** to give the *N*-centered radical **274**. A formal 1,5-sulfonyl migration, suggested to occur via a 6-membered transition state, leads to the expulsion of dinitrogen and the formation of the vinyl tosylate radical **275**. Abstraction of a hydrogen atom from the solvent, as confirmed via deuterium incorporation studies using $CDCl_3$, generates the final product **276** and a CCl_3 radical that promotes the regeneration of the photocatalyst $[Ru(bpy)_3]^{2+}$.

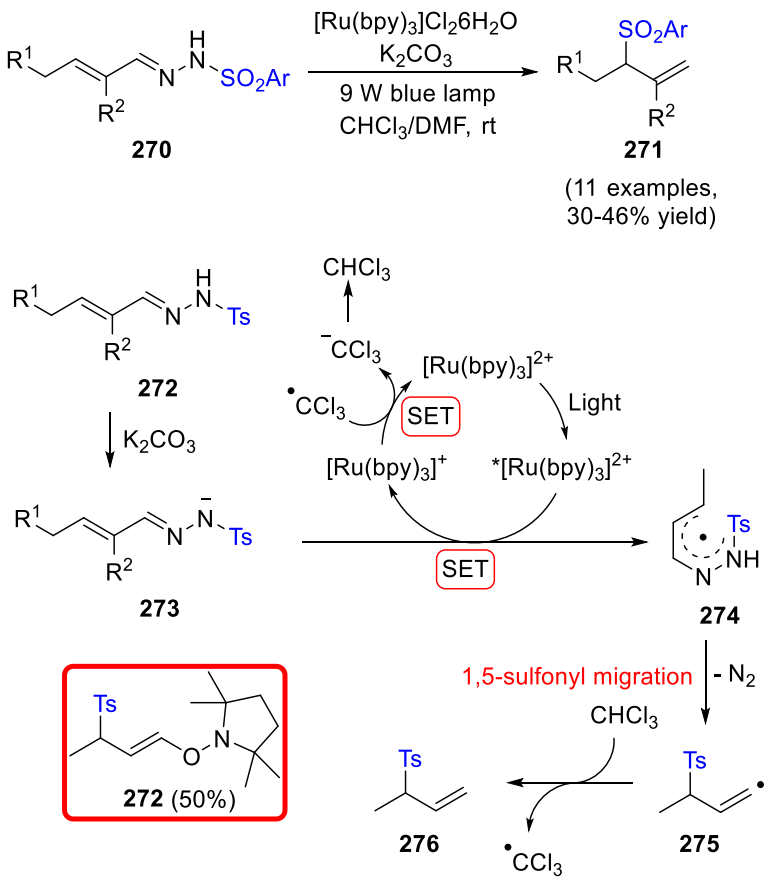

Scheme 1.39: Visible-light-mediated photocatalytic transformation of α,β-unsaturated *N*-sulfonylhydrazones to allylic sulfones

1.2.3. Non-metal-catalysed sulfonyl migration

In 1997, the Tamaru group reported the thermal [2+2] cycloaddition of allenesulfonamides with electron deficient alkenes and alkynes to yield substituted cyclobutene derivatives, for example the reaction of **277** with methyl acrylate afforded the cyclobutane **279** in 73% yield (**Scheme 1.40,** X = H).[62] In an extension of this study, the authors were surprised to find that when the alkene substrate was an enol ether, such as methyl β-methoxyacrylate **278** (X = OMe), that a completely different pathway was operational, with the tetrahydropyridine **280** isolated as the major product and no evidence for the expected cyclobutane product (**Scheme 1.40**, X = OMe).[63] Notably, this pathway involved an unexpected 1,3- nitrogen to carbon sulfonyl migration, while enol ethers including acyclic and cyclic aldehyde enol ethers and acyclic and cyclic ketone-enol ethers all reacted similarly. Using this methodology highly functionalised tetrahydropyridines could be accessed in moderate to excellent yields **(Scheme 1.41)**.[64]

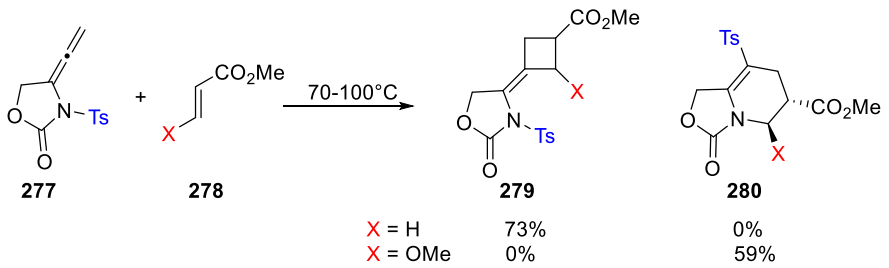

Scheme 1.40: Novel addition-cyclisation reaction of 4-vinylidene-1,3-oxazolidin-2-ones and enol ethers; observation of a 1,3-sulfonyl migration

The reaction mechanism is believed to proceed through the transition state **284** in which the cumulative effect of the electron density of the C1′–C2′ alkene bond being pushed into the sulfonamide moiety and the electron density being drawn away from the carbamate through conjugation with the C4′–C1′ alkene bond significantly weakens the N–S bond, allowing for the 1,3-sulfonyl migration and the generation of s-*trans*-1-azabutadiene **285**. Subsequent isomerisation of the terminal double bond to s-*cis* **285**, allows for a facile hetero-Diels–Alder reaction with the enol ether **282** to afford the tetrahydropyridine product **283 (Scheme 1.41, path A)**. In certain instances the enol ether was observed to isomerise during the reaction with the allenesulfonamides **281** with both *E*- and *Z*-isomers recoverable; however, no isomerisation was observed in the absence of **281**. In contrast, the allenesulfonamide **281** readily isomerised to 3-tosyl-4-vinyl-4-oxazolin-2-one under thermal conditions via a 1,3-H shift in the absence of enol ether highlighting that allenesulfonamide **281** promotes the isomerisation of the enol ether, while the enol ether is crucial in promoting the 1,3-sulfonyl migration. For enol ethers that are highly electron-donating (e.g., ketone enol ethers and furans) it is possible that pathway B could be operational to some extent due to being more able to stabilise the zwitterionic species **286**.

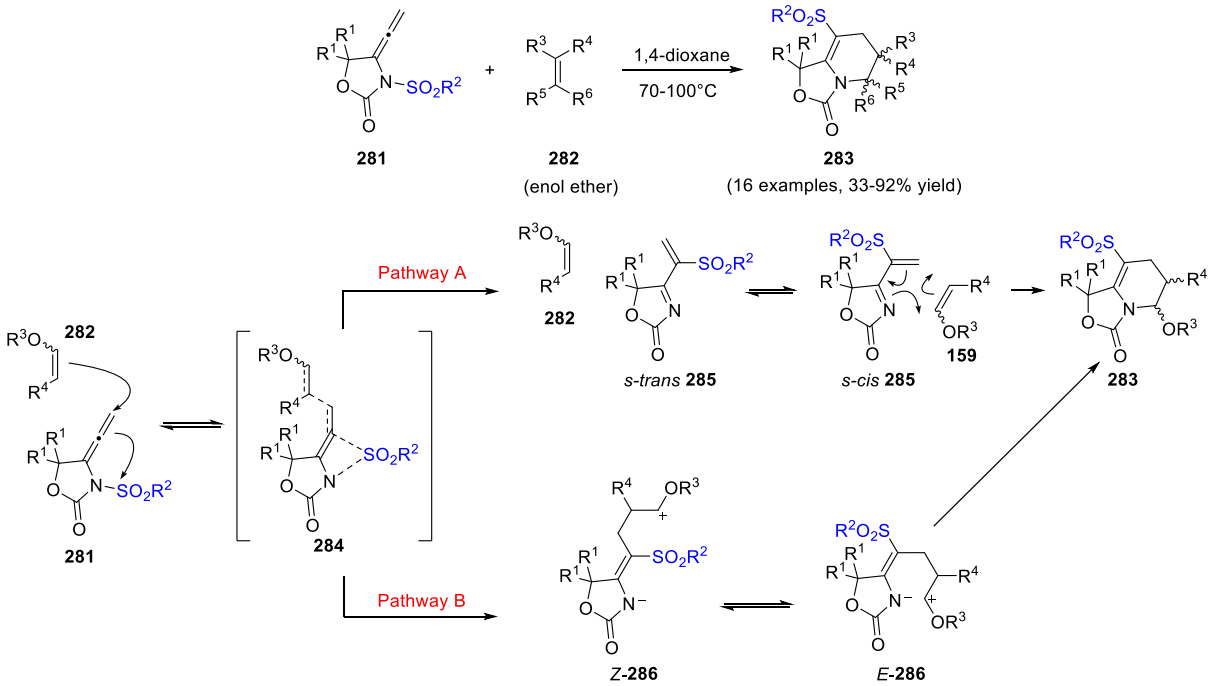

Scheme 1.41: Possible mechanistic pathways for the selective formation of tetrahydropyridines

Subsequent studies by the group highlighted that allyl silanes and hydrosilanes react in an analogous manner, albeit with reduced efficiency, despite being much poorer nucleophiles than enol ethers.[65] Further extension to hetero-nucleophiles including alcohols and thiols afforded both 1,3-sulfonyl migration products in addition to significant amounts of non-sulfonyl migration products as a result of simple addition to the Cα=Cβ bond. Indoles were observed to undergo a similar reaction profile, however the addition occurs through the alkenyl carbon, rather than the nitrogen atom, akin to an electrophilic aromatic substitution.[64]

Wudl reported the first example of an uncatalysed 1,3-sulfonyl migration from a sulfonamide **287** to a keteneimine **288** under thermal conditions.[66] Notably, the rearrangement of the ynamide **287**, which proceeds cleanly either in the melt or in solution at 100–120˚C, involves the migration of both the tosyl group and the *p*-methoxybenzyl (PMB) group from the nitrogen atom to the same β-carbon, to afford the nitrile **291** in an isolated yield of 92%. Variable temperature ^{1}H NMR was readily used to follow the progress of the rearrangement in the non-aromatic solvent decalin. This demonstrated that the rearrangement occurs via the observable intermediate **289**, which also demonstrates that the 1,3-sulfonyl migration occurs first. The identity of the keteneimine intermediate **288** was further inferred as it hydrolysed readily on contact with water to afford the amide **292**, which was characterised by X-ray crystallography. Quantum mechanical calculations suggest that strong resonance stabilisation of the transition state facilitates the sulfonyl migration **(Scheme 1.42)**. Both rearrangement processes were calculated to be thermodynamically favoured.

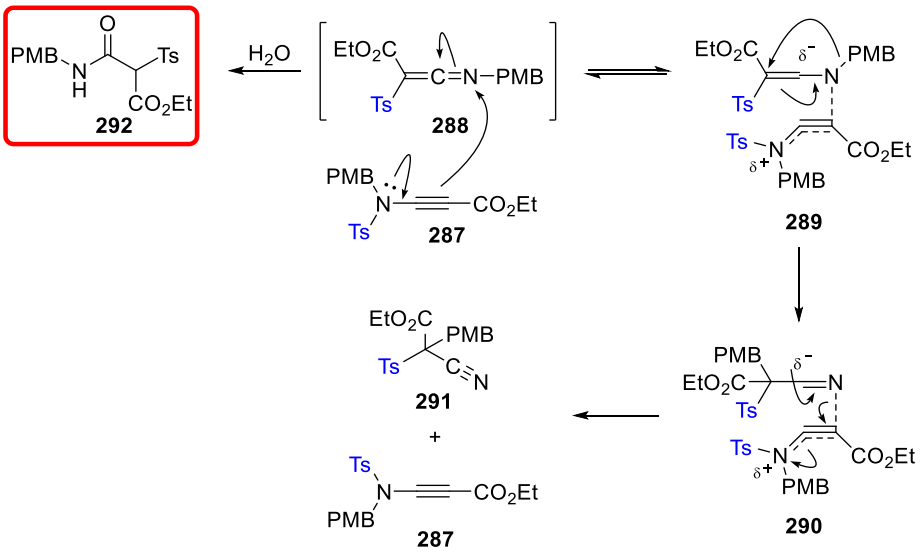

Scheme 1.42: 1,3-Sulfonyl migration of a sulfonyl group from sulfonamide to keteneimine

The Zhang group described the thermal aza-Claisen rearrangements of *N*-allyl ynamides **293** to allyl-keteneimine intermediate **295** via the aza-Claisen transition state **294**, with subsequent spontaneous 1,3-sulfonyl migrations affording quaternary nitriles **296** in moderate yields (7 examples, 45–64%) **(Scheme 1.43)**.[67] The sulfonyl migration was not observed when R^2 = TIPS, with the generated silyl keteneimine **298** sufficiently stable to not undergo subsequent sulfonyl migration. Monitoring of the reaction progress by ^{1}H NMR did not reveal any of the allyl-keteneimine intermediate **295,** suggesting rapid sulfonyl migration at 110˚C.

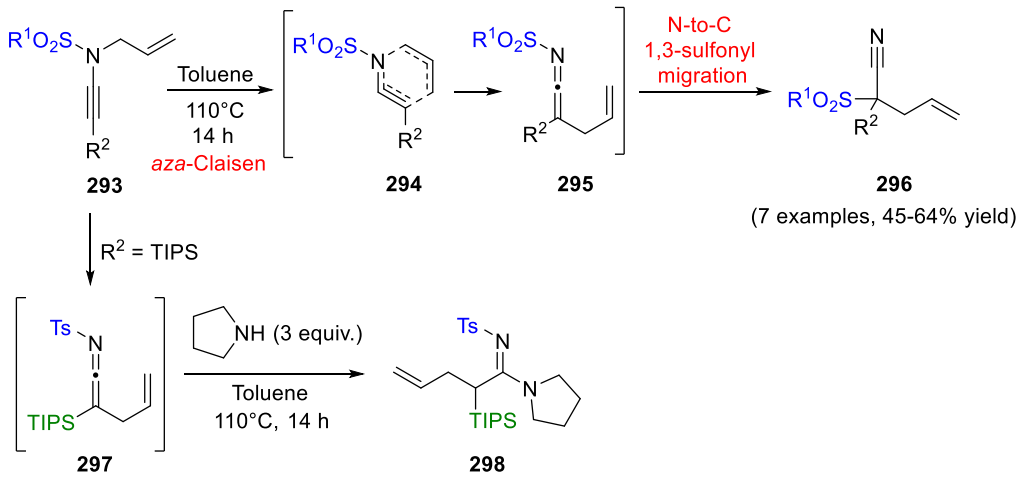

Scheme 1.43: Thermal aza-Claisen rearrangement of *N*-allyl ynamides and subsequent 1,3-sulfonyl migration

The authors attempted to extend this methodology to ynamides of type **299** possessing a propargylic stereocenter, with the possibility to undergo a stereoselective 1,3-sulfonyl migration leading to either **302** or **302'** **(Scheme 1.44)**. They reasoned that the conformational preference of the allyl-keteneimine intermediate **301** or **301'** would dictate the level of selectivity, with the $A^{1,2}$-strain present in **301** potentially meaning that the conformer **301'** would be preferred. If so, this preference could result in facially selective 1,3-sulfonyl migration to give **302'**. They further hypothesised that suitable modification of the protecting group (P) could lead to the conformational preference shown for **303'** in which anchimeric assistance could also result in facially selective 1,3-sulfonyl migration. In the event, however, the highest diastereomer ratio achieved was 2:1.

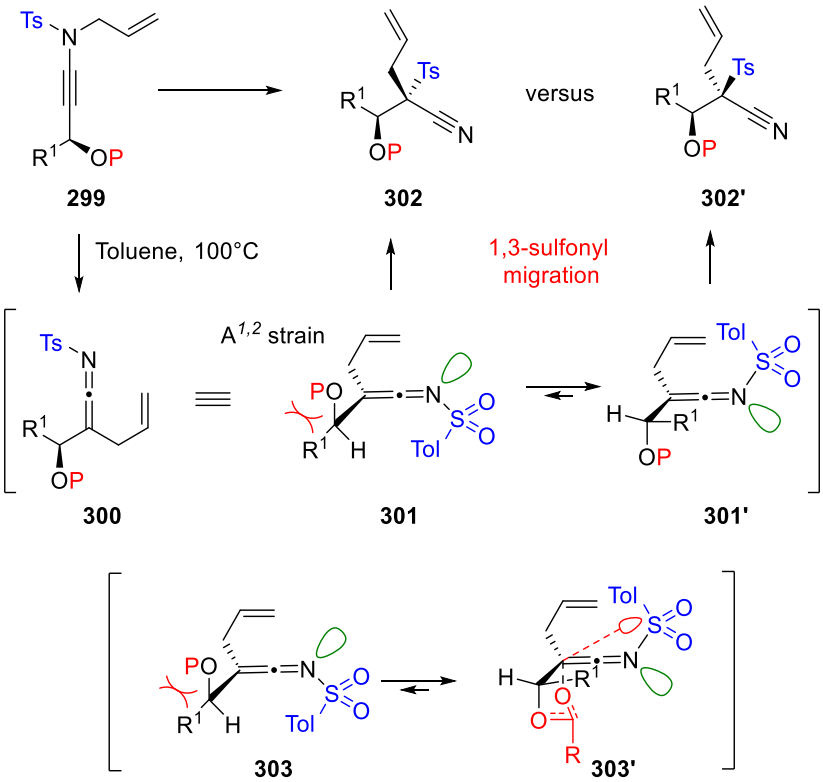

Scheme 1.44: Attempted diastereoselective N-to-C 1,3-sulfonyl migration

The Wan group reported the highly regioselective sulfonyl group migration in the synthesis of functionalised pyrroles.[68] A significant feature of the work is that the regioselectivity of the sulfonyl migration can be tuned with high selectivity for the formation of both α- and β-(arylsulfonyl)methyl pyrroles **306** and **305** in excellent yields **(Scheme 1.45)**. Under thermal conditions, the azaenyne derivative **304** is transformed into **307** via an aza-Claisen rearrangement. Due to the electron-withdrawing character of both the double bond and the sulfonyl group the nitrogen atom is rendered electrophilic, leading to ring closure to afford the zwitterionic intermediate **308** through nucleophilic attack of the allene moiety. Cleavage of the N–S bond leads to the ion pair **309**, which recombines to complete the 1,3-sulfonyl migration. The presence of the ion-pair **309**, and the intermolecular nature of the migration was confirmed by crossover experiments. Finally, isomerisation of **310** affords the α-(arylsulfonyl)-methyl pyrrole **306**.

In the presence of base, namely $CsCO_3$, β-(arylsulfonyl)methyl pyrroles **305** were the favoured rearrangement products indicative of an alternate mechanism for the transformation **(Scheme 1.45)**. Under basic conditions the propargyl group of **304** is converted to the allene intermediate **312** via protonation of **311**. Subsequent ring closing affords the zwitterionic intermediate **313**, with the electrophilic carbocation instead γ- to the nitrogen atom. Akin to the thermal reaction an intermolecular sulfonyl migration was elucidated, hence elimination of the sulfonyl moiety gives the ion-pair **314**, which on recombination completes the 1,4-sulfonyl migration. Isomerisation of **315** affords the β-(arylsulfonyl)methyl pyrrole **305**. The group subsequently reported that this methodology could be extended to the synthesis of 2-trifluoromethyl-4-(arylsulfonyl)methyl pyrroles **305** (R^4 = CF_3), with crossover and competition experiments indicating the likelihood of the same mechanism, however, in this instance CsOPiv was the optimal base **(Scheme 1.45)**.[29]

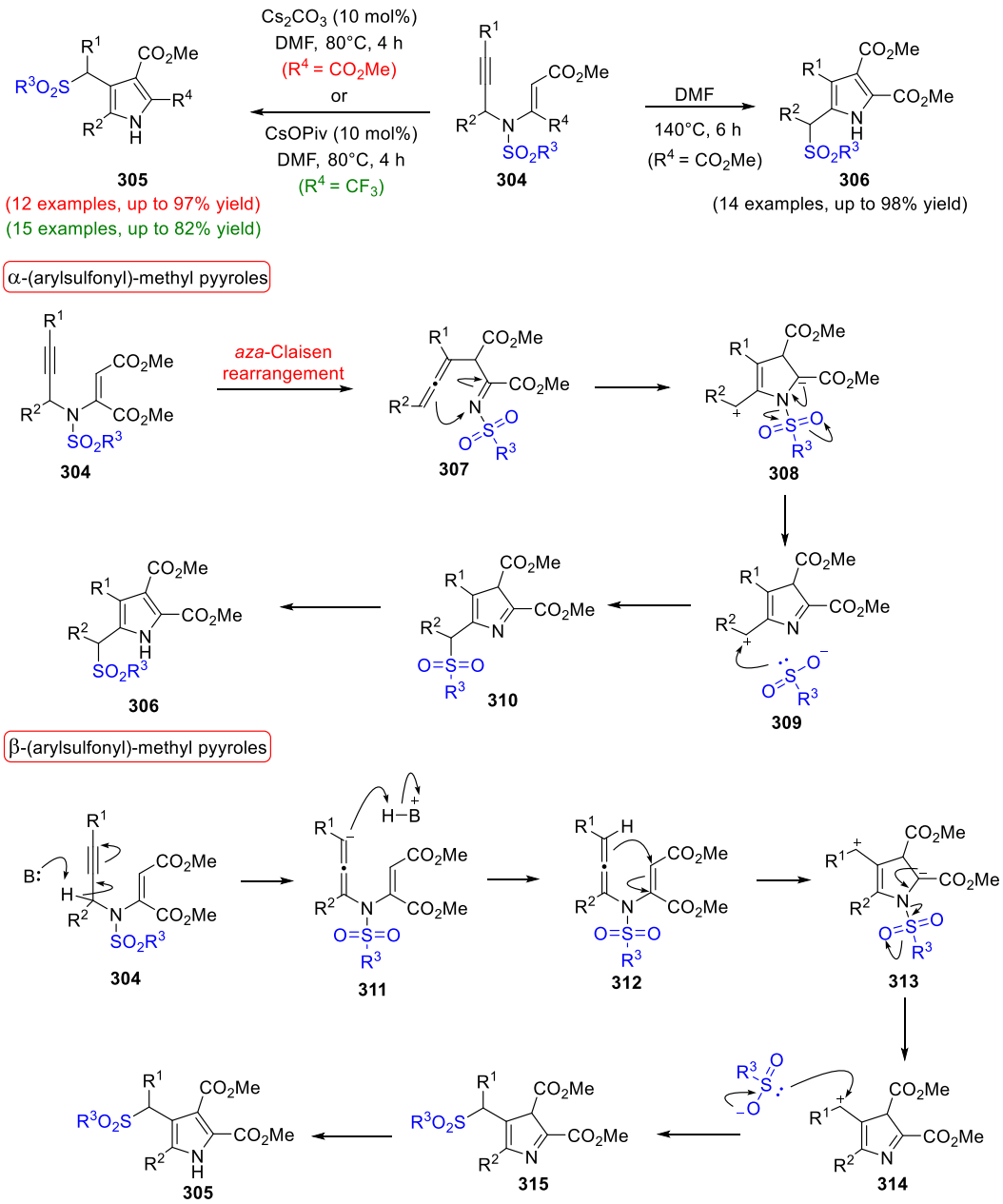

Scheme 1.45: 1,3- and 1,4-sulfonyl migration in the generation of both α- and β-(arylsulfonyl)methyl pyrroles under thermal and basic conditions respectively

Using this precedent, the authors reasoned that the replacement of the alkenyl group with an acyl group could provide a route towards base-catalysed cycloisomerisation to access sulfonylmethyl-substituted oxazoles. With this in mind the authors reacted a series of *N*-sulfonyl propargylamides **316** in the presence of catalytic DBU affording various 5-(sulfonylmethyl)oxazoles **317** in up to 98% yield.[69] The allene intermediate **318** was determined to be a key intermediate in the mechanistic cycle, while monitoring of the conversion process by HPLC highlighted the presence of a further intermediate, that despite not being isolable, the authors reasoned was the zwitterionic species **319**. Key to the mechanistic cycle is a formal 1,4-sulfonyl migration which by means of crossover experiments was determined to be an intermolecular process. While not fully understood, the DBU is likely pertinent to facilitating the dissociation of the sulfonyl group **(Scheme 1.46)**.

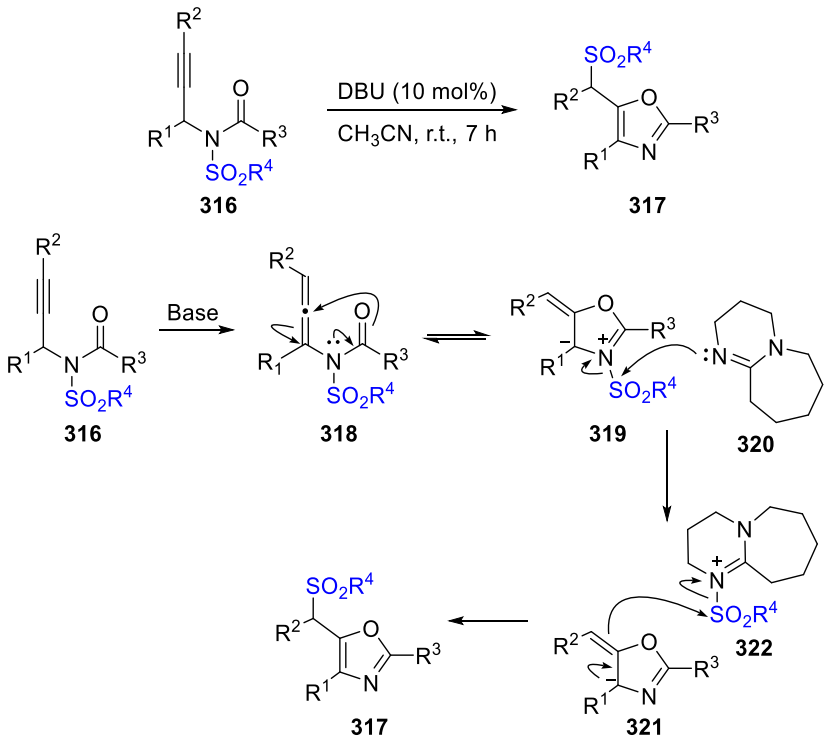

Scheme 1.46: DBU-catalysed cycloisomerisation of *N*-sulfonyl propylargylamides via 1,4-sulfonyl migration

In a further extension to this methodology the group rationalised that incorporating an additional methylene group at the C-7 position of 3-aza-1,5-enynes could be utilised in complex heterocycle synthesis. Accordingly, a series of 2-azabicyclo[3.2.0]hept-2-enes **325** were synthesised via base-catalysed cycloisomerisation of the requisite substrates **323** in moderate yields **(Scheme 1.47)**.[70] Similar to their previous studies, a 1,3-sulfonyl migration was observed. Consistent with the results of deuterium labelling experiments the following mechanism was formulated. Deprotonation of the less sterically hindered C-7 position (compared to the more acidic C-4 proton) generates the allene intermediate **326**. [2+2] Cycloaddition affords the bicyclic intermediate **327**, which undergoes sequential [1,3]-H shift and 1,3-sulfonyl migration to afford the desired 2-azabicyclo[3.2.0]hept-2-ene **325**. Interestingly, when the R^2 substituent in **323** is a phenoxy group the product formed is the vinyl-substituted pyrrole **324**, with 1,4-sulfonyl migration a crucial step **(Scheme 1.47)**. The mechanism for this transformation is thought to be the same as the one presented for the synthesis of β-(arylsulfonyl)-methyl pyrroles **305** in **Scheme 1.45**. Once the pyrrole **329** is formed elimination of phenol affords the vinyl group in the product **324**.

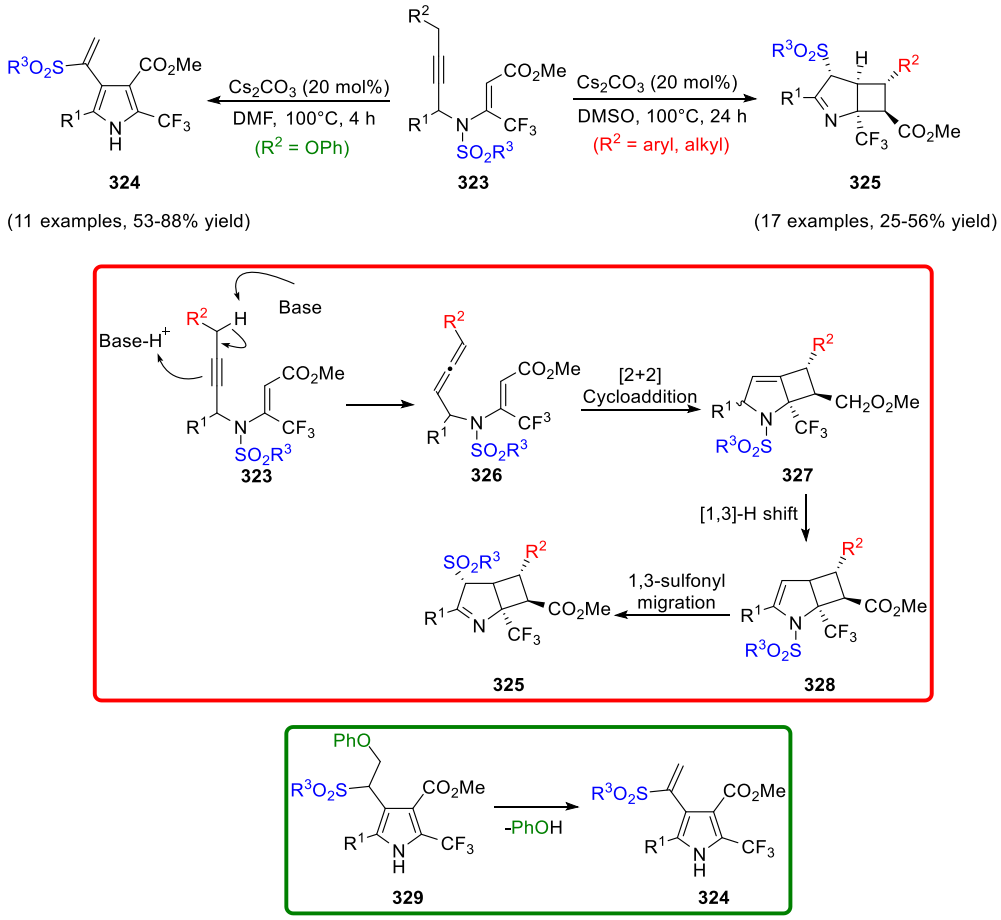

Scheme 1.47: Base-catalysed selective synthesis of 2-azabicyclo[3.2.0]hept-2-enes and sulfonyl vinyl-substituted pyrroles from 3-aza-1,5-enynes via 1,3- and 1,4-sulfonyl migrations respectively

The synthesis of tetrasubstituted imidazoles **333** via a two-step one-pot approach from the three-component reaction of propargyl amines **330**, sulfonyl azides **332** and alkynes **441** utilising 1,3-sulfonyl migration has been described **(Scheme 1.48)**.[71] Initially, the keteneimine **334** is generated in situ by means of a copper catalysed azide-alkyne cycloaddition between the alkyne and tosyl azide. Nucleophilic addition of the propargyl amine **335** to the ketenimine **334** affords the intermediate **336**. In the second step, the allene **337** is generated through the deprotonation of the propargyl moiety, which subsequently undergoes a 6π-electron electrocyclic ring closure (6π-ECR) to give the zwitterionic structure **338**. Finally, an intramolecular 1,3-sulfonyl migration completes the process affording the imidazole product **339**. Crossover experiments supported the intramolecular nature of the sulfonyl migration.

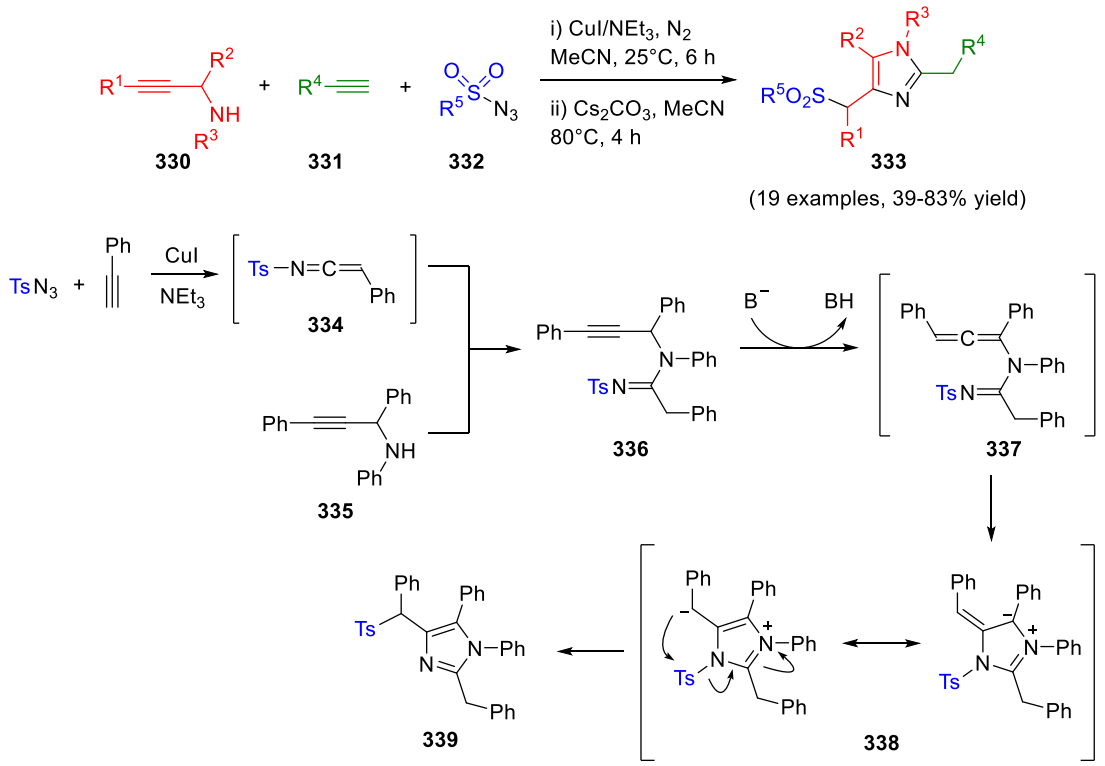

Scheme 1.48: One-pot synthesis of tetrasubstituted imidazoles utilising intramolecular 1,3-sulfonyl migration

Following the Zhan group's seminal report regarding the reactivity of *N*-propargylic sulfonylhydrazones in the presence of copper catalysts, they further demonstrated that compounds of this type could undergo Lewis base catalysed reaction to give 4-sulfonyl-1*H*-pyrazoles **341** in moderate to good yields, with allenic sulfonamide formation and 1,3-sulfonyl migration key steps in the transformation **(Scheme 1.49)**.[72] DMAP in a mixed solvent system of tetrahydrofuran and triethylamine at 80˚C proved to be the optimal conditions for the transformation with yields up to 92% achieved. As per their initial optimisation study, the allenic sulfonamide **342** was formed exclusively at room temperature in 0.5 h indicating that it is likely a key intermediate in the cascade process. This was confirmed by reacting the allenic sulfonamide **342** under the optimised conditions with the pyrazole **341** formed in 97% yield. Notably, in the absence of DMAP no reaction occurred at room temperature indicating that both the allenamide formation and cyclisation reactions are catalysed by DMAP.

Considering this the authors proposed the following mechanism **(Scheme 1.49)**. The propargylic amide moiety of **340** is transformed into the allenic sulfonamide intermediate **342** in the presence of DMAP. Nucleophilic addition of the Lewis base to the sp^2 terminus of the allene moves electron density towards the sulfonamide moiety to give the transition state **343**, leading to the breakage of the N–S bond forming **344**, completing an intramolecular 1,3-sufonyl migration as supported by crossover experiments. Elimination of the Lewis base affords the α,β-unsaturated imine **345** which undergoes intramolecular 1,4-addition to form the zwitterionic species **346**. Finally, 1,3-hydride shift and electron transfer occur to give the rearranged pyrazole **341**.

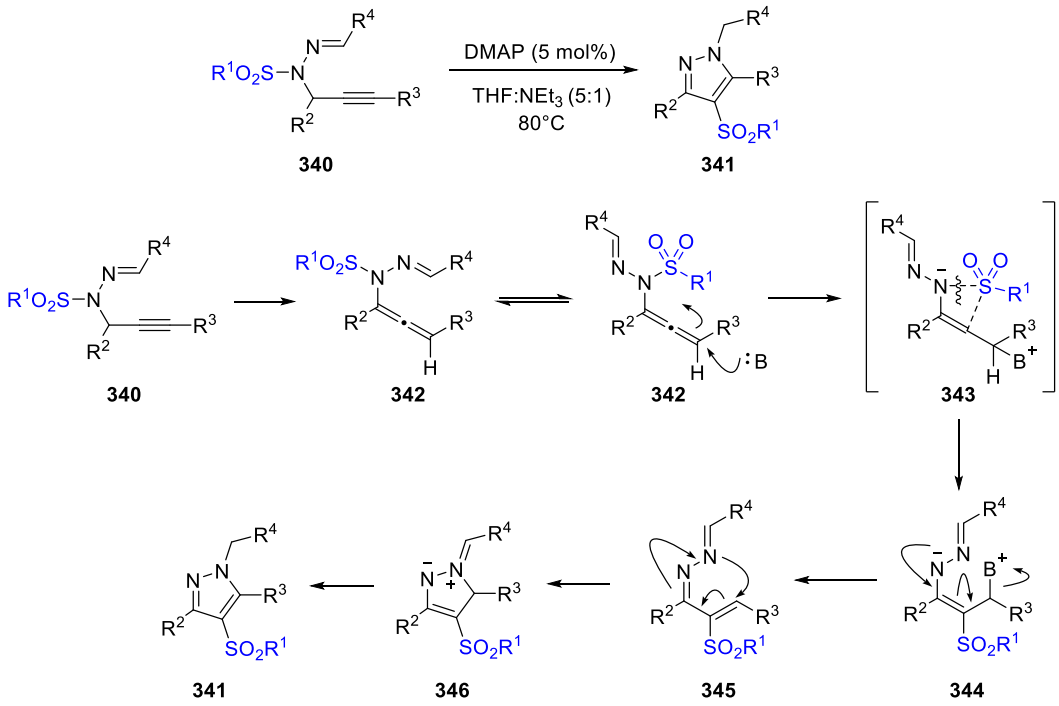

Scheme 1.49: Lewis base catalysed synthesis of 4-sulfonyl-1*H*-pyrazoles involving 1,3-sulfonyl migration

The base-mediated decomposition of a series of bicyclic amide-substituted furfuryl tosylhydrazones **347** was observed to lead to formal nitrogen to carbon 1,5-sulfonyl migration affording sulfone derivatives **348** with the furan ring remaining intact **(Scheme 1.50)**.[73] Competition experiments suggested that the sulfonyl migration most likely proceeds in an intermolecular manner. The authors postulated that the mechanism proceeds via the base-mediated generation of the anion **349** which decomposes to the diazo compound **350** with concomitant extrusion of the tosyl group. Loss of nitrogen from the diazo moiety affords the electrophilic carbene **351**, which mediates ring opening of the furan ring to generate the enynyl-ketoamide **352**. Regioselective nucleophilic addition of the tosyl group to the α,β-unsaturated system of **352** regenerates the furan ring giving **353** which is converted to the final rearranged product **348** following protonation and aromatisation.

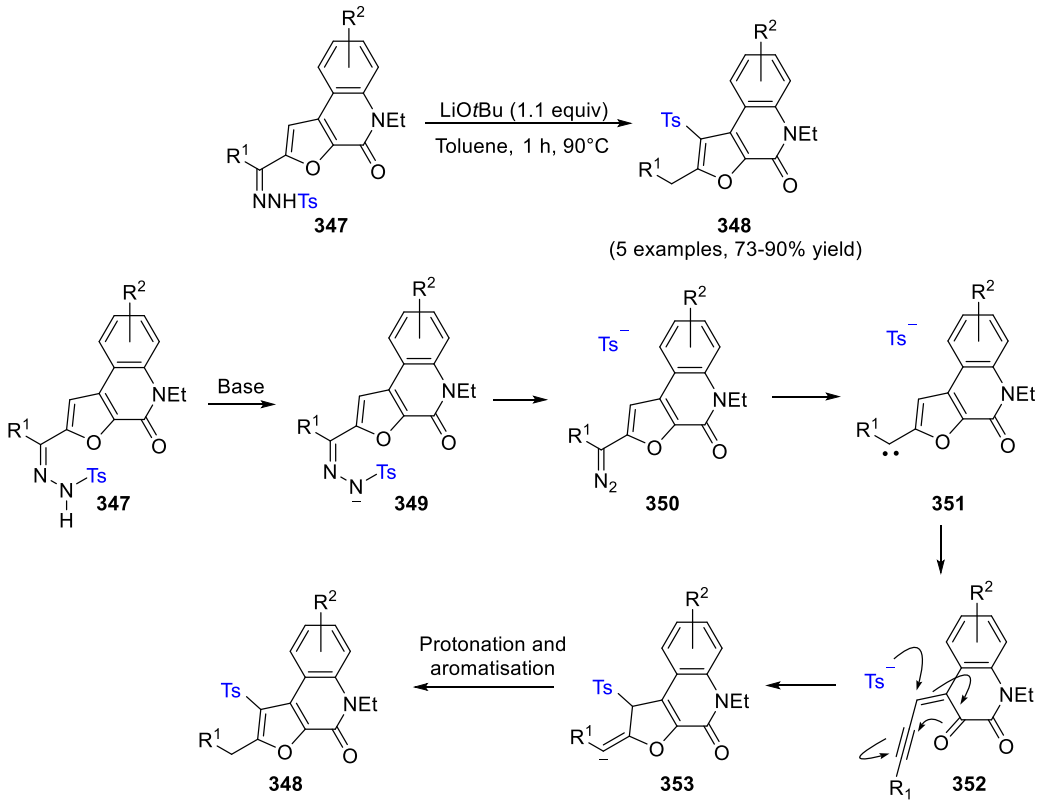

Scheme 1.50: Observation of a 1,5-nitrogen to carbon tosyl migration to afford sulfone derivatives from furfuryl tosylhydrazones

Li reported the diamination of the domino aryne precursor **354**[74-75] with sulfonamides, affording 1,3-diaminobenzenes **356** in moderate to good yields **(Scheme 1.51)**.[76] Interestingly, in their investigation to ascertain the origin of the proton at the 2-position, a deuterium-labeling experiment in MeCN-d_6 indicated that the proton comes from both the solvent and the N–H bond of the amine starting material (25% deuterium incorporation, compound **358**). The authors therefore rationalised that this methodology could be further applied to the synthesis of 1,2,3-trisubstituted benzenes **357** by capturing an electrophile rather than a proton. Indeed, by carrying out the reaction in the inert solvent toluene, and in the presence of K_2CO_3 and 18-crown-6 as activating agents, a formal 1,3 nitrogen to carbon sulfonyl migration of the triflyl group readily occurred in good yields. Extension of the methodology to the migration of a tosyl group proved unsuccessful.

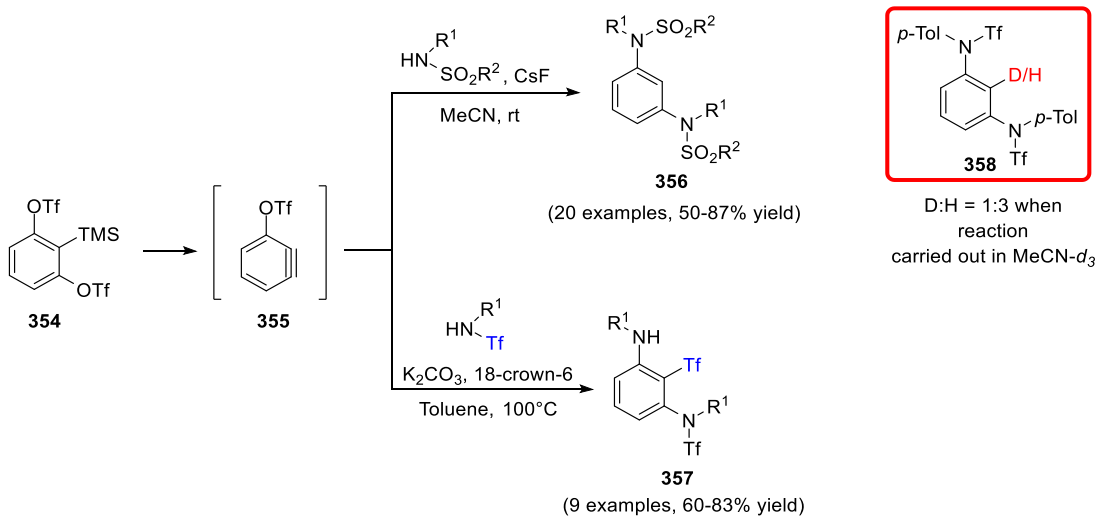

Scheme 1.51: 1,3-sulfonyl migration via aryne precursors

Kakiuchi's team developed a synthesis of α-functionalised enoximes **360** via nitrosoallenes **363**,[77] a group of compounds pioneered by the group,[78-79] through a fluoride-mediated deprotection of the silyl moiety and tandem elimination of sulfinate from *N*-sulfonyl hydroxylamines **359 (Scheme 1.52)**. Recombination of the sulfinate with the electrophilic moiety of the allene **363**, completes a formal intermolecular 1,3-sulfonyl migration, with subsequent *O*-protonation affording α-sulfonyl enoximes **360** in high yields. In some instances, where all substituents on the allenylamides **359** were aryl groups, 2-isoxazolines **361** were afforded as major products derived from the cyclocondensation of the initially fomed vinylsulfones **360**. The group further established that by adding an azodicarboxylate as a sulfinate scavenger that the protocol could be extended to allow functionalisation of the α-position by various nucleophiles in moderate to excellent yields (compounds **362**).

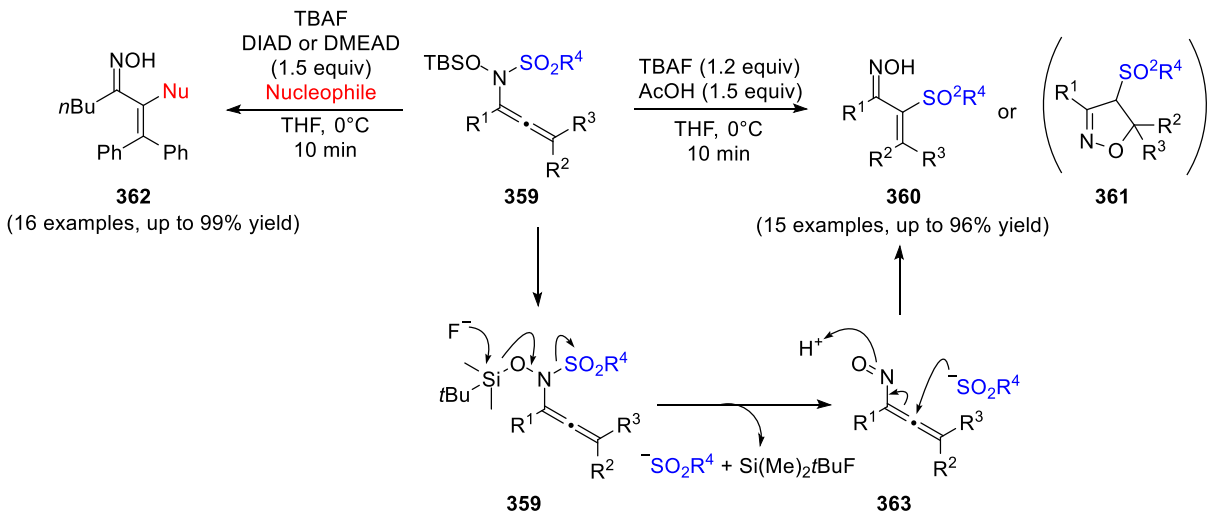

Scheme 1.52: Synthesis of α-substituted enoximes via fluoride mediated deprotection of nitrosoallenes

The utility of triflic anhydride-mediated amide activation of a series of α-aminoamides **364** to generate tetrasubstituted imidazoles **365** in moderate yields was demonstrated to proceed via a mechanistically intriguing [2,3]-sigmatropic rearrangement of a sulfinate intermediate, promoting a formal 1,2-

sulfonyl migration from nitrogen to carbon **(Scheme 1.53)**.[80] Quantum-chemical calculations were used to rationalise the overall mechanistic transformation. Initially, triflic anhydride activation of the α-aminoamide **364** and subsequent nucleophilic addition of acetonitrile to the keteneiminium ion **366** affords intermediate **367**. A 7-*endo*-dig cyclisation of **367** via nucleophilic attack of the sulfonamide oxygen onto the nitrilium moiety gives the intermediate **368**. Cleavage of the N–S bond ensues giving the sulfinate **369** which subsequently cyclises to **370** which then undergoes a [2,3]-sigmatropic rearrangement, reminiscent of a retro-Mislow–Evans-type rearrangement,[81] to complete the formal 1,2-sulfonyl migration to give **371**. Deprotonation of intermediate **371** affords the final rearranged imidazole **365** through aromatisation. While the computational analysis indicated that the 7-*endo*-dig cyclisation is endergonic ($\Delta G_{A\text{-}B}$ = + 14 kcal mol^{-1}), the subsequent cleavage of the N–S bond ($\Delta G_{B\text{-}C}$ = − 25.8 kcal mol^{-1}) and the [2,3]-sigmatropic rearrangement ($\Delta G_{D\text{-}E}$ = − 21.4 kcal mol^{-1}) provides significant thermodynamic stabilisation.

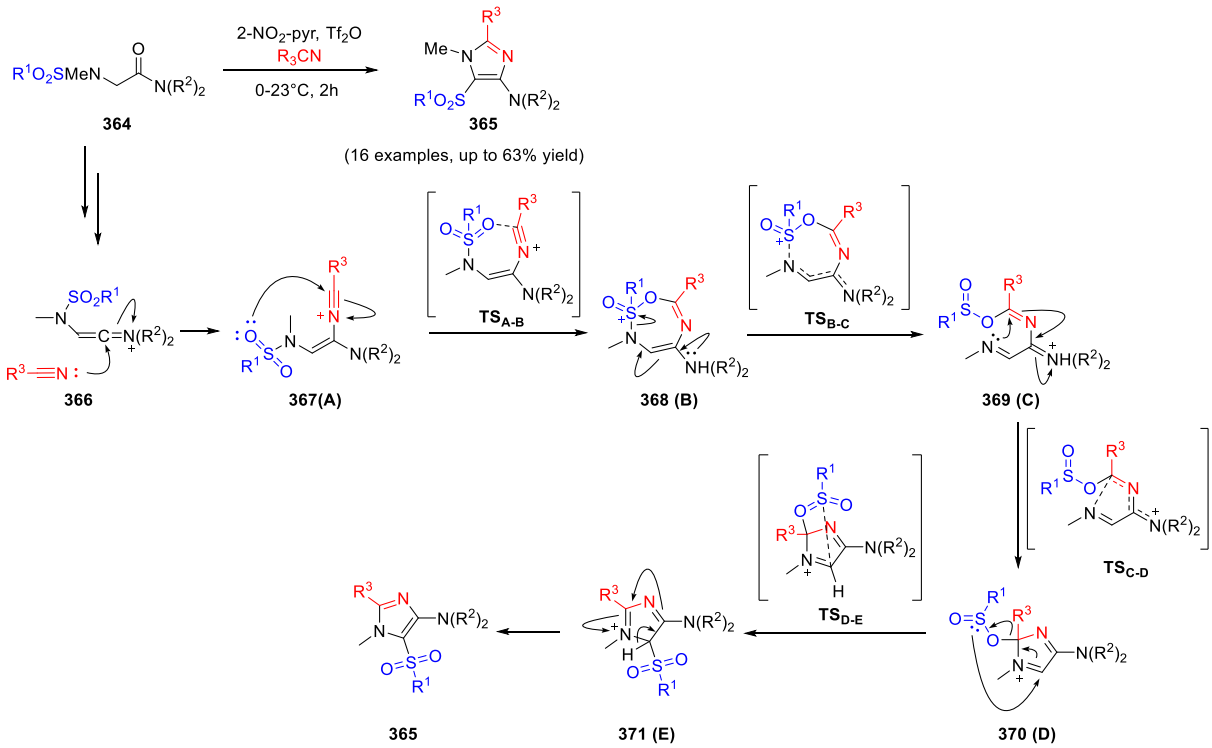

Scheme 1.53: Generation of tetrasubstituted 5-aminoimidazoles via formal 1,2-sulfonyl migration

The Bharatam group reported a mechanistically interesting 1,3-sulfonyl migration from nitrogen to carbon within the pyrrole framework, the first example of such a rearrangement for this heterocycle class. They demonstrated that *N*-sulfonyl-2-arylpyrroles **373** undergo a 1,3-sulfonyl migration in pivalic acid to afford 2-aryl-3-sulfonylpyrroles **374** in moderate to excellent yields.[82] They further realised that this sulfonyl migration could be incorporated into a one-pot tandem palladium-catalysed oxidative arylation of the 2-position of *N*-sulfonylpyrroles **372**, followed by regioselective sulfonyl migration **(Scheme 1.54)**.

While further clarity is required, the authors tentatively proposed an operative intramolecular nucleophilic displacement pathway based on a series of experimental observations and computational results. An intermolecular process was deemed unlikely based on crossover experiments. The addition of CsF, benzylsulfonate or benzenesulfonyl chloride to the *N*-sulfonylpyrroles **375**, **376** and **377** afforded neither **381** or **382**, which would be expected if an intimate ion-pair mechanism were

operational. The sulfonyl migration occurs readily in the presence of TEMPO, suggesting that the reaction does not involve the formation of a free-radical. Interestingly, when *N*-tosylpyrroles **383**–**385** (ie. unsubstituted, 2-substituted or 2,5-disubstituted without an aryl substituent) were heated under the optimised conditions no reaction was observed. Notably, the reaction was found to be completely inhibited in the absence of an aryl group at the 2-position, while blockage of the *ortho*-position of the aryl ring, as seen for the reaction of *N*-tosyl-2-pentafluorophenylpyrrole **389**, had the same effect. Deuterium incorporation studies indicated that C–H bond breaking was unlikely to be involved in the sulfonyl migration, but that an aryl group at the 2-position is crucial for the migration to occur, which suggests an intramolecular C-2 aryl group assisted sulfonyl migration is operational for this transformation.

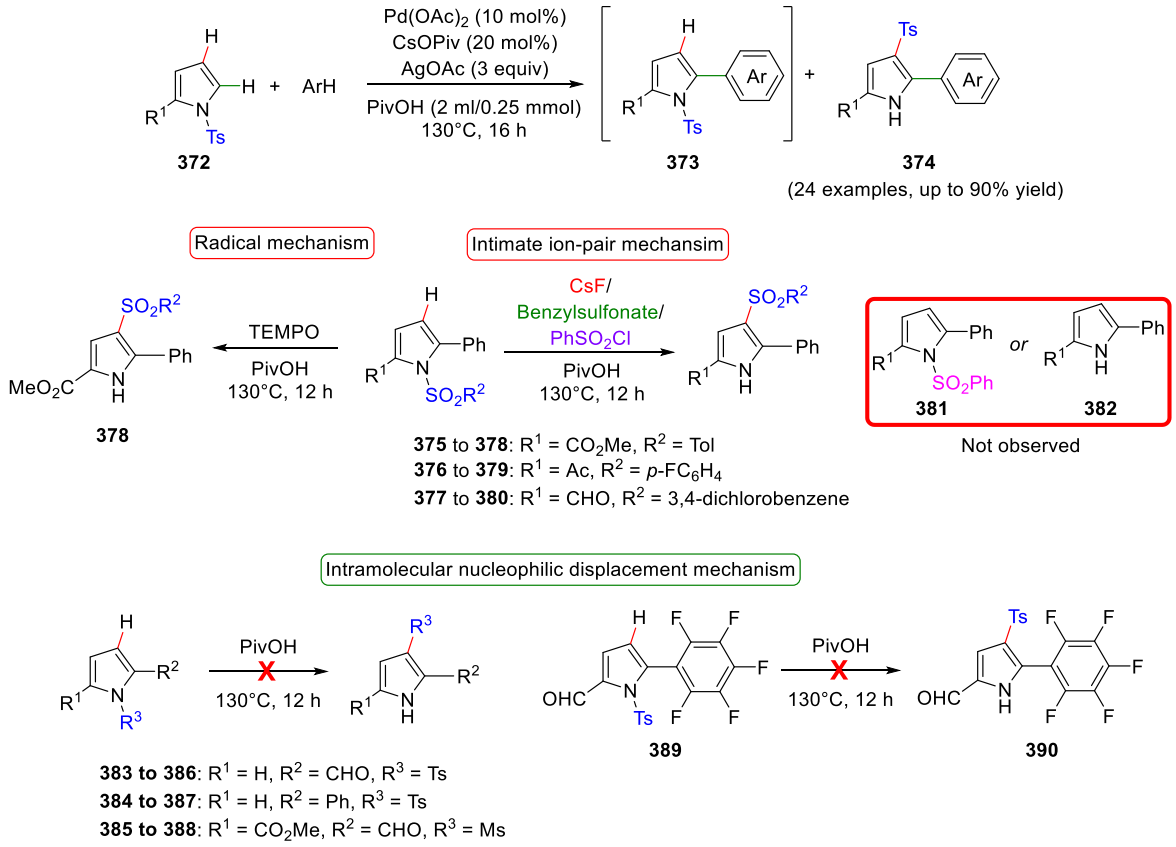

Scheme 1.54: One-pot tandem oxidative arylation and sulfonyl migration of pyrroles; mechanistic studies supporting an intramolecular nucleophilic displacement mechanism

Javorskis and Orentas described the chemoselective deprotection of neutral and electron-deficient sulfonamides **391** under acidic conditions using trifluoromethanesulfonic acid **(Scheme 1.55, A)**.[83] Interestingly, when this deprotection strategy was applied to electron-rich *N*-arylsulfonamides **393** a completely different reaction profile was observed, with a 1,3-sulfonyl migration preferred **(Scheme 1.55, B)**. Notably, mesyl, tosyl and nosyl substituents were well tolerated. An independent crossover experiment confirmed that this sulfonyl migration is most likely an intramolecular process. On the basis of the mechanism proposed for the hydrolysis of neutral and electron-deficient *N*-arylsulfonamides, which involves the formation of the mixed anhydride **399** as a side-product, the authors hypothesised that the high reactivity of the mixed anhydride **399** may facilitate an intermolecular sulfonyl group migration. Verification of this assumption was achieved via deprotection of the electron-deficient aniline **395** in the presence of electron-rich arenes, 1,3-

dimethoxybenzene and *m*-xylene, which afforded the sulfones **396** and **397** respectively through a Friedel–Crafts sulfonylation. In subsequent optimisation studies the *N*-sulfonylated urea **398** was determined to undergo desulfonylation much more readily, allowing access to the mixed anhydride **399** under more facile conditions.

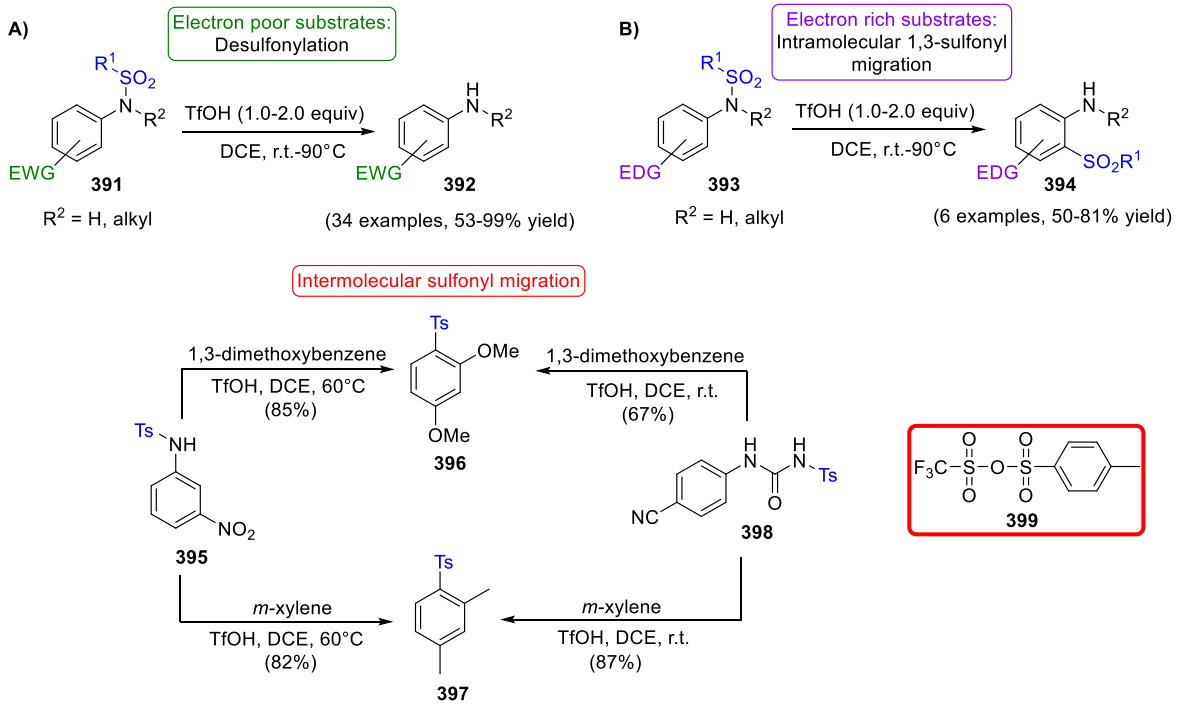

Scheme 1.55: Chemoselective deprotection of sulfonamides under acidic conditions; observation of a 1,3-sulfonyl migration

The Hoye group reported the generation of tetrahydroquinolines **402** from hexadehydro-Diels–Alder substrates **400** through a cascade cyclisation and sulfonyl migration.[84] For substrates **400** bearing a trimethylene linker between the alkyne and sulfonamide a newly fused piperidine ring is generated, with a formal 1,3-sulfonyl migration of a tosyl group also observed (6 examples, 83–92% yield) **(Scheme 1.56)**. Variation of the sulfonyl group in certain instances led to suppression of the sulfonyl migration **(Scheme 1.57)**. For mesyl substituted substrates **400**, the desulfonylated tetrahydroquinolines **406** were generated, through elimination of sulfene from the zwitterionic intermediate **405**. Substitution with a nosyl group afforded the expected rearrangement product **410** as the major product, but its formation was accompanied by the generation of the *p*-nitrophenyl-substituted biaryl compound **409** in which sulfur dioxide has been eliminated. This variant of the Truce–Smiles rearrangement[85] is thought to take place via ipso-attack para to the nitro group in **407**. The zwitterionic intermediate **408** loses SO_2 to form **409**. Interestingly, incorporation of the shorter dimethylene tether between the diyne moiety and the sulfonamide of **403** afforded exclusively desulfonylated indolines **404** regardless of the sulfonyl moiety (mesyl and tosyl both studied) **(Scheme 55)**. This was attributed to the increased strain in the transition state that would lead to the 5-membered zwitterion **411**, and hence the product **412** was not formed **(Scheme 1.57)**.

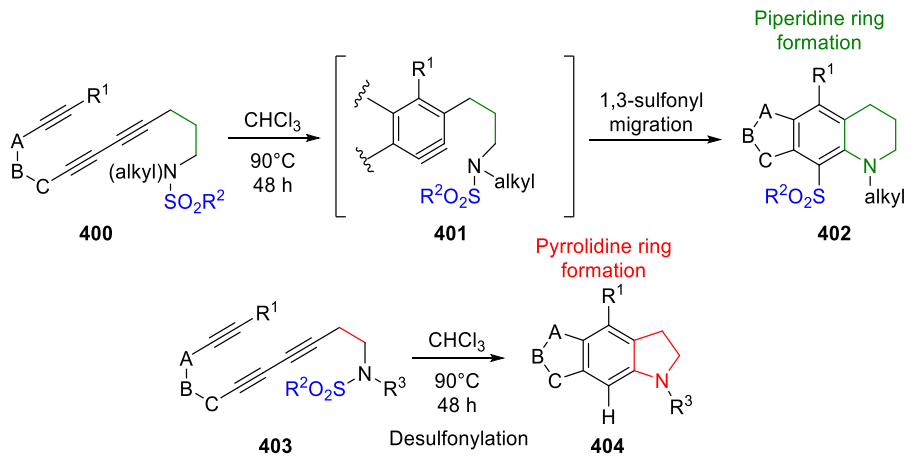

Scheme 1.56: Synthesis of tetrahydroquinolines and indolines accompanied by 1,3-sulfonyl migration or desulfonylation via sulfonamide-trapping reactions of thermally generated benzynes

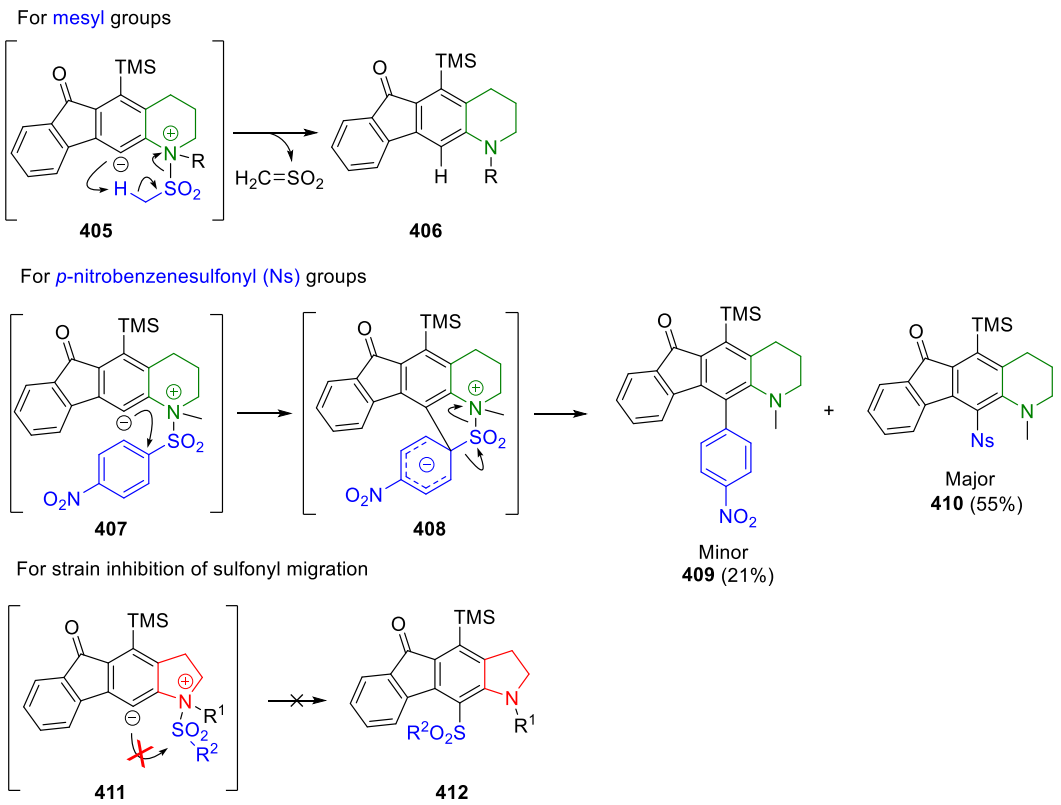

Scheme 1.57: Mechanistic rationales for desulfonylation of mesyl groups, migration of *p*-nitrobenzene from nosyl group and inhibition of sulfonyl migration for indoline derivatives

Selvaraj and Swamy reported the generation of 6-sulfonyl substituted α-carbolines **416** via a Bronsted acid-mediated reaction of 2-sulfonamidoindolines **414** and propargylic alcohols **413**, via a formal 1,6-tosyl migration **(Scheme 1.58)**.[86] Despite the moderate yields achieved (21–40%), and the selective formation of α-carbolines **417** via competing 1,2-aryl migration, this was the first example of the direct introduction of a sulfonyl moiety to the C-6 position of the indole framework in the absence of a metal catalyst. A crossover experiment between the conjugated sulfonamidoindoline **415** (R^1, R^2 = Tol; R^3 = Ph, R^4 = H) and sodium benzenesulfinate did not lead to the incorporation of the sulfonyl moiety at

the C-6 position of the indole system, while the migration product was acquired when **415** was heated to reflux in the presence of *p*-toluenesulfonic acid. Considering this, the authors suggested that the incorporated tosyl moiety has exclusively migrated from the indole framework.

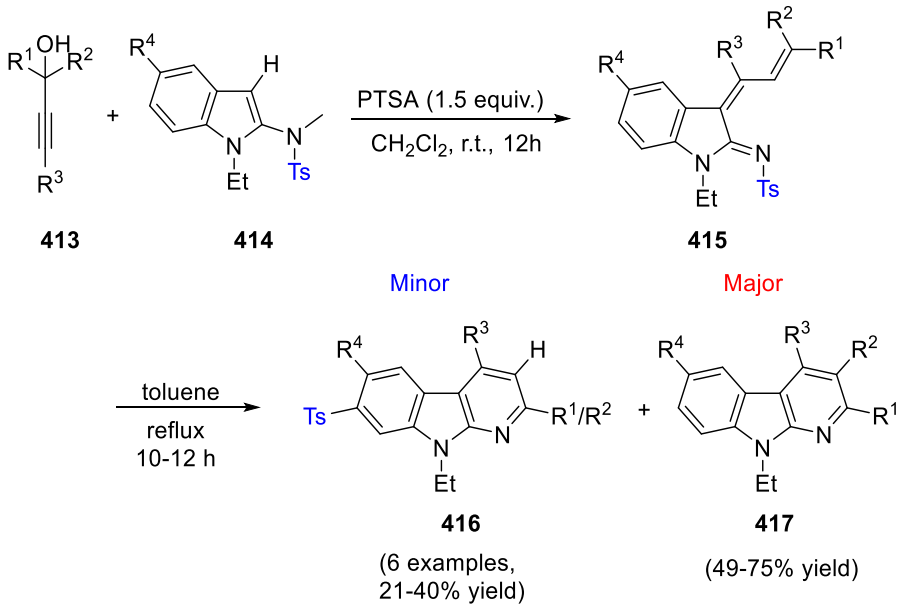

Scheme 1.58: Regioselective tosyl group migration from indole 2- to 6-position

In light of these observations the authors proposed the following mechanism to account for the observed tosyl migration **(Scheme 1.59)**. The allenic carbocation **418** is formed via Bronsted acid-mediated Meyer–Schuster rearrangement of **413**, which undergoes a Friedel–Crafts reaction with the indoline **414** to afford the conjugated intermediate **419**. Subsequent [1,5]-hydride shift affords the tosylimine **415**, which was isolable. A 6π-electrocyclic ring closure, followed by elimination of the tosylate anion gives the carbocation **421** which can undergo two divergent pathways. Firstly, and preferentially, a [1,2]-aryl shift affords **422** which upon aromatisation gives the major α-carboline product **417**. Alternatively, regioselective addition of the tosylate to the C-6 position of the indole affords **423**, with subsequent elimination of an aryl group affording the aromatised product **416**.

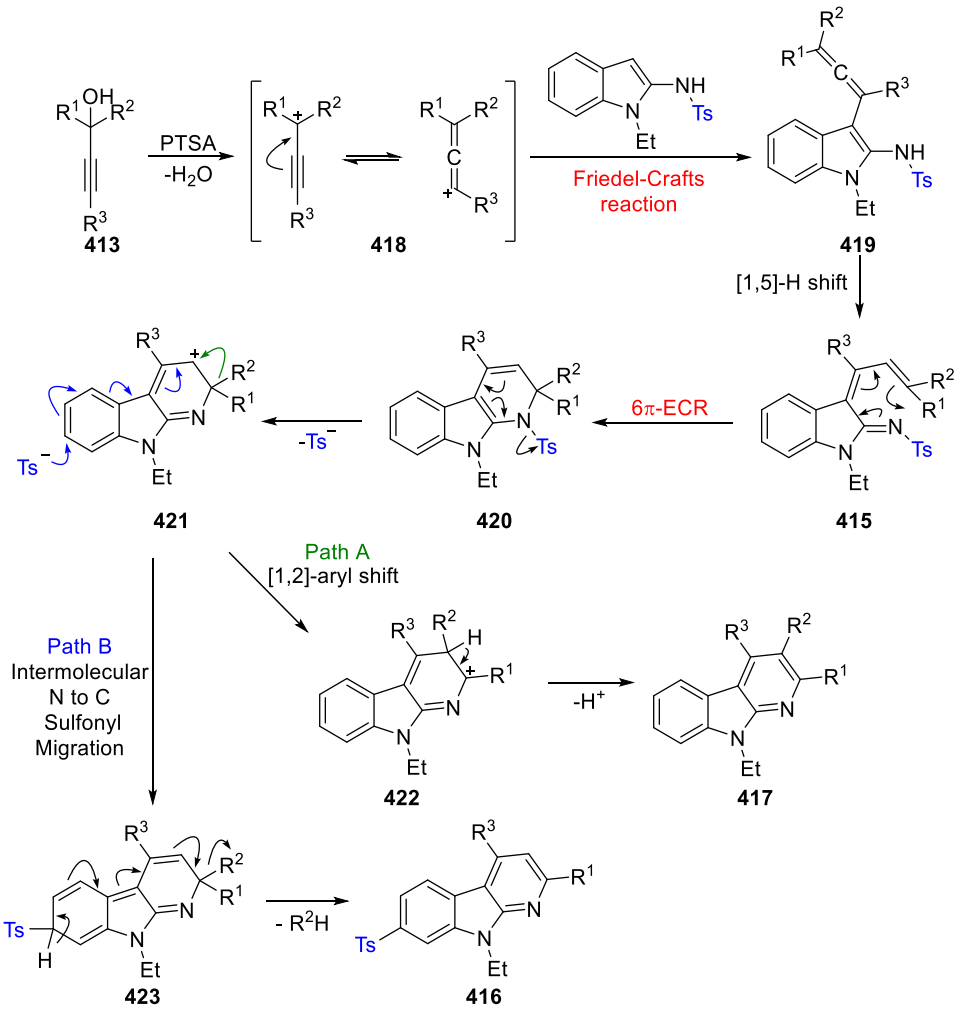

Scheme 1.59: Formation of α-carbolines from the reaction of propargyl alcohols and sulfonamido-indoles; observation of an unexpected 1,6-tosyl migration

Shen *et al*. reported the coupling of carboxylic acids **424** and ynamides **425** to form α-acyloxyenamides **428**, with subsequent 1,3-sulfonyl migration and Mumm rearrangement observed at high temperatures leading to imides **426** in moderate to excellent yields **(Scheme 1.60, A)**.[87] In the presence of base, the functionalised imides undergo additional rearrangement to give β-keto amides **427** in moderate to good yields in a one-pot process **(Scheme 1.60, B)**. Crossover experiments demonstrated that the thermally induced 1,3-sulfonyl migration of the α-acyloxyenamide **428** involves cleavage of the N–S bond, generating an ion pair **429** that undergoes intermolecular rearrangement to afford the intermediate **430 (Scheme 1.60)**.

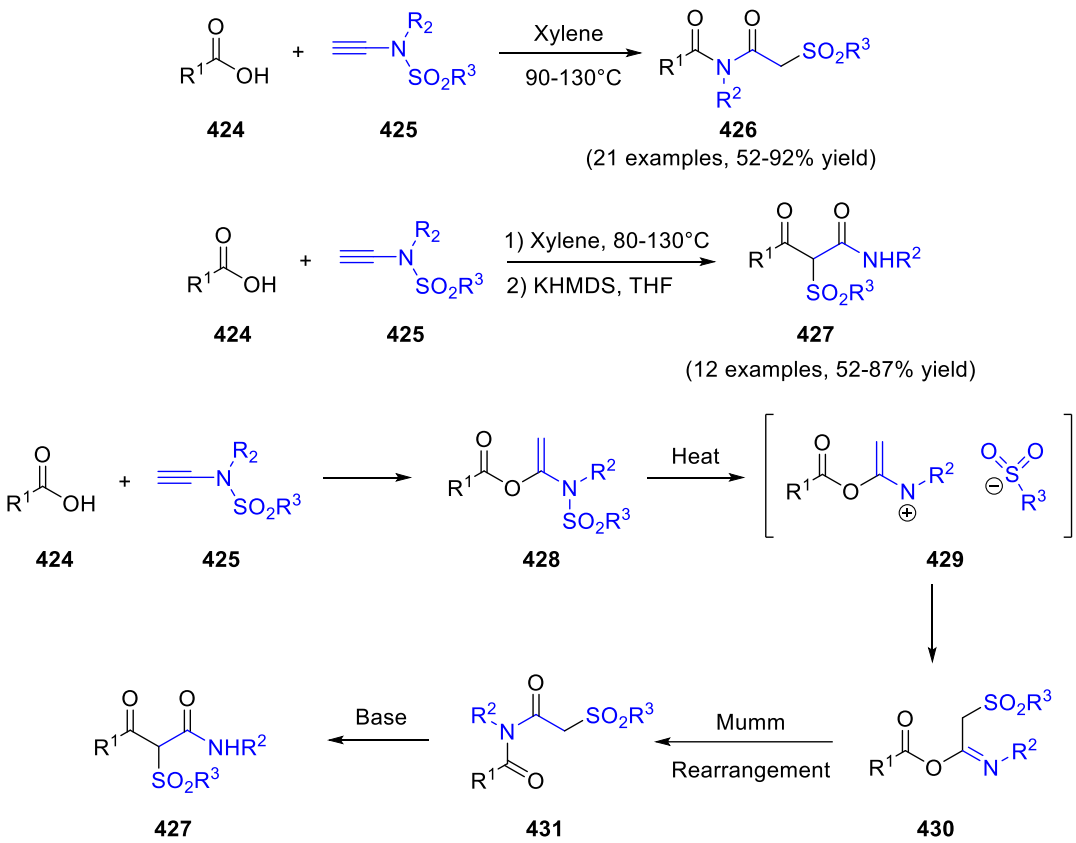

Scheme 1.60: Coupling of carboxylic acids with ynamides to afford imides and amides via sulfonyl migration and subsequent rearrangement

Sulfonyl-substituted trifluoroalanine derivatives **434** can be accessed in almost quantitative yields via nitrogen to carbon 1,2-sulfonyl migration from the reaction of vicinal sulfonyliminocarboxylates **432** and phosphites **433 (Scheme 1.61)**.[88] Monitoring the progress of the reaction by ^{31}P and ^{19}F NMR spectroscopy revealed the presence of two pentacoordinate phosphorus intermediates which were transformed over time to the iminophosphorane **434**. Based on the NMR data the authors assigned the intermediate stereoisomeric phosphorane **435**, generated through the 1,4-cycloaddition of **432** and **433**. Accordingly, it was proposed that the transformation from the intermediate **435** to **434** involves intramolecular nucleophilic attack of the sp^2-hybridised carbon on the sulfonyl moiety, which is favoured by the cumulative effect of the alkoxy and phosphoryloxy substituents, which on subsequent breakdown completes a formal 1,2-sulfonyl migration. Replacement of the ester moiety by a trifluoromethyl group completely inhibits the reaction, supporting the likelihood of intermediate **435** being generated via cycloaddition.

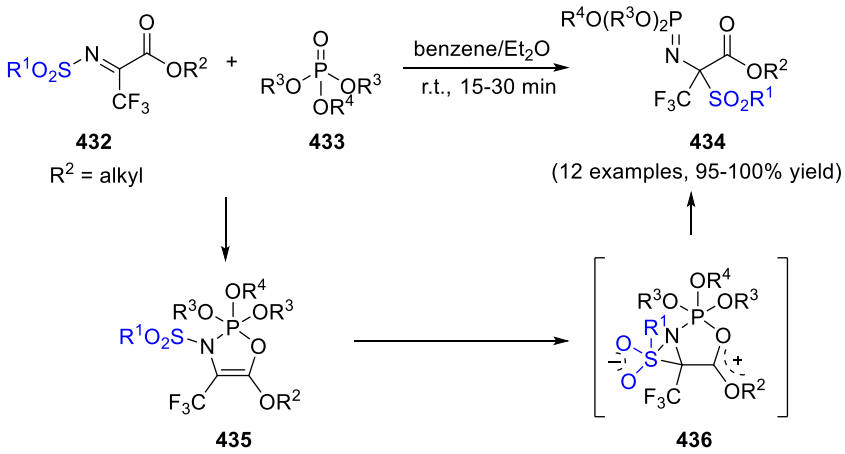

Scheme 1.61: Access to sulfonyl-substituted trifluroalanine derivatives via 1,4-cycloaddition and 1,2-sulfonyl migration

1.3. Nitrogen to Nitrogen Sulfonyl migration

Michaelidou and Koutentis observed a surprising 1,4- nitrogen to nitrogen tosyl migration in their attempts to detosylate the indoles **437** under basic conditions; 3-(*N*-tosylamino)indoles **438** were isolated in moderate to good yields **(Scheme 1.62)**.[89] While several mechanistic pathways can be considered to explain the transformation, the authors favoured **path B**, in which base-catalysed elimination of tosylate affords the imine **440 (Scheme 1.62)**. Their preference was for the ambidentate tosylate to directly add to the indolimine at the C-2 position through the oxygen atom to afford the sulfinate ester **442**. Subsequent isomerisation via either a concerted 2,3-sigmatropic rearrangement or a stepwise ion pair process affords the desired product, completing the formal 1,4- nitrogen to nitrogen tosyl migration. This proposed pathway was preferred as **path C** would involve a less favourable four-membered transition state to complete the 1,3-sulfonyl migration, compared to the five-membered analogue required for **path B**, while intermediate **442** would also be less sterically crowded than **443** at the C-2 indole position **(Scheme 1.62)**. The direct addition of tosylate to the indolimine **440** (**path A**) was disfavoured due to electrophilicity of the nitrogen atom being offset by the conflicting local dipole and lone pair repulsion centered at that atom.

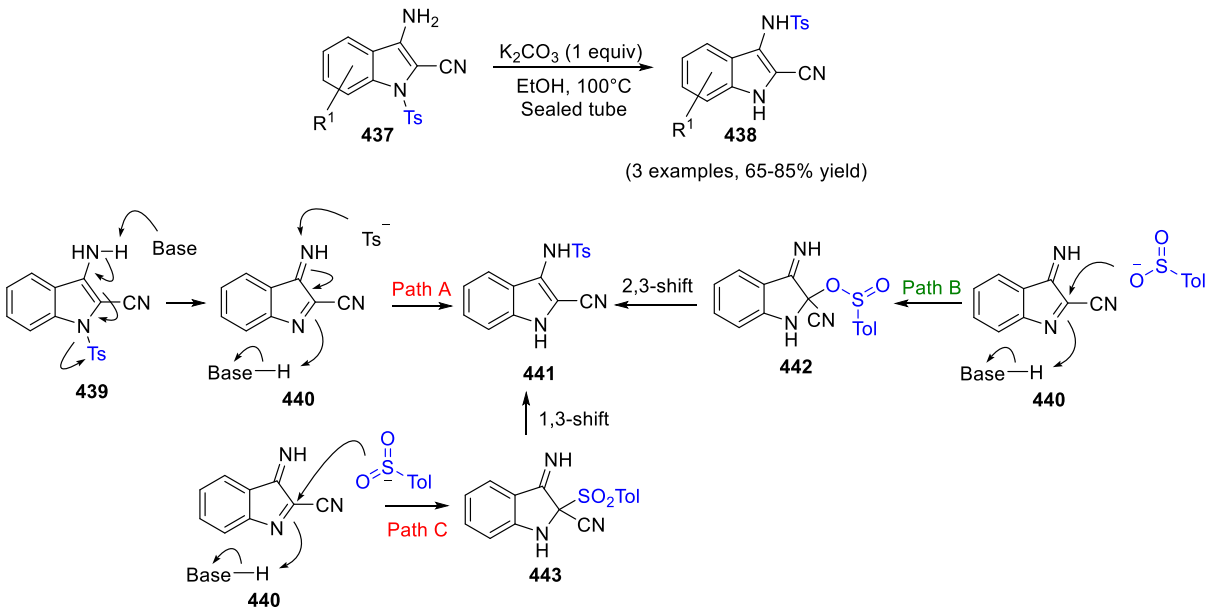

Scheme 1.62: Base-mediated 1,4-nitrogen to nitrogen tosyl migration of 3-amino-1-tosylindole-2-carbonitriles

The Lewis acid mediated tandem reaction of propargyl alcohols **444** and *N*-sulfonylhydrazones **445** to afford dihydropyrazoles **446** in moderate to good yields via a nitrogen to nitrogen 1,2-sulfonyl migration was reported by Wang and co-workers **(Scheme 1.63)**.[90] Lewis acid mediated conversion of the tertiary alcohol **444** to the allenic carbocation **448** occurs by Meyer–Schuster rearrangement.[91] The allenic carbocation **448** is trapped by *N*-sulfonylhydrazone **445** to afford the *N*-sulfonylallenamide **449**. Cyclisation via nucleophilic addition of the internal carbon of the allene to the electron-deficient carbon of the hydrazone can be envisaged to construct the cyclised intermediate **450**. The sequence is completed by intramolecular 1,2-sulfonyl migration to afford the dihydropyrazole **446** via **451**. The intramolecular nature of the sulfonyl migration was confirmed by the addition of sodium *p*-toluene sulfinate to the standard reaction conditions, with no incorporation of the tosyl group observed.

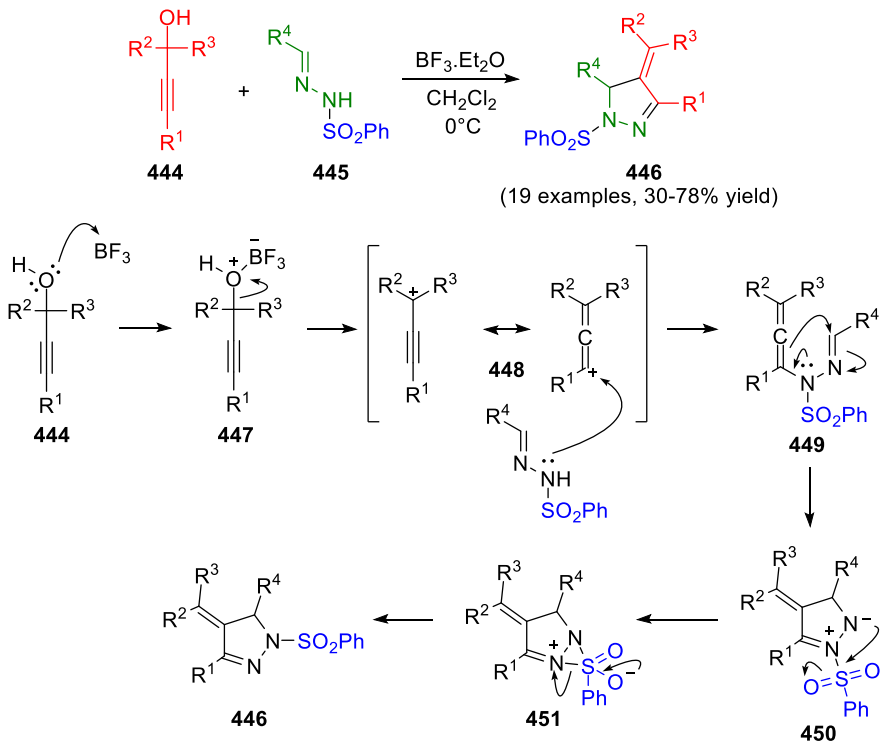

Scheme 1.63: Formation of dihydropyrazoles from the Lewis acid-catalysed tandem reaction of *N*-sulfonyl hydrazones and propargyl alcohols via intramolecular 1,2-nitrogen to nitrogen sulfonyl migration

In 2013, the Dong group reported the regioselective synthesis of polysubstituted 4-amino- and 6-amino-2-iminopyridines **452** via copper-catalysed three-component reaction of sulfonyl azides, alkynes, and 2-[(amino)methylene]malononitriles.[92] Subsequently, during examination of the synthetic potential of these substrates, the same group observed that that these pyridine derivatives readily undergo base-mediated regioselective ring opening to afford 5-oxo-pent-3-enimidamides **453** in high yields.[93] Under thermal conditions, rearrangement involving a rare nitrogen-to-nitrogen 1,3-sulfonyl migration affords 4-aminopyridines **454** in excellent yields **(Scheme 1.64)**. It is thought that **455'**, the enol tautomer of **453**, being a polysubstituted azatriene, undergoes a 6π-azaelectrocyclisation[94-96] at high temperatures to give the 1,2-dihydropyridine intermediate **456**. Subsequently, a 1,3-nitrogen-to-nitrogen tosyl migration generates the aromatic 4-aminopyridine **454**, after loss of water **(Scheme 1.64)**.

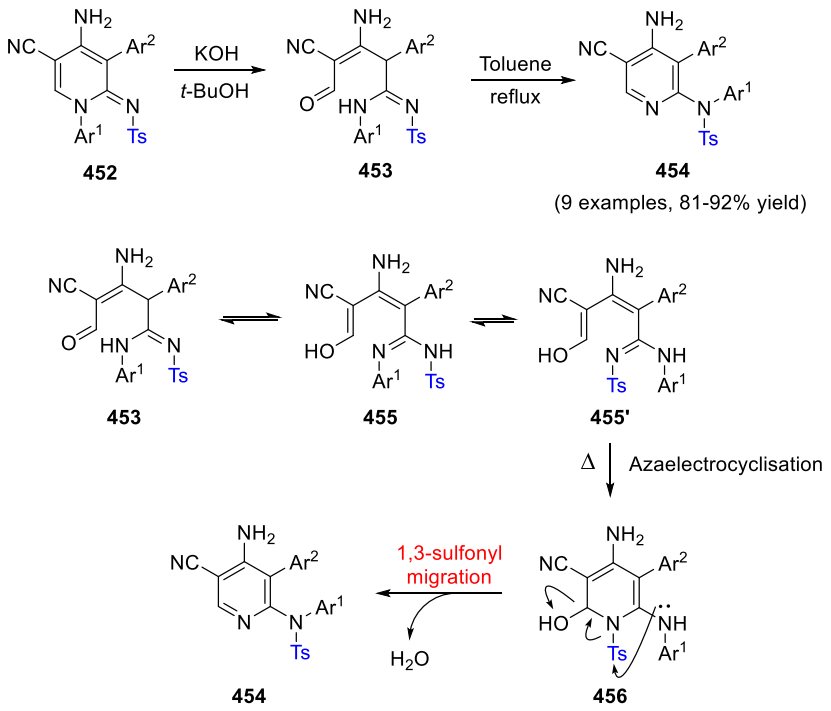

Scheme 1.64: Thermal rearrangement of 5-oxo-pent-3-enimidamides to 4-aminopyridines via 1,3-nitrogen-to-nitrogen sulfonyl migration

The thermal ring expansion of 2-sulfonylimidoyl-1-phthalimidoaziridines **457** to generate *N*-sulfonylimidazoles **458**, involving a 1,3-nitrogen to nitrogen sulfonyl migration, in moderate to good yields has been described **(Scheme 1.65)**.[97] To confirm the nitrogen to nitrogen sulfonyl migration the ^{15}N-labelled aziridine **462** was prepared, which when heated afforded the ^{15}N-labelled imidazole **463** with the tosyl group on the unlabelled nitrogen. By virtue of crossover experiments the sulfonyl migration was determined to be an intramolecular process. The mechanism is postulated to involve ring opening of the aziridine ring of **457,** which affords the azomethine ylide **459**. A 1,5-electrocyclisation to imidazoline **460** precedes elimination of the phthalimide moiety to give the sterically hindered imidazole **461**. Isomerisation via an in intramolecular 1,3-sulfonyl migration affords the less sterically hindered rearranged imidazole **458**.

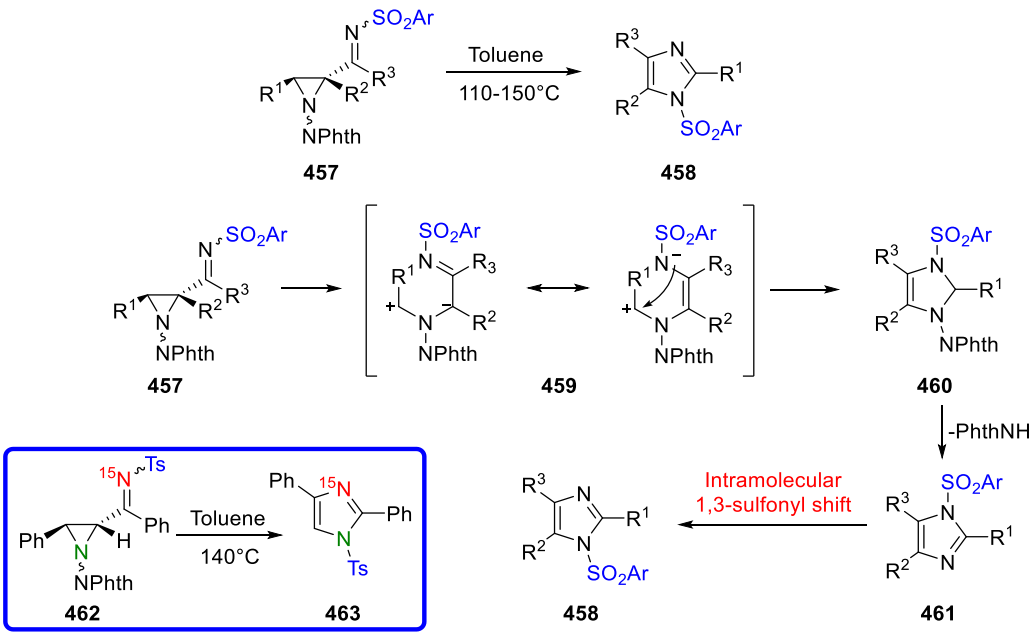

Scheme 1.65: Thermal ring expansion of 2-sulfonylimidoyl-1-phthalimidoaziridines into *N*-sulfonylimidazoles involving 1,3-nitrogen to nitrogen sulfonyl migration

Interestingly, while the Zhan group observed a 1,4-nitrogen to carbon sulfonyl migration for the $ZnCl_2$-mediated reaction of *N*-allenic sulfonylhydrazones **178** (see **Scheme 1.25**),[42] a 1,2-nitrogen to nitrogen sulfonyl migration was observed in the presence of $FeCl_3$ as a catalyst with the same substrate class **(Scheme 1.66)**.[42] As with the zinc-catalysed reaction, intermolecular sulfonyl migration was supported by crossover experiments. Analogous to the $ZnCl_2$ catalysed reaction, the intermediate **469** is generated in the same manner from **465**, however, under this set of conditions elimination of $FeCl_2$ facilitates direct nucleophilic addition of the nitrogen atom to tosyl chloride completing a formal 1,2-nitrogen to nitrogen sulfonyl migration to give the rearranged pyrazole **470**.

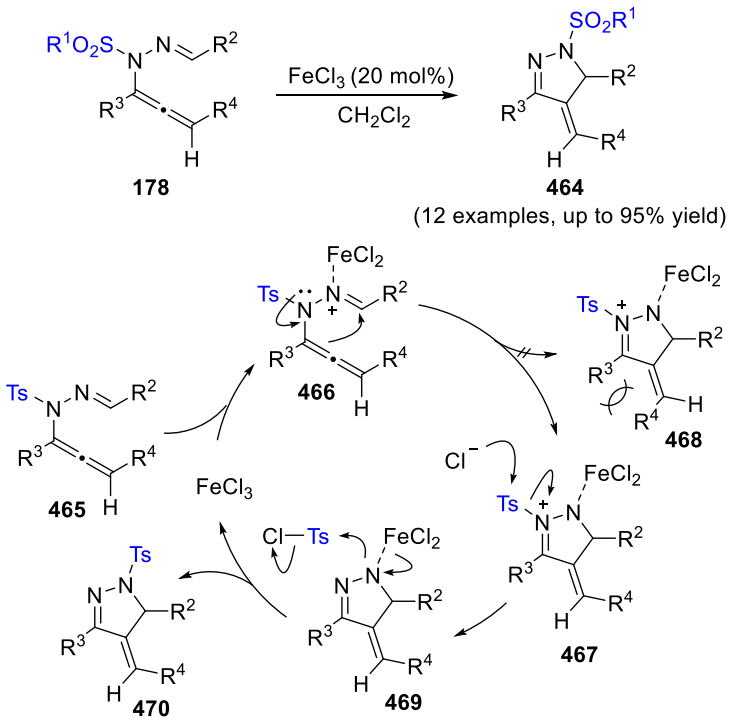

Scheme 1.66: Selective synthesis of (*E*)-4,5-dihydro-1*H*-pyrazoles from *N*-allenic sulfonylhydrazones via 1,2-nitrogen to nitrogen sulfonyl migration

The Beak group reported the application of the endocyclic restriction test in the evaluation of the geometries of nucleophilic substitutions at the sulfonyl moiety of aryl sulfonamides **471/472** to afford alkyl sulfonamides **473/474** via base-catalysed nitrogen to nitrogen migration **(Scheme 1.67)**.[98] By incorporating a short molecular tether (X = CH_2, **472**) linking the nucleophilic amine and the sulfonyl leaving group, the geometry is restrained. Therefore, the simultaneous apical entering of the nucleophile and leaving of the sulfonyl moiety affording a trigonal biypyramidal transition state structure is disfavoured; hence an intermolecular migration is most likely. In contrast a long tether [X = $O(CH_2)_{11}$, **471**] which is much more flexible would make such a transition state more likely, and as a result an intramolecular migration may become the operative pathway.

To test this assumption a double-labelled crossover experiment was performed between an equimolar mixture of unlabelled **471** and labelled **471-*d*$_{10}$** at 0.1 and 0.01 M. Following isolation and analysis of the isotopic composition of the products by FABMS it was determined that at a concentration of 0.1 M the sulfonyl migration occurs in both an intra- and intermolecular manner. However, at a dilution of 0.01 M a significant increase in intramolecular substitution is observed **(Scheme 1.67)**. This increase at higher dilution is consistent with a first-order (intramolecular) reaction which becomes competitive with a second-order (intermolecular) reaction which occurs more readily at higher concentrations. Repeating the double-labelled crossover experiment with the less flexible arylsulfonamides **472** and **472-*d*$_{10}$** at 0.01 M determined that the sulfonyl migration is instead an intermolecular process. These results are consistent with the requirement of an almost linear arrangement of the nucleophile and leaving group at sulfur in the transition state, with a trigonal bipyramidal structure **475** with a large bond angle between the incoming and leaving groups a reasonable candidate for the transition state for such reactions.

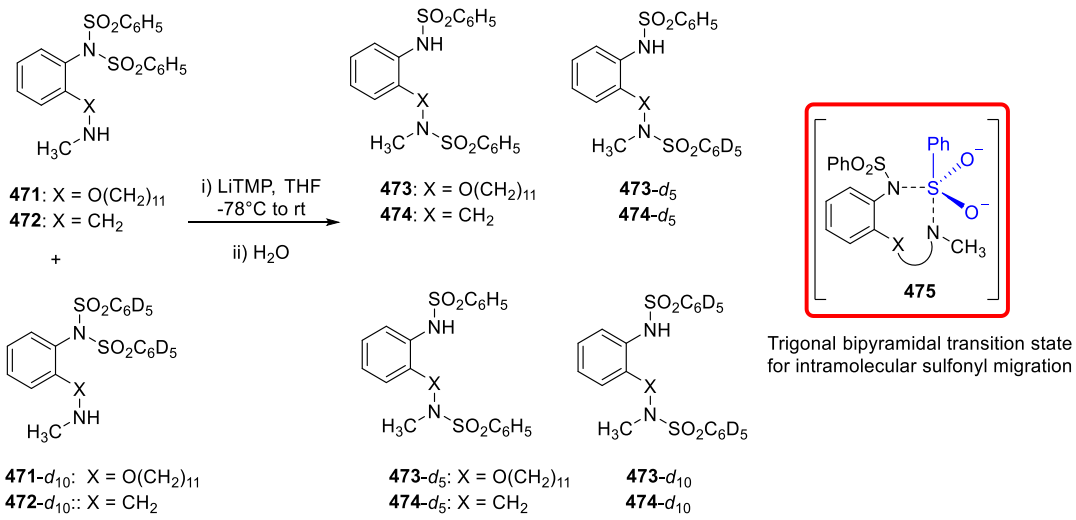

Scheme 1.67: Evaluation of the geometries of nucleophilic substitutions at the sulfonyl moiety of aryl sulfonamides using the endocyclic restriction test

1.4. Nitrogen to Oxygen Sulfonyl migration

1.4.1. Transition metal-catalysed sulfonyl migration

Boominathan *et al*. described the iron-catalysed cascade generation of 5*H*-benzo[*b*]carbazole derivatives **477** utilising an intramolecular 1,4-nitrogen to oxygen sulfonyl migration **(Scheme 1.68)**.[99] The following mechanism was tentatively suggested by the authors. Keto-enol tautomerisation of the ketone **476** occurs, with subsequent coordination of the iron catalyst to the alkyne **478** facilitating a 5-*exo*-dig cyclisation and protodemetallation to afford the vinylidene intermediate **479**. Keto-enol tautomerisation of this intermediate generates the enol **480**, which, after 6π-electrocyclisation gives the ring-closed intermediate **481**. Aerial oxidative aromatisation[100-103] gives the hydroxy 5*H*-benzo[*b*]carbazole intermediate **482**, which was isolable. Coordination of the iron catalyst with the sulfonyl group of intermediate **482** gives the intermediate **483**, which due to the increased electrophilicity at sulfur undergoes an intramolecular nucleophilic attack of the phenolic OH giving the 5-membered intermediate **484**. Finally, the iron-driven scission of the N–S bond completes the 1,4-sulfonyl migration from nitrogen to oxygen. The intramolecular nature of the sulfonyl migration was supported by the results of crossover experiments. Notably, no sulfonyl migration was observed for the reaction of the intermediate **482** in the absence of the iron catalyst, highlighting that the catalyst is required for both the cascade process and the sulfonyl migration.

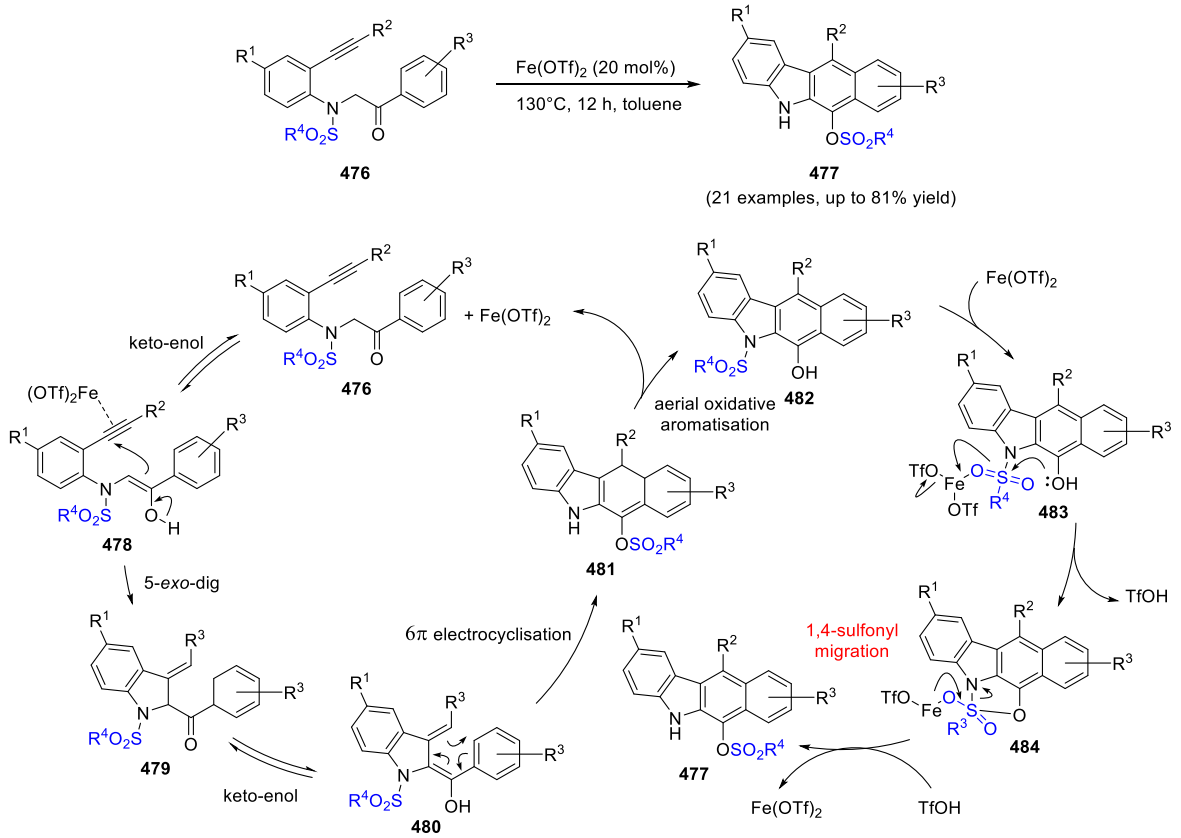

Scheme 1.68: Iron-catalysed cascade generation of benzo[*b*]carbazoles followed by 1,4-nitrogen to oxygen sulfonyl migration

The Blanc group reported the synthesis of 1-azabicycloalkane derivatives **487** via a gold-catalysed desulfonylative cyclisation.[104] Notably, *N*-sulfonyl azacyclic ynone derivatives **485** can readily undergo two divergent reaction pathways; the pathway followed is strongly dependant on whether a suitable protic oxygen-nucleophile is added, and the ability of the substrate to enolise **(Scheme 1.69)**.

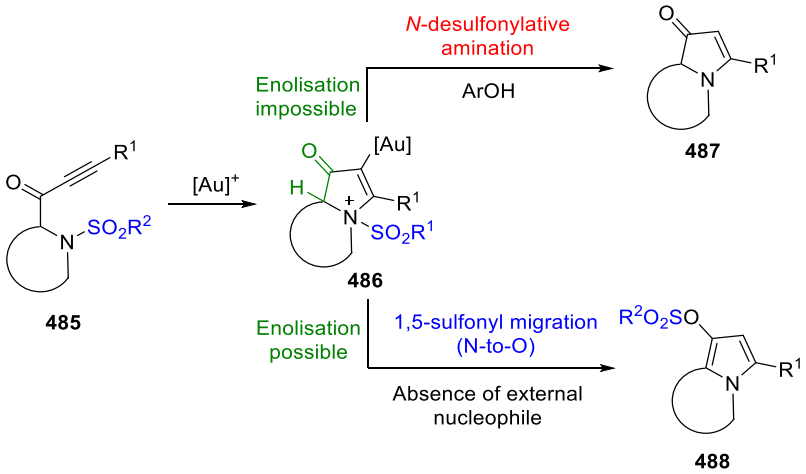

Scheme 1.69: Overview of gold(I)-catalysed *N*-desulfonylation or regioselective 1,5-sulfonyl migration

In the presence of $[Cy_3PAuCl]/AgBF_4$ as catalyst and an excess of *m*-nitrophenol, the azabicyclic products **490** were generated in moderate to good yields via *N*-desulfonylation of the ammonium intermediate **486 (Scheme 1.69/1.70 A)**. Expanding the scope of the reaction to more flexible substrates, which are more readily enolisable, an alternative 1,5-nitrogen to oxygen sulfonyl migration occurred in the presence of triphenylphosphine gold(I) triflimidate and in the absence of external nucleophile. Using this approach pyrrolizine or indolizine derivatives **492** were accessible in moderate to high yields **(Scheme 1.70, B)**. Crossover experiments unambiguously confirmed that the 1,5-sulfonyl migrations proceeds intramolecularly. Notably, enolisation could be used as a switch between the *N*-desulfonylation pathways as demonstrated by the subjection of enolisable compound **493** and non-enolisable compound **494** to the optimised desulfonylation conditions **(Scheme 1.70, C)**. As expected the *N*-desulfonylation product **496** was obtained from non-enolisable **394**, while the enolisable **493** readily afforded the 1,5-sulfonyl migration product **495** in 90% yield.

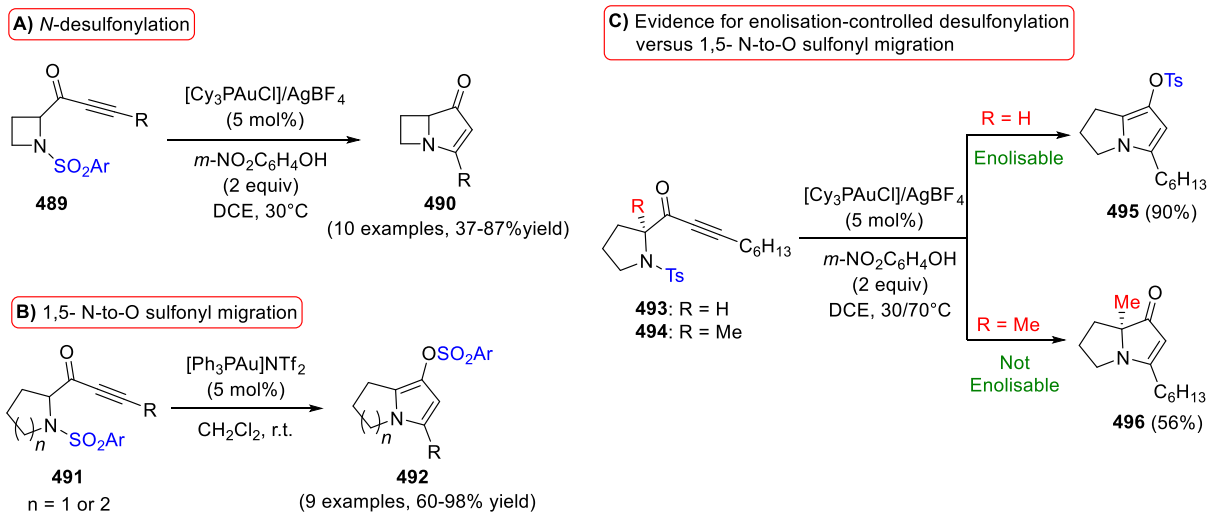

Scheme 1.70: Gold(I)-catalysed *N*-desulfonylation versus intramolecular 1,5-nitrogen to oxygen sulfonyl migration and the role of enolisation on the reaction outcome

The same group subsequently extended their gold-catalysed cycloisomerisation–sulfonyl migration cascade strategy to the formation of the key pyrrole ring in the total synthesis of the anticancer monoterpenoid indole alkaloid rhazinilam **500 (Scheme 1.71)**.[105] The required extension of the methodology to incorporate various *N*-alkylated *N*-sulfonyl 1-aminobut-3-yn-2-ones **497** proved successful, this time with the $JohnPhosAuNTf_2$ proving more efficient than the Gagosz catalyst for both acyclic and cyclic substrates. Using this methodology the substrates **497** formed the desired 1,2,4-trisubstituted pyrrolyl sulfonates **498** in high yields (up to 93%) in less than 10 minutes. Crucial to the total synthesis was the subsequent palladium-catalysed coupling of the pyrrolyl tosylates and related sulfonates with boronic acids, a first-in-class example of a challenging Suzuki–Miyaura coupling of pyrrolyl sulfonates.

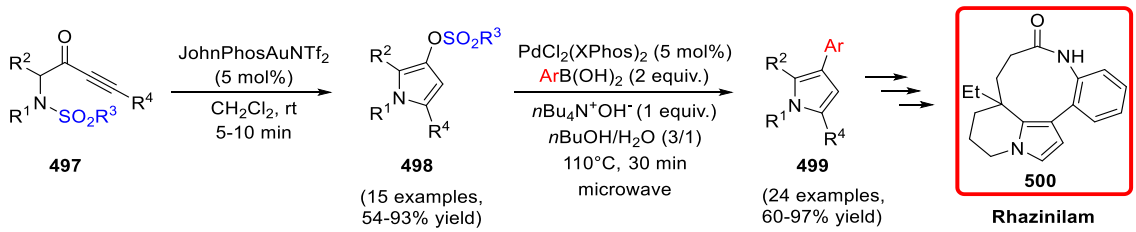

Scheme 1.71: Total synthesis of Rhazinilam through gold-catalysed cycloisomerisation–sulfonyl migration and palladium-catalysed Suzuki–Miyaura coupling of pyrrolyl sulfonates

1.4.2. Non-metal-catalysed sulfonyl migration

In studies on the Diels–Alder cycloadditions of 2-methyl- and 2,3-dimethyl-1,3-butadienes with 1-arylsulfonyl-2(1*H*)-pyridones **503** as dienophiles, Fujita and co-workers observed significant amounts of the 1,3-nitrogen to oxygen sulfonyl migration by-products **505 (Scheme 1.72).**[106] In a later study, the Yang group observed that the thermally driven sulfonyl migration of pyridones **506** can completely supress cycloaddition when using dienophiles such as dimethyl acetylenedicarboxylate **512**, methyl vinyl ketone **513**, ethyl vinyl ether **514** or methyl methacrylate **515**, whereas when methyl acrylate **507** is employed the cycloaddition is favoured albeit with significant amounts of sulfonyl migration product **510** also observed **(Scheme 1.73)**.[107]

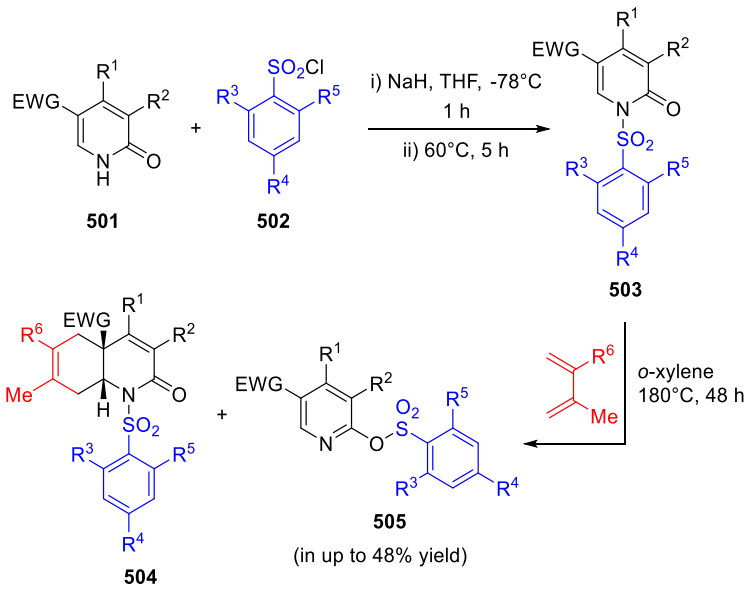

Scheme 1.72: Generation of sulfonate by-products **505** via thermal 1,3-nitrogen to oxygen sulfonyl migration in Diels–Alder cycloadditions between 1-arylsulfonylpyridones and dienes

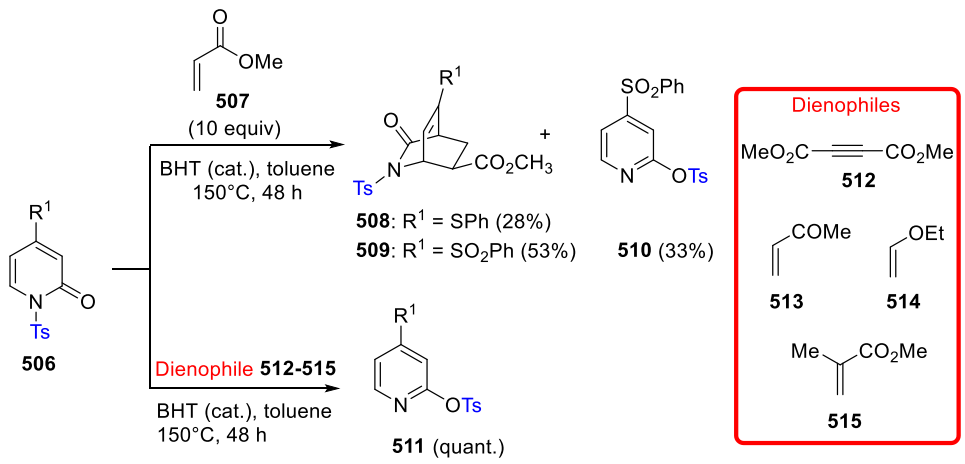

Scheme 1.73: Selective 1,3-nitrogen to oxygen tosyl migration of pyridones in the presence of dienophiles under thermal conditions

Perry and co-workers described an oxidative cascade, involving an oxidative ring expansion of α-furyl sulfonamides **516**, acid-catalysed aromatisation and a formal 1,4-sulfonyl migration from nitrogen to oxygen to generate 3-sulfonyloxypyridines **518** in moderate to excellent yields **(Scheme 1.74)**.[108] The authors propose that aromatisation of the pyridinone **517** occurs via acid-catalysed dehydration and enolisation to give the pyridinium salt intermediate **518**. Addition of triethylamine is believed to mediate the intermolecular 1,4-sulfonyl migration. When the reaction was quenched with methanol the 3-hydroxypyridine **519** was instead the major product, and sulfonyl migration product was not observed **(Scheme 1.74)**.

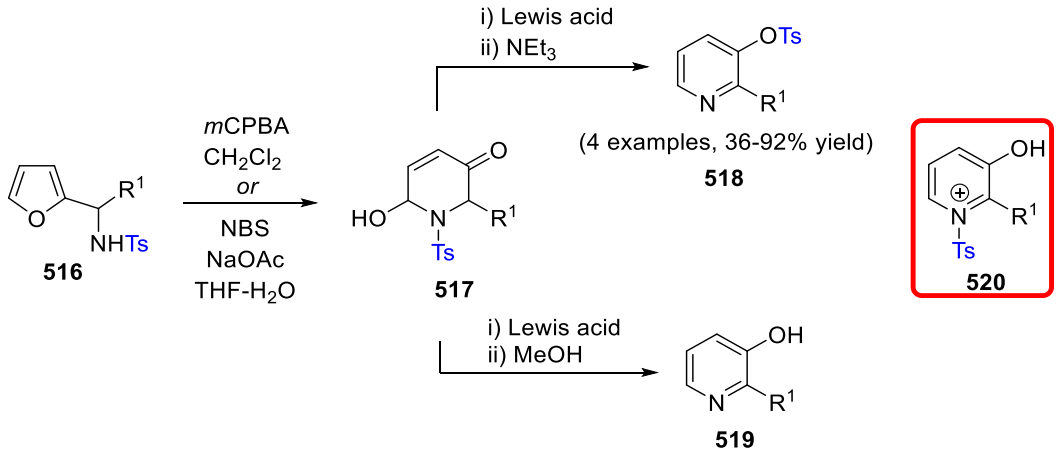

Scheme 1.74: Synthesis of 3-sulfonyloxypyridines via oxidative ring expansion of α-furyl sulfonamides and formal 1,4-sulfonyl migration

The Smith group developed an isothiourea-catalysed, one-pot synthesis of 2,4,6-substituted pyridines **523** bearing a 2-sulfonate moiety, amenable to further transformations, from (phenylthio)acetic acid **522** and a range of α,β-unsaturated ketimines **521 (Scheme 1.75)**.[109] This reaction involves intermolecular Michael addition/lactam formation, elimination of thiophenol, and finally 1,3- N-to O-sulfonyl migration. The results of crossover studies indicated that the sulfonyl migration is consistent with an intramolecular process.

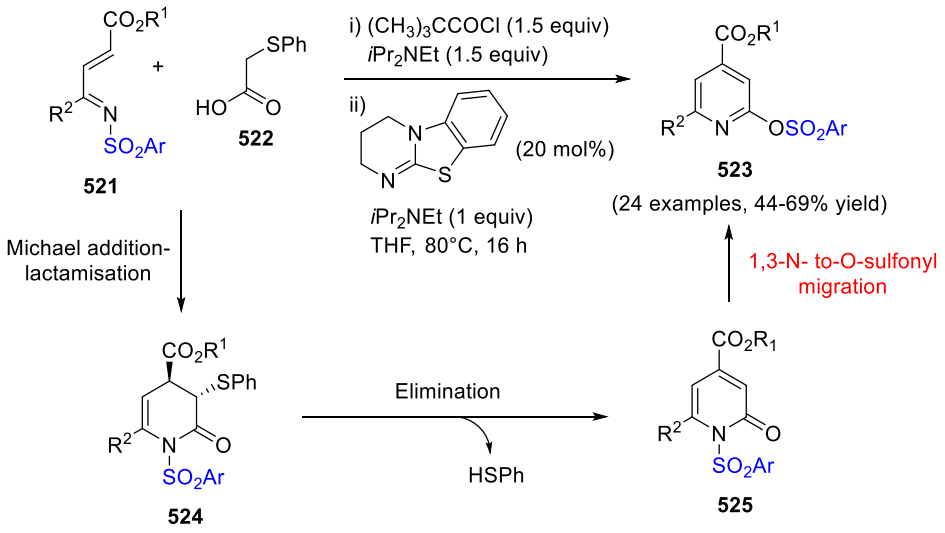

Scheme 1.75: Isothiourea-mediated one-pot synthesis of functionalised pyridines via 1,3-nitrogen to carbon sulfonyl migration

The group later extended this methodology by incorporating alkyl 2-[aryl(tosylimino)methyl]acrylates **526** as Michael acceptors to prepare 2,3,6-pyridine tosylates **529 (Scheme 1.76)**.[110] Utilising α-substituted pheylthioacetic acids **527** in combination with Michael acceptors bearing no β-substituent also facilitated the generation of 2,3,5,6-functionalised pyridines **529**. In these reactions the elimination of PhSH did not occur in either the presence of base or at elevated temperatures. To circumvent this, an additional oxidative step was added to the reaction sequence to generate the sulfoxide, which underwent elimination much more readily. Thermal conditions proved sufficient to enable the final *N*- to *O*-sulfonyl migration to afford the functionalised pyridines **529** in yields of 44–69% across three steps.

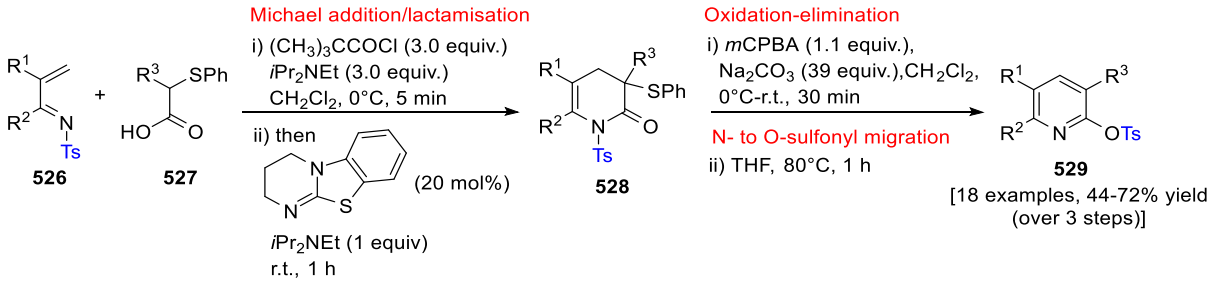

Scheme 1.76: Synthesis of di-, tri-, and tetrasubstituted pyridines from (phenylthio)carboxylic acids and 2-[aryl(tosylimino)methyl]acrylates

During a study relating to the sulfonylation of quinazoline-4(3*H*)-ones and related tetrahydrobenzothieno[2,3-*d*]pyrimidin-4(3*H*)-ones, Gütschow and co-workers observed an unexpected nitrogen to oxygen 1,3-sulfonyl migration during the cyclisation of **531** under thermal conditions; the O-sulfonylated isomer **533** was isolated as the major product, rather than the expected **532 (Scheme 1.77).**[111] The sulfonyl migration was further proved by heating **532** in acetonitrile and monitoring the reaction progress by HPLC. The sulfonyl migration was determined to proceed readily via first order kinetics to give the O-sulfonylated product **533**. However, the heating of **534**, bearing a hydrogen substituent at the 2-position, resulted in no reaction. These results support that the *N*-

sulfonylated products are the thermodynamically favoured isomers when the 2-position is unsubstituted, while for substituted derivatives the *O*-sulfonylated isomers are thermodynamically favoured. Crossover experiments indicated that the 1,3-sulfonyl migration is most likely an intramolecular process.

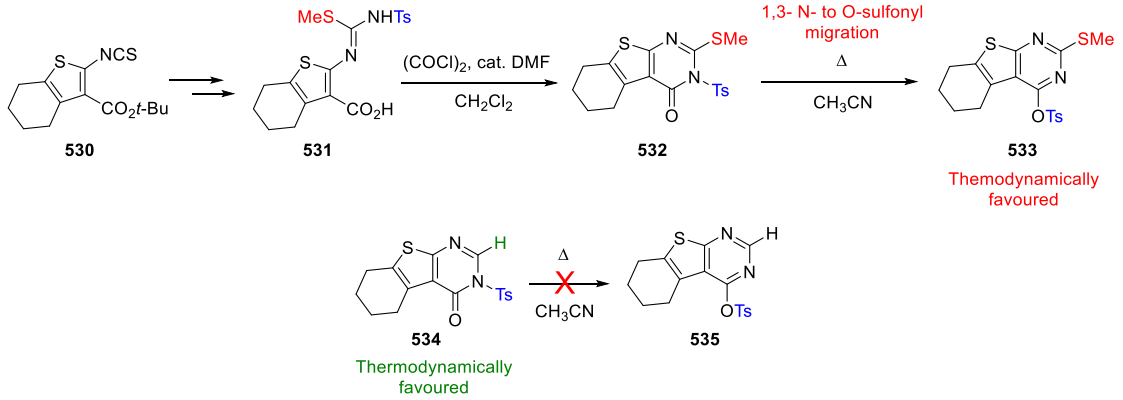

Scheme 1.77: Generation of *O*-sulfonylated thieno[2,3-*d*]pyrimidines via unexpected thermal intramolecular 1,3-sulfonyl migration

Chi and co-workers developed a one-step, chemo-, stereo- and enantioselective cascade reaction to synthesise multicyclic oxoquinoline-type heterocycles **538** via an *N*-heterocyclic carbene catalysed activation of the β sp^3-carbon atom of the ester **536** as a key step **(Scheme 1.78)**.[112] During derivatisation of the oxoquinoline **538**, the group demonstrated that a 1,3-N- to O-sulfonyl migration proceeds readily under thermal conditions to afford the quinoline derivative **539** in 92% yield. The enantiomeric and diastereomeric ratios remained intact through the migration.

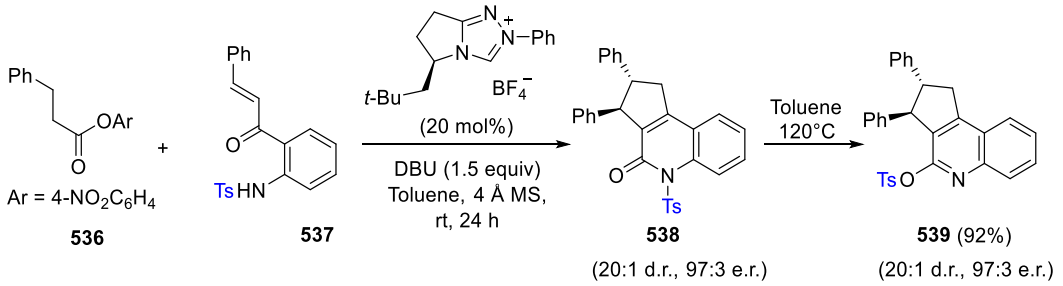

Scheme 1.78: Access to oxoquinoline heterocycles via *N*-heterocyclic carbene-catalysed ester activation for selective reaction with an enone

Trisubstituted pyridines **542**, bearing a 2-sulfonate moiety amenable to further synthetic manipulation, are accessible via a DMAP-catalysed activation of α-chloroacetic ester **540** in the presence of unsaturated imines **541** containing a tosyl protecting group that undergoes a thermal nitrogen- to oxygen 1,3-sulfonyl migration **(Scheme 1.79)**.[113] Optimal results were achieved using **541** bearing electron-withdrawing substituents, with a significant reduction in yield observed when electron-donating substituents were incorporated. Imines containing heterocyclic moieties also readily participated in the reaction, however the use of α-branched chloroacetates with an α-alkyl substituent completely inhibited the reaction pathway. The mechanism postulated involves the reaction of the DMAP-activated α-chloroacetic ester **540** with the unsaturated imine **541** leading to the lactam intermediate **543**. E2-elimination affords the adduct **544** which undergoes N- to O-sulfonyl

migration at elevated temperature to give the desired product **542**. It is likely that the driving force for the sulfonyl migration is the aromatisation of the heterocyclic ring.

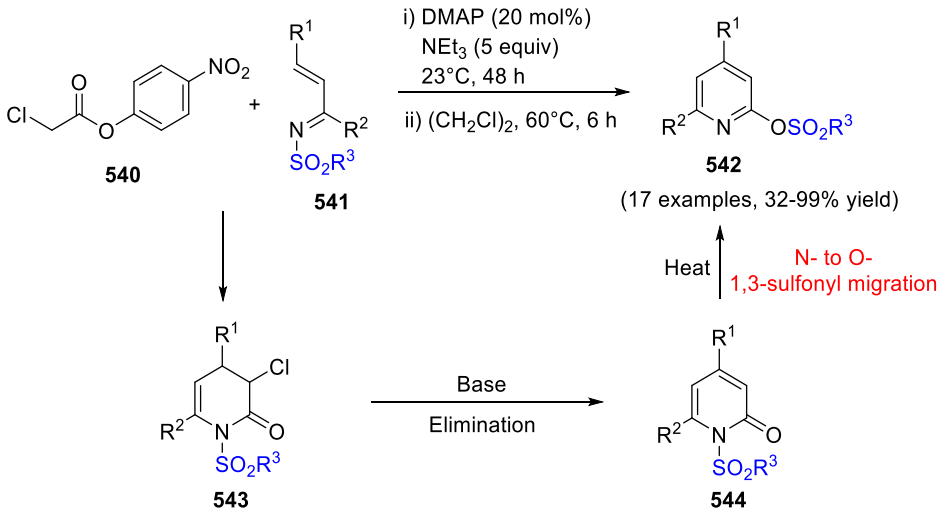

Scheme 1.79: Access to pyridines via DMAP-catalysed activation of α-chloroacetic ester with unsaturated imines

1.5. Oxygen to Carbon sulfonyl migration

1.5.1 Photoinduced sulfonyl migration

The photoinitiated radical fragmentation and rearrangement of vinyl tosylates resulting in efficient formation of aromatic and aliphatic β-ketosulfones **546** and **549** was reported by Xie *et al.*[114] Aromatic vinyl tosylates **545** and aliphatic vinyl tosylates **548** both underwent these visible-light promoted transformations with excellent and moderate to good yields respectively, albeit with different photoinitiators in each instance. Eosin B **547** proved optimal for the aromatic series, while 9-fluorenone **550** was preferable in the case of aliphatic vinyl tosylates **(Scheme 1.80)**.

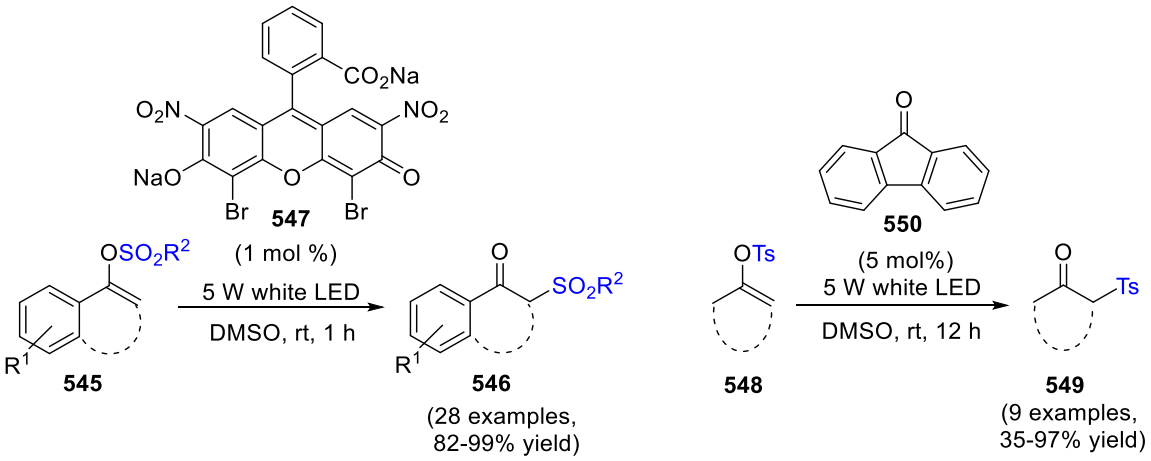

Scheme 1.80: Photoinduced rearrangement of vinyl tosylates to β-ketosulfones via 1,3-sulfonyl migration

A trapping experiment, using the radical scavenger TEMPO, revealed complete suppression of the reaction, and 99% recovery of the starting material, indicative of a radical mechanism. Crossover

experiments indicated that the 1,3-sulfonyl migration is an intermolecular process. A photoinduced chain mechanism was deemed likely as a result of quantum efficiency calculations, while DFT calculations for the initiation process were compatible with energy transfer between the initiator and the vinyl tosylate substrate. Considering this, the putative mechanistic pathway was presented **(Scheme 1.81)**. Homolytic cleavage of the O–S bond in the vinyl tosylate **551** occurs through energy transfer from the excited photosensitiser, to generate an enol radical **552** and a sulfonyl radical. The sulfonyl radical adds to another vinyl tosylate **551** affording the intermediate **553**, which on elimination of a further sulfonyl radical affords the β-ketosulfone **554** and sulfonyl radical for the subsequent reaction cycle.

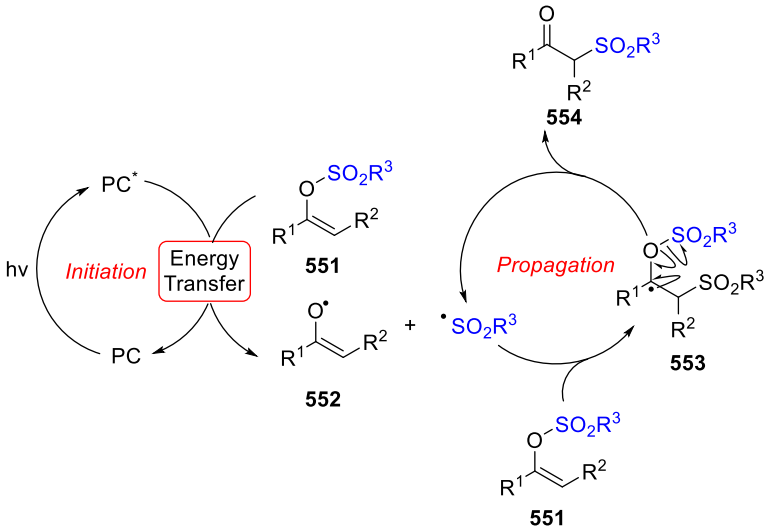

Scheme 1.81: Proposed mechanism for the photoinduced rearrangement of vinyl tosylates to β-ketosulfones via 1,3-sulfonyl migration

The Feng group reported an iridium-catalysed visible-light promoted oxo-sulfonylation of ynamides **555** with sulfonic acids **556**, leading to functionalised α-sulfonylated amides **557** in moderate to good yields **(Scheme 1.82)**.[115] Generally, ynamides bearing an electron-rich aromatic ring delivered the desired products in good yields, while substrates with an electron-deficient aromatic ring gave lower yields. Aryl halides, fused aromatics and heterocyclic substituents were well tolerated, while both electron-rich and electron-poor alkyl and aromatic sulfonic acid derivatives could be incorporated to furnish a diverse range of α-sulfonylated amides.

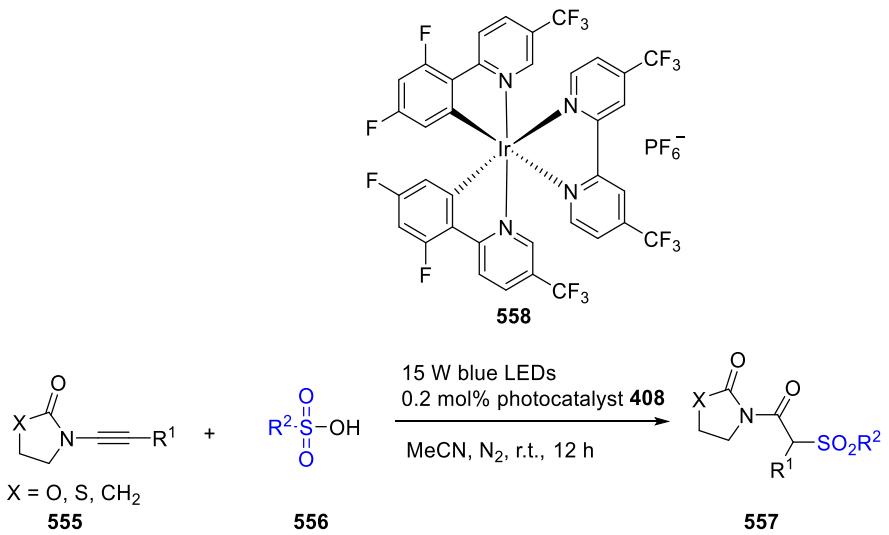

Scheme 1.82: Visible-light promoted oxo-sulfonylation of ynamides with sulfonic acids

In order to garner information regarding the mechanism the authors carried out a series of control experiments **(Scheme 1.83)**. Toluenesulfonic acid readily reacted with the ynamide **559** to give the vinyl tosylate **560** in almost quantitative yield **(Scheme 1.83, A)**. This vinyl tosylate could be converted into the α-sulfonylated amide **561** under the standard reaction conditions in high yields, confirming its role as an intermediate in the tandem reaction pathway **(Scheme 1.83, B)**. Performing the reaction in the presence of TEMPO, a radical scavenger, completely inhibited the reaction, supporting the generation of a radical intermediate in the rearrangement step **(Scheme 1.83, C)**. A radical mechanism was additionally confirmed through the reaction of **560** with dilauroyl peroxide as a radical initiator in place of the iridium photocatalyst **558** which also led to **561**, albeit in a significantly lower yield **(Scheme 1.83, D)**. Crossover experiments indicated that the sulfonyl migration was an intermolecular process.

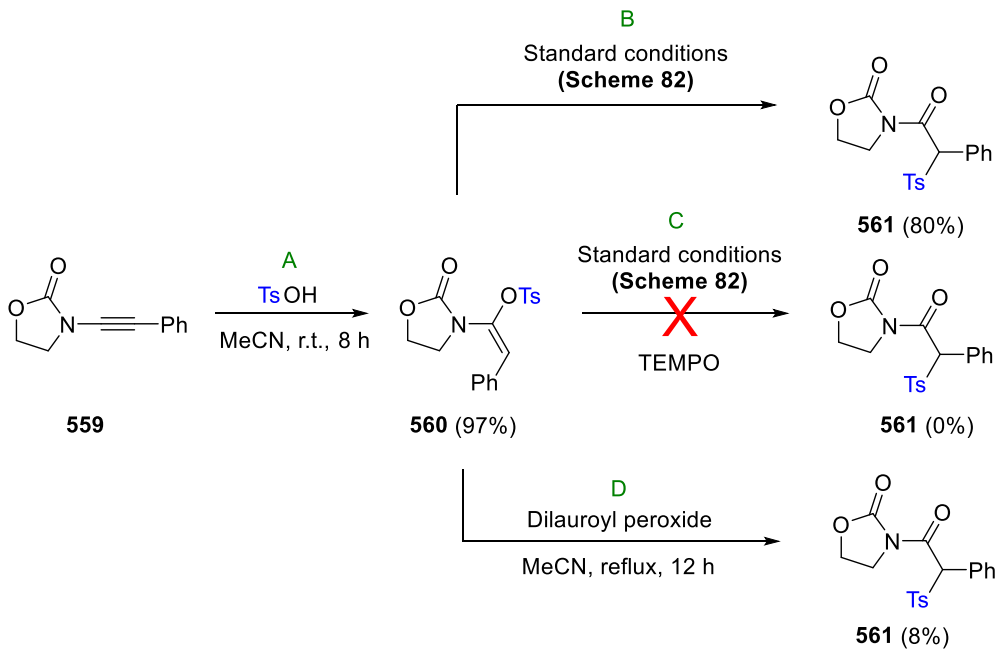

Scheme 1.83: Control experiments supporting a radical mediated oxygen to carbon sulfonyl migration in the synthesis of α-sulfonylated amides

In further investigation of the working mode of the photocatalyst (single electron transfer vs. energy transfer), cyclic voltammetry experiments indicated that the vinyl tosylate intermediate **560** has a higher reduction potential than the excited state of the photocatalyst (PC*), indicating that a single electron transfer cannot occur under the standard conditions. Stern–Volmer quenching experiments confirmed that the vinyl tosylate **560**, and not the ynamide **559** or tosic acid, could quench the excited photocatalyst. A DFT calculation of the triplet energy of **560** was calculated to be 100.1 kJ mol^{-1}, a value that is within the range expected to be accessed by the iridium photocatalyst (250.3 kJ mol^{-1}) as a triplet sensitiser. These results in combination support an energy transfer mechanism for the photocatalyst's working mode. Furthermore, a light on/off experiment confirmed that the reaction requires continuous irradiation to achieve reaction completion, while the quantum yield of 10.0 for the rearrangement of **560** to **561** indicated a radical chain propagation mechanism.

In light of these findings the following mechanism was proposed **(Scheme 1.84)**. Electrophilic addition of sulfonic acid to ynamide **555** gives vinyl sulfonate **562** in a regioselective manner. Subsequently, activation of the sulfonate **562** occurs through the energy transfer process from the excited photocatalyst (PC^*). Homolytic cleavage of the C–S bond of the activated vinyl sulfonate **562** generates the sulfonyl radical and enol radical **563**. Selective addition of the sulfonyl radical to the electron rich alkene group of vinyl sulfonate **562** leads to the α-sulfonylated amide **557** via β-scission of the radical intermediate **564**, which regenerates a sulfonyl radical enabling a radical chain propagation.

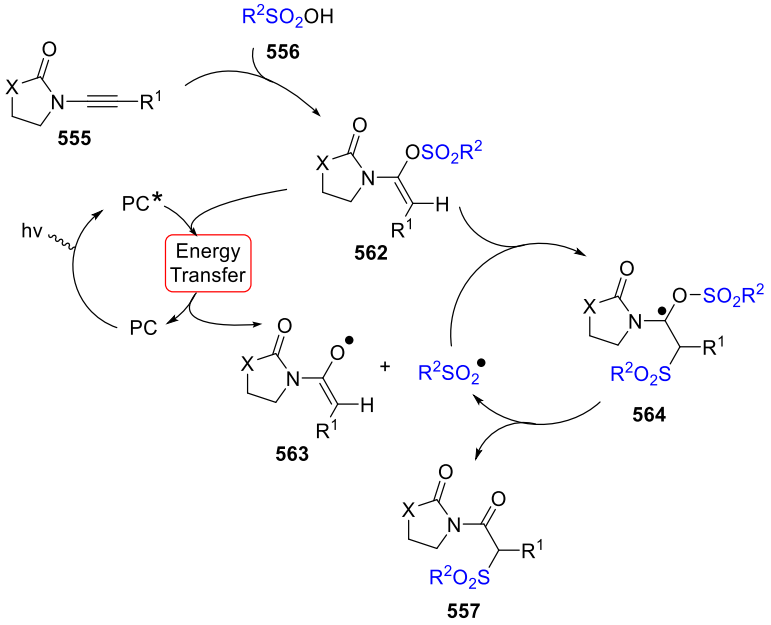

Scheme 1.84: Proposed mechanism for the visible-light-promoted oxo-sulfonylation of ynamides with sulfonic acids

1.5.2. Thia-Fries rearrangement

The thia-Fries rearrangement is a sulfur based sub-class of the well-known Fries rearrangement, in which aromatic sulfonates or sulfonanilides rearrange to afford ortho- or para-substituted hydroxy or amino sulfones respectively. The rearrangement, named after Karl Fries, who published the seminal report in 1908, has subsequently been demonstrated under cationic, anionic and radical/light-induced conditions. Notably, over the last 20 years the most significant highlight in this area was the development of the anionic-thia Fries rearrangement for sulfonates at both aromatics and

organometallics. An overview of the anionic Fries rearrangement, including the thia-Fries sub-class, was recently undertaken by Korb and Lang.[116] This section will further describe anionic and non-anionic thia-Fries rearrangement.

1.5.2.1. Anionic thia-Fries rearrangement

While attempting the palladium-catalysed cross-coupling of 1-chloro-2-naphthalene triflate **565** with a pyridyl zinc halide, generated *in situ* using LDA/$ZnCl_2$, a notable side product was identified as the *ortho*-hydroxyarylsulfone **566**. This result, reported by Lloyd-Jones in 2003, described the first example of an anionic thia-Fries rearrangement of aryl triflates.[117] Further optimisation revealed that it is in fact LDA, and hence a base, that mediates the rearrangement, with the *ortho*-hydroxyarylsulfone **566** obtained in 64% yield **(Scheme 1.85)**. Aryl triflates bearing moderately electron-withdrawing groups, particularly *ortho* to the triflate, readily underwent the thia-Fries rearrangement, whereas analogues containing electron-donating groups at the *ortho*-position favoured aryne generation. Notably, solvent effects are crucial in controlling the reaction outcome. For example, *o*-chlorophenyl triflate **567** exclusively affords the thia-Fries rearrangement product **570** in the presence of THF, however, the use of DIPA which is an effective aryne scavenger gives a mixture of both the mono- and bis-anilines **568** and **569 (Scheme 1.85)**. However, even in instances in which excess DIPA is not employed one must contend with the generation of DIPA from the deprotonation of the aryl triflate.

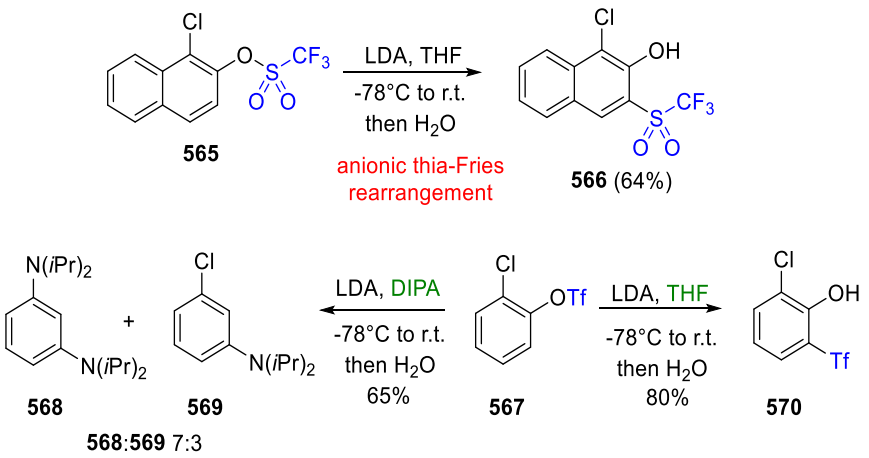

Scheme 1.85: Discovery of the first anionic this-Fries rearrangement

In order to rationalise the reactivity of aryl triflates towards thia-Fries rearrangement or elimination, Lloyd-Jones and co-workers carried out computational studies and labelling studies.[118] Gas phase and single point calculations, including a continuum description of the THF solvent, were performed for the pathways leading to the rearrangement and elimination of $[C_6H_4OTf]^-$ **(Scheme 1.86)**. The sulfonyl migration was predicted to be a highly exothermic process (62.0 kcal mol^{-1}), while a 1,2-oxethietane intermediate **576** could not be located. Instead, the sulfonyl migration was observed to proceed via a single and early transition state **574** in which the C–S and S–O bond distances shorten and lengthen respectively, relative to the reference starting material **571**. The significantly lower energy of the rearranged phenolate **575** relative to the reference substrate **571** excludes retro-Fries rearrangements as an operative mechanism. Alternatively, the loss of triflate is predicted to be only mildly exothermic (10.2 kcal mol^{-1}). Interestingly, the similar energies of the transition states **572** and **574** indicate that

a thermodynamic rather than a kinetic process may be operational, due to reversible elimination of triflate.

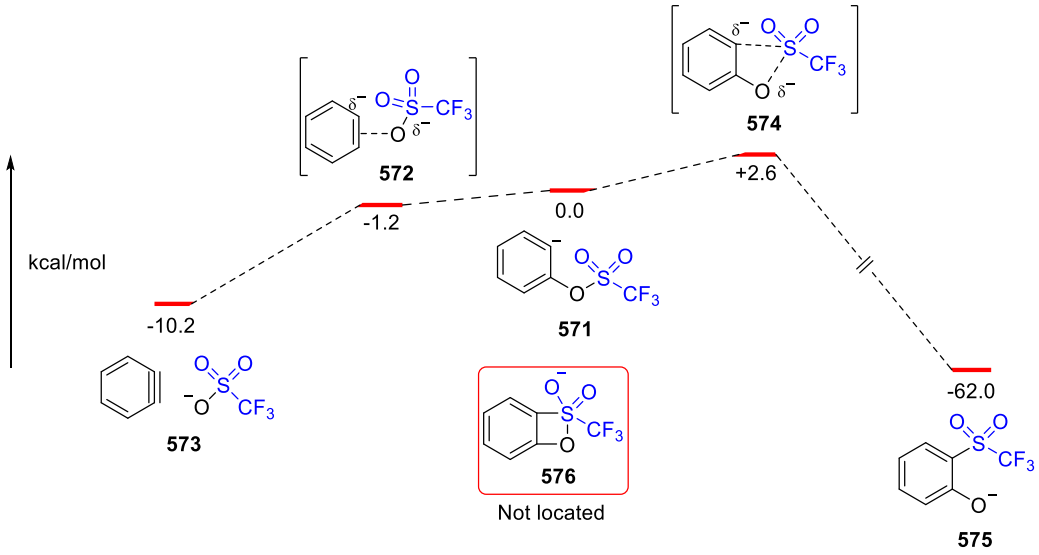

Scheme 1.86: Computed relative energies (in kcal mol^{-1}) for the elimination or thia-Fries rearrangement of **571** in a THF continuum

To test whether reversible addition/elimination of the triflate group to the aryne was occurring, ^{18}O-labelled triflate **577** was reacted under the standard conditions, however, only ^{18}O-labelled phenol **578**, generated through the expected anionic thia-Fries rearrangement was obtained, with no evidence for the ^{18}O/^{16}O scrambling product **579** that would be expected via a reversible process **(Scheme 1.87, A)**. A crossover experiment between ^{2}H-lablelled triflate **580** and ^{34}S-labelled triflate **581** did not generate any of the ^{2}H/^{34}S-lablled phenol **584** anticipated if an intermolecular mechanism was operational, hence the sulfonyl migration was deemed to be an intramolecular process **(Scheme 1.87, B)**.

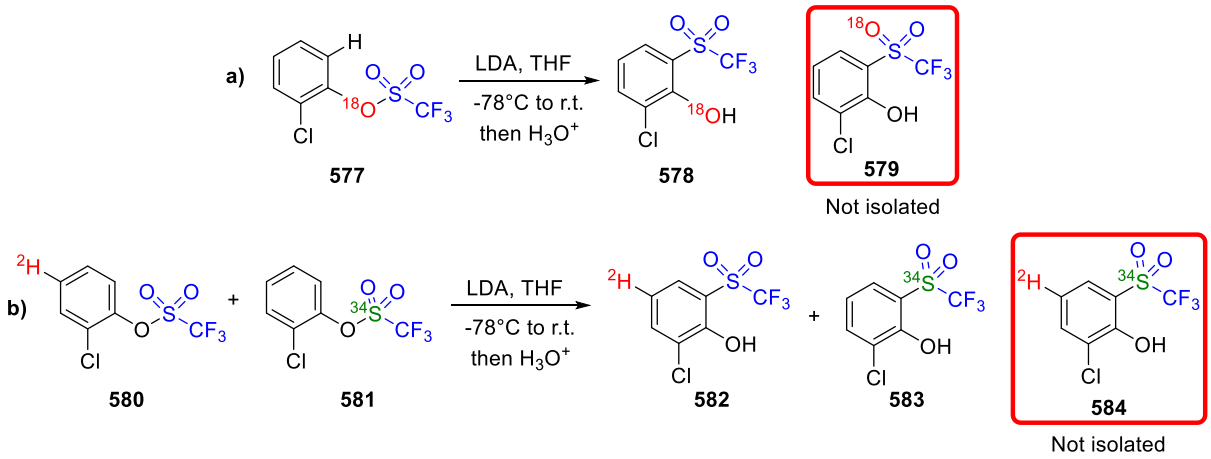

Scheme 1.87: a) ^{18}O-scrambling experiment eliminating reversible aryne formation mechanism; **b)** Crossover experiment indicating an intramolecular sulfonyl migration

The potential for a sulfinite based mechanism, in which one could consider an intramolecular attack of an anionic triflate at the sulfonyl oxygen to afford a trifluoromethylsulfinite **586**, via intermediate

585, was also investigated as a plausible route **(Scheme 1.88)**.[118] As organosulfinites undergo isomerisation to sulfones via heterolytic ion-pair recombination, it would be expected that isomerisation would readily occur for a trifluoromethylsulfinite and a phenolate **586**.[119] However, anionic thia-Fries rearrangement of the deuterium labelled **588** afforded exclusively **589**, with no evidence for isomerisation effectively ruling out the possibility of a sulfinite-based mechanism.

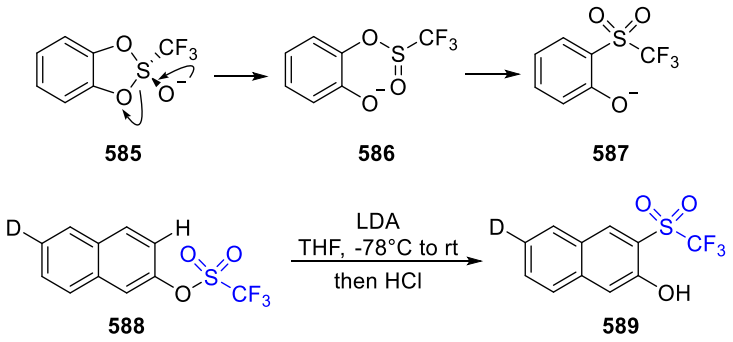

Scheme 1.88: Evidence disconfirming the likelihood of a sulfinite-based mechanism for the anionic thia-Fries rearrangement

Notably, while both the elimination and rearrangement processes nominally produce diisopropylamine (DIPA) from the reaction between the aryl triflate and LDA, the concentration of free base can have a significant impact on the course of the reaction outcome due to the strong complexation of the DIPA to the lithium cation in the rearranged product as well as its consumption by the aryne to produce ArN(*i*Pr)$_2$. Interestingly, carrying out the reaction of **588** in the presence of DIPA-free LDA affords the rearrangement product **589** in 30% yield and the aryne-derived amine **590** in 44% yield **(Scheme 1.89)**.[118] Repeating the reaction in the presence of 1,3-diphenylisobenzylfuran (DPIBF), an aryne trapping reagent, affords the naphthyne-DPIBF cycloadduct **591** in 99% yield with no thia-Fries rearrangement product **589** observed as a result of DPIBF bypassing DIPA consumption which leads to a rise in DIPA concentration **(Scheme 1.89)**. Therefore, the presence of a metalated compound, required for aryne generation, is favoured when the lithium cation is stabilised by the amine. The amine, in this instance DIPA, can be formed through either the deprotonation process or by being employed in excess. This finding, that DIPA catalyses aryne formation, is in agreement with Huisgen and Sauer's earlier work on the kinetics of aryne formation from Ar–X which highlighted that HNR$_2$ catalyses *ortho* metalation efficiently.[120]

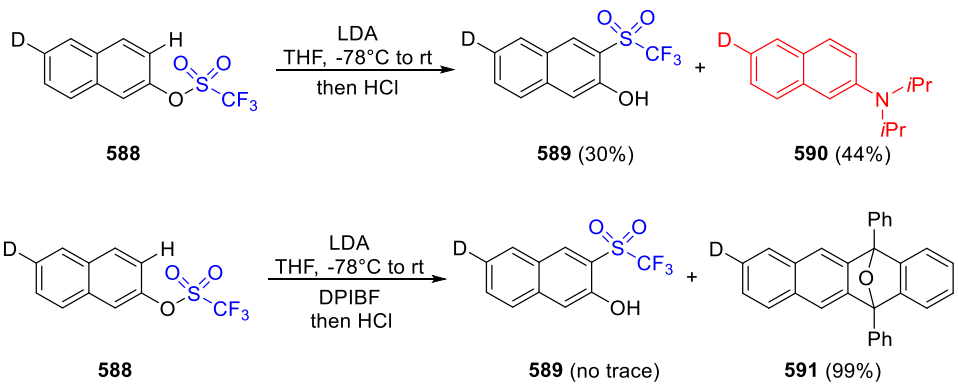

Scheme 1.89: Effect of concentration of free DIPA on anionic thia-Fries rearrangement and aryne generation

As a result of these findings two disparate mechanistic pathways are operational for the reaction of aryl triflates with LDA, namely an anionic pathway leading to anionic thia-Fries rearrangement and a DIPA-catalysed metalation pathway leading to aryne generation **(Scheme 1.90)**.[118] In the first instance, the anion **593** which can adopt two conformations of similar energies, plays a key role in the sulfonyl group migration. For unsubstituted aryl triflates (X = H) the cisoid conformation that is required for rearrangement is slightly higher in energy (+ 0.4 kcal mol^{-1}) than its transoid counterpart, however this can be overcome through the incorporation of electron withdrawing moieties *ortho* (and *para*) to the triflate group which inhibits competing metalation. In contrast, *meta* substituents actively destabilise the aryl anion **593** which favours elimination to **596** via **595**, while the employment of excess DIPA further facilitates elimination to generate the aryne **596**, with a concomitant decrease in the thia-Fries rearrangement product **594**.

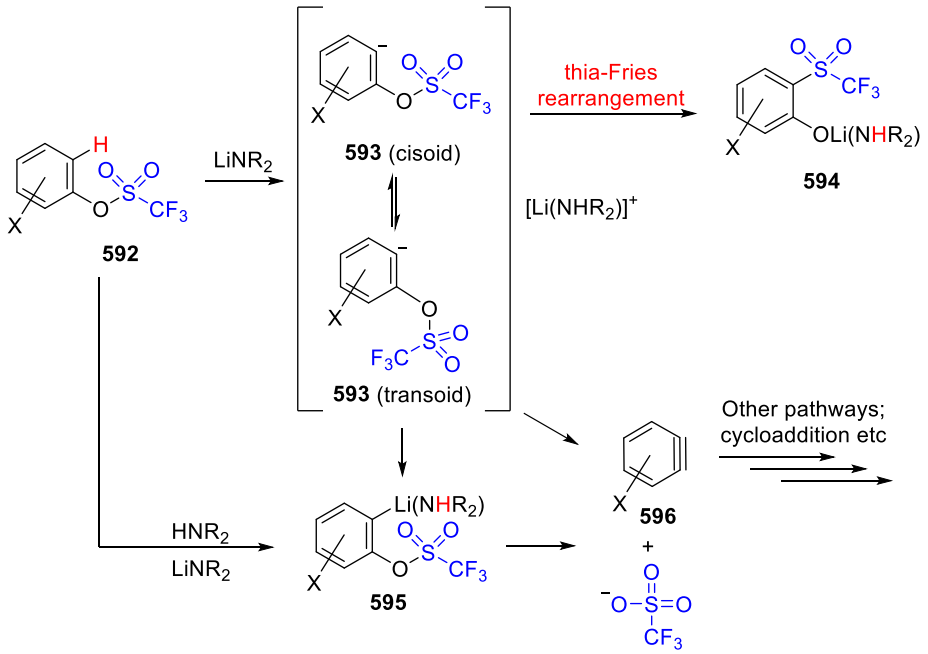

Scheme 1.90: Proposed mechanistic pathways for the reaction of aryl triflates with LDA; anionic thia-Fries rearrangement and aryne generation

In light of the clear evidence that metalation favours aryne generation the authors postulated that the use of more weakly coordinating metal cations, such as the larger potassium cation, would instead favour rearrangement. As such, by using potassium hexamethyldisilazane (KHMDS) as base in place of LDA, the aryl tosylates **597–600** which had previously exclusively afforded aryne-based products with LDA (as well as LiHMDS) afforded the thia-Fries rearrangement products **603–606** albeit in low to moderate yields, highlighting the key role that the metal cation plays in distinguishing between the two pathways **(Scheme 1.91)**.[118] In certain instances, the non-ionic base phosphazene **607**,[121] proved suitable in inducing thia-Fries rearrangement however stringently dry conditions are required or competing side reactions can occur.

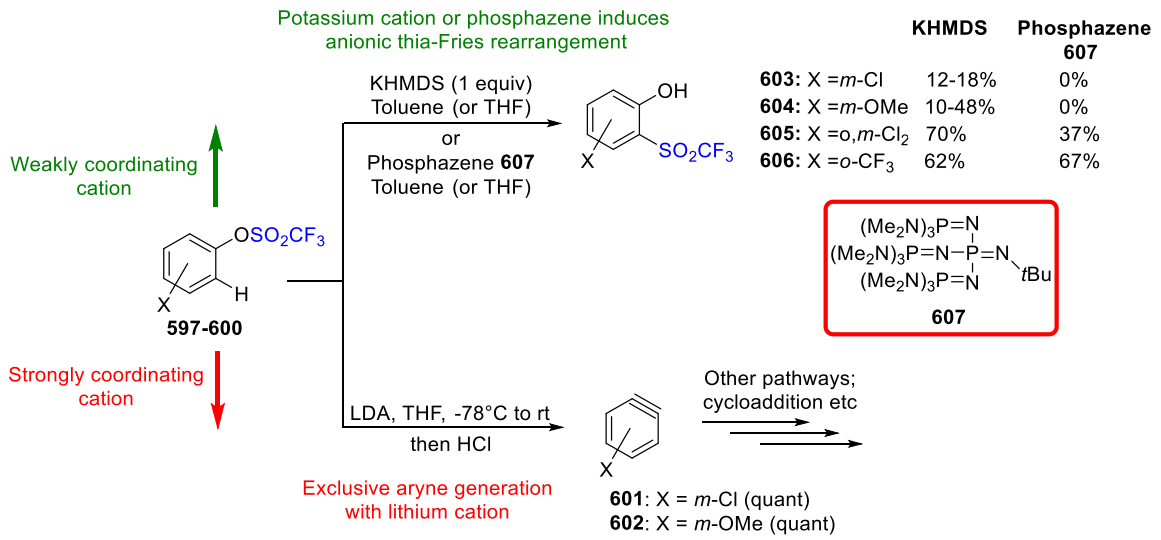

Scheme 1.91: Inhibition of aryne pathway via use of less coordinating metal cations; anionic thia-Fries rearrangement in the presence of KHMDS and phosphazene **607**

Notably, Lloyd-Jones and co-workers have successfully utilised the anionic-thia Fries rearrangement in the development of sulfone containing BINOL and BINAPHOS ligands for use in catalytic enantioselective indium-mediated allylations[122] and palladium-catalysed hydrophosphorylations.[123]

The first example of the application of the anionic thia-Fries rearrangement in heteroaromatic compounds was reported by Shibata and co-workers in 2012.[124] Using LDA as base a series of rearranged nitrogen containing heterocycles including oxindole **608**, pyrazolone **609**, quinoline **610** and pyridine triflones **611** was synthesised in moderate to good yields, with all products existing as the enol-tautomer rather than the amido form as confirmed by NMR studies **(Scheme 1.92)**. This transformation proceeds in higher yields than those in the pioneering work of Lloyd-Jones for the rearrangement of phenyl and naphthyl triflates.[117]

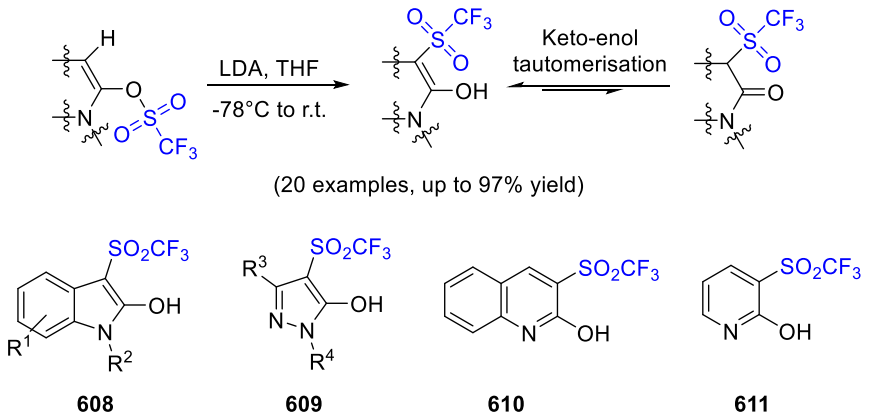

Scheme 1.92: Regioselective synthesis of heteroaryl triflones via LDA-mediated anionic thia-Fries rearrangement

In their studies on the reactivity of 3-triflyloxybenzyne **616**, the Hosoya group observed that in the absence of an arynophile, **616** reacted with the solvent rather than dimerizing **(Scheme 1.93)**.[125] Thus

the reaction in THF afforded the chlorobutoxy triflone **619**. The reaction proceeds by regioselective nucleophilic addition of THF to the benzyne **616** to afford the zwitterionic intermediate **617**, which subsequently undergoes anionic thia-Fries rearrangement to give **618**. Ring opening of the oxonium ion via addition of chloride from the Grignard reagent affords the rearranged triflone **619** upon protonation of the phenoxide anion **(Scheme 1.93).** The methodology was amenable to variation of the nucleophile; rearranged zwitterionic aryl triflones **613** and **614** were generated through regioselective nucleophilic addition of PPh_3 and Ph_2S to 3-triflyloxybenzyne **616**, while Bn_2S afforded the non-ionic triflone **615**, following debenzylation.

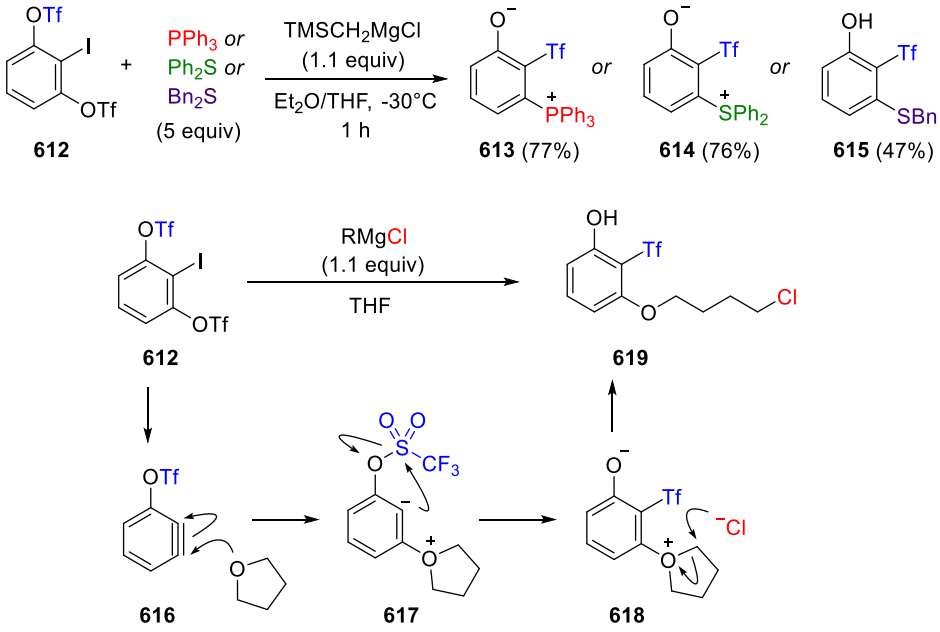

Scheme 1.93: Generation of aryl triflones via thia-Fries rearrangement

To broaden the applicability of 3-triflylbenzyne, the group further explored the reactivity in Diels–Alder cycloadditions of 3-triflyloxyarynes bearing an additional functionalisable group, such as a halide.[126] However, their initial attempt to generate the cycloadduct **621** from the triflate **620** and furan did not proceed efficiently using the previously optimised conditions, with a similar amount of the triflone **622** being generated via competing anionic thia-Fries rearrangement **(Table 1.1, Entry 1)**. The authors, therefore, screened for conditions to try to inhibit the thia-Fries rearrangement pathway. A significant improvement was attained by utilising non-polar solvents such as hexane and toluene, with further increases in yield and selectivity observed by increasing the amount of activator and decreasing the reaction temperature (**Table 1.1, Entries 6** and **7**). While not fully understood, it is likely that the non-polar solvents destabilise the anionic intermediate required for thia-Fries rearrangement, while enhancing the Mg–C bond formation which facilitates the elimination to the aryne.

Table 1.1: Influence of solvent on inhibition of thia-Fries rearrangement

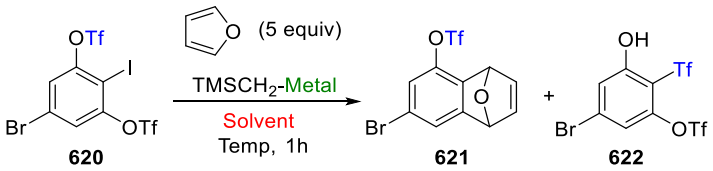

Entry	$TMSCH_2$-Metal (Equiv)	Solvent	Temp (°C)	Yield 621 (%)	Yield 622 (%)	621:622
1	$TMSCH_2MgCl$ (1.5)	Et_2O	-30	44	44	-
2	$TMSCH_2Li$ (1.5)	Et_2O	-30	32	24	57:43
3	$TMSCH_2MgCl.LiCl$ (1.5)	Et_2O	-30	25	19	57:43
4	$TMSCH_2MgCl.LiCl$ (1.5)	Toluene	-30	54	4	93:7
5	$TMSCH_2MgCl.LiCl$ (1.5)	*n*-hexane	-30	67	7	91:9
6	$TMSCH_2MgCl.LiCl$ (2.4)	Toluene	-50	70	4	95:5
7	$TMSCH_2MgCl.LiCl$ (2.4)	*n*-hexane	-30	83	4	95:5

In a subsequent publication the Hosoya group reported the isolation of the thia-Fries rearrangement by-product **626** in significant amounts (up to 32%) when using the 5,6-thienobenzyne precursor **624** in cycloaddition reactions **(Scheme 1.94)**.[127] It is likely that this side reaction is facilitated by the strongly electron-withdrawing trifluoromethyl group, which contributes by stabilising the anionic intermediate generated via the iodine-magnesium exchange reaction. Interestingly, the analogous cycloadditions of 6,7-thienobenzyne precursors under the same conditions proceed with significantly greater selectivity, with no evidence for thia-Fries rearrangement observed.

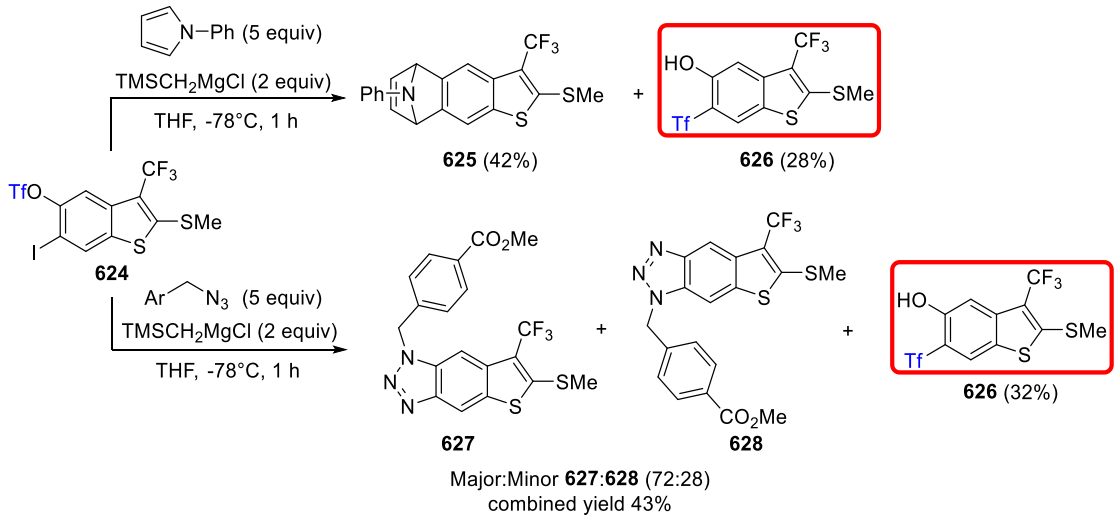

Scheme 1.94: [4+2] cycloadditions of 5,6-thienobenzyne precursors; competing anionic thia-Fries rearrangement of the phenylene ring

In 2013, Greaney and co-workers reported a tandem anionic thia-Fries rearrangement-cyclisation of 2-(trimethylsilyl)phenyl trifluoromethanesulfonate benzyne precursors **629** to form phenoxathiine-dioxide derivatives **630** in moderate yields as single regioisomers **(Scheme 1.95)**.[128] The phenoxathiine derivatives were only afforded when halogen substituents were present ortho to the triflate moiety, a result which is in line with Lloyd-Jones' earlier work that demonstrated that electron-withdrawing groups ortho to the sulfonate are crucial for anionic thia-Fries rearrangement.[117] However, in this

instance the halogenated triflates **629** can undergo both thia-Fries rearrangement and aryne generation in the same reaction and further react together in a tandem manner. This observation is in direct contrast with Lloyd-Jones' observation that the two processes are orthogonal to each other at low temperatures. Considering this, the following mechanism was postulated **(Scheme 1.95)**: C–Si bond cleavage is mediated by treatment with fluoride, which induces an anionic thia-Fries rearrangement of the resulting anion **631** to form the phenolate **632**. The aryne **633**, generated through the fluoride mediated elimination of the triflate and trimethylsilyl moieties, reacts with the phenolate **632** to generate the anionic intermediate **634**. Cyclisation of **634** via nucleophilic addition of the phenyl anion onto the trifluoromethane sulfonate moiety affords the phenoxathiine-dioxide product **630**. The dual mode of the triflate starting materials **629** with respect to anionic thia-Fries rearrangement and aryne formation in the one pot was supported via crossover experiments.

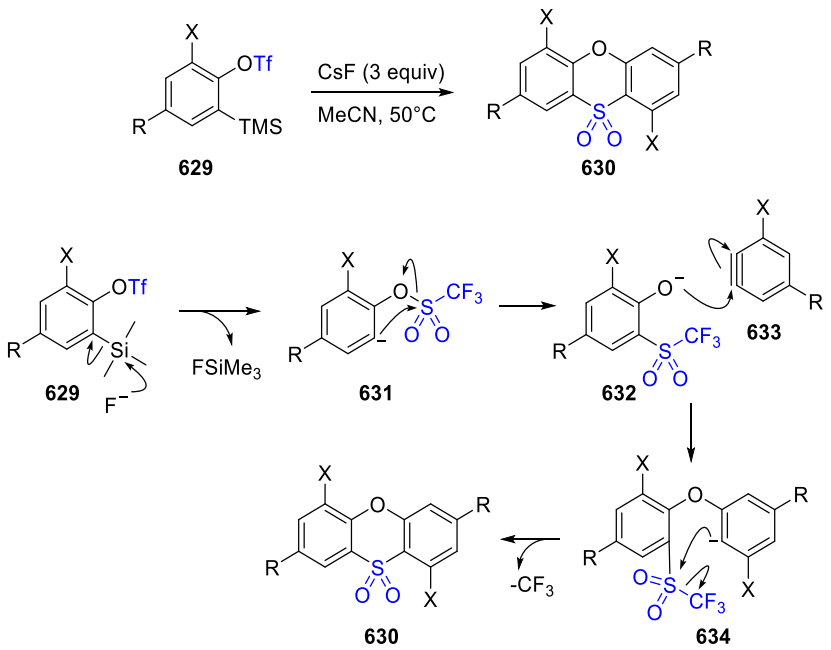

Scheme 1.95: Formation of phenoxathiine-dioxide derivatives via tandem anionic thia-Fries rearrangement-cyclisation of 2-(trimethylsilyl)phenyl trifluoromethanesulfonate benzyne precursors

1.5.2.2. Remote anionic thia-Fries rearrangement

The NaH-mediated remote anionic 1,5-thia-Fries rearrangement, which constitutes a formal 1,5-sulfonyl migration from oxygen to carbon, allowing the regioselective synthesis of 2-(2-hydroxyphenyl)-3-indole triflones and 3-sulfonyl indoles **636** was described by the Shibata group **(Scheme 1.96)**.[129] Notably, this first example of a remote anionic thia-Fries rearrangement tolerated both electron-withdrawing and electron-donating groups at various positions on the phenyl ring, while also tolerating the presence of bromo- and chloro-substituents due to the reaction not requiring strong alkyllithium bases. Strong base is not required for this reaction because, unlike conventional anionic Fries rearrangement, which is initiated by a carbanion, this method is initiated by a nitranion.

No migration was observed with either *N*-methylindole **639** or 3-methylindole **640** when subjected to the optimised conditions, while competition experiments demonstrated the likelihood of an intramolecular 1,5-sulfonyl migration. Therefore, the following mechanism was proposed **(Scheme 1.96)**. Deprotonation of **635** by NaH affords the nitrogen anion **637**, which undergoes intramolecular

1,5-sulfonyl migration to give intermediate **638,** which following protonation and tautomerisation affords the rearranged indole **636.**

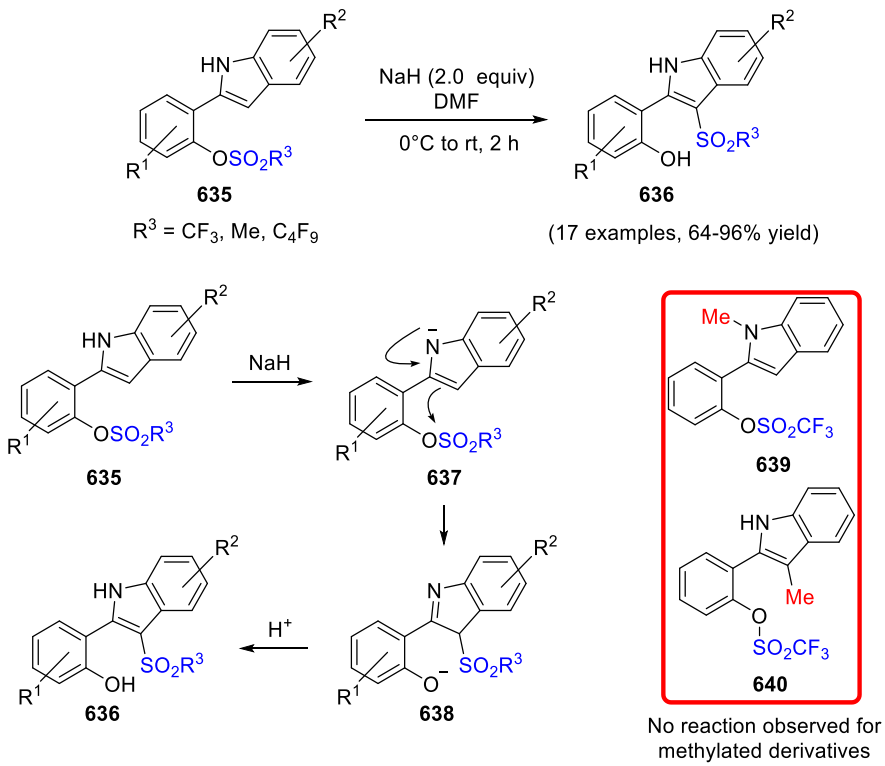

Scheme 1.96: Remote anionic Fries rearrangement of sulfonates: Regioselective synthesis of indole triflones

The Shibata group also demonstrated the synthesis of a series of vinyl triflones **642** in a stereoselective manner via remote anionic thia-Fries rearrangement from a series of *gem*-dibromovinyl substrates **(Scheme 1.97)**.[130] Employing two equivalents of *n*-BuLi, the requisite substrates **641** afforded exclusively *E*-vinyl triflones **642** in moderate to good yields, via 1,5-triflyl migration, with both electron-donating and electron-withdrawing substituents on the aryl ring well tolerated. The triflyl moiety was crucial to the transformation; no migration was observed for the analogous methanesulfonates. Interestingly, the indole derivative **643** also readily underwent rearrangement, and is the first example of an anionic 1,6-migration. The methodology could also be utilised in a tandem reaction with methyl formate as an electrophilic partner which led to cyclisation after the rearrangement, affording heteroaryl triflones **646** in moderate yields.

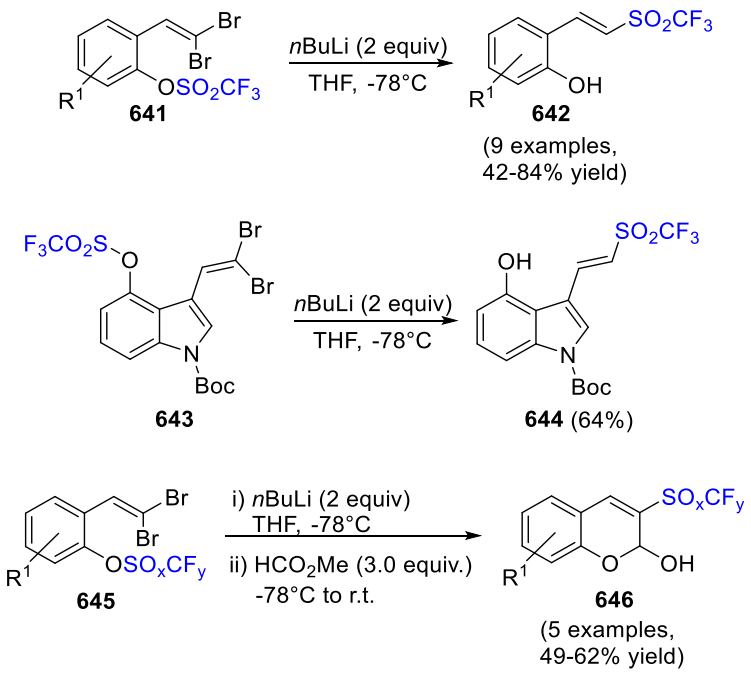

Scheme 1.97: 1,5- and 1,6-triflyl migration of *gem*-dibromovinyl compounds

Based on these results the authors postulated that lithium–bromine exchange of the substrate **641** and *n*-BuLi affords the anion **647 (Scheme 1.98)**, which undergoes remote anionic thia-Fries rearrangement, induced by the electron-withdrawing nature of the trifluoromethyl group, to afford the phenolate **648**. The presence of the electron-withdrawing triflyl moiety activates the remaining bromine in **648** to undergo lithium–bromine exchange with the second equivalent of *n*-BuLi to afford the intermediate **649** which rapidly isomerises to the more thermodynamically stable intermediate **650**. This isomerisation explains the stereoselective generation of the *E*-vinyl triflones **642** and the cyclised products **646**.

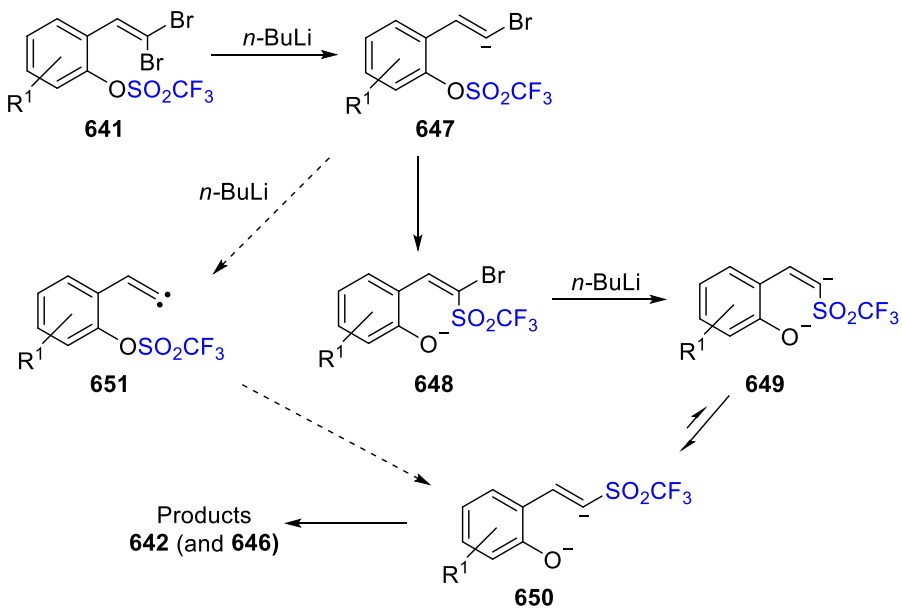

Scheme 1.98: Proposed mechanism for the 1,5-triflyl migration of *gem*-dibromovinyl compounds

1.5.2.3. Anionic thia-Fries rearrangement of organometallic complexes

In 2006, as part of their efforts to generate (η^6-aryne)chromiumtricarbonyl complexes, the Butenschön group studied the reactions of chromiumtricarbonyl complexes of arene triflates. They were surprised to find that none of the expected product **652** was observed under standard basic conditions. Instead, they uncovered the first examples of anionic thia-Fries rearrangement of organometallic substrates to afford a series of ortho-(trifluoromethylsulfonyl)phenol chromium complexes **653** in high yields **(Scheme 1.99)**.[131] Notably, the reaction tolerates both electron-rich and ortho-substituted substrates **651** that would normally be expected to favour elimination of the triflate. The preference for the thia-Fries rearrangement is likely attributable to the electron-withdrawing effect of the chromiumtricarbonyl moiety, which is better satisfied by the formation of the rearranged phenolate. The methodology was subsequently applied to the structurally complex estrone **654** **(Scheme 1.99)**. Under standard basic conditions regioselective thia-Fries rearrangement occurred to afford the phenolic estrone complex **655** in 77% yield. Iodine-mediated decomplexation afforded the desired steroid **656** in 97% yield.

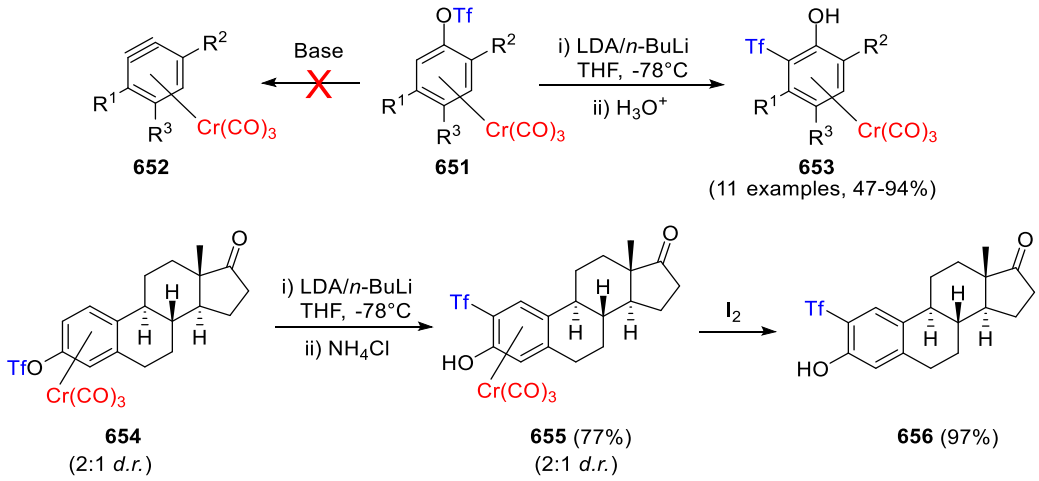

Scheme 1.99: First example of an anionic thia-Fries rearrangement at organometallics

In an attempt to compensate for the highly electron-withdrawing tricarbonylchromium moiety, which was believed to be the main factor inhibiting aryne generation, the authors hypothesised that the introduction of further strongly electron-donating groups may generate more electron-rich triflates more susceptible to elimination.[132] Therefore, the triflate **657**, bearing two methoxy substituents, was prepared and subjected to basic conditions in the presence of 2,5-dimethylfuran as trapping reagent **(Scheme 1.100)**. The desired cycloadduct **658** was isolated in quantitative yield demonstrating the suitability of triflate **657** to undergo base-mediated triflate elimination. On the other hand, the analogous reaction of the tricarbonylchromium complex **659** instantaneously afforded the anionic-thia Fries rearrangement product **660** exclusively, and upon acylation the product **661** was isolated in quantitative yield. As part of the same investigation, two (triphenylphosphine)dicarbonylchromium complexes, **662** and **663** were investigated. Despite the fact that it has been shown that replacement of one carbonyl ligand by triphenylphosphine reverses the electron-withdrawing effect of the chromium moiety,[133] when **662** or **663** were treated with LDA in THF at –78°C in the presence of trapping reagents, the anionic thia-Fries rearrangement was again the exclusive pathway, leading to **664** and **665** in almost quantitative yields **(Scheme 1.100)**.[132] As a result it can be concluded that electronics do not exert a significant effect on the outcome of the reaction, with organochromium complexes favouring anionic thia-Fries rearrangement.

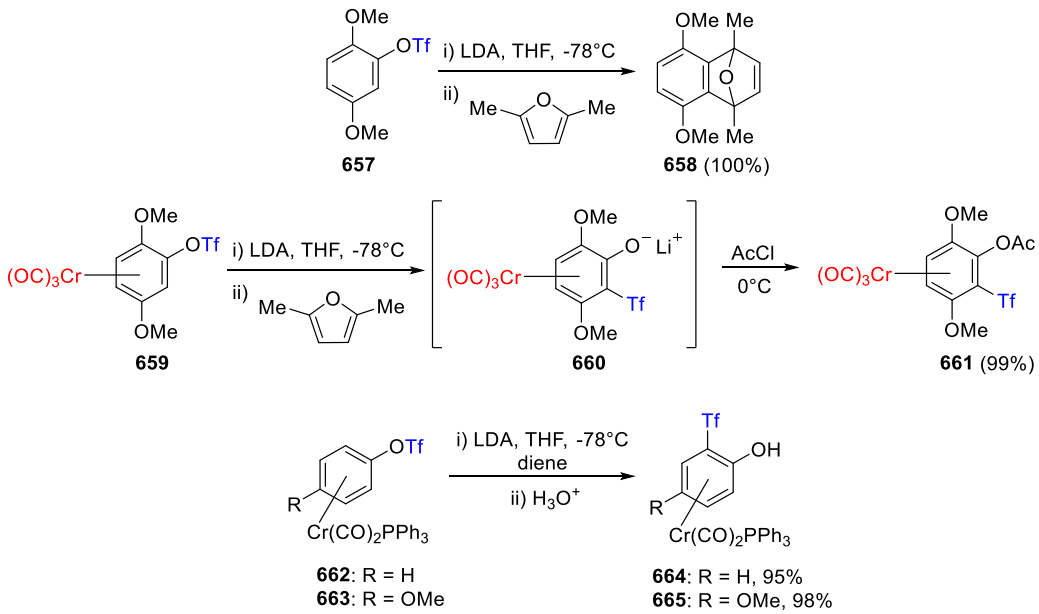

Scheme 1.100: Attempted compensation of the electron withdrawing effect of the tricarbonylchromium complex; no inhibition of the anionic thia-Fries rearrangement observed

In a further attempt to favour aryne formation, the Butenschön group attempted to use ferrocene derivatives in lieu of chromium complexes, hoping that the more electron-rich ferrocene derivatives might circumvent the problems encountered when using the highly electron-withdrawing tricarbonylchromium group. However, in spite of the more electron-rich substrate, ferrocenyl triflate **666** underwent a highly efficient anionic thia-Fries rearrangement instead of triflate elimination **(Scheme 1.101)**.[134] Lowering the temperature of the reaction from –78°C to as low as –117°C did not lead to any formation of ferrocyne product. This was the first example of an anionic thia-Fries rearrangement in a five-membered ring. The remarkable efficiency of the transformation was further demonstrated by the reaction of the more electron-poor ferrocene triflate **670**, which also readily underwent rearrangement in quantitative yields **(Scheme 1.101)**.

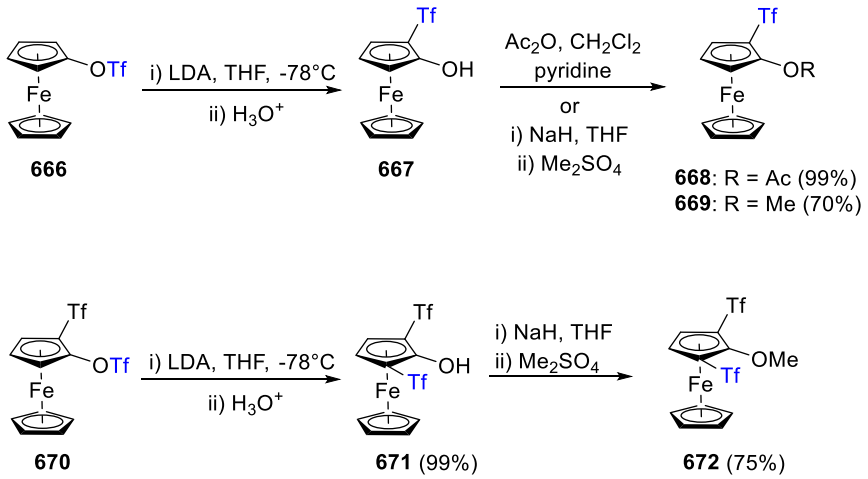

Scheme 1.101: Attempted use of electron-rich ferrocenyl triflate derivatives to achieve ferrocyne formation; first example of anionic thia-Fries rearrangement in a five-membered ring

Interestingly, when 1,1′ -ferrocenediyl ditriflate **673** was treated with 2.2 equivalents of LDA at –78°C a double anionic thia-Fries rearrangement occurred giving **676** in 85% yield.[134] Although this reaction could yield two diasteromeric rearrangement products, *meso*-**676** and *rac*-**677**, only the meso diastereomer was observed, i.e. the reaction proceeds with complete diastereoselectivity **(Scheme 1.102)**. To further probe this exceptional diastereoselectivity the authors attempted to obtain the single anionic thia-Fries rearrangement product **675** by instead using 1 equivalent of LDA**.** However, the reaction gave an almost equimolar mixture of the starting material **673** and the double rearrangement product **674** after acylation, highlighting that the rate of the second anionic thia-Fries rearrangement is significantly faster than that of the first **(Scheme 1.102)**.

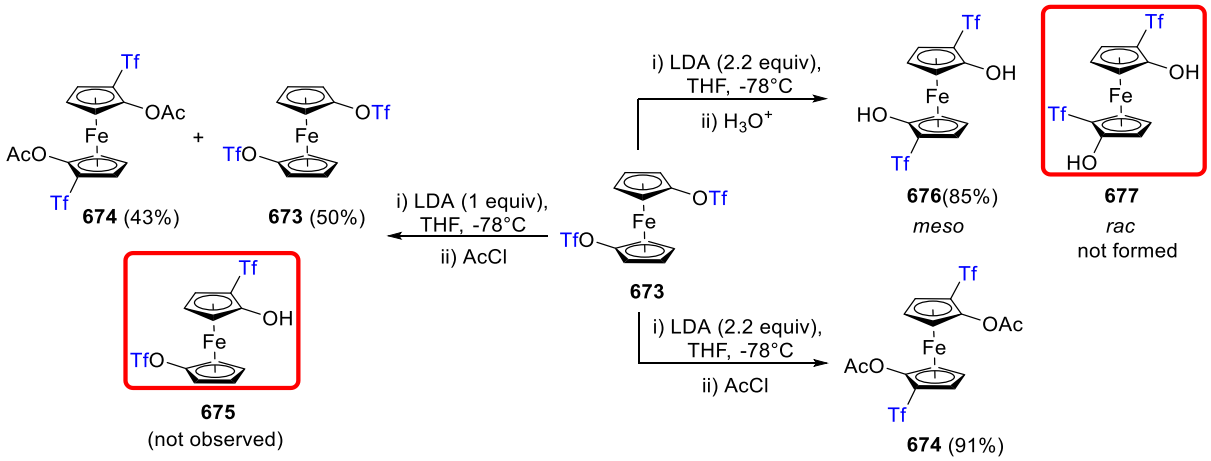

Scheme 1.102: Double anionic thia-Fries rearrangement of 1,1′-ferrocenediyl ditriflate **673**

In order to probe the effect of *ortho*-lithiation on the reaction outcome the authors prepared 2-(trimethylsilyl)ferrocenyl triflate **678** for comparison. Upon treatment with TBAF in acetonitrile at 25°C, exclusive anionic thia-Fries rearrangement occurred immediately to afford **679** in 84% yield **(Scheme 1.103)**.[135] Metalation of the *ortho*-position was considered as an alternative to anion formation, hence the tributylstannyl compound **680** was treated with *n*-BuLi to induce metal exchange to the respective lithio compound. However, exclusive anionic thia-Fries rearrangement was again observed affording **679** in quantitative yield **(Scheme 1.103)**. This was described as the first example of an anionic-thia Fries rearrangement induced by *ortho* metalation.

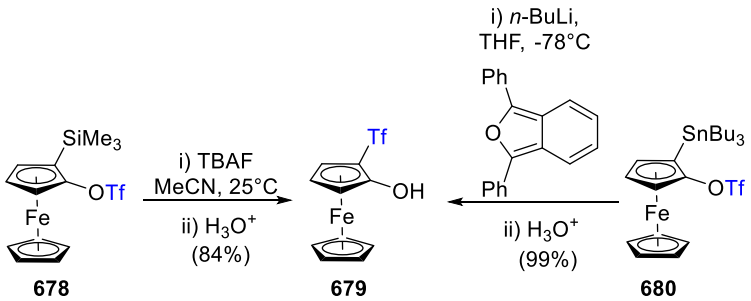

Scheme 1.103: First example of anionic thia-Fries rearrangement induced by *ortho* metalation

In light of the anionic thia-Fries rearrangement occurring for ferrocenyl triflates upon both *ortho* deprotonation as well as *ortho* metalation, the authors sought to determine how electron-rich the ferrocenyl triflate can be tailored to still allow the reaction. Even the more electron-rich methoxy

derivative **681** also afforded exclusively the anionic-thia Fries rearrangement product **683** in quantitative yield **(Scheme 1.104)**.[135] Therefore, it is clear that excess electron density in the ferrocene system does not prevent rearrangement. Sterics were hypothesised to be a possible factor that may favour ferrocyne formation via elimination, however, treatment of the trimethyl derivative **684** under standard basic conditions in the presence of anthracene as cycloaddition trapping reagent afforded exclusively the anionic thia-Fries rearrangement product **685 (Scheme 1.104)**. Notably, while triflate elimination is the most prominent method for the generation of arynes, there is little correlation between aromatic systems and their analogous organometallic derivatives. As a result, the procurement of organometallic arynes remains an ongoing research pursuit.

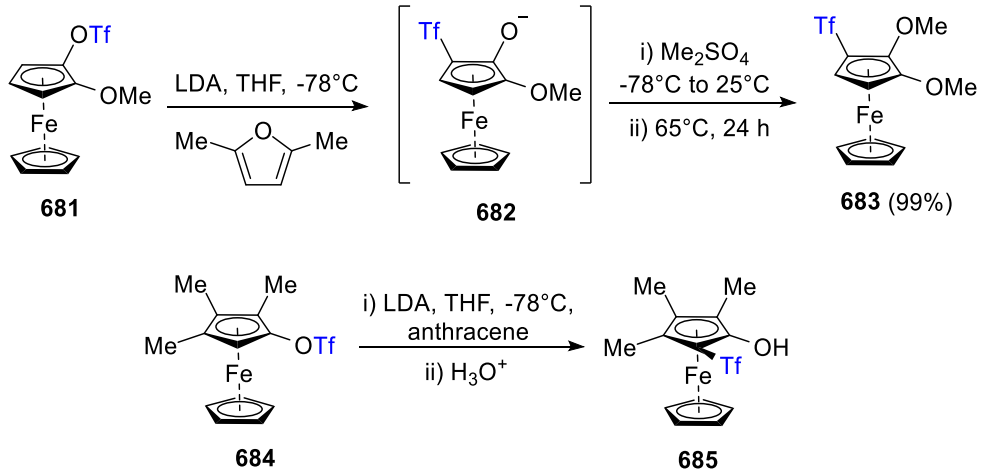

Scheme 1.104: Exclusive anionic thia-Fries rearrangement of ferrocenyl triflates despite incorporation of electron-donating groups

Prior to Lloyd-Jones' discovery of the anionic thia-Fries rearrangement in 2003, the Minami group observed an oxygen to carbon 1,3-sulfonyl migration of both phosphonates and sulfonates in cyclohexadiene systems **(Scheme 1.105)**.[136] Notably, iron coordination to the 1,3-diene with either a phosphate or sulfonate moiety allows ortho deprotonation of the C-3 position, which facilitates the overall 1,3-sulfonyl migration. The rearrangement proceeds rapidly and efficiently under basic conditions with **689** and **690** afforded in high yields after five minutes. However, when the migrating group contained acidic protons, e.g. a methanesulfonyl group, no migration was observed, and the iron dienol complex **691** was favoured instead. Crossover experiments for the phosphonate derivatives determined that the migration is likely an intramolecular process.

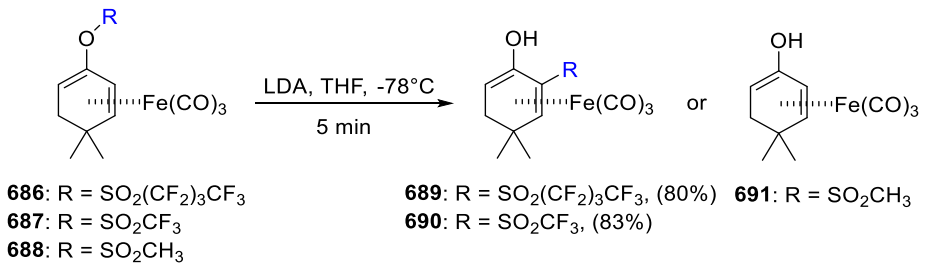

Scheme 1.105: O- to C-1,3-sulfonyl migration in iron-complexed non-aromatic cyclohexadienes

1.5.2.4. Non-anionic thia-Fries rearrangement

While the last two decades have seen considerable attention devoted to the development of the understanding of the anionic thia-Fries rearrangement, significantly less attention has been afforded to thia-Fries rearrangements via metal catalysis, microwave or photoirradiation techniques.

Moghaddam and Das almost simultaneously reported the high yielding thia-Fries rearrangement of aryl sulfonates **692** in the presence of anhydrous aluminium trichloride under microwave conditions **(Scheme 1.106, A)**.[137-138] Moghaddam's method involved using an $AlCl_3$–$ZnCl_2$ supported on silica gel in conjunction with microwave irradiation with similar efficiencies and yields. Das also demonstrated that the methodology could readily be used for the analogous reaction of aryl sulfonanilides with similar efficiencies and yields obtained. When Moghaddam *et al*. later attempted to extend their methodology to incorporate aryl benzylsulfonates, a pseudo-thia-Fries rearrangement was instead observed, with the *ortho*- and *para*-benzylated phenols **694**, and the dibenzylated phenols **695** isolated.[139] Unlike the photochemical thia-Fries rearrangement, which is known to proceed via a radical mechanism, the authors postulated that the reaction occurs via initial heterolytic cleavage of the O–S bond to generate a phenolate and a benzylsulfonyl cation which decomposes by elimination of SO_2 to afford the active benzyl cation **(Scheme 1.106)**. The cationic mechanism was supported by the capture of the hypothesised benzyl cation by the cation scavenger mesitylene to afford **702**. Furthermore, no evidence for the presence of the benzyl radical coupling product diphenylethane **703** was observed, also supporting the cationic mechanism. Benson *et al*. subsequently reported the $AlCl_3$-mediated thermal thia-Fries type rearrangement of aryl sulfamates **696** to generate aryl sulfonamides **697** and **698** in moderate to high yields **(Scheme 1.106, B)**.[140]

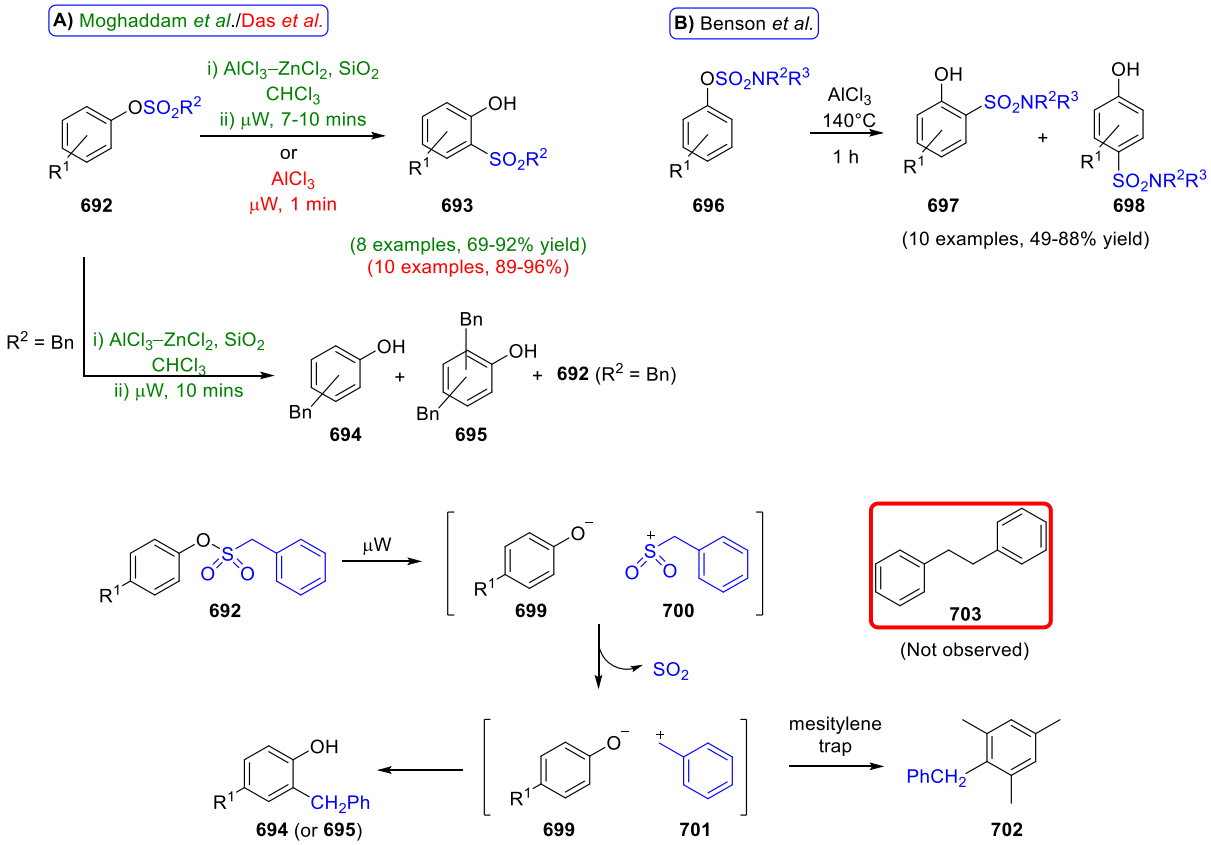

Scheme 1.106: Non-anionic thia-Fries rearrangement

Sharghi *et al*. reported the use of $Al_2O_3/MeSO_3H$,[141] and subsequently graphite/$MeSO_3H$[142] mixtures as novel reagents for a solvent-free thermal thia-Fries rearrangement of aryl tosylates **704** to afford hydroxy aryl sulfones in high yields **(Scheme 1.107, A)**. An intermolecular ionic mechanism was presented by the authors, with the presence of a sulfonyl cation intermediate, confirmed via trapping of the cation with electron-rich *m*-xylene. Furthermore electron-poor *meta*- and *para*-nitro derivatives **704** failed to undergo rearrangement providing further evidence for the proposed mechanism.

Crevatín *et al*. reported the photo-thia-Fries rearrangement for a series of 9*H*-carbazol-2-yl-sulfonates **707** to afford the respective alkyl- and arysulfones **708** and **709** **(Scheme 1.107, B)**.[143] Under photoirradiation, regardless of reaction solvent utilised (MeCN, MeOH, benzene, cyclohexane), the *ortho*-rearranged products **708** and **709** were obtained in a molar ratio of approx. 2:1, with **708** always being the favoured isomer. Semi-empirical and *ab initio* optimisation of the 2-hydroxy-9*H*-carbazole radical were used to rationalise the regioselectivity of the reaction, with a slightly higher charge density observed at C(1) when compared to C(3). Furthermore, hydrogen bonding with the carbazole N–H may assist with the migration to C(1); this is not possible for rearrangement to C(3) due to geometry.

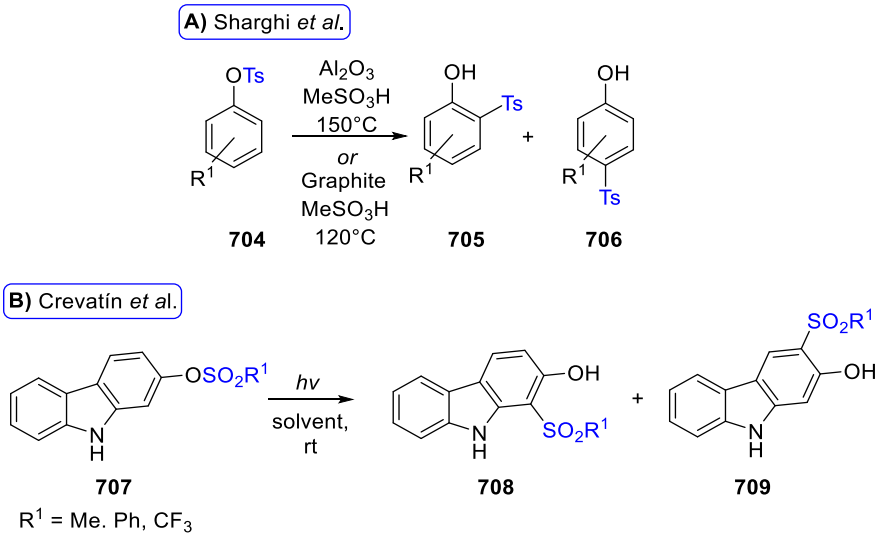

Scheme 1.107: Non-anionic thia-Fries rearrangement

1.6. Oxygen to Oxygen Sulfonyl Migration

Cavazza and Pietra reported the first examples of fluxional sulfonates, in which a formal thermal 1,4-oxygen to oxygen sulfonyl migration for tosyl and mesyl substituents was observed for troponoid **710** and colchicinoid **712** derivatives **(Scheme 1.108)**.[144] In all instances an equilibrium was observed. For example, when the tosylate of β-thujaplicine **710** was heated in DMF at 100°C a 1:1.09 mixture of **710** and 2-tosyloxy-6-isopropyltropone **711** was afforded after 2.5 hours. Isolation of pure **711**, followed by heating under the aforementioned conditions, again afforded a 1:0.9 mixture of **710:711** confirming the equilibrium process. A similar effect was observed for the colchicine **712**/isocolchicine **713** system, amongst other derivatives, in this case the equilibrium favoured the isomer bearing a double bond between C7a and C12a (**712:713** ca. 1:2.4) **(Scheme 1.108)**.

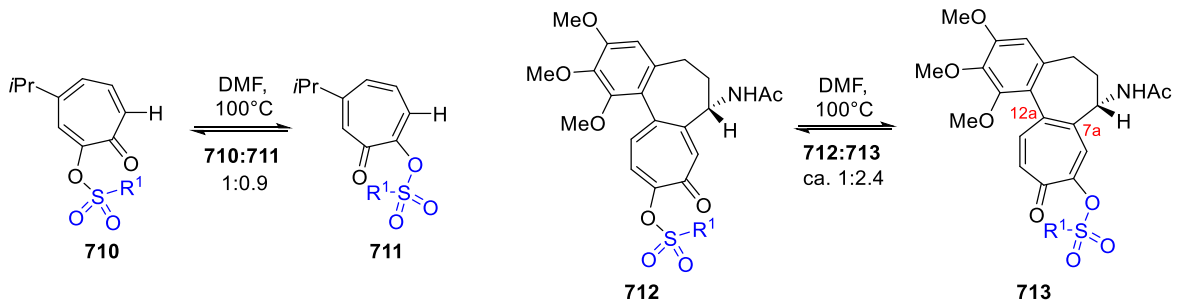

Scheme 1.108: Fluxional sulfonyl derivatives of troponoids and colchicinoids; observation of a formal 1,4-oxygen to oxygen sulfonyl migration

The mechanism can be rationalised via an intramolecular nucleophilic addition of the carbonyl oxygen atom to the electron-deficient sulfur atom of the sulfonyl moiety, generating a trigonal bipyramidal intermediate bearing negatively-charged oxygen atoms occupying the apical positions. Molecular mechanics calculations indicate that such an intermediate would have low strain, which is in contrast with the high strain that would be expected of a trigonal bipyramidal transition state formed via a concerted entering and leaving of the respective oxygen atoms. Also, the highly polarised character of the rate-determining transition state is borne out by the fact that a higher rate of reaction was observed in DMF than toluene.

In their efforts to access the aglaroxin C analogue **716**, of the rocaglate family of natural products, Zhang *et al*. hypothesised that the tosyl-enol rocaglate **714** could undergo base-mediated conjugate addition with benzamidine, followed by elimination of the tosyl moiety to give the enamine **715** which upon ring closure would afford the desired pyrimidinone product **716 (Scheme 1.109)**.[145] When the reaction was carried out using NaH as base, the isolated product was in fact the amidino-rocaglate **721**. The authors attributed this transformation to an intercepted retro-Nazarov reaction. Deprotonation of **714** affords the anionic intermediate **717** which undergoes an intramolecular 1,4-oxygen to oxygen tosyl migration to give the enolate **718**. Elimination of the tertiary tosylate generates the stabilised oxyallyl cation **719**. Nucleophilic addition of amidine and subsequent cyclisation affords the product **721**. Using this methodology, a series of amidino- and amino-rocaglates were synthesised (46 examples, up to 93% yield).

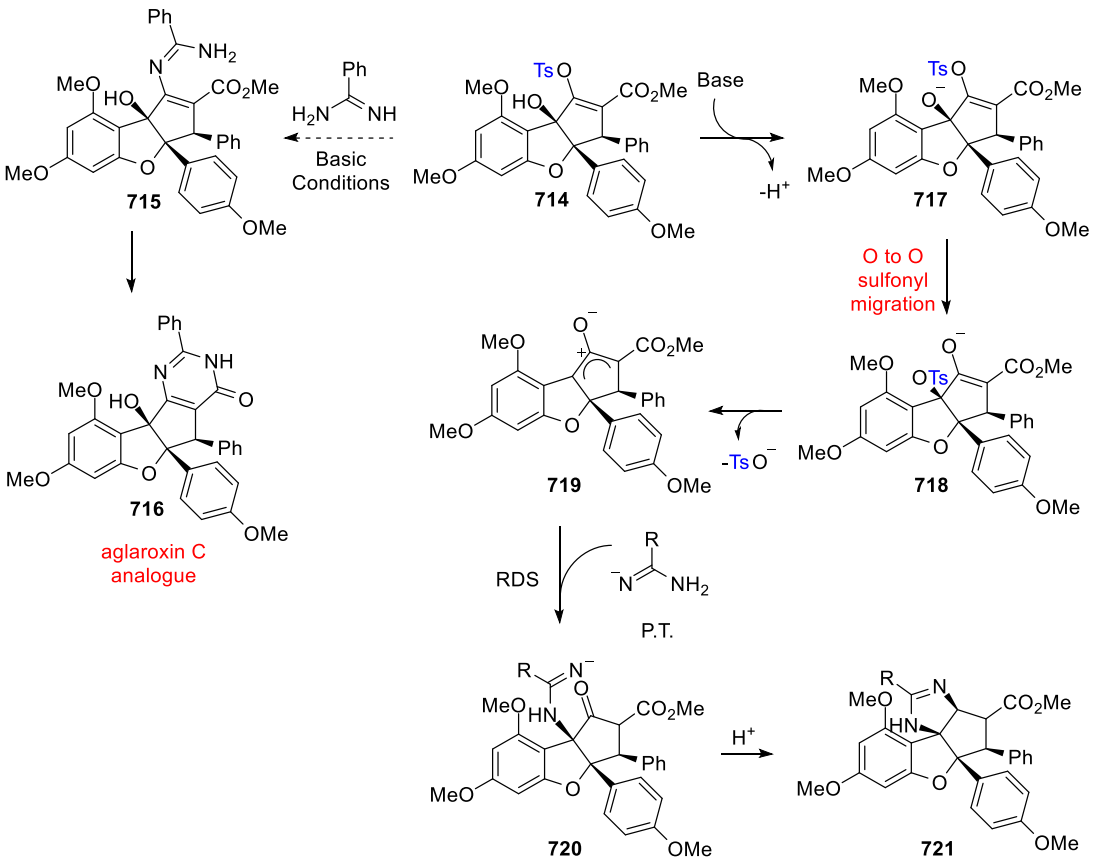

Scheme 1.109: Generation of amidino-rocaglate derivatives via an intercepted retro-Nazarov reaction; observation of a 1,4-oxygen to oxygen sulfonyl migration

1.7. Carbon to Carbon sulfonyl migration

1.7.1. *N*-Heterocyclic carbene-catalysed sulfonyl migration

Atienza *et al*. described the *N*-heterocyclic carbene (NHC) catalysed 1,2-sulfonyl migration of 1,1-bis(sulfonyl)ethylene derivatives **722** and their subsequent reactivity with 1,3-dipoles (predominantly nitrones **723**) to generate a series of highly functionalised isoxazolidine derivatives **724** as single diastereomers in good to excellent yields **(Scheme 1.110)**.[146] Mechanistic studies informed that the sulfonyl migration was an intermolecular process as supported by crossover experiments. Furthermore, the NHC catalyst **725** was not necessary for the [3+2]-dipolar cycloaddition to occur, however its presence was crucial for the isomerisation of the 1,1-bis(sulfonyl)ethylene derivative **722** to the rearranged *trans*-1,2-bis-alkene **731** as illustrated in **Scheme 1.110**. In addition, ^{13}C-labelling of **732** highlighted that the 1,2-sulfonyl migration occurs prior to the cycloaddition step as evidenced by isolation of a mixture of labelled products **734** and **735**. Notably, if only the ^{13}C-labelled vinyl sulfone isomer was present at the cycloaddition step isotopic labelling would only be observed at one position in the product.

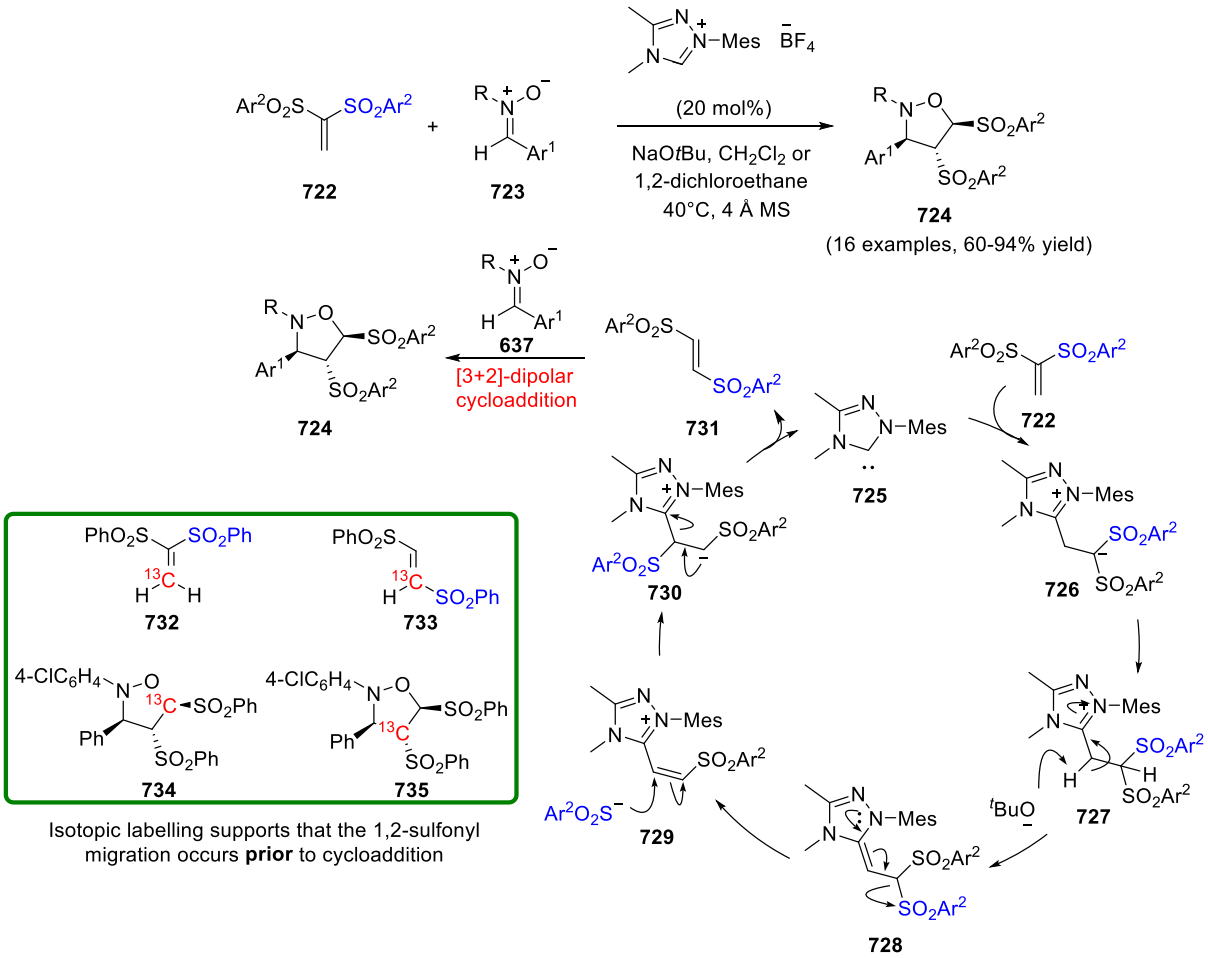

Scheme 1.110: *N*-heterocyclic carbene-catalysed 1,2-sulfonyl migration of vinyl sulfones

Yamada and co-workers described the *N*-heterocyclic-carbene-mediated cyclisation of sulfonylalkynols **736** with concomitant 1,2-sulfonyl migration to afford 5- and 6-membered oxacycles **737** in high yields **(Scheme 1.111)**.[147] While *N*-formylalkynamides cyclised smoothly under the same conditions, N-sulfonylalkynamide derivatives required the use of NHC **740** in conjunction with proton sponge as the base. The mechanism is believed to proceed via the allenyl sulfone intermediate **742** which is generated in situ on reaction of the sulfonylalkynol **741** with base. Applying this intermediate to the standard reaction conditions led to isolation of the desired product in high yield. Nucleophilic addition of the NHC to **742**, followed by a proton transfer affords the intermediate **743** which cyclises with accompanying tosylate extrusion to give **744**. This tosylate reacts with another equivalent of the allene intermediate **742** to give the intermediate **745**, which completes the formal 1,2-sulfonyl migration. A final cyclisation affords the desired vinyl sulfone **746**. That tosylate initiates the productive cycle was supported by carrying out the reaction in the presence of *p*-toluenesulfinate (2 mol%) in the absence of the NHC mediator. This experiment afforded the desired product **746** in 83% yield. The isolation of the disulfone **749** when the propargyl sulfone **747** was reacted under the standard conditions (in refluxing toluene) supports the formation of **745** as an intermediate in the reaction pathway. The group subsequently reported that the reaction can be carried out with either catalytic triphenylphosphine or DMAP in place of the *N*-heterocyclic carbene.[148]

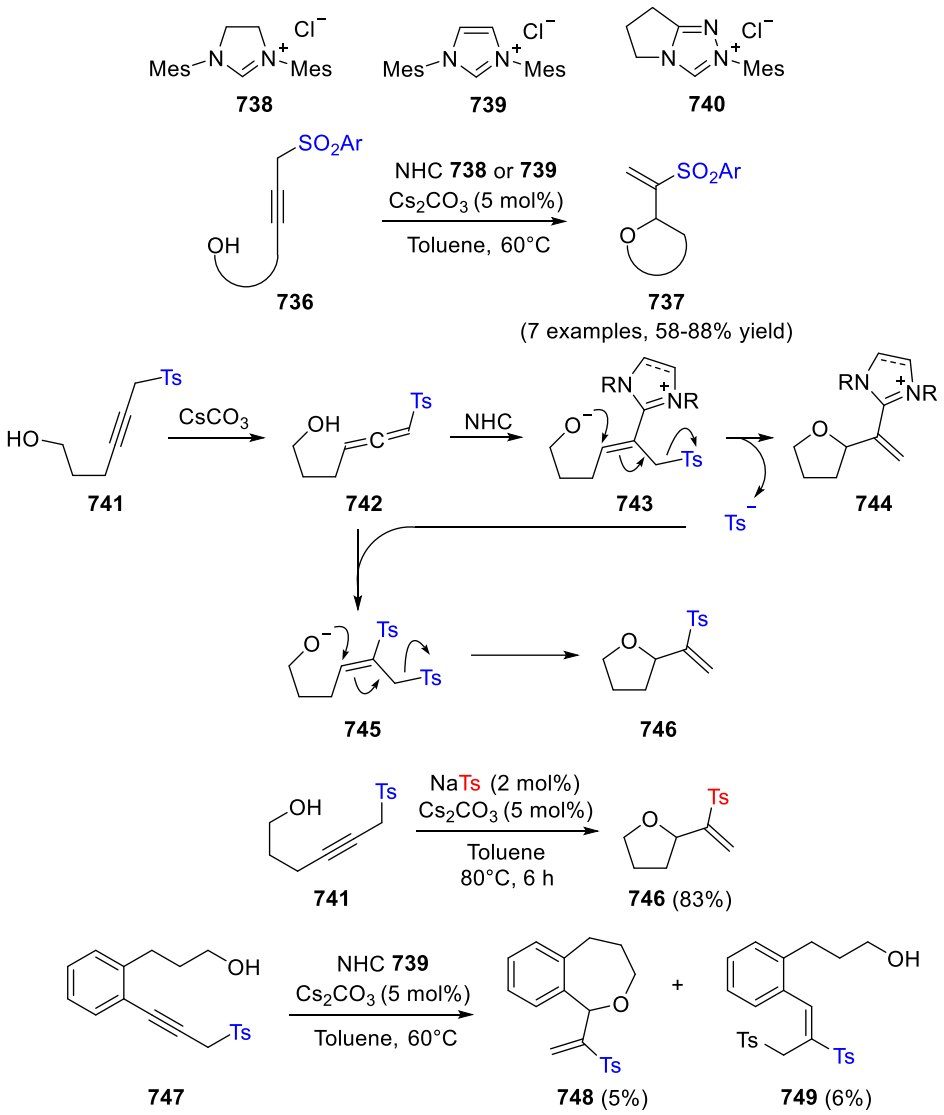

Scheme 1.111: NHC-mediated cyclisation of sulfonylalkynols forming oxacycles with accompanying 1,2-sulfonyl migration

1.7.2. Triphenylphosphine-catalysed sulfonyl migration

Lu *et al*. described the triphenylphosphine-catalysed 1,2-sulfonyl migration of electron-deficient allenes **751** in their reaction with active methylene compounds to give vinyl sulfones in moderate yields **(Scheme 1.112)**.[149] While mechanistic studies were not undertaken the authors postulated that the migration occurs via the in situ generation of the sulfinate anion as described in Scheme **112**. Upon its formation it is readily conceivable that the nucleophilic sulfinate could add to the allene **751** to form the vinyl anion **766**, which can deprotonate the active methylene compound **762** to form the allylic sulfone **767**. Subsequent addition of the anion **763** to **767** leads to elimination of the allylic sulfone, generating the desired rearranged product **768**.

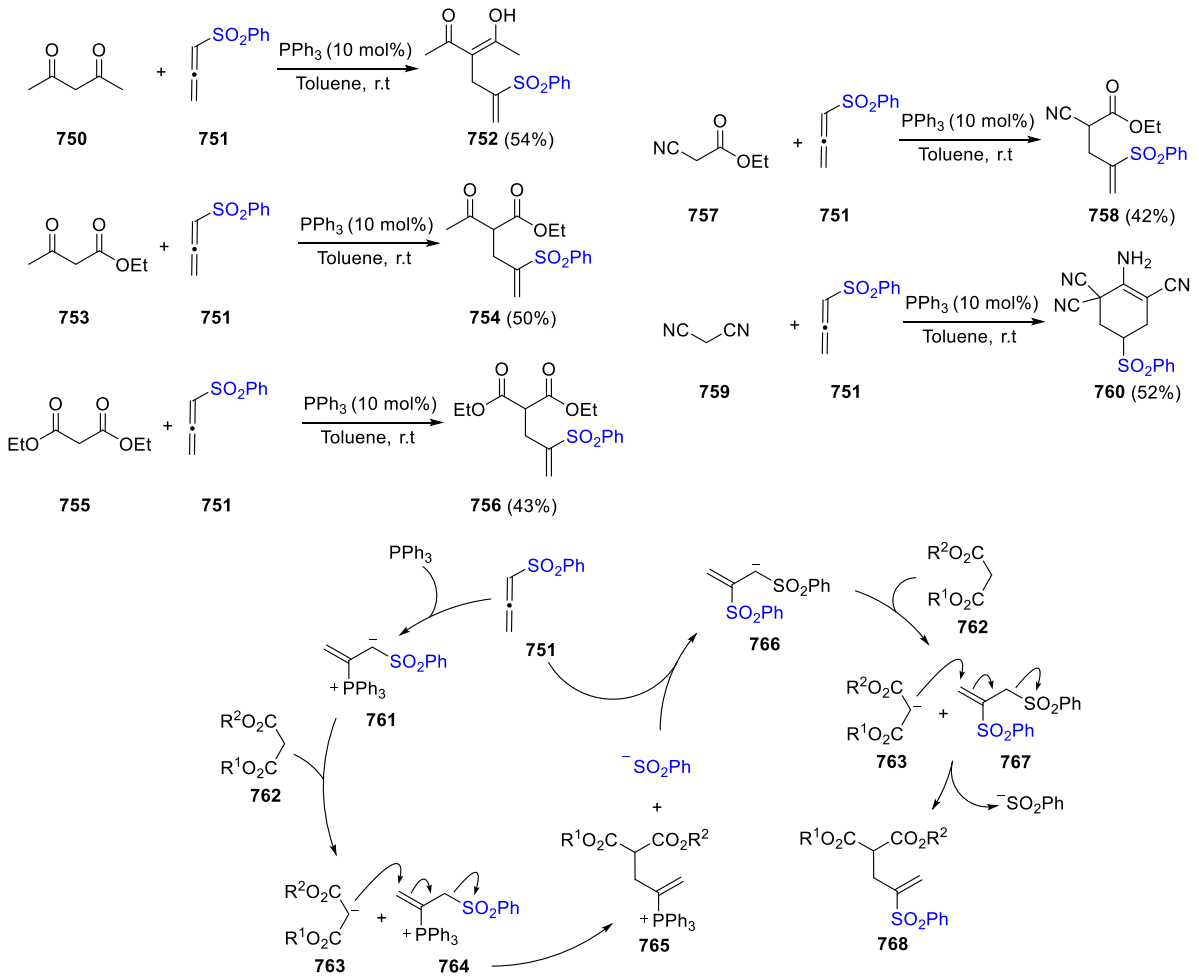

Scheme 1.112: Triphenylphosphine-catalysed 1,2-sulfonyl migration of electron-deficient allenes in their reaction with active methylene compounds affording vinyl sulfones

Hampton and Harmata reported the use of triphenylphosphine as a nucleophilic catalyst in the isomerisation of allenic sulfones **769** to afford 2-arylsulfonyl 1,3-dienes with catalytic phenol used as a proton shuttle **(Scheme 1.113)**.[150] The formal carbon to carbon 1,2-sulfonyl migration was rationalised by the following mechanism as previously described: nucleophilic addition of triphenylphosphine to the β-carbon of the allene substrate **771** affords **772** which is protonated by phenol to give the phosphonium salt **773**; the phenoxide anion deprotonates **773** which leads to the elimination of the tosylate anion, which undergoes nucleophilic addition to the β-carbon of the allene substrate **771** affording the anionic intermediate **775**; subsequent protonation by phenol, and deprotonation of **776** releases tosylate for the next catalytic cycle while generating the desired product **777**.

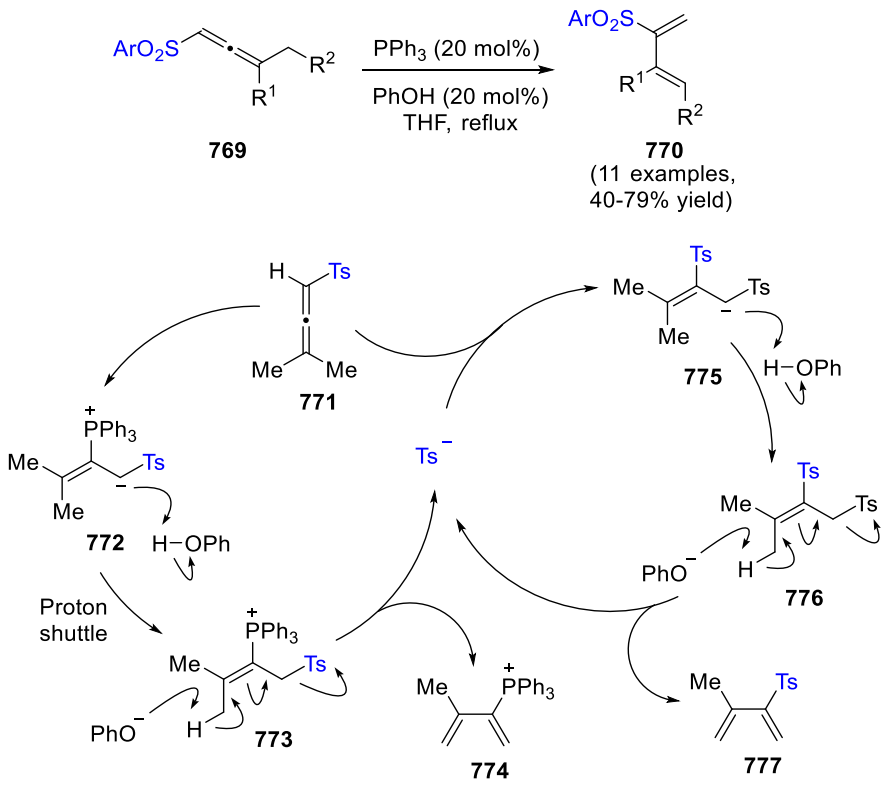

Scheme 1.113: Isomerisation of allenic sulfones affording 2-arylsulfonyl 1,3-dienes catalysed by triphenylphosphine

In a subsequent report the authors provided a series of supporting experiments confirming the likelihood of the presented mechanism **(Scheme 1.114)**.[151] Crossover experiments indicated an intermolecular sulfonyl migration, while the reaction was observed to proceed in the absence of triphenylphosphine when an external source of sulfinate anion was added in the presence of the proton shuttle phenol. While the phosphonium salt intermediates did not prove amenable to isolation, tentative evidence for the presence of either **778** or **779** was provided by ^{31}P NMR for the reaction of the allene **771** with one equivalent of triphenylphosphine. In this reaction, the proposed intermediate, the disulfone **780** was isolated in 12% yield. To ensure that this intermediate could lead to the dienyl product **777**, it was prepared independently and treated with in situ generated sodium phenoxide which afforded the desired product **777** in 91% yield. The authors were able to independently synthesise the phosphonium salt **782**, which compared favourably to the ^{31}P NMR data for the proposed intermediate **778** or **779**. To prove unequivocally that this salt was indeed an intermediate of the proposed reaction pathway it was reacted with the allene **781** in a crossover experiment in the presence of in situ generated sodium phenoxide. Notably, both **783** and **777** were formed consistent with the phosphonium salt **778** being an intermediate in the migratory process. DFT studies carried out by the Li group were consistent with the Harmata group's proposed mechanism for this process, and particularly support the role of phenol as proton shuttle.[152]

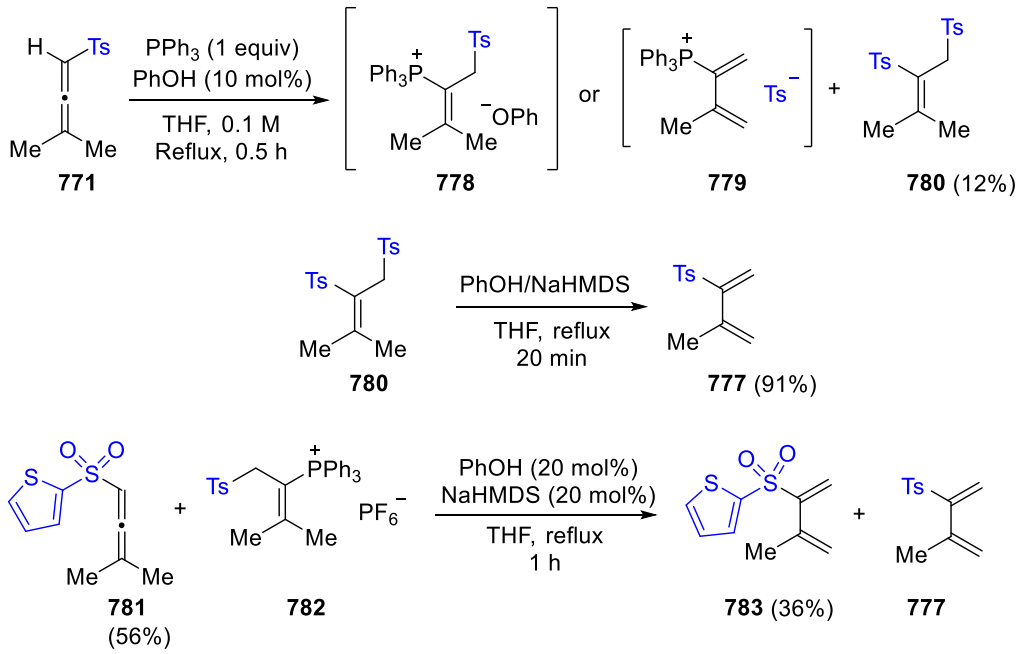

Scheme 1.114: Hampton and Harmata's supporting evidence for the proposed mechanism for the triphenylphosphine-catalysed isomerisation of allenic sulfones to 2-arylsulfonyl 1,3-dienes

1.7.3. Miscellaneous sulfonyl migration

Krasovsky *et al*. developed a novel electrophilic reagent, β-trifluoroacetylketene diphenyldithioacetal S,S'-tetroxide **783**, that allowed access to a range of previously undescribed 1,1,1-trifluoro-4-aryl-3-(phenylsulfonyl)but-3-en-2-ones **584**–**586**, **788** and **790** via Michael-like additions of electron-rich aromatic derivatives **(Scheme 1.115)**.[153] The highly electrophilic reagent **783** readily reacted with 1,3-dimethoxybenzene and 2-methylthiophene to afford the ketones **584**–**586** in high yields under mild conditions. Notably, the reaction occurs via an unusual 1,2-sulfonyl migration and elimination of one sulfonyl moiety. As such, the electrophilic ketone **783** is a synthetic equivalent for the cationic synthon **791** in reactions with electron-rich aromatics. Interestingly, reaction of **783** with the more electron-rich 2-methylindole and *N*-methylpyrrole occurred with rearrangement, but no elimination, at low temperatures to afford a mixture of diastereomeric ketones **787** and **788** with good stereoselectivity. Elimination of the β-phenylsulfonyl moiety could be induced thermally for pyrrole derived ketone **787**, whereas basic conditions were required for the analogous reaction of the indolyl derivative **789**. Mechanistic studies were not part of this investigation.

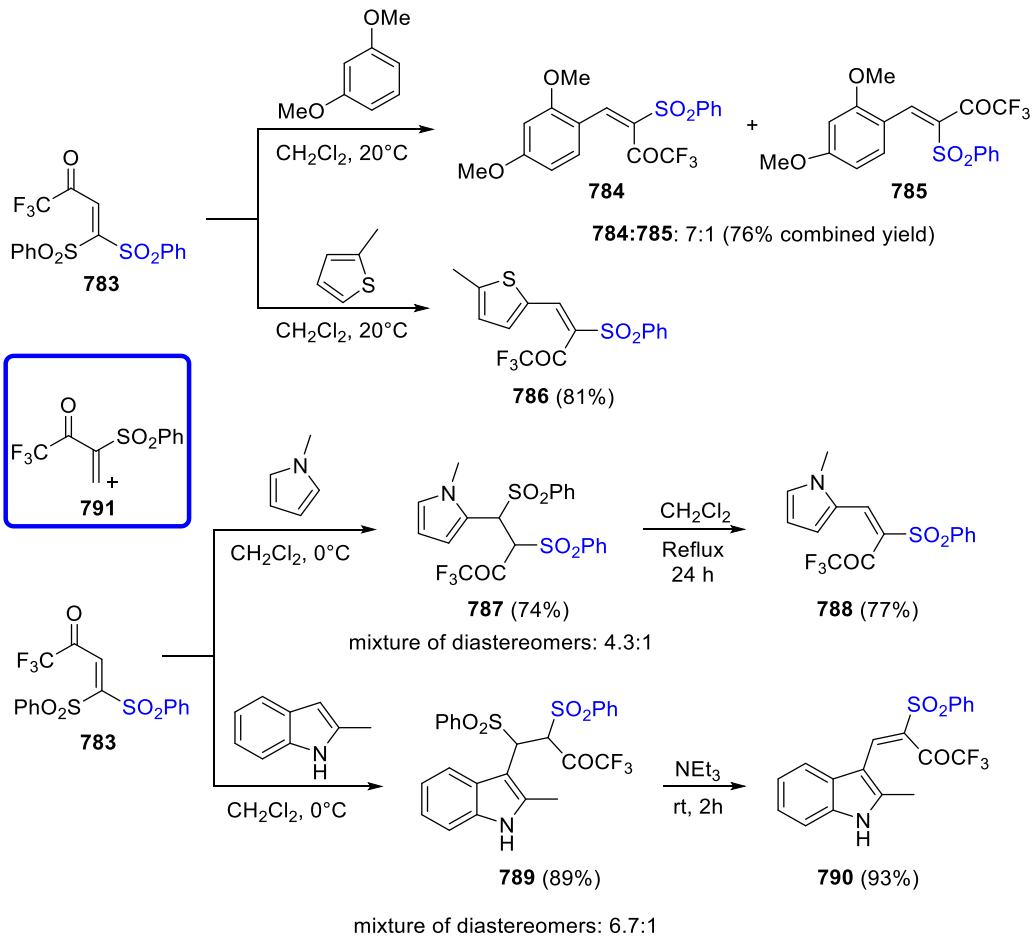

Scheme 1.115: β-trifluoroacetylketene diphenyldithioacetal S,S′-tetroxide as a synthetic equivalent for **791** in electrophilic aromatic substitution; observation of a 1,2-carbon to carbon sulfonyl migration

In their studies on the reactivity of carbanions derived from α-substituted-methyl tolyl sulfones with quinone methides **792** as Michael acceptors, Groszek and Lemek observed an unusual 1,2-tosyl migration when a *para*-nitro substituent was incorporated on the phenyl ring of the quinone scaffold **792 (Scheme 1.116)**.[154] The authors tentatively proposed the formation of the spirodienone **799** as an unstable intermediate, which undergoes a divergent reaction pathway due the electron-withdrawing nature of the nitro group. This nitro moiety significantly increases the acidity of the benzylic proton relative to the other substituents studied (Z = H, NMe_2, OMe). In the presence of excess base the nitro group facilitates deprotonation allowing the anion **800** to cyclise to the hypervalent sulfur intermediate **801** via nucleophilic addition to the sulfur of the sulfonyl moiety.[144, 155-156] Subsequent ring-opening and protonation leads to aromatisation and the acquisition of the rearranged product **795**.

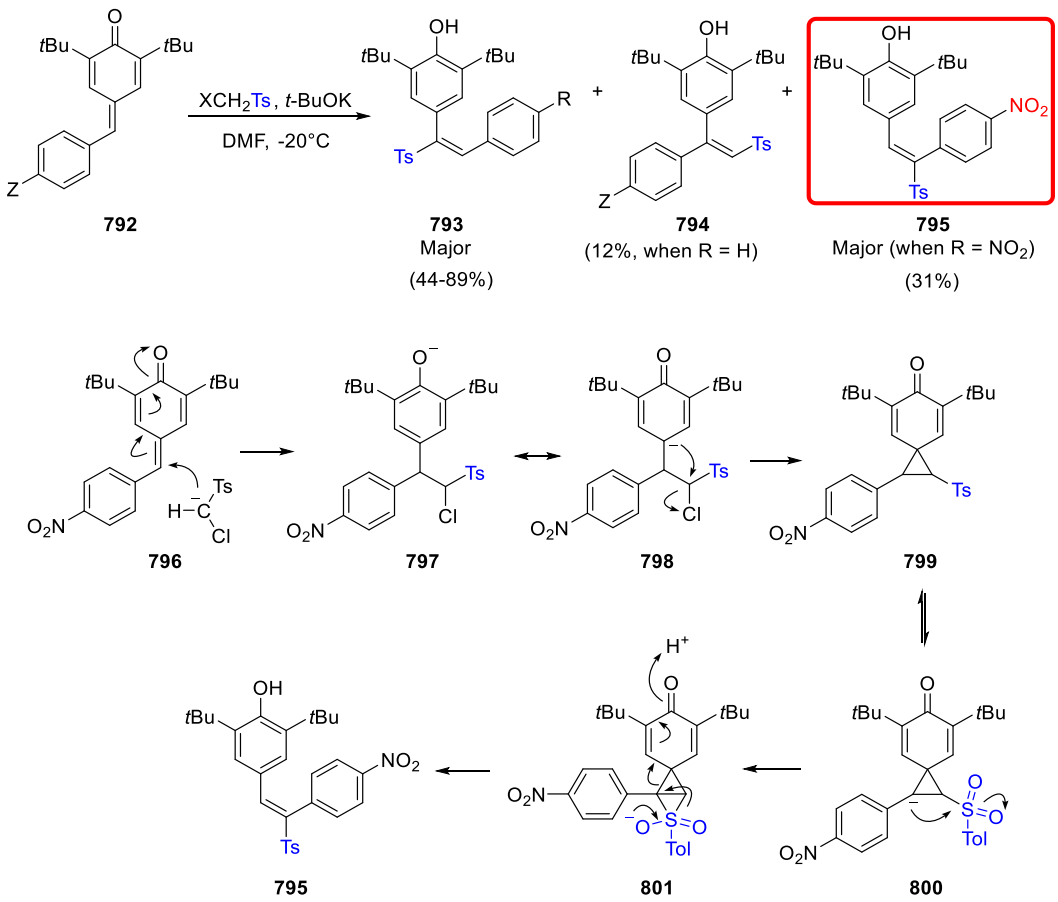

Scheme 1.116: Observation of a formal 1,2-sulfonyl migration from carbon to carbon via hypothesised hypervalent sulfur intermediate **801**

Following their success achieving the enantioselective generation of chiral cyclopropenes from ethyl diazoacetate and various terminal alkynes using the $Rh_2(OAc)(DPTI)_3$ catalyst,[157] the Corey group sought to extend this methodology to include tosyl derivatives to further study the effects of strain in unsaturated cyclopropenes. Using the highly selective rhodium catalyst the chiral tosyl substituted cyclopropenes **804**–**806** were afforded in 91%, 94% and 78% ee respectively **(Scheme 1.117)**.[158] Interestingly, when the 2-*n*-amyl-2-cyclopropenyl 4-tolyl sulfone **804** was purified by chromatography on silica gel, or allowed to stir with silica gel in benzene, complete racemisation was observed. Measurements of the kinetics of the thermal racemisation of **804** at 70°C in each of the solvents benzene, cyclohexane and acetonitrile afforded very similar first-order rate constants, indicating that a polar dissociation mechanism via the formation of a cyclopropenium toluene-sulfinate ion pair was unlikely. Instead, a reversible [2,3]-sigmatropic rearrangement was proposed by the authors **(Scheme 1.117)**. The reverse process, that is a sulfinate-sulfone allylic rearrangement, is well-known in the literature.

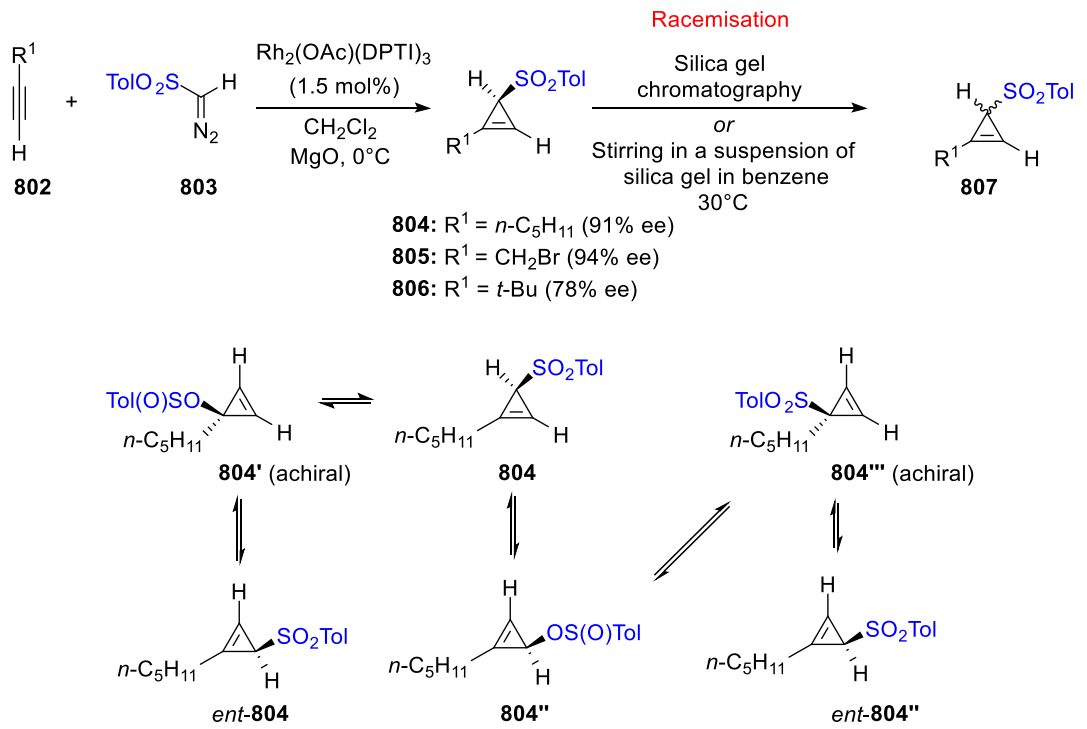

Scheme 1.117: Reversible 2,3-sulfone-sulfinate allylic rearrangement; formal 1,2-sulfonyl migration

Evidence supporting the reversible [2,3]-sigmatropic rearrangement of **804** in the solution phase was provided by carrying out a trapping experiment with anhydrous CD_3OD **(Scheme 1.118)**. Methanolysis of **804"** or *ent*-**804"** produced the isolable deuterated methyl toluenesulfinate **810**, and the cyclopropenol **808**, which despite being too unstable to isolate led to the β-deuterated α,β-enal **809** and the deuterated methyl acetal **811**. These results unequivocally support the generation of the sulfinate **804"**, formed via the first 2,3-sulfone-sulfinate allylic rearrangement. The instability of the cyclopropenol **808** is a direct consequence of high ring strain (approx. 55 kcal/mol) and the availability of a carbonyl-forming elimination process that can alleviate the strain. Ring strain can also explain the ring cleavage process that converts the sulfone **804'''** to the deuterated methoxy sulfone **813** via intermediate **812**. It is likely that the silica gel, acting as a weak protic acid, catalyses the racemisation through hydrogen bonding with one of the oxygen atoms of the migrating sulfonyl group in the transition state.

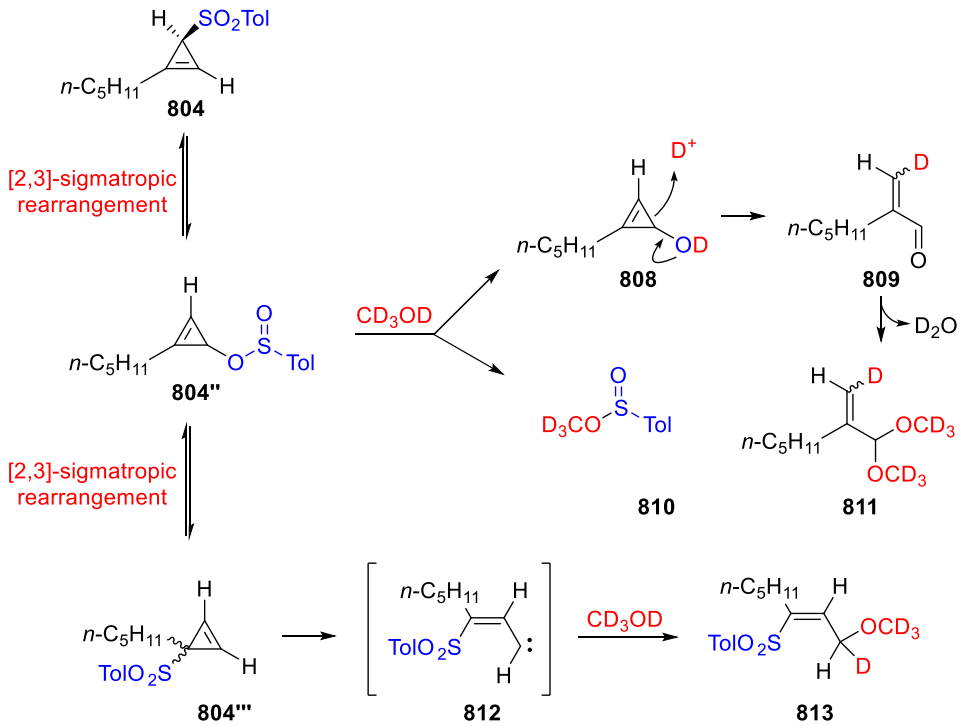

Scheme 1.118: Trapping experiment with CD_3OD confirming the sulfinate **804''** as an intermediate, evidence supporting a 2,3-sulfone-sulfinate allylic rearrangement

The synthetic value of sulfonyl migrations was utilised in Zakharov's enantioselective total synthesis of lycopodine **820**.[159-160] The observed 1,3-sulfonyl migration was the first example of a rearrangement of this type involving an α-sulfonyl imine. The proposed mechanism for the rearrangement is as follows **(Scheme 1.119)**. Treatment of the silyl enol ether **814** with zinc triflate likely affords the zinc complex **815** which can tautomerise to the metallo-enamine **816**, which is considered to be the intermediate that undergoes the 1,3-migration of the sulfonyl moiety from C8 to C14. This rearrangement might occur through (i) heterolytic or homolytic cleavage of the C–S bond to yield an intimate ion-pair or radical pair respectively, followed by recombination at the C14 position; (ii) [2,3]-sigmatropic rearrangement to a sulfinate ester which reorganises to the sulfone **817**; or (iii) formation of a 1,1-dioxothietane intermediate and subsequent ring opening. Protonation of the enamine in a diastereoselective fashion and epimerisation at C14 generates intermediate **818** which via an intramolecular Mannich reaction yields the tricyclic product **819**.

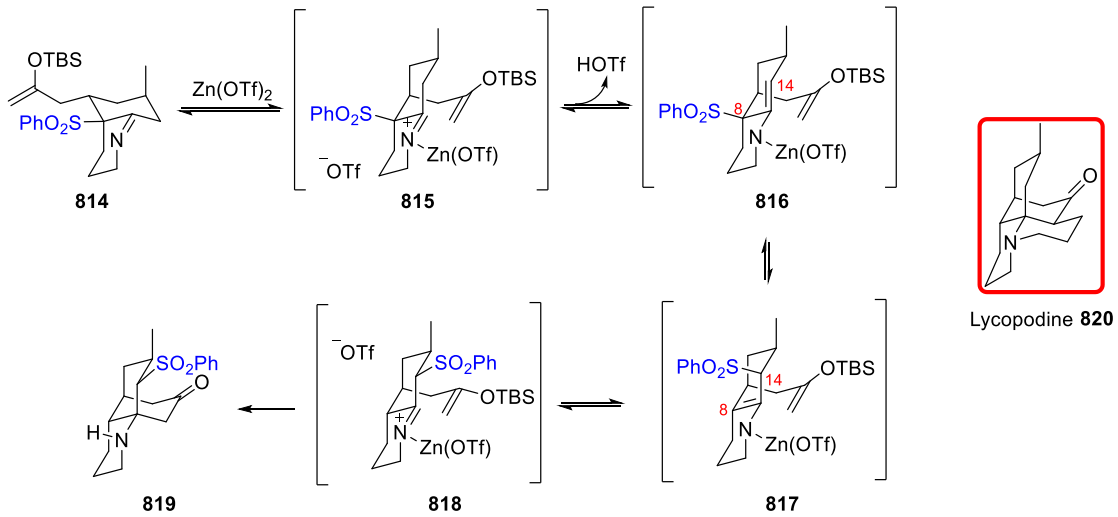

Scheme 1.119: The utilisation of a 1,3-sulfonyl migration in the enantioselective total synthesis of lycopodine

The Robina group reported a sulfonyl moiety catalysed anionic [3+2] cycloaddition of allenyl sulfones **751** and sulfonyl imines **821** to afford 2-aryl-4-phenylsulfonyl-3-pyrrolines **822** in moderate yields **(Scheme 1.120)**.[161] A nucleophilic mediator, in this instance $NaNO_2$, was required for the reaction to occur. The authors suggested that in order to rationalise the high regioselectivity of the transformation that the intermediate **826** must be involved in the process. They reasoned that this could be achieved via conjugate addition of in situ generated benzenesulfinate anion to the allenyl sulfone **751**. Nucleophilic addition of the anionic intermediate **823** to the *N*-sulfonylimine **824** forms the nitranion **825**. A 5-*endo*-trig cyclisation, and subsequent β-elimination of the sulfonyl moiety affords the desired rearranged pyrroline **822**. The route toward the initial formation of benzenesulfinate is unclear, however it is believed to be promoted by addition of the nucleophilic mediator $NaNO_2$ to **751**, which could then react via several pathways to afford the necessary sulfinate anion.

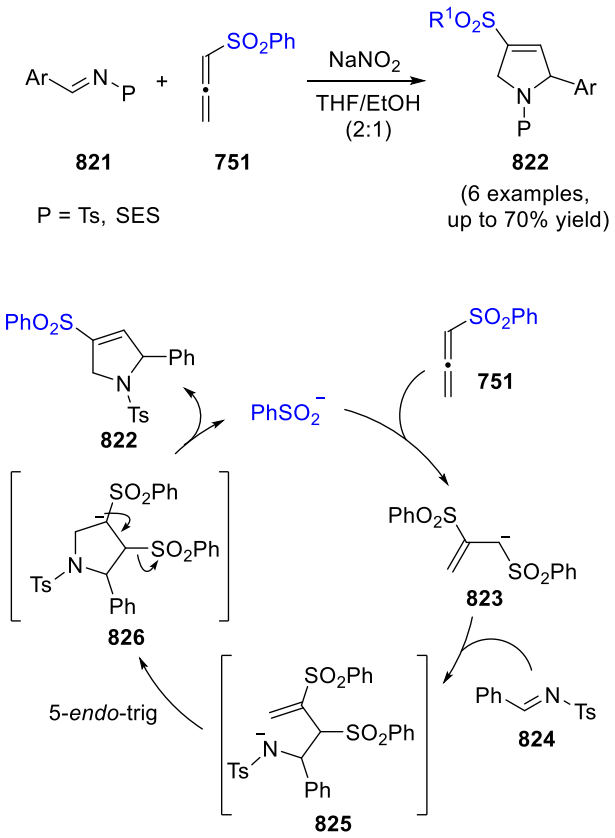

Scheme 1.120: Sulfonyl moiety-catalysed anionic [3+2] cycloaddition of allenyl sulfones and sulfonyl imines affording 2-aryl-4-phenylsulfonyl-3-pyrrolines

Alexakis reported an intriguing 1,2-carbon to carbon sulfonyl migration resulting from nucleophilic addition to bis activated vinyl-sulfones **828**.[162-163] Various nucleophiles including aldehydes, ketones, malonates, keto-esters and nitro-esters activated by different organocatalytic sources (enamine, Brønsted base, thiourea) can promote this migration in moderate to excellent yields and enantioselectivities **(Scheme 1.121)**. The authors reasoned that the mechanism likely proceeds via an anionic intermediate, formed upon Michael addition of the nucleophile and doubly activated vinyl sulfone. Indeed, anion trapping, by performing the reaction using *cis*-1,2-bis(phenylsulfonyl)ethene **832** in the presence of deuterium oxide, highlighted the existence of such an intermediate **837**, with the products **834–836** displaying deuterium incorporation at the α-, β- and γ-positions in 31%, 13% and 41% respectively **(Scheme 1.122)**. A control experiment using 1,1-bis-(phenylsulfone)ethene **833** led to deuterium incorporation at the α- and γ-positions only in 63% and 64% respectively.

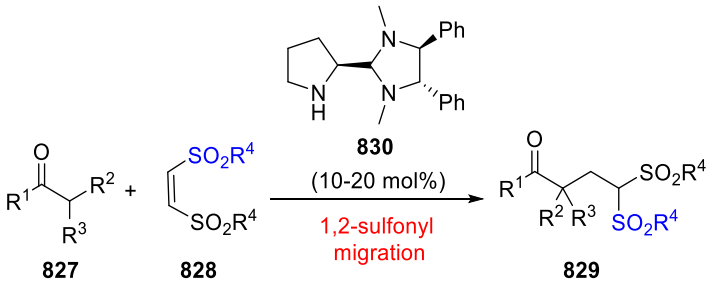

Scheme 1.121: Organocatalyst mediated 1,2-carbon to carbon sulfonyl migration resulting from nucleophilic addition to bis activated vinyl-sulfones

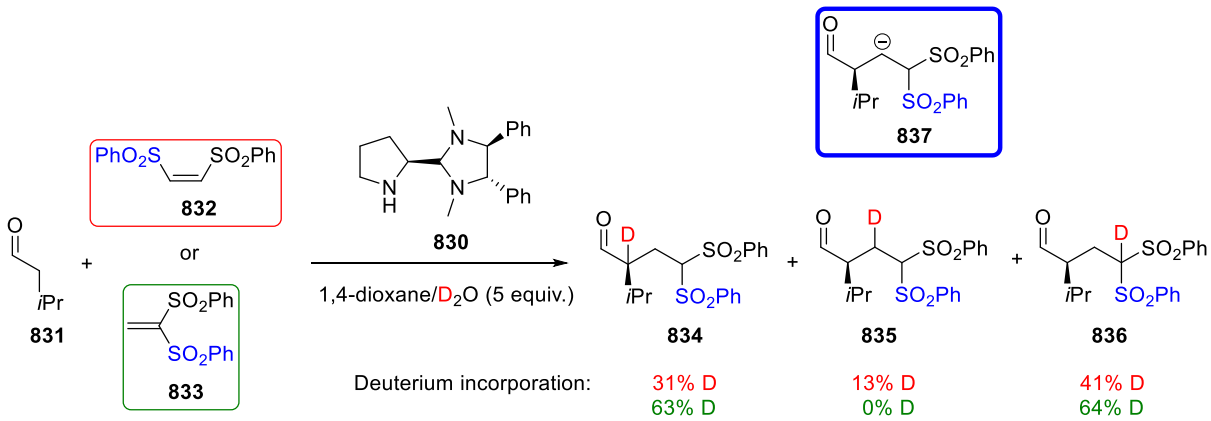

Scheme 1.122: Mechanistic studies supporting the formation of the anion intermediate **837**

Considering these observations, the following mechanism was postulated. Michael addition, or [2+2] cycloaddition, affords the anionic intermediate **839**. Depending on the substrate and the relative conformation of the sulfone and the adjacent anion, two disparate mechanistic outcomes can be considered. If the lone pair and the sulfone moiety are preferentially antiperiplanar after an *anti*-addition, as can be seen in the Newman projection **848**, the elimination of sulfinic acid will be favoured. Alternatively, if the lone pair is in the proximity of the sulfonyl moiety after a *syn* addition as is the case for **846**, then the 1,2-sulfonyl migration will preferentially occur **(Scheme 1.123)**. Protonation of the rearranged intermediate affords the desired product. Notably, the observation that the selectivity for the sulfonyl migration is enhanced by utilising larger nucleophiles is consistent with the proposed mechanism.

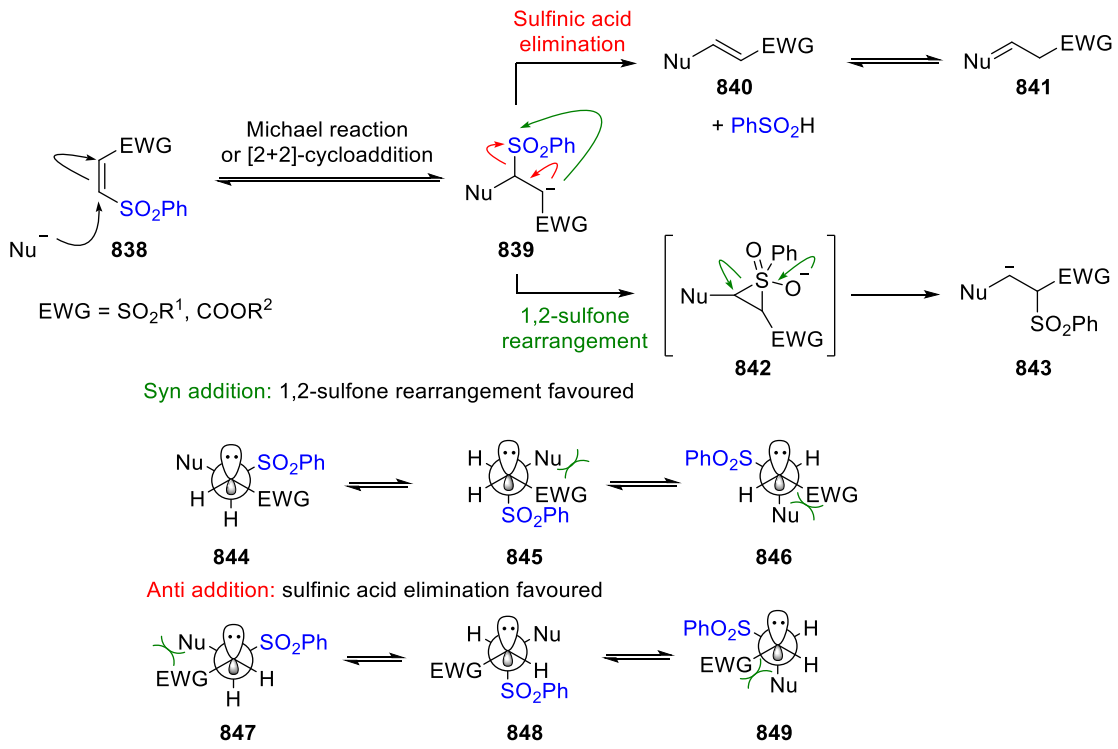

Scheme 1.123: Proposed mechanism for the 1,2-sulfonyl migration; stereochemistry of the transient anion

Subsequently, Rios demonstrated the application of this 1,2-sulfonyl migration in the asymmetric organocatalytic Michael addition of azlactones **850** to *cis*-1,2-bis(phenylsulfonyl)ethene **832** as a synthetically useful method for the generation of direct precursors to enantioenriched quaternary α-alkyl-α-amino acids **851 (Scheme 1.124)**.[164] The thiourea-based catalyst of Takemoto and co-workers (S,S)-**852** was determined to be the optimal catalyst for the transformation,[165] producing yields of up to 82% and enantiomeric excesses of up to 95%.

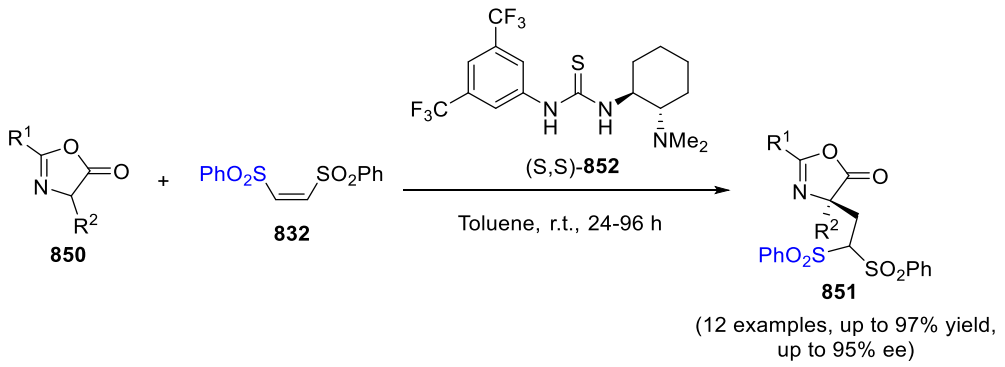

Scheme 1.124: Application of a 1,2-sulfonyl migration in the synthesis of direct precursors to enantioenriched quaternary α-alkyl-α-amino acids

2-(Sulfonylmethyl)arylpyrroles **855** were observed to be accessible from α-allyl-β-ketosulfones **853** via a $PdCl_2/CuCl_2/NH_4OAc$-mediated domino Wacker-type aminocyclisation via selective 1,4-sulfonyl migration with moderate to good yields **(Scheme 1.125)**.[166] Regardless of the conditions employed through optimisation, no evidence for the pyrrole **863**, derived from a 1,3-sulfonyl migration was observed. Complexation of the $PdCl_2/CuCl_2$-catalyst system to the olefin **854** was found to yield the Wacker oxidation product **856**. Condensation of **856** with NH_4OAc affords intermediate **857**, which subsequently undergoes desulfonylation, cyclisation and tautomerisation to give **860**. Elimination of ammonia leads to the generation of the fulvene skeleton **861**, which undergoes regioselective addition of the sulfinate, which gives the pyrrole product **862** via protonation of **861**, completing the overall 1,4-sulfonyl migration. Crossover experiments, whereby both the aryl group and the sulfonyl group were varied, supported the intermolecular nature of the sulfonyl migration and the presence of the fulvene skeleton **861** as a key intermediate.

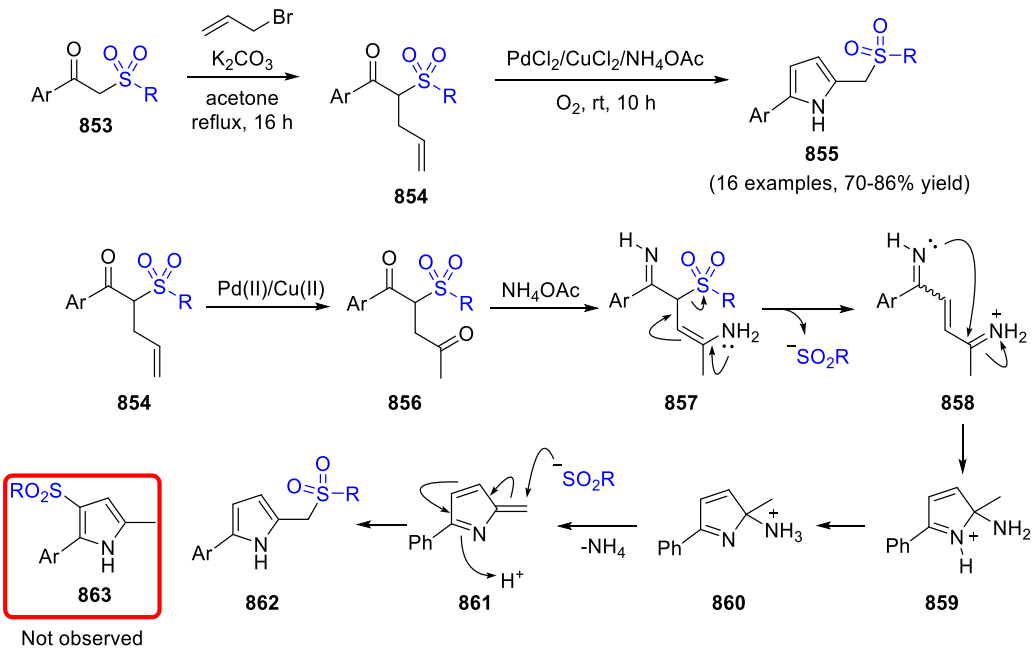

Scheme 1.125: $PdCl_2/CuCl_2/NH_4OAc$-mediated domino Wacker-type aminocyclisation of α-allyl-β-ketosulfones via selective 1,4-sulfonyl migration

The Yu group developed a copper-catalysed cyclisation of allenoates **864** with activated isocyanides **865**, that invloved 1,3-sulfonyl migration, leading to di- or tri-substituted pyrroles **866** in moderate to good yields **(Scheme 1.126)**.[167] The authors proposed that the transformation starts with Cu_2O mediated C–H bond activation of the isocycanide **867** to give the copper-isocyanide complex **868** with concomitant formation of H_2O. Subsequent [3+2]-dipolar cycloaddition of this intermediate with the allenoate **869** affords the intermediate **870**, which following protonolysis leads to the formation of **871** and the regeneration of the copper catalyst. A copper-assisted elimination of tosylate produces the cationic intermediate **872**, which upon recombination affords the rearranged pyrrole complex **873**. The intermolecular nature of the sulfonyl migration was further established by means of crossover experiments. Protonolysis of **873** leads to the final pyrrole product **874** and regeneration of the copper catalyst.

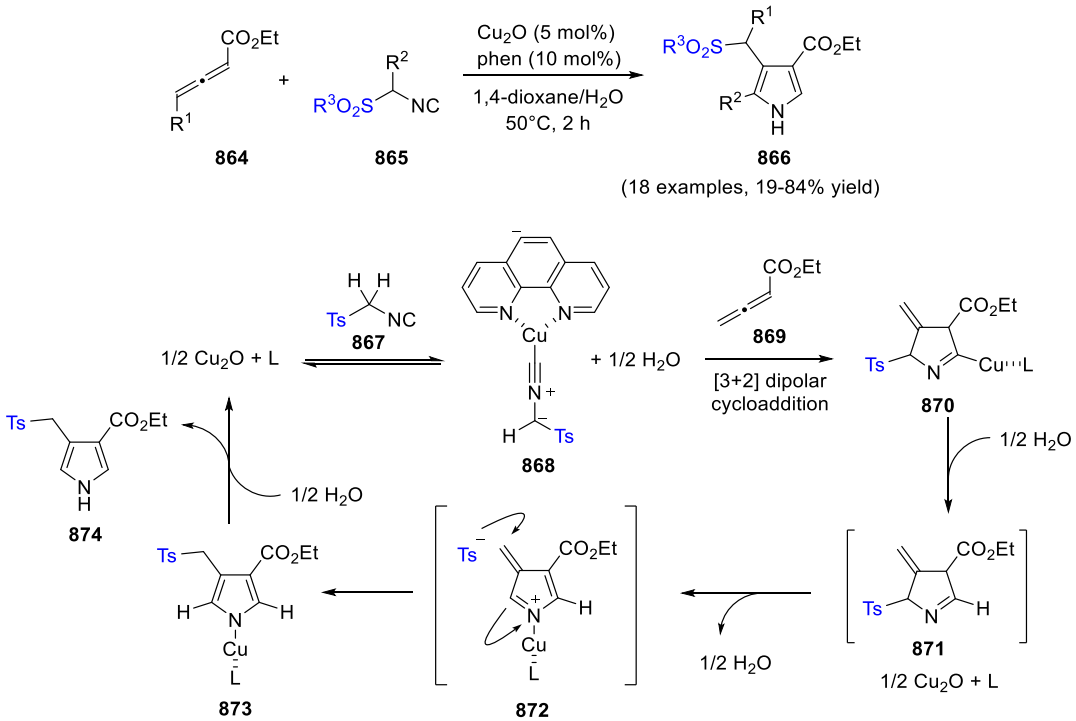

Scheme 1.126: Copper-catalysed cyclisation of allenoates with activated isocyanides featuring a carbon-carbon 1,3-sulfonyl migration

Bi and co-workers described the silver-catalysed generation of 1,4,5-trisubstituted imidazoles **877** via isocyanide–isocyanide [3+2]-dipolar cycloaddition in which a 1,2-tosyl migration was observed **(Scheme 1.127)**.[168] Notably, both electron-rich and electron-deficient aryl groups on the aryl isocyanides **875**, as well as sterically demanding groups, were well tolerated with moderate to high yields obtained in all instances. Furthermore, both aryl and alkyl α-substituted tosylmethyl isocyanide derivatives **876** reacted readily. The addition of either TEMPO or BHT did not inhibit the reaction, indicating that the mechanism does not proceed via a radical process **(Scheme 1.127)**. When the reaction was carried out in the presence of D_2O, 74% deuterium incorporation was observed, highlighting that trace amounts of water in the solvent may provide a proton in the imidazole products **877**. No deuterated imidazole [D]-**880** was isolated when the substrate [D]-**879** was reacted under standard conditions, confirming that the active methine group is involved in proton abstraction.

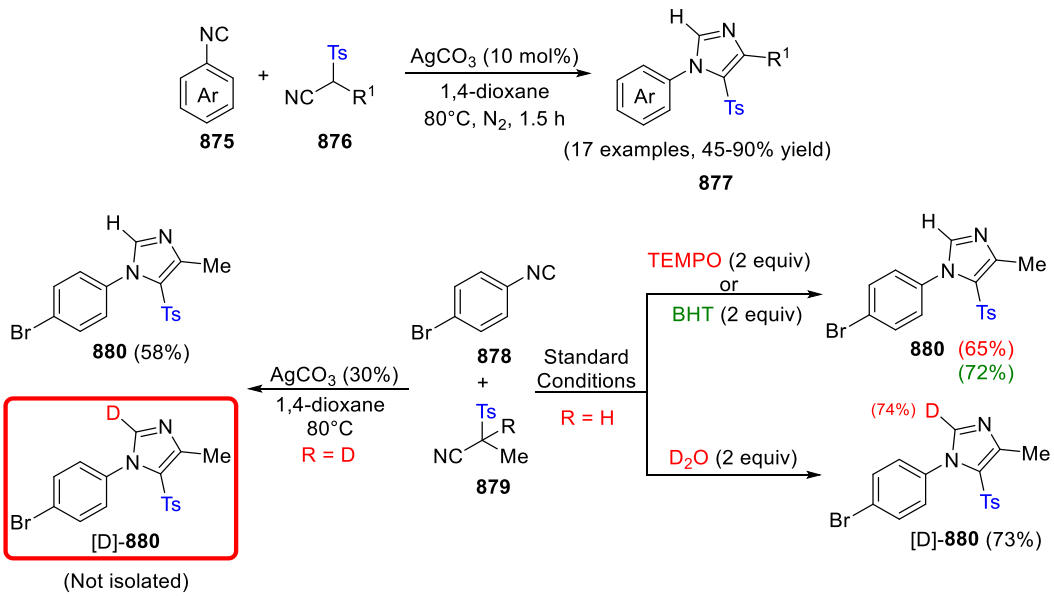

Scheme 1.127: Silver-catalysed formation of 1,4,5-trisubstituted imidazoles via isocyanide–isocyanide [3+2]-dipolar cycloaddition with accompanying 1,2-tosyl migration

The authors postulated that coordination of the silver catalyst to the isocyanides **878** and **879** generates the silver complexes **881** (following abstraction of a proton and concurrent generation of $AgHCO_3$) and **882**, which subsequently undergo [3+2]-dipolar cycloaddition to give the cyclic nitrilium ion **884 (Scheme 1.128)**. 1,2-Tosyl migration affords the carbocation intermediate **885** followed by loss of the silver cation and subsequent protonation forms the rearranged imidazoles **880** with concomitant regeneration of the silver catalyst.

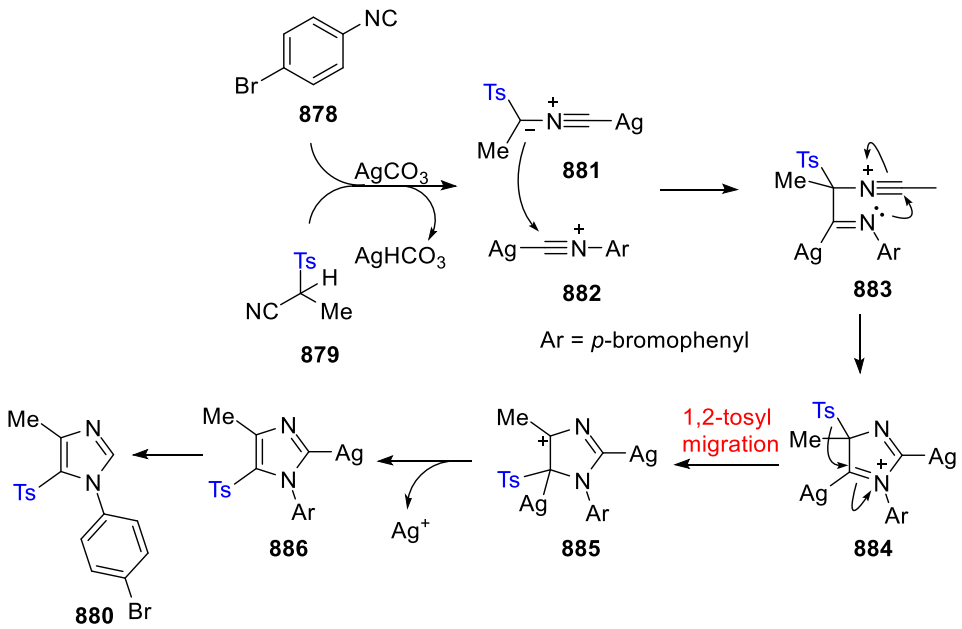

Scheme 1.128: Proposed mechanism for silver-catalysed formation of 1,4,5-trisubstituted imidazoles via isocyanide–isocyanide [3+2]-dipolar cycloaddition

The Xu group disclosed the first example of the preparation of *ortho*-alkylaryl triflones **889** via the insertion of arynes into C–SO_2CF_3 bonds through a tandem nucleophilic attack/intramolecular carbon to carbon 1,3-sulfonyl migration **(Scheme 1.129)**.[169] Using KF/18-crown-6 as fluoride source a series of *ortho*-alkylaryl triflones **889** were generated in moderate to high yields, with the presence of an electron-withdrawing substituent on the benzyl triflones **888** essential for efficient reaction. A plausible mechanism involves the fluoride-mediated generation of the aryne **890** and carbanion **891**, which upon nucleophilic addition forms the intermediate **892 (Scheme 1.129)**. Subsequent carbon to carbon 1,3-sulfonyl migration of the triflyl group, presumably via an intramolecular process, akin to an anionic thia-Fries rearrangement, affords the rearranged *ortho*-alkylaryl triflone **889**. Notably, the corresponding reaction of substituted benzyl methanesulfones did not afford the desired aryl methanesulfones, highlighting the importance of the triflyl group in the transformation.

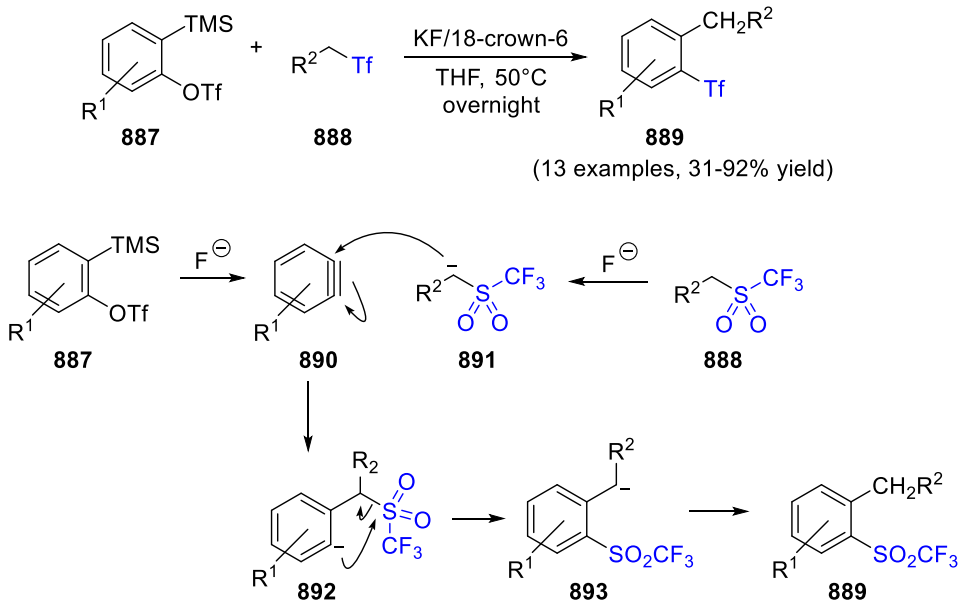

Scheme 1.129: Preparation of *ortho*-alkylaryl triflones via insertion of C–SO_2CF_3 bonds into arynes through a tandem nucleophilic attack/intramolecular carbon to carbon 1,3-sulfonyl migration

Access to novel atropisomeric 3-tosyl-1-enyl-cyclopropyl-diphenylphosphine oxide derivatives **896** and **897** via a one-pot transition metal free coupling of *N*-tosylhydrazones **894** and phosphinyl allenes **895** was recently developed by Wu and co-workers.[170] Notably, the multistep cascade reaction occurs by initial radical hydrazonyl N–S bond cleavage, followed by sequential radical C(sp^3)–OAr bond cleavage, carbon to carbon 1,3-sulfonyl migration and atropisomeric cyclopropanation to afford the desired products in moderate to high yields in excellent diastereoselectivity **(Scheme 1.130)**. The initial radical cleavage of the hydrazonyl N–S bond is enabled by the combination of catalytic 1,10-phenanthroline and potassium carbonate, and while significant attention was afforded to the elucidation of the mechanism for this step it is beyond the scope of this review. Consequently, we will focus exclusively on the attempts to elucidate the mechanism for the sulfonyl migration step. For clarity, the full proposed mechanism is included in **Scheme 1.131**.

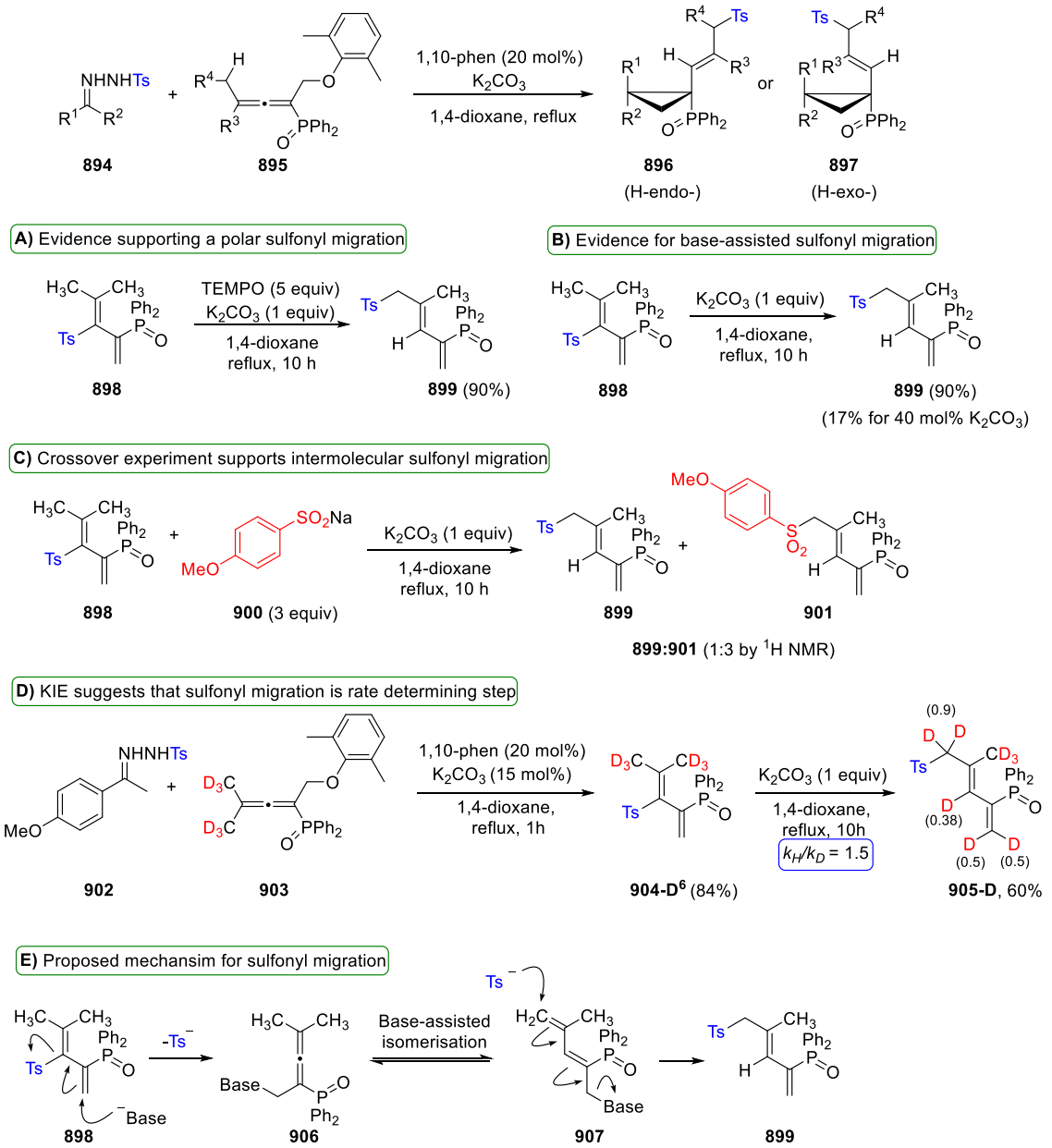

Scheme 1.130: Proposed mechanism for sulfonyl migration including experimental evidence

A radical mechanism was invalidated by the addition of TEMPO, under otherwise standard conditions, to the isolable intermediate **898** which afforded the rearranged product **899** with no inhibition observed **(Scheme 1.130, A)**. A stoichiometric amount of K_2CO_3 was shown to be necessary for optimal conversion to rearranged product, with a reduction in the amount of base inhibiting the cascade process **(Scheme 1.130, B)**. This finding strongly suggests that the base promotes the sulfonyl migration. A crossover experiment between **898** and sodium 4-methoxybenzenesulfinate **900** afforded a statistical mixture of products **899** and **901** supporting an intermolecular sulfonyl migration **(Scheme 1.130, C)**. A kinetic isotope effect value (k_H/k_D) of 1.5 was determined for the parallel reactions of **904** and **904-D^6** under standard conditions, with incorporation of deuterium observed over all the alkenyl positions **(Scheme 1.130, D)**. This KIE suggests that the rate-determining step probably involves the sulfonyl rearrangement but does not involve the previous C(sp^3)-H bond cleavage. With this experimental evidence in mind the following mechanism is postulated **(Scheme**

1.130, E): Base induced elimination of the tosyl moiety affords the tosyl anion and the allene **906**, which isomerises to **907** in the presence of stoichiometric base.[171] Nucleophilic addition of the tosyl anion promotes the elimination of the base and completes the formal 1,3-sulfonyl migration to afford **899**.

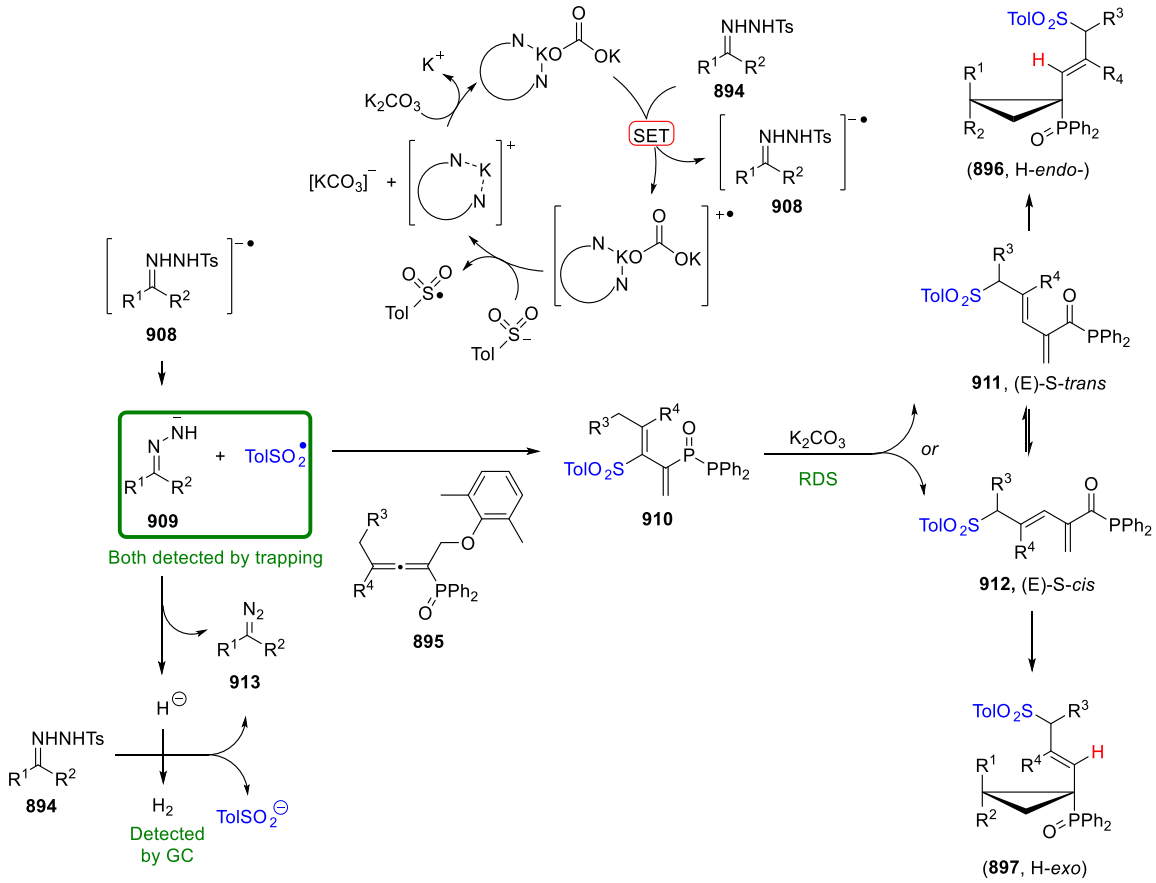

Scheme 1.131: Overall proposed mechanism for the synthesis of atropisomeric 3-tosyl-1-enyl-cyclopropyl-diphenylphosphine oxide derivatives

1.8. Summary and Outlook

In this introductory chapter, we have comprehensively compiled reports of sulfonyl migrations over the past 20 years, highlighted the development of insight into synthetic and mechanistic aspects of these sulfonyl shifts, and categorised them based on the migration type, namely nitrogen-carbon, nitrogen-oxygen, nitrogen-nitrogen, oxygen-carbon, oxygen-oxygen and carbon-carbon. While most sulfonyl migrations prior to the beginning of the 21st century were discovered as side reactions, and regularly as isolated cases, the last 20 years has seen a significant increase in the number of reports focusing on development of synthetic methodology based on the sulfonyl migration. Efforts to understand the mechanisms of these often 'unexpected' reactions have garnered significant recent attention including by means of crossover studies, competition experiments, isotopic-labelling, density functional theory calculations and electron paramagnetic resonance spectroscopy, although many sulfonyl migrations are only partially understood at this point. Despite progress in this area, the potential for formal 1,2-, 1,3-, 1,4-, 1,5-, 1,6- and 1,7-sulfonyl migrations, both in an inter- and intramolecular fashion, *via* both radical and polar processes render challenging the prediction of the outcome of such reactions in a manner that would facilitate their predictable use in synthesis.

Notwithstanding, the clear evidence discussed herein for the utility of sulfonyl migration, particularly in the synthesis of highly functionalised heterocycles, and notably in total synthesis, highlights the synthetic potential of sulfonyl migrations. Therefore, we believe that significant attention will be afforded to this expanding field of research in years to come.

Bibliography

1. E. J. Corey and X. M. Cheng, *The Logic of Chemical Synthesis*, Wiley, **1989**.
2. A. J. Flynn, A. Ford, U. B. R. Khandavilli, S. E. Lawrence and A. R. Maguire, *Eur. J. Org. Chem*, **2019**, 5368-5384.
3. *The Chemistry of Sulphones and Sulphoxides,* ed S. Patai, Z. Rappoport and C. Stirling, John Wiley & Sons, Chichester, **1988**.
4. B. M. Trost and C. A. Kalnmals, *Chem. Eur. J*, **2019**, 25, 11193-11213.
5. P. D. Magnus, *Tetrahedron*, **1977**, 33, 2019-2045.
6. N. S. Simpkins, *Chem. Soc. Rev.,* **1990**, 19, 335-354.
7. N. S. Simpkins, *Sulfones in Organic Synthesis*, Pergamon Press, Elmsford, NY, **1993**.
8. A. Padwa, Z. Ni and S. H. Watterson, *Pure Appl. Chem*, **1996**, 68, 831.
9. J.-E. Bäckvall, R. Chinchilla, C. Nájera and M. Yus, *Chem. Rev.*, **1998**, 98, 2291-2312.
10. P. L. Fuchs and T. F. Braish, *Chem. Rev.*, **1986**, 86, 903-917.
11. N. S. Simpkins, *Tetrahedron*, **1990**, 46, 6951-6984.
12. T. G. Back, K. N. Clary and D. Gao, *Chem. Rev.*, **2010**, 110, 4498-4553.
13. Y. M. Markitanov, V. M. Timoshenko and Y. G. Shermolovich, *J. Sulfur Chem.*, **2014**, 35, 188-236.
14. Y. Fang, Z. Luo and X. Xu, *RSC Adv.*, **2016**, 6, 59661-59676.
15. C. Stefan, S. Simon, W. Jean-Marc and P. Patrick, *Curr. Org. Synth.*, **2012**, 9, 806-827.
16. C. M. So and F. Y. Kwong, *Chem. Soc. Rev.*, **2011**, 40, 4963-4972.
17. S. Searles and S. Nukina, *Chem. Rev.*, **1959**, 59, 1077-1103.
18. I. Nakamura, U. Yamagishi, D. Song, S. Konta and Y. Yamamoto, *Angew. Chem. Int. Ed.*, **2007**, 46, 2284-2287.
19. I. Nakamura, U. Yamagishi, D. Song, S. Konta and Y. Yamamoto, *Chem. – Eur. J.*, **2008**, 3, 285-295.
20. I. Nakamura, Y. Mizushima, U. Yamagishi and Y. Yamamoto, *Tetrahedron*, **2007**, 63, 8670-8676.
21. A. Fürstner and P. W. Davies, *J. Am. Chem. Soc.*, **2005**, 127, 15024-15025.
22. W. Rao, D. Susanti and P. W. H. Chan, *J. Am. Chem. Soc.*, **2011**, 133, 15248-15251.
23. W. T. Teo, W. Rao, M. J. Koh and P. W. H. Chan, *J. Org. Chem.*, **2013**, 78, 7508-7517.
24. H.-S. Yeom, E. So and S. Shin, *Chem. – Eur. J*, **2011**, 17, 1764-1767.
25. J. Liu, P. Chakraborty, H. Zhang, L. Zhong, Z.-X. Wang and X. Huang, *ACS Catal.*, **2019**, 9, 2610-2617.
26. B. Prabagar, R. K. Mallick, R. Prasad, V. Gandon and A. K. Sahoo, *Angew. Chem. Int. Ed.*, **2019**, 58, 2365-2370.
27. Y. T. Lee and Y. K. Chung, *J. Org. Chem.*, **2008**, 73, 4698-4701.
28. Y. Hu, R. Yi, F. Wu and B. Wan, *J. Org. Chem.*, **2013**, 78, 7714-7726.
29. Y. Zhao, H. Wang, X. Li, D. Wang, X. Xin and B. Wan, *Org. Biomol. Chem.*, **2016**, 14, 526-541.
30. D. Arunprasath, B. Devi Bala and G. Sekar, *Adv. Synth. Catal.*, **2019**, 361, 1172-1207.
31. Y. Xia and J. Wang, *Chem. Soc. Rev.*, **2017**, 46, 2306-2362.
32. H. Wang, Y.-H. Deng and Z. Shao, *Synthesis*, **2018**, 50, 2281-2306.
33. S. Mao, Y.-R. Gao, X.-Q. Zhu, D.-D. Guo and Y.-Q. Wang, *Org. Lett.*, **2015**, 17, 1692-1695.
34. J. Ni, Y. Xue, L. Sun and A. Zhang, *J. Org. Chem.*, **2018**, 83, 4598-4605.
35. Q. Sun, L. Li, L. Liu, Q. Guan, Y. Yang, Z. Zha and Z. Wang, *Org. Lett.*, **2018**, 20, 5592-5596.
36. F. Wang, P. Xu, S.-Y. Wang and S.-J. Ji, *Org. Lett.*, **2018**, 20, 2204-2207.
37. Y. Zheng, L. Qiu, K. Hong, S. Dong and X. Xu, *Chem. – Eur. J*, **2018**, 24, 6705-6711.
38. P.-X. Zhou, Y.-Y. Ye, L.-B. Zhao, J.-Y. Hou, X. Kang, D.-Q. Chen, Q. Tang, J.-Y. Zhang, Q.-X. Huang, L. Zheng, J.-W. Ma, P.-F. Xu and Y.-M. Liang, *Chem. – Eur. J*, **2014**, 20, 16093-16096.
39. P.-X. Zhou, Y. Zhang, C. Ge, Y.-M. Liang and C. Li, *J. Org. Chem.*, **2018**, 83, 4762-4768.
40. B. Prasad, R. Adepu, S. Sandra, D. Rambabu, G. R. Krishna, C. M. Reddy, G. S. Deora, P. Misra and M. Pal, *Chem. Commun.*, **2012**, 48, 10434-10436.
41. Y. Zhu, T. Hai-Tao and Z.-P. Zhan, *Adv. Synth. Catal.*, **2013**, 355, 1291-1296.
42. Y. Zhu, J.-J. Hong, Y.-B. Zhou, Y.-W. Xiao, M. Lin and Z.-P. Zhan, *Org. Biomol. Chem.*, **2014**, 12, 3797-3801.
43. M. Padmanaban, L. C. R. Carvalho, D. Petkova, J.-W. Lee, A. S. Santos, M. M. B. Marques and N. Maulide, *Tetrahedron*, **2015**, 71, 5994-6005.
44. J. Wang, K.-I. Son and J. Xu, *Monatsh. Chem.*, **2016**, 147, 1637-1649.
45. R. Han, L. He, L. Liu, X. Xie and X. She, *Chem. – Eur. J.*, **2016**, 11, 193-197.
46. B. Wang, S. Jin, S. Sun and J. Cheng, *Org. Chem. Front.*, **2018**, 5, 958-961.
47. K. K. Park, J. J. Lee and J. Ryu, *Tetrahedron*, **2003**, 59, 7651-7659.

48. X. Hong, J. M. Mejía-Oneto, S. France and A. Padwa, *Tetrahedron Lett.*, **2006**, 47, 2409-2412.
49. X. Hong, S. France and A. Padwa, *Tetrahedron*, **2007**, 63, 5962-5976.
50. C. Simal, T. Lebl, A. M. Z. Slawin and A. D. Smith, *Angew. Chem. Int. Ed.*, **2012**, 51, 3653-3657.
51. P.-P. Yeh, J. E. Taylor, D. G. Stark, D. S. B. Daniels, C. Fallan, J. C. Walton and A. D. Smith, *Org. Biomol. Chem.*, **2017**, 15, 8914-8922.
52. I. Bernar, D. Blanco-Ania, S. J. Stok, L. Sotorríos, E. Gómez-Bengoa and F. P. J. T. Rutjes, *Eur. J. Org. Chem.*, **2018**, 5435-5444.
53. J. Wrobel, A. Dietrich, S. A. Woolson, J. Millen, M. McCaleb, M. C. Harrison, T. C. Hohman, J. Sredy and D. Sullivan, *J. Med. Chem.*, **1992**, 35, 4613-4627.
54. S. Zhang, L. Li, Y. Hu, Z. Zha, Z. Wang and T.-P. Loh, *Org. Lett.*, **2015**, 17, 1050-1053.
55. G. S. Lal, G. P. Pez and R. G. Syvret, *Chem. Rev.*, **1996**, 96, 1737-1756.
56. Y. Takeuchi, T. Suzuki, A. Satoh, T. Shiragami and N. Shibata, *J. Org. Chem.*, **1999**, 64, 5708-5711.
57. E. Torti, S. Protti, D. Merli, D. Dondi and M. Fagnoni, *Chem. – Eur. J*, **2016**, 22, 16998-17005.
58. E. Torti, S. Protti, M. Fagnoni and G. Della Giustina, *ChemistrySelect*, **2017**, 2, 3633-3636.
59. D. P. Ojha and K. R. Prabhu, *Org. Lett.*, **2015**, 17, 18-21.
60. Z. Luo, Y. Fang, Y. Zhao, X. Xu, C. Feng, Z. Li, X. Zhang and J. He, *Tetrahedron Lett.*, **2016**, 57, 4105-4108.
61. S. Parisotto, G. Garreffa, C. Canepa, E. Diana, F. Pellegrino, E. Priola, C. Prandi, V. Maurino and A. Deagostino, *ChemPhotoChem*, **2017**, 1, 56-59.
62. M. Kimura, Y. Horino, Y. Wakamiya, T. Okajima and Y. Tamaru, *J. Am. Chem. Soc.*, **1997**, 119, 10869-10870.
63. Y. Horino, M. Kimura, Y. Wakamiya, T. Okajima and Y. Tamaru, *Angew. Chem. Int. Ed.*, **1999**, 38, 121-124.
64. M. Kimura, Y. Horino, M. Mori and Y. Tamaru, *Chem. – Eur. J*, **2007**, 13, 9686-9702.
65. Y. Horino, M. Kimura, M. Naito, S. Tanaka and Y. Tamaru, *Tetrahedron Lett.*, **2000**, 41, 3427-3431.
66. M. Bendikov, H. M. Duong, E. Bolanos and F. Wudl, *Org. Lett.*, **2005**, 7, 783-786.
67. K. A. DeKorver, W. L. Johnson, Y. Zhang, R. P. Hsung, H. Dai, J. Deng, A. G. Lohse and Y.-S. Zhang, *J. Org. Chem.*, **2011**, 76, 5092-5103.
68. X. Xin, D. Wang, X. Li and B. Wan, *Angew. Chem. Int. Ed.*, **2012**, 51, 1693-1697.
69. X. Yu, X. Xin, B. Wan and X. Li, *J. Org. Chem.*, **2013**, 78, 4895-4904.
70. X. Xin, H. Wang, X. Li, D. Wang and B. Wan, *Org. Lett.*, **2015**, 17, 3944-3947.
71. Z. Jiang, P. Lu and Y. Wang, *Org. Lett.*, **2012**, 14, 6266-6269.
72. Y. Zhu, W.-T. Lu, H.-C. Sun and Z.-P. Zhan, *Org. Lett.*, **2013**, 15, 4146-4149.
73. F. Ji, H. Peng, X. Zhang, W. Lu, S. Liu, H. Jiang, B. Liu and B. Yin, *J. Org. Chem.*, **2015**, 80, 2092-2102.
74. J. Shi, D. Qiu, J. Wang, H. Xu and Y. Li, *J. Am. Chem. Soc.*, **2015**, 137, 5670-5673.
75. D. Qiu, J. Shi and Y. Li, *Synlett*, **2015**, 26, 2194-2198.
76. D. Qiu, J. He, X. Yue, J. Shi and Y. Li, *Org. Lett.*, **2016**, 18, 3130-3133.
77. H. Tanimoto, K. Yokoyama, Y. Mizutani, T. Shitaoka, T. Morimoto, Y. Nishiyama and K. Kakiuchi, *J. Org. Chem.*, **2016**, 81, 559-574.
78. H. Tanimoto, T. Shitaoka, K. Yokoyama, T. Morimoto, Y. Nishiyama and K. Kakiuchi, *J. Org. Chem.*, **2016**, 81, 8722-8735.
79. H. Tanimoto, S. Ueda, T. Morimoto and K. Kakiuchi, *J. Org. Chem.*, **2018**, 83, 1614-1626.
80. G. Di Mauro, B. Maryasin, D. Kaiser, S. Shaaban, L. González and N. Maulide, *Org. Lett.*, **2017**, 19, 3815-3818.
81. I. Colomer, M. Velado, R. Fernández de la Pradilla and A. Viso, *Chem. Rev.*, **2017**, 117, 14201-14243.
82. J. K. Laha, S. Sharma, R. A. Bhimpuria, N. Dayal, G. Dubey and P. V. Bharatam, *New J. Chem.*, **2017**, 41, 8791-8803.
83. T. Javorskis and E. Orentas, *J. Org. Chem.*, **2017**, 82, 13423-13439.
84. Y. Wang, L. Zheng and T. R. Hoye, *Org. Lett.*, **2018**, 20, 7145-7148.
85. A. R. P. Henderson, J. R. Kosowan and T. E. Wood, *Can. J. Chem.*, **2017**, 95, 483-504.
86. K. Selvaraj and K. C. K. Swamy, *J. Org. Chem.*, **2018**, 83, 15043-15056.
87. Y. Shen, Q. Li, G. Xu and S. Cui, *Org. Lett.*, **2018**, 20, 5194-5197.
88. P. P. Onys'ko, O. A. Suvalova, Y. V. Rassukana, T. I. Chudakova and A. D. Sinitsa, *Tetrahedron Lett.*, **2003**, 44, 1855-1857.
89. S. S. Michaelidou and P. A. Koutentis, *Tetrahedron*, **2010**, 66, 3016-3023.
90. Y. Zhu, S. Wen, G. Yin, D. Hong, P. Lu and Y. Wang, *Org. Lett.*, **2011**, 13, 3553-3555.
91. S. Swaminathan and K. V. Narayanan, *Chem. Rev.*, **1971**, 71, 429-438.

92. F. Zhou, X. Liu, N. Zhang, Y. Liang, R. Zhang, X. Xin and D. Dong, *Org. Lett.*, **2013**, 15, 5786-5789.
93. F. Zhou, N. Zhang, X. Xin, X. Zhang, Y. Liang, R. Zhang and D. Dong, *RSC Adv.*, **2014**, 4, 18198-18204.
94. H. Tsuchikawa, Y. Maekawa and S. Katsumura, *Org. Lett.*, **2012**, 14, 2326-2329.
95. Y. Maekawa, T. Sakaguchi, H. Tsuchikawa and S. Katsumura, *Tetrahedron Lett.*, **2012**, 53, 837-841.
96. X. Liu, N. Zhang, J. Yang, Y. Liang, R. Zhang and D. Dong, *J. Org. Chem.*, **2013**, 78, 3323-3328.
97. A. Stukalov, V. V. Suslonov and M. A. Kuznetsov, *Eur. J. Org. Chem*, **2018**, 1634-1645.
98. S. G. Jarboe, M. S. Terrazas and P. Beak, *J. Org. Chem.*, **2008**, 73, 9627-9632.
99. S. S. K. Boominathan, G. C. Senadi, J. K. Vandavasi, J. Y.-F. Chen and J.-J. Wang, *Chem. – Eur. J*, 2015, **21**, 3193-3197.
100. A. Diallo, Y.-L. Zhao, H. Wang, S.-S. Li, C.-Q. Ren and Q. Liu, *Org. Lett.*, **2012**, 14, 5776-5779.
101. T. Narender, S. Sarkar, K. Rajendar and S. Tiwari, *Org. Lett.*, **2011**, 13, 6140-6143.
102. G. G. Rajeshwaran and A. K. Mohanakrishnan, *Org. Lett.*, **2011**, 13, 1418-1421.
103. P. Xie, Y. Huang and R. Chen, *Chem. – Eur. J*, **2012**, 18, 7362-7366.
104. S. Miaskiewicz, B. Gaillard, N. Kern, J.-M. Weibel, P. Pale and A. Blanc, *Angew. Chem. Int. Ed.*, **2016**, 55, 9088-9092.
105. F. Sirindil, J.-M. Weibel, P. Pale and A. Blanc, *Org. Lett.*, **2019**, 21, 5542-5546.
106. R. Fujita, K. Watanabe, W. Ikeura, Y. Ohtake, H. Hongo, Y. Harigaya and H. Matsuzaki, *Tetrahedron*, **2001**, 57, 8841-8850.
107. S.-S. P. Chou, H.-C. Wang, P.-W. Chen and C.-H. Yang, *Tetrahedron*, **2008**, 64, 5291-5297.
108. R. Hodgson, A. Kennedy, A. Nelson and A. Perry, *Synlett*, **2007**, 1043-1046.
109. D. G. Stark, L. C. Morrill, P.-P. Yeh, A. M. Z. Slawin, T. J. C. O'Riordan and A. D. Smith, *Angew. Chem. Int. Ed.*, **2013**, 52, 11642-11646.
110. D. G. Stark, T. J. C. O'Riordan and A. D. Smith, *Org. Lett.*, **2014**, 16, 6496-6499.
111. M. D. Mertens, M. Pietsch, G. Schnakenburg and M. Gütschow, *J. Org. Chem.*, **2013**, 78, 8966-8979.
112. Z. Fu, K. Jiang, T. Zhu, J. Torres and Y. R. Chi, *Angew. Chem. Int. Ed.*, **2014**, 53, 6506-6510.
113. L. Hao, X. Chen, S. Chen, K. Jiang, J. Torres and Y. R. Chi, *Org. Chem. Front.*, **2014**, 1, 148-150.
114. L. Xie, X. Zhen, S. Huang, X. Su, M. Lin and Y. Li, *Green. Chem.*, **2017**, 19, 3530-3534.
115. L. Wang, C. Lu, Y. Yue and C. Feng, *Org. Lett.*, **2019**, 21, 3514-3517.
116. M. Korb and H. Lang, *Chem. Soc. Rev,*, 2019, **48**, 2829-2882.
117. J. P. H. Charmant, A. M. Dyke and G. C. Lloyd-Jones, *Chem. Commun.*, **2003**, 380-381.
118. A. M. Dyke, D. M. Gill, J. N. Harvey, A. J. Hester, G. C. Lloyd-Jones, M. P. Muñoz and I. R. Shepperson, *Angew. Chem. Int. Ed.*, **2008**, 47, 5067-5070.
119. S. Braverman and Y. Duar, *Tetrahedron*, **1990**, 46, 2975-2990.
120. R. Huisgen and J. Sauer, *Chem. Ber.*, **1959**, 92, 192-202.
121. R. Schwesinger and H. Schlemper, *Angew. Chem. Int. Ed. in English*, **1987**, 26, 1167-1169.
122. R. Kargbo, Y. Takahashi, S. Bhor, G. R. Cook, G. C. Lloyd-Jones and I. R. Shepperson, *J. Am. Chem. Soc*, **2007**, 129, 3846-3847.
123. K. Barta, G. Franciò, W. Leitner, G. C. Lloyd-Jones and I. R. Shepperson, *Adv. Synth. Catal.*, **2008**, 350, 2013-2023.
124. X.-H. Xu, X. Wang, G.-k. Liu, E. Tokunaga and N. Shibata, *Org. Lett.*, **2012**, 14, 2544-2547.
125. S. Yoshida, K. Uchida, K. Igawa, K. Tomooka and T. Hosoya, *Chem. Commun.*, **2014**, 50, 15059-15062.
126. K. Uchida, S. Yoshida and T. Hosoya, *Synthesis*, **2016**, 48, 4099-4109.
127. T. Morita, S. Yoshida, M. Kondo, T. Matsushita and T. Hosoya, *Chem. Lett.*, **2016**, 46, 81-84.
128. C. Hall, J. L. Henderson, G. Ernouf and M. F. Greaney, *Chem. Commun.*, **2013**, 49, 7602-7604.
129. X.-H. Xu, M. Taniguchi, A. Azuma, G. K. Liu, E. Tokunaga and N. Shibata, *Org. Lett.*, **2013**, 15, 686-689.
130. X.-H. Xu, M. Taniguchi, X. Wang, E. Tokunaga, T. Ozawa, H. Masuda and N. Shibata, *Angew. Chem. Int. Ed.*, **2013**, 52, 12628-12631.
131. Z. Zhao, J. Messinger, U. Schön, R. Wartchow and H. Butenschön, *Chem. Commun.*, **2006**, 3007-3009.
132. G. Werner and H. Butenschön, *Eur. J. Org. Chem*, **2012**, 3132-3141.
133. G. Jaouen and R. Dabard, *J. Organomet. Chem.*, **1974**, 72, 377-388.
134. G. Werner, C. W. Lehmann and H. Butenschön, *Adv. Synth. Catal.*, **2010**, 352, 1345-1355.
135. G. Werner and H. Butenschön, *Organometallics*, **2013**, 32, 5798-5809.
136. T. Okauchi, T. Teshima, K. Hayashi, N. Suetsugu and T. Minami, *J. Am. Chem. Soc*, **2001**, 123, 12117-12118.
137. F. M. Moghaddam and M. G. Dakamin, *Tetrahedron Lett.*, **2000**, 41, 3479-3481.
138. B. Das, P. Madhusudhan and B. Venkataiah, *J. Chem. Res.*, **2000**, 200-201.
139. F. M. Moghaddam, A. A. Hoor and M. G. Dekamin, *J. Sulf. Chem.*, **2004**, 25, 125-130.

140. G. A. Benson, P. J. Maughan, D. P. Shelly and W. J. Spillane, *Tetrahedron Lett.*, **2001**, 42, 8729-8731.
141. H. Sharghi and Z. Shahsavari-Fard, *Phosphorous, Sulfur, Silicon. Relat. Elem.*, **2005**, 180, 2491-2501.
142. H. Sharghi and Z. Shahsavari-Fard, *Helv. Chim.*, **2005**, 88, 42-52.
143. L. K. Crevatín, S. M. Bonesi and R. Erra-Balsells, *Helv. Chim.*, **2006**, 89, 1147-1157.
144. M. Cavazza and F. Pietra, *Tetrahedron Lett.*, **2003**, 44, 1895-1897.
145. W. Zhang, J. Chu, A. M. Cyr, H. Yueh, L. E. Brown, T. T. Wang, J. Pelletier and J. A. Porco, *J. Am. Chem. Soc.*, **2019**, 141, 12891-12900.
146. R. L. Atienza, H. S. Roth and K. A. Scheidt, *Chem. Sci.*, **2011**, 2, 1772-1776.
147. Y. Wang, R. Oriez, S. Kuwano, Y. Yamaoka, K. Takasu and K. Yamada, *J. Org. Chem.*, **2016**, 81, 2652-2664.
148. Y. Wang, R. Oriez, S. Ou, Y. Miyakawa, Y. Yamaoka, K. Takasu and K. Yamada, *Heterocycles*, **2017**, 95, 314-321.
149. C. Lu and X. Lu, *Tetrahedron*, **2004**, 60, 6575-6579.
150. C. S. Hampton and M. Harmata, *Org. Lett.*, **2014**, 16, 1256-1259.
151. C. S. Hampton and M. Harmata, *J. Org. Chem.*, **2015**, 80, 12151-12158.
152. B. Yuan, R. He, W. Shen, Y. Xu, X. Liu and M. Li, *ChemistrySelect*, **2016**, 1, 2971-2978.
153. A. L. Krasovsky, S. V. Druzhinin, V. G. Nenajdenko and E. S. Balenkova, *Tetrahedron Lett.*, **2004**, 45, 1129-1132.
154. G. Groszek, S. Błażej, A. Brud, D. Świerczyński and T. Lemek, *Tetrahedron*, **2006**, 62, 2622-2630.
155. A. E. Reed and P. v. R. Schleyer, *J. Am. Chem. Soc.*, **1990**, 112, 1434-1445.
156. D. V. Sevenard, A. A. Kolomeitsev, B. Hoge, E. Lork and G.-V. Röschenthaler, *J. Am. Chem. Soc.*, **2003**, 125, 12366-12367.
157. Y. Lou, T. P. Remarchuk and E. J. Corey, *J. Am. Chem. Soc.*, **2005**, 127, 14223-14230.
158. R. A. Weatherhead-Kloster, Corey, E. J., *Org. Lett.*, **2005**, 8, 171-174.
159. H. Yang, R. G. Carter and L. N. Zakharov, *J. Am. Chem. Soc.*, **2008**, 130, 9238-9239.
160. H. Yang and R. G. Carter, *J. Org. Chem.*, **2010**, 75, 4929-4938.
161. E. Moreno-Clavijo, A. T. Carmona, H.-U. Reissig, A. J. Moreno-Vargas, E. Alvarez and I. Robina, *Org. Lett.*, **2009**, 11, 4778-4781.
162. A. Quintard and A. Alexakis, *Chem. – Eur. J*, **2009**, 15, 11109-11113.
163. A. Quintard and A. Alexakis, *Org. Biomol. Chem.*, **2011**, 9, 1407-1418.
164. N. Bravo, A.-N. R. Alba, G. Valero, X. Companyó, A. Moyano and R. Rios, *New J. Chem.*, **2010**, 34, 1816-1820.
165. T. Okino, Y. Hoashi and Y. Takemoto, *J. Am. Chem. Soc.*, **2003**, 125, 12672-12673.
166. M.-Y. Chang, Y.-C. Cheng and Y.-J. Lu, *Org. Lett.*, **2014**, 16, 6252-6255.
167. K. Lu, F. Ding, L. Qin, X. Jia, C. Xu, X. Zhao, Q. Yao and P. Yu, *Chem. – Eur. J.*, **2016**, 11, 2121-2125.
168. H. Wang, R. K. Kumar, Y. Yu, L. Zhang, Z. Liu, P. Liao and X. Bi, *Chem. – Eur. J.*, **2016**, 11, 2841-2845.
169. X. Zhao, Y. Huang, F.-L. Qing and X.-H. Xu, *RSC Adv.*, **2017**, 7, 47-50.
170. Y.-Z. Chen, T. Liu, J. Zhu, H. Zhang and L. Wu, *Org. Chem. Front.*, **2018**, 5, 3567-3573.
171. L.-X. Shao, Y.-P. Zhang, M.-H. Qi and M. Shi, *Org. Lett.*, **2007**, 9, 117-120.

Chapter 2

Results & Discussion

[3+2] Dipolar Cycloadditions of α-Thio-β-Chloroacrylamides

Contents

2.1. Introduction 117
2.1.1. Project Background – Discovery of the α-Thio-β-Chloroacrylamide Reaction Cascade 117
2.1.2. Project Background – The Synthetic Utility of α-Thio-β-Chloroacrylamides 122
2.1.3. Project Background – The Importance of the Pyrazole Moiety 129
2.2. Project Objectives – The Synthesis of Densely Functionalised Pyrazoles 131
2.3. Generation of the Dipolarophile – Synthesis of the α-Sulfenyl- and α-Sulfinyl-β-Chloroacrylamide Scaffolds 133
2.3.1. Overview of Synthetic Approach 133
2.3.2. Preparation of α-Chloroamides 134
2.3.3. Preparation of α-Thioamides 135
2.3.4. Preparation of α-Thio-β-Chloroacrylamides 137
2.3.5. Synthesis of α-Thio-β-Chloroacrylate 142
2.3.6. Synthesis of α-Thio-β-Chlorothioester 144
2.3.7. Preparation of α-Sulfinyl-β-Chloroacrylamides 148
2.4. Generation of 1,3-Dipoles 151
2.4.1. Preparation of α-Diazosulfones 151
2.4.2. Preparation of *N*-Benzyl-α-Diazoacetamide 157
2.5. [3+2] Dipolar Cycloadditions 158
2.5.1. [3+2] Dipolar Cycloadditions α-Diazosulfones 158
2.5.2. [3+2] Dipolar Cycloadditions of α-Diazoacetates with α-Thio-β-Chloroacrylamides 163
2.5.3. [3+2] Dipolar Cycloadditions of α-Diazoacetates with α-Sulfinyl-β-Chloroacrylamides 171
2.5.4. [3+2] Dipolar Cycloadditions of α-Diazoacetates with α-Sulfonyl-β-Chloroacrylamides 176
2.5.5. [3+2] Dipolar Cycloaddition of *N*-Benzyl-α-Diazoacetamide 183
2.6. Spectroscopic Determination of the Tautomeric Composition of 3,4,5-Substituted Pyrazoles 184
2.7. Further Derivatisation of the Pyrazole Scaffold 190
2.8. Conclusions 192
2.9. Experimental 194
2.9.1. General Procedures 194
2.9.2. Synthesis of α-Chloroamides 195
2.9.3. Synthesis of α-Thioamides 197
2.9.4. Synthesis of α-Thio-β-Chloroacrylamides 201
2.9.5. Synthesis of 2,3,3-Trichloro-2-(phenylthio)-*N*-(4-methylphenyl)propanamide 206
2.9.6. Synthesis of α-Thio-β-Chloroacrylate 206
2.9.7. Synthesis of α-Thio-β-Chlorothioester 207
2.9.8. Synthesis of α-Sulfinyl- β-Chloroacrylamides 208
2.9.9. Synthesis of 1,3-Dipoles 212
2.9.9.1. Synthesis of α-Diazomethyl Phenylsulfone 212
2.9.9.2. Synthesis of Tosyl Diazomethane 213
2.9.9.3. Synthesis of *N*-Benzyl-α-Diazoacetamide 215
2.9.10. [3+2] Dipolar Cycloadditions 216
2.9.10.1. [3+2] Dipolar Cycloadditions of α-Diazosulfones 216
2.9.10.2. [3+2] Dipolar Cycloadditions of α-Diazoacetates with α-Thio-β-Chloroacrylamides 218
2.9.10.3. [3+2] Dipolar Cycloadditions of α-Diazoacetates with α-Sulfinyl-β-Chloroacrylamides 226
2.9.10.4. [3+2] Dipolar Cycloadditions of α-Diazoacetates with α-Sulfonyl-β-Chloroacrylamides 231
2.9.10.5. [3+2] Dipolar Cycloaddition of *N*-Benzyl-α-Diazoacetamide 236
2.9.11. Synthesis of the α-Sulfonyl-β-Chloroacrylamide of the Weinreb amide 237
2.9.12. Synthesis of 3-Ethyl 4,5-Dimethyl 1*H*-Pyrazole-3,4-5-Tricarboxylate 238
2.9.13. Derivatisation of the Pyrazole Scaffold 239
Bibliography 246

2.1 Introduction

The focus of this work was to utilise [3+2] dipolar cycloaddition methodology for the synthesis of structurally diverse sulfur containing pyrazole derivatives. Specifically, this work investigates the use of electron deficient terminal α-diazocarbonyl compounds, and related α-diazosulfones, as functionalised 1,3-dipoles in conjunction with unique dipolarophilic scaffolds pioneered in our group, α-thio-β-chloroacrylamides, α-sulfinyl-β-chloroacrylamides and α-sulfonyl-β-chloroacrylamides. This introduction outlines firstly our group's initial discovery of the α-thio-β-chloroacrylamides including the elucidation of its complex reaction mechanism via a *N*-chlorosuccinimide mediated chlorination cascade. Secondly, the synthetic application of these compounds is described, highlighting their considerable synthetic potential, with particular emphasis afforded to their application in the synthesis of heterocyclic scaffolds.

2.1.1 Project background – Discovery of the α-Thio-β-Chloroacrylamide Reaction Cascade

In 1993, the γ-lactam **1** was required as part of a synthetic research programme in our laboratory **(Scheme 2.1)**.[1] A retrosynthetic analysis of this target identified the α-chloroamide **2** as a suitable precursor that could undergo intramolecular electrophilic aromatic substitution in the presence of a Lewis acid catalyst.

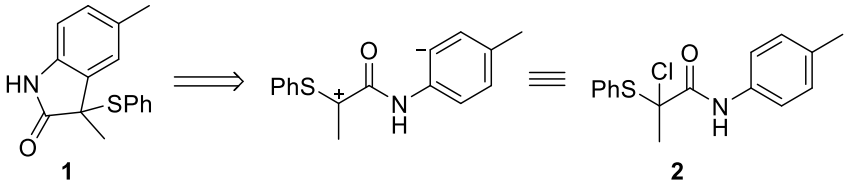

Scheme 2.1: Retrosynthetic analysis of γ-lactam **1**

Indeed, McKervey *et al*. had previously reported the intermolecular electrophilic aromatic alkylation between *p*-hydroxy dihydrocinnamate **3** and methyl-2-(butylthio)propanoate **4** in the presence of zinc chloride to give the γ-lactone **5 (Scheme 2.2)**.[2-3] With this in mind, attention turned to the generation of α-chloroamide **2**.

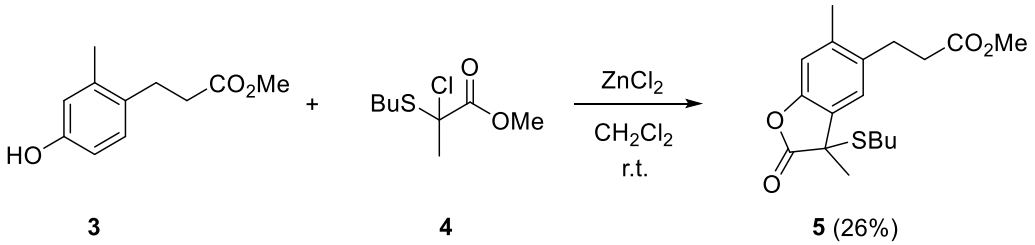

Scheme 2.2: Intermolecular electrophilic aromatic alkylation using α-chloroester **4**

The α-chlorination of sulfides with numerous chlorinating agents is described, with the use of *N*-chlorosuccinimide (NCS) particularly attractive due to its ease of handling and facile removal of the reaction by-product succinimide.[4-5] Consequently, NCS was initially screened to chlorinate α-thioamide **6**, however, in addition to the formation of the expected α-chloroamide **2**, a much more

complex reaction pathway was uncovered **(Scheme 2.3)**, with the stereoselective formation of the α-thio-β-chloroacrylamide **9** of particular interest.[6-7]

As illustrated in **Scheme 2.3**, it was established that careful control of the reaction parameters could be utilised to obtain a variety of products with significant synthetic potential. For example, the original α-chloroamide **2** of interest, was formed exclusively when the α-thioamide **6** was treated with one equivalent of NCS in carbon tetrachloride at 0°C. Further investigations led to the observation that at room temperature, after 24 h, the same amount of NCS gave an essentially equimolar mixture of α-chloroamide **2** and acrylamide **7**. When the number of equivalents of NCS was increased to two, under otherwise identical reaction conditions, the major compound formed was the dichloride **8**, although minor amounts of the acrylamide **7** were also present. Most interestingly, is that when this crude reaction mixture was treated with an excess of zinc chloride in a mixture of nitromethane/dichloromethane two major products were observed and isolated, the α-thio-β-chloroacrylamide **9** and α,β-dithioacrylamide **10**.

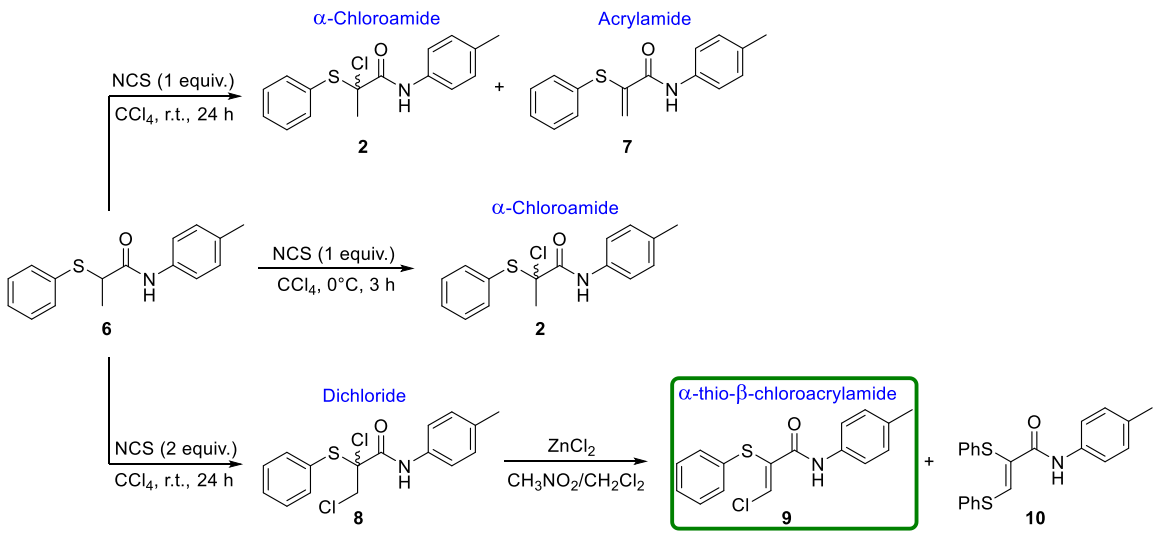

Scheme 2.3: Initial observation of the unexpected NCS mediated highly stereoselective formation of α-thio-β-chloroacrylamide **9**

The serendipitous discovery of α-thio-β-chloroacrylamide **9** attracted our group's attention as a synthetically versatile intermediate, potentially undergoing a range of different transformations depending on the reaction conditions. Ultimately, these compounds were considered to be potentially valuable highly functionalised acrylamide derivatives, bearing an exceptionally electrophilic β-carbon due to the combined electron-withdrawing character of the amide and chlorine moieties. Accordingly, a range of synthetically powerful reaction pathways were envisaged with these highly functionalised derivatives including Diels–Alder cycloadditions,[8] [3+2] dipolar cycloadditions,[9-10] sulfur oxidation,[11-13] and nucleophilic substitution[14] amongst many others. These transformations will be discussed in detail in **Section 2.1.2**.

Accordingly, an extensive programme of research has been undertaken within our group to optimise the yield of this transformation, explore its scope and investigate the mechanism of this unexpected transformation. The single-step transformation of α-thioamides to α-thio-β-chloroacrylamides has since been optimised within the group for a wide range of substituents, offering a simple stereoselective route to the novel β-chloroacrylamides in good yields and purities **(Scheme 2.4)**.[7, 15-16]

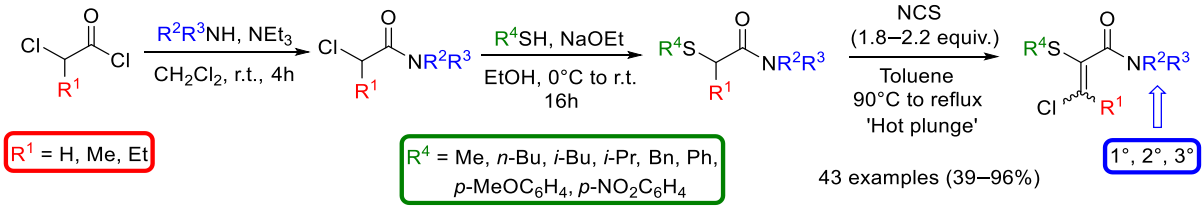

Scheme 2.4: Previously optimised batch synthesis of α-thio-β-chloroacrylamides

Notably, the single step one-pot transformation of α-thioamides to α-thio-β-chloroacrylamides converts an unreactive sp^3 hybridised β-carbon to a highly activated sp^2 hybridised β-carbon with excellent stereocontrol and significant synthetic potential. As a result, the reaction mechanism of this stereoselective transformation has been extensively investigated within our group **(Scheme 2.5)**.

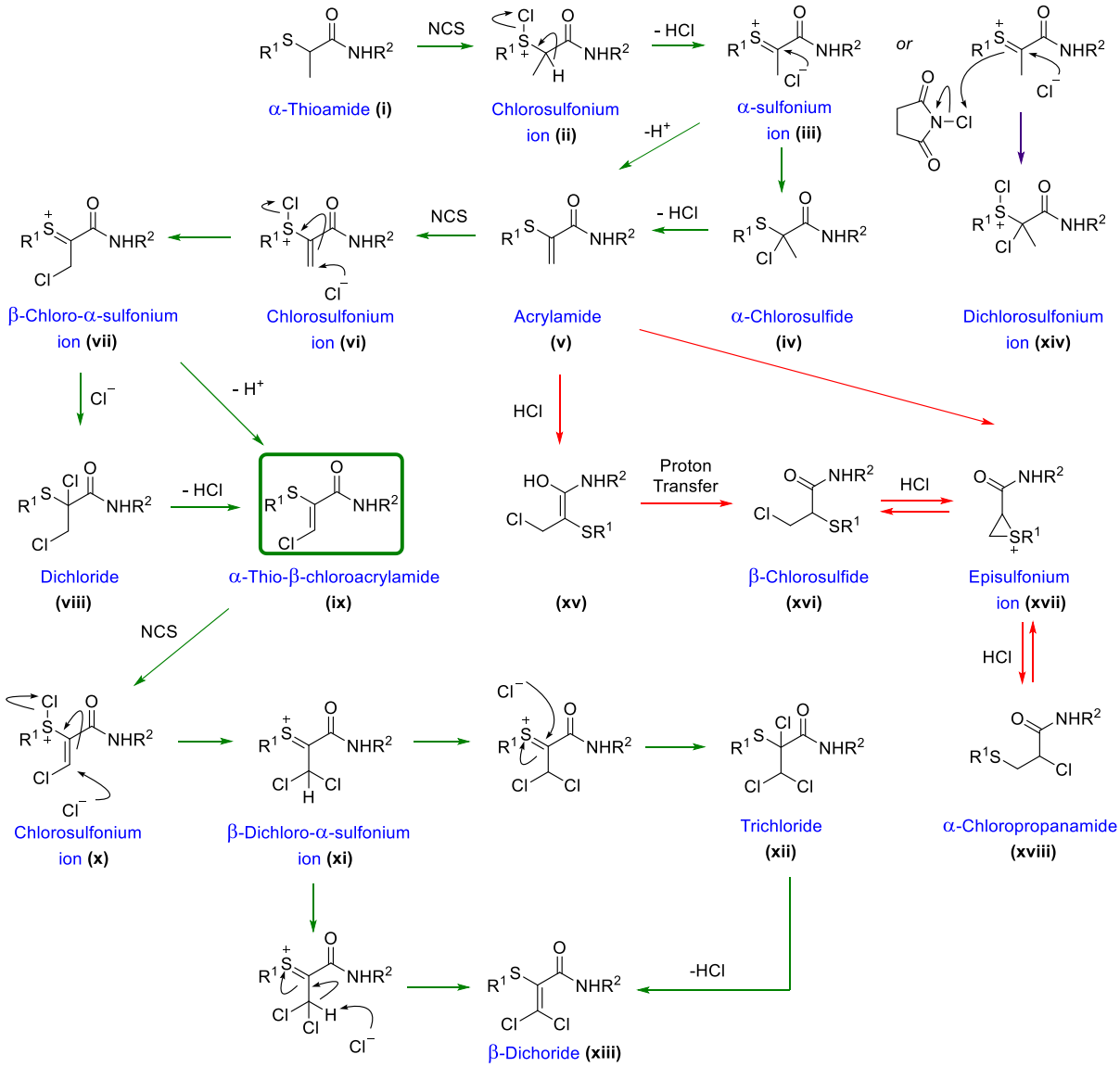

Scheme 2.5: Overview of NCS mediated chlorination pathway of α-thioamides. Mechanistic pathway highlighted in green determined by Murphy *et al.*,[7, 15] mechanistic pathway highlighted in purple determined by Foley *et al.*,[17] and mechanistic pathway highlighted in red determined by Cacheux *et al.*[18]

Chlorination of the α-thioamide **(i)** by the first equivalent of NCS generates the chlorosulfonium ion **(ii)**, which readily undergoes 1,2-elimination of hydrogen chloride to generate the resulting sulfur stabilised cation **(iii)**. Subsequent nucleophilic addition of chloride at the α-position of **(iii)** generates the α-chlorosulfide **(iv)**. A second elimination of hydrogen chloride forms the acrylamide **(v)**. A second equivalent of NCS chlorinates the sulfur substituent on the acrylamide **(v)** generating the chlorosulfonium ion **(vi)**. With no α-proton available to trigger elimination of hydrogen chloride, nucleophilic addition of chloride at the β-position occurs promoting chloride elimination to form the β-chloro-α-sulfonium ion **(vii)**. Further chloride addition at the α-position of **(vii)** generates the dichloride **(viii)**, with subsequent elimination of hydrogen chloride producing the α-thio-β-chloroacrylamide **(ix)** in a stereoselective manner. The α-thio-β-chloroacrylamide **(ix)** can also be generated directly through deprotonation of the β-chloro-α-sulfonium ion **(vii)**. Through careful tailoring of the reaction conditions to enhance the formation of a particular compound in the cascade, each of the intermediates **(iv)**, **(v)**, **(viii)** and **(xiii)** has been isolated and identified.[7, 15]

In the presence of an additional equivalent of NCS further chlorination of the α-thio-β-chloroacrylamide scaffold can occur to generate the chlorosulfonium ion **(x)**. Addition of chloride at the β-carbon promotes elimination of chloride to form the β-dichloro-α-sulfonium ion **(xi)**. Subsequent chloride addition at the α-carbon generates the trichloride **(xii)**. It is plausible that elimination of HCl from the trichoride **(xiii)** could form the more stable β-dichloride **(xiii)**. Alternatively, abstraction of a proton on the β-carbon of **(xi)** can be envisaged, leading to the β-dichloride **(xiii)**. To date the trichloride **(xii)** has not been isolated pure and has only been tentatively assigned.

Subsequent studies by Foley *et al*. using ^{1}H ReactNMR and ReactIR *in situ* monitoring enabled direct observation of each of the intermediates in the α-thio-β-chloroacrylamide cascade pathway, including those that had proved too labile to isolate.[17] Notably, this work highlighted the formation of a previously unobserved reaction byproduct when the reaction was carried out in carbon tetrachloride at 25°C, namely the dichlorosulfonium ion **12** [**Figure 2.1** and **Scheme 2.5 (xiv)**]. Interestingly, once formed the dichlorosulfonium ion **12** does not undergo further transformations and hence is a competitive pathway that is a reaction 'cul-de-sac' that has implications in terms of yield reduction.

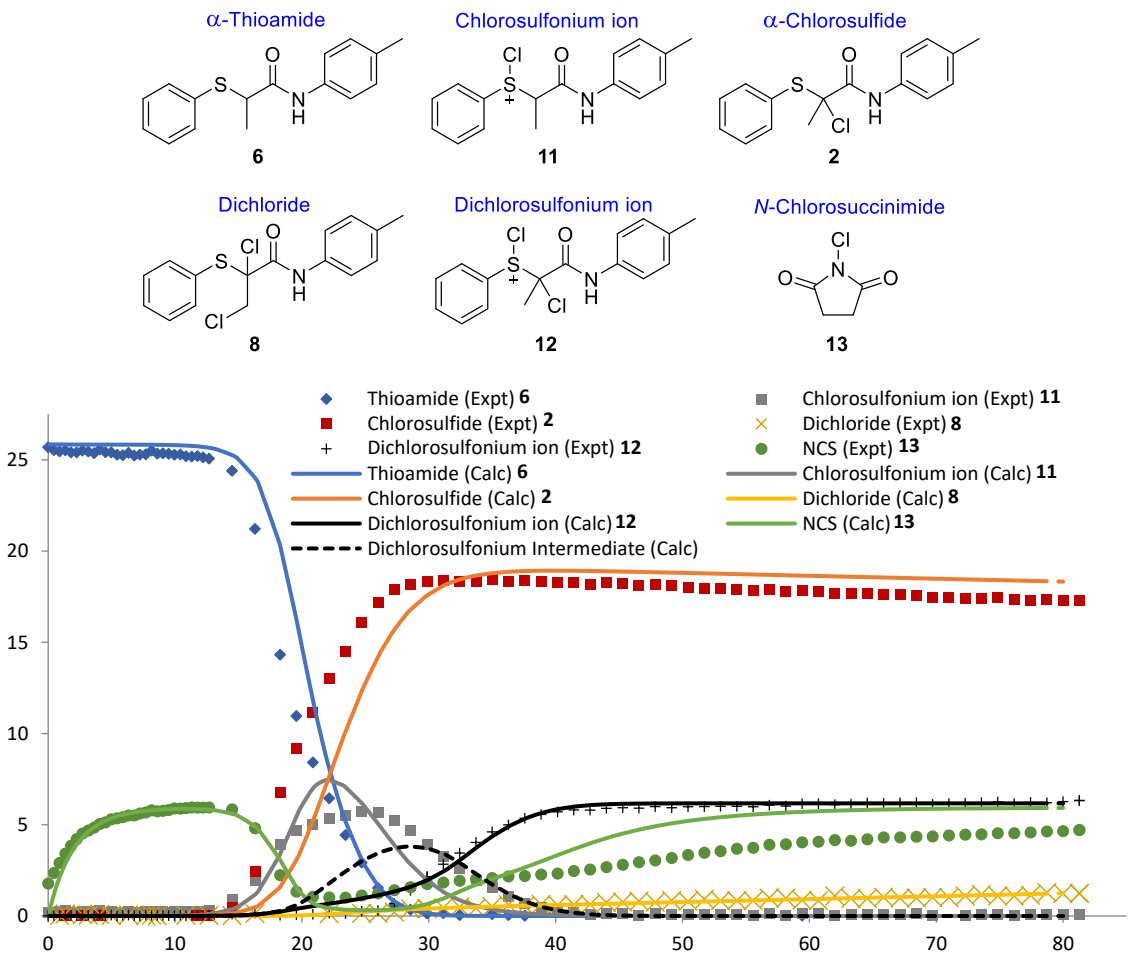

Figure 2.1: Reaction profile of NCS mediated transformation of α-thioamide **6** in carbon tetrachloride at 25°C using React NMR technology. Experimental data are displayed as symbols and the corresponding computationally optimised data are displayed as solid lines. Figure reproduced from reference.[17]

Synthetically important was the observation that the chlorosulfonium ion **11** and dichlorosulfonium ion **12** were only detectable when the reaction was carried out in carbon tetrachloride, but not in toluene-d_8 or acetonitrile-d_3.[17] Therefore, the rate of hydrogen chloride elimination and the subsequent elimination step is solvent dependant, presumably due to differences in solvent polarity. It is postulated that in carbon tetrachloride that the α-sulfonium ion **(iii)** undergoes an additional reaction with NCS to form the dichlorosulfonium ion **(xiv) (Scheme 2.5)**. In addition, it should be noted that an elevation of temperature to 40°C was determined to be necessary to promote hydrogen chloride elimination from the dichloride **(vii)** to form the desired α-thio-β-chloroacrylamide **(ix)**.[17]

Cacheux also demonstrated that the acrylamide intermediate **(v)** can be used to access β-chlorosulfides **(xvi)** with careful control of the reaction conditions **(Scheme 2.5)**.[18] Using 1.1 equivalent of NCS in carbon tetrachloride (or in certain instances toluene) at room temperature the α-thioamide **(i)** is converted to a mixture of the acrylamide **(v)** and β-chlorosulfide **(xvi)**, however, these compounds proved inseparable by column chromatography. While the mechanism of this transformation is not known, and requires further investigation, Cacheux hypothesised that any potential mechanism would utilise the acrylamide **(v)** as the starting point. Accordingly, two mechanisms have been proposed. Firstly, addition of *in situ* generated hydrochloric acid to the acrylamide **(v)** could directly produce the

β-chlorosulfide **(xvi)**. Alternatively (or in addition), the mechanism could proceed via an episulfonium ion intermediate **(xvii)** formed by attack of the electron rich sulfur atom. Subsequent ring-opening by attack at the terminal carbon gives the anti-Markovnikov β-chlorosulfide **(xvi)**. Interestingly, the Markovnikov product, α-chloro-β-thiopropanamide **(xviii)**, was also observed in this work, highlighting the likelihood of an episulfonium ion intermediate.

As mentioned above, the protocol for the batch synthesis of α-thio-β-chloroacrylamides has been previously optimised within our group **(Scheme 2.4)**. Notably, it was found that a 'hot plunge' was crucial in ensuring the efficiency of the NCS mediated chlorination cascade.[7] According to this method, immediately following the addition of NCS, the reaction vessel was plunged into a pre heated oil bath at the requisite temperature. By doing so, rapid heating of the reaction mixture could be ensured, which allows optimal transformation of the α-thioamide **6**, to the acrylamide **7**, the dichloride **8** and finally the α-thio-β-chloroacrylamide **9** (see **Scheme 2.5**). Although this protocol performs well, giving 91% yield on a ca. 5g scale, the rapid heating required limits the scalability of the transformation. With poor heat transfer, less rapid transformation of intermediates occurs, giving rise to elongated reaction times and/or higher recovery of intermediates, which consequently reduces the yield of the reaction. Considering this Dennehy *et al*. investigated the use of continuous flow processing as an alternative means of scale up for the α-thio-β-chloroacrylamide cascade, due to its improved capacity for excellent temperature control.[19] Following optimisation, continuous flow processing was successfully applied to the transformation of α-thioamide **6** to α-thio-β-chloroacrylamide **9** on a 30 g scale **(Scheme 2.6)**. Advantageously, this method obviates the need for chromatography and affords the final product **9** on more than three times the scale that can be obtained in batch over the same reaction time.

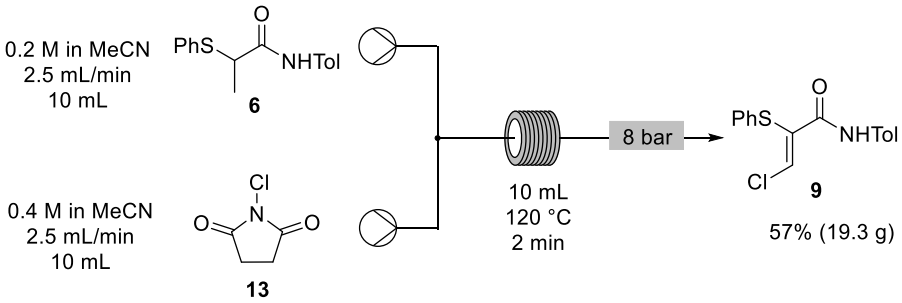

Scheme 2.6: Optimised scale-up of NCS mediated chlorination of α-thioamide **6** using continuous flow processing

2.1.2 Project background – The Synthetic Utility of α-Thio-β-Chloroacrylamides

α-Thio-β-chloroacrylamides are a synthetically versatile, highly functionalised class of compounds that can undergo a large range of transformations due to the electronic character of their substituents. Particularly important is the combined electronic effects of the amide and chloride groups, that in addition lead to an exceptionally potent electrophilic β-carbon. Due to the rich functionality incorporated on the α-thio-β-chloroacrylamide scaffold several synthetically useful reaction pathways can be envisaged, not limited to **a)** radical addition, **b)** 1,2-reduction, **c)** [3+2] dipolar cycloaddition,[9-10] **d)** Diels–Alder cycloaddition,[8] **e)** desulfurisation, **f)** reductive dichlorination, **g)** sulfur oxidation,[11-13] and **h)** addition-substitution **(Scheme 2.7)**.[14]

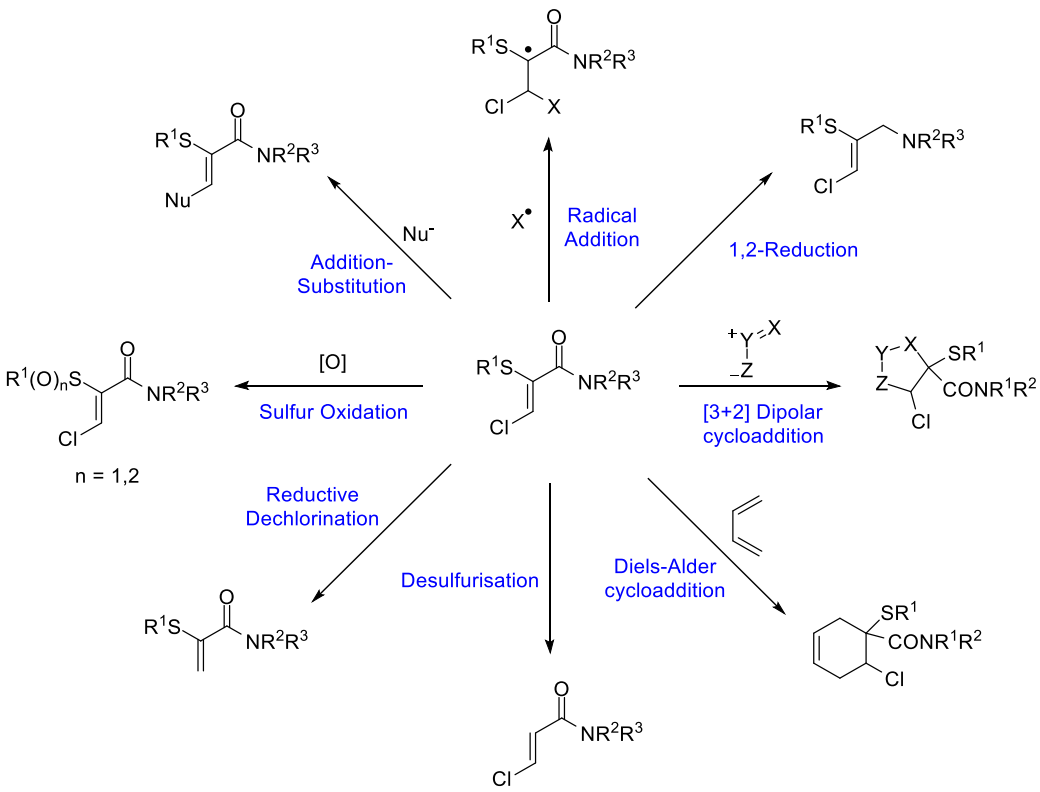

Scheme 2.7: Potential synthetic utility of the α-thio-β-chloroacrylamide scaffold

Murphy investigated the reactivity of the α-thio-β-chloroacrylamides as Michael acceptors in nucleophilic addition/substitution reactions. Conjugate addition readily occurs for a range of carbon, nitrogen, oxygen and sulfur based nucleophiles **(Scheme 2.8)**.[14-15] In most instances, the nucleophile replaces the chloro substituent to give mono substitution with retention of stereochemistry. Reaction with alkoxides, however, favour a second addition which leads to the generation of acetals. Chopra[20] and Kissane,[21] extended the scope of the nitrogen-based nucleophiles by exploring their reactivity with the sulfoxide and sulfone derivatives respectively. For nitrogen based nucleophiles, the stereochemistry of the resulting enamine derivatives is strongly dependent on the nature of the amine employed, the degree of sulfur oxidation of the β-chloroacrylamide as well as their substituents.[14, 20-21] Notably, of all the addition/substitution reactions investigated in our group it is only the enamine derivatives of the α-thio-β-chloroacrylamides that display a significant degree of interconversion between *E*- and *Z*-isomers, with the thermodynamic equilibrium depending on the derivatives substitution pattern. [14, 20-21]

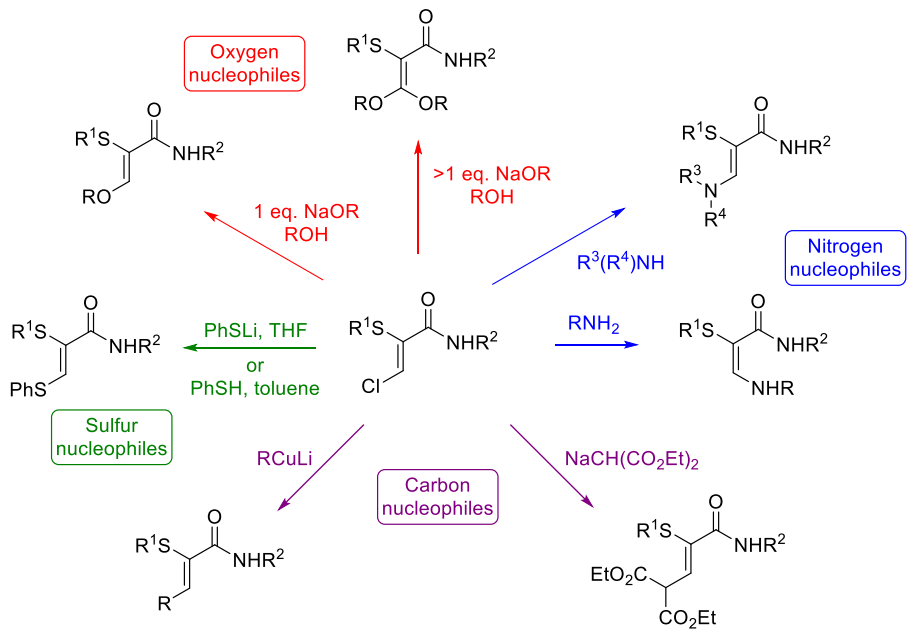

Scheme 2.8: Summary of nucleophilic addition/substitution reactions using oxygen, nitrogen, carbon and sulfur nucleophiles.

The synthetic potential of the sulfur moiety was initially explored by Murphy,[15] with chemoselective oxidation to the racemic sulfoxide readily achieved, a process subsequently optimised by Lynch **(Scheme 2.9)**.[12, 16] A number of synthetic methods for the enantioselective oxidation of the α-thio-β-chloroacrylamides were examined, including the Kagan and Bolm oxidations. Using titanium catalysis, Lynch demonstrated that the Kagan method affords moderate enantioselectivity (up to 53% *ee*).[16] Chopra subsequently demonstrated that the Bolm method, particularly when using vanadium catalysis in conjunction with Schiff base ligands, leads to improved enantioselectivities (up to 71% *ee*) for this family of sulfur compounds.[20] *m*CPBA was demonstrated to be the only oxidant to result in oxidation of the sulfoxide to the sulfone, however, isolation of analytically pure samples proved challenging due to instability attributable to their significant Michael acceptor character. Kissane circumvented this issue by adding morpholine to the crude sulfones, triggering an addition-substitution process to the β-amino derivatives which are readily isolable as pure compounds **(Scheme 2.9)**.[12, 21]

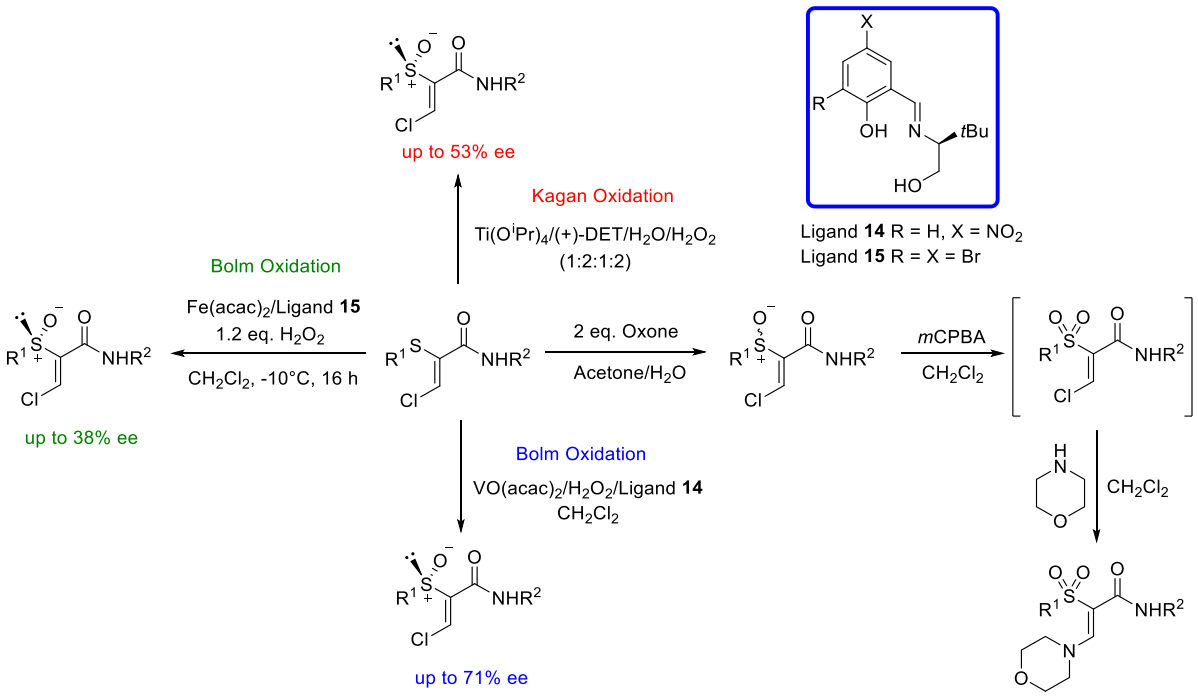

Scheme 2.9: Chemoselective and enantioselective oxidation of α-thio-β-chloroacrylamides

Kissane later investigated the diastereoselective sulfur oxidation of a range of α-thio-β-chloroacrylamide derivatives containing some simple chiral amide auxiliaries **(Scheme 2.10)**.[11, 21] Using Oxone® as oxidant in acetone and water at room temperature, diastereoselectivities of up to 53% *de* were achieved, with the highest levels of diastereoselection observed in systems constrained by intramolecular hydrogen bonding. The effect of amide auxiliary on diastereoselective sulfur oxidation is summarised in **Scheme 2.10**.

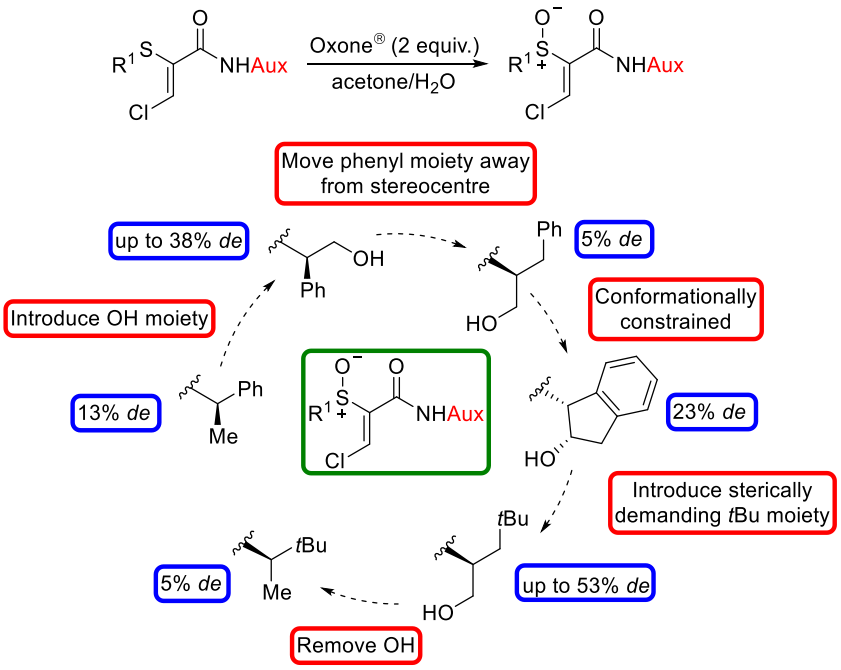

Scheme 2.10: Effect of amide auxiliary of diastereoselective oxidation of α-thio-β-chloroacrylamides

Kissane also demonstrated that diastereoselective sulfur oxidation of related α-thio-β-chloropropenyloxazolidin-2-ones occurs in modest diastereocontrol. However, via a combination of diastereoselective oxidation and subsequent kinetic resolution via selective oxidation of the minor sulfoxide **17b** to the sulfone **18**, diastereoselectivities of up to 94% *de* can be achieved **(Scheme 2.11)**.[13, 21]

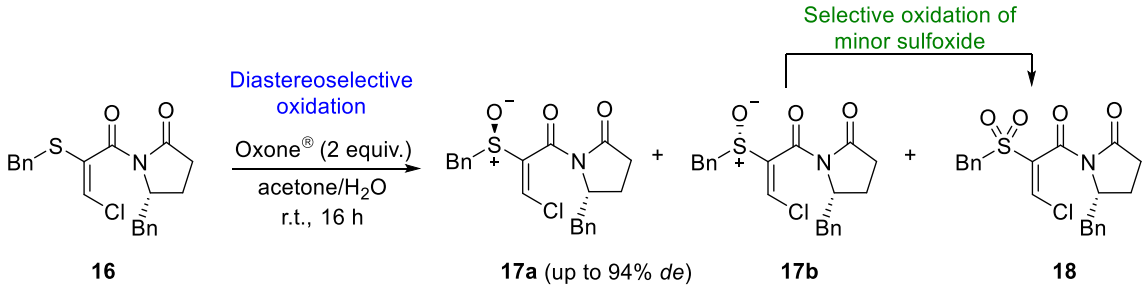

Scheme 2.11: Diastereoselective oxidation of (*E*)-**16** with subsequent kinetic resolution

A preliminary investigation by Murphy demonstrated that α-thio-β-chloroacrylamide **23**, containing an in-built oxygen-based nucleophile can undergo intramolecular addition-substitution to generate the oxathiin **25**.[15] Cacheux further optimised the generation of 1,4-oxathiin, demonstrating how Maguire's NCS mediated β-chlorination methodology can be used in the synthesis of biologically relevant heterocycles **(Scheme 2.12,** highlighted in red).[18] Similarly, the 1,4-thiazine can be generated using similar conditions **(Scheme 2.12,** highlighted in blue). Crucially, it was observed that unlike for the oxathiin series Boc protection of the amine was critical to generate the α-thioamide **27**. Extension of this methodology to benzothiazines and dithiins was unsuccessful.

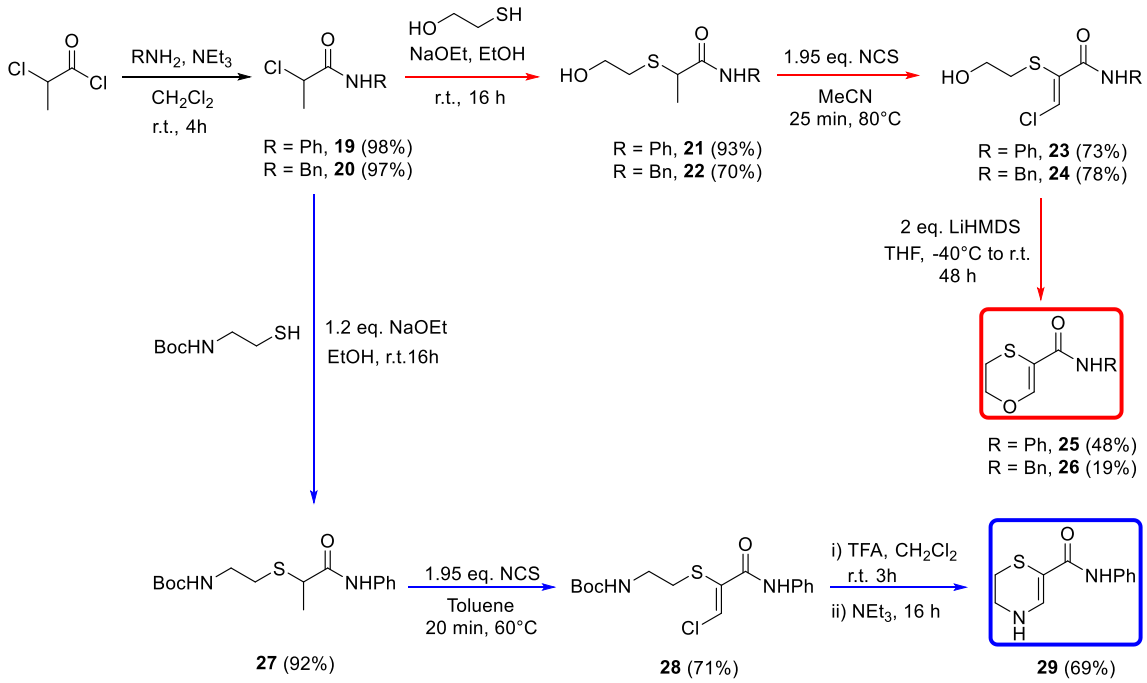

Scheme 2.12: 1,4-Oxathiin and 1,4-thiazine formation using NCS mediated chlorination cascade

Lynch explored the dienophilic character of the α-thio-β-chloroacrylamides in the Diels–Alder cycloaddition with cyclopentadiene **(Scheme 2.13)**.[8, 16] Initial attempts to achieve cycloaddition at the

sulfide oxidation level under thermal conditions proved unsuccessful. Activation of the α-thio-β-chloroacrylamide scaffold toward cycloaddition was achieved through oxidation to the sulfoxide derivatives, following which a mixture of two diastereomeric cycloadducts with negligible diastereoselectivity was observed under thermal conditions, albeit in good to excellent combined yields. Notably, the addition of Lewis acid catalysts, such as $CuCl_2$ or $Cu(OTf)_2$, was observed to improve the diastereoselectivity to synthetically useful ratios. Considering this, Lynch re-examined the cycloaddition with the sulfide derivatives in the presence of $CuCl_2$. Interestingly, although the cycloaddition occurred, albeit with prolonged reaction times, poor diastereoselectivity was observed indicating the importance of the sulfoxide moiety in establishing diastereoselective control.

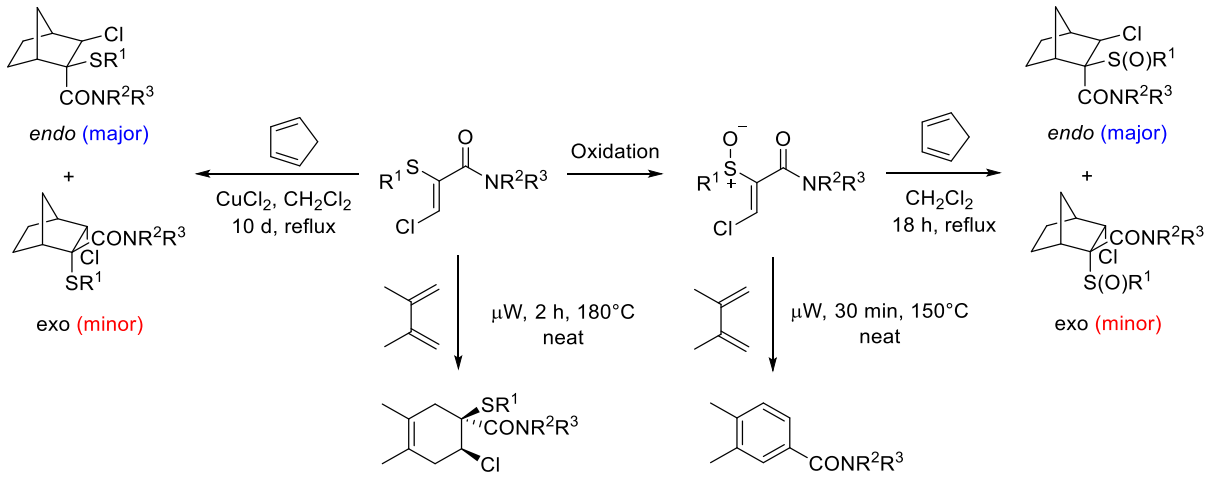

Scheme 2.13: Diels-Alder cycloadditions of α-sulfenyl- and α-sulfinyl-β-chloroacrylamides under thermal, catalytic and microwave conditions

Kissane, later attempted to extend this methodology to the acyclic diene 2,3-dimethyl-1,3-butadiene, however neither thermal conditions or Lewis acid catalysis proved successful.[8, 21] Interestingly, however, the microwave assisted Diels–Alder cycloaddition with α-sulfinyl-β-chloroacrylamides proved very successful, with complete conversion to the trisubstituted aromatic adducts observed **(Scheme 2.13)**. Extension to the less reactive sulfide derivatives using microwave conditions efficiently formed cyclohexene cycloadducts in synthetically useful yields.

Kissane explored the use of both α-thio-β-chloroacrylamides and α-sulfinyl-β-chloroacrylamides as dipolarophiles in [3+2] dipolar cycloadditions with benzonitrile oxide and nitrones.[10, 21] Notably, the cycloadditions with benzonitrile oxide **30** were highly regioselective, as well as being exceptionally stereoselective, with the isoxazoline cycloadducts obtained as a single diastereomer (**Scheme 2.14, a**). Cycloadditions with nitrone **31** and α-sulfinyl-β-chloroacrylamides were explored using both thermal and microwave conditions, with similar yields achieved under both conditions, however the microwave mediated reactions were advantageous due to significantly shorter reaction times. Interestingly, with this dipole, the major products are substituted piperidines, rather than the expected isoxazolidines **(Scheme 2.14, b)**.

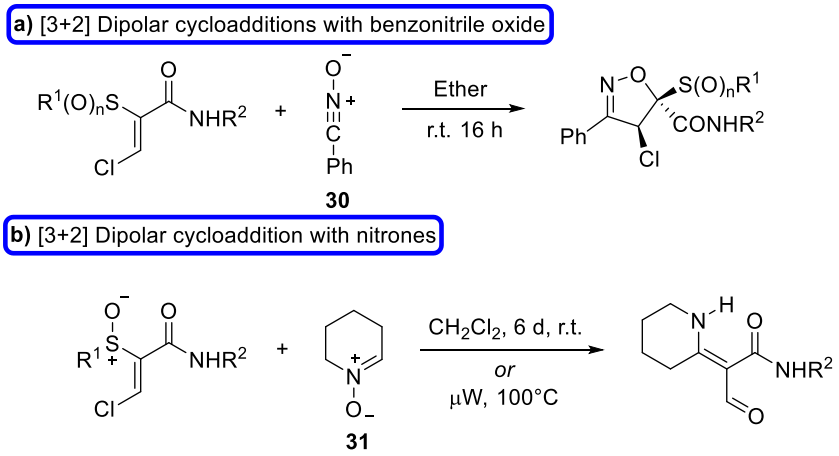

Scheme 2.14: [3+2] Dipolar cycloadditions with **a)** benzonitrile oxide and **b)** nitrones

Kissane investigated further the dipolarophilic behaviour of the α-thio-β-chloroacrylamides at both the sulfide and sulfoxide level towards the highly reactive diazoalkanes, namely diazoethane, diazomethane, trimethylsilyldiazomethane and phenyldiazomethane **(Scheme 2.15)**.[9, 21] Interestingly, the pyrazoline or pyrazole products isolated from the [3+2] dipolar cycloadditions were found to be dependent on a combination of factors including choice of dipole, the level of sulfur oxidation and the substituents on the α-thio-β-chloroacrylamide. In all instances, the cycloadditions proceeded in a highly regioselective manner, with the carbon terminus of the diazoalkane adding to the β-carbon of the β-chloroacrylamide. Particularly interesting, in several instances, was the observation that for pyrazoline cycloadducts, that were too unstable to isolate, the sulfinyl group eliminates while the sulfide group migrates, highlighting the main mechanistic difference between the sulfide and sulfoxide derivatives.

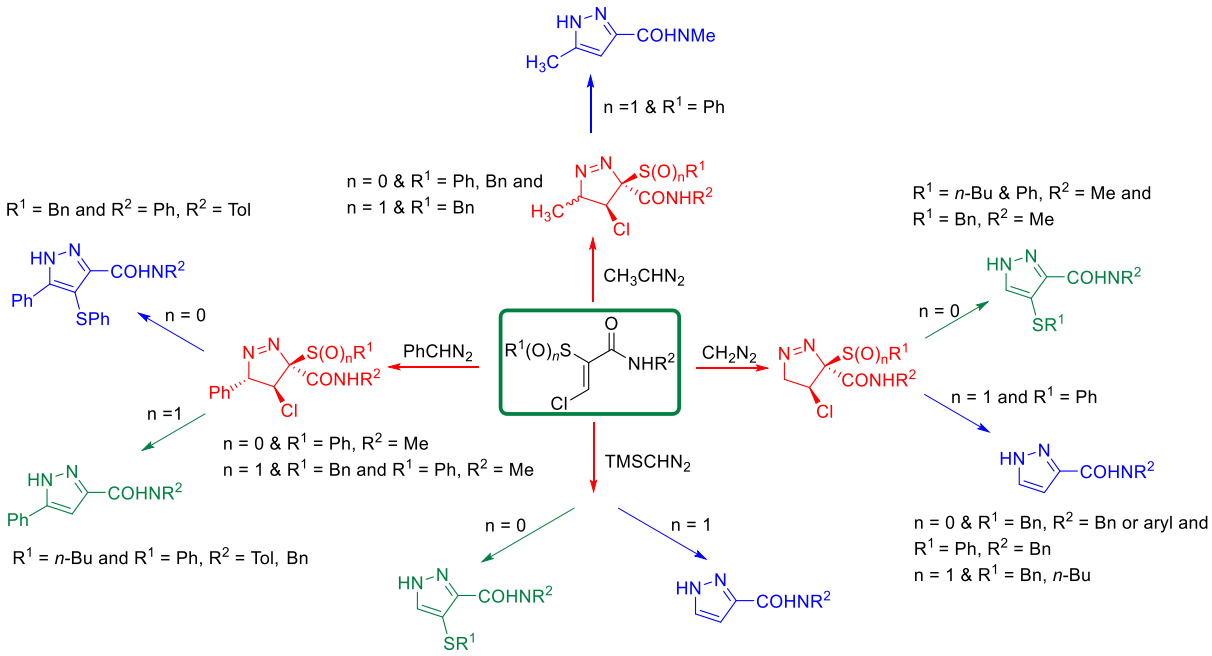

Scheme 2.15: [3+2] Dipolar cycloaddition of diazoalkanes with α-thio-β-chloroacylamides and α-sulfinyl-β-chloroacrylamides

For a more comprehensive overview of our group's portfolio of work on the stereoselective synthesis of α-thio-β-chloroacrylamides and investigation of their reactivity please see Kissane and Maguire's 2011 review.[22]

2.1.3 Project background – The Importance of the Pyrazole Moiety

Heterocycles are an indispensable and ubiquitous class of compounds; notably they make up more than half of all known organic compounds and have a broad range of biological, chemical and physical properties spanning an expansive spectrum of reactivity and stability.[23-29] Among heterocycles, the pyrazole moiety and its derivatives are an important class of nitrogen containing five-membered heterocyclic compounds that have garnered significant interest in recent times predominantly due to their usefulness as targets in drug discovery.[30-33] Notably, several commercialised synthetic pyrazoles have come to prominence in recent decades highlighting the diverse biological effects associated with this critical scaffold. Celecoxib **32**, a COX-2 inhibitor is widely used as a non-steroidal anti-inflammatory drug;[34] sildenafil **33** is used for the treatment of erectile dysfunction and pulmonary hypertension,[35] rimonabant **34** was used in the treatment of obesity by acting as an inverse agonist of the cannabinoid receptor CB1 prior to its withdrawal from market,[36-37] tartrazine **35** is a synthetic lemon azo dye primarily used as a food colouring,[38] and fipronil **36** is a broad spectrum insecticide that acts on GABA-gated and glutamate-gated chloride channels in the insect nervous system **(Figure 2.2)**.[39] Of significant interest is the presence of highly functionalised diversified substituents bonded to the pyrazole nucleus, many of which are electron withdrawing groups, that are critical to the compound's activity.

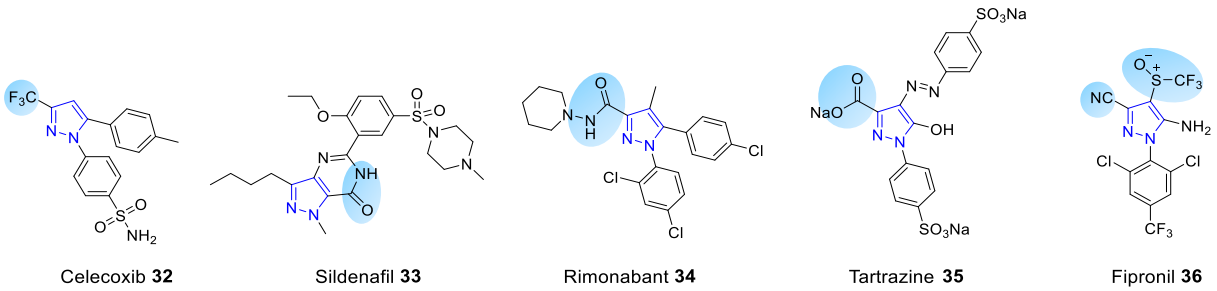

Figure 2.2: Commercialised substances containing the pyrazole moiety highlighting the biological application of incorporating electron-withdrawing substituents at the C(3), C(4) and C(5) positions

Markedly, the condensation of 1,3-dicarbonyl compounds with hydrazine derivatives remains the prevailing synthetic route towards formation of the pyrazole scaffold despite its numerous associated limitations, most notably limited functional group diversity **(Scheme 2.16)**. The incorporation of functionalised substituents, such as carbonyl derivatives, at each the C(3), C(4) and C(5) positions of the pyrazole ring is not feasible using this methodology as their presence in the requisite 1,3-dicarbonyl compound would lead to additional chemoselectivity and regioselectivity issues. As a result, substituents tend to be limited to alkyl or aryl groups, which possess limited synthetic potential. Further constraints include the multistep sequences (in many instances) required to generate the desired starting materials, harsh reaction conditions and poor regioselectivities **(Scheme 2.16)**.[40] Furthermore, the safety aspects of using hydrazines and its derivatives, known for its associated mutagenicity, must also be considered.[41] Additionally, the use of substituted hydrazines, leads to

alkylation of the N(1) position in the pyrazole product, and hence imposes further limitations regarding the synthetic versatility of this position.

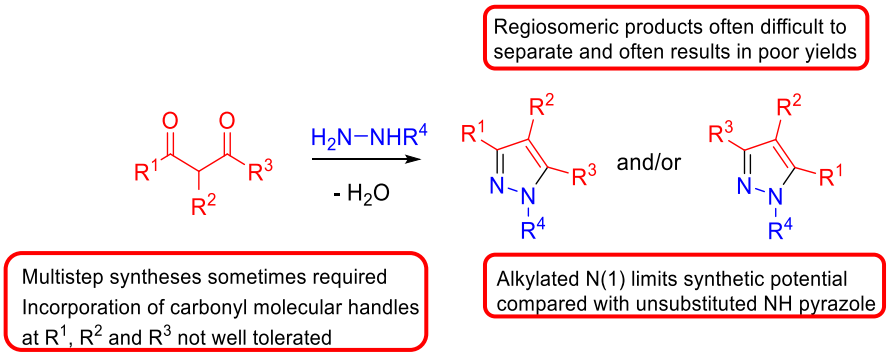

Scheme 2.16: Hydrazine condensation route towards 3,4,5-substituted pyrazoles highlighting associated limitations of the methodology

The [3+2] dipolar cycloaddition offers a unique atom-economical solution to many of the aforementioned problems with excellent regioselectivities and tolerance of functional group diversity characteristic of the reaction.[42] The [3+2] dipolar cycloaddition of alkenes with highly reactive electron-rich diazoalkanes is well-documented generally forming a 1-pyrazoline that readily isomerises to the more thermodynamically stable 2-pyrazoline, however a further oxidative step is usually required to form the pyrazole **(Scheme 2.17)**.[43-45] While this methodology is an exceptionally powerful protocol for the synthesis of pyrazoline and pyrazole structures the presence of an alkyl moiety on the diazo precursor limits further derivatisation of this substituent in the final product.

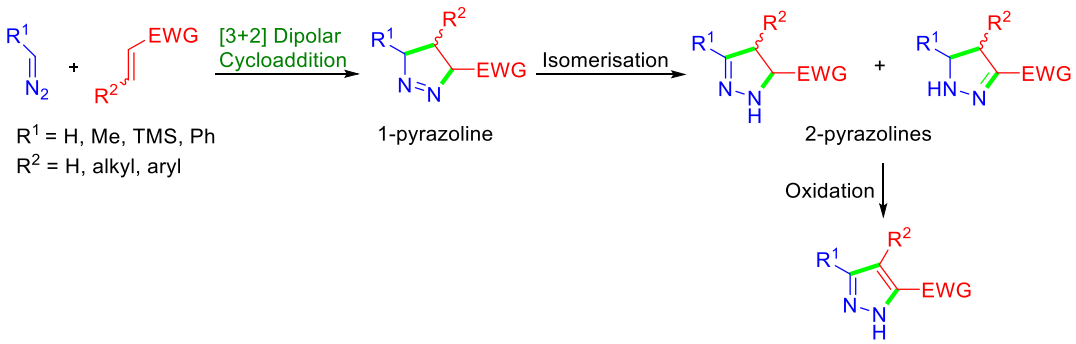

Scheme 2.17: [3+2] Dipolar cycloaddition of diazoalkanes with alkenes to form pyrazolines and pyrazoles

Notably, however, this problem can be circumvented by employing diazo compounds with an in-built synthetic handle that is retained through the cycloaddition, that can much more readily undergo further synthetic transformations. Furthermore, a major advantage of the [3+2] dipolar cycloaddition is that the dipolarophile can be tuned to incorporate a range of functionality that would otherwise be a difficult task using traditional methods.

2.2 Project Objectives – The Synthesis of Densely Functionalised Pyrazoles

While the reactivity and scope of the [3+2] dipolar cycloaddition of diazoalkanes is well documented in the literature,[9, 46-49] the use of terminal electron deficient diazo compounds such as α-diazoesters, α-diazoacetamides and α-diazosulfones remain much less explored presumably due to the inherent difficulty of overcoming the increased HOMO–LUMO energy gap between the dipole and dipolarophile, which is considerably greater relative to related α-diazoalkanes. However, a significant shortcoming of pyrazoles generated through [3+2] dipolar cycloaddition of α-diazoalkanes and dipolarophiles is that further functionalisation of the C(3) position bearing an alkyl substituent is not trivial, hence the use of these electron-deficient diazo compounds is attractive from a synthetic and biological point of view.

In light of Kissane's pioneering work on [3+2] dipolar cycloadditions using α-thio-β-chloroacrylamides as dipolarophiles,[9-10, 21] the Maguire group recognised the potential to generate a series of highly functionalised sulfur substituted pyrazoles not readily accessible via other synthetic routes. Interestingly, in most of the reports describing [3+2] dipolar cycloadditions of α-diazoacetates for example, the dipolarophiles tend to be structurally simple. In contrast, the α-thio-β-chloroacrylamide framework is a structurally complex. Most notably, this scaffold contains a halide capable of acting as a leaving group, which in combination with the presence of a nucleophilic sulfide provides access to a potential source of functional group migrations, which is rare in reports regarding cycloadditions of diazo compounds.

To further demonstrate the synthetic application of this methodology the following research objectives were investigated:

- To investigate whether electron deficient terminal α-diazosulfones, α-diazoacetates, and α-diazoacetamides will undergo [3+2] dipolar cycloadditions in a synthetically useful manner with a series of α-thio-β-chloroacrylamides and related derivatives at each of the sulfide, sulfoxide and sulfone oxidation levels analogous to α-diazoalkanes (**Scheme 2.18** and **Figure 2.3**).

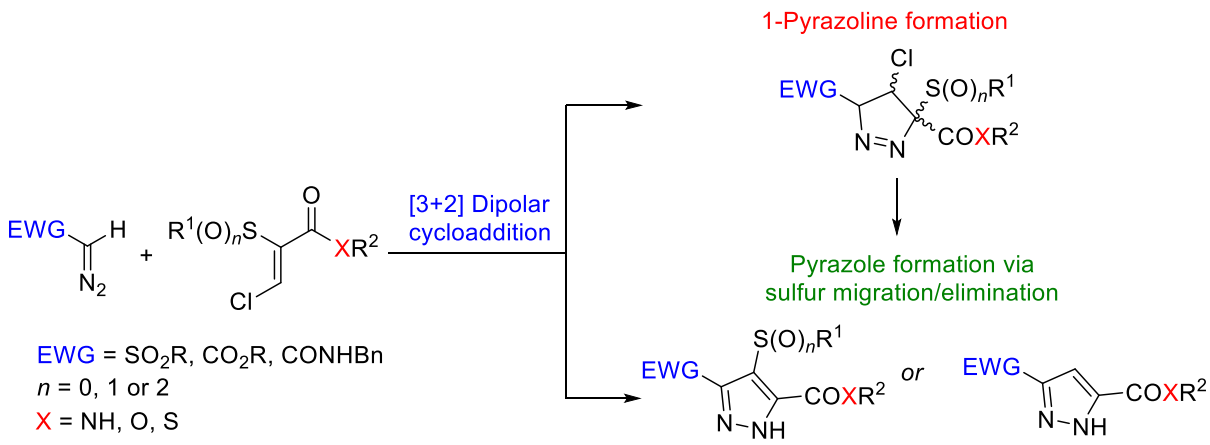

Scheme 2.18: [3+2] Dipolar cycloadditions utilising electron deficient diazo compounds in conjunction with structurally and electronically complex α-thio-β-chloroacrylamide derivatives; potential access to functional group migrations due to leaving group ability of the chlorine substituent

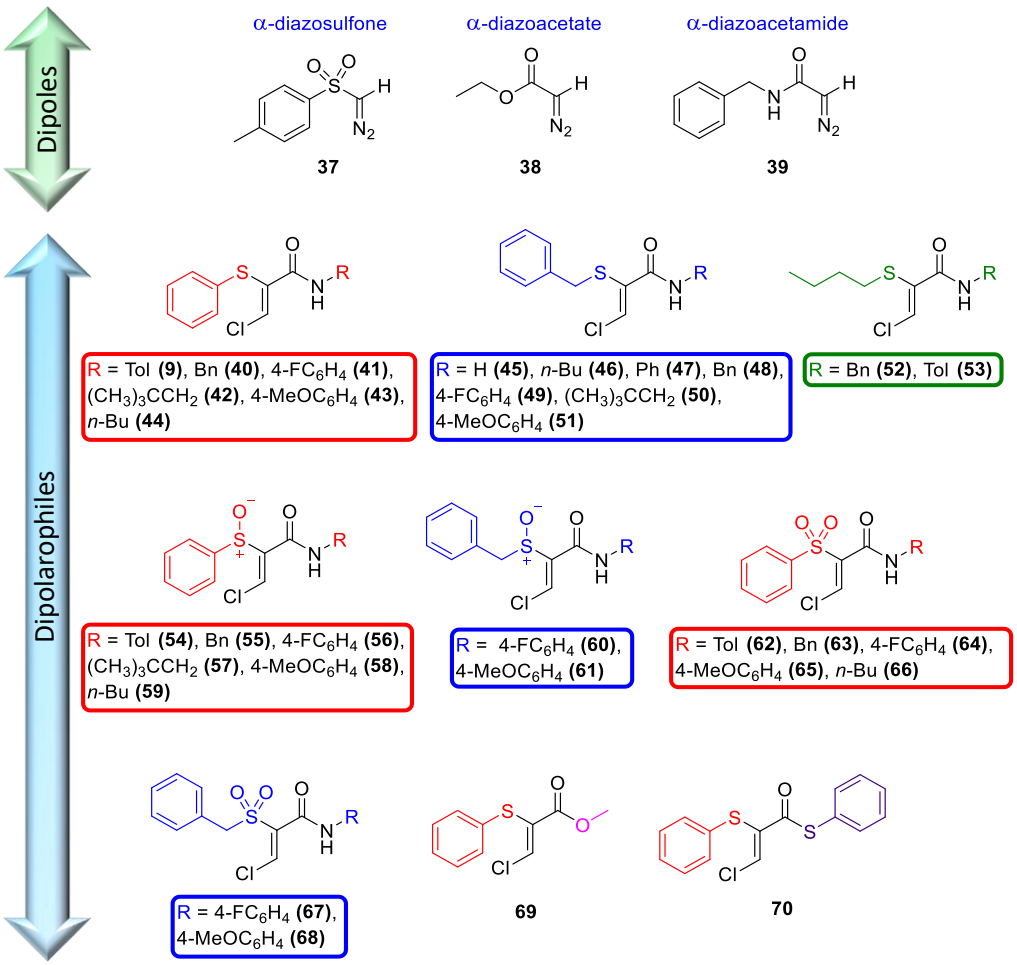

Figure 2.3: Dipoles and dipolarophiles utilised in this work to investigate their application in [3+2] dipolar cycloadditions

- To further probe the synthetic utility of using dipolarophiles bearing halides capable of acting as a leaving group in [3+2] dipolar cycloadditions, and to explore their role in subsequent functional group migrations at the sulfide, sulfoxide and sulfone oxidation levels of the dipolarophile **(Scheme 2.18)**.
- To generate, isolate and characterise a series of novel densely functionalised 3,4,5-substituted pyrazoles analogous to that illustrated in **Figure 2.4**.
- To explore the tautomeric composition of the pyrazole cycloadducts in a variety of solvents enabling facile characterisation of the C(3), C(4) and C(5) carbons by ^{1}H and ^{13}C NMR spectroscopy **(Scheme 2.19)**.

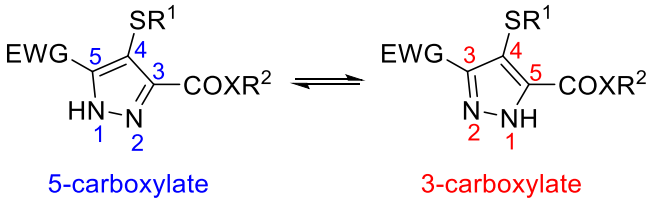

Scheme 2.19: Possible tautomeric forms of 3,4,5-substituted pyrazoles

- To explore the enhanced synthetic potential of the novel 3,4,5-substituted pyrazoles via a range of reactions including alkylations, oxidations, hydrolysis and coupling reactions **(Figure 2.4)**.

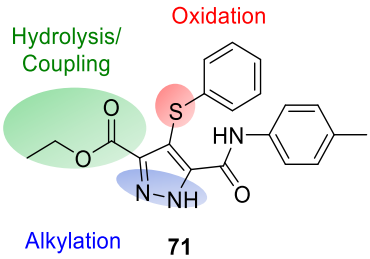

Figure 2.4: Further derivitisation of the pyrazole scaffold **71**

2.3 Generation of the Dipolarophile – Synthesis of the α-sulfenyl- and α-sulfinyl-β-chloroacrylamide scaffolds

2.3.1 Overview of synthetic approach

The first stage of this project involved the generation of the α-thio-β-chloroacrylamides and α-sulfinyl-β-chloroacrylamides precursors that would subsequently be used as dipolarophiles in [3+2] dipolar cycloadditions. The synthesis of the α-thio-β-chloroacrylamide scaffold has been extensively optimised within our group and involves an efficient three-step protocol **(Scheme 2.20)**.[6-7, 15, 19] Initial addition-substitution of 2-chloropropionyl chloride **(i)** with the requisite amine affords the α-chloroamide **(ii)**. Subsequent nucleophilic substitution with the thiolate anion affords the α-thioamide **(iii)**. NCS mediated chlorination of **(iii)** gives the desired α-thio-β-chloroacrylamide **(iv)**. Finally, oxidation of the sulfide to sulfoxide is achieved using Oxone® as oxidant, affording the α-sulfinyl-β-chloroacrylamide **(v)**.[12, 15-16] This approach was used exclusively for the formation of all α-sulfenyl-β-chloroacrylamide and α-sulfinyl-β-chloroacrylamide derivatives, unless otherwise stated, and is discussed in detail in **Sections 2.3.2–2.3.7**.

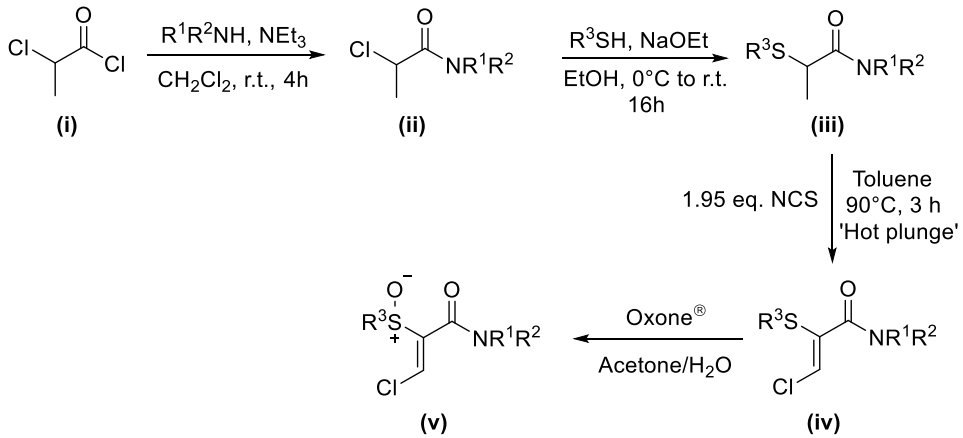

Scheme 2.20: Overview of synthetic approach to α-sulfenyl- and α-sulfinyl-β-chloroacrylamide dipolarophile precursors

2.3.2 Preparation of α-Chloroamides

Previous work within our group optimised the synthesis of the α-chloroamides.[15-16] Early studies by Murphy involved treating one equivalent of the commercially available 2-chloropropionyl chloride in dichloromethane with an excess of the amine (1.5 equivalents) in dichloromethane.[15] The excess amine neutralises the hydrogen chloride generated during the reaction. However, depending on the amine used, particularly for high molecular weight amines or chiral amines, this method was deemed unsatisfactory due to the lack of atom economy and potential cost. Further improvements to the methodology included reducing the loading of the amine to 1 equivalent to generate the amide, with the prior addition of 1 equivalent of triethylamine to ensure the neutralisation of the liberated hydrochloric acid.[16]

This optimised procedure, as developed by Lynch,[16] outlined above was employed in the synthesis of six α-chloroamides in this work. The α-chloroamides were chosen to incorporate amides that would allow electronic and steric effects to be studied in the later [3+2] dipolar cycloadditions of α-sulfenyl- and α-sulfinyl-β-chloroacrylamides (see **Section 2.5**). A minor deviation was made regarding the number of equivalents of 2-chloropropionyl chloride and triethylamine used (both 1.01 equivalents) to ensure that the amine reacted to completion. In order to control the exotherm generated from the liberation of hydrogen chloride during the reaction the acid chloride in dichloromethane was added dropwise over 20 minutes to a stirring solution of the amine and triethylamine in dichloromethane at 0˚C. On completion of the addition, a white precipitate of triethylamine hydrochloride was always observed. The crude products were sufficiently pure after alkaline work up using *sat*. sodium bicarbonate to be used without further purification. This methodology was routinely conducted on multigram quantities, with almost quantitative yields of between 94–98% obtained in all instances **(Scheme 2.21)**.

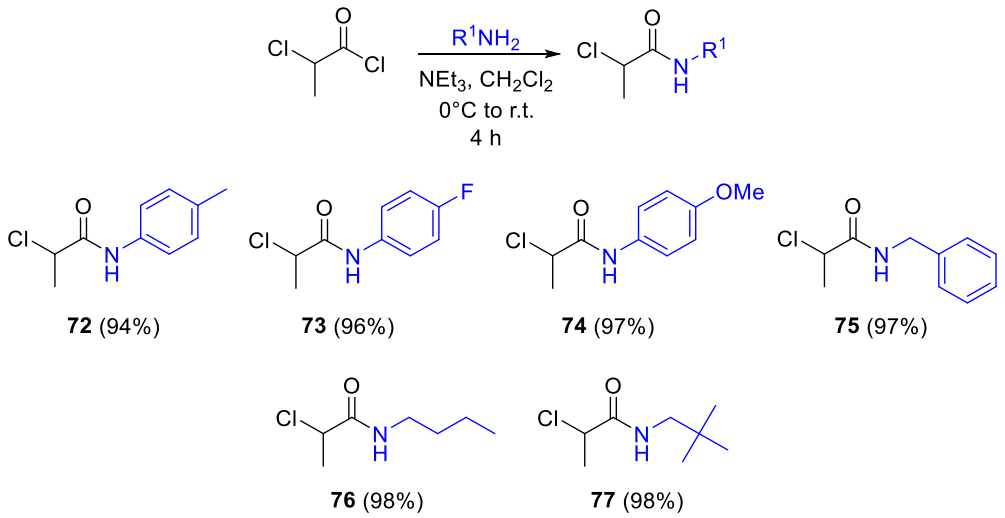

Scheme 2.21: Preparation of α-chloroamides (Yields quoted are crude yields, no purification required).

The α-chloroamides **72**, **73**, and **75**–**76** have been previously synthesised within our group,[15-16, 20-21] amide **74** has been synthesised in the literature using a similar procedure,[50] while amide **77** is novel and was fully characterised in this work. The α-chloroamides' spectroscopic characteristics were consistent with those already reported, with comparable yields obtained in all cases.

The ^{1}H NMR spectra of the α-chloroamides contain a number of distinctive signals **(Figure 2.5)**. A doublet is observed at δ_H 1.71–1.80 ppm for the β-methyl group while a quartet is observed at δ_H 4.42–4.53 ppm for the proton bonded to the α-carbon. Notably, these signals are observed consistently slightly further downfield for the aryl substituted α-chloroamides **72**–**74** than the corresponding alkyl substituted derivatives **75**–**77**, presumably due to the additional electron-withdrawing effect of the aryl moiety. Furthermore, the alkyl substituted amide derivatives **75**–**77** are readily identified by the presence of a distinct pair of doublet of doublets, or in the case of **76** a doublet of triplets, indictive of the diasterotopic methylene protons that result from the presence of an ABX system.

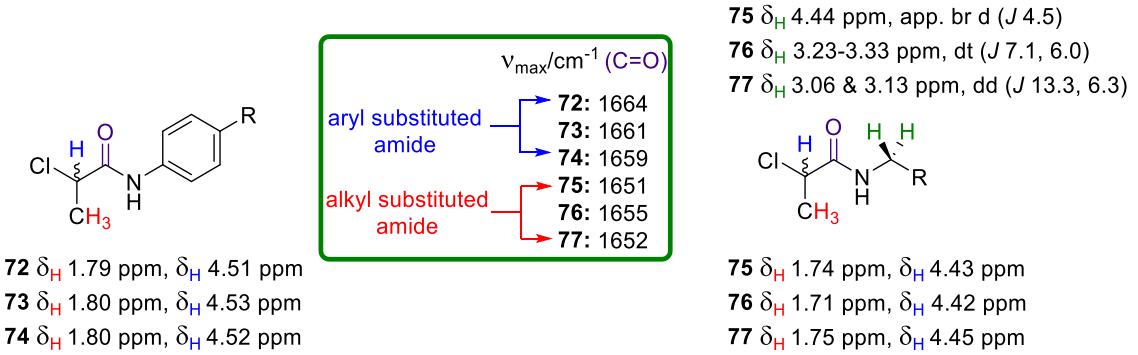

Figure 2.5: ^{1}H NMR (in $CDCl_3$ at 300 MHz) and IR (ATR) spectroscopic characteristics of the α-chloroamides

In the IR spectra, notable differences were observed between the *N*-alkyl and *N*-aryl derivatives for the carbonyl stretching frequency shift, with the *N*-alkyl derivatives **75**–**77** observed approximately 10 wavenumbers lower than the corresponding *N*-aryl derivatives **72**–**74 (Figure 2.5)**. This is due to a decrease in the carbonyl bond order as delocalisation in the *N*-alkyl derivatives can is more efficient.

2.3.3 Preparation of α-Thioamides

The preparation of α-thioamides from α-chloroamides has received significant attention in our group, with a comprehensive range of primary, secondary *N*-alkyl, *N*-aryl, tertiary *N*,*N*-alkyl amides generated in various combinations with *S*-alkyl and *S*-aryl derivatives.[15-16, 18, 20-21] Early studies by Murphy and Lynch demonstrated that α-chloroamides bearing an *N*-aryl or *N*-benzyl substituent can be efficiently sulfenylated in ethanol by reaction with freshly prepared sodium ethoxide.[15-16] While this method was highly efficient, extension of this methodology to include *N*-alkyl derivatives required more forcing conditions to obtain similar efficiencies and yields. Accordingly, for these derivatives it was oftentimes necessary to generate the requisite thiolate using sodium hydride in anhydrous DMF.[16] However, in subsequent studies, Kissane highlighted that this was not consistently the case when synthesising *N*-alkyl α-thioamides, and that in certain instances the use of sodium ethoxide in ethanol readily afforded complete conversion.[21]

In this work the α-thioamides **6**, **78**–**80** and **83**–**85** were prepared using a modified version of Lynch and Murphy's optimised method as described above. In this method the requisite thiolate is firstly prepared by treating the thiol with freshly prepared sodium ethoxide in ethanol at 0°C. This solution was stirred for twenty minutes prior to the addition of the α-chloroamide, however, Cacheux subsequently demonstrated that this hold-time was not necessary, and that its removal from the protocol did not negatively impact on the efficiency of the transformation.[18] Therefore, in this work,

the addition of the α-chloroamide was made immediately after the addition of thiol. Using this method **(Method A)**, the known α-thioamides **6**, **78**–**80** and **83**–**85** were prepared in 72–93% yield following flash column chromatography **(Table 2.1)**.

Notably, during this work in a parallel programme of research, Dennehy *et al*. reported an improved batch process for the transformation of α-chloroamide **72** to α-thioamide **6** using sodium hydroxide in an ethanol/water mixture at reflux.[19] Using this method, problems associated with reaction efficiencies were obviated, with quantitative conversion observed. Furthermore, the rate of the reaction was significantly improved to only 1 hour, and unfavourable disulfide formation was eliminated. Most favourably, however, was that the α-thioamide **6** was isolable in high yields via filtration following the further addition of water, circumventing the need for oftentimes laborious column chromatography. In light of this report, we successfully extended this protocol to the preparation of the novel α-thioamides **81**, **82**, **86** and **87 (Method B)**. While the α-thioamides **81**, **82** and **86** are solids and were readily isolated in high purity by suction filtration, the α-thioamide **87** is an oil and was instead isolated pure following partitioning between dichloromethane and aqueous sodium hydroxide (2M).

Table 2.1: Preparation of α-Thioamides

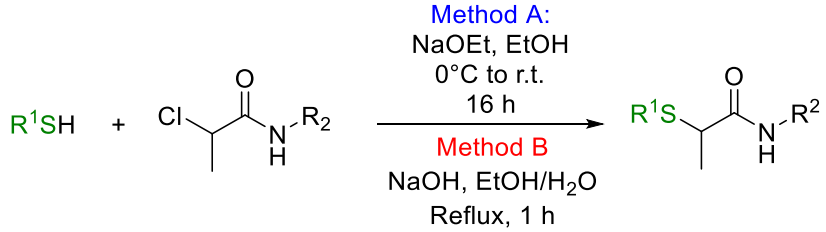

Entry	α-chloroamide	R^1	R^2	Method[a]	α-chloroamide: α-thioamide:[b]	Yield (%)[c]	α-thioamide
1	**72**	Ph	Tol	A	0 : 100	93[d]	**6**[7, 15, 21]
2	**75**	Ph	Bn	A	18 : 82	72	**78**[6, 15, 21]
3	**76**	Ph	*n*-Bu	A	16 : 84	81[e]	**79**[7, 15, 21]
4	**73**	Ph	4-FC_6H_4	A	0 : 100	80	**80**[7, 15, 21]
5	**74**	Ph	4-$MeOC_6H_4$	B	0 : 100	89[f]	**81**
6	**77**	Ph	Neopentyl	B	0 :100	98[f]	**82**
7	**75**	Bn	Bn	A	16 : 84	88	**83**[7, 21]
8	**76**	Bn	*n*-Bu	A	2 : 98	82	**84**[7, 21]
9	**73**	Bn	4-FC_6H_4	A	0 : 100	89	**85**[7, 21]
10	**74**	Bn	4-$MeOC_6H_4$	B	0 : 100	86[f]	**86**
11	**77**	Bn	Neopentyl	B	0 : 100	94[g]	**87**

a) **Method A:** 1.2 equiv. thiol, 1.2 equiv. sodium ethoxide generated freshly from sodium metal in absolute ethanol, 18 h; **Method B**: 1.04 equiv. thiol in ethanol, 2 equiv. aqueous sodium hydroxide (0.8 M), 1h.
b) Ratio of α-chloroamide: α-thioamide determined by ^{1}H NMR analysis of the crude reaction mixture.
c) Percentage yield isolated post column chromatography on silica gel unless otherwise stated.
d) The crude α-thioamide was sufficiently pure to be used without further purification.
e) The purified product contained 5% unreacted *N*-*n*-butyl-2-chloropropanamide **76** that was inseparable from the product **79** by chromatography. This material was carried forward to the next step without further purification.
f) Percentage yield isolated following suction filtration.
g) Percentage yield isolated following aqueous alkaline work-up.

As outlined in **Table 2.1**, all the transformations of α-chloroamides to α-thioamides performed in this work proceeded in good to excellent yields on multigram scales, hence no further efforts were made

to optimise the reactions. That said, several observations were consistent with reports previously described in our group. The α-chloroamides bearing an *N*-butyl or *N*-benzyl substituent did not proceed to completion; however, this only prevented the isolation of the *N*-*n*-butyl substituted α-thioamide **79** in pure form **(Table 2.1**, **Entry 3)**. While our group has previously observed that the reaction of *N*-alkyl α-chloroamides with thiols can be forced to completion using sodium hydride in DMF,[16] based on the observation in this work that Dennehy's method[19] was suitable to fully convert the *N*-alkyl α-chloroamide **77** to the α-thioamides **82** and **87** using thiophenol and benzyl mercaptan respectively, then it is reasonable to assume that this method would be suitable for related *N*-alkyl derivatives. Accordingly, it appears that Dennehy's method is optimal for the transformation of α-chloroamides to α-thioamides regardless of substitution on the amide moiety.

Kissane initially explored the synthesis of α-benzylthioamides,[21] with subsequent investigations carried out by Cacheux.[18] Interestingly, when preparing these derivatives both researchers observed the formation of dibenzyldisulfide **88** when using benzyl mercaptan. This observation was consistent with this work using **Method A**, with the appearance of a singlet at δ_H 3.59 ppm in the ^{1}H NMR spectra of the crude products in **Entries 7–9 (Table 2.1)** corresponding to the methylene hydrogens adjacent to sulfur **(Figure 2.6)**. The formation of dibenzyldisulfide **88** was not observed using Dennehy's optimised method **(Method B)** (**Entries 10** and **11, Table 2.1**), highlighting that the increased rate of reaction may prevent its formation.

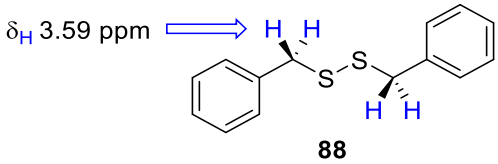

Figure 2.6: Dibenzyldisulfide **88** by-product formed in the preparation of α-benzylthioamides

An attribute worthy of note is the increased reactivity of the benzylthiolate when compared with arythiolates, such as thiophenolate used in this work, in the preparation of α-thioamides. While for arylthiolates the negative charge can be readily delocalised into the aromatic system, the presence of a methylene group between the sulfur anion and the aromatic system prevents delocalisation of the electron density for the benzylthiolate anion. Consequently, the benzylthiolate anion is a much more reactive nucleophile than that corresponding aryl thiolates, and it is likely this increased nucleophilicity readily contributes to the enhanced formation of dibenzyldisulfide **88** relative to corresponding aryl thiols. The p*K*a of benzyl mercaptan (15.3) and thiophenol (10.3) in DMSO supports this analysis, with the more reactive thiolate derived from benzyl mercaptan.[51]

2.3.4 Preparation of α-Thio-β-Chloroacrylamides

Since the serendipitous discovery of the α-thio-β-chloroacrylamides,[6] significant efforts have been made in the Maguire group to optimise their formation with significant improvements made regarding the selectivity of the NCS mediated cascade, reaction times and safety profile of the reaction.[7, 15-16, 21] A large library of these synthetically versatile compounds have been previously generated by various members of our team with diverse combinations of primary, secondary and tertiary amides, bearing both alkyl and aryl substituents, and *S*-alkyl, *S*-benzyl and *S*-aryl derivatives all extensively explored **(Figure 2.7)**. This methodology was also readily extended to α-thio-β-chloroacrylates,[16, 52] α-thio-β-chloroacrylonitriles[16, 52] and most recently α-thio-β-chloroenones.[53-54]

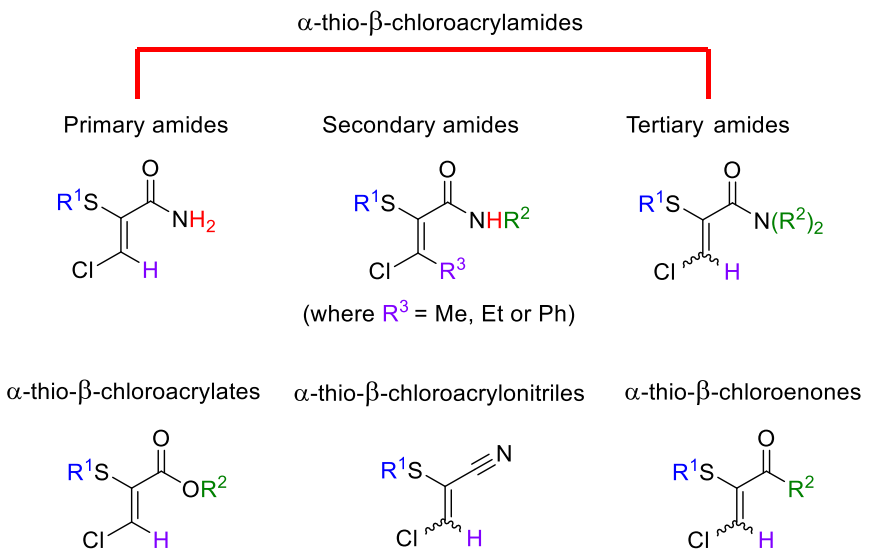

Figure 2.7: Overview of α-thio-β-chloroacrylamide and related derivatives generated in the Maguire group since its discovery via the NCS mediated cascade.

While the initial investigations utilised carbon tetrachloride as solvent, efforts to generate a greener process, and avoid the use of a suspected carcinogen, led to the development that toluene can be used with either similar or improved reaction efficiencies observed in most instances. Not only does the use of toluene enable much quicker reactions, with our optimised batch method reaching completion in 3 hours at 90°C, but its use is particularly beneficial due to the insolubility of the succinimide by-product at low temperatures (i.e. 0°C) which facilitates its almost quantitative removal by simple filtration. While in the original studies Murphy utilised recrystallised NCS,[6, 15] it was later established by Lynch that commercial unrecrystallised NCS was equally as effective as recrystallised material, further highlighting the robust nature of the transformation.[16] Temperature was observed to be a crucial factor in the reproducibility and overall efficiencies of the chlorination cascade particularly in regards to scale-up. Of major interest in the early work was the poor efficiencies when the reaction mixture was heated to the required temperature, most oftentimes 90°C, starting from room temperature, which became particularly problematic on scale-up due to the longer times it took for the reaction medium to reach the requisite temperature. Therefore, the utilisation of a 'hot-plunge' method in which the reaction mixture is immediately lowered into a preheated oil bath at the desired temperature was a significant step forward in the optimisation of our batch procedure. Ultimately, this procedure leads to more rapid heating of the reaction mixture and enables more efficient transformation of the α-thioamide, to the acrylamide, to the dichloride, and finally, to the α-thio-β-chloroacrylamide.

That the transformation occurs stereoselectively, and in the majority of cases forms exclusively the Z-isomer (see **Table 2.2**), was confirmed by single crystal X-ray diffraction of the *N*-benzyl derivative **48**.[7, 15] In the work described herein, and for all other derivatives previously prepared in our group, as highlighted in **Figure 2.7**, stereochemistry is assigned by analogy to this derivative.

The optimised conditions developed for the batch generation of α-thio-β-chloroacrylamides was developed by Lynch,[16] following on from Murphy's initial report.[6, 15] The general optimised conditions are 1.95 equivalents of NCS at 90°C, although for some derivatives the optimised conditions have been observed to vary slightly. As mentioned in **Section 2.1.1**, **Scheme 2.6**, our group has further optimised this process via continuous flow methodology,[19] however, the optimised batch conditions were used

exclusively for the preparation of all α-thio-β-chloroacrylamides in this work. These results are illustrated in **Table 2.2**.

Table 2.2: Preparation of α-thio-β-chloroacrylamides

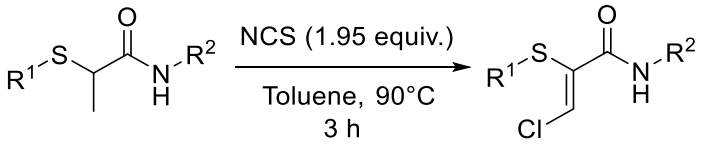

Entry	α-Thioamide	R^1	R^2	Yield (%)[a]	(*Z*)-α-Thio-β-chloroacrylamide
1	**6**	Ph	Tol	82	**9**[7]
2[b]	**78**	Ph	Bn	57	**40**[7]
3	**79**	Ph	*n*-Bu	72	**44**[7]
4[c]	**80**	Ph	4-FC_6H_4	71	**41**[7]
5	**81**	Ph	4-$MeOC_6H_4$	34[h]	**43**
6	**82**	Ph	Neopentyl	77	**42**
7[d]	**83**	Bn	Bn	61[e]	**48**[7, 21]
8[f]	**84**	Bn	*n*-Bu	75[g]	**46**[7, 21]
9	**85**	Bn	4-FC_6H_4	70	**49**[7, 21]
10	**86**	Bn	4-$MeOC_6H_4$	40[h]	**51**
11	**87**	Bn	Neopentyl	65	**50**

a) Isolated yield after chromatography on silica gel.
b) ^{1}H NMR analysis of the crude spectrum indicated a mixture of α-thio-β-chloroacrylamide **40** to trichloride **89** (82:18).
c) ^{1}H NMR analysis of the crude spectrum indicated a mixture of α-thio-β-chloroacrylamide **41** to tentatively assigned acrylamide **90** (93:7).
d) ^{1}H NMR analysis of the crude spectrum indicated a mixture of α-thio-β-chloroacrylamide **48** to tentatively assigned *E*-isomer **91** (93:7).
e) Co-eluting fraction containing a 73:27 ratio of α-thio-β-chloroacrylamide **48** to tentatively assigned *E*-isomer **91** also isolated. This fraction was used to tentatively assign the *E*-isomer **91**. δ_H ($CDCl_3$, 300 MHz) 3.85 (2H, s, SCH_2), 4.48 (2H, d, *J* 5.9, $C\underline{H_2}NH$), 6.44 [1H, s, ClHC(3)=], 6.62 (1H, br t, unresolved coupling, NH) ppm.
f) ^{1}H NMR analysis of the crude spectrum indicated a mixture of α-thio-β-chloroacrylamide **46** to tentatively assigned trichloride **92** (92:8).
g) Purified product **46** contained 5% of the trichloride **92**. δ_H ($CDCl_3$, 300 MHz) 3.32 [2H, dt appears as a q, *J* 6.9, 6.2, C(1′)H_2], 6.22 (1H, br s, NH), 6.44 [1H, s, C(3)] ppm.
h) The lower yields of α-thio-β-chloroacrylamides **43** and **51** were due in part to solubility issues encountered during column chromatography, however, the ^{1}H NMR spectra of the crude product mixtures indicated efficient transformation.

The α-thio-β-chloroacrylamides **9**, **40**, **41**, **44**, **46**, **48** and **49** are known compounds that have been previously synthesised in our group, with yields obtained in this work comparable to those in previous reports.[7, 21] Interestingly, it was observed that the selectivity of the reaction was particularly poor for the α-thioamide **78 (Entry 2)**, an observation also made by Kissane in earlier work under identical conditions.[21] Notably, while this was not discussed in any detail by Kissane, this work highlights that overchlorination to the trichloride **89** was the major contributing factor for the lower yield obtained in this work, with analysis of the ^{1}H NMR spectrum highlighting a ratio of circa. 82:18 α-thio-β-chloroacrylamide **40** to trichloride **89**, excluding minor impurities related to the NCS cascade **(Scheme 2.22)**. Following flash column chromatography the α-thio-β-chloroacrylamide **40** and the less polar novel trichloride **89** were isolated as white solids in 57% and 9% yield respectively in high purity.

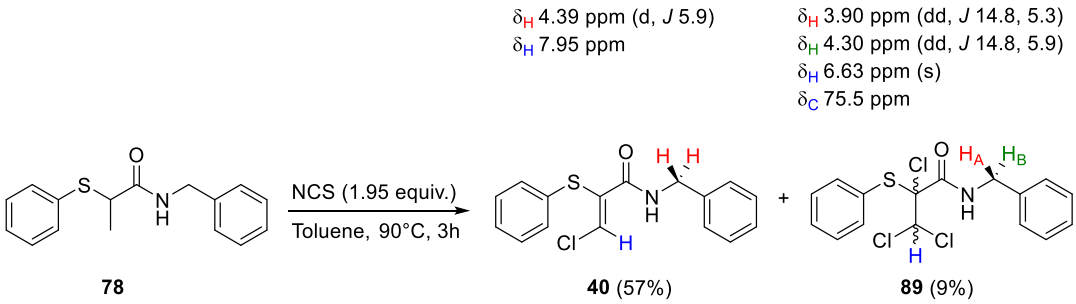

Scheme 2.22: NCS mediated transformation of α-thioamide **78** to form α-thio-β-chloroacrylamide **40** and trichloride **89**

The trichloride **89** is a novel compound and was fully characterised in this work. Significantly, in the ^{1}H NMR spectrum of the trichloride **89** the β-hydrogen is observed at 6.63 ppm, which is considerably more shielded than the α-thio-β-chloroacrylamide **40**, despite the accumulative electron-withdrawing effects of geminal and vicinal chlorine atoms. In addition, the benzylic protons, illustrated as H_A and H_B in **Scheme 2.22**. are diasterotopic due to the stereocentre formed at the α-carbon. It is known that the β-hydrogen of the E-isomer of the α-thio-β-chloroacrylamides is significantly shielded compared to that in the Z-isomer. Accordingly, great care must be taken when assigning the trichloride and/or E-isomer. While the observation of the ABX system in the trichloride **89** for the benzylic hydrogens confirms the presence of a stereocentre, and therefore excludes the presence of the E-isomer, further evidence is provided by the lack of an sp^{2} hybridised C–H signal for the β-carbon in the ^{13}C NMR spectra. Instead the β-carbon is observed at 75.5 ppm indicative of a strongly deshielded sp^{3} hybridised carbon **(Scheme 2.22)**.

The α-thio-β-chloroacrylamides **42**–**43** and **50**–**51** are novel compounds and were fully characterised in this work. The low yields of the 4′-methoxyphenyl derivatives **43** and **51** (**Entries 5** and **10**, **Table 2.2**) are attributable primarily due to solubility issues encountered during chromatography, while the crude product mixtures indicated efficient transformation. In both cases, the α-thio-β-chloroacrylamides crystallised out during chromatography in hexane: ethyl acetate. Consequently, significant amounts of dichloromethane had to be added to the eluent system to resolubilise the compounds, which prevented facile separation from other by-products.

While significant attention has been afforded to the elucidation of the mechanism of the NCS mediated cascade of α-thioamides, with the α-thioamide **6** used as the model substrate for these studies, we have never previously isolated the trichloride **93** in pure form for characterisation purposes despite observing its formation for other derivatives. This would suggest that the α-thio-β-chloroacrylamide **9** is particularly stable to further chlorination. While not essential for this research, as a curiosity, it was decided to investigate if the chlorination of α-thio-β-chloroacrylamide **9** could be effected by using a large excess of NCS under the otherwise optimised conditions. Accordingly, the chlorination of α-thioamide **6** was carried out using 3.96 equivalents of NCS, approximately double that of the standard conditions **(Scheme 2.23)**. ^{1}H NMR spectroscopic analysis of the crude reaction product indicated an almost equimolar mixture of α-thio-β-chloroacrylamide **9** and trichloride **93** (46:54) with **93** formed from further reaction of **9**. Following repeated flash column chromatography on silica gel, due to the similar retention factors of the two compounds, the novel trichloride **93** was isolated as a white solid in 18% yield. Clearly, further chlorination of the α-thio-β-chloroacrylamide **9** is not particularly efficient, with an almost two-fold increase in NCS not driving the reaction completely to the trichloride **93** product. This result further highlights the importance of ensuring the

minimisation of impurities in the NCS cascade as evidenced by the laborious column chromatography required to isolate the desired trichloride **93**. As the focus of the chromatography was to recover a pure sample of **93** the α-thio-β-chloroacrylamide **9** was not recovered from this column.

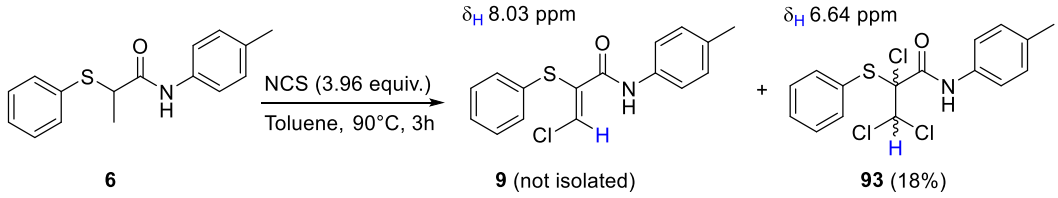

Scheme 2.23. Preparation of previously hypothesised novel trichloride **93**

In light of obtaining the trichloride **93**, each of the α-chloroamide, acrylamide, dichloride and trichloride impurities have been isolated for our model reaction exploring the NCS mediated chlorination cascade of α-thioamide **6**. Notably, the ^{1}H and ^{13}C NMR spectra of the trichloride **93** are distinctly similar to other trichlorides isolated in our group over the years, as evidenced by the chemical shift of the β-hydrogen at 6.64 ppm **(Figure 2.7)**, which compares closely with that in trichloride **89** also isolated in this work.

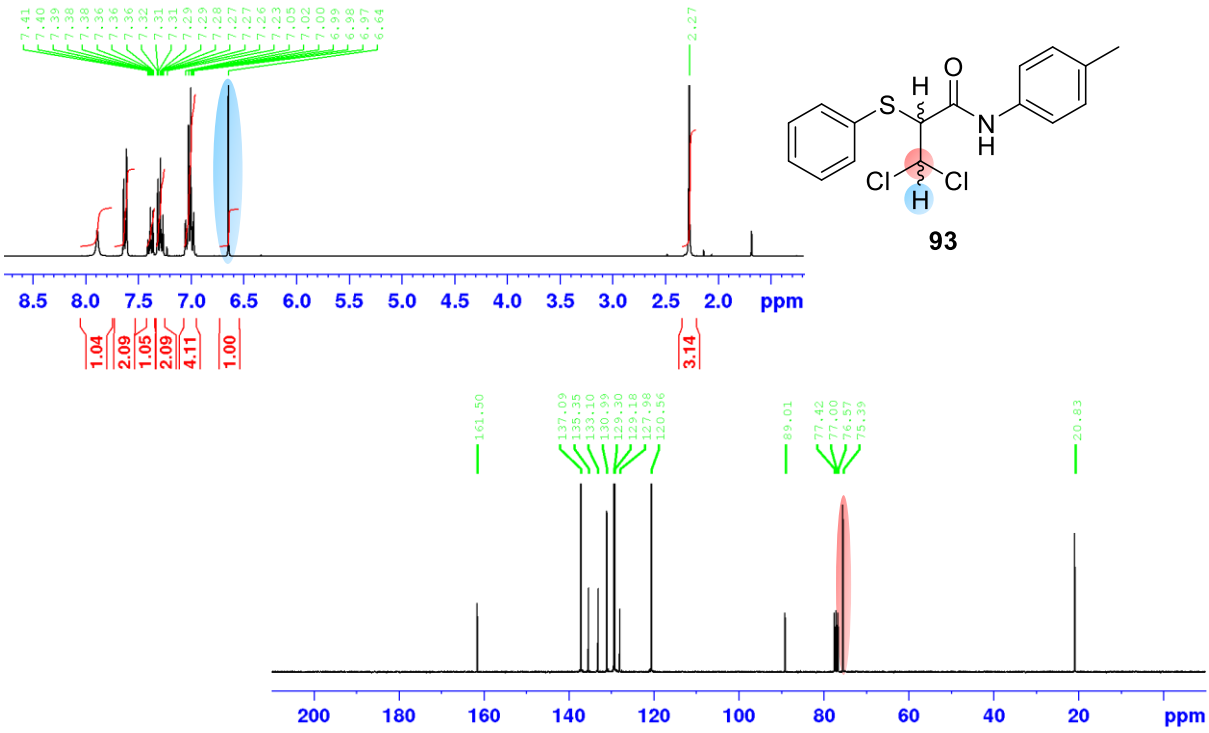

Figure 2.7: ^{1}H and ^{13}C NMR spectra for novel trichloride **93** in $CDCl_3$ at 300 MHz

For clarity the signals observed for the tentatively assigned impurities **90**–**92**, that were observed in the ^{1}H NMR spectra of the crude product mixtures in **Entries 4**, **7** and **8** in **Table 2.2** are illustrated in **Figure 2.8**. These compounds were not isolated in this work and were assigned by analogy to comparable derivatives isolated and characterised in our group.[7, 15-16]

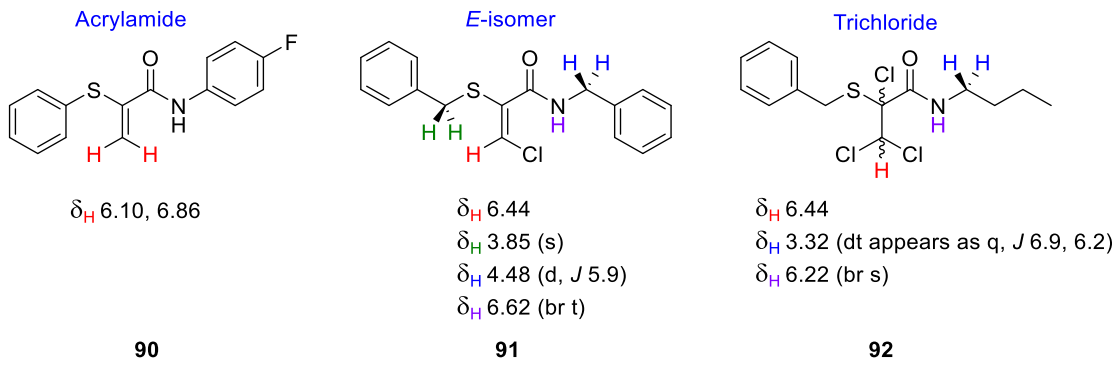

Figure 2.8: Tentatively assigned impurities **90**, **91** and **92** observed in ^{1}H NMR spectra (in $CDCl_3$ at 300 MHz) of crude reaction mixtures as highlighted in **Table 2.2**.

2.3.5. Synthesis of α-Thio-β-Chloroacrylate

To further expand the scope of the methodology alteration of the dipolarophile to include the α-thio-β-chloroacrylate **69** was also considered, as incorporation of an ester moiety in pyrazoline and/or pyrazole products is highly desirable due to the ease of manipulation of the ester functionality, particularly when compared to amides. The preparation of α-thio-β-chloroacrylate **69** has previously been optimised by Lynch,[16] and has subsequently been prepared by Kissane.[21, 52] Notably, Kissane reported that the α-thio-β-chloroacrylate **69** is an equally efficacious dipolarophile as the α-thio-β-chloroacrylamides in [3+2] dipolar cycloadditions with electron rich diazoalkanes.[9, 21]

The preparation of the ester derivatives is very similar to that of the α-thio-β-chloroacrylamides, with one major difference due to the increased stability of the dichloride **97** for the ester series, and in addition 2.1 equivalents of NCS at 130°C was employed for the chlorination step. As highlighted in **Scheme 2.24**, the synthesis requires four steps including **i)** preparation of the α-chloroester **95**, **ii)** nucleophilic displacement of the chloride to give the α-thioester **96**, **iii)** formation of the dichloride **97** as the major product via the NCS chlorination cascade, and finally **iv)** Lewis acid mediated decomposition of the dichloride to give the α-thio-β-chloroacrylate **69**. The yields obtained in this work are included in **Scheme 2.24**.

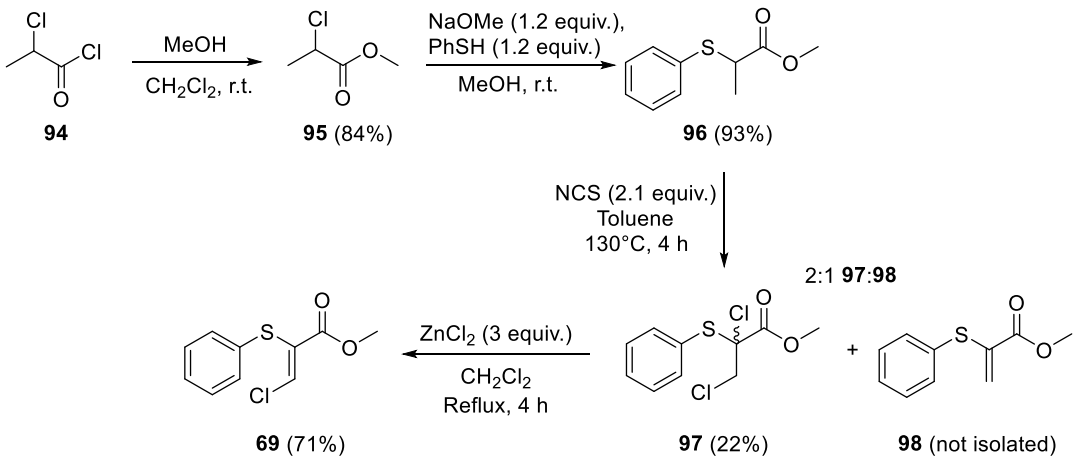

Scheme 2.24: Preparation of α-thio-β-chloroacrylate **69**

The α-chloroester **95** was firstly prepared by treatment of a dichloromethane solution of 2-chloropropionyl chloride **94** with an excess of methanol in dichloromethane **(Scheme 2.24)**. After aqueous work-up the resulting ester **95**, which is volatile, was isolated in 84% yield following removal of dichloromethane by concentration under reduced pressure. To ensure minimal loss of yield the temperature of the water bath was maintained lower than 30°C. The α-chloroester **95** was sufficiently pure by ^{1}H, ^{13}C NMR and IR to use without purification.

Sulfenylation of the α-chloroester **95** was achieved using 1.2 equivalents of freshly prepared sodium methoxide and 1.2 equivalents of thiophenol, to give the corresponding α-thioester **96** as a clear oil in 93% yield. Further purification of the α-thioester **96** was not required. The dichloride **97** was synthesised using Lynch's optimised method;[16, 52] 2.1 equivalents of NCS was added to a solution of the α-thioester **96** in toluene and the reaction was immediately lowered into a pre-heated oil bath at 130°C, with heating maintained while stirring for four hours **(Scheme 2.24)**. Following removal of the succinimide by-product by filtration, ^{1}H NMR spectroscopy of the crude product indicated a 2:1 mixture of dichloride **97**: acrylate **98**. This contrasts with Lynch's observation, in which complete conversion to the dichloride **97** was described. Following purification by flash column chromatography the dichloride was isolated as a colourless oil in 22% yield. The poor yield in this instance was associated with the difficulty in finding suitable conditions to separate the acrylate **98** and dichloride **97** by column chromatography, with a mixed fraction also isolated, containing a 74:26 ratio of dichloride **97** to acrylate **98** accounting for a further 24% yield of the dichloride **97**. The dichloride **97** was readily assigned by the presence of a distinctive AB quartet at δ_H 3.91 and 4.00 ppm (*J* 11.6 Hz) in the ^{1}H NMR spectrum of **97**. The acrylate **98**, although not isolated pure, was readily identified by its characteristic singlet signals at δ_H 5.24 and 6.33 ppm for the respective β-hydrogens in the ^{1}H NMR spectrum of the crude product.

Notably, the dichloride **97** is significantly more stable than the corresponding dichloride of the α-thio-β-chloroacrylamide series, which under the same conditions readily eliminates hydrogen chloride to give the α-thio-β-chloroacrylamide. Kissane and Lynch have previously hypothesised that the increased stability of the ester containing dichloride relative to that of the amide is as a result of conformational differences between the two types of derivative. Their rationale for this was that in the amides the intramolecular hydrogen bond could hold the compound in a conformation in which loss of chloride from the α-carbon is favoured through captodative stabilisation of the resulting sulfur-stabilised carbocation **(Figure 2.9)**.[55] In contrast, for the ester derivative there is no restriction on the conformation, and therefore, the chlorosulfide could adopt a different conformation from which loss of the chloride is disfavoured.

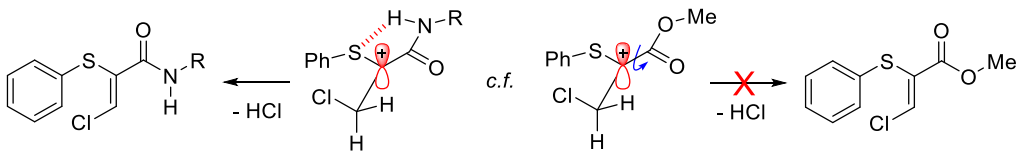

Figure 2.9: Kissane and Lynch's hypothesis that intramolecular hydrogen bonding in the amide series holds the dichloride in a conformation that favours elimination

However, this does not take into account our group's observations that tertiary α-thioamides, with no hydrogen bond donor, undergo the NCS mediated chlorination cascade to afford α-thio-β-chloroacrylamides usually as a mixture of E- and Z-isomers. Therefore, it is more likely that that the increased stability of the esters is simply due to the increased electron withdrawing effect of the ester

relative to the amide, which acts to destabilise the build-up of a carbonium ion at the α-carbon **(Figure 2.10)**.

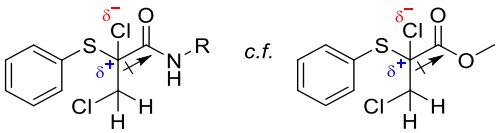

Figure 2.10: Postulated greater destabilisation of carbonium ion build-up in ester derivative due to more electron withdrawing ester moiety when compared to an amide derivative

Based on Murphy's observation that the α-thio-β-chloroacrylamide **9** was generated when the dichloride **8** was treated with zinc chloride **(Scheme 2.3**, **Section 2.1.1)** Lynch envisaged that this pathway may provide a more forcing means of achieving hydrogen chloride elimination, and hence formation of the desired α-thio-β-chloroacrylate **69**.[16, 52] Following optimisation, this was proved to be correct, with Lynch outlining that the optimal conditions for the transformation involve heating a dichloromethane solution of **97** with three equivalents of zinc chloride at reflux for 4 hours. Accordingly, these conditions were utilised in this work, and following purification by column chromatography the α-thio-β-chloroacrylate **69** was isolated as a pale yellow oil in 71% yield. Spectroscopic characteristics for the α-chloroacrylate **95**, α-thioacrylate **96**, dichloride **97** and α-thio-β-chloroacrylate **69** were identical to those reported.[16, 52]

2.3.6. Synthesis of α-Thio-β-Chlorothioester

While our group has extensively explored the synthesis of α-thio-β-chloroacrylamides via the NCS mediated chlorination cascade,[7, 15] and have readily extended this methodology to the preparation of corresponding ester,[52] nitrile,[52] and more recently ketone derivatives, we have never included thioesters in the scope of this transformation. Thioesters are a unique scaffold, that are critical acylating agents in biosynthesis,[56-57] and are crucial moieties in many biologically active compounds.[58-59] Thioesters are also exceptionally reactive compounds, which makes this functional group particularly amenable to further transformations. Accordingly, in this work, attempts were firstly made to determine whether a thioester moiety could undergo the NCS mediated chlorination cascade, and if so, if the α-thio-β-chlorothioester **70** could act as an effective dipolarophile in [3+2] dipolar cycloadditions.

Using the same methodology as outlined for the α-thio-β-chloroacrylamides the first step involved nucleophilic displacement of the chlorine atoms. Unlike for the α-thio-β-chloroacrylamides, however, in which an amine nucleophile is utilised prior to a thiolate, in this case both nucleophiles are a thiolate. In light of this, and taking into consideration the malodorous nature of thiols, a one-pot thiolation of both the acid chloride and alkyl chloride components of 2-chloropropionyl chloride **94** was envisaged to reduce the number of steps involving handling and purification of thiols. Considering this, a solution of 2-chloropropionyl chloride **94** in dichloromethane was added to a solution of thiophenol (2 equiv.) and triethylamine (4 equiv.) in dichloromethane. An excess of triethylamine was required to facilitate deprotonation of thiophenol and consume any hydrochloric acid produced. Following purification by flash column chromatography the novel α-thiothioester **99** was isolated in 64% yield **(Scheme 2.25)**.

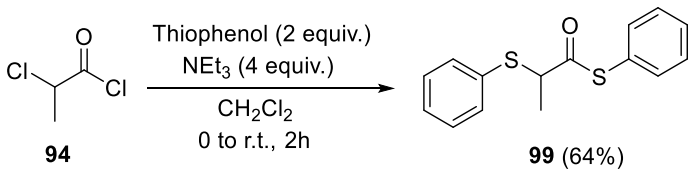

Scheme 2.25: Preparation of the α-thiothioester **99**

Notably, the signal for the carbon of the carbonyl moiety in the α-thiothioester **99** is observed at δ_C 197.9 ppm, making it significantly more deshielded than its ester counterpart **96** (δ_C 173.0 ppm), highlighting the considerably poorer resonance delocalisation that occurs in the thioester moiety relative to an ester due to decreased efficiency of orbital overlap.

With the α-thiothioester **99** in hand, it was decided to investigate whether the NCS mediated chlorination reaction cascade to afford α-thio-β-chlorothioester **70** occurs in an analogous manner to that of the α-thio-β-chloroacrylamides and/or α-thio-β-chloroacrylates. Therefore, the reaction was investigated using various conditions in an attempt to identify the respective α-chlorothioester **100**, thioacrylate **101**, dichloride **102** intermediates and isolate α-thio-β-chlorothioester **70**. We initially investigated the transformation under the optimised conditions for the chlorination of α-thioamides, that is using 1.95 equivalents of NCS in toluene at 90°C. Using this method no α-thio-β-chlorothioester **70** was observed. ^{1}H NMR spectroscopic analysis of the crude product indicated an 87:13 ratio of α-chlorothioester **100** to dichloride **102 (Entry 1**, **Table 2.3)**. Purification of the reaction intermediates by column chromatography was unsuccessful, with co-elution preventing the isolation of pure products. Despite this, each of the intermediates **100** and **102** survived flash column chromatography on silica gel and were isolated as mixtures. Identification and assignment of the intermediates was made by analogy with the corresponding signals from the ^{1}H NMR data for the related amide and ester series, for which there was considerable similarity (see **Figure 2.12**).

Table 2.3: Attempted NCS mediated chlorination of α-thiothioester **99**

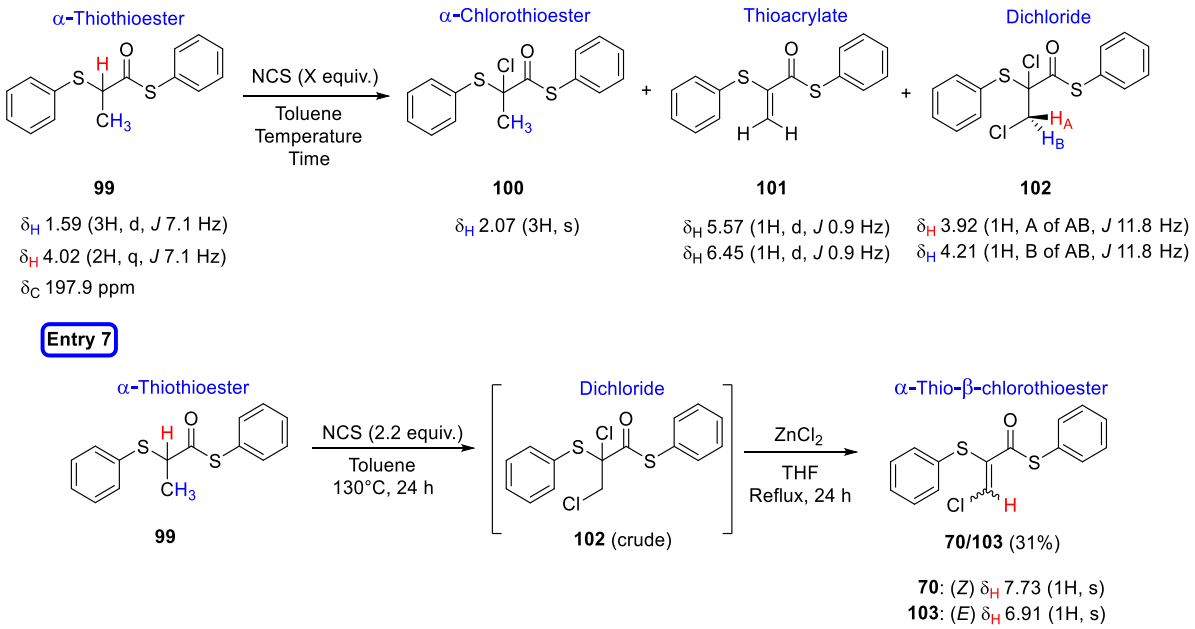

Entry	α-Thiothioester 99 (mmol)	NCS (equiv.)	Time (h)	Temp. (°C)	99 : 100 : 101 : 102[a]	$ZnCl_2$/THF (equiv.)	Yield[c] (%) 70/103
1	1	1.95	3	90	0 : 87 : 0 : 13[b]	No	-
2	1	0.5	3	90	83 : 17 : 0 : 0	No	-
3	1	1.0	3	90	44 : 56 : 0 : 0	No	-
4	0.5	1.5	3	90	37 : 47 : 0 : 16	No	-
5	0.5	3	3	90	0 : 55 : 0 : 45	No	-
6	0.5	3	20	130	0 : 2 : 30 : 68	No	-
7	1	2.2	24	130	-	Yes (5)	31[d]

a) Ratio determined by integration of relevant signals in the crude ^{1}H NMR spectra
b) A mixed fraction containing a 39:61 ratio of α-chlorothioester **100** and dichloride **102** was collected following flash column chromatography on silica gel. A second mixed fraction containing a 91:9 ratio of α-chlorothioester **100** and dichloride **102** was collected following flash column chromatography on silica gel.
c) Isolated yield following purification by flash column chromatography.
d) Isolated as a 90:10 mixture of tentatively assigned Z- and E-isomers **70** and **103** respectively.

Using 0.5 equivalents of NCS only 17% α-chlorothioester **110** was observed with 83% of unreacted α-thiothioester **99 (Entry 2)**. A singlet at δ_H 2.07 ppm was characteristic of the methyl β-hydrogens for the α-chlorothioester **100**. Increasing the equivalents of NCS to one moderately improved the consumption of the α-thiothioester **99**, with 56% α-chlorothioester **100** indicated by ^{1}H NMR spectroscopic analysis of the crude reaction mixture, albeit no evidence for the corresponding thioacrylate **101** or dichloride **102** was observed **(Entry 3)**. Only at 1.5 equivalents of NCS did any noticeable formation of the dichloride occur **(Entry 4)**, as indicated by the AB system at δ_H 3.92 and 4.21 ppm (*J* 11.8 Hz), however, even using three equivalents of NCS a mixture of α-chlorothioester **100** and dichloride **102** was obtained (55:45) with no evidence observed for α-thio-β-chlorothioester **70 (Entry 5)**. Therefore, it appeared that the dichloride **102** unsurprisingly shows a similar stability trend to that of the corresponding ester derivatives. To attempt to drive the reaction to complete conversion to the dichloride **102** the reaction was repeated using a three-fold excess of NCS at 130°C **(Entry 6)**. Following stirring under reflux for 24 hours 68% dichloride **102** was observed by ^{1}H NMR spectroscopy, with significant amounts of the thioacrylate also present (30%). As Lynch had reported that 2.1 equivalents of NCS under reflux was sufficient to afford the dichloride ester derivatives, in a very clean

transformation, a reaction using 2.2 equivalents was subsequently carried out **(Entry 7)**. After stirring under reflux for 24 hours, the reaction mixture was concentrated under reduced pressure to dryness, and resolubilised in THF. Zinc chloride in THF (5 equiv.) was added to promote the decomposition of the dichloride **102** to the α-thio-β-chlorothioester **70**, and the reaction mixture was subsequently stirred under reflux for 24 hours.

Following purification by column chromatography the α-thio-β-chlorothioester was isolated otherwise cleanly as mixture of *E*-**103** and *Z*-**70** isomers (10:90) in 31% yield, with the major product tentatively assigned as the *Z*-isomer by analogy with the α-thio-β-chloroacrylamides, for which the β-hydrogen is always observed to be more deshielded than its corresponding *E*-isomer. The ^{1}H NMR spectrum of this mixture is illustrated in **Figure 2.11**. Notably, as summarised in **Figure 2.12** the β-hydrogen signal in the ^{1}H NMR spectrum for the thioester derivative **70** is in very close agreement with that for the corresponding ester derivative **69**.

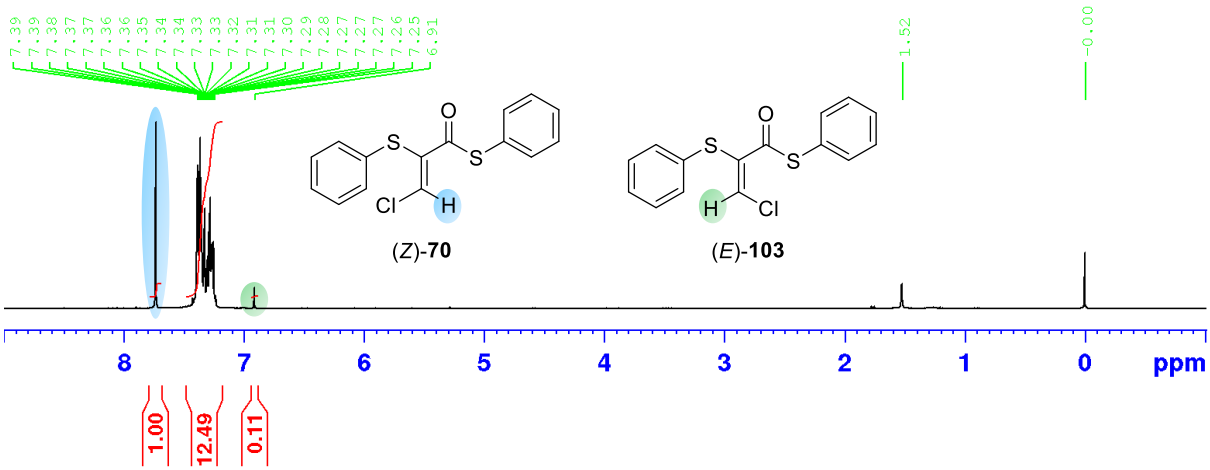

Figure 2.11: ^{1}H NMR spectrum of isolated mixture of tentatively assigned (*Z*)- and (*E*)-α-thio-β-chlorothioester **70** and **103**, in $CDCl_3$ at 300MHz.

With the generation of the α-thio-β-chlorothioester **70**, albeit as an inseparable mixture with the E-isomer **103**, the Maguire group has successfully applied the NCS mediated chlorination cascade to α-thioamides, α-thioesters, α-thionitriles, α-thioketones and now α-thiothioesters, with each mechanistic pathway observed to proceed via similar reaction intermediates as readily identified by their distinct characteristic ^{1}H NMR spectroscopic data. A complete summary of these intermediates and their key ^{1}H NMR signals are illustrated in **Figure 2.12**.

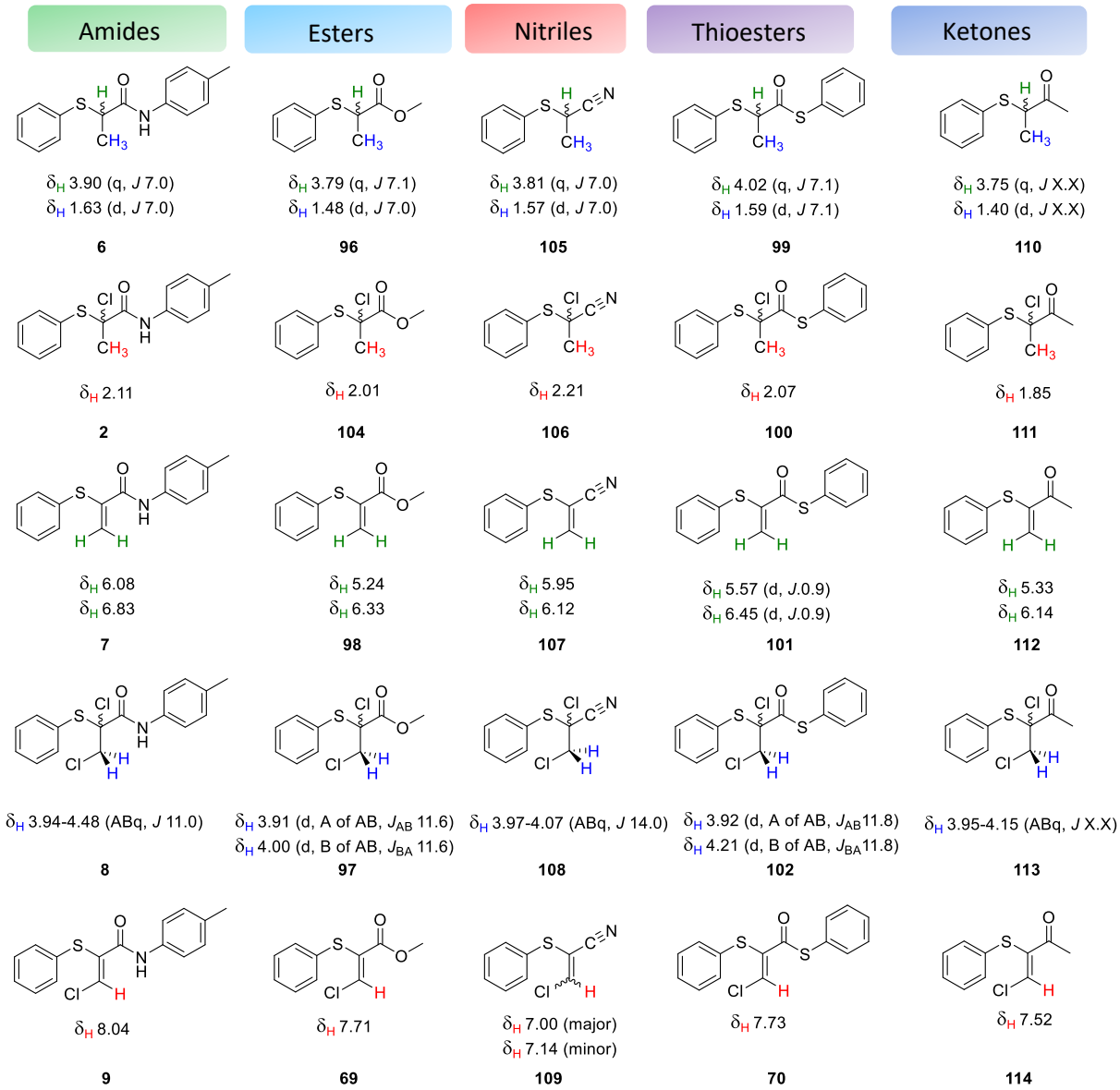

Figure 2.12: Summary of Maguire's NCS mediated chlorination cascade for amides, esters, nitriles, thioesters and ketones highlighting relevant ^{1}H NMR spectroscopy data.

2.3.7 Preparation of α-Sulfinyl-β-chloroacrylamides

Murphy initially explored the oxidation of the α-thio-β-chloroacrylamides to the corresponding racemic α-sulfinyl-β-chloroacrylamides using both *m*CPBA and Oxone® as oxidants **(Scheme 2.26)**.[15]

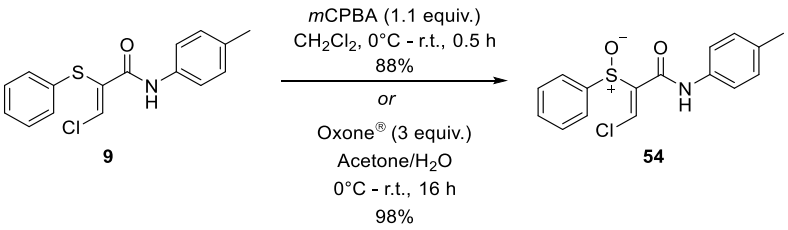

Scheme 2.26: Murphy's initial experiments on the oxidation of the α-thio-β-chloroacrylamides to the corresponding α-sulfinyl-β-chloroacrylamides

While on first inspection both methods appeared to be chemoselective for the sulfoxide, subsequent investigations by Lynch highlighted that the *m*CPBA mediated oxidation was not as selective as first thought, with typical product mixtures consisting of the unoxidized α-thio-β-chloroacrylamide, sulfoxide and sulfone.[16] Also problematic was the poor reproducibility observed when using *m*CPBA. Lynch subsequently highlighted that employment of two equivalents of Oxone® in an acetone/water mixture at room temperature for two hours were the optimised conditions for the chemoselective oxidation to the sulfoxide.

Oxone® is a stoichiometric commercially available oxidant that was first reported by Kennedy and Stock in 1960.[60] It is a triple salt consisting of two moles of potassium peroxymonosulfate, one mole of potassium bisulfate and one mole of potassium sulfate. The active oxygen transfer reagent dimethyldioxirane **115** is generated from the reaction of potassium peroxymonosulfate and acetone as illustrated in **Scheme 2.27**.[61] The mechanism for the oxidation of sulfides to their corresponding sulfoxides and sulfones using dioxiranes has received significant attention in the literature,[61-67] with both a concerted single step mechanism and a two-step process operational dependent on the reaction conditions. While a concerted process is favoured for dimethyldioxirane **115** in acetone or mixtures of acetone with aprotic co-solvents, a two-step process is favoured for dimethyldioxirane **115** in aqueous acetone of sufficient water content (20% v/v).[67] The latter process involves nucleophilic attack of the sulfur on the dioxirane **115** to give the intermediate betaine **(i) (Scheme 2.27, b)**. When the reaction is performed in aqueous acetone, specific solvation of **(i)** by water, via electron-pair donation to the partial positive charge on sulfur, and hydrogen bonding to the partial negative charge on oxygen in the dioxirane, leads to an increase in the reaction rate. Subsequent elimination of acetone from **(i)** affords the desired sulfoxide.

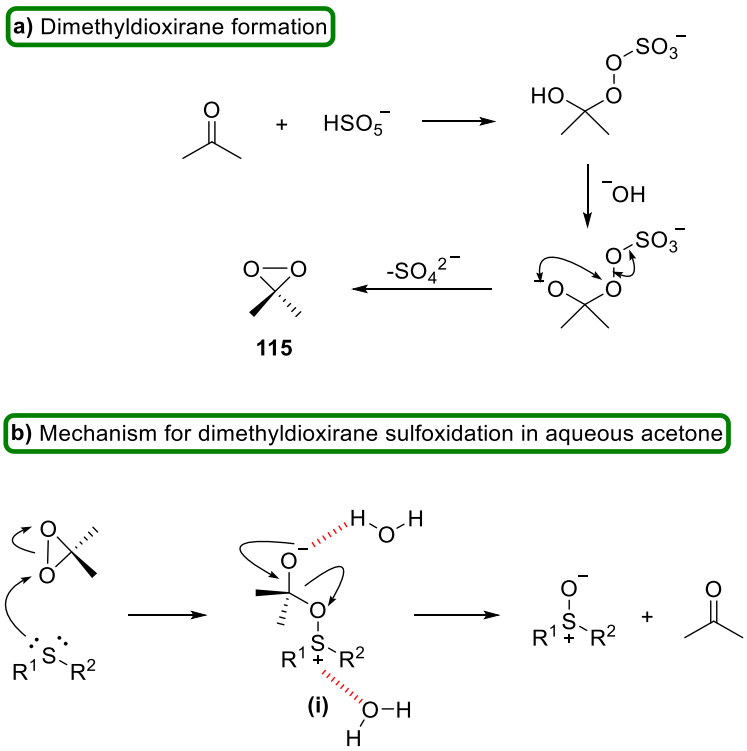

Scheme 2.27: a) Formation of dimethyldioxirane **115** from Oxone® and acetone **b)** mechanism for dimethyldioxirane sulfoxidation in aqueous acetone

In this work, Lynch's general optimised conditions using Oxone® as oxidant was used to generate a series of racemic known and novel α-sulfinyl-β-chloroacrylamides **54–61** and **116–117 (Table 2.4)**. In most instances, oxidation of the α-thio-β-chloroacrylamides exclusively afforded the desired α-sulfinyl-β-chloroacrylamides, with no evidence by ^{1}H NMR spectroscopy of over-oxidation to the sulfone, and hence were isolated in high purity following aqueous work-up in up to 97% yield. In instances in which the E-isomer appeared during the oxidation (tentatively assigned by ^{1}H NMR spectroscopy of the crude products), column chromatography was required to enable isolation of analytically pure sulfoxide derivatives.

Table 2.4: Preparation of racemic α-sulfinyl-β-chloroacrylamides

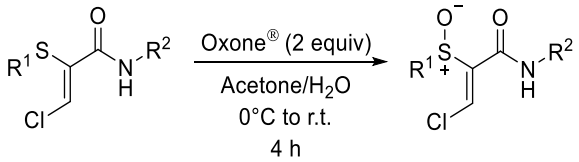

Entry	α-Thio-β-chloroacrylamide	R^1	R^2	Yield (%)[a/b]	α-Sulfinyl-β-chloroacrylamide
1	**9**	Ph	Tol	94[a]	**54**[12]
2	**40**	Ph	Bn	97[a]	**55**[12]
3	**41**	Ph	4-FC_6H_4	98[a]	**56**[12]
4	**42**	Ph	Neopentyl	96[a]	**57**
5	**43**	Ph	4-$MeOC_6H_4$	79[b]	**58**
6	**44**	Ph	*n*-Bu	95[a]	**59**[12]
7	**48**	Bn	Bn	87[b]	**116**[12]
8	**46**	Bn	*n*-Bu	80[b]	**117**[12]
9	**49**	Bn	4-FC_6H_4	93[a]	**60**[12]
10	**51**	Bn	4-$MeOC_6H_4$	92[b]	**61**

a) Crude product was sufficiently pure to be used without further purification.
b) Yield following purification by flash column chromatography.

The relative stereochemistry of the α-thio-β-chloroacrylamides was retained in all instances for the isolated α-sulfinyl-β-chloroacrylamides on oxidation from the sulfide to the sulfoxide; Lynch confirmed the Z-stereochemistry of the *N*-ethyl derivative **118** by single crystal X-ray diffraction and the sulfoxides prepared in this work were assigned Z by analogy **(Figure 2.13)**.[12]

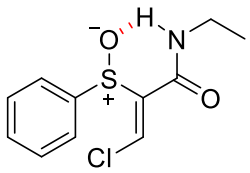

118

Figure 2.13: Z stereochemistry of α-sulfinyl-β-chloroacrylamides assigned by analogy with **118** whose structure was determined by single crystal PXRD.[12]

Yields and spectroscopic data for all resynthesised α-sulfinyl-β-chloroacrylamides in this work were consistent with those previously reported.[12, 16, 21] The sulfoxides **57**, **58** and **61** are novel compounds and were fully characterised in this work **(Figure 2.14)**. For the *Z*-sulfoxides, an upfield shift in the ^{1}H NMR spectra of the β-hydrogen of approximately 0.15 ppm occurred on oxidation of the α-thio-β-chloroacrylamides, reflecting that the oxidation has a significant impact on the extent of resonance delocalisation in the acrylamide system. The signal for the SCH_2 group of the benzylsulfinyl derivatives is shifted downfield by approximately 0.3 ppm in the ^{1}H NMR spectra, while the corresponding signal in the ^{13}C NMR spectra appears approximately 20 ppm downfield when compared to the analogous signal for the benzylthio derivatives. This is due to the increase in the inductive electron-withdrawing effect on going from the sulfides to the sulfoxides. The frequency of the carbonyl stretch in the IR spectra increased by 20–30cm^{-1} on oxidation of the α-thio-β-chloroacrylamides **(Figure 2.14)**. The decreased electron delocalisation in the acrylamide system due to the inductive effect of the sulfoxide accounts for this effect.

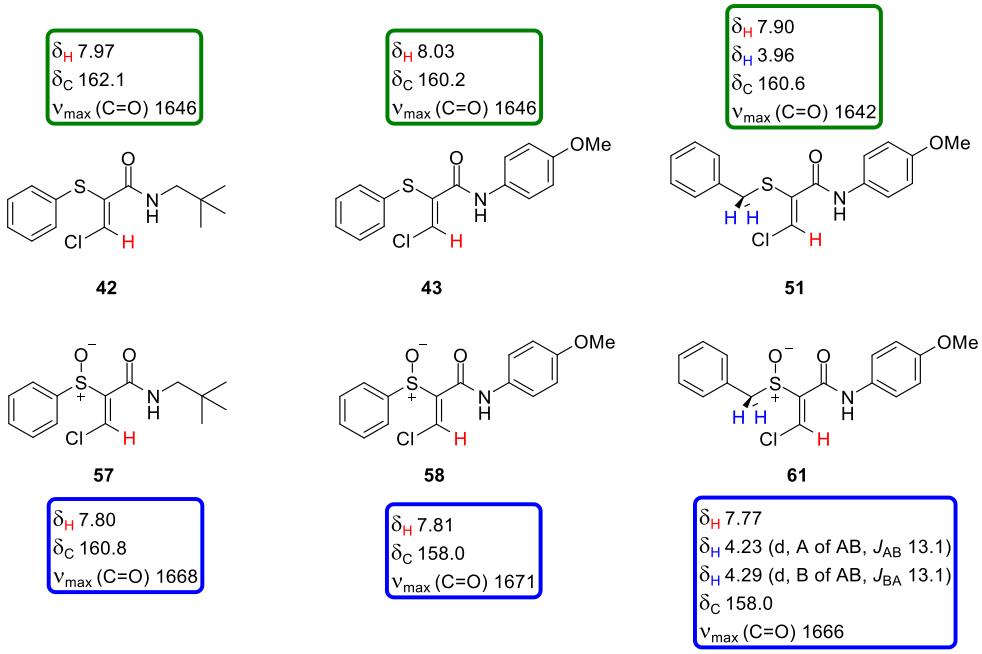

Figure 2.14: Comparison of ^{1}H, ^{13}C NMR (in $CDCl_3$ at 300 MHz) and IR (ATR) data for novel α-thio-β-chloroacrylamides and α-sulfinyl-β-chloroacrylamides

2.4 Generation of 1,3-Dipoles

2.4.1 Preparation of α-Diazosulfones

The use of terminal α-diazosulfones in [3+2] dipolar cycloadditions, at time of writing, is unexplored in the literature, however, due to the exceptional synthetic versatility of the sulfone moiety, and their prevalence in biologically active compounds, we envisaged that their incorporation into pyrazoline and/or pyrazole heterocycles in a regioselective manner via cycloaddition methodology would be advantageous. The synthesis of terminal α-diazosulfones has been reported by several groups, with aluminium oxide mediated debenzoylation[68] or deacylation[69] of α-diazo-β-ketosulfones, and the decarboxylation of *N*-nitroso compounds most popular **(Scheme 2.28)**.[70-73] The use of *N*-nitroso compounds however, is preferably avoided due to the inherent toxicity of these derivatives. More recently, Yan *et al*. extended this methodology to include a decarboxylation strategy,[74] in which the

ester moiety of α-diazo-β-sulfonylacetates is readily cleaved by aluminium oxide **(Scheme 2.28)**, however, the complexity of the 3,5,5-trimethylcyclohex-2-enol derived ester **122** required for this transformation was initially off-putting as a viable synthetic route.

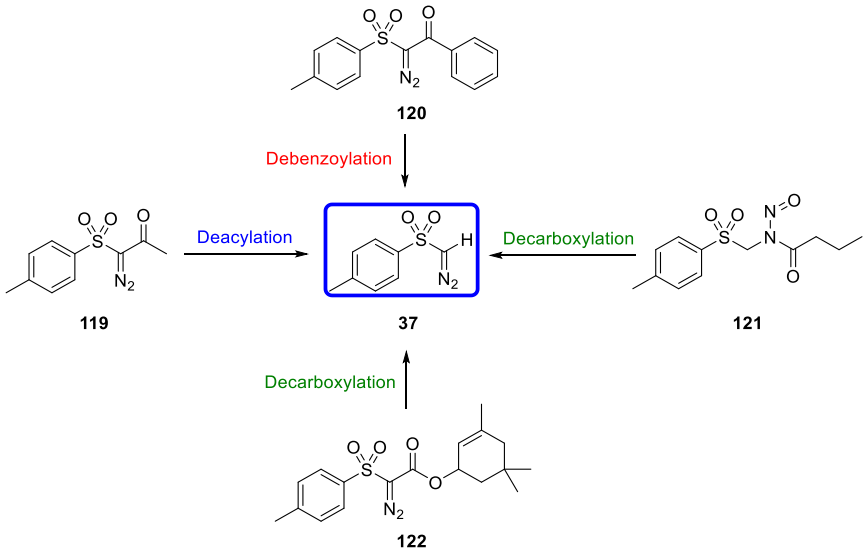

Scheme 2.28: Alumina mediated primary synthetic routes toward the generation of terminal α-diazosulfones

In order to avoid the use of highly toxic *N*-nitroso derivatives we initially explored the practicality of the debenzoylation strategy, with the known α-diazosulfone **127** chosen as our model compound.[68, 74] In this work the route employed to this compound is illustrated in **Scheme 2.29**. Due to large range of commercially available thiophenols it was envisaged that this route would allow access to a large library of terminal α-diazosulfones.

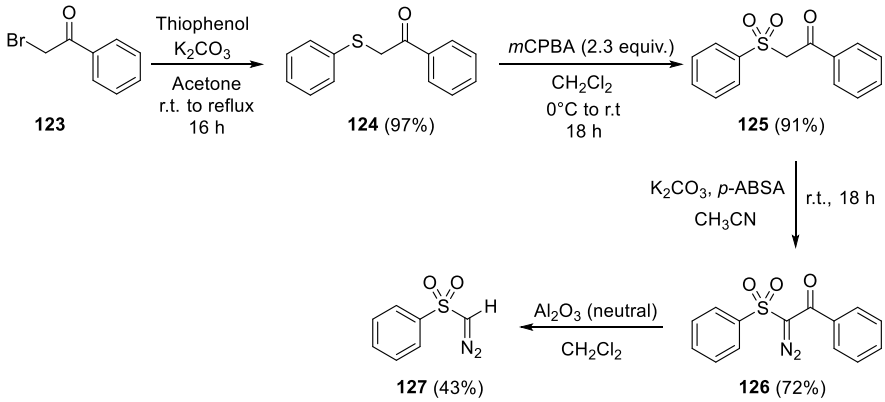

Scheme 2.29: Preparation of α-diazo-β-ketosulfone **127**

Initial thiolation of 2-bromoacetophenone **123** afforded the known β-ketosulfone **124** in almost quantitative yield (97%) following flash column chromatography.[75] Oxidation to the known sulfone **125** was efficiently achieved in 91% yield using an excess of *m*CPBA (2.3 equiv.) in dichloromethane, with ^{1}H NMR spectroscopy of the crude product following alkaline work-up indicating that no further purification was required.[76] Subsequently, Regitz diazo transfer using *p*-ABSA and K_2CO_3 in acetonitrile, conditions previously optimised in our group for the generation of similar α-diazo-β-ketosulfones,

afforded **126** in moderate yield (72%).[77] With the α-diazo-β-ketosulfone in hand we were interested in a report by Korneev and Richter, in which they described the selective benzoyl cleavage of **126** using neutral aluminium oxide **(Scheme 2.30)**, however, the reaction in their hands did not proceed to completion.[68]

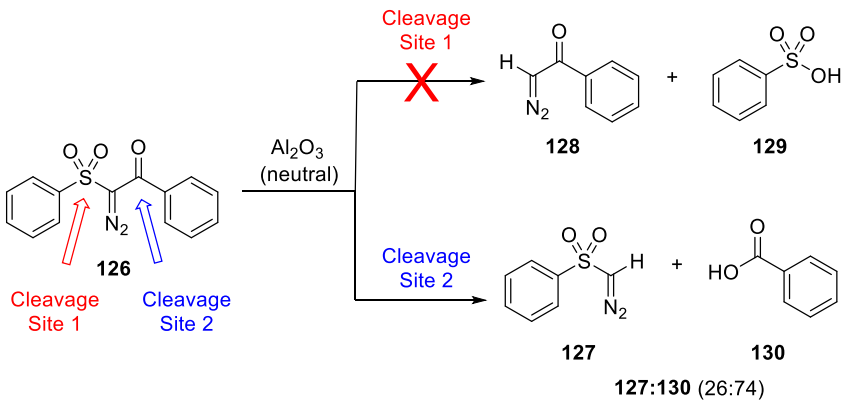

Scheme 2.30: Korneev and Richter's route towards α-diazosulfone **127**

Accordingly, we attempted to use this method for the preparation of α-diazosulfone **127**. In the first instance, as a preliminary investigation, 50 mg of α-diazo-β-ketosulfone **126** was loaded onto a column (diameter 1.5 cm, height 5 cm) of Al_2O_3 (6 g, activated, neutral, Brockmann 1) with dichloromethane as eluent. As α-diazosulfones are known to be light-sensitive the column was wrapped in tin-foil to ensure exposure to light was minimised. The products of the transformation were eluted slowly by gravity and the UV active fractions, readily identified by the yellow-tinge of the collected fractions, and were concentrated under reduced pressure in a round bottom flask also covered in tin foil at no greater than 30°C. In agreement with Korneev and Richter's observation the reaction had not reached completion with ^{1}H NMR spectroscopy of the crude product mixture indicating a mixture of 69:31 of **126**:**127 (Figure 2.15)**. Therefore, the process was repeated on the same column a further two times, the results of which are indicated in **Figure 2.15**, but ultimately highlighting that the reaction remained incomplete. Therefore, in order to attempt to force the transformation to completion, the reaction mixture was transferred to a column (diameter 2 cm, height 10 cm) of Al_2O_3 (16 g) under otherwise identical conditions, after which ^{1}H NMR spectroscopy of the isolated fractions confirmed that that the α-diazosulfone **127** had been obtained in pure form, albeit in low yield (32%).

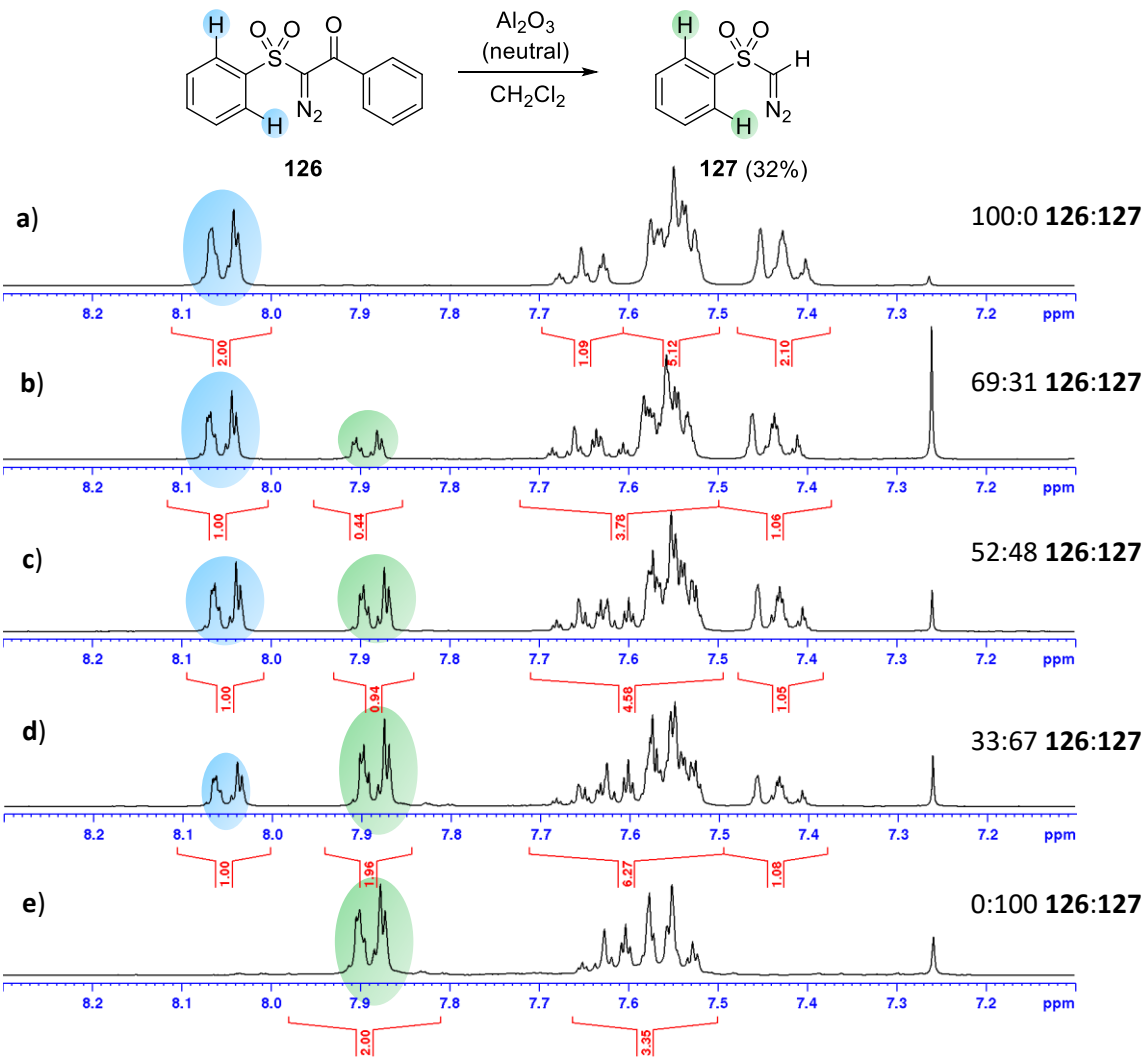

Figure 2.15: ^{1}H NMR spectra (in $CDCl_3$ at 300 MHz) of attempted debenzoylation of α-diazo-β-ketosulfone **126**; **a)** pure α-diazo-β-ketosulfone **126, b)** crude reaction mixture after passing through first column of alumina **c)** crude reaction mixture after passing through column of alumina a second time **d)** crude reaction mixture after passing through column of alumina a third time **e)** pure α-diazosulfone **127** after passing through column of alumina (16 g).

Despite the inefficiency of the transformation the reaction was scaled up in order to obtain enough α-diazosulfone **127** for preliminary [3+2] dipolar cycloaddition investigations. The reaction was repeated using 1 g of α-diazo-β-ketosulfone **126** and 100 g of alumina as described above, however, although the transformation went to 85% completion, a second column was required to complete the process in 43% yield **(Scheme 2.29)**. This process, however, did not prove to be robust with challenges encountered in reproducing the yield as described above. In other attempts, under similar conditions, with slight variations in the amount of Al_2O_3, isolation of the pure product was hampered by the presence of impurities likely due to degradation of the α-diazosulfone **127** due to extended contact with the Al_2O_3. Notably, the alumina turns a faint shade of pink throughout the transformation which has been postulated to be due to degradative pathways in the literature.[73] Despite this, enough material was obtained for the initial cycloaddition investigations, and hence was used in the early work as described in **Section 2.5.1**. However, due to the issues encountered in preparing synthetically useful amounts of α-diazosulfone **127** alternative routes were considered.

In this regard, the synthesis of α-tosyldiazomethane **37** has received significant attention in the literature, with an *Organic Syntheses* procedure published by van Leusen and Strating in 1977.[71] This procedure was more recently optimised by the Fischer group,[73] who demonstrated that difficulties in reproducibility could be greatly alleviated by first heating the alumina at ca. 300°C, and stringently excluding water from the final decomposition of the *N*-nitroso compound **121**. Furthermore, the use of highly toxic gaseous nitrosyl chloride in a neat manner was circumvented by instead using *iso*-amyl nitrite in the presence of trimethylsilyl chloride. Accordingly, this method was used for the preparation of α-tosyldiazomethane **37** and is illustrated in **Scheme 2.31**. Yields quoted in **Scheme 2.31** are yields that were obtained in this work.

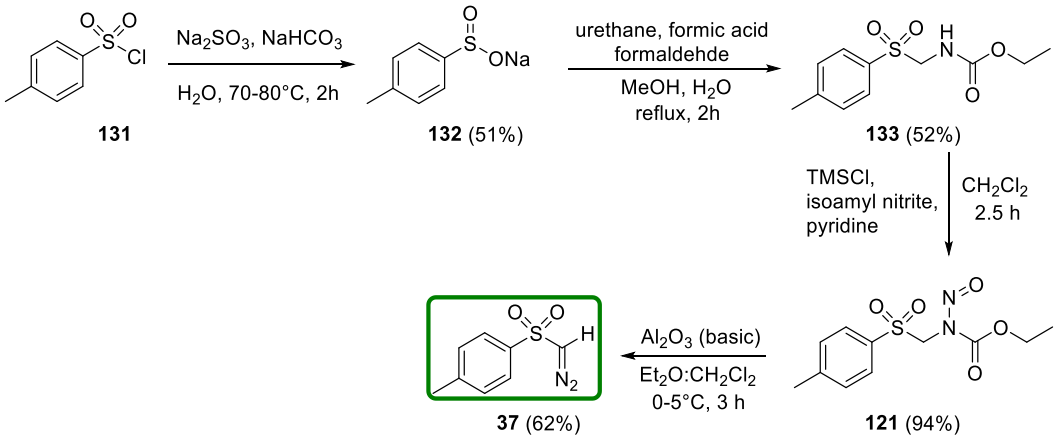

Scheme 2.31: Synthesis of α-tosyldiazomethane **37**

The sodium sulfinate **132** was firstly prepared in 51% yield via the reduction of the sulfonyl chloride **131** using sodium sulfite in the presence of sodium bicarbonate at elevated temperatures in water. The carbamate **133** was generated in 52% yield through a Mannich-type alkylation of the sulfinate **132**. Interestingly, the ^{1}H NMR spectrum of the pure product **133** indicated the presence of rotamers, despite being reported as a single rotameric species in the literature. It is known that amides and carbamates can exist as *syn*- or *anti*-rotamers about the C–N bond.[78] Typically, for secondary alkyl carbamates the fraction of *syn*-rotamer is approximately 10%, with the *anti*-rotamer more stable by approximately 1 kcal/mol.[79] Based on this observation, ^{1}H NMR analysis of the carbamate **133** in $CDCl_3$ at 20˚C indicated the presence of circa. 20% of the *syn*-rotamer, easily characterised by the signal broadening observed for the *syn*-rotamer as a result of restricted rotation **(Figure 2.16)**. It should be noted that it is not uncommon for the identification of the *syn*-rotamer to be difficult as the extent of signal broadening can cause their peaks to blend into the baseline. Observation of both the *syn*- and *anti*-rotamers strongly suggests that, in the non-interacting solvent $CDCl_3$, rotation around the C–N bond is slow on the NMR timescale. To ensure that it was indeed rotamers being observed, and not an impurity, ^{1}H NMR spectroscopy was also carried out in the hydrogen bond acceptor solvent, DMSO-d_6 at 20˚C. It was thought that if C–N bond rotation is slow on the NMR timescale in $CDCl_3$, it would be further slowed in the hydrogen bonding acceptor solvent DMSO-d_6. Interestingly, however, no substantial change in the ratio of *anti*- and *syn*-rotamers was observed. Broad signals corresponding to the minor *syn*-rotamer were also observed in the ^{13}C NMR spectrum of **133**, further supporting the presence of a rotameric mixture.

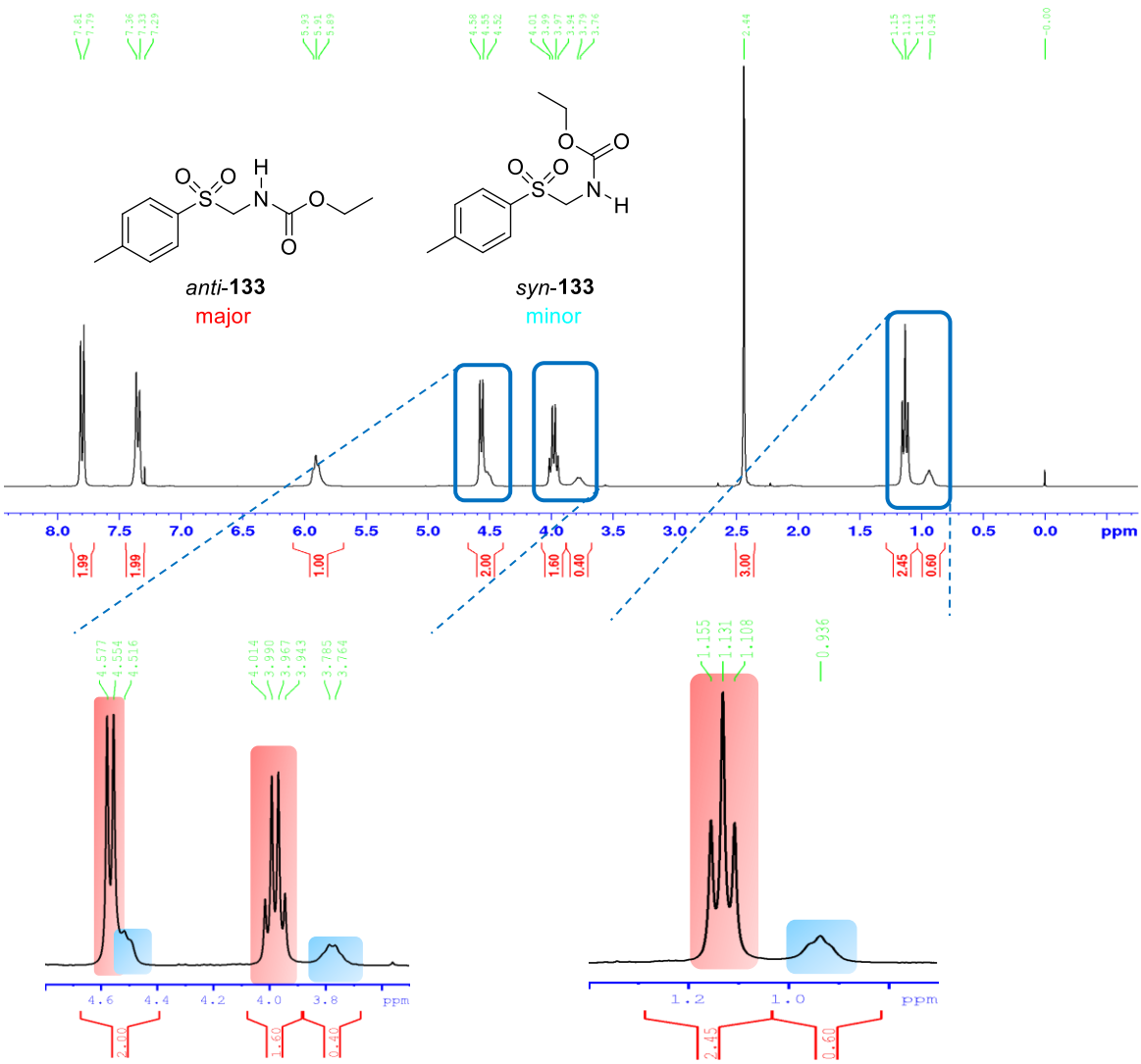

Figure 2.16: Previously unreported rotameric effect observed in the ^{1}H NMR (300 MHz) spectrum of carbamate **133** in $CDCl_3$ at 20˚C; tentatively assigned major *anti*-rotamer highlighted in red; minor *syn*-rotamer highlighted in blue

Next, the *N*-nitroso derivative **121** was formed in 94% yield by treating the carbamate **133** with an excess of isoamyl nitrite, trimethylsilyl chloride and pyridine in dichloromethane. Using this method, the handling of neat gaseous nitrosyl chloride is avoided by generating it in *situ* as highlighted in **Scheme 2.31.** Finally, transformation of the *N*-nitroso derivative to α-tosyldiazomethane **37** was achieved in 62% yield by stirring in a mixture of basic Al_2O_3 (activated by heating to 300°C) in dichloromethane: diethyl ether for 3 hours at 0–5°C. All compounds highlighted in **Scheme 2.31** are known compounds and their physical and spectroscopic characteristics were consistent with literature reports,[71] with the exception of the NMR spectroscopic data for the carbamate **133 (Figure 2.16)**. The generated batch of α-tosyldiazomethane **37** was stored in the dark, in the freezer, and showed no appreciable degradation over a one year period. This is in contrast with the α-diazosulfone **127**, which in our hands was observed to be much more labile with degradation occurring over a matter of days even when stored under identical conditions. This difference in stability may be due to differences in the physical properties of the two compounds; α-tosyldiazomethane **37** is a solid while the α-diazosulfone **127** is an oil.

2.4.2. Preparation of *N*-Benzyl-α-Diazoacetamide

Current methods to generate diazo compounds are numerous and include **a)** diazo transfer,[80-81] **b)** diazotization,[82-83] **c)** decomposition or oxidation of hydrazones,[84-87] **d)** fragmentation of 1,3-disubstituted alkyl aryl triazenes,[88-89] and **f)** rearrangement of *N*-alkyl *N*-nitroso compounds.[90] For this work a high yielding 'deimidogenation' reaction, a term coined by Raines and Myres, was used to generate the terminal α-diazoacetamide **39**.[91] Our preparation of *N*-benzyl-α-diazoacetamide, based on this report, is illustrated in **Scheme 2.32**.

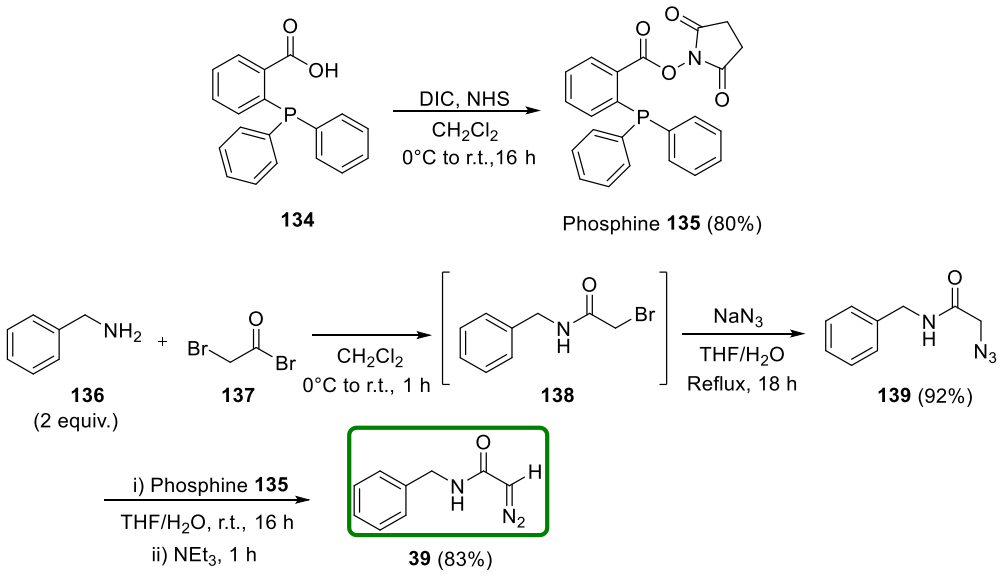

Scheme 2.32: Preparation of *N*-benzyl-α-diazoacetamide

The phosphine **135** was firstly prepared via coupling of the carboxylic acid **134** and *N*-hydroxysuccinimide in the presence of *N,N'*-diisopropylcarbodiimide in dichloromethane. Following flash column chromatography the pure known phosphine **134** was isolated in 80% yield, the purity of which was confirmed by ^{31}P NMR spectroscopy [{δ_P} – 4.5 ppm].

N-Benzyl-2-bromoacetamide **138** was prepared by treatment of bromoacetyl bromide **137** with an excess of benzyl amine **136** (2 equiv.) in dichloromethane for 1 h. Analogous to the formation of the α-chloroamides, as discussed in **Section 2.3.2**, the addition-substitution reaction occurs chemoselectively at the acyl bromide. The second equivalent of benzyl amine consumes the hydrochloric acid produced during the reaction, as evidenced by the formation of a white precipitate immediately on the addition of bromoacetyl bromide. Following work up the crude α-bromoacetamide **138** was reacted with sodium azide in a mixture of tetrahydrofuran/water under reflux for 18 h to afford the pure α-azidoacetamide **139** in 92% yield.

The 'deimidogenation' reaction for the conversion of pure α-azidoacetamide **139** to the desired α-diazoacetamide **39** proceeded in excellent yield (83%), comparable to that obtained in the original report (85%).[91] The solid α-diazoacetamide **39** was accessible on multigram scale, can be stored without evident degradation and was readily characterised by various spectroscopic techniques. The presence of the diazo functionality was confirmed by IR spectroscopy, with a stretch at 2096 cm^{-1} consistent with literature reports. Furthermore, in the ^{1}H NMR spectrum a characteristic 1H singlet was observed for the CHN_2 signal at 4.81 ppm, highlighting the cumulative electron-withdrawing effect of the amide and diazo moieties. The mechanism for this reaction is not fully understood but isolation

of an acyl triazene derivative in the reported work supports the mechanism postulated in **Scheme 2.33**.[91] While the preparation of diazo compounds via the fragmentation of triazenes is uncommon, there are a few isolated reports of this transformation that further support the likelihood of this transformation.[88-89] The final transformation from acyl triazene **142** to diazo product **39** has been hypothesised to involve either thermal or base catalysed fragmentation of the acyl triazene **142**, however, further mechanistic studies are required to confirm this rationale.

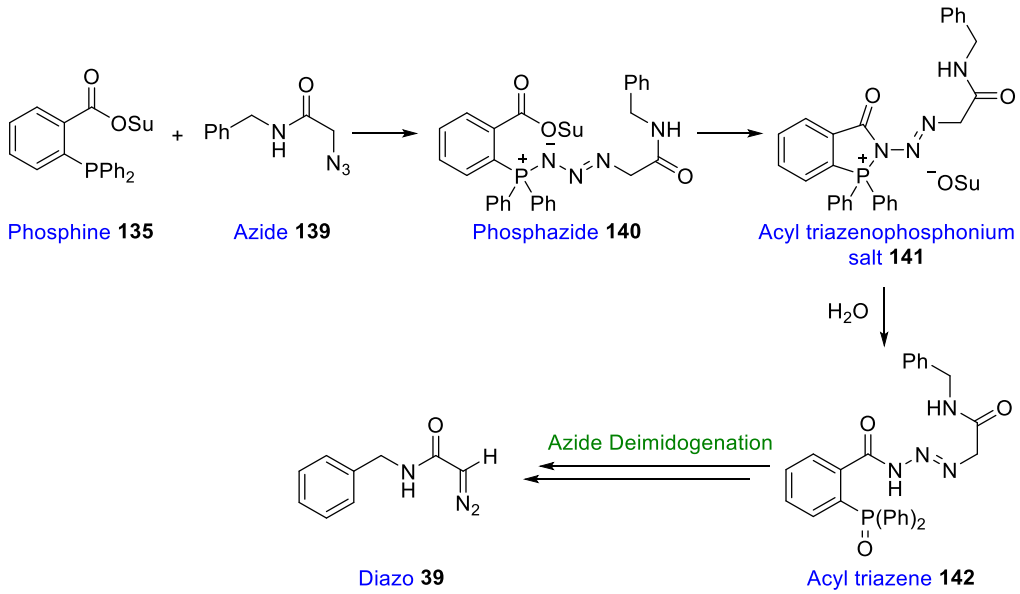

Scheme 2.33: Overview of the 'deimidogenation' reaction for the conversion of pure α-azidoacetamide **139** to the α-diazoacetamide **39**.

2.5. [3+2] Dipolar Cycloadditions

2.5.1. [3+2] Dipolar Cycloadditions of α-Diazosulfones

The [3+2] dipolar cycloaddition of α-diazosulfone **127** with α-thio-β-chloroacrylamide **52**, provided by Cacheux at the outset of this work,[18] was initially explored. In Kissane's related work using the considerably more reactive diazoalkanes a large excess of diazo was utilised (approx. 6-7 equivalents) to ensure reaction completion.[9, 21] Accordingly, an excess of an ethereal solution of α-diazosulfone **127** (6.8 equiv.) was added dropwise to an ethereal solution of α-thio-β-chloroacrylamide **52** at 0°C under nitrogen in the dark **(Scheme 2.34)**. Following stirring for 16 h, the reaction progress was checked by ^{1}H NMR spectroscopy, however, no evidence for the formation of either the pyrazoline **144** or pyrazole **145** was observed. Despite the lack of evidence for cycloaddition, significant consumption of the α-thio-β-chloroacrylamide **52** had in fact occurred, with a 52:48 ratio of **52** to the unexpected oxidised product α-sulfinyl-β-chloroacrylamide **143**. This determination was made by observation of the distinctive ^{1}H NMR data for the known α-sulfinyl-β-chloroacrylamide **143** as illustrated in **Scheme 2.34** which allowed the sulfoxide's unambiguous assignment.[12]

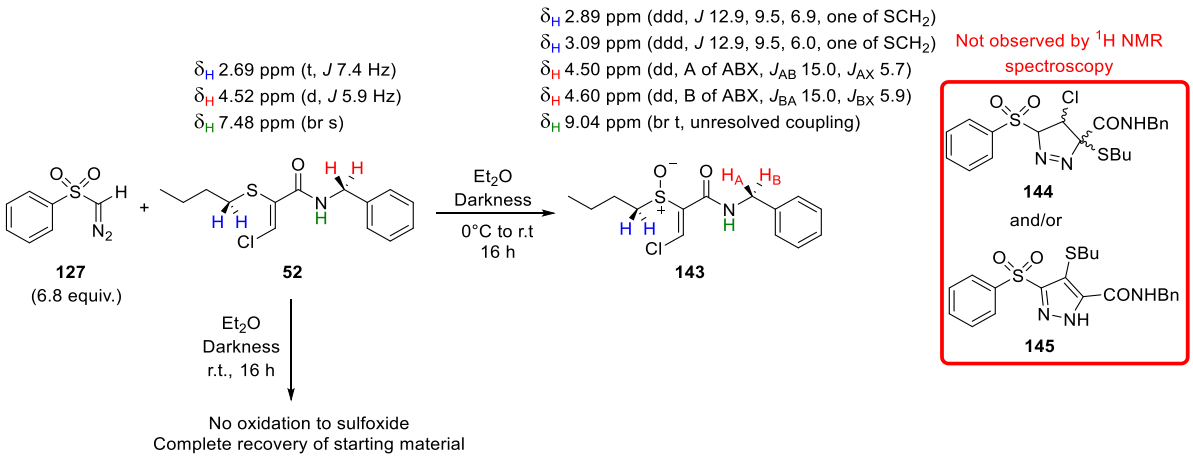

Scheme 2.34: Attempted [3+2] dipolar cycloaddition of α-diazosulfone **127** and α-thio-β-chloroacrylamide **52**

Interestingly, when the reaction was repeated in the absence of α-diazosulfone **127** no oxidation was observed with complete recovery of the α-thio-β-chloroacrylamide **52**, highlighting that the diazo compound was actuating oxidation rather than peroxides in the ether **(Scheme 2.34)**. As mentioned in **Section 2.4.1**, in our hands the α-diazosulfone **127** was observed to be a very labile compound, degrading readily over time if not stored in a freezer under nitrogen. It is likely that the degradation pathway involves loss of dinitrogen leading to carbene formation. As such, it is plausible that the oxidation of α-thio-β-chloroacrylamide **52** was mediated via the formation of the sulfonium ylide **(i)** **(Scheme 2.35)**. Notably, the use of carbenes in the formation of sulfur ylides has been extensively explored by Ando and his co-workers,[92] with the majority of their research using carbenes with strongly electron-withdrawing substituents. This type of substitution is known to have a stabilising effect on the resulting ylides so that they can often be isolated and thoroughly characterised.[93] In our case, no evidence for the ylide was observed, however its formation can readily be used to rationalise the oxidation process. A tentatively proposed mechanism is proposed in **Scheme 2.35**, however, as the objective of this work involved cycloadditions the mechanism of this transformation was not pursued. While oxygen transfer from the sulfone could be envisaged, it is likely that adventitious water plays a key role in the hydrolysis of the sulfonium ylide, while the methyl phenyl sulfonyl moiety would act as an excellent leaving group due to the extensive delocalisation of the anion through the sulfonyl moiety. That said, no evidence for the formation of methyl phenyl sulfone **146** was observed in the ^{1}H NMR spectrum of the crude product.

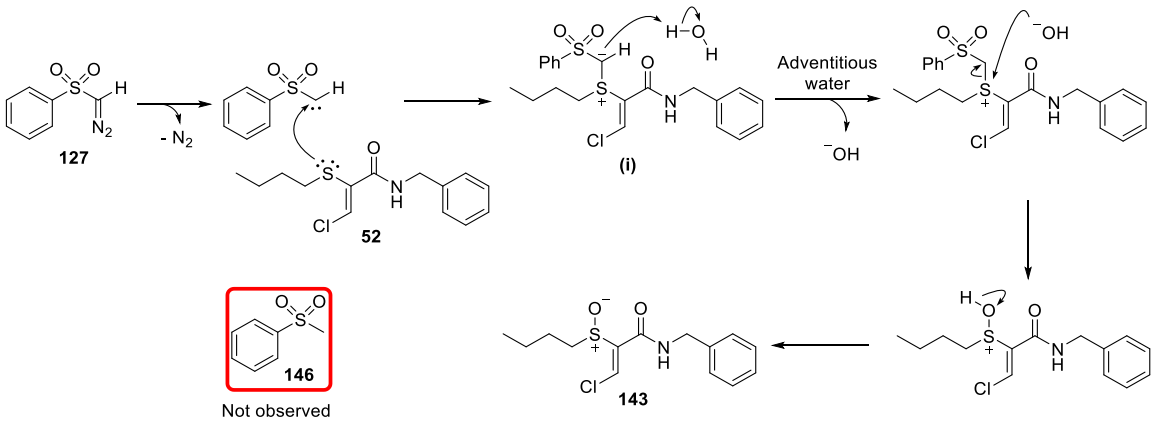

Scheme 2.35: Tentatively proposed mechanism for the α-diazosulfone **127** promoted oxidation of α-thio-β-chloroacrylamide **52**

In order to evaluate whether competing dipolar cycloaddition could be mediated by increasing the temperature of the reaction, the α-diazosulfone **127** was reacted with α-thio-β-chloroacrylamide **147**, chosen to allow facile monitoring of the benzylic hydrogens by ^{1}H NMR spectroscopy, at 30°C in diethyl ether. Following stirring for 36 h, ^{1}H NMR spectroscopy of the crude reaction mixture indicated that oxidation had again occurred, with coinciding degradation of the α-diazosulfone **127**, with the absence of any evidence for cycloaddition **(Scheme 2.36)**.

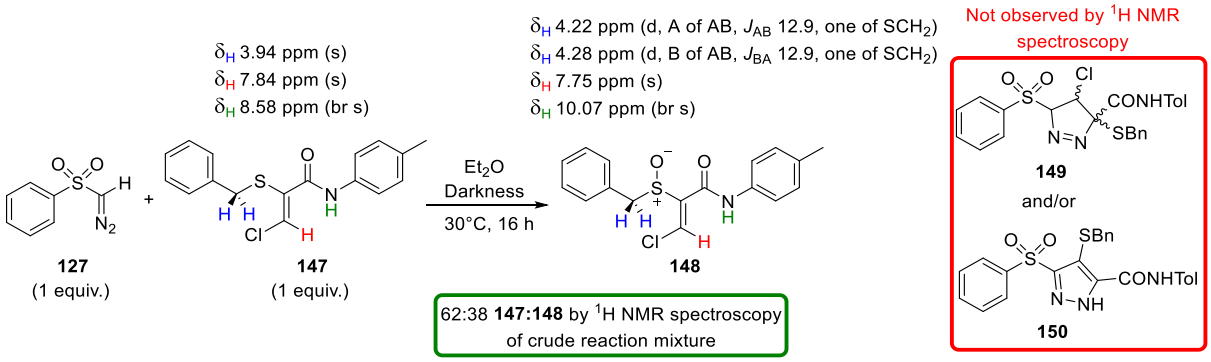

Scheme 2.36: Attempted [3+2] dipolar cycloaddition of α-diazosulfone **127** and α-thio-β-chloroacrylamide **147** at 30°C. α-Thio-β-chloroacrylamide **147** provided by Cacheux at the commencement of these studies.[18]

Clearly carbene formation was problematic from the perspective of maintaining the diazo moiety to undergo dipolar cycloaddition. The degradation of diazo compounds to the corresponding carbene under thermal conditions, or to the carbenoid via transition metal catalysis are well known processes, with similar by-products observed using both methods. For example, Corey and co-workers demonstrated that rhodium catalysed degradation of tosyl diazomethane **37** forms a mixture of the carbene dimerization products *cis*-**151** and *trans*-**152** as well as the unexpected thiosulfonate **153** **(Scheme 2.37, a)**.[94] Therefore, in this work, to investigate the thermal stability of the α-diazosulfone **127**, the compound was stirred in ether under reflux for 16 hours. Analysis of the crude reaction mixture by ^{1}H NMR spectroscopy indicated complete consumption of the α-diazosulfone, with a 95:5 mixture of the dimerisation products *trans*-**154** and *cis*-**155**, both of which are known compounds **(Scheme 2.37, b)**.[95]

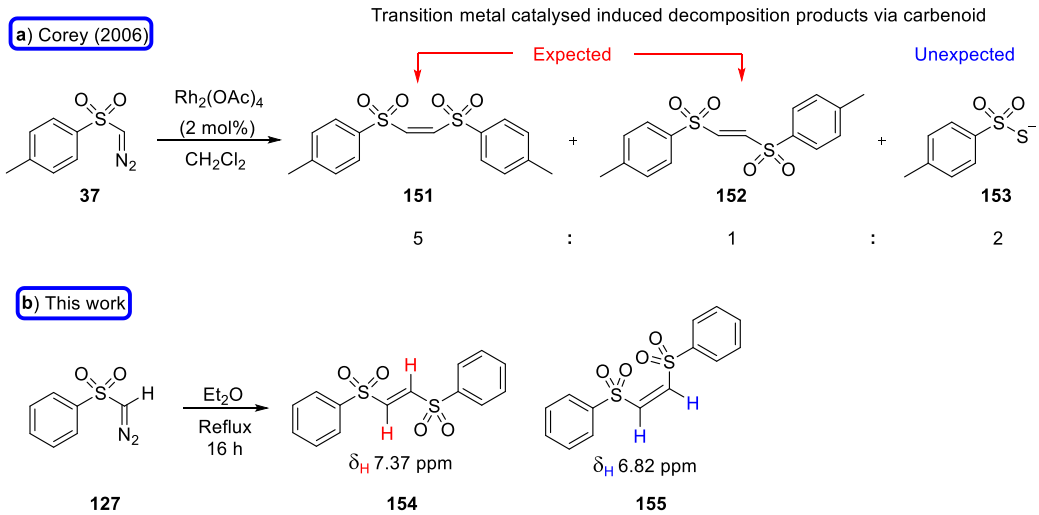

Scheme 2.37: a) Rhodium catalysed degradation of tosyl diazomethane **37**, and
b) Thermal degradation of α-diazosulfone **127**

Consequently, the use of heat to overcome the $HOMO_{(Dipole)}$–$LUMO_{(Dipolarophile)}$ and/or $HOMO_{(Dipolarophile)}$–$LUMO_{(Dipole)}$ energy difference was not pursued further. In light of not observing any evidence for the formation of either a pyrazoline or pyrazole structure, and the lack of literature reports describing the [3+2] dipolar cycloadditions of α-diazosulfones, we envisaged that the highly electron-withdrawing nature of the sulfonyl moiety may restrict entirely its supposed dipole character. However, thus far in this work, the only dipolarophiles investigated were α-thio-β-chloroacrylamides, which are both electronically and sterically complex. Therefore, it was decided to determine whether α-diazosulfone **37** could indeed undergo [3+2] dipolar cycloaddition by reacting it with a known highly reactive dipolarophile. In this regard dimethyl acetylenedicarboxylate **156** (DMAD) was chosen, as electron deficient alkynes are known to be exceptionally reactive in $HOMO_{(Dipole)}$–$LUMO_{(Dipolarophile)}$ cycloadditions. Accordingly, one equivalent of DMAD **156** was added neat to a solution of two equivalents of the α-diazosulfone **37** at 0°C, in case of an exotherm, in the dark under nitrogen **(Scheme 2.38)**. The ice-bath was removed, and the reaction mixture was warmed slowly to room temperature and stirred for 24 h. ^{1}H NMR spectroscopy indicated that the reaction had gone to completion, in a very clean manner. Following purification by flash column chromatography the novel pyrazole **157** was isolated as a white solid in 92% yield and fully characterised.

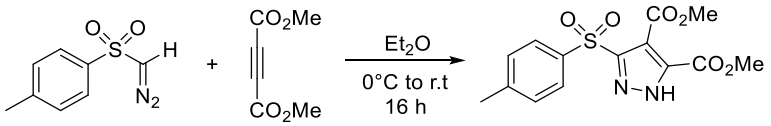

Scheme 2.38: [3+2] Dipolar cycloaddition with electron deficient alkynyl dipolarophile DMAD **156**

While alkynes bearing electron withdrawing groups are excellent dipoalrophiles for $HOMO_{(dipole)}$–$LUMO_{(dipolarophile)}$ cycloadditions they are structurally and electronically dissimilar to the α-thio-β-chloroacrylamides utilised in this work. Therefore, we subsequently investigated whether the α-diazosulfone **37** would react with a more closely related dipolarophile. In this context, *N*-phenyl maleimide **158** was utilised as dipolarophile, under otherwise identical conditions **(Figure 2.17)**. Notably, the locked conformation of the dipolarophile in this instance enabled facile [3+2] dipolar cycloaddition, with ^{1}H NMR spectroscopy of the crude reaction mixture indicating a clean conversion to the 1-pyrazoline **159 (Figure 2.17**, **a)**. Following purification by flash column chromatography on silica gel, however, the novel 1-pyrazoline **159** had completely tautomerised to the thermodynamically more stable 2-pyrazoline **160 (Figure 2.17**, **b)**. The novel 2-pyrazoline **160** was isolated as a white solid in 53% yield. A D_2O exchange confirmed that the broad singlet at 7.26 ppm, which overlaps with the residual $CDCl_3$ signal, corresponds to the hydrogen of the N–H moiety in **160 (Figure 2.17, c)**.

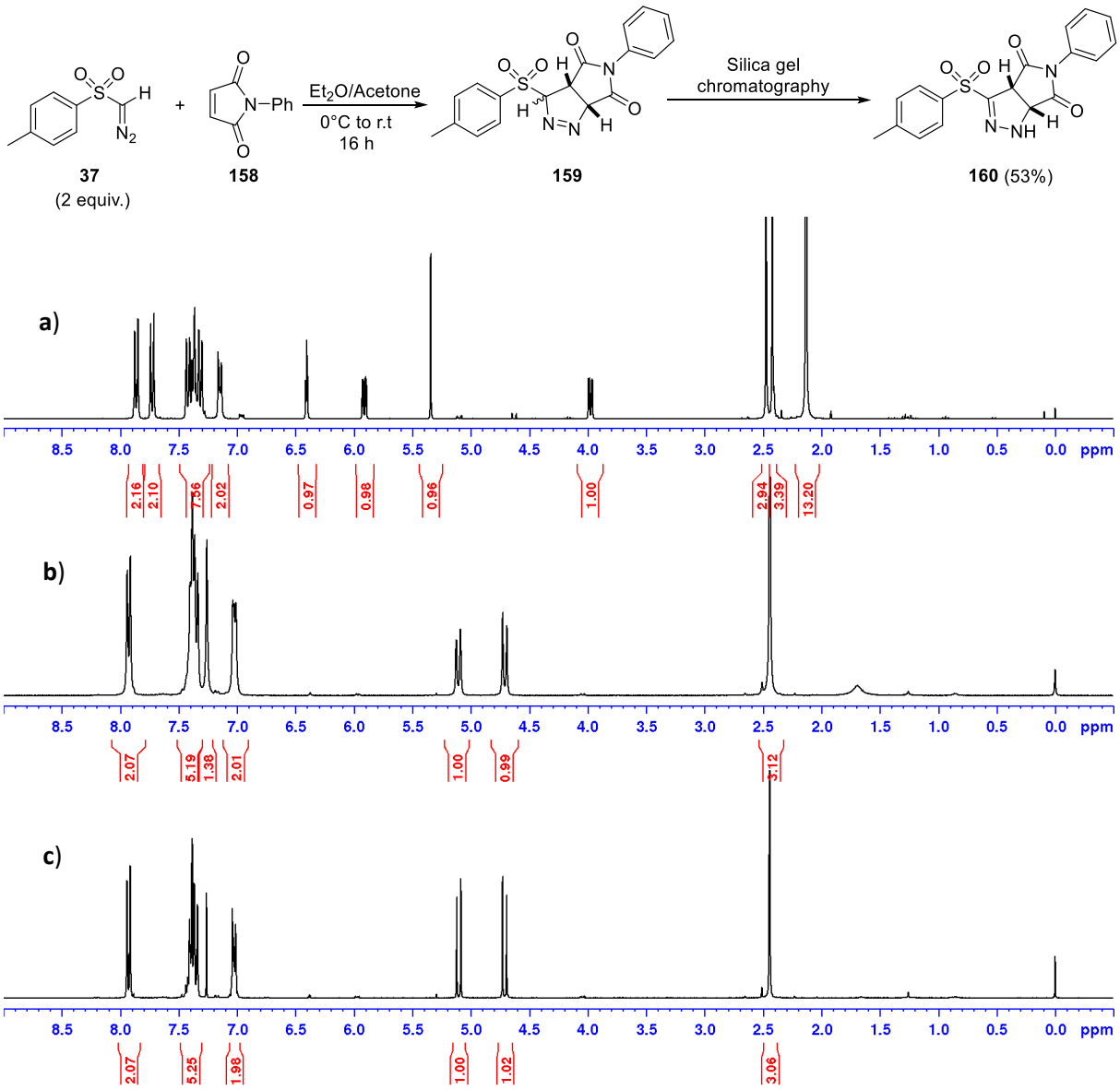

Figure 2.17: [3+2] Dipolar cycloaddition of α-diazosulfone **37** and *N*-phenyl maleimide **158**. ^{1}H NMR spectra (in $CDCl_3$, 300 MHz) of **a)** crude reaction mixture highlighting clean conversion to the 1-pyrazoline **159**, **b)** pure 2-pyrazoline **160** following flash column chromatography on silica gel, and **c)** D_2O exchange

To further increase the similarity of the dipolarophile to the α-thio-β-chloroacylamides, we next utilised 2-methyl-*N*-phenylmaleimide **161**, however, in this instance the incorporation of a methyl substituent substantially decreased the rate of reaction; ^{1}H NMR spectroscopy of the crude reaction mixture indicated a 21% conversion to the tentatively assigned 1-pyrazoline **162** after 24 hours **(Scheme 2.39)**. Attempts to improve the conversion of the reaction by increasing the reaction time to one week and increasing the amount of α-diazosulfone **37** to 4 equivalents, did not prove beneficial with degradation of the α-diazosulfone **37** becoming more problematic overtime. The 1-pyrazoline **162** was not isolated as a result of the poor conversions, however, tentatively assigned signals from the ^{1}H and ^{13}C NMR spectra of the crude reaction mixture compare favourably to those observed for the 1-pyrazoline **159 (Figure 2.17)**.

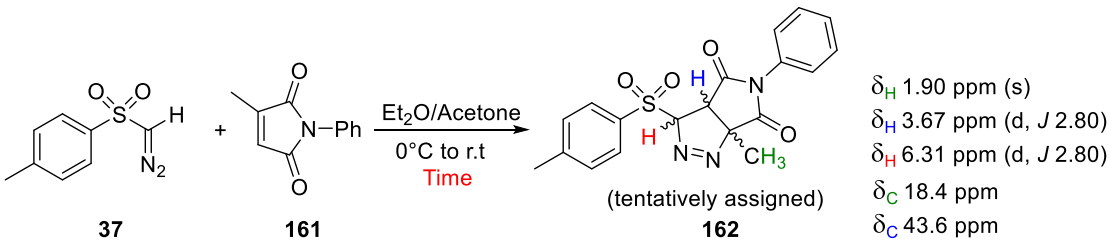

Entry 1	(2 equiv.)	24 h	21% conversion
Entry 2	(4 equiv.)	7 days	Significant degradation

Scheme 2.39: Attempted [3+2] dipolar cycloaddition of α-diazosulfone **37** and 2-methyl-*N*-phenylmaleimide **161**

Due to the profound effect that the incorporation of a methyl substituent had on the [3+2] dipolar cycloaddition of 2-methyl-*N*-phenylmaleimide **161**, the labile nature of the α-diazosulfones at temperatures above 30°C, and the observation that oxidation of the sulfide moiety occurs in preference to cycloaddition for the α-thio-β-chloroacrylamides it was concluded that the [3+2] dipolar cycloaddition of α-diazosulfones and α-thio-β-chloroacrylamides was not possible under thermal conditions. Notably, Lynch observed that α-thio-β-chloroacrylamides were also unreactive as dienophiles in Diels–Alder cycloadditions, under thermal conditions, however, the corresponding α-sulfinyl-β-chloroacrylamides were considerably more reactive presumably due to the sulfoxide moiety lowering the LUMO of the dienophile.[8, 16] In light of this a final attempt to effect cycloaddition was attempted by utilising the α-sulfinyl-β-chloroacrylamide **54**, in order to increase the reactivity of the dipolarophile, however no cycloaddition or oxidation was observed, despite evidence for degradation of the α-diazosulfone **37 (Scheme 2.40)**.

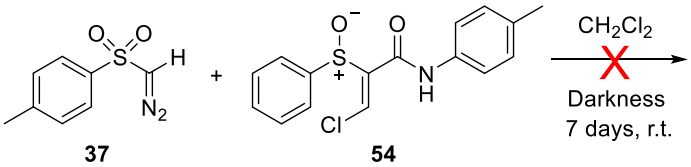

Scheme 2.40: Attempted [3+2] dipolar cycloaddition of α-diazosulfone **37** and α-sulfinyl-β-chloroacrylamide **54**

2.5.2. [3+2] Dipolar Cycloadditions of α-Diazoacetates with α-Thio-β-Chloroacrylamides

Significantly, as described above, the use of terminal α-diazosulfones as dipolarophiles in [3+2] dipolar cycloadditions are extremely restricted by virtue of their poor thermal stabilities. Notably, in a study of the thermal stabilities of the diazo moiety in a series of acyldiazomethanes, Regitz and Maas highlighted that α-diazosulfones are extremely labile under thermal conditions relative to other related derivatives **(Figure 2.18)**.[96] Terminal α-diazoacetates, however, have a much higher thermal stability and hence their use as 1,3-dipoles at elevated temperatures is well explored.[97-107] The difference in thermal stabilities is readily rationalised by studying the various resonance contributors of the respective 1,3-dipoles. As illustrated for ethyl diazoacetate **38** and tosyl diazomethane **37** in **Scheme 2.41**, the activated form for dinitrogen cleavage is represented by the resonance contributor **B**. In this state both dinitrogen and the carbene **C** are 'preformed'. Accordingly, delocalisation of excess electron density at the diazo carbon by electron-withdrawing groups will undoubtably favour fragmentation. Notably, the sulfonyl moiety is considerably more inductively electron withdrawing than the corresponding ester, and hence the α-diazosulfone is much less stable under thermal

conditions than the α-diazoester. With this in mind our attention turned to the [3+2] dipolar cycloadditions of α-diazoacetates with the α-thio-β-chloroacrylamides.

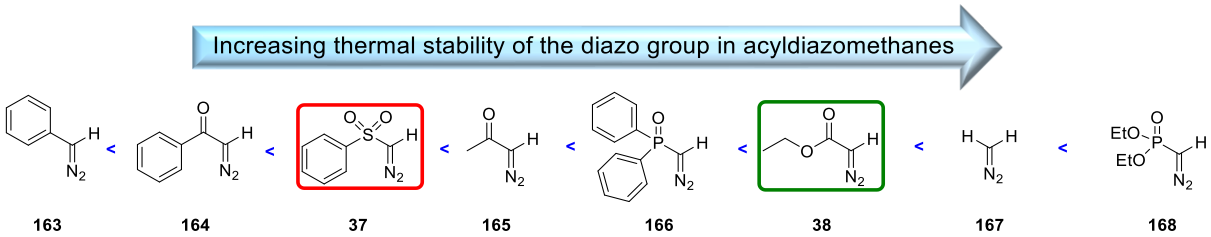

Figure 2.18: Comparison of thermal stabilities of terminal acyldiazomethanes and related derivatives.[96]

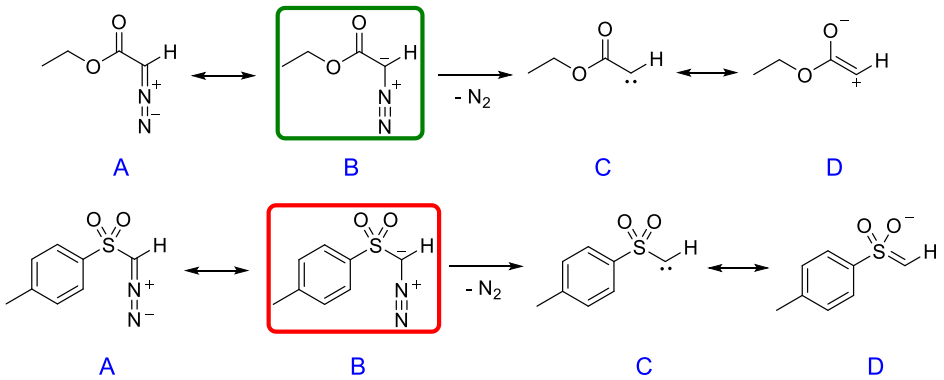

Scheme 2.41: Rationale for increased thermal stability of α-diazoacetates compared to α-diazosulfones[96]

In the first instance, an excess of ethyl diazoacetate **38** (4 equiv.) was added in one portion to a stirring solution of α-thio-β-chloroacrylamide **9** in toluene at room temperature **(Table 2.5**, **Entry 1)**; however, no reaction was observed by ^{1}H NMR spectroscopy after 24 hours. Increasing the reaction temperature to 50°C under otherwise identical conditions also lead to no consumption of either starting material **(Entry 2)**. When the reaction temperature was increased to 100°C, however, following the removal of an aliquot after 2 hours, tentative evidence supporting the formation of a pyrazoline or pyrazole was observed by ^{1}H NMR spectroscopy with a broad singlet at δ_H 9.83 ppm, presumably due to the presence of a new N–H bond. After 2 hours the reaction appeared to be 8% complete by integration of the methyl hydrogens of the tolyl group of the α-thio-β-chloroacrylamide **9** and what was subsequently determined to be the rearranged pyrazole product **71 (Entry 3)**. After stirring for a further 22 h, however, the reaction was still incomplete despite full consumption of the diazo **38**. Consequently, the number of equivalents of ethyl diazoacetate **38** was increased to 8 and following a combination of flash column chromatography on silica gel followed by trituration with diethyl ether the novel rearranged pyrazole **71** was obtained as a white solid in 64% yield **(Entry 4)**.

Table 2.5: Preliminary investigation of [3+2] dipolar cycloaddition of ethyl diazoacetate **38** and α-thio-β-chloroacrylamide **9**

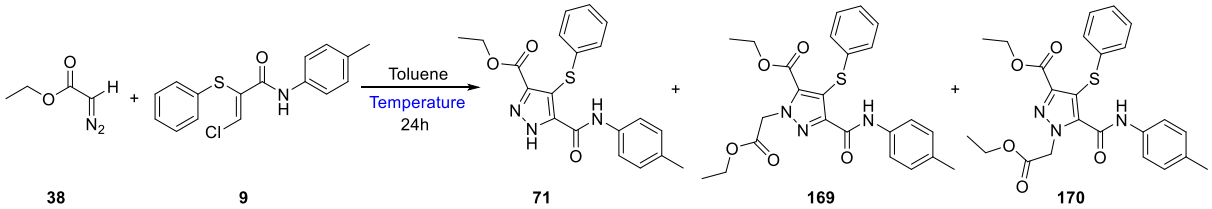

Entry	Temp. (°C)	Equiv.	9 : 71 : 169 + 170[b]	38[d]	Yield 71 (%)[e]
1	r.t.	4	100 : 00 : 00	Yes	-
2	50	4	100 : 00 : 00	Yes	-
3[a]	100	4	48 : 43 : 9	No	-
4	100	8	-[c]	-	64

a) An aliquot was removed after 2 h, concentrated under reduced pressure, and analysed by ^{1}H NMR spectroscopy which indicated a 92:8 ratio of α-thio-β-chloroacrylamide **9** to pyrazole **71**.

b) Estimated % conversion of α-thio-β-chloroacrylamide **9** to pyrazole **71** and combined N–H insertion products **169**+**170** were calculated from the ^{1}H NMR spectra of the crude product in $CDCl_3$ taken after 24 h. Estimated by integration of the β-H signal of **9,** the pyrazole **71** NH signal, and the 2H, methylene NCH_2CO signals of the N–H insertion products **169** and **170**.

c) ^{1}H NMR spectroscopy of the crude reaction mixture was not recorded in this instance.

d) Yes: Unreacted ethyl diazoacetate **38** was present in crude reaction mixture; No: Ethyl diazoacetate **38** was completely consumed in the reaction.

e) Isolated yield after column chromatography on silica gel using hexane: ethyl acetate as eluent followed by trituration using diethyl ether.

In light of this result the dipolarophilic reactivity of the α-thio-β-chloroacrylamides **40–53** towards ethyl diazoacetate as the 1,3-dipole was subsequently investigated as illustrated in **Table 2.6**. An excess (8 equivalents) of ethyl diazoacetate was added in one portion to a stirring solution of the α-thio-β-chloroacrylamide in toluene (0.2 M) at room temperature. The reaction solution was heated gradually to 100 °C and this temperature was maintained for 24 h. After 24 h the reaction mixture was cooled to room temperature and an aliquot was concentrated under reduced pressure and analysed by ^{1}H NMR spectroscopy. The ^{1}H NMR spectra indicated incomplete consumption of α-thio-β-chloroacrylamide in all instances except for the α-thio-β-chloroacrylamide **41** which leads to formation of pyrazole **173**; however, at this point characteristic methylene NCH_2 signals for the two regioisomeric N–H insertion by-products **(iii)** and **(iv)** were observed in most instances. As a result, despite evidence for residual α-thio-β-chloroacrylamide remaining after 24 hours, further ethyl diazoacetate was not added to avoid increased formation of the N–H insertion by-products **(iii)** and **(iv)**.

Table 2.6: [3+2] Dipolar cycloaddition of α-diazoacetates and α-thio-β-chloroacrylamides (and related derivatives):

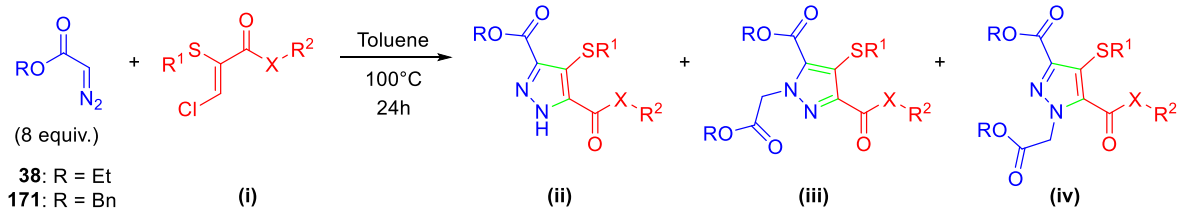

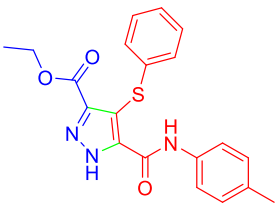

71 (64%)

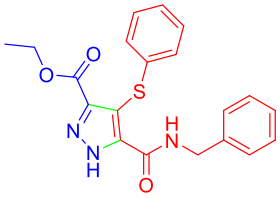

172 (39%)

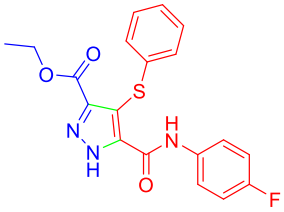

173 (55%)

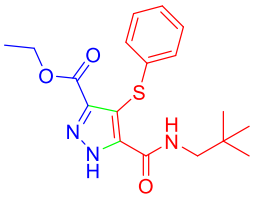

174 (27%)

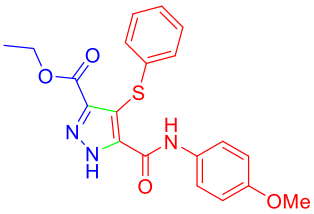

175 (40%)

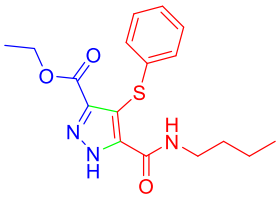

176 (67%)

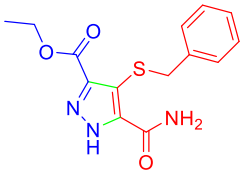

177 (71%)

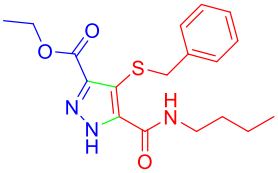

178 (52%)

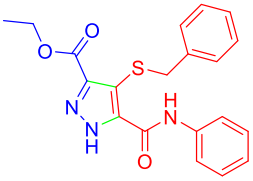

179 (28%)

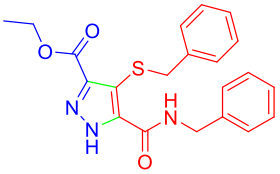

180 (60%)

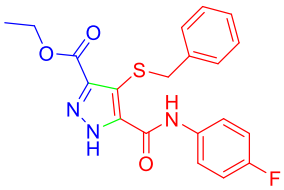

181 (19%)

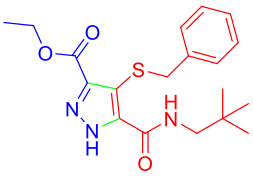

182 (59%)

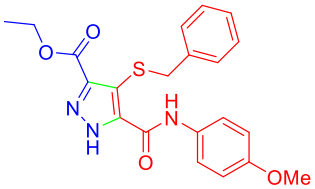

183 (55%)

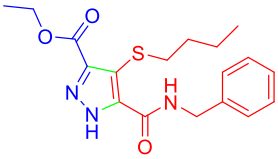

184 (44%)

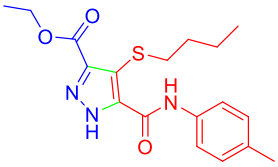

185 (35%)

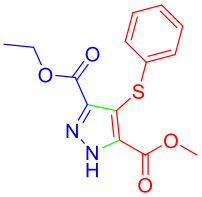

186 (49%)

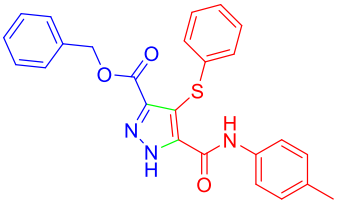

187 (63%)

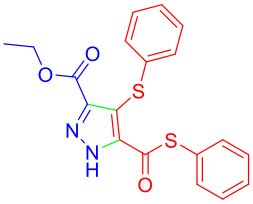

188 (n.d)

Entry	R	α-thio-β-chloro-acrylamide	R^1	X	R^2	Conversion[b,c,d,e,f] (i) : (ii) : (iii) + (iv)	Pyrazole	Yield (%)[h,i,j,k]	Pyrazole Recovery (%)[l]
1	Et	**9**	Ph	NH	Tol	-[d]	**71**	64[h]	-
2	Et	**40**	Ph	NH	Bn	2 : 66 : 32	**172**	39[h]	60
3	Et	**41**	Ph	NH	4-FC_6H_4	0 : 82 : 18	**173**	55[h]	67
4	Et	**42**	Ph	NH	$(CH_3)_3CCH_2$	6 : 44 : 50	**174**	27[i]	62
5	Et	**43**	Ph	NH	4-$MeOC_6H_4$	12 : 66 : 22	**175**	40[h]	60
6	Et	**44**	Ph	NH	*n*Bu	7 : 78 : 15	**176**	67[i]	85
7	Et	**45**[a]	Bn	NH_2	-	8 : 86 : 5	**177**	71[j,k]	83
8	Et	**46**	Bn	NH	*n*Bu	17 : 70 : 13	**178**	52[i]	74
9	Et	**47**[a]	Bn	NH	Ph	5 : 74 : 21	**179**	28[i]	38
10	Et	**48**	Bn	NH	Bn	12 : 79 : 9	**180**	60[h]	76
11	Et	**49**	Bn	NH	4-FC_6H_4	3 : 38 : 58	**181**	19[i]	49
12	Et	**50**	Bn	NH	$(CH_3)_3CCH_2$	24 : 68 : 8	**182**	59[i]	87
13	Et	**51**	Bn	NH	4-$MeOC_6H_4$	39 : 61 : 0	**183**	55[h]	90
14	Et	**52**[a]	*n*Bu	NH	Bn	9 : 77 : 14	**184**	44[i]	57
15	Et	**53**[a]	*n*Bu	NH	Tol	2 : 84 : 14	**185**	35[h]	42
16	Et	**69**	Ph	O	Me	15 : 77 : 8	**186**	49[i]	64
17	Bn	**9**	Ph	NH	Tol	-[f]	**187**	63[h,k]	-
18	Et	**70**	Ph	S	Ph	-[g]	**188**	-	-

a) α-Thio-β-chloroacrylamides **45**, **47**, **52** and **53** synthesised by Kissane were used.[7, 21]
b) **(i)** α-Thio-β-chloroacrylamide, **(ii)** pyrazole, **(iii)** N–H insertion by-product (5-carboxylate) and **(iv)** N–H insertion by-product (3-carboxylate).
c) Estimated % conversion of α-thio-β-chloroacrylamide **(i)** to pyrazole **(ii)** and combined N–H insertion products **(iii)+(iv)** were calculated from the ^{1}H NMR spectra of the crude product in $CDCl_3$ taken after 24 h. Estimated by integration of the β-H signal of **(i)**, the pyrazole **(ii)** NH signal, and the 2H, methylene NCH_2CO signals of the N–H insertion products **(iii)** and **(iv)**.
d) ^{1}H NMR spectroscopic analysis of the crude reaction mixture for the generation of pyrazole **71** was not recorded.
e) N–H insertion products **(iii)** and **(iv)** were not isolated except for **169** and **170** (see **Table 2.5**); assignment of the N–H insertion products **(iii)** and **(iv)** in the crude ^{1}H NMR was made tentatively by analogy using the methylene NCH_2CO signals of **169** and **170**.
f) Estimated % conversion for [3+2] dipolar cycloaddition of α-thio-β-chloroacrylamide **9** with benzyl diazoacetate **171** not recorded as N–H insertion products **(iii)** and **(iv)** (R = Bn, not isolated) could not be readily identified from the ^{1}H NMR spectrum of the crude reaction mixture.
g) No evidence for formation of the pyrazole **188** by ^{1}H NMR spectroscopy of the crude reaction mixture despite complete consumption of α-thio-β-chlorothioester **70**.
h) Isolated yield after column chromatography on silica gel using hexane: ethyl acetate as eluent followed by trituration using diethyl ether.
i) Isolated yield after column chromatography (twice) on silica gel, first using hexane: ethyl acetate as eluent then dichloromethane: ethyl acetate.
j) Isolated yield by filtration of the reaction mixture.
k) As the NMR spectra of pyrazoles **177** and **187** were recorded in DMSO-d_6 both the 3-, and 5-carboxylate tautomers were observed (see **Experimental** section for full characterisation details).
l) Calculated % recovery of pyrazole **(ii)** based on ratio of pyrazole **(ii)** in the ^{1}H NMR spectrum of the crude product mixture.

The novel pyrazoles **71** and **172**–**187** were isolated in moderate to good yields across the α-thio-β-chloroacrylamides **9** and **40**–**53** substrate range, predominantly as solids that proved stable on storage. Interestingly, variation of the steric and electronic properties on either the sulfur or amide substituent did not have a noticeable impact on the outcome of the cycloaddition, highlighting the generality of the method. In some instances (**Entries 2**, **4** and **11**, **Table 2.6**) the formation of the N–H insertion products **(iii)** and **(iv)**, through further reaction of the rearranged pyrazoles with ethyl diazoacetate **38** was significant; extensive optimization of the reaction conditions was not attempted. In addition to variation of the amide and sulfide substituents across **71** and **172**–**187**, the [3+2] dipolar cycloaddition between benzyl diazoacetate **169** and α-thio-β-chloroacrylamide **9** afforded the pyrazole **187** in 63% yield **(Entry 17)**, while the α-thio-β-chloroacrylate **69** also underwent

cycloaddition with ethyl diazoacetate to give the C(3) and C(5) substituted dicarboxylate **186** in 49% yield **(Entry 16)**. Extension to the α-thio-β-chlorothioester **70** proved to be unsuccessful with a complex mixture obtained under the general conditions, with no evidence for the formation of the pyrazole **188** or either of its potential corresponding N–H insertion by-products **(Entry 18)**. This is despite complete consumption of the thioester being observed by ^{1}H NMR spectroscopy. As such, it is likely that the thioester moiety is too labile to survive the rearrangement process which involves the loss of HCl.

In line with the [3+2] dipolar cycloadditions of α-diazoalkanes with α-thio-β-chloroacrylamides, the reactions of **9**, **40–53** and α-thio-β-chloroacrylate **69** were found to proceed with complete regiocontrol, the carbon atom of ethyl diazoacetate **38** adding to the electrophilic β-carbon of the α-thio-β-chloroacrylamide, followed by rearrangement to form the novel pyrazoles **71** and **172–187**. From literature precedent, [3+2] dipolar cycloadditions of α-diazoacetates to alkenes bearing electron withdrawing groups in direct conjugation with the dipolarophilic component are generally dipole-HOMO controlled, hence the predominant interaction involves the two atoms with the largest orbital coefficients in the dipole and dipolarophile respectively, which accounts for the regiocontrol observed **(Scheme 2.42)**.[108-109]

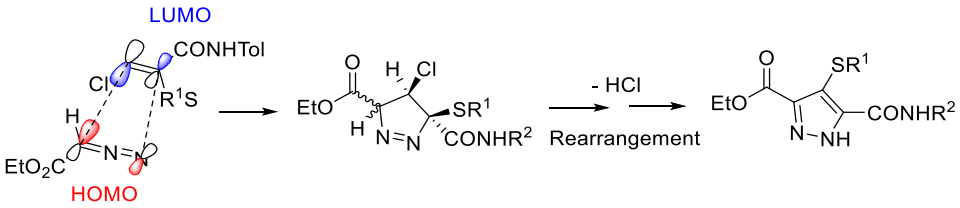

Scheme 2.42. Regiochemistry of the [3+2] dipolar cycloaddition of ethyl diazoacetate with α-thio-β-chloroacrylamide.

The lower yields of pyrazoles **174**, **178**, **179, 182** and **184** were attributable in part to their co-elution during column chromatography with the pyrazoline by-product **190** derived from the thermal decomposition of excess ethyl diazoacetate **(Scheme 2.43)**.[110] Notably, Basato *et al*. have demonstrated that both *cis*- and *trans*-**189** undergoes facile [3+2] dipolar cycloaddition with ethyl diazoacetate **38** at only 20°C to give the pyrazoline **190** in high yields.[111]

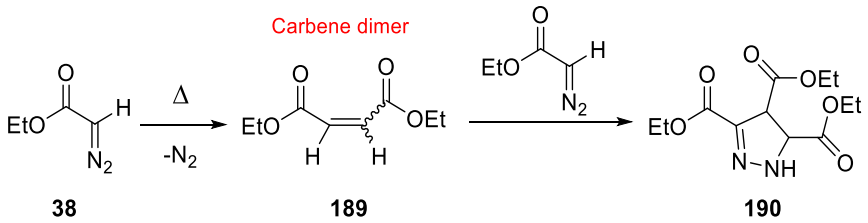

Scheme 2.43. Thermal decomposition of ethyl diazoacetate **38** and subsequent formation of pyrazoline **190**.

The novel N–H insertion by-products **169** and **170** were isolated to facilitate structural assignment, however, the other derivatives **(iii)** and **(iv)** were not isolated and characterised **(Scheme 2.44)**. In all instances the pyrazole **(iii)** is observed in the ^{1}H NMR spectrum of the crude product in greater amounts than **(iv)** indicating that N–H insertion preferentially occurs to give the 5-carboxylate **(iii)**.

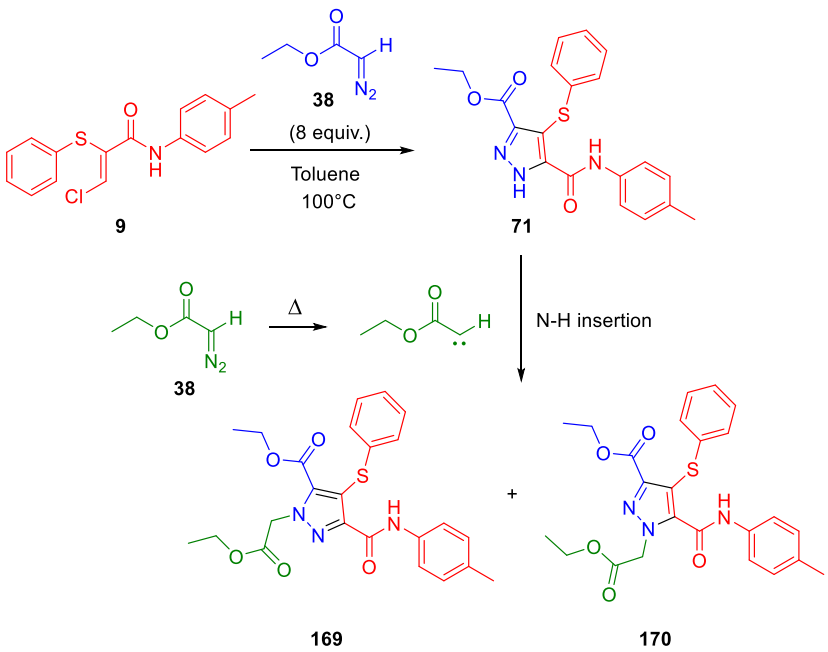

Scheme 2.44. Formation of the 5-carboxylate **169** and 3-carboxylate **170** by N–H insertion

^{1}H-^{13}C Heteronuclear multiple bond correlation (HMBC) spectroscopy was used to determine the regiochemistry of the two N–H insertion products **169** and **170 (Figure 2.19)**. The NMR experiment revealed that the methylene protons at 5.58 ppm and the amide NH at 10.01 ppm in pyrazole **170** both correlated to the same C(5) ring carbon at 138.8 ppm. In pyrazole **169** the methylene protons at 5.38 ppm correlated to the C(5) ring carbon at 137.2 ppm, however, there was no correlation between the amide NH at 9.07 ppm and C(5). Therefore, the pyrazole **170** was assigned as the 3-carboxylate and pyrazole **169** as the 5-carboxylate **(Figure 2.19)**. As illustrated in **Figure 2.19**, the ^{13}C NMR chemical shifts of the C(3), C(4) and C(5) carbons of the pyrazole ring are predominantly influenced by the regiochemistry of the pyrazole, with limited impact of alteration of the substituent. It should be noted that the correlation observed between the amide NH at 10.01 ppm and the C(5) ring carbon at 138.8 ppm in pyrazole **170** was very weak, and was not consistently observed in other similar alkylated derivatives generated in this work (see **Section 2.7**). X-ray crystallography of pyrazole **169** following recrystallisation from dichloromethane unambiguously confirmed the assignment of pyrazole **169** as the 5-carboxylate **(Figure 2.20)**.

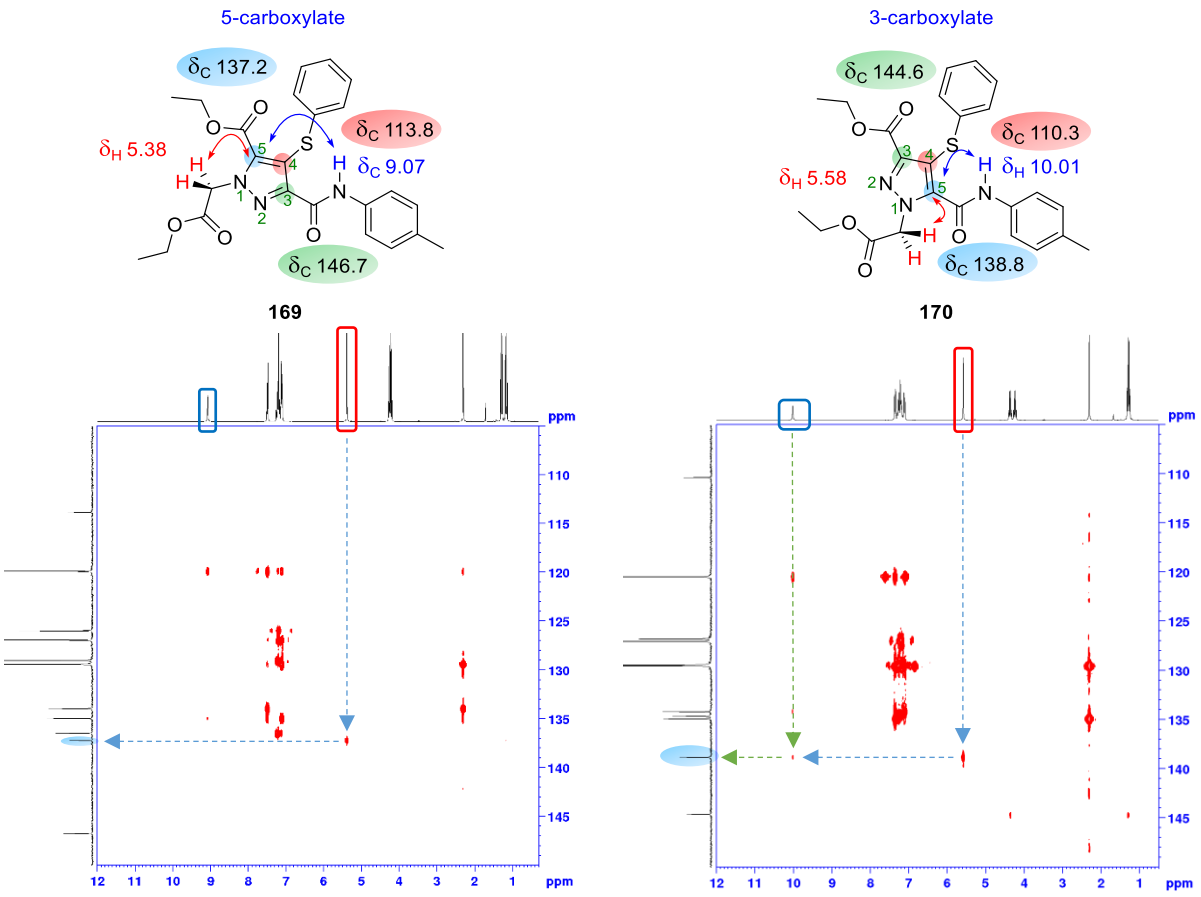

Figure 2.19: ^{1}H-^{13}C HMBC ($CDCl_3$) three bond correlations indicating the assignments of N–H insertion products **169** and **170** including relevant ^{1}H and ^{13}C NMR chemical shifts (in ppm).

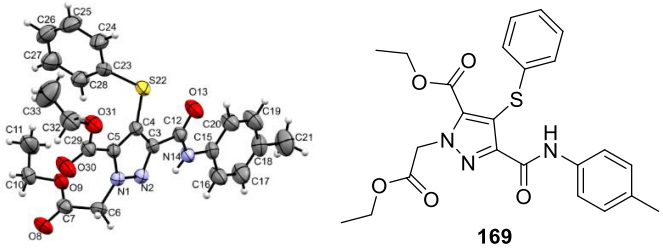

Figure 2.20: X-ray structure of pyrazole **169** (anisotropic displacement parameters drawn at the 50% probability level).[112]

Two potential mechanisms can be envisaged for the formation of the rearranged pyrazoles **71** and **172**–**187**. Firstly, using the α-thio-β-chloroacrylamide **9** as an example, thermally induced regiospecific [3+2] dipolar cycloaddition of ethyl diazoacetate **38** with the α-thio-β-chloroacrylamide leads to the initial pyrazoline cycloadduct **(i)**. In the first instance an E_1 elimination can be considered, with loss of chloride to form a sulfur stabilised carbocation [**Scheme 2.45**, **Mechanism A**, **(ii)**]. Subsequent generation of an episulfonium ion intermediate **(iii)**, followed by deprotonation of the acidic *α*-carbon leads to ring opening of the episulfonium ion and completes the sulfur migration to form **(iv)**. Finally, tautomerisation leads to aromatisation and the rearranged pyrazole **71**.

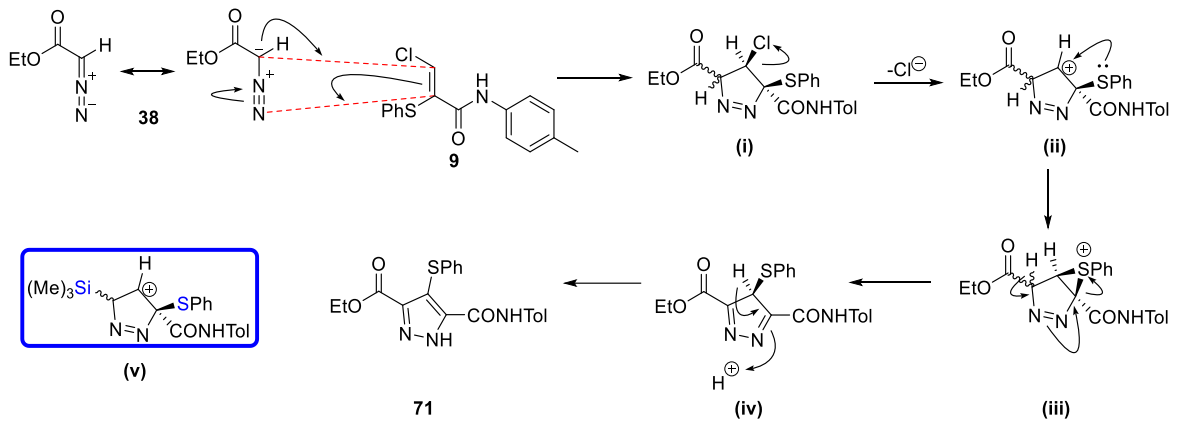

Scheme 2.45 (Mechanism A): E_1 elimination.

Alternatively, the following $E_{1C}B$-like mechanism is postulated to be more likely **(Scheme 2.46, Mechanism B)**. Deprotonation of the acidic α-carbon, adjacent to the ester moiety, in the initial pyrazoline cycloadduct **(i)** generates an enolate **(ii)** that is stabilised through extended conjugation. Subsequent elimination of chloride generates the anti-aromatic pyrazole **(iii)**. The sulfur migration can be envisaged to occur through an intramolecular conjugate addition to generate the episulfonium ion intermediate **(iv)**, that subsequently ring opens to complete the sulfur migration to form **(v)**. Tautomerisation affords the aromatic pyrazole **71**. It is believed that the driving force for the sulfur migration in both mechanistic pathways is the restoration of the pyrazole aromaticity. In our earlier work with trimethylsilyldiazomethane, formation of the carbocation **(v)** analogous to **(ii)** **(Scheme 2.45)** was readily envisaged due to the β-silicon effect, however in the ester derivative the formation of the carbocation **(ii)** is less likely and as a result, the mechanistic details may be altered by the different substituents on the 1,3-dipole.[9, 21]

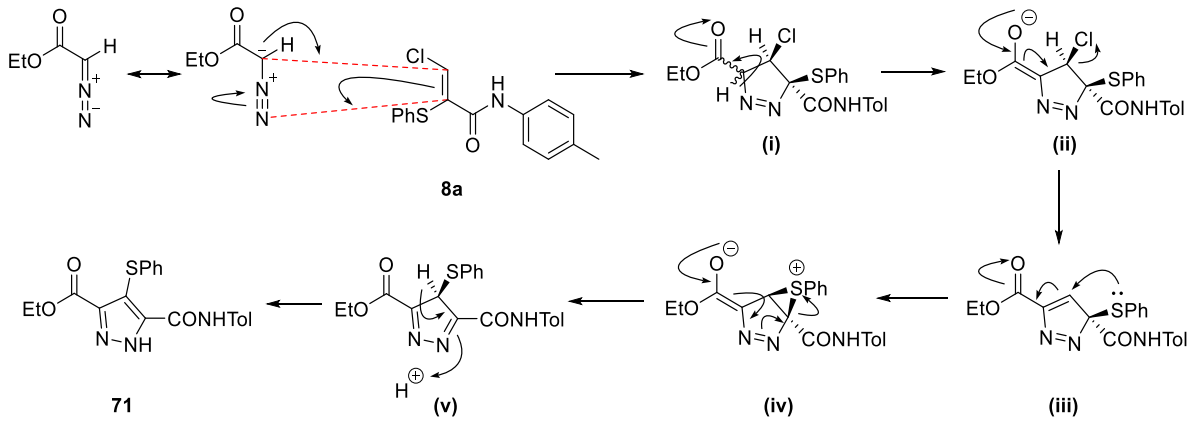

Scheme 2.46. (Mechanism B). $E_{1C}B$-like elimination.

2.5.3. [3+2] Dipolar Cycloadditions of α-Diazoacetates with α-Sulfinyl-β-chloroacrylamides

Dipolar cycloadditions using diazoalkanes, including ethyl diazoacetate, are generally dipole HOMO controlled, therefore the presence of electron-withdrawing groups on the dipolarophile should accelerate the cycloaddition by lowering the LUMO energy of the dipolarophile.[108] Therefore, we envisaged that oxidation of the α-thio-β-chloroacrylamides to the corresponding α-sulfinyl-β-

chloroacrylamides would provide a more reactive dipolarophile by virtue of creating a much more electrophilic alkene due to the presence of a more electron withdrawing sulfoxide moiety **(Figure 2.21)**. By doing so we envisaged that the high temperatures that were required to actuate cycloaddition for the α-thio-β-chloroacrylamide series may be circumventable.

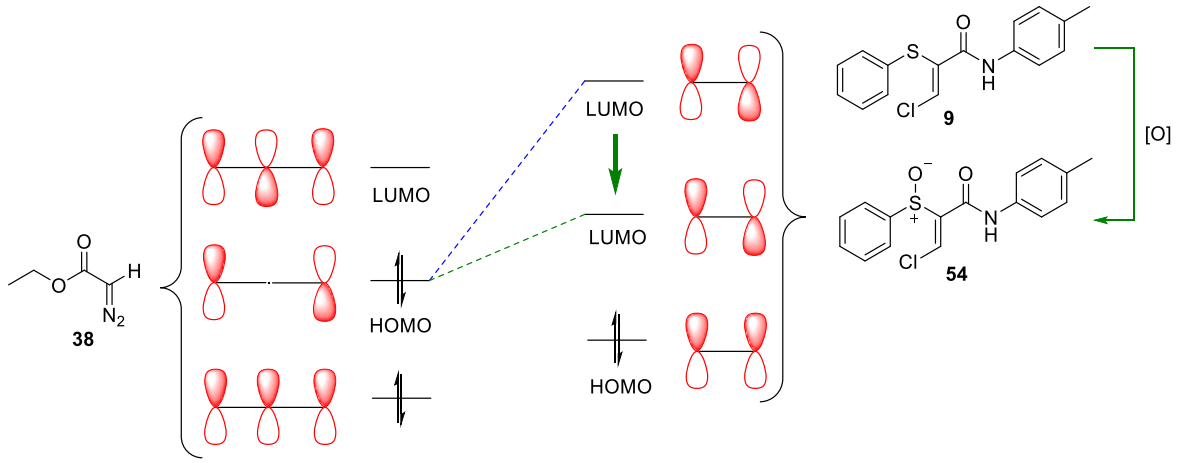

Figure 2.21: Postulated frontier molecular orbital analysis of the [3+2] dipolar cycloaddition of ethyl diazo acetate **38** and the α-thio-β-chloroacrylamide **9** relative to the α-sulfinyl-β-chloroacrylamide **54**

Initial attempts to achieve [3+2] dipolar cycloaddition of ethyl diazoacetate **38** and α-sulfinyl-β-chloroacrylamide **54** at room temperature, or at reflux in dichloromethane, did not result in cycloaddition and/or any competing reactions. Reverting to toluene at 100 °C resulted in full consumption of the sulfoxide dipolarophile after 48 h, however, with concomitant degradation, hence the ^{1}H NMR spectrum of the crude product mixture was complex, hindering accurate determination of product ratios. To attempt to reduce the degree of competing degradation the reaction was repeated at 50°C, 60°C, 70°C and 80°C; however, reaction progress was severely hindered in all instances particularly at the lower temperatures **(Scheme 2.47)**. Furthermore, the reduced reaction temperatures did not reduce the degradation profile of the transformation to any meaningful extent. It should be noted that ethyl diazoacetate **38** was not observed (by ^{1}H NMR spectroscopy) to degrade whatsoever in toluene at 100°C over 24 hours, hence the degradation observed is likely due to the formation of benzenesulfinyl chloride (see below for discussion of reaction mechanism).

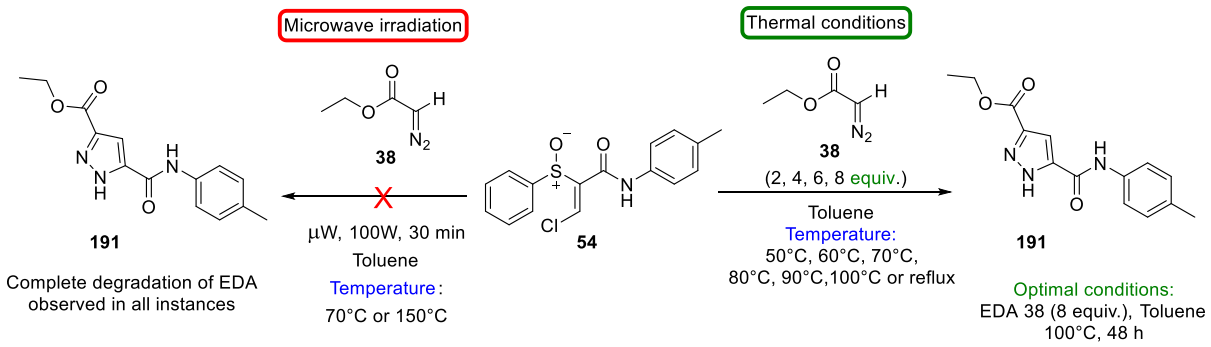

Scheme 2.47: Thermal and microwave irradiation conditions investigated for [3+2] dipolar cycloaddition of ethyl diazoacetate **38** and α-sulfinyl-β-chloroacrylamide **54**

Due to the prolonged heating of the reaction medium likely being associated with the degradation profile of the reaction we attempted to investigate whether microwave irradiation could be utilized

to actuate more uniform heating of the reaction media, and hence improve the rate of the reaction while also leading to less by-products/decomposition products. However, in both instances, there was no evidence for formation of any cycloadduct by ^{1}H NMR spectroscopy of the crude product, suggesting that complete degradation of ethyl diazoacetate **38** occurred within 30 minutes at either 70°C or 150°C preventing cycloaddition **(Scheme 2.47)**.

Despite the complex reaction mixtures obtained, a series of α-benzenesulfinyl-β-chloroacrylamides were treated with ethyl diazoacetate **38** and benzyl diazoacetate **171** to afford the novel pyrazoles **191**–**199** in yields of 13–47% **(Table 2.7)**. However, in most instances the 3,5-substituted pyrazoles generated proved to be insoluble in toluene allowing isolation by filtration from the reaction mixture on cooling **(Table 2.7)**. Analysis of the mother liquors demonstrated some loss of product through the filtration process, however, only to a very minor extent. In cases in which no precipitate formed, the pyrazoles were purified by column chromatography, i.e. pyrazoles **194** and **196** (**Entries 4** and **6**). The low yields of the desulfinylated pyrazoles may be attributable to the generation of benzenesulfinyl chloride which could result in side reactions, or to the enhanced reactivity of the α-sulfinyl-β-chloroacrylamides relative to the α-thio-β-chloroacrylamides. Notably, the [3+2] dipolar cycloadditions of α-diazoacetates and α-sulfinyl-β-chloroacrylamides occur in an analogous manner to the corresponding cycloadditions using the more reactive diazoethane or trimethylsilyldiazomethane under far milder conditions, highlighting that the sulfinyl moiety plays a key role in the reaction outcome. Yields in this work were comparable to those obtained by Kissane in our groups's earlier work for the dipolar cycloadditions of α-benzenesulfinyl-β-chloroacrylamides.[9, 21]

Table 2.7: [3+2] Dipolar cycloadditions using α-benzenesulfinyl-β-chloroacrylamides

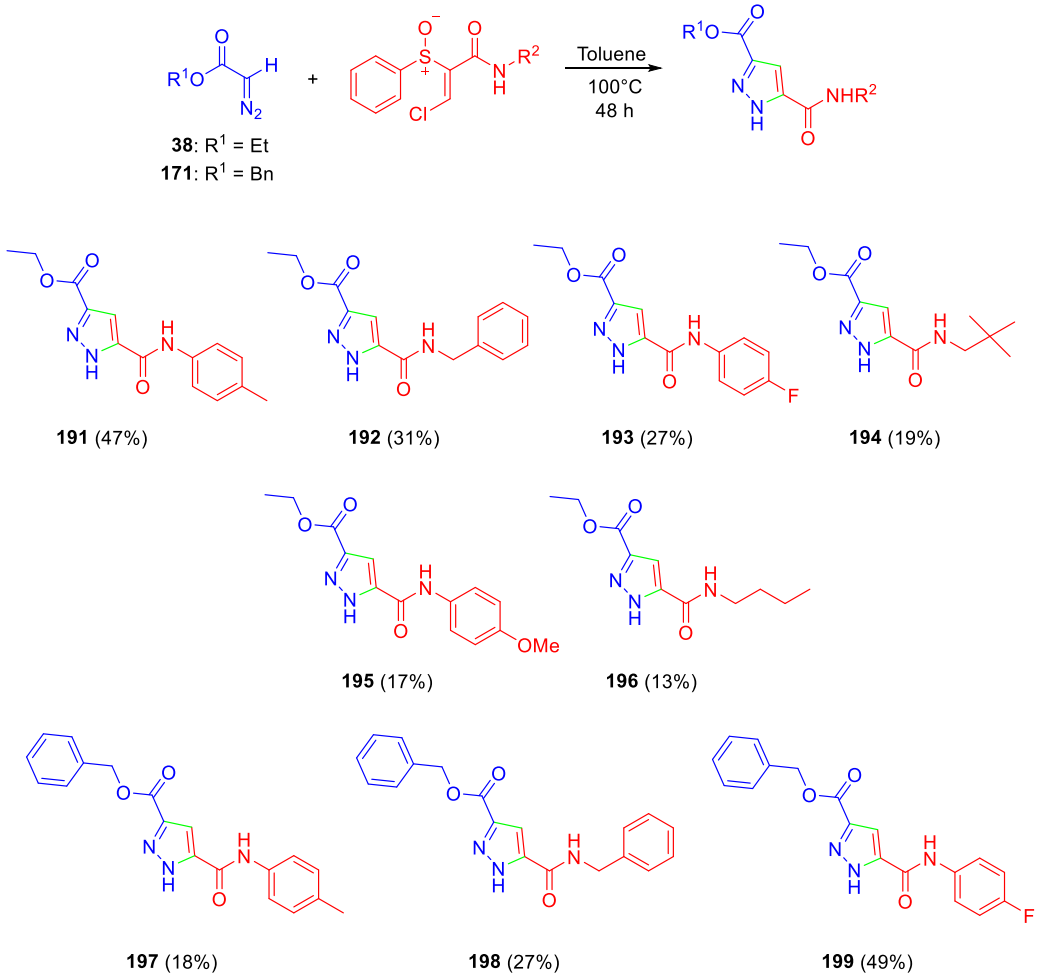

Entry	R^1	α-Sulfinyl-β-chloroacrylamide	R^2	Pyrazole	Yield (%)[a,c]
1	Et	**54**	Tol	**191**	47
2	Et	**55**	Bn	**192**	31
3	Et	**56**	4-FC_6H_4	**193**	27
4	Et	**57**	$(CH_3)_3CCH_2$	**194**	19[b]
5	Et	**58**	4-$MeOC_6H_4$	**195**	17
6	Et	**59**	*n*Bu	**196**	13[b]
7	Bn	**54**	Tol	**197**	18
8	Bn	**55**	Bn	**198**	27
9	Bn	**56**	4-FC_6H_4	**199**	49

a) Isolated yield collected by filtration of the reaction mixture unless otherwise stated.
b) Isolated yield after column chromatography.
c) As the ^1H and ^{13}C NMR spectra were recorded in DMSO-d_6 (unless otherwise stated) the 3- and 5-carboxylate tautomers were observed (see **Experimental** section for more details).

In all instances complete regiocontrol was observed, with the α-carbon of the α-diazoacetate adding to the β-carbon of the dipolarophile, with concomitant desulfinylation and aromatisation to the 3,5-disubstituted pyrazoles observed. The regiochemistry of the pyrazoles **191–199** was assigned by comparison of the characteristic C(4) ring carbon of the ^{13}C NMR spectra to literature values for related compounds.[9, 21] Two mechanisms of pyrazole formation can be considered for the cycloaddition and desulfinylation process. Firstly, regioselective [3+2] dipolar cycloaddition of ethyl diazoacetate **38** and

α-sulfinyl-β-chloroacrylamide **54** forms the initial pyrazoline **(i) (Scheme 2.48**, **Mechanism A)**. Analogous to the cycloadditions of the sulfide derivatives an $E_{1c}B$-type elimination of HCl can be envisaged to give the intermediate **(iii)** via **(ii).** Subsequent nucleophilic addition of chloride to the electrophilic sulfinyl moiety triggers the elimination of benzenesulfinyl chloride and aromatization to **191** via the intermediate **(iv)**. However, when the reaction was carried out in the presence of trimethyl orthoformate, a known non-nucleophilic acid scavenger,[113] using the otherwise general conditions, comparable formation of the **191** was observed by ^{1}H NMR spectroscopy. Consequently, we believe that it is unlikely that this is the operative mechanism.

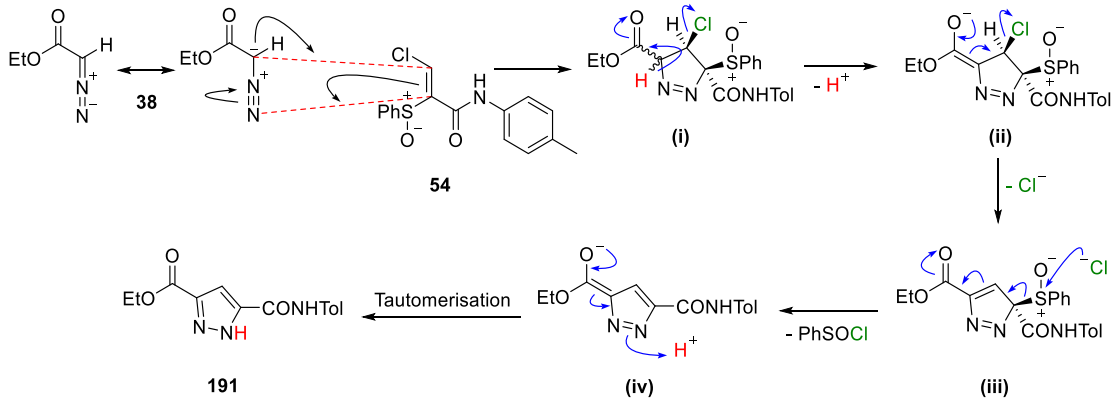

Scheme 2.48 (Mechanism A): Postulated formation of desulfinylated pyrazole **191** via dipolar cycloaddition

Alternatively, [3+2] dipolar cycloaddition to form the initial pyrazoline cycloadduct **(i)** is envisaged, followed by spontaneous *syn*-elimination of benzenesulfinyl chloride from the pyrazoline intermediate **(i)**, leading to the desulfinylated cycloadduct **(ii)**. Subsequent tautomerisation affords the aromatic pyrazole **191 (Scheme 2.49)**.

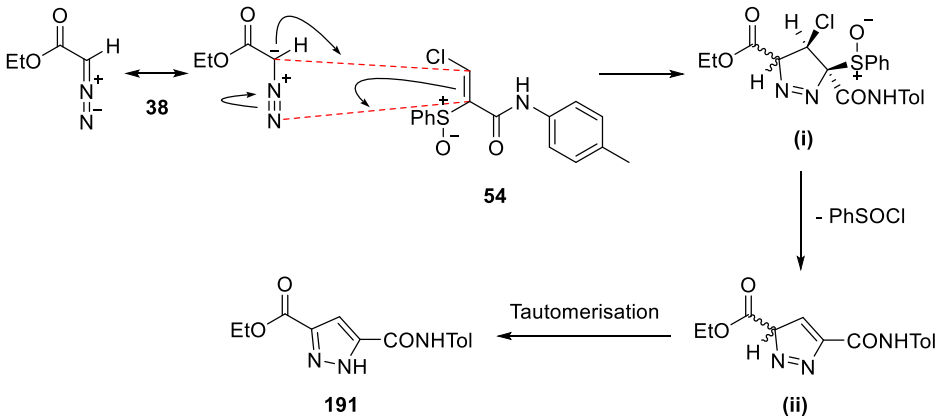

Scheme 2.49 (Mechanism B): Mechanistic route toward desulfinylated 3,5-substituted pyrazoles through 1,2-elimination of benzenesulfinyl chloride.

Formation of a stoichiometric amount of the reactive by-product benzenesulfinyl chloride can be envisaged to lead to side products through reaction with the initial cycloadducts.

2.5.4. [3+2] Dipolar Cycloadditions of α-Sulfonyl-β-chloroacrylamides

Vinyl sulfones are among the most reactive and versatile dipolarophiles,[114] owing to the strongly electron withdrawing character of the sulfone moiety. Namboothiri *et al*. have reported extensively on the base-mediated [3+2] dipolar cycloaddition of phosphorylated and sulfonylated dipoles, specifically α-diazosulfones, with various dipolarophiles, including vinyl sulfones, to generate functionalised C(3)-substituted sulfonylpyrazoles.[115-116] However, in light of our methodology forming the C(4)-substituted sulfenylpyrazoles **(Table 2.6**, **Section 2.5.2)** we were keen to explore whether α-sulfonyl-β-chloroacrylamides would undergo cycloaddition with *α*-diazoacetates. Based on the work at the sulfide and sulfoxide level of oxidation the fate of the initial cycloadduct was of interest to see if elimination would occur as seen with the sulfoxides, or migration as seen with the sulfides (considered unlikely), or if an alternative reaction pathway would be observed at this level of oxidation.

Preliminary studies into the oxidation of the α-thio-β-chloroacrylamides to the sulfone level of oxidation were conducted by Lynch,[16] however, despite investigating the efficiencies of a range of oxidants including H_2O_2, peracetic acid, $KMnO_4$, Oxone®, MMPP and *m*CPBA, no oxidant was observed to oxidise the sulfides directly to the sulfones. In light of this Lynch turned his attention to the one-step oxidation of the α-sulfinyl-β-chloroacrylamides to sulfones, however, of all the oxidants listed above only *m*CPBA afforded synthetically useful amounts of the α-sulfonyl-β-chloroacrylamides. Lynch found that employment of 4 equivalents of *m*CPBA in dichloromethane at reflux for 16 hours or 2 equivalents of *m*CPBA in dichloromethane at room temperature for 48 hours led to complete conversion to the α-sulfonyl-β-chloroacrylamide **200 (Scheme 2.50)**. However, the reproducibility of this transformation was deemed to be quite poor.

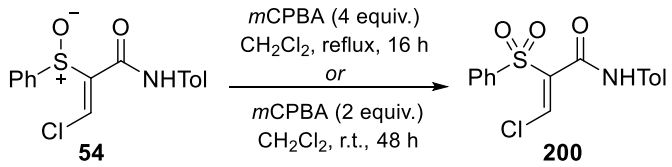

Scheme 2.50: Lynch's optimized conditions for the oxidation of α-sulfinyl-β-chloroacrylamide **54** to α-sulfonyl-β-chloroacrylamide **200**

Despite being able to obtain complete conversion, isolation of the α-sulfonyl-β-chloroacrylamide **200** from the reaction mixture proved to be complex.[16] While the majority of the *m*-chlorobenzoic acid by-product was removable by washing with aqueous sodium sulfite and sodium bicarbonate, its complete removal via washings proved unsuccessful. Purification by column chromatography on silica gel led to significant degradation of the α-sulfonyl-β-chloroacrylamide **200,** presumably due to the interaction of the silica gel and the sulfone which is a potent Michael acceptor. Kissane further explored the purification strategies for the isolation of α-sulfonyl-β-chloroacrylamide **201** (in which the tolyl group in **200** is replaced with 4-FC_6H_4).[21] In her hands the crude sulfone **201** did not survive washings with saturated sodium bicarbonate. Efforts to purify the sulfone by column chromatography on silica gel using chilled eluent, and a combination of chilled eluent with a column surrounded by ice, also did not prevent degradation. Using an alumina stationary phase in place of silica was also unsuccessful, therefore, it was determined that the α-sulfonyl-β-chloroacrylamides are too labile to survive chromatographic purification.

Despite this, our group has previously demonstrated that the crude α-sulfonyl-β-chloroacrylamides can undergo further reactions without purification as exemplified by the successful Diels–Alder cycloaddition between cyclopentadiene and sulfone **200** (**Scheme 2.51**).[8]

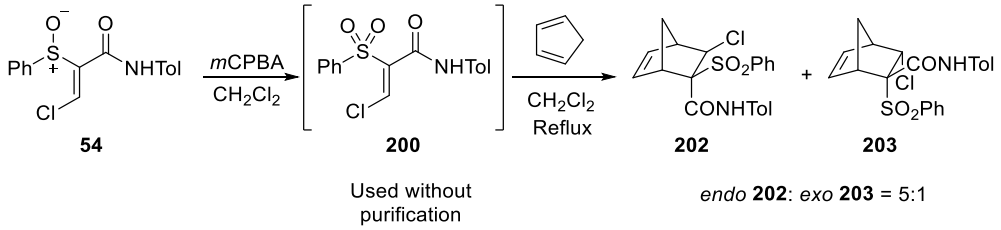

Scheme 2.51: Diels–Alder cycloaddition with crude α-sulfonyl-β-chloroacrylamide **200** and cyclopentadiene

In light of this, in this work the sulfoxide **54** was treated with *m*CPBA (2 equiv.) in dichloromethane at room temperature for 43 h. Reaction monitoring by ^{1}H NMR spectroscopy over several time increments indicated that the oxidation did not go to completion, and that over time the impurity profile deteriorated. For this reason, addition of ethyl diazoacetate **38** was made once the level of impurities was observed to significantly increase relative to the increase of sulfone **200**. At this point the reaction mixture appeared to contain 78% sulfone **200**, 8% sulfoxide **54**, and 14% of an unknown impurity by ^{1}H NMR spectroscopy in addition to *m*CPBA and the corresponding benzoic acid **(Scheme 2.52)**. After the addition the reaction mixture was stirred overnight at room temperature. The loading of ethyl diazoacetate was decreased to 4 equivalents relative to the 8 equivalents used at the sulfide and sulfoxide levels of cycloaddition due to the anticipated increased reactivity of the dipolarophile. The ^{1}H NMR spectrum of the crude reaction mixture was very complex, however, no evidence for residual sulfone **200** was apparent. Notably, following repeated column chromatography the novel rearranged 4-sulfonylpyrazole **204** was isolated in pure form as a white solid in 16% yield over two steps (**Scheme 2.52** and **Table 2.8**, **Entry 1**), highlighting an unprecedented formal 1,2-sulfonyl migration.

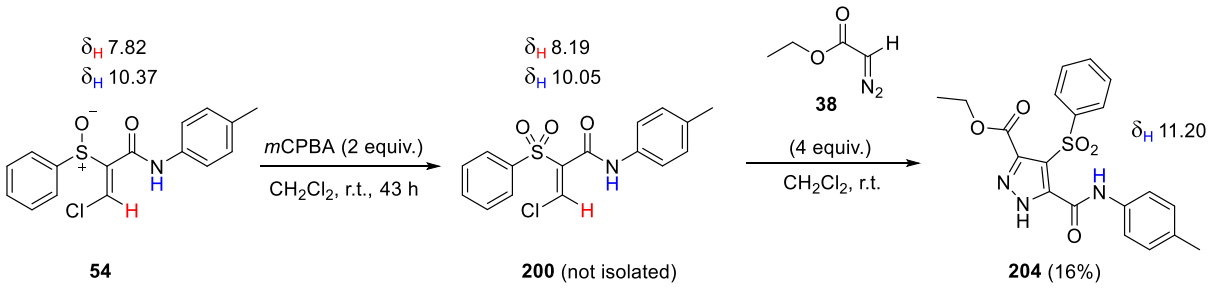

Scheme 2.52: [3+2] Dipolar cycloaddition of *in situ* generated α-sulfonyl-β-chloroacrylamide **200** and ethyl diazoacetate **38**; observation of an unprecedented 1,2-sulfonyl migration

As the oxidation to form the sulfone is a limiting factor in the overall transformation, optimisation was undertaken including variation of time and/or increasing the reaction temperature to reflux in dichloromethane. While it is clear that the sulfone is sensitive to prolonged heating at reflux in dichloromethane, with close monitoring of the reaction mixture by ^{1}H NMR spectroscopy, optimal conversions can be achieved within 10–14 hours, leading to comparable results to when the oxidation was conducted for 48 hours at room temperature. Accordingly, extension of this methodology to a range of α-sulfonyl-β-chloroacrylamides with varying electronic and steric properties at both the sulfone and amide was undertaken leading to a series of novel 4-sulfonylpyrazoles **204** and **210**–**215**,

albeit in low yields of 14–18%, confirming that the sulfone migration was consistent across a series of compounds **(Table 2.8)**.

Table 2.8: [3+2] Dipolar cycloadditions with α-sulfonyl-β-chloroacrylamides

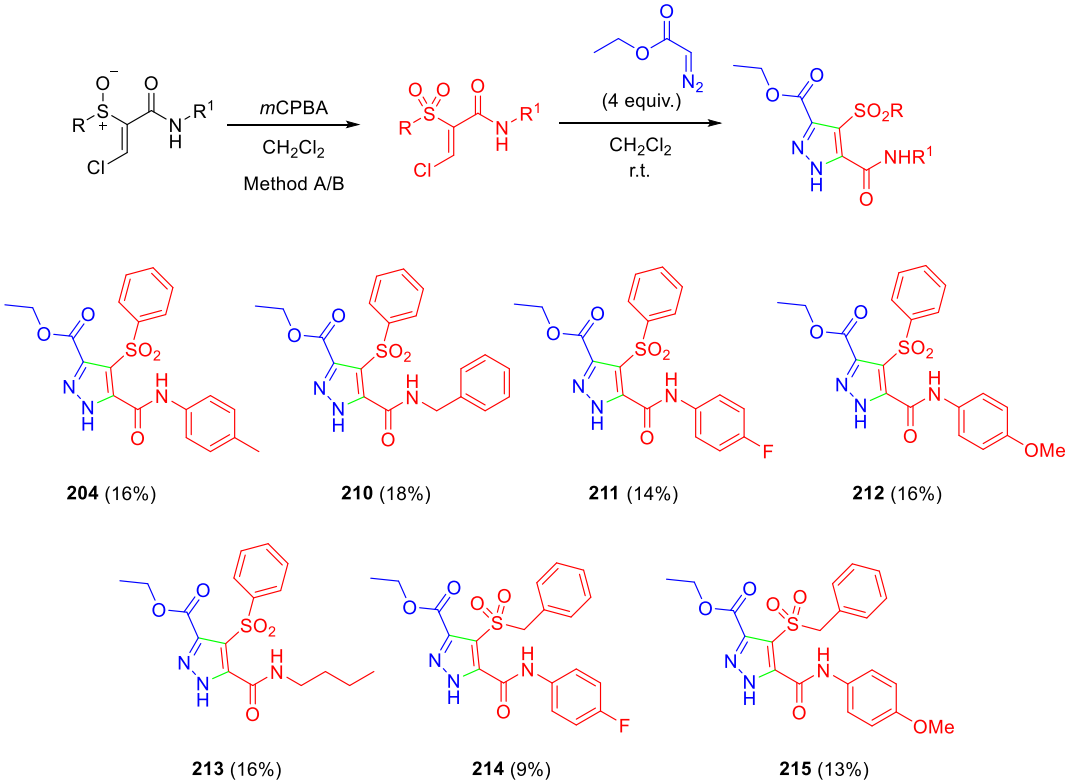

Entry	R	R^1	α-sulfonyl-β-chloroacrylamide	Method[a]	% α-sulfonyl-β-chloroacrylamide[b]	Pyrazole	Yield (%)[c]
1	Ph	Tol	**200**	A	78	**204**	16
2	Ph	Bn	**205**	B	71	**210**	18
3	Ph	4-FC_6H_4	**201**	B	63	**211**	14
4	Ph	4-$MeOC_6H_4$	**206**	B	30	**212**	16
5	Ph	*n*-Bu	**207**	B	-[d]	**213**	16
6	Bn	4-FC_6H_4	**208**	B	-[d]	**214**	9
7	Bn	4-$MeOC_6H_4$	**209**	B	-[d]	**215**	13

a) **Method A:** *m*CPBA (2 equiv.) in dichloromethane was added dropwise to a stirring solution of α-sulfinyl-β-chloroacrylamide in dichloromethane at room temperature under nitrogen. The reaction mixture was stirred for up to 48 h. **Method B:** *m*CPBA (2 equiv.) in dichloromethane was added dropwise to a stirring solution of α-sulfinyl-β-chloroacrylamide in dichloromethane at room temperature under nitrogen. The reaction mixture was heated to gentle reflux and stirred at this temperature for 10–14 h. Both methods were monitored by ^{1}H NMR spectroscopy at regular time intervals.

b) Estimated % of α-sulfonyl-β-chloroacrylamide present in the reaction mixture prior to the addition of ethyl diazoacetate **38**. Determined from the ^{1}H NMR spectra of an aliquot withdrawn from the reaction mixture.

c) Isolated yield calculated over two steps after purification by repeated column chromatography.

d) % Conversion could not be accurately determined due to the complexity of the ^{1}H NMR spectrum of the reaction mixture.

The regiochemistry of the [3+2] dipolar cycloaddition and subsequent rearrangement of novel pyrazole **204** was determined by single X-ray crystallography following recrystallisation from dichloromethane **(Figure 2.22)**. Furthermore, the X-ray crystal structure confirms that migration of the sulfone moiety has occurred, with the sulfone at the C(4) position analogous to that of the sulfide

migration (see **Table 2.6, Section 2.5.2**). The regiochemistry of the 4-sulfenylpyrazole **71** was further confirmed by independently oxidising **71** to the 4-sulfonylpyrazole **204** using *m*CPBA in refluxing dichloromethane (see **Table 2.9**, **Section 2.7**).

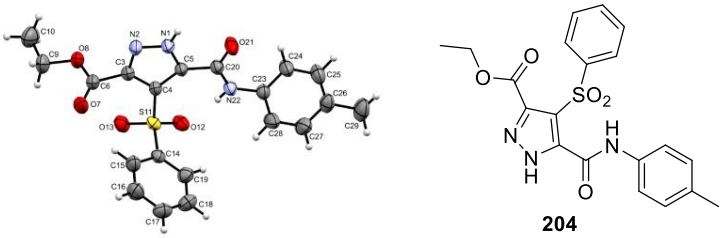

Figure 2.22: X-ray structure of pyrazole **204** (anisotropic displacement parameters drawn at the 50% probability level).[117]

To the best of our knowledge, at the time of writing, carbon to carbon 1,2-sulfonyl migration in pyrazolines is unprecedented, thus the rearrangement leading to **204** involving a formal 1,2-sulfonyl migration is highly unusual. The mechanism for the formation of the rearranged 4-sulfonylpyrazoles **204** and **210**–**215** is not well understood, but several mechanistic routes can be considered based on the confirmed regiochemistry of the products. Using the formation of the 4-sulfonylpyrazole **204** as an example, regioselective [3+2] dipolar cycloaddition of the crude α-sulfonyl-β-chloroacrylamide **200** leads to the initial pyrazoline cycloadduct **(i)**, which readily undergoes elimination of HCl to give the intermediate cycloadduct **(ii) (Scheme 2.54)**. While the sulfur migration at the sulfide level can be readily understood due to the nucleophilic character of the sulfide, extending this to rationalise the unprecedented 1,2-sulfonyl shift is not feasible.

In light of the following two reports a [1,5]-sigmatropic shift can be considered to rationalise the sulfonyl migration. Fuchs *et al*. reported the thermally induced rearrangement of a γ-sulfonyl enone **216** to the rearranged sulfone **218** in almost quantitative yields **(Scheme 2.53, A)**.[118] The authors rationalised the transformation through the formation of the enol intermediate **217** which undergoes a [1,5]-sigmatropic rearrangement. Notably, however, this reaction was carried out in toluene at 145 °C in a sealed tube which constitutes significantly harsher conditions than those employed in this work. Recently, Valdés *et al*. reported the synthesis of chiral pyrazoles **221** and **222** through the [3+2] dipolar cycloaddition of α-chiral tosylhydrazones **219** with alkynes **(Scheme 2.53, B)**.[119] Interestingly, they observed that the initial cycloadduct **220** underwent [1,5]-sigmatropic rearrangement with migration of the alkyl group. Significantly in their study, they observed that the [1,5]-sigmatropic rearrangement, which has two regioisomeric outcomes, preferentially, but not exclusively, migrates to nitrogen rather than the C(4) carbon. However, forcing reaction conditions (110 °C in 1,4-dioxane) were also required in this instance.

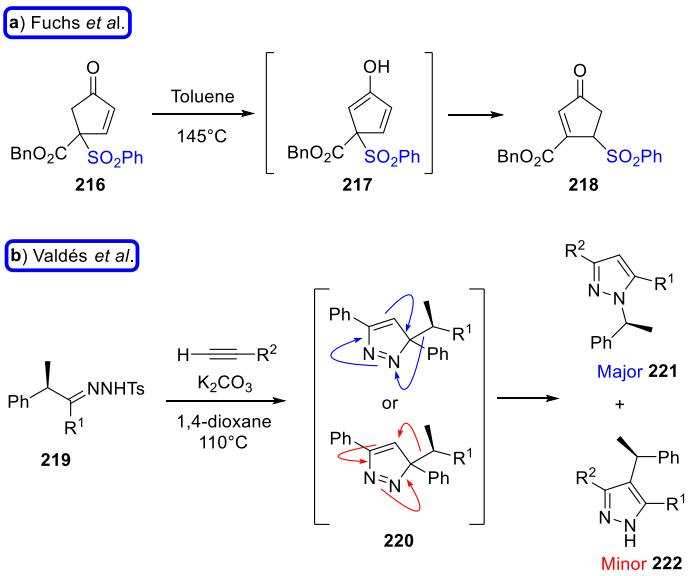

Scheme 2.53: Literature examples of **a)** [1,5]-sigmatropic shift of sulfone moiety leading to formal 1,2-shift in five membered carbocyclic ring, and **b)** [1,5]-sigmatropic shift of alkyl group in pyrazole system

Considering these reports, we note that the pyrazole **204,** and its related derivatives, could be generated through a [1,5]-sigmatropic shift of the sulfonyl moiety **(Scheme 2.54**, **Mechanistic Pathway A)**. However, the [3+2] dipolar cycloadditions in this work were carried out at room temperature, while [1,5]-sigmatropic shifts generally require much higher temperatures as can be seen above. While the *N*(1)-substituted sulfone was not isolated or observed, since the recoveries were very low it is impossible to exclude its formation.

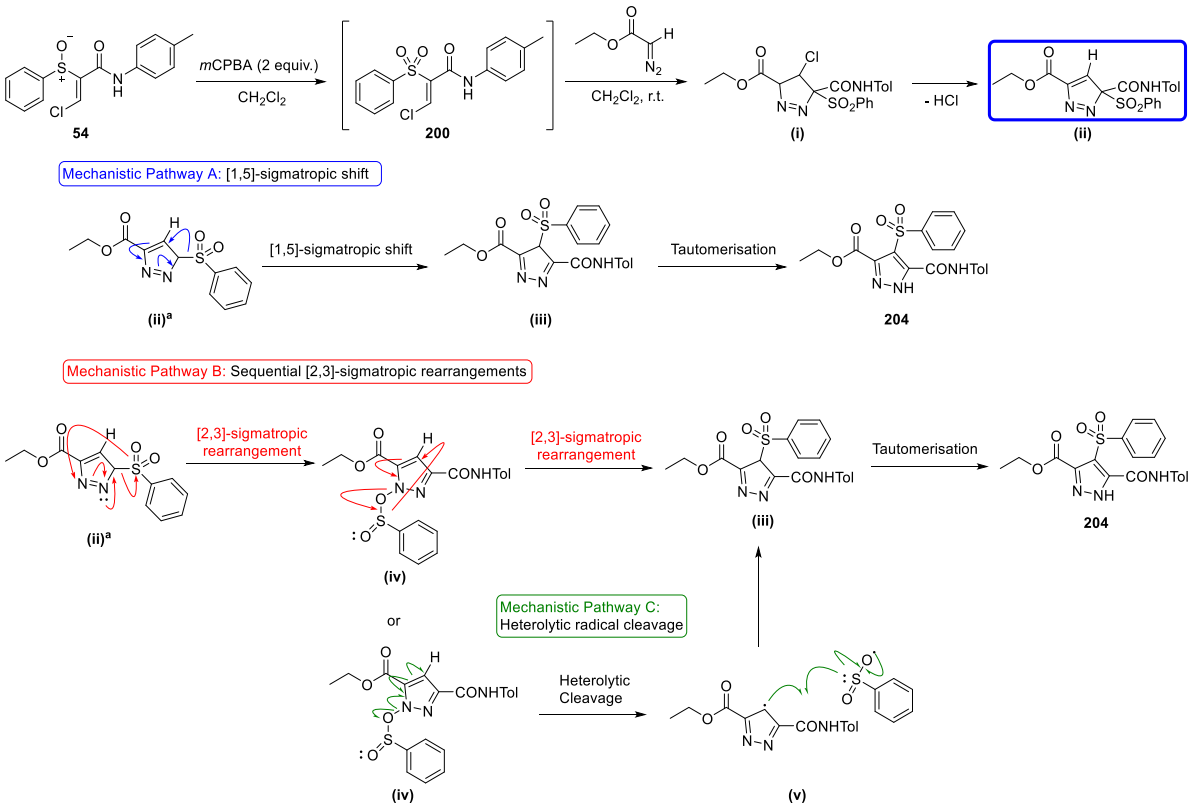

Scheme 2.54: Tentatively proposed mechanistic routes for sulfone migration [**a**) CONHTol substituent not shown in intermediate **(ii)**]

An alternative mechanistic pathway can be envisaged with two sequential [2,3]-sigmatropic rearrangements of the sulfonyl moiety as illustrated in **Scheme 2.54** (**Mechanistic Pathway B**) followed by re-aromatisation via tautomerisation at the end of the sequence to afford the rearranged pyrazole **204**. The second [2,3]-sigmatropic rearrangement is somewhat akin to an allylic sulfinate-sulfone rearrangement.[120] Alternatively, from the intermediate **(iv)**, homolytic cleavage of the weak N–O bond could be envisaged generating a radical pair which on recombination forms the more stable C–S bond (**Scheme 2.54, Mechanistic Pathway C**).

A major difficulty in elucidating the operative mechanism for the 1,2-sulfonyl migration was the complexity of the ^{1}H NMR spectra of the crude reaction mixtures, which made the monitoring of specific signals, and hence the reaction progress, extremely challenging. This complexity was deemed to be predominantly due to the impurity profile following the initial oxidation, but also in part to the use of an excess of ethyl diazoacetate **38**. Accordingly, attempts to circumvent these problems were pursued, to allow more facile detection of potential rection intermediates/by-products.

While the oxidation of α-sulfinyl-β-chloroacrylamides bearing secondary amides, and the subsequent isolation of the corresponding α-sulfonyl-β-chloroacrylamides was previously determined to be a non-trivial task by several researchers in our group, isolation of tertiary amides was successful. Notably, Lynch previously synthesised and isolated the Weinreb amide containing α-sulfonyl-β-chloroacrylamide **228**.[16, 52] Accordingly, using our group's previously optimised conditions, the Weinreb amide **228** was resynthesised and isolated in pure form by column chromatography as illustrated in **Scheme 2.55**. Yields and spectroscopic characteristics were consistent with those previously reported by Lynch.[16, 52]

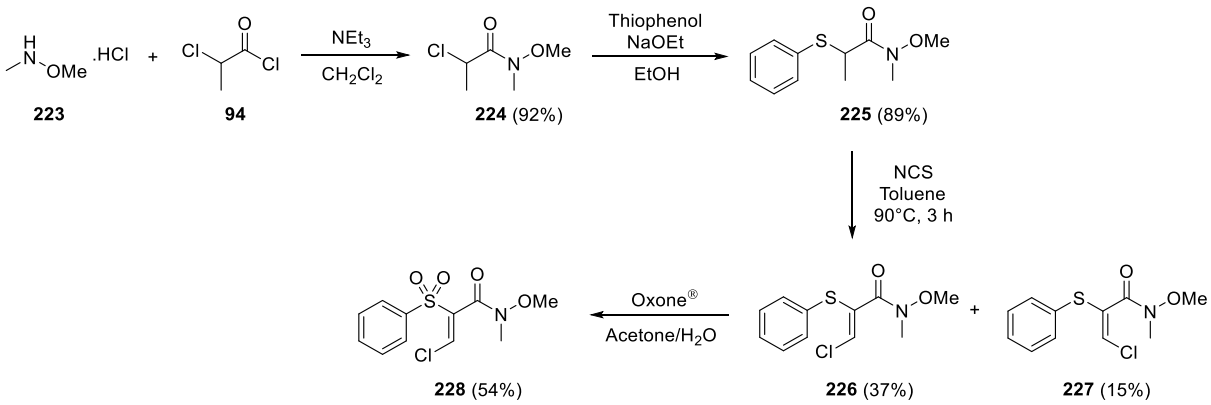

Scheme 2.55: Synthesis of analytically pure sample of α-sulfonyl-β-chloroacrylamide **225** (Yields quoted are from this work)

Subsequently the α-sulfonyl-β-chloroacrylamide **228** was reacted with an excess of ethyl diazoacetate (2.5 equiv.) in dichloromethane at room temperature, however, unexpectedly no reaction was observed **(Scheme 2.56)**. Increasing the reaction conditions to reflux in dichloromethane also proved unsuccessful. To ensure that *m*CPBA was not playing a role in the cycloaddition 0.1 equivalent of *m*CPBA was added to the reaction mixture, however, no cycloaddition was observed. Repeating the reaction in toluene at 100°C, the conditions utilised for the dipolar cycloadditions of both the α-thio-β-chloroacrylamides and the α-sulfinyl-β-chloroacrylamides, also proved unsuccessful. The α-thio-β-chloroacrylamides, α-sulfinyl-β-chloroacrylamides and α-sulfonyl-β-chloroacrylamide containing either a primary or secondary amide are conformationally constrained due to the intramolecular

hydrogen bond between the amide and the respective sulfide, sulfoxide or sulfone, and as such they adopt an S-*cis* conformation **(Scheme 2.56)**. The absence of cycloaddition in the Weinreb amide derivative **228** suggests that in the absence of an intramolecular hydrogen bond and the resulting conformational flexibility, the orbital overlap between the alkene and carbonyl group of the acrylamide is significantly reduced, and consequently the reactivity towards dipoles is reduced.

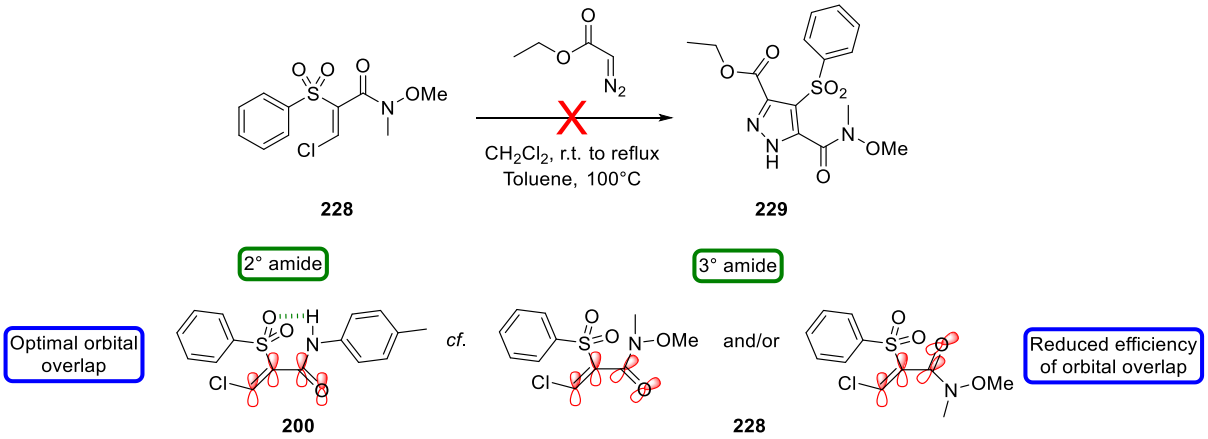

Scheme 2.56: Attempted [3+2] dipolar cycloaddition of **228** and ethyl diazoacetate; comparison of conformational properties of secondary and tertiary amide containing α-sulfonyl-β-chloroacrylamides **200** and **228** respectively

In order to minimize the potential impact of using excess ethyl diazoacetate on the impurity profile of the cycloaddition, trapping of excess dipole with highly reactive DMAD **156** was attempted. Firstly, an independent sample of the known pyrazole product **230**[121] was prepared via a literature procedure described for similar compounds,[98] by treating DMAD **156** (1.2 equiv.) in dichloromethane with ethyl diazoacetate **38** (1 equiv.) at 0°C under nitrogen, and subsequently heating the reaction mixture under reflux for 1 h. Following flash column chromatography the known pyrazole **230** was isolated in quantitative yield. Spectroscopic details were consistent with literature reports **(Scheme 2.57)**.[121]

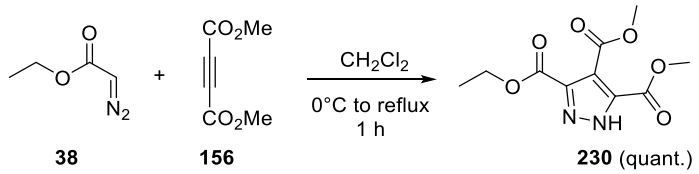

Scheme 2.57: Preparation of known pyrazole **230** using [3+2] dipolar cycloaddition methodology

Subsequently, the [3+2] dipolar cycloaddition of *in situ* generated α-sulfonyl-β-chloroacrylamide **200** and ethyl diazoacetate **38** (4 equiv.) was carried out **(Scheme 2.58)**. After stirring for 4 hours in dichloromethane at room temperature ^{1}H NMR spectroscopy of an aliquot indicated complete consumption of the α-sulfonyl-β-chloroacrylamide **200**, hence at this point 3 equivalents of DMAD **156** was added in one portion to quench any unreacted ethyl diazoacetate, and stirring was continued for an additional 24 hours. Despite clear spectroscopic evidence for the formation of the pyrazole **230**, and complete consumption of ethyl diazoacetate, the crude ^{1}H NMR spectrum remained very complex. Following repeated flash column chromatography on silica gel, the desired rearranged pyrazole **204** was isolated as a 40:60 mixture with the pyrazole **230**, which proved to be inseparable using both eluent systems employed [column 1: ethyl acetate: hexane (60:40); column 2: ethyl acetate: dichloromethane (90:10)]. This experiment establishes two features: firstly the low yield in

the cycloadditions are not due to degradation of ethyl diazoacetate when added directly to the *m*CPBA mediated oxidation solution (as formation of **230** is consistent with the presence of excess ethyl diazoacetate), and secondly the complex by-product mixture is not due to side reactions from excess ethyl diazoacetate. Accordingly, the poor efficiency of these cycloadditions is predominantly due to the lability of the α-sulfonyl-β-chloroacrylamides.

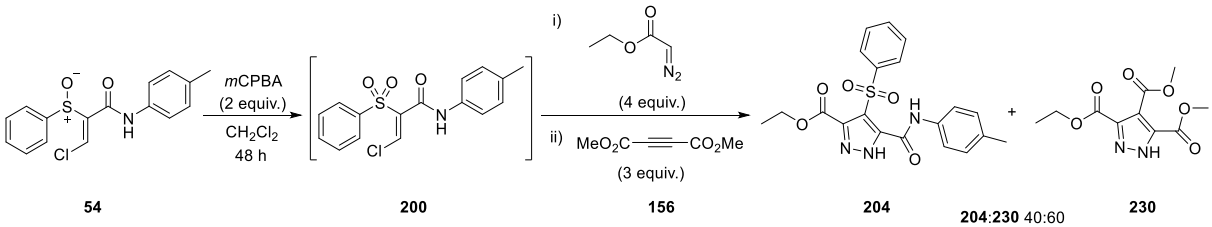

Scheme 2.58: Attempted minimisation of reaction impurities by trapping of excess ethyl diazoacetate

Attempts to obtain experimental evidence to support one of our postulated mechanisms for this unprecedented transformation proved unsuccessful, primarily due to the significant impurity profile of the reaction, however, due to its unusual nature this transformation warrants further investigation in future. In this regard, future efforts in our group may focus on the use of considerably more reactive α-diazoalkanes in conjunction with with tertiary amide containing α-sulfonyl-β-chloroacrylamides, which may potentially overcome the conformational issues preventing cycloaddition in this instance.

2.5.5. [3+2] Dipolar Cycloaddition of *N*-Benzyl-α-Diazoacetamide

We subsequently briefly explored whether *N*-benzyl-α-diazoacetamide **39** would react with the α-thio-β-chloroacrylamides in an analagous manner to ethyl diazoacetate **38**. In this regard, an excess of *N*-benzyl-α-diazoacetamide **39** (4 equiv.) was reacted with the α-thio-β-chloroacrylamide **9** under the otherwise general conditions **(Scheme 2.59)**. It was envisaged that less equivalents of the dipole could be utilised in this instance due to the greater degree of resonance delocalisation from the nitrogen lone pair into the carbonyl moiety most likely rendering the α-carbon of the α-diazoacetamide **39** more nucleophilic than the corresponding α-carbon of ethyl diazoacetate **38**. After 24 h, in contrast to the cycloadditions with ethyl diazoacetate, a white precipitate had formed. Following filtration, and washing with diethyl ether and hexane, ^{1}H NMR spectroscopy indicated the presence of the two N–H insertion products **232** and **233** in a ratio of approx. 45:55 confirming that [3+2] cycloaddition occurs in an analagous manner to the α-diazoacetates. ^{1}H NMR spectroscopy of the mother liquor confirmed that the N–H insertion products were the major products of the reaction, with minimal evidence for the presence of pyrazole **231** observed, however, a significant amount of unreacted α-thio-β-chloroacrylamide **9** remained. Following flash column chromatography on silica gel of the isolated precipiate the two novel N–H insertion products **232** and **233** were isolated in 9% and 16% yield respectively.

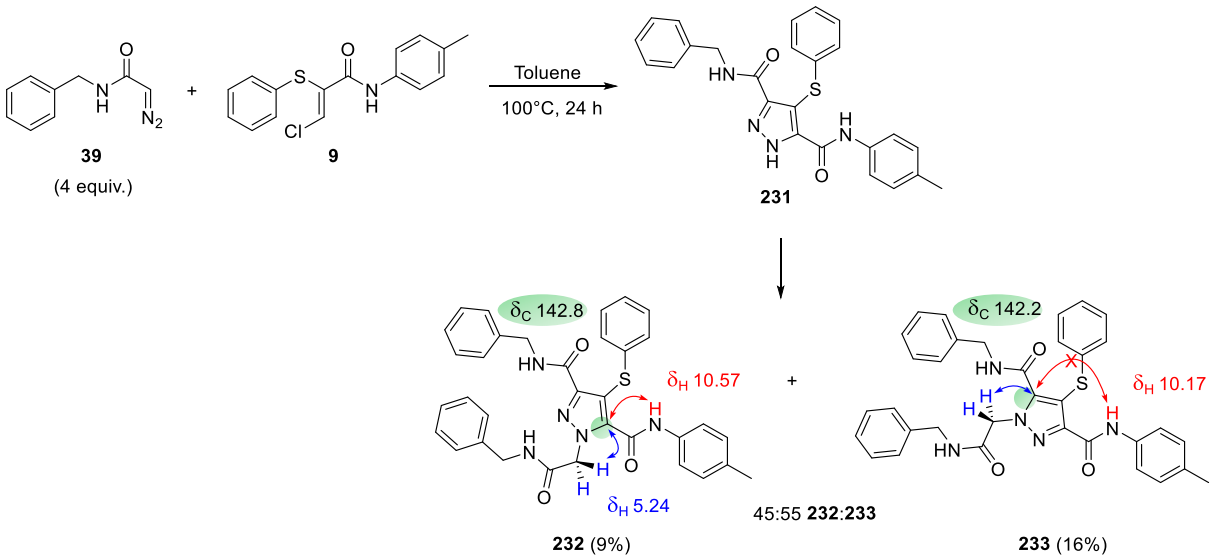

Scheme 2.59: [3+2] Dipolar cycloaddition using α-diazo-*N*-benzylacetamide **39**

Analagous to the pyrazoles **169** and **170**, ^{1}H-^{13}C HMBC spectroscopy was used to determine the regiochemistry of the two N–H insertion products **232** and **233 (Scheme 2.59)**. The NMR experiment revealed that the methylene protons at 5.24 ppm and the amide NH at 10.57 ppm in pyrazole **232** both correlated to the same C(5) ring carbon at 142.8 ppm. In pyrazole **233** the methylene protons at 5.27 ppm correlated to the C(5) ring carbon at 142.2 ppm, however, there was no correlation between the amide NH at 10.17 ppm and C(5). The [3+2] dipolar cycloadditions of α-diazo-*N*-benzylacetamide **39** was not pursued any further, however, it is likely that the use of lower temperatures would enable the isolation of the pyrazole **231** in synthetically useful yields, as the thermal stability of α-diazo-*N*-benzylacetamide **39** was the major limiting factor that prevented complete consumption of the α-thio-β-chlroroacrylamide **9**, as well as the subsequent formation of the N–H insertion products **232** and **233**.

2.6. Spectroscopic Determination of the Tautomeric Composition of 3,4,5-Substituted Pyrazoles

Definitive spectroscopic analysis of unsubstituted N–H pyrazole scaffolds is complicated by the dynamic tautomeric nature of these compounds. For this reason, significant attention has been paid in the literature to the spectroscopic analysis of these compounds particularly using ^{1}H-^{13}C HMBC and NOE experiments, often in conjunction with each other.[122] Unambiguous assignment of the ^{13}C NMR signals for the C(3), C(4) and C(5) carbons is particularly challenging, especially in the absence of an adjoining proton **(Figure 2.23)**. In order to conclusively characterise our novel pyrazoles an in-depth ^{13}C NMR study was performed.

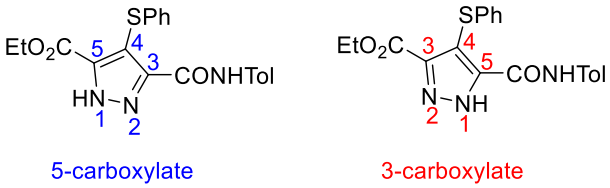

Figure 2.23: Tautomeric forms of pyrazole **71** in solution

The elucidation of the C(3), C(4) and C(5) pyrazole ring carbon chemical shifts by ^{13}C NMR at 75.5 MHz for pyrazoles **71** and **172**–**187** in $CDCl_3$ proved to be challenging, with the C(3) and C(5) carbons not observed at this field strength, believed to be due to dynamic tautomerism in conjunction with the absence of either direct or indirect coupling to hydrogen. In most instances, however, a weak signal was observed for the C(4) carbon as the chemical shift of this carbon remains largely unaffected by tautomerism. In contrast, at 150.9 MHz broad signals were observed for C(3), C(4) and C(5). Interestingly when the spectra of the pyrazoles **71**, **172**–**176** and **178**–**186** were recorded at 150.9 MHz in the noninteracting solvent $CDCl_3$ only a single set of carbon signals are seen indicating one of the following possibilities:

A) one exclusive tautomer in solution, *or*
B) tautomers rapidly interconverting on the NMR timescale, *or*
C) two tautomers in dynamic equilibrium with the equilibrium highly favouring one tautomer with the concentration of the minor tautomer so negligible that it is not detectable by ^{13}C NMR.

Due to the broadening of the signals for the C(3), C(4) and C(5), it is unlikely that one tautomer exists exclusively in solution, although the signal broadening could be due in part to the quadrupolar moment of ^{14}N rather than tautomerism only. Furthermore, the ^{13}C NMR spectra of the pyrazoles **169** and **170** could readily be obtained at 75.5 MHz with each of the C(3), C(4) and C(5) ring carbons observed as sharp signals, consistent with the pyrazoles **169** and **170** being unable to undergo prototropic tautomerism due to the alkylation of the respective N(1) positions **(Figure 2.24)**. This strongly suggests that the signal broadening observed in pyrazole **71** is not due to the ^{14}N quadrupolar moment. Direct comparison of the sp^2 region of the ^{13}C NMR spectra of the pyrazole **71** and the two N–H insertion products **169** and **170** demonstrated that the chemical shifts in pyrazole **71** and **170** were remarkably similar, and substantially different to those of pyrazole **169 (Figure 2.24)**. This observation allowed assignment of the major tautomer of **71** in $CDCl_3$ to be identified as the 3-carboxylate, however, it is not the exclusive tautomer as both *N*-alkylated pyrazoles **169** and **170** are formed through the N–H insertion reaction. This allows us to conclude that for pyrazoles **71**, **172**–**176** and **178**–**186** in the non-interacting solvent $CDCl_3$ that the tautomers exist in dynamic equilibrium albeit with the 5-carboxylate form present in undetectable concentrations. An alternative possible explanation for the signal broadening could be due to the presence of amide rotamers; comparison of the ^{13}C NMR spectra of pyrazole **71** with the two N–H insertion products **169** and **170**, however, highlights that the signal broadening is due to tautomers, with no dynamic effects observed in the ^{13}C NMR spectra of **169** and **170**.

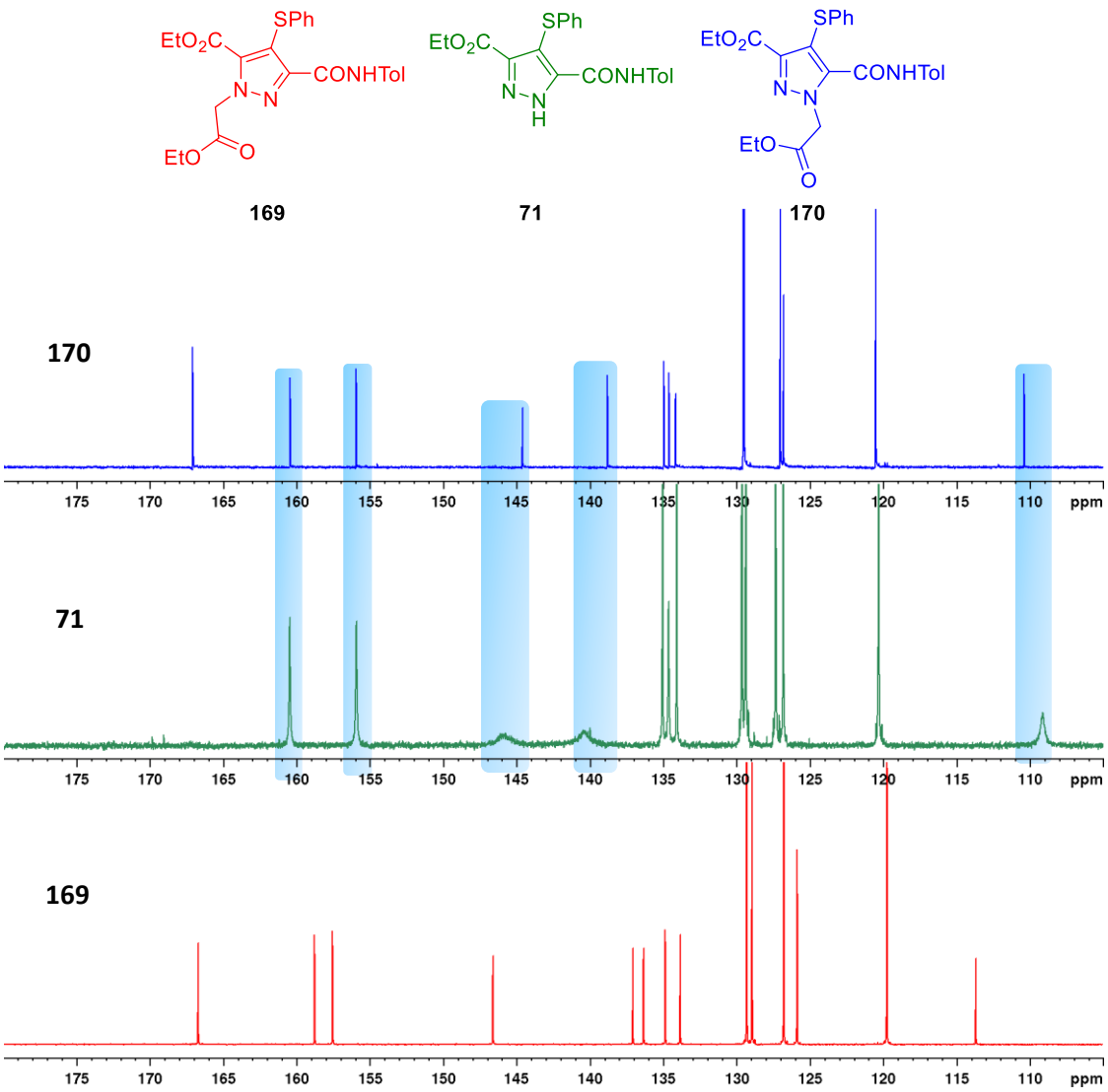

Figure 2.24: ^{13}C NMR (150.9 MHz) spectra of pyrazole **71** and N–H insertion products **169** and **170** illustrating that the major tautomer of pyrazole **71** in $CDCl_3$ is the 3-carboxylate

While it appears that the dynamic equilibrium in $CDCl_3$ favors the 3-carboxylate tautomeric form it is interesting that it is, in fact, the minor tautomer that undergoes N–H insertion more readily to give the pyrazole **169** as the major regioisomer. To test whether this was due to the minor tautomer being more reactive or whether the dynamic equilibrium tended towards the 5-carboxylate in the reaction solution, ^{13}C NMR spectra for the pyrazole **71** and the N–H insertion products **169** and **170** were recorded in toluene-d_8, the solvent used for the cycloaddition, at 150.9 MHz **(Figure 2.25)**. As was observed in $CDCl_3$, substantial overlap of the signals was observed with those for N–H insertion product **170**, indicating that the major tautomer present in toluene-d_8, and presumably the reaction medium, is the 3-carboxylate. Therefore, despite the observation that the equilibrium between the 3-carboxylate and 5-carboxylate tautomers in non-interacting solvents strongly favours the 3-carboxylate tautomer, isolation of the 5-carboxylate as the major N–H insertion product **169** suggests that the minor tautomer is significantly more reactive.

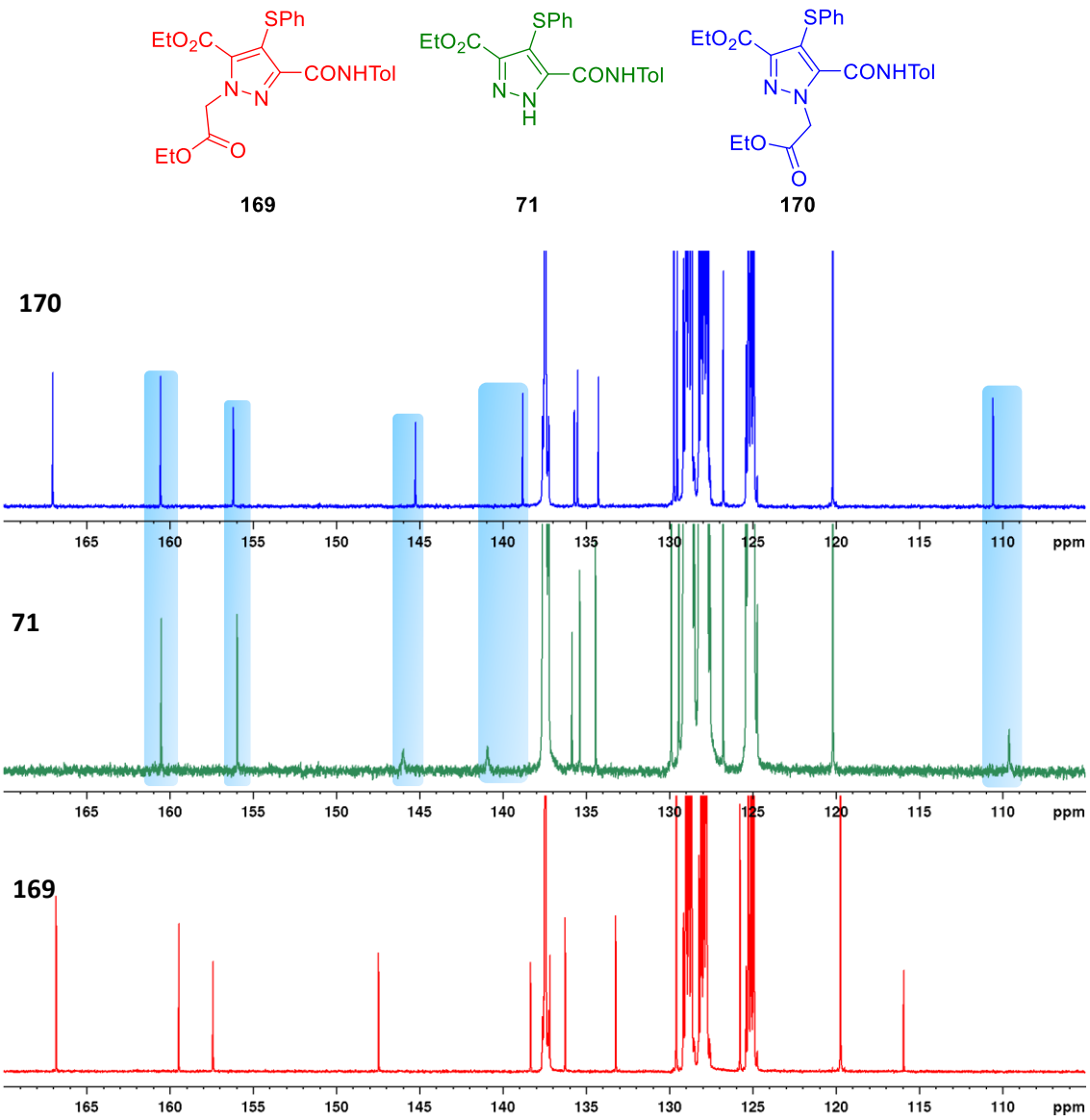

Figure 2.25: ^{13}C NMR (150.9 MHz) spectra of pyrazole **71** and N–H insertion products **169** and **170** illustrating that the major tautomer of pyrazole **71** in toluene-d_8 is the 3-carboxylate

As pyrazoles **177** and **187** were insoluble in $CDCl_3$ their NMR spectra were recorded in DMSO-d_6 with broad signals for both tautomers observed in each instance. Considering this, the solvent dependency on the position of equilibrium was studied by comparing the ^{13}C NMR spectra for pyrazoles **71**, **169** and **170** in DMSO-d_6 with those in $CDCl_3$. Notably in DMSO-d_6, two distinct sets of broad signals were observed for pyrazole **71** at 150.9 MHz **(Figure 2.26)**, characteristic of both the 3-carboxylate and 5-carboxylate tautomer, with the 5-carboxylate predominating as the major tautomer in solution as evidenced by comparison of carbon signals with that of pyrazole **169**.

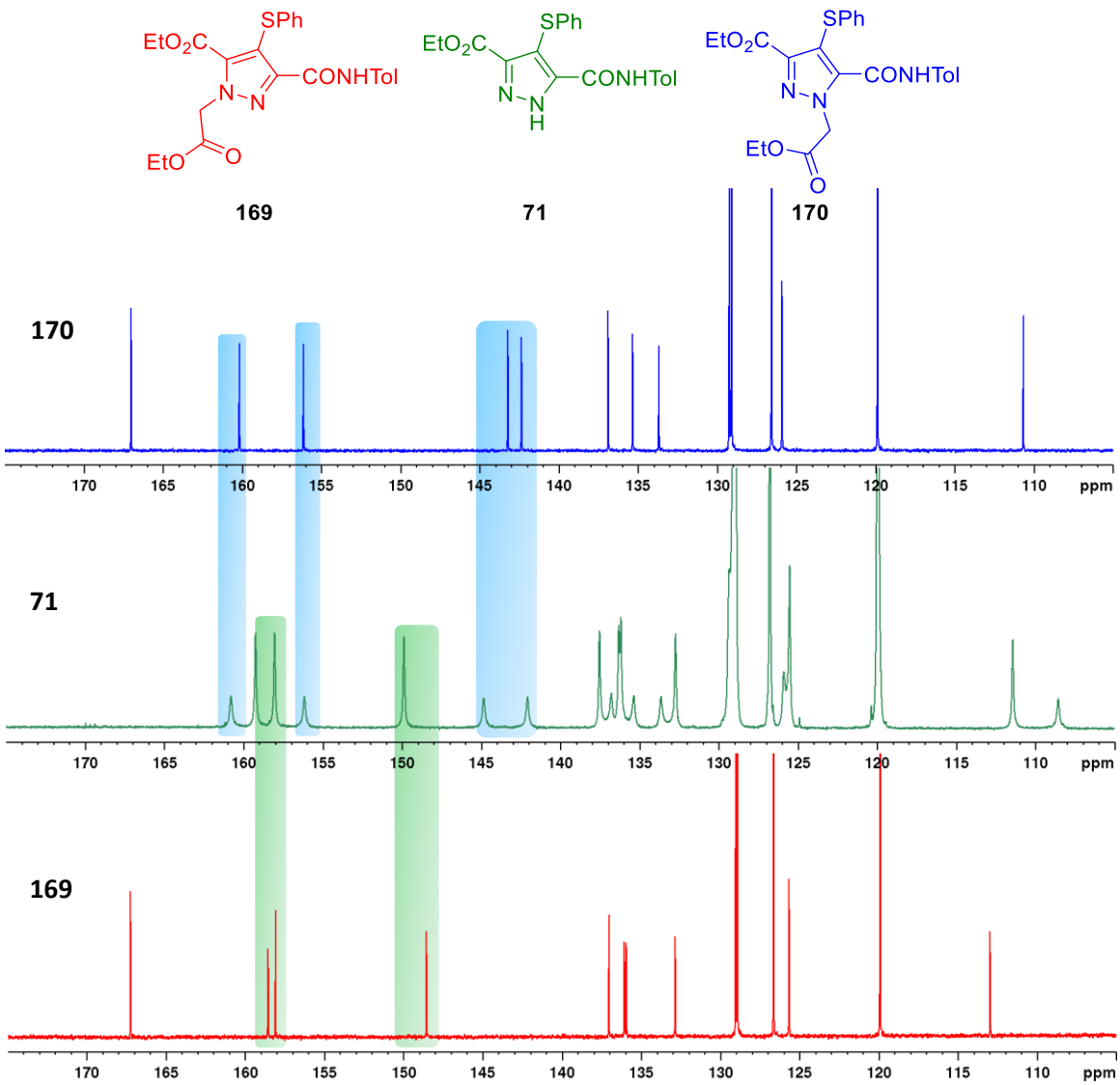

Figure 2.26: ^{13}C NMR (150.9 MHz) spectra of pyrazole **71** and N–H insertion products **169** and **170** illustrating that the major and minor tautomers of pyrazole **71** in DMSO-d_6 are the 5- and 3-carboxylates respectively

For tautomer assignment one of the characteristic features is that the C(4) chemical shift for the 5-carboxylate tautomer is always more deshielded than that for the 3-carboxylate. Accordingly, in the experimental section, the pyrazoles **177** and **187** are characterised as a mixture of the 3- and 5-carboxylate tautomers while pyrazoles **71**, **172**–**176** and **178**–**186** were characterised as the major 3-carboxylate tautomer as their spectra were recorded in $CDCl_3$ **(Figure 2.27)**. The impact of solvent on the dynamic equilibrium between the 3- and 5-carboxylate tautomers for pyrazole **71** is summarised in **Scheme 2.60**.

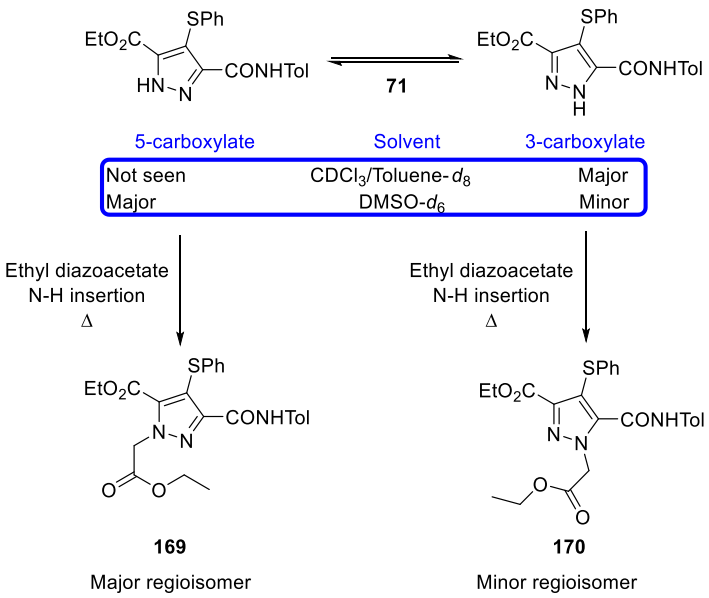

Scheme 2.60: Summary of solvent effects on the dynamic equilibrium between the 3- and 5-carboxylate tautomers for pyrazole **71**.

Pyrazoles **191–199** were significantly less soluble than their 3,4,5-substituted counterparts, and DMSO-d_6 was required to solubilise these compounds for NMR spectroscopy. The NMR spectra of **196** could be recorded in $CDCl_3$. Pyrazole **196** exhibited one set of broad signals in the ^{13}C NMR spectrum at 150.9 MHz in $CDCl_3$, while splitting of both the NH pyrazole and NH amide signals, into major and minor components, was observed in the ^{1}H NMR spectrum at 600 MHz. Two sets of broad signals were observed in the ^{13}C NMR spectra for pyrazoles **191–195** and **197–199** recorded in DMSO-d_6, indicative of the 3-carboxylate and 5-carboxylate, however, comparison of the ^{13}C NMR spectra of 4-sulfenylpyrazoles (i.e. **71**) and desulfinylated pyrazoles (i.e. **191**) in DMSO-d_6 strongly suggests that the dynamic equilibrium shifts towards the 3-carboxylate on removal of the sulfur moiety at the C(4) position. Therefore, similar solvent effects on the dynamic equilibrium are observed for both the 3,5-substituted and 3,4,5-substituted pyrazoles, however, with the 5-carboxylate predominating for the 3,4,5-substuted pyrazoles and the 3-carboxylate predominating for the 3,5-substituted pyrazoles in DMSO-d_6. Accordingly, the pyrazoles **191–199** are characterised as their 3-carboxylates in this work **(Figure 2.27)**.

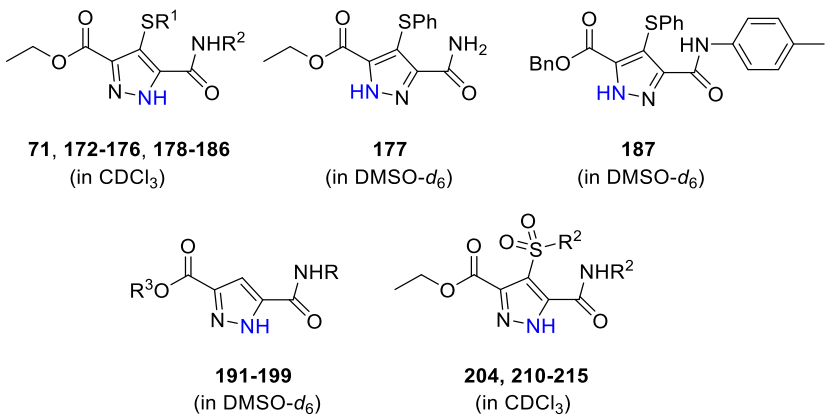

Figure 2.27: Principal tautomers of the 3,4,5-substituted pyrazoles and 3,5-substituted pyrazoles generated in this work illustrating the importance of solvent on the dynamic equilibrium. Structures are named and numbered accordingly in the **Experimental Section**.

In the solid state, the 4-sulfonylpyrazole **204** exists as the tautomer with the carboxylate at the C(3) position (Figure 4). As is the case for the pyrazoles formed at sulfide oxidation level, one set of ^{13}C NMR signals is observed for the 4-sulfonylpyrazoles in the non-interacting solvent $CDCl_3$, however the C(4) carbon is considerably sharper and more deshielded for this set of compounds than for the sulfide analogues. The C(3) and C(5) carbons remain very broad, suggesting that the pyrazoles are also in dynamic equilibrium, with the 3-carboxylate the favoured tautomer, and the 5-carboxylate tautomer undetectable in the ^{13}C NMR spectra as seen at the sulfide level of cycloaddition. The 4-sulfonylpyrazoles are assigned as the major 3-carboxylate tautomer in this work **(Figure 2.27)**.

2.7. Further Derivatisation of the Pyrazole Scaffold

The [3+2] dipolar cycloaddition of *α*-diazoacetates is a powerful synthetic methodology that, when compared to the more standard hydrazine condensation, has the advantage that it allows incorporation of highly functionalised substituents at each the C(3), C(4) and C(5) positions of the pyrazole core. As there are very few examples of 3,4,5-trisubstituted pyrazoles (particularly bearing a sulfur moiety), with each substituent bearing functionalisable groups, investigation of the synthetic potential of these compounds was briefly undertaken utilising pyrazole **71** as a standard substrate. For this purpose, the pyrazole NH, the ester moiety and the sulfide were chosen for further derivatisation **(Figure 2.28)**.

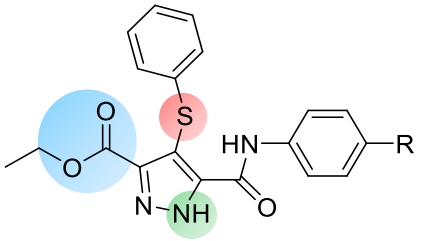

Figure 2.28: Synthetic handles chosen for further functionalisation

As summarised in **Table 2.9**, selective oxidation of the sulfide in pyrazole **71** to either the sulfoxide **234** or sulfone **201** can be achieved using *m*CPBA as oxidant, with the extent of oxidation controlled by reaction temperature and/or stoichiometry. Thus, exposure of pyrazole **71** to 2 equivalents of *m*CPBA overnight led to a mixture of 85:15 of the sulfoxide **234** and sulfone **204**, while use of 2.5 equivalents of *m*CPBA at reflux afforded exclusively the sulfone **204.** Application of these conditions to pyrazoles **175** and **176** similarly led to sulfoxide **235** and sulfone **213** respectively highlighting the generality of this approach. As discussed in **Section 2.5.2** oxidation of the 4-sulfenylpyrazole **71** to the 4-sulfonylpyrazole **201**, whose structure was confirmed crystallographically **(Figure 2.22)**, enabled confirmation of the regiochemistry of the rearranged pyrazoles from the α-thio-β-chloroacrylamide cycloadditions. While access to the 4-sulfinyl- and 4-sulfonylpyrazoles through direct cycloaddition at the appropriate oxidation level was challenging (sulfoxide elimination occurs leading to pyrazoles **191**–**199** in place of 4-sulfinylpyrazoles, while yields of the 4-sulfonylpyrazoles **204** and **210**–**215** were very low), combining the robust [3+2] dipolar cycloaddition at the sulfide level leading to 4-sulfenylpyrazoles, with the selective oxidation protocols, provides access to 4-sulfinyl and 4-sulfonylpyrazoles in a synthetically useful manner.

Table 2.9. Sulfur oxidation of pyrazoles

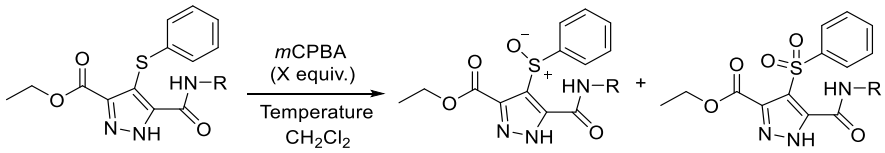

Entry	Pyrazole	R	Temp.	Equiv. *m*CPBA	Sulfoxide: Sulfone[a]	Sulfoxide	Sulfone	Yield (%)[b]
1	**71**	Tol	r.t.	2	85 : 15	**234**	-	66[c]
2	**71**	Tol	Reflux	2.5	0 : 100	-	**204**	82
3	**175**	4-$MeOC_6H_4$	r.t.	1	100 : 0	**235**	-	94
4	**176**	*n*-Bu	Reflux	2.5	0 : 100	-	**213**	78

a) Conversion calculated by analysis of the ^{1}H NMR spectra of the crude products.
b) Isolated yield after basic work up unless otherwise stated.
c) Isolated yield after flash column chromatography.

We subsequently explored the synthetic potential of the acidic pyrazole N–H bond via a series of regioselective alkylations of the pyrazole **71**. Following a procedure reported by Zheng,[123] a series of alkylation reactions using potassium carbonate, dimethyl sulfoxide and a variety of alkyl bromides as electrophiles, was carried out to give the novel pyrazoles **169**, **170**, and **236**–**240** in high yields **(Table 2.10)**.[124-125] Interestingly, the regioselectivity of the alkylations was consistent with the regioselectivities observed for the N–H insertion reactions (approximately 3:1 by ^{1}H NMR spectroscopy), favouring the 5-carboxylate regioisomer. The *N*-alkylated regioisomers **236**–**240** were assigned by comparison to the ^{1}H NMR spectra of the N–H insertion products **169** and **170** (see **Section 2.5.2**). The distinctive methylene NCH_2 signal and the amide NH signal for the major regioisomer, the 5-carboxylate, for the pyrazoles generated in this study are significantly more shielded in their respective ^{1}H NMR spectra than the corresponding signals in the 3-carboxylate regioisomer. Notably, as mentioned previously, the major tautomer of **71** in DMSO-d_6 is the 5-carboxylate, hence the alkylations proceed preferentially through the major tautomer in solution for this set of reaction conditions.

Table 2.10. Regioselective alkylation of the pyrazole **71**

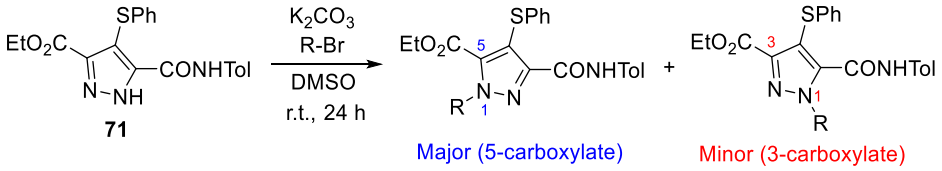

Entry[a]	R	Major: Minor[b]	Major	Minor	Yield[e] (%)
1	Bn	78 : 22	**236**	**237**[c]	76
2	CH_2COOEt	72 : 28	**169**	**170**	92
3	CH_2COPh	75 : 25	**238**	**239**	84
4	Et	94 : 6	**240**	-[d]	70

a) Reaction conditions: Pyrazole **71** (0.393 mmol), K_2CO_3 (0.512 mmol), electrophile (0.472 mmol) and anhydrous DMSO (3 ml).
b) Ratios of major and minor regioisomers were calculated from the ^{1}H NMR spectra of the crude reaction mixtures using the 2H methylene NCH_2 signals for **Entries 1–3**; the NH amide signal was used for **Entry 4**.
c) Pyrazole **237** was isolated in 87% purity containing 13% of the regioisomer **236**.
d) Not isolated.
e) Total isolated yield for the combined *N*-alkylated regioisomers following column chromatography, however, compounds **169**, **170**, **236** and **238–240** were isolated as pure compounds as described in the **Experimental section**.

Finally, the synthetic potential of the ester moiety was explored via a two-step hydrolysis and amide coupling strategy **(Scheme 2.61)**. Firstly, hydrolysis of the ester moiety in pyrazole **71** was efficiently achieved in the presence of sodium hydroxide affording the novel carboxylic acid **241** in 91% yield. Subsequent coupling with *p*-anisidine afforded the novel 3,5-dicarboxamide **242** in 64% yield without optimisation illustrating the synthetic potential for variation of the ester moiety introduced to the pyrazole through the dipole.

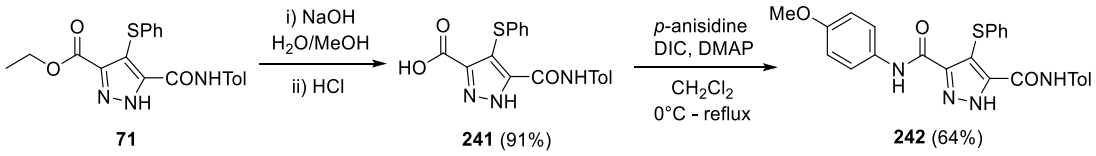

Scheme 2.61. Derivatisation of the ester moiety through hydrolysis and subsequent coupling.

While only briefly explored in this work, the high yielding derivatisations of pyrazole **71** herein discussed highlights the significant synthetic potential of utilising α-diazoacetates as 1,3-dipoles in conjunction with α-thio-β-chloroacrylamides as dipolarophiles to access not only highly functionalised pyrazoles in the first instance, but importantly functionalised pyrazoles readily amenable to significant further synthetic transformations.

2.8. Conclusions

In summary, we have presented herein highly regioselective synthetic methodology leading to densely functionalised C(3), C(4) and C(5) substituted pyrazoles **71**, **172–187**, **204** and **210–215** via thermal [3+2] dipolar cycloaddition of α-diazoacetates and α-thio-β-chloroacrylamides, at the sulfide, sulfoxide and sulfone levels of oxidation. Significantly, this work allows access to C(4) sulfenyl or sulfonyl pyrazoles, through migration of the sulfur substituent at the sulfide and sulfone oxidation levels, while elimination of the sulfinyl group is observed, leading to 3,5-disubstituted pyrazoles **191–**

199. Notably, use of highly functionalised dipolarophiles, and in particular a chloro substituent which can act as a leaving group, enables the key rearrangement following cycloaddition to provide the synthetically versatile pyrazoles, where each of the three substituents has the potential for orthogonal functional group interconversion.

While the sulfide migration to the electron deficient carbon is readily rationalised, the analogous carbon–carbon 1,2-sulfonyl migration is unprecedented and mechanistically intriguing. Notably, we have found that the [3+2] dipolar cycloaddition is remarkably insensitive to the nature of the substituent present on both the amide (secondary) and sulfide, however, tertiary amides at the sulfone oxidation level do not undergo cycloaddition highlighting the importance of conformation in the dipolarophilic species, with the presence of a hydrogen bond in both primary and secondary amides critical to pyrazole formation.

Extension of the methodology to include α-thio-β-chloroesters was also possible as illustrated by the successful formation of the pyrazole **186**, however, our attempts to extend this methodology to the novel α-thio-β-chlorothioester scaffold proved to be unsuccessful presumably due to the labile nature of the thioester moiety. While moderate to good yields are obtained using the dipolarophiles at the sulfide level of oxidation, efficiencies are decreased when conducted using the sulfoxide or sulfone, reflecting the labile nature of the reactants and products under the reaction conditions. Despite this, from a synthetic perspective, accessing both 4-sulfinyl and 4-sulfonylpyrazoles is a straightforward process via simple *m*CPBA mediated oxidation of the requisite 4-sulfenyl precursor, highlighting a synthetically useful method for the generation of these highly functionalised heterocycles.

In contrast to alternative synthetic methods leading to pyrazoles, such as hydrazine condensation, this methodology offers distinct synthetic advantage enabling access to highly substituted and structurally diverse pyrazoles with functionality amenable to further selective synthetic transformations. In this regard, we have demonstrated that the pyrazole **71** can undergo a range of further reactions with selective oxidation, regioselective alkylation, and ester hydrolysis with subsequent coupling described in this work in high yields.

Isolation of the *N*-alkylated pyrazoles **169** and **170** as by-products from the cycloaddition through further reaction of the pyrazole **71** with excess α-diazoacetate, proved useful in rationalising the tautomeric behaviour evident in the NMR spectra of the pyrazoles, with the position of the tautomeric equilibrium influenced by solvent and substituents.

The use of terminal α-diazosulfones **37** and **127** as 1,3-dipoles was briefly investigated, but these compounds were observed to be incompatible with both α-thio-β-chloroacrylamides and α-sulfinyl-β-chloroacrylamides, with no cycloaddition observed. Instead, for the α-thio-β-chloroacrylamides oxidation to the corresponding sulfoxide was observed, mediated by likely carbene derived sulfonium ylide formation. Despite this, the α-diazosulfones **37** successfully underwent cycloaddition with a range of structurally and electronically simple dipolarophiles. α-Diazoacetamides were also observed to undergo dipolar cycloaddition with α-thio-β-chloroacrylamides in an analogous manner to the α-diazoacetates, however, undesirable N–H insertion becomes significant at elevated temperatures.

2.9. Experimental

2.9.1. General Procedures

All solvents were distilled prior to use by the following methods: dichloromethane was distilled from phosphorous pentoxide, and in certain intances was futher distilled from calcium hydride; ethyl acetate was distilled from potassium carbonate; toluene was distilled from sodium benzophenone ketyl and stored over 4Å molecular sieves; tetrahydrofuran was distilled from sodium benzophenone ketyl; and hexane was distilled before use. Molecular sieves were dried by heating at 150 °C overnight. Organic phases were dried using anhydrous magnesium sulfate. All commercial reagents were used without further purification unless otherwise stated.

^{1}H NMR (300 MHz) and ^{13}C (75.5 MHz) NMR spectra were recorded on a Bruker Avance 300 NMR spectrometer. ^{1}H NMR (400 MHz) and ^{13}C (100 MHz) NMR spectra were recorded on a Bruker Avance 400 NMR spectrometer. ^{1}H NMR (600 MHz) and ^{13}C (150.9 MHz) NMR spectra were recorded on a Bruker Avance 600 NMR spectrometer. All spectra were recorded at room temperature (300K) in deuterated chloroform ($CDCl_3$), unless otherwise stated using tetramethylsilane (TMS) as an internal standard. ^{1}H NMR spectra that were recorded in deuterated dimethyl sulfoxide (DMSO-d_6) were assigned using the DMSO peak as the reference peak. ^{13}C NMR spectra were calibrated using the solvent signal, i.e., $CDCl_3$ δ_C 77.0 ppm, DMSO-d_6 39.5 ppm, toluene-d_8 20.4 ppm. Chemical shifts (δ_H and δ_C) are reported in parts per million (ppm) relative to TMS, and coupling constants are expressed in Hertz (Hz). Splitting patterns in ^{1}H NMR spectra are designated as s (singlet), br s (broad singlet), d (doublet), t (triplet), br t (broad triplet), q (quartet), dd (doublet of doublets), AB (AB system), ABX (ABX system) and m (multiplet). ^{13}C NMR spectra were assigned with the aid of DEPT experiments. Compounds which were assigned with the aid of DEPT experiments were assigned by identifying both the carbon, designated as CH_3, CH_2, CH, or C, and also the atom number of the carbon, for example, [CH, C(2)H]. A number of spectra were assigned with the aid of 2D NMR correlation experiments including COSY, HSQC and HMBC. On occasion, *J* values measured from the spectra do not exactly match up, but always fall within experimental error. The values recorded are those that are measured. All spectroscopic details for compounds previously made were in agreement with those previously reported unless otherwise stated.

Infrared spectra were measured using a FTIR UATR2 spectrometer or were recorded as films on sodium chloride plates on a PerkinElmer Paragon 1000 FT-IR spectrometer. Flash column chromatography was carried out using Kieselgel silica gel 60, 0.035–0.075 mm (Merck).

Thin-layer chromatography (TLC) was carried out on precoated silica gel plates (Merck 60 PF254). Visualization was achieved by UV (254 nm) light absorption.

The Microanalysis Laboratory, National University of Ireland, Cork, performed elemental analysis using a PerkinElmer 240 and Exeter Analytical CE440 elemental analysers.

Low-resolution mass spectra (LRMS) was recorded on a Waters Quattro Micro triple quadrupole instrument in electrospray ionization (ESI) mode using 50% acetonitrile/water containing 0.1% formic acid as eluent. High resolution (precise) mass spectra (HRMS) were recorded on a Waters LCT Premier Time of Flight LC–MS instrument in electrospray ionization (ESI) mode using 50% acetonitrile/water containing 0.1% formic acid as eluent. High-resolution (precise) mass spectra (HRMS) were also recorded on an Agilent 6530B Accurate Mass Q-TOF LC/MS instrument in electrospray ionisation mode using 50% acetonitrile/water containing 0.1% formic acid as eluent. Samples were prepared for either LRMS or HRMS by employing acetonitrile as solvent.

Melting points were obtained using a Unimelt Thomas–Hoover capillary melting point apparatus and are uncorrected.

Single-crystal X-ray analysis was performed on a Bruker APEX II DUO diffractometer at room temperature using graphite monochromatic Mo K_α (λ = 0.7107 Å) radiation. All calculations and refinement were made using the APEX software,[126] containing the SHELX suite of programs[127] and diagrams prepared with Mercury 3.10.[128] All non-hydrogen atoms were located and refined with anisotropic thermal parameters. Hydrogen atoms were included in calculated positions or were located and refined with isotropic thermal parameters.

2.9.2 Synthesis of α-Chloroamides

2-Chloro-*N*-(4-methylphenyl)propanamide 72[7, 16, 19]

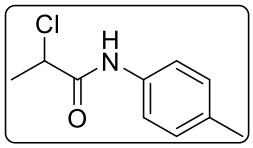

2-Chloropropionyl chloride (20 g, 0.157 mol) in dichloromethane (100 ml) was added dropwise over 20 min to a solution of *p*-toluidine (16.59 g, 0.155 mol) and triethylamine (21.90 ml, 0.157 mol) in dichloromethane at 0°C, while stirring under nitrogen. On completion of the addition, the reaction solution was removed from the ice bath and stirred at room temperature for 4 h. Water (200 ml) was added and the layers separated. The organic layer was washed with a saturated solution of sodium bicarbonate (2 x 150 ml), water (200 ml), and brine (200 ml), dried, filtered and concentrated under reduced pressure to give the α-chloroamide **72** as a white solid (28.75 g, 94 %) which required no further purification; mp 117-121°C (lit.[19] 120-122°C); ν_{max}/cm^{-1} (ATR) 3251 (NH), 3187 (CH), 1664 (C=O), 1543, 1367 (CN stretch); δ_H (300 MHz, $CDCl_3$) 1.81 [3H, d, *J* 7.0 Hz, C(3)H_3], 2.32 (3H, s, ArH), 4.53 [1H, q, *J* 7.0 Hz, C(2)H], 7.14 (2H, d, *J* 8.2 Hz, ArH), 7.38-7.44 (2H, m, ArH), 8.24 (1H, br s, NH) ppm; δ_C (75.5 MHz, $CDCl_3$) 20.9 (CH_3, $ArCH_3$), 22.7 [CH_3, C(3)H_3], 56.2 [CH, C(2)H], 120.1 (CH, CH_{Ar}),129.5 (CH, CH_{Ar}), 134.4 (C, $C_{Ar(q)}$), 134.8 (C, $C_{Ar(q)}$), 167.3 (C, C=O) ppm.

2-Chloro-*N*-(4-fluorophenyl)propanamide 73[7, 16]

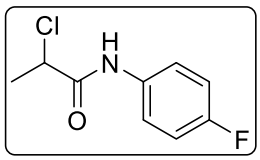

The title compound was prepared following the procedure described for **72** from 2-chloropropionyl chloride (7.36 g, 57.97 mmol), 4-fluroaniline (6.38 g, 57.40 mmol) and triethylamine (5.87 g, 57.97 mmol) in dichloromethane (120 ml) to give the α-chloroamide **73** as a pale orange solid (11.06 g, 96 %) which required no further purification; mp 80-83°C (lit.[129] 83-84°C); ν_{max}/cm^{-1} (ATR) 3250 (NH), 1661 (C=O), 1542 (NH bend), 1507, 1374 (CN stretch); δ_H (300 MHz, $CDCl_3$) 1.80 [3H, d, *J* 7.1 Hz, C(3)H_3], 4.53 [1H, q, *J* 7.1 Hz, C(2)H], 6.97-7.06 (2H, m, ArH), 7.45-7.54 (2H, m, Ar-H), 8.37 (1H, br s, NH) ppm; δ_C (75.5 MHz, $CDCl_3$) 22.4 [CH_3, C(3)H_3], 55.8 [CH, C(2)H], 115.7 [CH, d, $^2J_{CF}$ 22.6 Hz, C(3′)H_{Ar}], 122.1 [CH_r, d, $^3J_{CF}$ 8.0 Hz, C(2′)H_{Ar}], 132.9 [C, d, $^4J_{CF}$ 2.9 Hz, C(1′)$_{Ar(q)}$NH], 159.7 [C, d, $^1J_{CF}$ 244.6 Hz, C(4′)$_{Ar(q)}$F], 167.6 (C, C=O) ppm.

2-Chloro-*N*-(4-methoxyphenyl)propanamide 74[129-130]

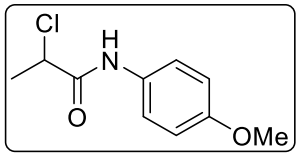

The title compound was prepared following the procedure described for **72** from 2-chloropropionyl chloride (7.90 g, 62.22 mmol), *p*-anisidine (61.60 g, 61.60 mmol) and triethylamine (6.30 g, 62.22 mmol) in dichloromethane (120 ml) to give the α-chloroamide **74** as a grey solid (12.77 g, 97 %) which required no further purification; mp 104-107°C (lit.[129] 105-106°C); ν_{max}/cm^{-1}

(ATR) 3254 (NH), 2970 (CH), 1659 (C=O), 1542 (NH bend), 1509, 1456 (CN stretch); δ_H (300 MHz, $CDCl_3$) 1.80 [3H, d, *J* 7.0 Hz, C(3)H_3], 3.78 (3H, s, ArOCH_3), 4.52 [1H, q, *J* 7.0, C(2)H], 6.83-6.90 (2H, m, ArH), 7.40-7.46 (2H, m, ArH), 8.26 (1H, br s, NH) ppm; δ_C (75.5 MHz, $CDCl_3$) 22.5 [CH_3, C(3)H_3], 55.4 (CH_3, ArOCH_3), 56.0 (CH, C(2)H), 114.1 (CH, CH_{Ar}), 121.9 (CH, CH_{Ar}), 130.0 [C, $C_{Ar(q)}$NH], 156.9 [C, $C_{Ar(q)}$OMe], 167.3 (C, C=O) ppm.

_N_-Benzyl-2-chloropropanamide 75[7, 16]

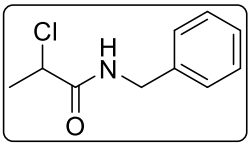

The title compound was prepared following the procedure described for **72** from 2-chloropropionyl chloride (10.25 g, 80.7 mmol), benzylamine (8.56 g, 79.9 mmol) and triethylamine (8.17 g, 80.7 mmol) in dichloromethane (150 ml) to give the α-chloroamide **75** as a white solid (15.38 g, 98 %) which required no further purification; mp 77-79°C (lit.[131] 80-82°C); ν_{max}/cm^{-1} (ATR) 3268 (NH), 3066 (CH), 2974 (CH), 1651 (C=O), 1547 (NH bend), 1454 (CN stretch); δ_H (300 MHz, $CDCl_3$) 1.74 [3H, d, *J* 7.1 Hz, C(3)H_3], 4.43 [1H, q, *J* 7.1 Hz, C(2)H], 4.44 (2H, d, *J* 5.8 Hz, NCH_2) 6.97 (1H, br s, NH), 7.22-7.38 (5H, m, ArH) ppm; δ_C (75.5 MHz, $CDCl_3$) 22.6 [CH_3, C(3)H_3], 43.8 (CH_2, CH_2NH), 55.7 (CH, C(2)H), 127.5 (CH, CH_{Ar}) 127.6 (CH, CH_{Ar}), 128.7 (CH, CH_{Ar}), 137.4 (C, $C_{Ar(q)}$), 169.4 (C, C=O) ppm.

_N-n_-Butyl-2-chloropropanamide 76[7, 16]

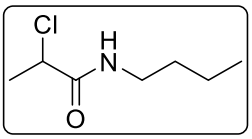

The title compound was prepared following the procedure described for **72** from 2-chloropropionyl chloride (7.35 g, 57.89 mmol), *n*-butylamine (4.19 g, 57.32 mmol) and triethylamine (5.86 g, 57.89 mmol) in dichloromethane (100 ml) to give the α-chloroamide **76** as a yellow oil (15.38 g, 98 %) which required no further purification; ν_{max}/cm^{-1} (ATR) 3288 (NH), 3090 (CH), 2960 (CH), 1655 (C=O), 1552 (NH bend), 1373 (CN stretch); δ_H (300 MHz, $CDCl_3$) 0.94 [3H, t, *J* 7.3 Hz, C(4′)H_3], 1.30-1.44 [2H, m, C(3′)H_2], 1.47-1.60 [2H, m, C(2′)H_2], 1.71 [3H, d, *J* 7.0 Hz, C(3)H_3], 3.28 [2H, dt, *J* 7.1, 6.0 Hz, C(1′)$\underline{H_2}$], 4.42 [1H, q, *J* 7.0 Hz, C(2)H], 6.94 (1H, br s, NH) ppm; δ_C (75.5 MHz, $CDCl_3$) 13.4 [CH_3, C(4′)H_3], 19.7 [CH_2, C(3′)H_2], 22.3 [CH_3, C(3)H_3], 31.1 [CH_2, C(2′)H_2], 39.4 [CH_2, C(1′)H_2], 55.4 [CH, C(2)H], 169.3 (C, C=O) ppm.

2-Chloro-_N_-(2′,2′-dimethylpropyl)propanamide 77

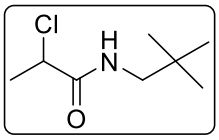

The title compound was prepared following the procedure described for **72** from 2-chloropropionyl chloride (7.61 g, 59.94 mmol), 2,2-dimethylpropylamine (5.17 g, 59.35 mmol) and triethylamine (6.07 g, 59.94 mmol) in dichloromethane (100 ml) to give the α-chloroamide **77** as a grey solid as a white solid (15.38 g, 97 %) which required no further purification; mp 79-81˚C; ν_{max}/cm^{-1} (ATR) 3255 (NH), 3093 (CH), 2957 (CH), 1652 (C=O), 1574, 1374 (CN stretch); δ_H (300 MHz, $CDCl_3$) 0.94 [9H, s, C(CH_3)$_3$], 1.75 [3H, d, *J* 7.1 Hz, C(3)H_3], 3.06 [1H, dd, A of ABX system, J_{AB} 13.3 Hz, J_{AX} 6.3 Hz, one of C$\underline{H_2}$NH], 3.13 [1H, dd, B of ABX system, J_{BA} 13.3 Hz, J_{BX} 6.4 Hz, one of C$\underline{H_2}$NH], 4.45 [1H, q, *J* 7.1 Hz, C(2)H], 6.70 (1H, br s, NH) ppm; δ_C (75.5 MHz, $CDCl_3$) 22.8 [CH_3, C(3)H_3], 27.0 [CH_3, C($\underline{C}H_3$)$_3$], 31.9 [C, $\underline{C}$(CH_3)$_3$], 50.8 (CH_2, CH_2NH), 56.3 [CH, C(2)H], 169.4 (C=O) ppm; HRMS (ES+): Exact mass calculated for $C_8H_{16}NO^{35}Cl$ $[M+H]^+$ 178.0993. Found 178.0995; m/z (ES+) 180.3 {[($C_8H_{16}NO^{37}Cl$)+H^+], 30%}, 178.3 {[($C_8H_{16}NO^{35}Cl$)+H^+], 100%}.

2.9.3 Synthesis of α-Thioamides

_N_-(4-Methylphenyl)-2-(phenylthio)propanamide 6[7, 15, 21]

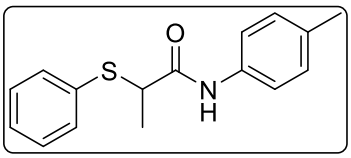

Thiophenol (16.9 ml, 0.166 mol) was added to a solution of freshly prepared sodium ethoxide [prepared from sodium (3.81 g, 0.166 mol) in dry ethanol (250 ml) at 0°C] while stirring under nitrogen. Immediately a solution of 2-chloro-*N*-(4-methylphenyl)propanamide **72** (27.21 g, 0.138 mol) in dry ethanol (50 ml) was added to the reaction mixture. Upon completion of the addition the ice bath was removed. Following stirring at room temperature for 18 h, the reaction was quenched by addition of water (200 ml) and dichloromethane (200 ml). The phases were separated and the aqueous layer was extracted with dichloromethane (2 x 80 ml). The combined organic layers were washed with aqueous sodium hydroxide (1M, 2 x 80 ml), water (100 ml) and brine (100 ml), dried, and concentrated under reduced pressure to give *N*-(4-methylphenyl)-2-(phenylthio)propanamide **6** as a white solid (34.80 g, 93 %) which did not require further purification; mp 108-111°C (lit.[7] 112-113°C); ν_{max}/cm^{-1} (ATR) 3291 (NH), 3123 (CH), 2924 (CH), 1160 (C=O), 1527, 1444 (CN stretch); δ_H (300 MHz, $CDCl_3$) 1.59 [3H, d, *J* 7.3 Hz, C(3)H_3], 2.28 (3H, s, ArCH_3), 3.87 (1H, q, *J* 7.3 Hz, C(2)H], 7.08 (2H, d, *J* 8.1 Hz, ArH), 7.17-7.41 (7H, m, ArH), 8.38 (1H, br s, NH) ppm; δ_C (75.5 MHz, $CDCl_3$) 18.2 [CH_3, C(3)H_3], 20.8 (CH_3, ArCH_3), 47.9 [CH, C(2)H], 119.9 (CH, CH_{Ar}), 127.6 (CH, CH_{Ar}), 129.2 (CH, CH_{Ar}), 129.5 (CH, CH_{Ar}), 130.7 (CH, CH_{Ar}), 133.3 (C, $C_{Ar(q)}$), 134.2 (C, $C_{Ar(q)}$), 134.9 (C, $C_{Ar(q)}$), 170.0 (C, C=O) ppm.

_N_-Benzyl-2-(phenylthio)propanamide 78[6, 15, 21]

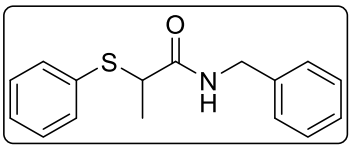

The title compound was prepared following the procedure described for **6** using *N*-benzyl-2-chloropropanamide **75** (7.57 g, 38.4 mmol), thiophenol (4.70 ml, 46.1 mmol), and sodium (1.06 g, 46.1 mmol) in dry ethanol (100 ml). The reaction mixture was stirred for 16 h before work up as described for **6** gave the crude sulfide as a white solid. Purification by flash column chromatography on silica gel using hexane: ethyl acetate as eluent (gradient elution 20-40% ethyl acetate) gave pure *N*-benzyl-2-(phenylthio)propanamide **78** (7.93 g, 72 %) as a white solid; mp 45-47 °C (lit.[21] 43-45°C); ν_{max}/cm^{-1} (ATR) 3315 (NH), 3061 (CH), 2963 (CH), 1655 (C=O), 1527, 1473; δ_H (300 MHz, $CDCl_3$) 1.57 [3H, d, *J* 7.3 Hz, C(3)H_3], 3.87 [1H, q, *J* 7.3, C(2)H], 4.33 [1H, dd, A of ABX system, J_{AB} 14.9 Hz, J_{AX} 5.6, one of C$\underline{H}_2$NH], 4.43 [1H, dd, B of ABX system, J_{BA} 14.9 Hz, J_{BX} 6.1, one of C$\underline{H}_2$NH], 6.91 (1H, br s, NH), 7.03-7.12 (2H, m, ArH), 7.17-7.34 (8H, m, ArH) ppm; δ_C (75.5 MHz, $CDCl_3$) 18.2 (CH_3, C(3)H_3), 43.6 (CH_2, CH_2NH), 46.8 [CH, C(2)H], 127.1 (CH, CH_{Ar}), 127.4 (CH, CH_{Ar}), 127.5 (CH, CH_{Ar}), 128.6 (CH, CH_{Ar}), 129.1 (CH, CH_{Ar}), 130.1 (CH, CH_{Ar}), 133.8 [C, $C_{Ar(q}$], 137.8 [C, $C_{Ar(q)}$], 171.7 (C, C=O) ppm.

_N-n_-Butyl-2-(phenylthio)propanamide 79[7, 15, 21]

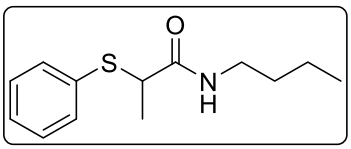

The title compound was prepared following the procedure described for **6** using *N-n*-butyl-2-chloropropanamide **76** (4.32 g, 26.5 mmol), thiophenol (3.24 ml, 31.8 mmol), and sodium (0.73 g, 31.8 mmol) in dry ethanol (80 ml). The reaction mixture was stirred for 16 h before work up as described for **6** gave the crude sulfide as a yellow oil. Purification by flash column chromatography on silica gel using hexane: ethyl acetate as eluent (gradient elution 15-40% ethyl acetate) gave pure *N-n*-butyl-2-(phenylthio)propanamide **79** (5.08 g, 81 %)* as a colourless oil; δ_H (300

MHz, $CDCl_3$) 0.84 [3H, t, *J* 7.3 Hz, C(4′)H_3], 1.13-1.27 [2H, m, C(3′)H_2], 1.30-1.43 [2H, m, C(2′)H_2], 1.55 [3H, d, *J* 7.3, C(3)H_3], 3.10-3.32 [2H, m, C(1′)H_2], 3.82 [1H, q, *J* 7.3 Hz, C(2)H], 6.63 (1H, br s, NH), 7.17-7.36 (5H, m, ArH) ppm; δ_C (75.5 MHz, $CDCl_3$) 13.6 [CH_3, C(4′)H_3], 18.3 [CH_3, C(3)H_3], 19.8 [CH_2, C(3′)H_2], 31.4 [CH_2, C(2′)H_2], 39.3 [CH_2, C(1′)H_2NH], 46.8 [CH, C(2)H], 127.0 (CH, CH_{Ar}), 129.1 (CH, CH_{Ar}), 129.8 (CH, CH_{Ar}), 134.1 [C, $C_{Ar(q)}$], 171.5 (C, C=O) ppm.

** The purified product contained 5 % unreacted N-n-butyl-2-chloropropanamide **76** that was inseparable from the product **79*** by chromatography. *This material was carried forward to the next step without further purification.*

_N_-4-Fluorophenyl-2-(phenylthio)propanamide 80[7, 15, 21]

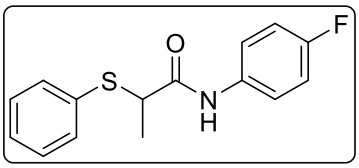

The title compound was prepared following the procedure described for **6** using 2-chloro-*N*-(4-fluorophenyl)propanamide **73** (5.39 g, 26.8 mmol), thiophenol (3.28 ml, 32.2 mmol), and sodium (0.74 g, 32.2 mmol) in dry ethanol (80 ml). The reaction mixture was stirred for 16 h before work up as described for **6** gave the crude sulfide as a pale-yellow solid. Purification by flash column chromatography on silica gel using hexane: ethyl acetate as eluent (gradient elution 20-40% ethyl acetate) gave pure *N*-4-fluorophenyl-2-(phenylthio)propanamide **80** (5.92 g, 80 %) as a white solid; mp 91-93°C (lit.[16] 90-91°C); ν_{max}/cm^{-1} (ATR) 3263 (NH), 3147 (CH), 2975 (CH), 1660 (C=O), 1544, 1507, 1406; δ_H (300 MHz, $CDCl_3$) 1.61 [3H, d, *J* 7.3 Hz, C(3)H_3], 3.89 [1H, q, *J* 7.3 Hz, C(2)H], 6.91-7.03 (2H, m, ArH), 7.19-7.46 (7H, m, ArH), 8.39 (1H, br s, NH) ppm; δ_C (75.5 MHz, $CDCl_3$) 18.1 (CH_3, C(3)H_3), 47.7 [CH, C(2)H], 115.6 [CH, d, $^2J_{CF}$ 22.6 Hz, C(3′)H], 121.7 [CH, d, $^3J_{CF}$ 8.0 Hz, C(2′)H], 127.7 (CH, CH_{Ar}), 129.3 (CH, CH_{Ar}), 130.8 (CH, CH_{Ar}), 133.2 [C, $C_{Ar(q)}$S], 133.4 [C, d, $^4J_{CF}$ 2.8 Hz, C_{Ar}(1′)NH], 159.5 (C, d, $^1J_{CF}$ 243.6 Hz, C_{Ar}(4′)F], 170.0 (C, C=O) ppm.

_N_-4′-Methoxyphenyl-2-(phenylthio)propanamide 81

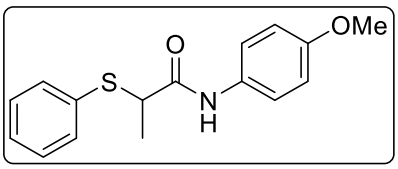

Thiophenol (3.11 ml, 30.5 mmol) in ethanol (23 ml) was added to a solution of aqueous sodium hydroxide (0.8 M, 74 ml, 58.66 mmol). Immediately, a solution of 2-chloro-*N*-(4′-methoxyphenyl)propanamide **74** (6.25 g, 29.33 mmol) in ethanol (80 ml) was added gradually over 15 minutes to the reaction mixture. Following heating under reflux for 1 h, the reaction was cooled in an ice bath and was quenched by the addition of water (70 ml). The solid precipitate was isolated by suction filtration to give pure *N*-4′-methoxyphenyl-2-(phenylthio)propanamide **81** as a grey solid (7.52 g, 89 %); mp 67-69 ˚C; ν_{max}/cm^{-1} (ATR) 3250 (NH), 1656 (C=O), 1526, 1511, 1439 (CN stretch); δ_H (300 MHz, $CDCl_3$) 1.56 [3H, d, *J* = 7.3 Hz, C(3)H_3], 3.71 (3H, s, ArOCH_3), 3.87 [1H, q, *J* = 7.3 Hz, C(2)H], 6.74-6.82 (2H, m, ArH), 7.16-7.42 (7H, m, ArH) ppm; δ_C (75.5 MHz, $CDCl_3$) 17.9 [CH_3, C(3)H_3], 47.4 [CH, C(2)H], 55.2 [CH_3, ArOCH_3], 113.9 (CH, CH_{Ar}), 121.8 (CH, CH_{Ar}), 127.4 (CH, CH_{Ar}), 129.0 (CH, CH_{Ar}), 130.4 [C, $C_{Ar(q)}$], 131.0 (CH, CH_{Ar}), 133.2 [C, $C_{Ar(q)}$], 156.4 [C, $C_{Ar(q)}$], 169.9 (C, C=O) ppm; HRMS (ES+): Exact mass calculated for $C_{16}H_{17}NO_2S$ $[M+H]^+$ 288.1058. Found 288.1052; m/z (ES+) 288.3 {$[(C_{16}H_{17}NO_2S)+H^+]$, 100%}.

_N_-(2′,2′-Dimethylpropyl)-2-(phenylthio)propanamide 82

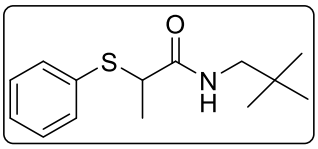

The title compound was prepared following the procedure described for **81** using 2-chloro-*N*-(2′,2′-dimethylpropyl)-propanamide **77** (4.80 g, 27.10 mmol), thiophenol (2.89 ml, 28.2 mmol) and aqueous sodium hydroxide (0.8 M, 78 ml, 54.20 mmol) in ethanol (60 ml). Following heating under reflux for 1 h, the reaction mixture was cooled in an ice bath and was quenched by the addition of water (70 ml). The solid precipitate was isolated by suction filtration to give pure *N*-(2′,2′-dimethylpropyl)-2-(phenylthio)propanamide **82** as a white solid (6.67 g, 98 %); mp 87-89˚C; ν_{max}/cm^{-1} (ATR) 3272 (NH), 2964 (CH), 2953 (CH), 1640 (C=O), 1564, 1203; δ_H (300 MHz, $CDCl_3$) 0.78 [9H, s, $C(CH_3)_3$], 1.56 [3H, d, *J* = 7.3 Hz, $C(2)H_3$], 2.95 [1H, dd, A of ABX system, J_{AB} = 13.3 Hz, J_{AX} = 6.0 Hz, one of $C\underline{H}_2NH$], 3.06 [1H, dd, B of ABX system, J_{BA} = 13.3 Hz, J_{BX} = 6.7, one of $C\underline{H}_2NH$], 3.91 [1H, q, *J* = 7.4 Hz, C(2)H], 6.79 (1H, br s, NH), 7.15-7.36 (5H, m, ArH) ppm; δ_C (75.5 MHz, $CDCl_3$) 18.3 [CH_3, $C(3)H_3$], 26.9 [CH_3, $C(CH_3)_3$] 31.6 [C, $C(CH_3)_3$], 46.6 [CH, C(2)H], 50.6 (CH_2, CH_2NH), 126.7 (CH, CH_{Ar}), 129.0 (CH, CH_{Ar}), 129.1 (CH, CH_{Ar}), 134.1 [C, $C_{Ar(q)}$], 171.5 (C=O) ppm; HRMS (ES+): Exact mass calculated for $C_{14}H_{21}NOS$ $[M+H]^+$ 252.1422. Found 252.1428; m/z (ES+) 252.4 {[($C_{14}H_{21}NOS$)+H^+], 100%}.

_N_-Benzyl-2-(benzylthio)propanamide 83[7, 21]

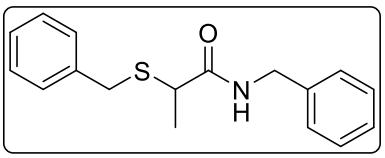

The title compound was prepared following the procedure described for **6** using *N*-benzyl-2-chloropropanamide **75** (7.53 g, 38.2 mmol), benzyl mercaptan (5.38 ml, 45.9 mmol), and sodium (1.06 g, 45.9 mmol) in dry ethanol (100 ml). The reaction mixture was stirred for 18 h before work up as described for **6** gave the crude sulfide as a white solid. Purification by flash column chromatography on silica gel using hexane: ethyl acetate as eluent (gradient elution 10-20% ethyl acetate) gave pure *N*-benzyl-2-(benzylthio)propanamide **83** (9.58 g, 88 %) as a white solid; mp 66-68°C (lit.[7] 66-67°C); ν_{max}/cm^{-1} (ATR) 3287 (NH), 3031 (CH), 1641 (C=O), 1553, 693; δ_H (300 MHz, $CDCl_3$) 1.47 [3H, d, *J* 7.3 Hz, $C(3)H_3$], 3.35 [1H, q, *J* 7.3, C(2)H], 3.69 (2H, s, SCH_2), 4.34 [1H, dd, A of ABX system, J_{AB} 14.8 Hz, J_{AX} 5.8, one of $C\underline{H}_2NH$], 4.41 [1H, dd, B of ABX system, J_{BA} 14.9 Hz, J_{BX} 6.1, one of $C\underline{H}_2NH$], 6.85 (1H, br s, NH), 7.17-7.39 (10H, m, ArH) ppm; δ_C (75.5 MHz, $CDCl_3$) 18.5 (CH_3, $C(3)H_3$), 36.3 (CH_2, SCH_2), 43.7 (CH_2, CH_2NH), 44.2 [CH, C(2)H], 127.3 (CH, CH_{Ar}), 127.6 (CH, CH_{Ar}), 127.7 (CH, CH_{Ar}), 128.66 (CH, CH_{Ar}), 128.74 (CH, CH_{Ar}), 128.8 (CH, CH_{Ar}), 137.3 [C, $C_{Ar(q)}$], 138.2 [C, $C_{Ar(q)}$], 172.1 (C=O) ppm.

_N-n_-Butyl-2-(benzylthio)propanamide 84[7, 21]

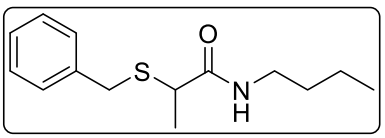

The title compound was prepared following the procedure described for **6** using *N-n*-butyl-2-chloropropanamide **76** (3.99 g, 24.4 mmol), benzyl mercaptan (3.44 ml, 29.3 mmol), and sodium (0.77 g, 29.3 mmol) in dry ethanol (80 ml). The reaction mixture was stirred for 16 h before work up as described for **6** gave the crude sulfide as an orange oil. Purification by flash column chromatography on silica gel using hexane: ethyl acetate (80:20) as eluent gave pure *N-n*-butyl-2-(benzylthio)propanamide **84** (5.01 g, 81.6 %) as a white low melting point solid; ν_{max}/cm^{-1} (ATR) 3276 (NH), 2957 (CH), 2931 (CH), 1641 (C=O), 1543, 703; δ_H (300 MHz, $CDCl_3$) 0.93 [3H, t, *J* 7.3 Hz, $C(4')H_3$], 1.27-1.52 [7H, m, overlapping $C(3')H_2$, $C(2')H_2$ and $C(3)H_3$; $C(3)H_3$ could be distinguished as a strong doublet at 1.43 (*J* 7.3 Hz)], 3.10-3.27 [2H, m, $C(1)H_2NH$], 3.30 [1H, q, *J* 7.3 Hz, C(2)H], 3.72 (2H, s, SCH_2), 6.58 (1H, br s, NH), 7.20-7.38 (5H, m, ArH) ppm; δ_C (75.5 MHz, $CDCl_3$) 13.7 [CH_3, $C(4')H_3$], 18.6 [CH_3, $C(3)H_3$], 20.0 [CH_2, $C(3')H_2$], 31.5 [CH_2, $C(2')H_2$], 36.3 (CH_2, SCH_2), 39.3 [CH_2,

C(1′)H_2], 44.4 [CH, C(2)H], 127.3 (CH, CH_{Ar}), 128.6 (CH, CH_{Ar}), 128.8 (CH, CH_{Ar}), 137.4 [C, $C_{Ar(q)}$], 172.0 (C, C=O) ppm.

2-(Benzylthio)-*N*-(4-flurophenyl)propenamide 85[7, 21]

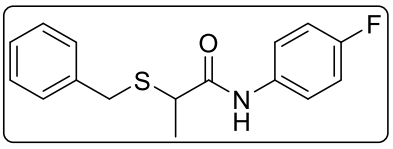

The title compound was prepared following the procedure described for **6** using 2-chloro-*N*-(4-fluorophenyl)propenamide **73** (5.42 g, 27.0 mmol), benzyl mercaptan (3.80 ml, 32.4 mmol), and sodium (0.74 g, 32.4 mmol) in dry ethanol (80 ml). The reaction mixture was stirred for 16 h before work up as described for **6** gave the crude sulfide as a brown solid. Purification by column chromatography on silica gel using hexane: ethyl acetate as eluent (gradient elution 5-40% ethyl acetate) gave pure *N*-4-fluorophenyl-2-(benzylthio)propanamide **85** (6.91 g, 89 %) as a white solid; mp 98-100°C (lit.[7] 99-101°C); ν_{max}/cm^{-1} (ATR) 3294 (NH), 2975 (CH), 1654 (C=O), 1551, 1504, 1210, 833, 693; δ_H (300 MHz, $CDCl_3$) 1.52 [3H, d, *J* 7.4 Hz, C(3)H_3], 3.43 [1H, q, *J* 7.4 Hz, C(2)H], 3.77 (2H, s, SCH_2), 6.95-7.05 (2H, m, ArH), 7.16-7.31 (5H, m, ArH), 7.36-7.44 (2H, m, ArH) ppm; δ_C (75.5 MHz, $CDCl_3$) 18.5 (CH_3, C(3)H_3), 36.5 (CH_2, SCH_2), 45.1 [CH, C(2)H], 115.5 [CH, d, $^2J_{CF}$ 22.7 Hz, C(3′)H], 121.4 [CH, d, $^3J_{CF}$ 7.9 Hz, C(2′)H], 127.4, 128.8 (2 x CH, 3 x CH_{Ar}), 133.6 [C, d, $^4J_{CF}$ 2.8 Hz, C_{Ar}(1′)NH], 137.2 [C, $C_{Ar(q)}$], 159.4 (C, d, $^1J_{CF}$ 243.8 Hz, C_{Ar}(4′)F], 170.3 (C, C=O) ppm.

***N*-4′-Methoxyphenyl-2-(benzylthio)propanamide 86**

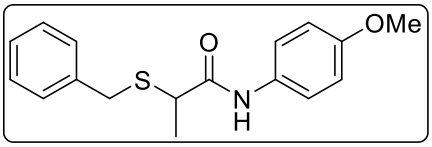

The title compound was prepared following the procedure described for **81** using 2-chloro-*N*-(4′-methoxyphenyl)-propanamide **74** (6.40 g, 30.04 mmol), benzyl mercaptan (3.67 ml, 31.24 mmol) and aqueous sodium hydroxide (0.8 M, 75 ml, 60.08 mmol) in ethanol (82 ml). Following heating under reflux for 1 h, the reaction mixture was cooled in an ice bath and was quenched by the addition of water (70 ml). The solid precipitate was isolated by suction filtration to give pure *N*-4′-methoxyphenyl-2-(benzylthio)propanamide **86** as a metallic grey solid (7.79 g, 86 %); mp 79-81˚C; ν_{max}/cm^{-1} (ATR) 3256 (NH), 2933 (CH), 1651 (C=O), 1511, 1454, 1245, 1165, 1027; δ_H (300 MHz, $CDCl_3$) 1.50 [3H, d, *J* 7.3 Hz, C(3)H_3], 3.41 [1H, q, *J* 7.4, C(2)H], 3.77 (5H, s, overlapping $ArOCH_3$ and SCH_2), 6.76-6.88 (2H, m, ArH), 7.16-7.31 (5H, m, ArH), 7.33-7.40 (2H, m, ArH), 8.35 (1H, br s, NH) ppm; δ_C (75.5 MHz, $CDCl_3$) 18.4 [CH_3, C(3)H_3], 36.2 (CH_2, SCH_2), 44.9 [CH, C(2)H], 55.4 [CH_3, $ArOCH_3$], 114.0 (CH, CH_{Ar}), 121.4 (CH, CH_{Ar}), 127.3 (CH, CH_{Ar}), 128.6 (CH, CH_{Ar}), 128.7 (CH, CH_{Ar}), 130.6 [C, $C_{Ar(q)}$], 137.2 [C, $C_{Ar(q)}$], 156.4 [C, $C_{Ar(q)}$], 170.1 (C, C=O) ppm; HRMS (ES+): Exact mass calculated for $C_{17}H_{19}NO_2S$ $[M+H]^+$ 302.1215. Found 302.1215; m/z (ES+) 302.3 {$[(C_{17}H_{19}NO_2S)+H^+]$, 82%}.

***N*-(2′,2′-Dimethylpropyl)-2-(benzylthio)propanamide 87**

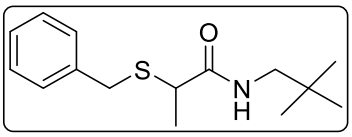

The title compound was prepared following the procedure described for **81** using 2-chloro-*N*-(2′,2′-dimethylpropyl)propenamide **77** (4.65 g, 26.26 mmol), benzyl mercaptan (3.21 ml, 27.31 mmol) and aqueous sodium hydroxide (0.8 M, 66 ml, 52.51 mmol) in ethanol (81 ml). Following heating under reflux for 1 h, the reaction mixture was cooled in an ice bath and was quenched by the addition of water (70 ml). No precipitate was observed in this instance, hence dichloromethane (100 ml) was added and the layers separated. The organic layer was washed with sodium hydroxide (2M, 3 x 100 ml), brine (100 ml), and was concentrated under reduced pressure to give *N*-(2′,2′-dimethylpropyl)-2-(benzylthio)propanamide **87** as a golden oil which solidified to a white solid overnight (6.53 g, 94 %); mp 57-59°C; Found C, 67.91; H, 8.56; N, 5.41. $C_{15}H_{23}NOS$ requires C,

67.88; H, 8.73; N, 5.28; ν_{max}/cm^{-1} (ATR) 3313 (NH), 2955 (CH), 1657 (C=O), 1548, 1205, 696; δ_H (300 MHz, $CDCl_3$) 0.92 [s, 9H, $C(CH_3)_3$], 1.45 [3H, d, *J* 7.3 Hz, $C(2)H_3$], 2.96 [1H, dd, A of ABX system, J_{AB} 13.3 Hz, J_{AX} 6.1 Hz, one of $C\underline{H}_2NH$], 3.07 [1H, dd, B of ABX system, J_{BA} 13.3 Hz, J_{BX} 6.6, one of $C\underline{H}_2NH$], 3.34 [1H, q, *J* 7.3 Hz, C(2)H], 3.74 (2H, s, SCH_2), 6.74 (1H, br s, NH), 7.19-7.37 (5H, m, ArH) ppm; δ_C (75.5 MHz, $CDCl_3$) 18.8 [CH_3, $C(3)H_3$], 27.2 [CH_3, $C(\underline{C}H_3)_3$], 31.8 [C, $\underline{C}(CH_3)_3$], 36.4 (CH_2, SCH_2), 44.6 [CH, C(2)H], 50.6 (CH_2, CH_2NH), 127.3 (CH, CH_{Ar}), 128.6 (CH, CH_{Ar}), 128.8 (CH, CH_{Ar}), 137.3 [C, $C_{Ar(q)}$], 172.1 (C, C=O) ppm; HRMS (ES+): Exact mass calculated for $C_{15}H_{23}NOS$ $[M+H]^+$ 266.1579. Found 266.1574; m/z (ES+) 266.4 {[($C_{15}H_{23}NOS$)+H^+], 100%}.

2.9.4. Synthesis of α-Thio-β-Chloroacrylamides

_N_-(4-Methylphenyl)-_Z_-3-chloro-2-(phenylthio)propenamide 9[6-7, 19]

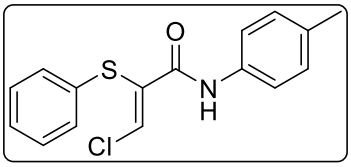

Unrecrystallised *N*-chlorosuccinimide (9.83 g, 73.58 mmol) was added in one portion to a solution of *N*-(4-methylphenyl)-2-(phenylthio)-propanamide **6** (10.23 g, 37.74 mmol) in toluene (120 ml). The flask was immediately immersed in an oil bath at 90 °C and heating was maintained with stirring for 3 h. The reaction mixture was cooled to 0 °C and the succinimide by-product was removed by filtration. The solvent was removed at reduced pressure to give the crude product as an orange solid. Following purification by flash column chromatography on silica gel using hexane: ethyl acetate (98:2) as eluent, the pure β-chloroacrylamide **9** (9.38 g, 82 %) was isolated as a white solid; mp 110-112°C (lit.[7] 110-111°C); ν_{max}/cm^{-1} (ATR) 3334 (NH), 3060 (CH), 1653 (C=O), 1564, 1524 (NH bend), 1402 (CN stretch); δ_H (300 MHz, $CDCl_3$) 2.28 (3H, s, $ArCH_3$), 7.05-7.12 (2H, m, ArH), 7.16-7.38 (5H, m, Ar-H), 8.03 [1H, s, ClHC(3)=], 8.61 (1H, br s, NH) ppm; δ_C (75.5 MHz, $CDCl_3$) 20.8 (CH_3, $ArCH_3$), 120.2 (CH, CH_{Ar}), 127.3 (CH, CH_{Ar}), 128.2 (CH, CH_{Ar}), 129.5 (CH, CH_{Ar}), 129.6 (CH, CH_{Ar}), 130.7 (C, $C_{Ar(q)}$ or SC=), 132.5 (C, $C_{Ar(q)}$ or SC=), 134.4 (C, $C_{Ar(q)}$ or SC=), 134.7 (C, $C_{Ar(q)}$ or SC=), 140.5 [CH, ClHC(3)=], 160.2 (C, C=O) ppm.

_N_-Benzyl-_Z_-3-chloro-2-(phenylthio)propenamide 40[6-7]

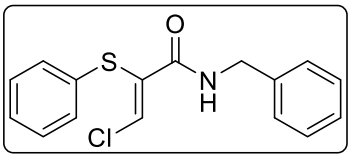

The title compound was prepared following the procedure described for **9** using *N*-benzyl-2-(phenylthio)propenamide **78** (7.10 g, 24.9 mmol), *N*-chlorosuccinimide (6.48 g, 48.5 mmol), and toluene (120 ml). The reaction mixture was heated at 90 °C for 3 h. Following filtration and evaporation of the solvent at reduced pressure, the crude reaction mixture was obtained as an orange oil. ^{1}H NMR spectroscopic analysis of the crude reaction mixture indicated a 82:18 ratio of α-thio-β-chloroacrylamide **40** to trichloride **89.** Purification by flash column chromatography on silica gel using hexane: ethyl acetate (gradient elution 2-10% ethyl acetate) as eluent afforded the more polar pure product **40** (4.32 g, 57 %) as a white solid; mp 75-77°C (lit.[7] 78-80°C); ν_{max}/cm^{-1} (ATR) 3406 (NH), 3053, 2927 (CH), 1661 (C=O), 1560, 1496; δ_H (300 MHz, $CDCl_3$) 4.39 (2H, d, *J* 5.9 Hz, CH_2NH), 6.87-6.94 (2H, m, ArH), 7.08-7.34 [9H, m, overlapping NH and ArH (8H)], 7.95 [1H, s, ClHC(3)=] ppm; δ_C (75.5 MHz, $CDCl_3$) 43.9 (CH_2, CH_2NH), 127.0 (CH, CH_{Ar}), 127.2 (CH, CH_{Ar}), 127.3 (CH, CH_{Ar}), 128.0 (CH, CH_{Ar}), 128.5 (CH, CH_{Ar}), 129.5 (CH, CH_{Ar}), 130.3 [C, $C_{Ar(q)}$ or C(2)S], 132.8 [C, $C_{Ar(q)}$ or C(2)S], 137.2 [C, $C_{Ar(q)}$ or C(2)S], 139.5 [CH, ClHC(3)=], 162.2 (C, C=O) ppm.

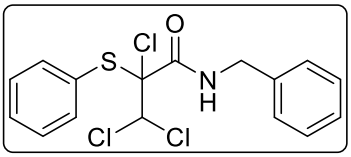

The less polar trichloride, *N*-benzyl-2,3,3-trichloro-2-(phenylthio)propenamide **89**, was also isolated as a white solid (0.85 g, 9 %); mp 84-86°C; ν_{max}/cm^{-1} (ATR) 3341 (CH stretch), 1664 (C=O), 1518, 746; δ_H (300 MHz, $CDCl_3$) 3.91 [1H, dd, A of ABX system, J_{AB} 14.8,

J_{AX} 5.3 Hz, one of C<u>H</u>$_2$NH], 4.30 [1H, dd, B of ABX system, J_{BA} 14.8, J_{BX} 5.3 Hz, one of C<u>H</u>$_2$NH], 6.61 (1H, br s, NH), 6.63 [1H, s, C(3)H], 6.91-7.00 (2H, m, ArH), 7.22-7.30 (3H, m, ArH), 7.32-7.41 (2H, m, ArH), 7.44-7.52 (1H, m, ArH), 7.60-7.67 (2H, m, ArH) ppm; δ_C (75.5 MHz, $CDCl_3$) 44.5 (CH_2, CH_2NH), 75.5 [CH, C(3)H], 89.2 [C, C(2)S], 127.6 (CH, CH_{Ar}), 127.8 (CH, CH_{Ar}), 128.3 (C, $C_{Ar(q)}$), 128.7 (CH, CH_{Ar}), 129.2 (CH, CH_{Ar}), 131.0 (CH, CH_{Ar}), 136.2 (C, $C_{Ar(q)}$), 137.2 (CH, CH_{Ar}), 163.5 (C, C=O) ppm; HRMS (ES+): Exact mass calculated for $C_{16}H_{14}NOSCl_3$ $[M+H]^+$ 373.9940. Found 373.9935.

_N_-(4′-Flurophenyl)-_Z_-3-chloro-2-(phenylthio)propenamide 41[7, 16, 21]

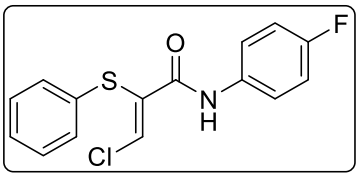

The title compound was prepared following the procedure described for **9** using *N*-4′-fluorophenyl-2-(phenylthio)propanamide **80** (5.72 g, 20.8 mmol), *N*-chlorosuccinimide (5.41 g, 40.5 mmol), and toluene (100 ml). The reaction mixture was heated at 90 °C for 3 h. Following filtration and evaporation of the solvent at reduced pressure, the crude reaction product was obtained as an orange oil. ^{1}H NMR spectroscopy of the crude reaction mixture indicated a mixture of α-thio-β-chloroacrylamide **41** to tentatively assigned acrylamide **90** (93:7). This was purified by flash column chromatography on silica gel using hexane: ethyl acetate (95:5) as eluent to give the pure product **41** (4.56 g, 71 %) as a white solid; mp 94-96°C (lit.[7] 96-97°C); ν_{max}/cm^{-1} (ATR) 3333 (NH), 3059 (CH), 1656 (C=O), 1520, 1508, 1405, 1212; δ_H (300 MHz, $CDCl_3$) 6.93-7.03 (2H, m, ArH), 7.20-7.40 (7H, m, ArH), 8.05 [1H, s, ClHC(3)=], 8.63 (1H, br s, NH) ppm; δ_C (75.5 MHz, $CDCl_3$) 115.7 [CH, d, $^2J_{CF}$ 22.6 Hz, C(3′)H], 122.1 [CH, d, $^3J_{CF}$ 8.0 Hz, C(2′)H], 127.4 (CH, CH_{Ar}), 128.1 (CH, CH_{Ar}), 129.7 (CH, CH_{Ar}), 130.4 [C, $C_{Ar(q)}$ or SC(2)=], 132.4 [C, $C_{Ar(q)}$ or SC(2)=], 133.0 [C, d, $^4J_{CF}$ 2.8 Hz, C_{Ar}(1′)NH], 159.8 (C, d, $^1J_{CF}$ 244.8 Hz, C_{Ar}(4′)F], 160.4 (C, C=O) ppm.

_N_-(2′,2′-Dimethylpropyl)-_Z_-3-chloro-2-(phenylthio)propenamide 42

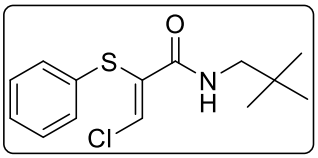

The title compound was prepared following the procedure described for **9** using *N*-(2′,2′-dimethylpropyl)-2-(phenylthio)propanamide **82** (5.01 g, 19.95 mmol), *N*-chlorosuccinimide (5.19 g, 38.90 mmol), and toluene (110 ml). The reaction mixture was heated while stirring at 90 °C for 3 h. Following filtration and evaporation of the solvent at reduced pressure, the crude product was obtained as a brown solid. This was purified by flash column chromatography on silica gel using hexane: ethyl acetate (95:5) as eluent to give the pure α-thio-β-chloroacrylamide **42** as a white solid (4.13 g, 77 %); mp 79-82°C; Found C, 59.39; H, 6.35; N, 4.96. $C_{14}H_{18}NOSCl$ requires C, 59.25; H, 6.39; N, 4.94; ν_{max}/cm^{-1} (ATR) 3382 (NH), 2955 (CH), 1646 (C=O), 1519, 1232; δ_H (300 MHz, $CDCl_3$) 0.68 [9H, s, C(CH_3)$_3$], 3.02 (2H, d, *J* 6.4 Hz, C<u>H</u>$_2$NH), 6.92 (1H, br s, NH), 7.16-7.33 (5H, m, ArH), 7.97 [1H, s, ClHC(3)=] ppm; δ_C (75.5 MHz, $CDCl_3$) 26.8 [CH_3, C(<u>C</u>H_3)$_3$], 31.7 [C, <u>C</u>(CH_3)$_3$], 51.1 (CH_2, CH_2NH), 127.0 (CH, CH_{Ar}), 127.8 (CH, CH_{Ar}), 129.5 (CH, CH_{Ar}), 130.4 [C, SC(2)=], 133.0 (C, $C_{Ar(q)}$), 139.7 [CH, C(3)HCl=], 162.1 (C, C=O) ppm; HRMS (ES+): Exact mass calculated for $C_{14}H_{18}NOS^{35}Cl$ $[M+H]^+$ 284.0858. Found 284.0866; m/z (ES+) 286.3 {[($C_{14}H_{18}NOS^{37}Cl$)+H^+], 40%}, 284.3 {[($C_{14}H_{18}NOS^{35}Cl$)+H^+], 100%}.

_N_-(4′-Methoxyphenyl)-_Z_-3-chloro-2-(phenylthio)propenamide 43

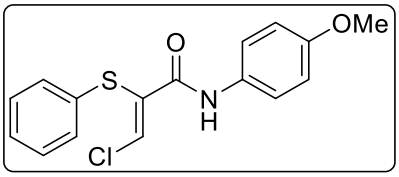

The title compound was prepared following the procedure described for **9** using *N*-4′-methoxyphenyl-2-(phenylthio)-propanamide **81** (6.50 g, 22.65 mmol), *N*-chlorosuccinimide (5.90 g, 44.18 mmol), and toluene (120 ml). The reaction mixture was heated while stirring at 90 °C for 3 h. Following filtration and evaporation of the solvent at reduced pressure, the crude product was obtained as a brown oil. This was purified by flash column chromatography on silica gel using hexane: ethyl acetate (gradient elution 5-10% ethyl acetate) as eluent, followed by trituration using hexane to give the pure α-thio-β-chloroacrylamide **43** as a white solid (2.43 g, 34 %); mp 110-112°C; Found C, 60.09; H, 4.46; N, 4.33; $C_{16}H_{14}NO_2SCl$ requires C, 60.09; H, 4.41; N, 4.38; ν_{max}/cm^{-1} (ATR) 3306 (NH), 2951 (CH), 1646 (C=O), 1519, 1235, 1030; δ_H (300 MHz, $CDCl_3$) 3.76 (3H, s, $ArOCH_3$), 6.78-6.85 (2H, m, ArH), 7.19-7.36 (7H, m, ArH), 8.03 [1H, s, ClHC(3)=], 8.56 (1H, br s, NH) ppm; δ_C (75.5 MHz, $CDCl_3$) 55.4 (CH_3, $ArOCH_3$), 114.2 (CH, CH_{Ar}), 122.0 (CH, CH_{Ar}), 127.3 (CH, CH_{Ar}), 128.1 (CH, CH_{Ar}), 129.6 (CH, CH_{Ar}), 130.1 (C, $C_{Ar(q)}$), 130.6 [C, SC(2)=], 132.6 (C, $C_{Ar(q)}$), 140.4 [CH, C(3)HCl=], 156.9 (C, $C_{Ar(q)}$), 160.2 (C, C=O) ppm; HRMS (ES+): Exact mass calculated for $C_{16}H_{14}NO_2S^{35}Cl$ $[M+H]^+$ 320.0500. Found 320.0503; m/z (ES+) 322.2 {[($C_{16}H_{14}NO_2S^{37}Cl$)+H^+], 44%}, 320.2 {[($C_{16}H_{14}NO_2S^{35}Cl$)+H^+], 100%}.

_N-n_-Butyl-_Z_-3-chloro-2-(phenylthio)propenamide 44[7, 15-16]

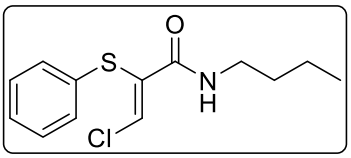

The title compound was prepared following the procedure described for **9** using *N-n*-butyl-2-(phenylthio)propanamide **79** (4.99 g, 21.05 mmol), *N*-chlorosuccinimide (5.48 g, 41.04 mmol), and toluene (90 ml). The reaction mixture was heated at 90 °C for 3 h. Following filtration and evaporation of the solvent at reduced pressure, the crude product was obtained as an orange oil. This was purified by flash column chromatography on silica gel using hexane: ethyl acetate (95:5) as eluent to give the pure product **44** (4.08 g, 72 %) as a clear oil; ν_{max}/cm^{-1} (ATR) 3359 (NH), 2955 (CH), 2926 (CH), 2870, 1638 (C=O), 1562, 1439; δ_H (300 MHz, $CDCl_3$) 0.78 [3H, t, *J* 7.3 Hz, C(4′)H_3], 1.00-1.15 [2H, m, C(3′)H_2], 1.22-1.36 [2H, m, C(2′)H_2], 3.20 [2H, dt (appears as a q), *J* 6.9, 6.0, C(1′)H_2], 6.84 (1H, br s, NH), 7.16-7.37 (5H, m, ArH), 7.90 (1H, s, ClHC(3)=) ppm; δ_C (75.5 MHz, $CDCl_3$) 13.5 (CH_3, C(4′)H_3), 19.6 [CH_2, C(3′)H_2], 31.1 [CH_2, C(3′)H_2], 39.6 [CH_2, C(1′)H_2], 126.9 (CH, CH_{Ar}), 127.8 (CH, CH_{Ar}), 129.4 (CH, CH_{Ar}), 130.5 [C, $C_{Ar(q)}$ or SC(2)=], 132.9 [C, $C_{Ar(q)}$ or SC(2)=], 138.9 [CH, C(3)HCl=], 162.0 (C, C=O) ppm.

_N-n_-Butyl-Z-3-chloro-2-(benzylthio)propenamide 46[7, 21]

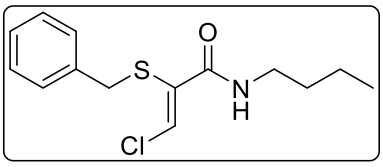

The title compound was prepared following the procedure described for **9** using *N-n*-butyl-2-(benzylthio)propenamide **84** (4.88 g, 19.42 mmol), *N*-chlorosuccinimide (5.06 g, 37.86 mmol), and toluene (60 ml). The reaction mixture was heated at 90 °C for 3 h. Following filtration and evaporation of the solvent at reduced pressure, the crude reaction mixture was obtained as an orange oil. ^{1}H NMR spectroscopy of the crude reaction mixture indicated a mixture of α-thio-β-chloroacrylamide **46** to tentatively assigned trichloride **92** (92:8). This was purified by flash column chromatography on silica gel using hexane: ethyl acetate (90:10) as eluent to give the pure product **46** as a yellow oil (4.13 g, 75 %);* ν_{max}/cm^{-1} (ATR) 3300 (NH), 2957 (CH), 2930 (CH), 1644 (C=O), 1560, 1514; δ_H (300 MHz, $CDCl_3$) 0.90 [3H, t, *J* 7.2 Hz, C(4′)H_3], 1.17-1.42 [4H, m, overlapping C(3′)H_2 and C(2′)H_2], 3.12 [2H, dt (appears as a q), *J* 6.8, 6.1, C(1′)H_2], 3.91 (2H, s, SCH_2), 6.82 (1H, br s, NH), 7.18-7.35 (5H, m, ArH), 7.80 (1H, s, ClHC(3)=) ppm; δ_C

(75.5 MHz, $CDCl_3$) 13.6 [CH_3, C(4')H_3], 19.9 [CH_2, C(3')H_2], 31.2 [CH_2, C(2')H_2], 38.3 (CH_2, CH_2N or SCH_2), 39.6 (CH_2, CH_2N or SCH_2), 127.6 (CH, CH_{Ar}), 128.65 (CH, CH_{Ar}), 128.67 (CH, CH_{Ar}), 131.1 [C, $C_{Ar(q)}$ or SC(2)=], 137.1 [C, $C_{Ar(q)}$ or SC(2)=], 138.8 [CH, C(3)HCl=], 162.6 (C, C=O) ppm.

Purified product **46 contained 5% of the trichloride **92**; δ_H ($CDCl_3$, 300 MHz) 3.32 [2H, dt (appears as a q), J 6.9, 6.2, C(1')H_2], 6.22 (1H, br s, NH), 6.44 [1H, s, C(3)] ppm.*

N-Benzyl-Z-3-chloro-2-(benzylthio)propenamide 48[7, 21]

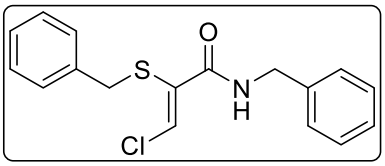

The title compound was prepared following the procedure described for **9** using *N*-benzyl-2-(benzylthio)propanamide **83** (8.57 g, 28.40 mmol), *N*-chlorosuccinimide (7.39 g, 55.37 mmol), and toluene (100 ml). The reaction mixture was heated at 90 °C for 3 h. Following filtration and evaporation of the solvent at reduced pressure, the crude reaction mixture was obtained as an orange solid. ^{1}H NMR spectroscopy of the crude mixture indicated a mixture of α-thio-β-chloroacrylamide **48** to tentatively assigned *E*-isomer **91** (93:7). This was purified by flash column chromatography on silica gel using hexane: ethyl acetate (90:10) as eluent to give the pure product **48** as a white solid; mp 70-72°C (lit.[7] 69-72°C); ν_{max}/cm^{-1} (ATR) 3341 (NH), 3030 (CH), 1642 (C=O), 1555, 1515; δ_H (300 MHz, $CDCl_3$) 3.88 (2H, s, SCH_2), 4.30 (2H, d, *J* 6.0 Hz, C$\underline{H}_2$NH), 7.09-7.36 [11H, m, overlapping NH and ArH (10H)], 7.83 (1H, s, ClHC(3)=) ppm; δ_C (75.5 MHz, $CDCl_3$) 38.2 (CH_2, SCH_2), 44.0 (CH_2, CH_2NH), 127.48, 127.53, 127.57, 128.61, 128.64, (5 x CH, 5 x CH_{Ar}, 5 signals for 6 carbons), 130.8, 136.8 [C, $C_{Ar(q)}$ or C(2)S], 137.4 [C, $C_{Ar(q)}$ or C(2)S], 139.2 [CH, ClHC=], 162.7 (C, C=O) ppm.

*A co-eluting fraction containing a 73:27 ratio of α-thio-β-chloroacrylamide **48** to tentatively assigned E-isomer **91** also isolated. This fraction was used to tentatively assign the E-isomer **91**; δ_H ($CDCl_3$, 300 MHz) 3.85 (2H, s, SCH_2), 4.48 (2H, d, J 5.9, C$\underline{H}_2$NH), 6.44 [1H, s, ClHC(3)=], 6.62 (1H, br t, unresolved coupling, NH) ppm.*

N-(4'-Flurophenyl)-Z-3-chloro-2-(benzylthio)propenamide 49[7, 21]

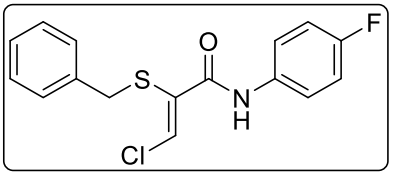

The title compound was prepared following the procedure described for **9** using *N*-4'-fluorophenyl-2-(benzylthio)-propanamide **85** (6.77 g, 26.33 mmol), *N*-chlorosuccinimide (6.856 g, 51.35 mmol), and toluene (120 ml). The reaction mixture was heated at 90 °C for 3 h. Following filtration and evaporation of the solvent at reduced pressure, the crude product was obtained as an orange solid. This was purified by flash column chromatography on silica gel using hexane: ethyl acetate (97:3) as eluent to give the pure product **49** as a white solid (5.98 g, 70%); mp 80-82°C (lit.[7] 81-82°C); ν_{max}/cm^{-1} (ATR) 3320 (NH), 3052 (CH), 1646 (C=O), 1518 (NH bend), 1506, 1406 (CN stretch); δ_H (300 MHz, $CDCl_3$) 3.97 (2H, s, SCH_2), 6.92-7.04 (2H, m, ArH), 7.14-7.34 (7H, m, ArH), 7.94 [1H, s, ClHC(3)=], 8.55 (1H, br s, NH) ppm; δ_C (75.5 MHz, $CDCl_3$) 38.7 (CH_2, SCH_2), 115.5 [CH, d, $^2J_{CF}$ 23 Hz, C(3')H_{Ar}], 121.7 [CH, d, $^3J_{CF}$ 8 Hz, C(2')H_{Ar}], 127.8 (CH, CH_{Ar}), 128.7 (CH, CH_{Ar}), 128.9 (CH, CH_{Ar}), 131.2 [C, $\underline{C}_{Ar(q)}CH_2S$ or C(2)S], 133.1 [C, d, $^4J_{CF}$ 3 Hz, C(1')$_{Ar(q)}$], 137.0 [C, $\underline{C}_{Ar(q)}CH_2S$ or C(2)S], 140.9 [CH, ClHC(3)=], 159.6 [C, d, $^1J_{CF}$ 244 Hz, C(4')$_{Ar(q)}$F], 161.2 (C, C=O) ppm.

_N_-(2′,2′-Dimethylpropyl)-_Z_-3-chloro-2-(benzylthio)propenamide 50

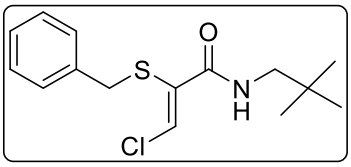

The title compound was prepared following the procedure described for **9** using *N*-(2′,2′-dimethylpropyl)-2-(benzylthio)propanamide **87** (6.30 g, 23.77 mmol), *N*-chlorosuccinimide (6.19 g, 46.35 mmol), and toluene (100 ml). The reaction mixture was heated while stirring at 90 °C for 3 h. Following filtration and evaporation of the solvent at reduced pressure, the crude product was obtained as an orange oil. This was purified by flash column chromatography on silica gel using hexane: ethyl acetate (9:1) as eluent to give the pure α-thio-β-chloroacrylamide **50** as a pale golden oil which solidified overnight to a white solid (4.62 g, 65 %); mp 49-51°C; Found C, 60.49; H, 6.69; N, 4.83. $C_{15}H_{20}ClNOS$ requires C, 60.49; H, 6.77; N, 4.70; ν_{max}/cm^{-1} (ATR) 3236 (NH stretch), 2958 (CH stretch), 1637 (C=O amide), 1556 (NH bend), 1293, 693; δ_H (300 MHz, $CDCl_3$) 0.83 [9H, s, $C(CH_3)_3$], 2.94 (2H, d, *J* 6.4 Hz, $C\underline{H}_2NH$), 3.94 (2H, s, SCH_2), 6.99 (1H, br s, NH), 7.18-7.34 (5H, m, ArH), 7.85 [1H, s, ClHC(3)=] ppm; δ_C (75.5 MHz, $CDCl_3$) 27.1 [CH_3, $C(\underline{C}H_3)_3$], 31.7 [C, $\underline{C}(CH_3)_3$], 38.3 (CH_2, SCH_2), 51.1 (CH_2, CH_2NH), 127.6 (CH, CH_{Ar}), 128.7 (CH, CH_{Ar}), 128.8 (CH, CH_{Ar}), 131.1 [C, SC(2)=], 137.0 (C, $C_{Ar(q)}$), 139.1 [CH, C(3)HCl=], 162.7 (C, C=O) ppm; HRMS (ES+): Exact mass calculated for $C_{15}H_{20}NOS^{35}Cl$ $[M+H]^+$ 298.1032. Found 298.1034; m/z (ES+) 300.2 {[($C_{15}H_{20}NOS^{37}Cl$)+H^+], 40%}, 298.2 {[($C_{15}H_{20}NOS^{35}Cl$)+H^+], 100%}.

_N_-(4′-Methoxyphenyl)-_Z_-3-chloro-2-(benzylthio)propenamide 51

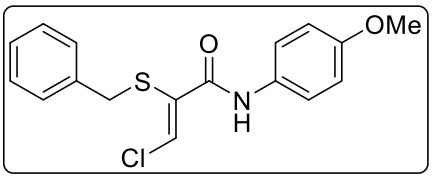

The title compound was prepared following the procedure described for **9** using *N*-4′-methoxyphenyl-2-(benzylthio)-propanamide **86** (7.16 g, 23.79 mmol), *N*-chlorosuccinimide (6.20 g, 46.39 mmol), and toluene (120 ml). The reaction mixture was heated while stirring at 90 °C for 3 h. Following filtration and evaporation of the solvent at reduced pressure, the crude product was obtained as a yellow solid. This was purified by flash column chromatography on silica gel using hexane: ethyl acetate (gradient elution 5-10 % ethyl acetate) as eluent to give the pure α-thio-β-chloroacrylamide **51** as a white solid (3.15 g, 40 %); mp 121-123°C; Found C, 61.20; H, 4.84; N, 4.02. $C_{17}H_{16}NO_2SCl$ requires C, 61.16; H, 4.83; N, 4.20; ν_{max}/cm^{-1} (ATR) 3305 (NH stretch), 3054 (CH stretch), 1642 (C=O), 1519 (NH bend), 1235, 1029; δ_H (300 MHz, $CDCl_3$) 3.77 (3H, s, $ArOCH_3$), 3.96 (2H, s, SCH_2), 6.79-6.86 (2H, m, ArH), 7.15-7.33 (7H, m, ArH), 7.90 [1H, s, ClHC(3)=], 8.51 (1H, br s, NH) ppm; δ_C (75.5 MHz, $CDCl_3$) 38.6 (CH_2, SCH_2), 55.4 (CH_3, $ArOCH_3$), 114.0 (CH, CH_{Ar}), 121.6 (CH, CH_{Ar}), 127.8 (CH, CH_{Ar}), 128.7 (CH, CH_{Ar}), 128.8 (CH, CH_{Ar}), 130.2 (C, $C_{Ar(q)}$), 131.4 [C, SC(2)=], 137.0 (C, $C_{Ar(q)}$), 140.0 [CH, C(3)HCl=], 156.7 (C, $C_{Ar(q)}$), 160.6 (C, C=O) ppm; HRMS (ES+): Exact mass calculated for $C_{17}H_{16}NO_2S^{35}Cl$ $[M+H]^+$ 334.0666. Found 334.0662; m/z (ES+) 336.2 {[($C_{17}H_{16}NO_2S^{37}Cl$)+H^+], 42%}, 334.2 {[($C_{17}H_{16}NO_2S^{35}Cl$)+H^+], 100%}.

2.9.5 Synthesis of 2,3,3-Trichloro-2-(phenylthio)-*N*-(4′-methylphenyl)propanamide

2,3,3-Trichloro-2-(phenylthio)-*N*-(4-methylphenyl)propanamide 93

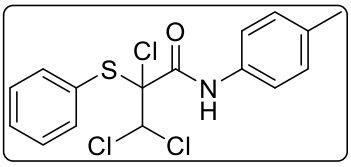

The title compound was prepared following the procedure described for **9** using *N*-(4′-methylphenyl)-2-(phenylthio)propanamide **6** (1.21 g, 9.06 mmol), *N*-chlorosuccinimide (2.36 g, 17.67 mmol), and toluene (40 ml). The reaction mixture was heated while stirring at 90 °C for 3 h. Following filtration and evaporation of the solvent at reduced pressure, the crude reaction mixture was obtained as a yellow solid. ^{1}H NMR spectroscopy of the crude reaction mixture indicated a 46:54 ratio of α-thio-β-chloroacrylamide **9** to trichloride **93**. Following purification by flash column chromatography on silica gel using hexane: ethyl acetate (gradient elution 5-10 % ethyl acetate) as eluent, followed by a second column using hexane: ethyl acetate (98:2) as eluent the pure more polar trichloride **93** was isolated as a white solid (0.61 g, 18 %); mp 90-91°C; ν_{max}/cm^{-1} (ATR) 3312 (CH stretch), 2996 (CH), 1664 (C=O), 1517, 746; δ_H (300 MHz, $CDCl_3$) 2.27 (3H, s, $ArCH_3$), 6.64 [1H, s, C(3)H], 6.95-7.07 (4H, m, ArH), 7.24-7.43 (3H, m, ArH), 7.58-7.67 (2H, m, ArH), 7.89 (1H, br s, NH) ppm; δ_C (75.5 MHz, $CDCl_3$) 20.8 (CH_3, $ArCH_3$), 75.4 [CH, C(3)H], 89.0 [C, C(2)S], 120.6 (CH, CH_{Ar}), 128.0 [C, $C_{Ar(q)}$], 129.2 (CH, CH_{Ar}), 129.3 (CH, CH_{Ar}), 131.0 (CH, CH_{Ar}), 133.1 (C, $C_{Ar(q)}$), 135.3 (C, $C_{Ar(q)}$), 137.1 (CH, CH_{Ar}), 161.5 (C, C=O) ppm; HRMS (ES+): Exact mass calculated for $C_{16}H_{14}NOSCl_3$ $[M+H]^+$ 373.9940. Found 373.9933.

2.9.6 Synthesis of α-Thio-β-Chloroacrylate

Methyl 2-chloropropanoate 95[3, 16, 21]

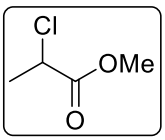

2-Chloropropionyl chloride (3.94 ml, 39.4 mmol) in dichloromethane (25 ml) was added slowly to a solution of methanol (8.10 ml) in dichloromethane (75 ml) at 0 °C. On completion of the addition, the ice bath was removed and the reaction solution was warmed to room temperature. After stirring at room temperature for 17 h, distilled water (100 ml) was added and the layers were separated. The organic layer was washed with brine (100 ml), dried, filtered and concentrated under reduced pressure (keeping the bath temperature below 30 °C) to give the volatile ester **95** (3.86 g, 80 %)* as a colourless oil. Further purification was not required; ν_{max}/cm^{-1} (ATR) 2957 (CH), 1743 (C=O), 1448; δ_H (300 MHz, $CDCl_3$) 1.70 [3H, d, *J* 7.0 Hz, C(3)H_3], 3.79 (3H, s, OCH_3), 4.42 [1H, q, *J* 6.9 Hz, C(2)H] ppm; δ_C (75.5 MHz, $CDCl_3$) 21.3 [CH_3, C(3)H_3], 52.2 [CH, C(2)H] , 52.8 [CH_3, OCH_3], 170.4 (C, C=O) ppm.

**A yield of 84% was obtained for a batch that was synthesised later.*

Methyl 2-(phenylthio)propanoate 96[3, 16, 21]

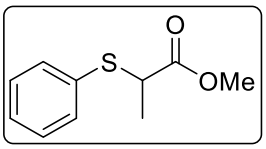

Thiophenol (3.64 ml, 35.7 mmol) was added to a freshly prepared solution of sodium methoxide [made from sodium (0.82 g, 35.7 mmol) in dry methanol (70 ml) at 0 °C while stirring under nitrogen. After stirring for 10 min at room temperature, methyl 2-chloropropanoate **95** (3.63 g, 29.8 mmol) in methanol (20 ml) was added slowly. Following stirring at room temperature for 16 h, the reaction was quenched by addition of water (100 ml) and dichloromethane (80 ml). The phases were separated and the aqueous layer was extracted with dichloromethane (2 x 30 ml). The combined organic layers were washed with sodium hydroxide (1 M, 80 ml), water (80 ml) and brine (80 ml), dried and concentrated

under reduced pressure to give methyl 2-(phenylthio)propanoate **96** (5.45 g, 93 %) as a colourless oil. Further purification was not required; ν_{max}/cm^{-1} (ATR) 2951 (CH), 1732 (C=O), 1438; δ_H (300 MHz, $CDCl_3$) 1.48 [3H, d, *J* 7.1 Hz, C(3)H_3], 3.66 (3H, s, OCH_3), 3.79 [1H, q, *J* 7.1 Hz, C(2)H], 7.22-7.36 (3H, m, ArH), 7.40-7.52 (2H, m, ArH) ppm; δ_C (75.5 MHz, $CDCl_3$) 17.4 [CH_3, C(3)H_3], 45.2 [CH, SC(2)H], 52.2 [CH_3, OCH_3], 127.5 (C, $C_{Ar(q)}$), 128.0 (CH, CH_{Ar}), 128.9 (CH, CH_{Ar}), 133.0 (CH, CH_{Ar}), 173.0 (C, C=O) ppm.

Methyl 2,3-dichloro-2-(phenylthio)propanoate 97[16, 21, 52]

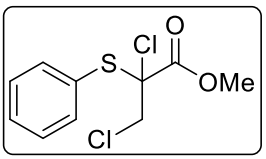

N-Chlorosuccinimide (7.64 g, 57.2 mmol) was added in one portion to a stirring solution of the sulfide **96** (5.34 g, 27.3 mmol) in toluene (70 ml). The flask was carefully lowered into a pre-heated oil bath at 130 °C and heated for 4 h. The reaction solution was then cooled to 0 °C and the succinimide by-product was removed by filtration. The toluene was removed by evaporation at reduced pressure to give the crude dichloride as an orange oil. Purification by flash column chromatography on silica gel using hexane: ethyl acetate 97:3 as eluent afforded a 2:1 mixture of dichloride **97**: acrylate **98**. Following flash column chromatography of this mixture on silica gel using dichloromethane: hexane : ethyl acetate 100:40:1 as eluent the dichloride **97** (1.57 g, 22 %) was obtained as a colourless oil; ν_{max}/cm^{-1} (ATR) 2954 (CH), 1749 (C=O), 1439, 1284, 1255; δ_H (300 MHz, $CDCl_3$) 3.80 (3H, s, OCH_3), 3.91 (1H, d, A of AB system, J_{AB} 11.6 Hz, one of CH_2Cl), 4.00 (1H, d, B of AB system, J_{BA} 11.6 Hz, one of CH_2Cl), 7.35-7.56 (3H, m, ArH), 7.61-7.70 (2H, m, ArH) ppm; δ_C (75.5 MHz, $CDCl_3$) 49.1 (CH_2, CH_2Cl), 54.0 (CH_3, OCH_3), 78.2 [C, SC(2)], 127.7 (C, $C_{Ar(q)}$), 129.2 (CH, CH_{Ar}), 130.9 (CH, CH_{Ar}), 137.3 (CH, CH_{Ar}), 166.0 (C, C=O) ppm.

Note: *Evidence for the acrylate **98** in the ^{1}H NMR spectrum of the crude product was seen at δ_H 3.81 (3H, s, OCH_3), 5.24 (1H, s, one of CH_2), 6.33 (1H, s, one of CH_2) ppm.*[16] *A mixed fraction (2.34 g) was also collected following the second column containing a 74:26 ratio of dichloride: acrylate.*

Methyl Z-3-chloro-2-(phenylthio)propenoate 69[16, 21, 52]

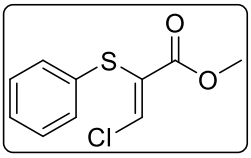

A solution of zinc chloride in tetrahydrofuran (51.4 ml of a 0.5 M solution, 25.68 mmol) was added to a stirring solution of the dichloride **97** (2.26 g, 8.56 mmol) in dichloromethane (50 ml) and the resulting solution was heated at reflux for 18 h. The reaction was quenched by addition of water (70 ml) and the phases were separated. The organic layer was washed with water (70 ml) and brine (70 ml), dried and concentrated at reduced pressure to give the crude product as a brown oil. Purification by flash column chromatography on silica gel using hexane: ethyl acetate (gradient elution 1-2% ethyl acetate) as eluent afforded the acrylate **69** as a pale yellow oil (1.39 g, 71 %); ν_{max}/cm^{-1} (ATR) 3062 (CH), 2952 (CH), 1718 (C=O), 1557, 1268, 1235; δ_H (300 MHz, $CDCl_3$) 3.66 (3H, s, OCH_3), 7.19-7.36 (5H, m, ArH), 7.69 [1H, s, ClHC(3)=] ppm.

2.9.7 Synthesis of α-Thio-β-Chlorothioester

***S*-Phenyl 2-(phenylthio)propanethioate 99**

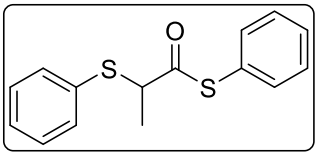

2-Chloropropionyl chloride (3.82 ml, 39.38 mmol) in dichloromethane (30 ml) was added dropwise over 20 min to a solution of thiophenol (8.03 ml, 78.76 mmol) and triethylamine (11.1 ml, 79.15 mmol) in dichloromethane (70 ml) at 0°C, while stirring under nitrogen. On

completion of the addition, the reaction solution was removed from the ice bath and heated under reflux for 2 h. Water (100 ml) was added and the layers separated. The organic layer was washed with water (2 x 100 ml), and brine (100 ml), dried, filtered and concentrated under reduced pressure to give *S*-phenyl 2-(phenylthio)propanethioate **99** as a yellow oil (6.91 g, 64%) which required no further purification; ν_{max}/cm^{-1} (ATR) 3059 (CH stretch), 1694 (C=O), 1477, 1439, 927, 744, 647; δ_H (300 MHz, $CDCl_3$) 1.58 [3H, d, *J* 7.1 Hz, C(3)H_3], 4.02 [1H, *J* 7.2 Hz, C(2)H], 7.28-7.42 (8H, m, ArH), 7.47-7.53 (2H, m, ArH) ppm; δ_C (75.5 MHz, $CDCl_3$) 18.0 [CH_3, C(3)H_3], 53.4 [CH, C(2)H], 127.8 (C, $C_{Ar(q)}$), 128.2 (CH, CH_{Ar}), 129.1 (CH, CH_{Ar}), 129.2 (CH, CH_{Ar}), 129.4 (CH, CH_{Ar}), 132.8 (CH, CH_{Ar}), 132.9 (C, $C_{Ar(q)}$), 134.5 (CH, CH_{Ar}), 197.9 (C, C=O) ppm. HRMS (ES+): Exact mass calculated for $C_{15}H_{14}S_2O$ $[M+H]^+$ 256.0564. Found 256.0560.

_S_-Phenyl (_Z_)-3-chloro-2-(phenylthio)prop-2-enethioate 70

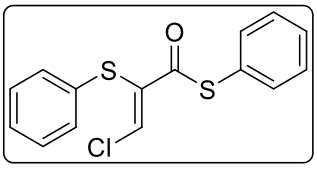

Unrecrystallised *N*-chlorosuccinimide (294 mg, 2.2 mmol) was added in one portion to a solution of *S*-phenyl 2-(phenylthio)propanethioate **99** (274 mg, 1 mmol) in toluene (15 ml). The flask was immediately immersed in an oil bath at 130 °C and heating was maintained with stirring for 24 h. The reaction mixture was cooled to 0 °C and the succinimide by-product was removed by filtration. The solvent was removed at reduced pressure to give the crude dichloride **102**. The crude dichloride was dissolved in THF (5 ml) and a solution of $ZnCl_2$ in THF (10 ml of a 0.5 M solution, 5 mmol) was added. The resulting solution was then heated under reflux for 24 h. After cooling to room temperature the sample was concentrated under reduced pressure. Dichloromethane (15 ml) and water (15 ml) was added and the phases separated. The organic layer was washed with water (15 ml) and brine (15 ml), dried, concentrated under reduced pressure to give the crude product as a yellow oil. Following purification by flash column chromatography on silica gel using hexane: ethyl acetate (95:5) as eluent, the α-thio-β-chlorothioester (95 mg, 31%) was isolated as a yellow oil, as a 9:1 mixture of tentatively assigned (*Z*)-**70** and (*E*)-**103**; ν_{max}/cm^{-1} (ATR) 3057 (CH stretch), 1682 (C=O), 1546, 1477, 1440, 1076; δ_H (300 MHz, $CDCl_3$) 7.20-7.44 (10H, m, ArH), 7.74 [1H, s, ClC(3)H=] ppm; δ_C (75.5 MHz, $CDCl_3$) 127.3 (CH, CH_{Ar}), 128.0 (C, $C_{Ar(q)}$), 129.2 (CH, CH_{Ar}), 129.3 (CH, 2 x CH_{Ar}), 129.6 (CH, CH_{Ar}), 133.1 (C, $C_{Ar(q)}$), 134.5 (CH, CH_{Ar}), 136.3 [C, SC(2)], 137.6 [CH, ClC(3)H=], 188.9 (C, C=O) ppm; HRMS (ES+): Exact mass calculated for $C_{15}H_{11}S_2OCl$ $[M+H]^+$ 307.0018. Found 307.0012. A singlet was observed at δ_H 6.91 ppm for the tentatively assigned (*E*)-isomer.

2.9.8 Synthesis of α-Sulfinyl-β-Chloroacrylamides

_N_-(4′-Methylphenyl)-Z-3-chloro-2-(benzenesulfinyl)propenamide 54[12, 21]

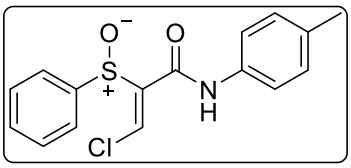

A solution of Oxone® (2.35 g, 7.65 mmol) in water (15 ml) was added dropwise to a stirring solution of *N*-(4′-methylphenyl)-*Z*-3-chloro-2-(phenylthio)propenamide **9** (1.16 g. 3.82 mmol) in acetone (60 ml) at room temperature. A colourless precipitate formed immediately. The reaction mixture was stirred for 16 h. Water (100 ml) was added and the aqueous solution was extracted with dichloromethane (3 x 50 ml). The organic layers were combined and washed with water (2 x 50 ml) and brine (50 ml), dried, filtered and concentrated at reduced pressure to give the sulfoxide **54** as a white solid (1.14 g, 94 %) which required no further purification; mp 125-128°C (lit.[12] 128-129.5°C); ν_{max}/cm^{-1} (ATR) 3041 (NH), 2924 (CH), 1672 (C=O), 1610, 1514 (NH bend), 1034 (SO); δ_H (300 MHz, $CDCl_3$) 2.30 (3H, s, ArCH_3), 7.11 (2H, m, ArH), 7.37-7.54

(5H, m, ArH), 7.65-7.74 (2H, m, ArH), 7.81 [1H, s, ClHC(3)=], 10.36 (1H, br s, NH) ppm; δ_C (75.5 MHz, $CDCl_3$) 20.9 (CH_3, $ArCH_3$), 120.7 (CH, CH_{Ar}), 124.1 (CH, CH_{Ar}), 129.5 (CH, CH_{Ar}), 129.8 (CH, CH_{Ar}), 131.9 (CH, CH_{Ar}), 134.6 [C, $C_{Ar(q)}$ or SC(2)=], 134.7 [C, $C_{Ar(q)}$ or SC(2)=], 137.6 [CH, C(3)HCl=], 138.6 [C, $C_{Ar(q)}$ or SC(2)=], 140.8 [C, $C_{Ar(q)}$ or SC(2)=], 158.1 (C=O) ppm.

_N_-Benzyl-Z-3-chloro-2-(benzenesulfinyl)propenamide 55[12]

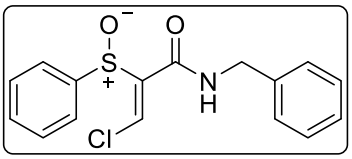

The title compound was prepared following the procedure described for **54** using *N*-benzyl-*Z*-3-chloro-2-(phenylthio)propenamide **40** (3.30 g, 10.82 mmol) in acetone (120 ml) and Oxone® in water at (30 ml). The reaction was stirred at room temperature for 14 h and following work up, the crude sulfoxide **55** was obtained as a white solid (3.33 g, 97 %), which required no further purification; mp 84-85°C (lit.[12] 80-82°C); ν_{max}/cm^{-1} (ATR) 3278 (NH), 3083 (CH), 1657 (C=O), 1543, 1028 (SO); δ_H (300 MHz, $CDCl_3$) 4.23-4.35 [1H, A of ABX system, J_{AB} 14.9, J_{AX} 5.0 Hz, one of $C\underline{H}_2NH$], 4.54-4.64 [1H, B of ABX system, J_{BA} 14.9, J_{BX} 6.6 Hz, one of $C\underline{H}_2NH$], 7.04-7.13 (2H, m, ArH), 7.22-7.30 (3H, m, ArH), 7.41-7.58 (5H, m, ArH), 7.79 (1H, s, ClHC(3)=), 8.74 (1H, br s, NH) ppm; δ_C (75.5 MHz, $CDCl_3$) 43.2 (CH_2, CH_2NH), 124.0 (CH, CH_{Ar}), 127.4 (CH, CH_{Ar}), 127.6 (CH, CH_{Ar}), 128.6 (CH, CH_{Ar}), 129.6 (CH, CH_{Ar}), 131.5 (CH, CH_{Ar}), 137.3 [C, $C_{Ar(q)}$ or SC(2)=], 137.5 [CH, C(3)HCl=], 138.5 [C, $C_{Ar(q)}$ or SC(2)=], 140.8 [C, $C_{Ar(q)}$ or SC(2)=], 160.5 (C=O) ppm.

_N_-(4′-Flurophenyl)-Z-3-chloro-2-(benzenesulfinyl)propenamide 56[12, 21]

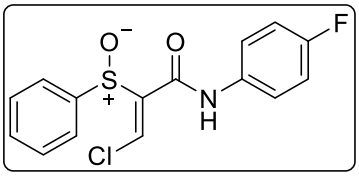

The title compound was synthesised following the procedure outlined for **54** using *N*-(4′-fluorophenyl)-Z-3-chloro-2-(benzylthio)propenamide **41** (3.15 g, 10.26 mmol) in acetone (160 ml) and Oxone® (6.31 g, 20.52 mmol) in water (40 ml). The reaction mixture was stirred at room temperature for 18 h and following work up, the sulfoxide **56** was obtained as a white solid (3.26 g, 98 %), which required no further purification; mp 105-108°C (lit.[12] 99-101°C); ν_{max}/cm^{-1} (ATR) 3063 (NH), 1674 (C=O), 1621, 1508 (NH bend), 1215, 1027 (SO); δ_H (300 MHz, $CDCl_3$) 6.95-7.05 (2H, m, ArH), 7.45-7.56 (5H, m, ArH), 7.65-7.73 (2H, m, ArH), 7.83 (1H, s, ClHC(3)=), 10.43 (1H, br s, NH) ppm; δ_C (75.5 MHz, $CDCl_3$) 115.7 [CH, d, $^2J_{CF}$ 23 Hz, C(3′)H_{Ar}], 122.3 [CH, d, $^3J_{CF}$ 7.9 Hz, C(2′)H_{Ar}], 124.0 (CH, CH_{Ar}), 129.8 (CH, CH_{Ar}), 131.9 (CH, CH_{Ar}), 133.1 [CH, d, $^4J_{CF}$ 3 Hz, C(1′)NH], 137.9 [CH, C(3)HCl=], 138.3 [C, $C_{Ar(q)}$ or SC(2)=], 140.7 [C, $C_{Ar(q)}$ or SC(2)=], 158.3 (C, C=O), 159.6 [C, d, $^1J_{CF}$ 244.7 Hz, $C_{Ar(q)}$(4′)F] ppm.

_N_-(2′,2′-Dimethylpropyl)-_Z_-3-chloro-2-(benzenesulfinyl)propenamide 57

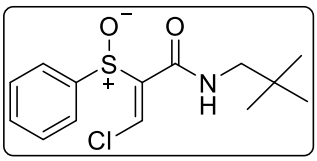

The title compound was prepared following the procedure described for **54** using *N*-(2′,2′-dimethylpropyl)-Z-3-chloro-2-(phenylthio)-propenamide **42** (3.08 g, 10.88 mmol) in acetone (120 ml) and Oxone® (6.69 g, 21.76 mmol) in water at (20 ml). The reaction was stirred at room temperature for 18 h and following work up, the sulfoxide **57** (3.13 g, 96%) was obtained as a clear oil, which required no further purification; ν_{max}/cm^{-1} (ATR) 3267 (NH stretch), 3059 (CH stretch), 2957 (CH), 1668 (C=O), 1556 (NH bend), 1030 (SO); δ_H (300 MHz, $CDCl_3$) 0.82 [9H, s, $C(CH_3)_3$], 2.91-3.00 [1H, dd, A of ABX system, J_{AB} 13.3, J_{AX} 5.5 Hz, one of $C\underline{H}_2NH$], 3.10-3.19 [1H, dd, B of ABX system, J_{BA} 13.3, J_{BX} 6.5 Hz, one of $C\underline{H}_2NH$], 7.47-7.70 (5H, m, ArH), 7.80 [1H, s, ClHC(3)=], 8.34 (C, C=O) ppm; δ_C (75.5 MHz, $CDCl_3$) 27.2 [CH_3, $C(\underline{C}H_3)_3$], 31.7 [C, $\underline{C}(CH_3)_3$], 50.8 (CH_2, CH_2NH), 124.2 (CH, CH_{Ar}), 129.6 (CH, CH_{Ar}), 131.6 (CH, CH_{Ar}), 137.5 [CH, C(3)HCl=], 138.7 [C, SC(2)=],

141.2 (C, $C_{Ar(q)}$), 160.8 (C, C=O) ppm; HRMS (ES+): Exact mass calculated $C_{14}H_{18}NO_2S^{35}Cl$ $[M+H]^+$ 300.0820. Found 300.0827; m/z (ES+) 302.2 {[($C_{14}H_{18}NO_2S^{37}Cl$)+H^+], 40%} 300.2 {[($C_{14}H_{18}NO_2S^{35}Cl$)+H^+], 100%}.

***N*-(4′-Methoxyphenyl)-Z-3-chloro-2-(benzenesulfinyl)propenamide 58**

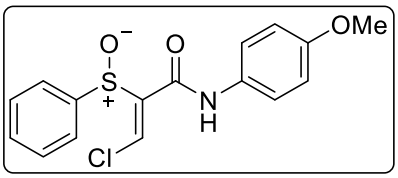

The title compound was prepared following the procedure described for **54** using *N*-(4′-methoxyphenyl)-*Z*-3-chloro-2-(phenylthio)propenamide **43** (1.86 g, 5.83 mmol) in acetone (80 ml) and Oxone® (3.59 g, 11.65 mmol) in water (20 ml). Following stirring at room temperature for 16 h and aqueous work up the crude sulfoxide **XX** was obtained as a yellow solid. Purification by column chromatography on silica gel using hexane: ethyl acetate (90:10) as eluent gave the pure sulfoxide **58** as a pale yellow solid (1.55 g, 79 %); mp 130-132°C; Found C, 57.14; H, 4.20; N, 4.17. $C_{16}H_{14}NO_3SCl$ requires C, 57.23; H, 4.20; N, 4.17; ν_{max}/cm^{-1} (ATR) 3057 (NH stretch), 1671 (C=O), 1509 (NH bend), 1237, 1023 (SO); δ_H (300 MHz, $CDCl_3$) 3.77 (3H, s, $ArOCH_3$), 6.81-6.88 (2H, m, ArH), 7.41-7.56 (5H, m, ArH), 7.66-7.74 (2H, m, ArH), 7.81 [1H, s, ClHC(3)=], 10.31 (1H, br s, NH) ppm; δ_C (75.5 MHz, $CDCl_3$) 55.4 (CH_3, $ArOCH_3$), 114.2 (CH, CH_{Ar}), 122.2 (CH, CH_{Ar}), 124.1 (CH, CH_{Ar}), 129.8 (CH, CH_{Ar}), 130.3 (C, $C_{Ar(q)}$), 131.9 (CH, CH_{Ar}), 137.4 [CH, C(3)HCl=], 138.5 [C, SC(2)=], 140.9 (C, $C_{Ar(q)}$), 156.8 (C, $C_{Ar(q)}$), 158.0 (C, C=O) ppm; HRMS (ES+): Exact mass calculated for $C_{16}H_{14}NO_3S^{35}Cl$ $[M+H]^+$ 336.0461. Found 336.0464; m/z (ES+) 338.1 {[($C_{16}H_{14}NO_3S^{37}Cl$)+H^+], 18%}, 336.1 {[($C_{16}H_{14}NO_3S^{35}Cl$)+H^+], 50%}.

***N*-*n*-Butyl-Z-3-chloro-2-(benzenesulfinyl)propenamide 59**[12, 21]

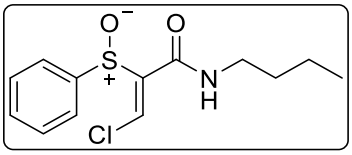

The title compound was prepared following the procedure described for **54** using *N*-*n*-butyl-*Z*-3-chloro-2-(phenylthio)propenamide **44** (2.06 g, 7.64 mmol) in acetone (80 ml) and Oxone® (4.70 g, 15.28 mmol) in water at (20 ml). The reaction was stirred at room temperature for 18 h and following work up, the sulfoxide **59** was obtained as a clear oil (2.06 g, 95%), which required no further purification; ν_{max}/cm^{-1} (ATR) 3286 (NH), 3056, 2957 (CH), 1651 (C=O), 1538, 1444, 1032 (SO); δ_H (300 MHz, $CDCl_3$) 0.87 [3H, t, *J* 7.3 Hz, C(4′)H_3], 1.12-1.52 [4H, m, C(2′)H_2 and C(3′)H_2], 3.09-3.38 [2H, m, C(1′)H_2], 7.46-7.69 (5H, m, ArH), 7.75 [1H, s, ClHC(3)=], 8.33 (1H, br s, NH) ppm; δ_C (75.5 MHz, $CDCl_3$) 13.6 [CH_3, C(4′)H_3], 19.9 [CH_2, C(3′)H_2], 31.2 [CH_2, C(2′)H_2], 39.0 [CH_2, C(1′)H_2], 124.0 (CH, CH_{Ar}), 129.5 (CH, CH_{Ar}), 131.5 (CH, CH_{Ar}), 137.0 [CH, C(3)HCl=], 138.7 [C, $C_{Ar(q)}$ or SC(2)=], 141.0 [C, $C_{Ar(q)}$ or SC(2)=], 160.3 (C, C=O) ppm.

2.10.8.1 Synthesis of α-Benzylsulfinyl-β-Chloroacrylamides

***N*-(4-Flurophenyl)-Z-3-chloro-2-(benzylsulfinyl)propenamide 60**[12, 21]

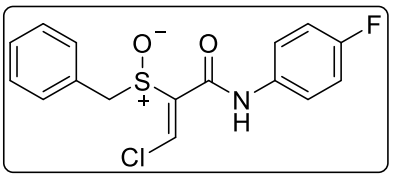

The title compound was prepared following the procedure described for **54** using *N*-(4-flurophenyl)-Z-3-chloro-2-(benzylthio)propenamide **49** (3.00 g, 9.34 mmol) in acetone (80 ml) and Oxone® (5.74 g, 18.68 mmol) in water at (20 ml). The reaction was stirred at room temperature for 18 h and following work up, the sulfoxide **60** (2.93 g, 93%) was obtained as a white solid, which required no further purification; mp 118-120°C (lit.[12] 121-122°C); ν_{max}/cm^{-1} (ATR) 3212 (NH), 3064 (CH), 1671 (C=O), 1573 (NH bend), 1406 (CN stretch), 1026 (SO); δ_H (300 MHz, $CDCl_3$) 4.27 (2H, s, SCH_2), 6.91-7.00 (2H, m,

ArH), 7.18-7.40 (8H, m, ArH), 7.80 [1H, s, ClHC(3)=], 10.08 (1H, br s, NH) ppm; δ_C (75.5 MHz, $CDCl_3$) 58.4 (CH_2, SCH_2), 115.5 [CH, d, $^2J_{CF}$ 23 Hz, C(3′)H_{Ar}], 122.3 [CH, d, $^3J_{CF}$ 8 Hz, C(2′)H_{Ar}], 127.7 (C, $C_{Ar(q)}$), 128.9 (CH, CH_{Ar}), 129.2 (CH, CH_{Ar}), 130.6 (CH, CH_{Ar}), 133.2 [C, d, $^4J_{CF}$ 3 Hz, $C_{Ar(q)}$(1′)], 135.0 [C, C(2)S], 137.0 [CH, ClHC(3)=], 158.4 (C, C=O), 159.6 [C, d, $^1J_{CF}$ 245 Hz, $C_{Ar(q)}$(4′)F] ppm.

***N*-(4′-Methoxyphenyl)-Z-3-chloro-2-(benzylsulfinyl)propenamide 61**

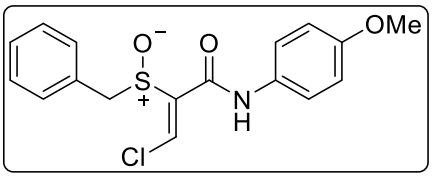

The title compound was prepared following the procedure described for **54** using *N*-(4′-methoxyphenyl)-*Z*-3-chloro-2-(benzylthio)propenamide **51** (2.05 g, 6.16 mmol) in acetone (140 ml) and Oxone® (3.78 g, 12.31 mmol) in water (20 ml). Following stirring at room temperature for 16 h and aqueous work up the crude sulfoxide **61** was obtained as a yellow oil. Purification by flash column chromatography on silica gel using hexane: ethyl acetate (60:40) as eluent gave the pure sulfoxide **61** (1.98 g, 92%) as a white solid; mp 112-114°C; Found C, 58.39; H, 4.62; N, 3.93. $C_{17}H_{16}NO_3SCl$ requires C, 58.37; H, 4.61; N, 4.00; ν_{max}/cm^{-1} (ATR) 3058 (NH), 3002 (CH), 1666 (C=O), 1567 (NH bend), 1510, 1238, 1022 (SO); δ_H (300 MHz, $CDCl_3$) 3.77 (3H, s, $ArOCH_3$), 4.23 (1H, d, A of AB system, J_{AB} 13.1, one of CH_2SO), 4.29 (1H, d, B of AB system, J_{BA} 13.1 Hz, one of CH_2SO), 6.77-6.84 (2H, m, ArH), 7.19-7.37 (7H, m, ArH), 7.77 [1H, s, ClHC(3)=], 10.02 (1H, br s, NH) ppm; δ_C (75.5 MHz, $CDCl_3$) 55.3 (CH_3, $ArOCH_3$), 58.4 (CH_2, CH_2SO), 113.9 (CH, CH_{Ar}), 122.1 (CH, CH_{Ar}), 127.8 (C, $C_{Ar(q)}$), 128.8 (CH, CH_{Ar}), 129.0 (CH, CH_{Ar}), 130.3 (C, $C_{Ar(q)}$), 130.5 (CH, CH_{Ar}), 135.2 [C, SC(2)=], 136.5 [CH, C(3)HCl=], 156.6 (C, $C_{Ar(q)}$), 158.0 (C, C=O) ppm; HRMS (ES+): Exact mass calculated for $C_{17}H_{16}NO_3S^{35}Cl$ $[M+H]^+$ 350.0616. Found 350.0612; m/z (ES+) 352.1 {[($C_{17}H_{16}NO_3S^{37}Cl$)+H^+], 20%}. 350.1 {[($C_{17}H_{16}NO_3S^{35}Cl$)+H^+], 44%}.

***N*-Benzyl-Z-3-chloro-2-(benzylsulfinyl)propenamide 116**[12, 21]

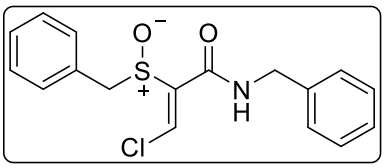

The title compound was prepared following the procedure described for **54** using *N*-benzyl-Z-3-chloro-2-(benzylsulfinyl)-propenamide **48** (1.93 g, 6.09 mmol) in acetone (60 ml) and Oxone® (3.74 g, 12.18 mmol) in water (20 ml). Following stirring at room temperature for 14 h and aqueous work up the crude sulfoxide **116** was obtained as a clear oil. Purification by flash column chromatography on silica gel using hexane: ethyl acetate (85:15) as eluent gave the pure sulfoxide **116** as a clear oil (1.76 g, 87%); ν_{max}/cm^{-1} (ATR) 3250 (NH), 3059 (CH), 1666 (CO), 1574 (NH bend), 1495, 1454 (CN stretch), 1029 (SO); δ_H (300 MHz, $CDCl_3$) 4.16 (1H, d, A of AB system, J_{AB} 12.6 Hz, one of $SOCH_2$), 4.23 (1H, dd, A of ABX, J_{AB} 15.0, J_{AX} 5.7 Hz, one of CH_2NH), 4.26 (1H, d, B of AB system, J_{AB} 12.6 Hz, one of $SOCH_2$), 4.43 (1H, dd, B of ABX, J_{AB} 15.0, J_{AX} 5.7 Hz, one of CH_2NH), 7.18-7.38 (10H, m, ArH), 7.72 [1H, s, ClHC(3)=], 8.63 (1H, br s, NH) ppm; δ_C (75.5 MHz, $CDCl_3$) 43.8 (CH_2, NCH_2), 58.8 (CH_2, SCH_2), 127.9 (CH, CH_{Ar}), 128.1 (CH, CH_{Ar}), 128.5 (C, $C_{Ar(q)}$), 129.1 (CH, CH_{Ar}), 129.3 (CH, CH_{Ar}), 129.4 (CH, CH_{Ar}),131.0 (CH, CH_{Ar}), 135.8 [C, $C_{Ar(q)}$ or SC(2)=], 137.0 [CH, C(3)HCl=], 137.9 [C, $C_{Ar(q)}$ or SC(2)=], 161.1 (C, C=O) ppm.

***N*-*n*-Butyl-Z-3-chloro-2-(benzylsulfinyl)propenamide 117**[12, 21]

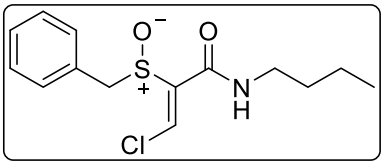

The title compound was prepared following the procedure described for **54** using *N*-*n*-butyl-Z-3-chloro-2-(benzylthio)-propenamide **46** (0.75 g, 2.64 mmol) in acetone (30 ml) and Oxone® (1.62 g, 5.27 mmol) in water (10 ml). Following stirring at room temperature for 16 h and aqueous work up the crude sulfoxide **117** was obtained as a clear oil. Purification by flash column chromatography on silica gel

using hexane: ethyl acetate (80:20) as eluent gave the pure sulfoxide **117** (1.98 g, 92%) as a clear oil; ν_{max}/cm^{-1} (ATR) 3230 (NH), 3054 (CH), 2985 (CH), 1657 (C=O), 1568 (NH bend), 1405 (CN stretch), 1026 (SO); δ_H (300 MHz, $CDCl_3$) 0.91 [3H, t, *J* 7.2 Hz, C(4')H_3], 1.22-1.48 [4H, m, overlapping C(3')H_2 and C(2')H_2], 3.00-3.27 [2H, m, C(1')$\underline{H_2}$], 4.19 (1H, d, A of AB system, J_{AB} 12.9 Hz, one of $SOCH_2$), 4.26 (1H, d, B of AB system, J_{BA} 12.9 Hz, one of $SOCH_2$), 7.20-7.45 (5H, m, ArH), 7.68 [1H, s, ClHC(3)=], 8.19 (1H, br s, NH) ppm; δ_C (75.5 MHz, $CDCl_3$) 13.7 [CH_3, C(4')H_3], 20.2 [CH_2, C(3')H_2], 31.1 [CH_2, C(2')H_2], 39.1 [CH_2, C(1')H_2], 58.4 (CH_2, $SOCH_2$), 128.2 (C, $C_{Ar(q)}$), 128.8 (CH, CH_{Ar}), 128.9 (CH, CH_{Ar}), 130.6 (CH, CH_{Ar}), 135.5 [C, C(2)S], 136.0 [CH, ClHC(3)=], 160.5 (C, C=O) ppm.

2.9.9 Synthesis of 1,3-Dipoles

2.9.9.1 Synthesis of α-Diazomethyl Phenylsulfone

1-Phenyl-2-(phenylthio)ethanone 124[75]

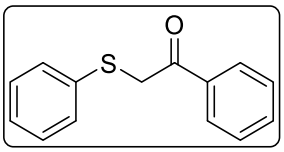

Thiophenol (5.11 ml, 50 mmol) was added in one portion to a stirring solution of potassium carbonate (7.60 g, 55 mmol) in acetone (70 ml), at room temperature, under nitrogen. The reaction mixture was stirred for 15 minutes. Phenacyl bromide **123** (9.95 g, 50 mmol) was then added in one portion at room temperature and upon completion of the addition the reaction mixture was heated under reflux for 16 h. The reaction mixture was cooled to room temperature, filtered through a bed of Celite®, concentrated under reduced pressure to afford the crude sulfide as a red oil. Purification by flash column chromatography on silica gel using hexane: ethyl acetate (60:40) as eluent afforded the β-ketosulfide **124** as a yellow solid (11.04 g, 97%); m.p. 51-53°C (lit.[132] 52-53°C); ν_{max}/cm^{-1} (ATR) 3055 (CH), 2953 (CH), 2921, 1670 (C=O), 1578, 1272, 740, 686; ^{1}H NMR ($CDCl_3$, 300 MHz) 4.20 (2H, s, SCH_2), 7.08-7.26 (3H, m, ArH), 7.28-7.40 (4H, m, ArH), 7.42-7.51 (1H, m, ArH), 7.83-7.92 (2H, m, ArH) ppm; ^{13}C NMR ($CDCl_3$, 75.5 MHz) 40.9 (CH_2, SCH_2), 126.8 (CH, CH_{Ar}), 128.4 (CH, CH_{Ar}), 128.9 (CH, CH_{Ar}), 130.2 (CH, CH_{Ar}), 133.2 (CH, CH_{Ar}), 134.7 (C, $C_{Ar(q)}$), 135.2 (C, $C_{Ar(q)}$), 193.8 (C, C=O) ppm.

2-(Phenylsulfonyl)acetophenone 125[76]

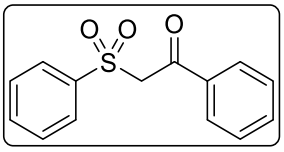

A solution of *m*CPBA (77%, 15.46 g, 69 mmol) in dichloromethane (150 ml) was added dropwise to a solution of 1-phenyl-2-(phenylthio)ethenone **124** (6.84 g, 30 mmol) in dichloromethane (50 ml) over 10 min at 0°C. The solution was stirred for a further 18 h while warming slowly to room temperature. The crude mixture was washed with aqueous sodium bicarbonate (10%, 3 x 50 ml) brine (50 ml), dried, concentrated under reduced pressure to give 2-(phenylsulfonyl)acetophenone **125** (7.10 g, 91%) as a white solid; mp 92-94°C (lit.[133] 93-95°C); ν_{max}/cm^{-1} (ATR) 3070 (CH stretch), 2998 (CH), 2941 (CH), 1672 (C=O), 1307 (asymmetric SO_2), 1154 (symmetric SO_2); ^{1}H NMR ($CDCl_3$, 300 MHz) 4.74 (2H, s, SO_2CH_2), 7.42-7.70 (6H, m, ArH), 7.86-7.97 (4H, m, ArH) ppm; ^{13}C NMR ($CDCl_3$, 75.5 MHz) 63.4 (CH_2, SCH_2), 128.5 (CH, CH_{Ar}), 128.8 (CH, CH_{Ar}), 129.15 (CH, CH_{Ar}), 129.22 (CH, CH_{Ar}), 134.2 (CH, CH_{Ar}), 134.3 (CH, CH_{Ar}), 135.7 (C, $C_{Ar(q)}$), 138.7 (C, $C_{Ar(q)}$), 187.9 (C, C=O) ppm.

2-Diazo-1-phenyl-2-(phenylsulfonyl)ethenone 126[68]

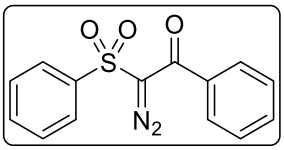

Potassium carbonate (0.54 g, 3.9 mmol) was added to a stirring solution of 2-(phenylsulfonyl)acetophenone **125** (0.78 g, 3 mmol) in acetonitrile (30 ml) at room temperature. A solution of *p*-ABSA (0.72 g, 3 mmol) in acetonitrile (5 ml) was added dropwise over 5 min and then for a further 18 h. Diethyl ether (10 ml) and hexane (10 ml) was added to precipitate the sulfonamide salts, and the reaction mixture was filtered through a bed of Celite®. The crude reaction was concentrated under reduced

pressure to give the crude product as an orange solid. Purification by flash column chromatography on silica gel using hexane: ethyl acetate (60:40) as eluent afforded the α-diazo-β-ketosulfone **126** (0.62 g, 72 %) as a yellow solid; m.p. 126-129°C (lit.[134] 128-130°C); ν_{max}/cm^{-1} (ATR) 3097 (CH stretch), 2113 (N_2), 1632 (C=O), 1327 (asymmetric SO_2), 1146 (symmetric SO_2), 727; ^{1}H NMR ($CDCl_3$, 300 MHz) 7.38-7.48 (2H, m, ArH), 7.50-7.60 (5H, m, ArH), 7.62-7.71 (1H, m, ArH), 8.01-8.11 (2H, m, ArH) ppm; ^{13}C NMR ($CDCl_3$, 75.5 MHz) 83.2 (C, C=N_2) 127.3 (CH, CH_{Ar}), 128.0 (CH, CH_{Ar}), 128.8 (CH, CH_{Ar}), 129.0 (CH, CH_{Ar}), 132.9 (CH, CH_{Ar}), 134.1 (CH, CH_{Ar}), 135.7 (C, $C_{Ar(q)}$), 141.3 (C, $C_{Ar(q)}$), 182.5 (C, C=O) ppm.

α-Diazomethyl Phenylsulfone 127[68]

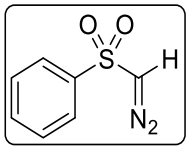

2-Diazo-1-phenyl-2-(phenylsulfonyl)ethenone **126** (50 mg, 0.175 mmol) in dichloromethane (2 ml) was loaded onto a column (diameter 1.5 cm, height 5 cm) of alumina (6 g, activated, neutral, Brockmann 1) in dichloromethane as eluent. The column was wrapped in tin-foil to avoid light mediated degradation of the α-diazosulfone **127**. The α-diazosulfone was eluted slowly by gravity and the UV active fractions, readily identified by the yellow-tinge of the collected fractions, were collected, concentrated under reduced pressure in a round bottom flask, also covered in tin foil at no greater than 30°C. As the transformation progressed a pinkening of the alumina was observed. ^{1}H NMR spectroscopy of the collected fractions indicated a 69:31 mixture of α-diazo-β-ketosulfone **126**: α-diazosulfone **127**, therefore the mixture was loaded again to the same column and allowed elute slowly by gravity. This process was repeated for a total of three times at which point ^{1}H NMR spectroscopy of the collected fractions indicated a 33:67 mixture of α-diazo-β-ketosulfone **126**: α-diazosulfone **127**. The mixture was then applied to a fresh column (diameter 2 cm, height 10 cm) of Al_2O_3 (16 g) under otherwise identical conditions, after which ^{1}H NMR spectroscopy of the isolated fractions confirmed that that the α-diazosulfone **127** had been obtained in pure form as a yellow oil (9.9 mg, 32 %); ^{1}H NMR ($CDCl_3$, 300 MHz) 5.27 (1H, s, CH), 7.47-7.65 (3H, m, ArH), 7.81-7.90 (2H, m, ArH) ppm; ^{13}C NMR ($CDCl_3$, 75.5 MHz) 57.7 (CH, br, CH), 126.2 (CH, CH_{Ar}), 129.4 (CH, CH_{Ar}), 133.3 (CH, CH_{Ar}) ppm.

α-Diazomethyl phenylsulfone **127** was subsequently prepared using the method described above using α-diazo-β-ketosulfone **126** (1 g, 3.50 mmol) and alumina (100 g) in dichloromethane as eluent. In this instance two runs through the column was required to afford the α-diazosulfone **127** (274 mg, 43%). Spectroscopic details were consistent with those outlined above.

2.9.9.2 Synthesis of Tosyl Diazomethane

Sodium *p*-Toluenesulfinate 131[135]

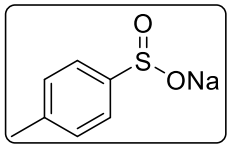

Tosyl chloride **131** (54.83 g, 0.29 mol), sodium sulfite (68.68 g, 0.55 mol) and sodium bicarbonate (48.35 g, 0.58 mol) were charged to a 1L round bottom flask in 400ml of water. The mixture was heated gradually to 70–80°C at which point the reaction mixture was stirred for 2 h. The temperature was maintained by a thermostat set to 75°C. After cooling to room temperature, the solvent was removed under vacuum while maintaining the water bath at 80°C. The crude product was washed thoroughly with ethanol and filtered through a sintered glass funnel. The ethanolic solution was concentrated under reduced pressure to afford pure sodium *p*-toluenesulfinate **132** (25.86 g, 51 %) as a white solid; m.p. >300°C ν_{max}/cm^{-1} (ATR) 3404 (CH stretch), 1685, 1022, 1015, 975, 815; δ_H (300 MHz, D_2O) 2.41 (3H, s, $ArCH_3$), 7.39 (2H, d, J 8.0 Hz, ArH), 7.58 (2H, d, *J* 8.0 Hz, ArH) ppm; δ_C (75.5 MHz, D_2O) 20.5 (CH_3, $ArCH_3$), 123.5 (CH, CH_{Ar}), 129.6 (CH, CH_{Ar}), 141.2 (C, $\underline{C}_{Ar(q)}CH_3$), 150.5 (C, $C_{Ar(q)}SO_2Na$) ppm.

(Toluene-4-sulfonylmethyl)-carbamic acid ethyl ester 133[71, 73]

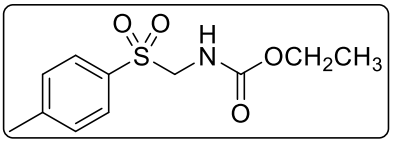

Formaldehyde (40 weight % in water, 14.83 ml, 0.165 mol), ethyl carbamate (12.22 g, 0.137 mol, 1 equiv.) and formic acid (30 ml) were added to a solution of sodium *p*-toluenesulfinate **132** (24.42 g, 0.137 mol) in water (160 ml), and the reaction mixture was heated to a gentle reflux for 2 h. The reaction mixture was allowed cool to room temperature before being further cooled to 0°C for 2 h. The white precipitate was collected by suction filtration and washed thoroughly with hexane to afford (toluene-4-sulfonylmethyl)-carbamic acid ethyl ester **133** as a white solid (18.34 g, 52 %); mp 107-110°C (lit.[71] 109-111°C); ν_{max}/cm^{-1} (ATR) 3359 (NH stretch), 1721 (C=O), 1526 (NH bend), 1313 (asymmetric SO_2), 1246, 1137 (symmetric SO_2), 1035; δ_H (300 MHz, $CDCl_3$) 0.94 (0.59H, br t, unresolved coupling, minor rotamer of $OCH_2C\underline{H}_3$), 1.13 (2.41H, t, *J* 7.1 Hz, major rotamer, $OCH_2C\underline{H}_3$), 2.44 (3H, s, $ArCH_3$), 3.77 (0.41H, br q, unresolved coupling, minor rotamer of $OC\underline{H}_2CH_3$), 3.98 (1.59H, *J* 7.1 Hz, major rotamer of $OC\underline{H}_2CH_3$), 4.43-4.66 [2H, overlapping doublet at 4.57, *J* 7.0 Hz and br m, CH_2SO_2], 5.91 (1H, br t, unresolved coupling, NH), 7.40 (2H, d, *J* 8.0 Hz, ArH), 7.80 (2H, d, *J* 8.3 Hz, ArH) ppm; δ_H (300 MHz, DMSO-d_6) 0.96 (0.5H, br t, unresolved coupling, minor rotamer, $OCH_2C\underline{H}_3$), 1.16 (2.5H, t, *J* 7.1 Hz, major rotamer, $OCH_2C\underline{H}_3$), 3.74 (0.38H, br q, unresolved coupling, minor rotamer, $OC\underline{H}_2CH_3$), 3.99 (1.62H, *J* 7.1 Hz, major rotamer, $OC\underline{H}_2CH_3$), 4.63 (2H, d, *J* 6.6 Hz, CH_2SO_2), 7.53 (2H, d, *J* 8.0 Hz, ArH), 7.81 (2H, d, *J* 8.3 Hz, ArH), 8.01 (0.18H, br t, unresolved coupling, minor rotamer, NH), 8.34 (0.82H, t, *J* 6.6 Hz, major rotamer, NH) ppm; δ_C (75.5 MHz, $CDCl_3$) 13.8 (CH_3, br, minor rotamer, $OCH_2\underline{C}H_3$), 14.2 (CH_3, major rotamer, $OCH_2\underline{C}H_3$), 21.5 (CH_3, $ArCH_3$), 61.7 (CH_2, major rotamer, $O\underline{C}H_2CH_3$), 62.3 (CH_2, CH_2SO_2), 63.1 (CH_2, br, minor rotamer, $O\underline{C}H_2CH_3$), 128.8 (CH, CH_{Ar}), 129.7 (CH, CH_{Ar}), 133.8 (C, $C_{Ar(q)}$), 145.2 (C, $C_{Ar(q)}$), 155.2 (C, major rotamer, C=O), 154.3 (C, br, minor rotamer, C=O) ppm.

**This compound displayed a previously unreported rotameric effect in its ^{1}H and ^{13}NMR spectrum. Assignment of the ^{1}H NMR data was made in conjunction with HSQC analysis.*

***N*-Nitroso-(toluene-4-sulfonylmethyl)-carbamic acid ethyl ester 121**[71, 73]

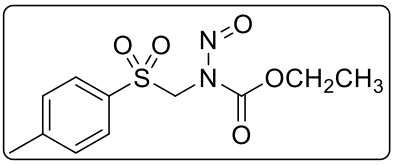

Pyridine (6.82 ml, 84.72 mmol), isoamyl nitrite (11.38 ml, 84.72 mmol) and trimethylsilyl chloride (18.64 ml, 146.85 mmol) were added to a solution of (toluene-4-sulfonylmethyl)-carbamic acid ethyl ester **133** (14.52 g, 56.48 mmol) in dichloromethane (60 ml) in a flame dried flask under nitrogen. The reaction progress was monitored by thin layer chromatography for consumption of starting material. After 2.5 h the reaction was observed to be complete. The reaction mixture was then poured slowly into a 10% aq. $NaHCO_3$ solution (200 ml) and stirred for 30 minutes. The heterogenous mixture was diluted with diethyl ether (500 ml) and the organic layer was washed with water (250 ml), 1 M HCl (250 ml), water (250 ml), 10% aq. $NaHCO_3$ (250 ml), water (250 ml) and brine (250 ml). The light-yellow organic phase was dried with $MgSO_4$, concentrated under reduced pressure to give the crude product **121** as a yellow solid. Purification by trituration with hexane afforded *N*-nitroso-(toluene-4-sulfonylmethyl)-carbamic acid ethyl ester **121** (15.20 g, 94%) as a yellow solid; δ_H (300 MHz, $CDCl_3$) 1.43 (3H, t, *J* 7.2 Hz, $OCH_2C\underline{H}_3$), 2.47 (3H, s, $ArCH_3$), 4.52 (2H, q, *J* 7.2 Hz, $OC\underline{H}_2CH_3$), 5.12 (2H, s, SO_2CH_2), 7.33-7.40 (2H, m, ArH), 7.67-7.74 (2H, m, ArH) ppm; δ_C (75.5 MHz, $CDCl_3$) 14.1 (CH_3, $OCH_2\underline{C}H_3$), 21.7 (CH_3, $ArCH_3$), 58.3 (CH_2, $O\underline{C}H_2CH_3$), 65.4 (CH_2, SO_2CH_2), 128.5 (CH, CH_{Ar}), 130.1 (CH, CH_{Ar}), 135.1 (C, $C_{Ar(q)}$), 145.8 (C, $C_{Ar(q)}$), 152.5 (C, C=O) ppm.

Note: *Due to the highly toxic nature of N-nitroso compounds no melting point or IR data were recorded for this compound. All handling of this compound was carried out in a well ventilated fumehood.*

Tosyl diazomethane 37[71, 73]

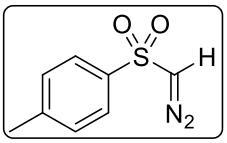

Aluminium oxide (activated, Brockmann 1, standard grade, 50-200 µm, 60 Å, 10 g) was added to a flame dried 2 neck round bottom flask and placed under a flow of nitrogen, cooled to 0°C, and slurried in anhydrous diethyl ether (40 ml). To this was added *N*-nitroso-(toluene-4-sulfonylmethyl)-carbamic acid ethyl ester **121** (1 g) in ddDCM. The reaction mixture, shielded from light by tin-foil, was mechanically stirred at 0°C-5°C for 3h at which point the starting material was determined to be completely consumed by TLC analysis. The reaction mixture at this point was bright yellow and the Al_2O_3 had pinkened slightly. The yellow solution was decanted and the Al_2O_3 was thoroughly washed with diethyl ether until the yellow colour indicative of the diazosulfone **37** could no longer be observed. The solution was filtered and concentrated under reduced pressure (water bath was maintained no higher than room temperature) to give a yellow oil which solidified over 2 h sitting at -20°C in the freezer. The yellow solid was triturated with cold hexane and the solution decanted to afford pure tosyl diazomethane **37** (0.33 g, 48%)*; mp 35-37°C (lit.[73] 34-35°C); ν_{max}/cm^{-1} (ATR) 3071 (CH stretch) 2107 (CN_2),1327, 1150, 1084, 810; δ_H (300 MHz, $CDCl_3$) 2.45 (3H, s, $ArCH_3$), 5.27 (1H, s, SO_2CHN_2), 7.34 (2H, d, *J* 8.4 Hz, ArH), 7.76 (2H, d, *J* 8.4 Hz, ArH) ppm; δ_C (75.5 MHz, $CDCl_3$) 21.5 (CH_3, $ArCH_3$), 57.7 (CH, SO_2CHN_2), 126.2 (CH, CH_{Ar}), 129.9 (CH, CH_{Ar}), 141.3 (C, $C_{Ar(q)}$), 144.3 (C, $C_{Ar(q)}$) ppm.

Precautions*: Efforts were made to ensure that the all reagents used were moisture free. The Al_2O_3 was dried at 140°C overnight prior to use. The diethyl ether (HPLC grade) was taken from a freshly opened bottle, and was subsequently stored over molecular sieves. Doubly distilled DCM (ddDCM) was used rather than distilled DCM. Tosyl diazomethane is both heat and light sensitive hence all glassware was covered in foil prior to commencing the reaction. All glassware was flame-dried prior to use.*

** A yield of 62% was obtained for a batch of **37** that was later synthesised on a 10.7 g: 100 g scale of N-nitroso-(toluene-4-sulfonylmethyl)-carbamic acid ethyl ester **121**: aluminium oxide.*

2.9.9.3 Synthesis of *N*-Benzyl-α-Diazoacetamide

2,5-Dioxopyrrolidin-1-yl-2-(diphenylphosphanyl)benzoate 135[91, 136]

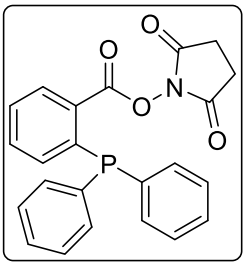

2-(Diphenylphosphanyl)benzoic acid **134** (16.94 g, 55.41 mmol) was dissolved in dichloromethane (200 ml), and the solution was cooled to 0 °C. *N*-Hydroxysuccinimide (12.76 g, 110.83 mmol) and *N*,*N'*-diisopropylcarbodiimide (7.69 g, 60.95 mmol) were added, and the mixture was allowed to warm to room temperature and stirred overnight under nitrogen. The resulting suspension was filtered and the filtrate was concentrated under reduced pressure. Purification by flash column chromatography on silica gel using hexane: ethyl acetate (70:30) as eluent gave 2,5-diisopyrrolidin-1-yl-2-(diphenylphosphanyl)benzoate **135** (17.89 g, 80 %) as a crystalline pale yellow solid; mp 155-158°C; ν_{max}/cm^{-1} (ATR) 1763 (C=O), 1737 (C=O), 1432, 1197, 997, 748, 696; δ_H (300 MHz, $CDCl_3$) 2.79 (4H, s, $COC\underline{H_2}C\underline{H_2}CO$), 6.96-7.06 [1H, m, ArH], 7.16-7.39 (10H, m, ArH), 7.43-7.53 [2H, m, ArH], 8.26-8.37 [1H, m, ArH] ppm; $\{\delta_P\}$ (121.5 MHz, $CDCl_3$) -4.5 ppm.

2-Azido-*N*-(phenylmethyl)acetamide 139[91, 137]

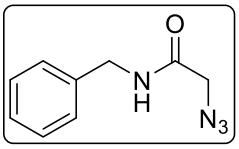

Benzyl amine **136** (6.55 ml, 60 mmol) in dichloromethane (60 ml) were added to a flame dried round bottomed flask under nitrogen and the resulting solution was cooled to 0°C using an ice bath. Bromoacetyl bromide **137** (2.61 ml, 30 mmol) was added to the solution dropwise over 5 minutes. A white precipitate was observed almost immediately upon the commencement of the addition. Upon completion of the addition the ice bath was removed, the reaction mixture was warmed to room temperature, and the stirred for 1 h. The precipitate was removed by filtration, and the organic phase was washed with hydrochloric acid (2M, 2 x 100 ml), water (100 ml) and brine (100 ml). The organic layer was dried, filtered and concentrated under reduced pressure to afford *N*-benzyl-2-bromoacetamide **138** as a white solid. This solid was dissolved in tetrahydrofuran (80 ml) and water (30 ml). Sodium azide (9.75 g, 150 mmol) was added, and the resulting mixture was stirred vigorously under reflux for 18 h. The organic layer was separated, washed with brine (2 x 100 ml), dried, filtered and concentrated under reduced pressure to give 2-azido-*N*-(phenylmethyl)acetamide **139** as a clear oil (5.22 g, 92%) that was used without further purification; ν_{max}/cm^{-1} (ATR) 3288 (NH stretch), 3065 (CH), 2100 (N_3), 1657 (C=O), 1532 (NH bend), 1251, 697; δ_H (300 MHz, $CDCl_3$) 3.97 (2H, s, CH_2N_3), 4.45 (2H, d, *J* 5.8 Hz, CH_2NH), 6.73 (1H, br s, NH), 7.22-7.39 (5H, m, ArH) ppm; δ_C (75.5 MHz, $CDCl_3$) 43.4 (CH_2, CH_2NH), 52.5 (CH_2, CH_2N_3), 127.66 (CH, CH_{Ar}), 127.74 (CH, CH_{Ar}), 128.7 (CH, CH_{Ar}), 137.4 (C, $C_{Ar(q)}$), 166.5 (C, C=O) ppm.

***N*-Benzyl-2-diazoacetamide 39**[91]

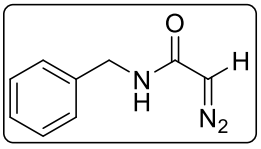

2-Azido-*N*-benzylacetamide **139** (4.99 g, 26.25 mmol) was dissolved in tetrahydrofuran/water (60 mL/7.5 ml). To this solution was added phosphine **135** (11.12 g, 27.56 mmol), and the resulting solution was stirred overnight under nitrogen. Triethylamine (7.32 ml, 52.50 mmol) was then added, and the mixture was stirred for 1 h. The mixture was then diluted with brine (70 mL) and extracted with dichloromethane (2 x 70 ml). The organic layers were combined, dried, filtered, and evaporated under reduced pressure. The residue was purified by flash chromatography on silica gel using hexane: ethyl acetate (70:30) as eluent to give *N*-benzyl-2-diazoacetamide **39** (3.83 g, 83%) as a yellow solid; mp 94-96°C (lit.[138] 100-103°C); ν_{max}/cm^{-1} (ATR) 3285 (NH stretch), 3091 (CH stretch), 2096 (C=N_2), 1606 (C=O), 1544 (NH bend), 1390, 1235; δ_H (300 MHz, $CDCl_3$) 4.34 (2H, d, *J* 5.9 Hz, $C\underline{H_2}NH$), 4.81 (1H, s, CHN_2), 6.33 (1H, br s, NH), 7.15-7.37 (5H, m, ArH) ppm; δ_C (75.5 MHz, $CDCl_3$) 43.7 (CH_2, CH_2NH), 46.9 (CH, CHN_2), 127.3 (CH, CH_{Ar}), 127.4 (CH, CH_{Ar}), 128.5 (CH, CH_{Ar}), 138.3 (C, $C_{Ar(q)}$), 165.9 (C, C=O) ppm.

2.9.10 [3+2] Dipolar Cycloadditions

2.9.10.1 [3+2] Dipolar Cycloadditions of α-Diazosulfones

Dimethyl 3-tosyl-1*H*-pyrazole-4,5-dicarboxylate 157

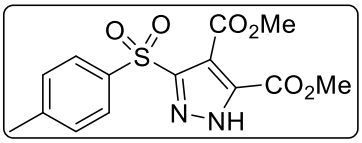

Tosyl diazomethane **37** (196 mg, 1 mmol) was added neat to a stirring solution of dimethyl acetylenedicarboxylate **156** (73.1 mg, 0.51 mmol) in diethyl ether (1 ml) at 0°C under nitrogen. The round bottomed flask (25 ml) was covered with tin foil to prevent light mediated decomposition of the diazo compound **37**. The reaction mixture was stirred for 16 h under nitrogen, and then concentrated under reduced pressure to afford the crude product. Purification by flash column chromatography on silica gel using hexane: ethyl acetate (60:40) as eluent gave the pyrazole **157** as a white solid (155 mg, 92 %); mp 145-147°C; ν_{max}/cm^{-1} (ATR) 3301 (NH), 2958 (CH),

1718 (C=O), 1331 (asymmetric SO_2), 1155 (symmetric SO_2), 670; δ_H (300 MHz, $CDCl_3$) 2.40 (3H, s, $ArCH_3$), 3.88 (3H, s, one of CO_2CH_3), 3.97 (3H, s, one of CO_2CH_3), 7.30 (2H, d, *J* 8.3 Hz, ArH), 7.92 (2H, d, *J* 8.3 Hz, ArH) ppm; δ_C (75.5 MHz, $CDCl_3$) 21.6 (CH_3, $ArCH_3$), 53.1 (CH_3, one of CO_2CH_3), 53.2 (CH_3, one of CO_2CH_3), 117.2 [C, C(4)], 128.4 (CH, CH_{Ar}), 129.8 (CH, CH_{Ar}), 134.6 [C, C(5)], 136.6 (C, $C_{Ar(q)}$), 145.3 (C, $C_{Ar(q)}$), 150.0 [C, C(3)], 157.9 (C, one of $\underline{C}O_2CH_3$), 162.1 (C, one of $\underline{C}O_2CH_3$) ppm; HRMS (ES+): Exact mass calculated for $C_{14}H_{14}N_2O_6S$ $[M+H]^+$ 339.0647. Found 339.0642.

5-Phenyl-3-tosyl-3a,6a-dihydropyrrolo[3,4-c]pyrazole-4,6(1*H*,5*H*)-dione 160

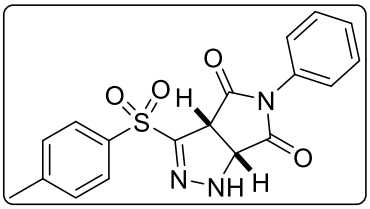

The title compound was prepared following the procedure outlined for **157** using tosyl diazomethane **37** (196 mg, 1 mmol) and *N*-phenylmaleimide **158** (86 mg, 0.5 mmol) in 50:50 diethyl ether/acetone (1 ml). After 16 h the reaction mixture was concentrated under reduced pressure to afford a 1:1 mixture of the pyrazoline **159*** and unreacted tosyldiazomethane **3**. Purification by flash column chromatography on silica gel using hexane: ethyl acetate (60:40) as eluent afforded the pyrazole **160** (196 mg, 53 %) as a white solid; ν_{max}/cm^{-1} (ATR) 3333 (CH stretch), 1715 (C=O), 1324 (asymmetric SO_2), 1155 (symmetric SO_2); mp 93-96°C; δ_H (300 MHz, $CDCl_3$) 2.44 (3H, s, $ArCH_3$), 4.71 [1H, d, *J* 10.6 Hz, one of C(4)H or C(5)H], 5.10 [1H, d, *J* 10.6 Hz, one of C(3)H or C(5)H], 6.98-7.07 (2H, m, ArH), 7.26 (1H, br s, NH), 7.32-7.46 (5H, m, ArH), 7.90-7.96 (2H, m, ArH) ppm; δ_C (75.5 MHz, $CDCl_3$) 21.7 (CH_3, $ArCH_3$), 51.7 [CH, one of C(3)H or C(4)H], 65.0 [CH, one of C(3) or C(5)H], 129.0 (CH, CH_{Ar}), 129.1 (CH, CH_{Ar}), 129.2 (CH, CH_{Ar}), 129.9 (CH, CH_{Ar}), 130.8 [C, $C_{Ar(q)}$], 135.4 [C, $C_{Ar(q)}$], 145.6 [C, C(3)], 169.4 (C, one of C=O), 172.9 (C, one of C=O) ppm; HRMS (ES+): Exact mass calculated for $C_{18}H_{15}N_3O_4S$ $[M+H]^+$ 370.0862. Found 370.0857.

** ^1H and ^{13}C NMR spectra were recorded for the crude reaction mixture indicating the formation of the pyrazoline **159**. These signals are tentatively outlined below despite not being isolated in pure form.*

5-Phenyl-3-tosyl-3a,6a-dihydropyrrolo[3,4-c]pyrazole-4,6(3*H*,5*H*)-dione 159

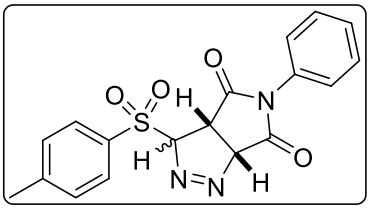

δ_H (300 MHz, $CDCl_3$) 2.42 (3H, s, $ArCH_3$), 3.98 [1H, dd, *J* 7.7, 2.7 Hz, pyrazoline ring CH], 5.92 [1H, dd, *J* 7.7, 2.7 Hz, pyrazoline ring CH], 6.42 [1H, dd (appears as t), *J* 2.6 Hz, pyrazoline ring CH], 7.10-7.20 (2H, m, ArH), 7.16-7.31 (5H, m, ArH), 7.63 (2H, d, *J* 8.4 Hz, ArH) ppm; δ_C (75.5 MHz, $CDCl_3$) 21.2 (CH_3, $ArCH_3$), 38.7 [CH, C(4)H], 94.5 [CH, C(5)H], 106.8 [CH, C(3)H], 125.9 (CH, CH_{Ar}), 128.8 (CH, CH_{Ar}), 128.9 (CH, CH_{Ar}), 129.2 (CH, CH_{Ar}), 129.7 (CH, CH_{Ar}), 130.5 (C, $C_{Ar(q)}$), 132.8 (C, $C_{Ar(q)}$), 146.6 (C, $C_{Ar(q)}$), 166.8 (C, C=O), 171.5 (C, C=O) ppm.

2.9.10.2 [3+2] Dipolar Cycloadditions of α-Diazoacetates with α-Thio-β-Chloroacrylamides

Ethyl 4-(phenylthio)-5-(4′-methylphenylcarbamoyl)-1*H*-pyrazole-3-carboxylate (major tautomer) and **ethyl 4-(phenylthio)-3-(4′-methylphenylcarbamoyl)-1*H*-pyrazole-5-carboxylate** (minor tautomer) **71**

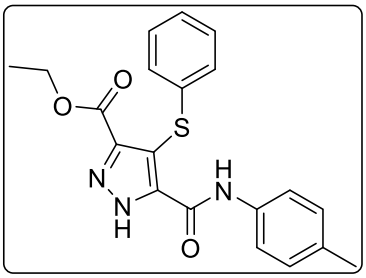

Ethyl diazoacetate (0.97 ml, 8 mmol, 87% in dichloromethane) was added in one portion to a solution of *N*-(4′-methylphenyl)-*Z*-3-chloro-2-(phenylthio)propenamide **9** (303 mg, 1 mmol) in toluene (5 ml) at room temperature. The solution was heated gradually to 100 °C and stirred under nitrogen for 24h. The cooled reaction mixture in toluene was transferred directly onto a silica gel column to prevent any potential degradation of unreacted EDA if concentrated. Purification by flash column chromatography using hexane: ethyl acetate (gradient elution 20-30% ethyl acetate) as eluent, followed by trituration with diethyl ether gave the pyrazole **71** as a white solid (245 mg, 64%); mp 155-158 °C; ν_{max}/cm^{-1} (ATR) 3188 (NH), 1717 (C=O ester), 1661 (C=O amide), 1235, 817, 737; δ_H (600 MHz, $CDCl_3$) 1.28 (3H, t, *J* 7.1 Hz, $OCH_2C\underline{H}_3$), 2.32 (3H, s, $ArCH_3$), 4.35 (2H, q, *J* 7.1 Hz, $OC\underline{H}_2CH_3$), 7.15 (2H, d, *J* 8.3 Hz, ArH), 7.17-7.30 (5H, m, ArH), 7.49 (2H, d, *J* 8.3 Hz, ArH), 9.95 (1H, br s, NH amide), 13.08 (1H, br s, NH pyrazole) ppm; δ_H (600 MHz, DMSO-d_6) 1.13 (3H, t, 7.1 Hz, $OCH_2C\underline{H}_3$), 2.25 (3H, s, $ArCH_3$), 4.20 (2H, q, *J* 7.0 Hz, $OC\underline{H}_2CH_3$), 7.11 (5H, app. t, unresolved coupling, ArH), 7.23 (2H, app. t, unresolved coupling, ArH), 7.51-7.61 (2H, m, ArH), 10.27 (1H, br s, NH amide), 14.80 (1H, br s, NH pyrazole) ppm; δ_H (600 MHz, Toluene-d_8) 1.01 (3H, t, *J* 7.1 Hz, $OCH_2C\underline{H}_3$), 2.04 (3H, s, $ArCH_3$), 4.07 (2H, q, *J* 7.1 Hz, $OC\underline{H}_2CH_3$), 6.74-6.92 (5H, m, ArH), 7.12-7.17 (2H, m, ArH), 7.55-7.60 (2H, m, ArH), 9.83 (1H, s, NH amide), 12.63 (1H, br s, NH pyrazole) ppm; δ_C (150.9 MHz, $CDCl_3$) 14.0 (CH_3, $OCH_2\underline{C}H_3$), 20.9 (CH_3, $ArCH_3$), 61.5 (CH_2, $O\underline{C}H_2CH_3$), 109.1 [C, br, C(4)], 120.3 (CH, CH_{Ar}), 126.8 (CH, CH_{Ar}), 127.4 (CH, CH_{Ar}), 129.3 (CH, CH_{Ar}), 129.6 (CH, CH_{Ar}), 134.1 (C, $C_{Ar(q)}$), 134.7 (C, $C_{Ar(q)}$), 135.0 (C, $C_{Ar(q)}$), 140.4 [C, br, one of C(3) or C(5)], 145.8 [C, br, one of C(3) or C(5)], 156.0 (C, C=O amide), 160.5 (C, C=O ester) ppm; δ_C (150.9 MHz, DMSO-d_6) 13.8 (CH_3, $OCH_2\underline{C}H_3$), 20.5 (CH_3, $ArCH_3$), 60.5 (CH_2, minor tautomer, $O\underline{C}H_2CH_3$), 61.3 (CH_2, major tautomer, $O\underline{C}H_2CH_3$), 108.5 [C, minor tautomer, C(4)], 111.4 [C, major tautomer, C(4)], 120.0 (CH, CH_{Ar}), 125.5 (CH, CH_{Ar}), 125.9 (CH, CH_{Ar}), 126.7 (CH, CH_{Ar}), 128.9, 129.0 129.3 (CH, overlapping broad signals, major and minor tautomers, CH_{Ar}), 132.7 (C, major tautomer, $C_{Ar(q)}$), 133.6 (C, minor tautomer, $C_{Ar(q)}$), 135.3 (C, minor tautomer, $C_{Ar(q)}$), 136.2 (C, major tautomer, $C_{Ar(q)}$),136.3 (C, major tautomer, $C_{Ar(q)}$), 136.8 (C, minor tautomer, $C_{Ar(q)}$), 137.5 [C, major tautomer, one of C(3) or C(5)],142.1 [C, minor tautomer, one of C(3) or C(5)], 144.8 [C, minor tautomer, one of C(3) or C(5)], 149.9 [C, major tautomer, one of C(3) or C(5)], 156.2 (C, minor tautomer, C=O amide), 158.0 (C, major tautomer, C=O amide), 159.2 (C, major tautomer, C=O ester), 160.8 (C, minor tautomer, C=O ester) ppm; δ_C (150.9 MHz, Toluene-d_8) 14.1 (CH_3, $OCH_2\underline{C}H_3$), 20.8 (CH_3, $ArCH_3$), 61.0 (CH_2, $O\underline{C}H_2CH_3$), 109.6 [C, br, C(4)], 120.2 (CH, CH_{Ar}), 126.8 (CH, CH_{Ar}), 129.4 (CH, CH_{Ar}), 129.9 (CH, CH_{Ar}), 134.4 (C, $C_{Ar(q)}$), 135.4 (C, $C_{Ar(q)}$), 135.8 (C, $C_{Ar(q)}$), 140.9 [C, br, one of C(3) or C(5)], 146.0 [C, br, one of C(3) or C(5)], 156.0 (C, C=O amide), 160.5 (C, C=O ester) ppm; HRMS (ES+): Exact mass calculated for $C_{20}H_{19}N_3O_3S$ $[M+H]^+$ 382.1208. Found 382.1215; m/z (ES+) 382.2 {$[(C_{20}H_{19}N_3O_3S)+H^+]$, 48%}, 782.7 (100%).

Note: *4 x CH_{Ar} signals observed for 5 x CH_{Ar} signals in ^{13}C NMR spectrum of pyrazole **71** in toluene-d_8. 1 CH_{Ar} signal overlapping with toluene-d_8 residual solvent peaks.*

Ethyl 5-(benzylcarbamoyl)-4-(phenylthio)-1*H*-pyrazole-3-carboxylate 172

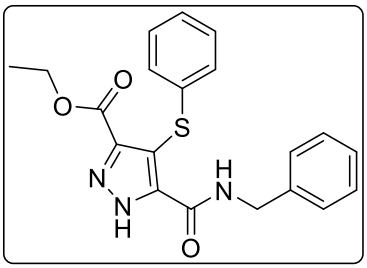

The title compound was prepared following the procedure described for **71** using ethyl diazoacetate (0.97 ml, 8 mmol, 87% in dichloromethane) and *N*-benzyl-*Z*-3-chloro-2-(phenylthio)-propenamide **40** (304 mg, 1 mmol) in toluene (5 ml). Purification by column chromatography on silica gel using hexane-ethyl acetate (gradient elution 20-40% ethyl acetate), followed by trituration with diethyl ether gave the pyrazole **172** as a white solid (149 mg, 39 %); mp 137-139˚C; ν_{max}/cm^{-1} (ATR) 3147 (NH stretch), 3060 (CH), 2940 (CH), 1720 (C=O ester), 1646 (C=O amide), 1557, 1224, 741; δ_H (600 MHz, $CDCl_3$) 1.28 (3H, t, *J* 7.0 Hz, $OCH_2C\underline{H}_3$), 4.34 (2H, q, *J* 7.0 Hz, $OC\underline{H}_2CH_3$), 4.66 (2H, d, *J* 5.4 Hz, CH_2NH), 6.98-7.33 (10H, m, ArH), 8.51 (1H, br s, NH amide), 13.52 (1H, br s, NH pyrazole) ppm; δ_C (150.9 MHz, $CDCl_3$) 14.0 (CH_3, OCH_2CH_3), 43.6 (CH_2, CH_2NH), 61.4 (CH_2, OCH_2CH_3), 109.0 [C, br, C(4)], 126.5 (CH, CH_{Ar}), 127.0 (CH, CH_{Ar}), 127.5 (CH, CH_{Ar}), 127.6 (CH, CH_{Ar}), 128.7 (CH, CH_{Ar}), 129.2 (CH, CH_{Ar}), 134.8 (C, $C_{Ar(q)}$), 136.7 (C, $C_{Ar(q)}$), 139.7 [C, br, one of C(3) or C(5)], 146.2 [C, br, one of C(3) or C(5)], 158.2 (C, C=O amide), 160.7 (C, C=O ester) ppm; HRMS (ES+): Exact mass calculated for $C_{20}H_{19}N_3O_3S$ $[M+H]^+$ 382.1220. Found 382.1225; m/z (ES+) 382.2 {$[(C_{20}H_{19}N_3O_3S)+H^+]$, 100%}.

Ethyl 5-((4′-fluorophenyl)carbamoyl)-4-(phenylthio)-1*H*-pyrazole-3-carboxylate 173

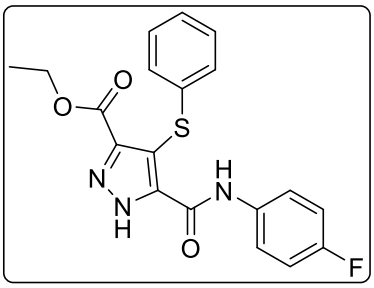

The title compound was prepared following the procedure described for **71** using ethyl diazoacetate (0.97 ml, 8 mmol, 87% in dichloromethane) and *N*-(4′-fluorophenyl)-*Z*-3-chloro-2-(phenylthio)propenamide **41** (307 mg, 1 mmol) in toluene (5 ml). Purification by flash column chromatography on silica gel using hexane: ethyl acetate (gradient elution 20-30% ethyl acetate), followed by trituration with diethyl ether gave the pyrazole **173** as a white solid (210 mg, 55 %); mp 151-154 °C; Found C, 58.75; H, 4.26; N, 10.59; $C_{19}H_{16}N_3O_3SF$ requires C, 59.21; H, 4.18; N, 10.90 %; ν_{max}/cm^{-1} (ATR) 3376 (NH stretch), 3246 (NH), 3059 (CH), 1686 (C=O amide), 1529, 1208, 747; ν_{max}/cm^{-1} (NaCl) 3266 (NH) stretch, 1727 (C=O ester), 1677 (C=O amide), 1509, 1215; δ_H (600 MHz, $CDCl_3$) 1.27 (3H, t, *J* 7.1 Hz, $OCH_2C\underline{H}_3$), 4.34 (2H, q, *J* 7.1 Hz, $OC\underline{H}_2CH_3$), 7.03 (2H, t, *J* 8.5 Hz, ArH), 7.12-7.40 (5H, m, ArH), 7.47-7.66 (2H, m, ArH), 9.98 (1H, br s, NH amide), 13.22 (1H, br s, NH pyrazole) ppm; δ_C (150.9 MHz, $CDCl_3$) 13.9 (CH_3, $OCH_2\underline{C}H_3$), 61.6 (CH_2, $O\underline{C}H_2CH_3$), 109.4 [C, br, C(4)], 115.8 [CH, d, $^2J_{CF}$ 22.7 Hz, C(3′)H], 122.1 [CH, d, $^3J_{CF}$ 8.0 Hz, C(2′)H], 126.8 (CH, CH_{Ar}), 127.3 (CH, CH_{Ar}), 129.4 (CH, CH_{Ar}), 132.7 [C, d, $^4J_{CF}$ 2.7 Hz, $C(1')_{Ar(q)}NH$], 134.6 (C, $C_{Ar(q)}$), 140.3 [C, br, one of C(3) or C(5)], 145.5 [C, br, one of C(3) or C(5)], 156.2 (C, C=O amide), 158.4 [C, d, $^1J_{CF}$ 243.4 Hz, $C(4')_{Ar(q)}F$], 160.3 (C, C=O ester) ppm; HRMS (ES+): Exact mass calculated for $C_{19}H_{16}N_3O_3SF$ $[M+H]^+$ 386.0975. Found 386.0965; m/z (ES+) 386.2 {$[(C_{19}H_{16}N_3O_3SF)+H^+]$, 60%}, 790.6 (100%).

Ethyl 5-(2′,2′-dimethylpropylcarbamoyl)-4-(phenylthio)-1*H*-pyrazole-3-carboxylate 174

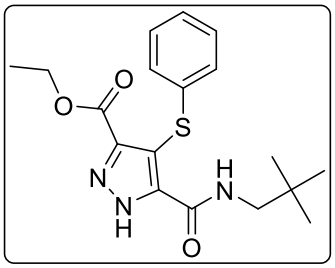

The title compound was prepared following the procedure described for **71** using ethyl diazoacetate (0.97 ml, 8 mmol, 87% in dichloromethane) and *N*-(2′,2′-dimethylpropyl)-*Z*-3-chloro-2-(phenylthio)propenamide **42** (283 mg, 1 mmol) in toluene (5 ml). Purification by column chromatography on silica gel using hexane: ethyl acetate (gradient elution 15-25% ethyl acetate), followed by trituration with diethyl ether gave a 41:59 mixture of pyrazole **174** and pyrazoline

190 as a white solid. Further purification by flash column chromatography on silica gel using dichloromethane: ethyl acetate (gradient elution 15-20% ethyl acetate) gave the pyrazole **174** as a white solid (97 mg, 27 %); mp 175-178°C; ν_{max}/cm^{-1} (ATR) 3293 (NH stretch), 3152 (CH), 1725 (C=O ester), 1651 (C=O amide), 1223, 739; δ_H (600 MHz, $CDCl_3$) 0.87 [9H, s, $C(CH_3)_3$], 1.28 (3H, t, *J* 7.1 Hz, $OCH_2C\underline{H}_3$), 3.29 (2H, d, *J* 6.2 Hz, $C\underline{H}_2NH$), 4.34 (2H, q, *J* 7.1 Hz, $OC\underline{H}_2CH_3$), 7.10 (2H, d, *J* 7.6 Hz, ArH), 7.17 (1H, t, *J* 7.4 Hz, ArH), 7.26 (2H, t, *J* 7.7 Hz, ArH), 8.31 (1H, br s, NH amide), 13.54 (1H, br s, NH pyrazole) ppm; δ_C (150.9 MHz, $CDCl_3$) 14.0 (CH_3, $OCH_2\underline{C}H_3$), 27.1 [CH_3, $C(\underline{C}H_3)_3$], 31.6 [C, $\underline{C}(CH_3)_3$], 50.9 (CH_2, CH_2NH), 61.3 (CH_2, $O\underline{C}H_2CH_3$), 107.8 [C, br, C(4)], 126.3 (CH, CH_{Ar}), 126.4 (CH, CH_{Ar}), 129.2 (CH, CH_{Ar}), 134.8 (C, $C_{Ar(q)}$), 140.1 [C, br, one of C(3) or C(5)], 146.4 [C, br, one of C(3) or C(5)], 158.3 (C, C=O amide), 160.7 (C, C=O ester) ppm; HRMS (ES+): Exact mass calculated for $C_{18}H_{23}N_3O_3S$ $[M+H]^+$ 362.1521. Found 362.1521; m/z (ES+) 362.2 {$[(C_{18}H_{23}N_3O_3S)+H^+]$, 68%}.

Ethyl 5-((4′-methoxyphenyl)carbamoyl)-4-(phenylthio)-1*H*-pyrazole-3-carboxylate 175

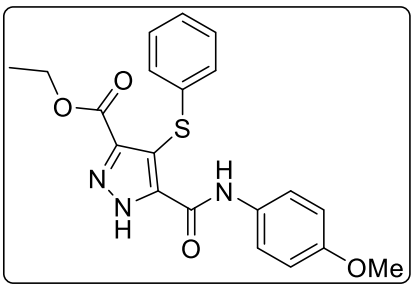

The title compound was prepared following the procedure described for **71** using ethyl diazoacetate (0.97 ml, 8 mmol, 87% in dichloromethane) and *N*-(4′-methoxyphenyl)-*Z*-3-chloro-2-(phenylthio)propenamide **43** (319 mg, 1 mmol) in toluene (5 ml). Purification by flash column chromatography on silica gel using hexane: ethyl acetate (gradient elution 20-30% ethyl acetate), followed by trituration with diethyl ether gave the pyrazole **175** as a white solid (159 mg, 40 %); mp 152-156°C; Found C, 60.24; H, 4.86; N, 10.45. $C_{20}H_{19}N_3O_4S$ requires C, 60.44; H, 4.82; N, 10.57 %; ν_{max}/cm^{-1} (ATR) 3154 (NH), 2950 (CH), 1722 (C=O ester), 1651 (C=O amide), 1508, 1232, 828, 739; δ_H (600 MHz, $CDCl_3$) 1.28 (3H, t, *J* 7.2 Hz, $OCH_2C\underline{H}_3$), 3.79 (3H, s, OCH_3), 4.35 (2H, q, *J* 7.2 Hz, $OC\underline{H}_2CH_3$), 6.85-6.91 (2H, m, ArH), 7.15-7.32 (5H, m, ArH), 7.48-7.56 (2H, m, ArH), 9.93 (1H, br s, NH amide), 13.31 (1H, br s, NH pyrazole) ppm; δ_C (150.9 MHz, $CDCl_3$) 14.0 (CH_3, $OCH_2\underline{C}H_3$), 55.4 (CH_3, $ArOCH_3$), 61.5 (CH_2, $O\underline{C}H_2CH_3$), 108.9 [C, br, C(4)], 114.2 (CH, CH_{Ar}), 122.0 (CH, CH_{Ar}), 126.8 (CH, CH_{Ar}), 127.2 (CH, CH_{Ar}), 129.4 (CH, CH_{Ar}), 129.7 (C, $C_{Ar(q)}$), 134.7 (C, $C_{Ar(q)}$), 140.1 [C, br, one of C(3) or C(5)], 146.1 [C, br, one of C(3) or C(5)], 155.9 (C, C=O amide), 157.1 (C, $C_{Ar(q)}$), 160.5 (C, C=O ester) ppm; HRMS (ES+): Exact mass calculated for $C_{20}H_{19}N_3O_4S$ $[M+H]^+$ 398.1175. Found 398.1166; m/z (ES+) 398.2 {$[(C_{20}H_{19}N_3O_4S)+H^+]$, 70%}, 814.7 (100%).

Ethyl 5-(*n*-butylcarbamoyl)-4-(phenylthio)-1*H*-pyrazole-3-carboxylate 176

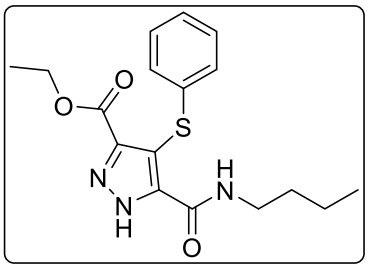

The title compound was prepared following the procedure described for **71** using ethyl diazoacetate (0.97 ml, 8 mmol, 87% in dichloromethane) and *N*-*n*-butyl-*Z*-3-chloro-2-(phenylthio)-propenamide **44** (269 mg, 1 mmol) in toluene (5 ml). Purification by flash column chromatography on silica gel using hexane: ethyl acetate (gradient elution 35-40% ethyl acetate) afforded the pyrazole **176** with minor impurities. Further purification by flash column chromatography on silica gel using dichloromethane-ethyl acetate (gradient elution 10-30% ethyl acetate) gave the pyrazole **176** as a white solid (231 mg, 67 %); mp 93-95˚C; ν_{max}/cm^{-1} (ATR) 3327 (NH stretch), 3099, 2930 (CH), 1722 (C=O ester), 1642 (C=O amide), 1218, 738; δ_H (600 MHz, $CDCl_3$) 0.87 (3H, t, *J* 7.3 Hz, $C(4')H_3$], 1.21-1.33 [5H, m, $OCH_2C\underline{H}_3$ and $C(3')H_2$], 1.44-1.55 [2H, m, $C(2')H_2$], 3.47 [2H, q, *J* 6.9 Hz, $C(1')H_2$], 4.34 (2H, q, *J* 7.1 Hz, $OC\underline{H}_2CH_3$), 7.13 (2H, d, *J* 7.6 Hz, ArH), 7.18 (1H, t, *J* 7.3 Hz, ArH), 7.26 (2H, app. t, unresolved coupling, ArH), 8.16 (1H, br s, NH amide), 13.46 (1H, br s, NH pyrazole) ppm; δ_C (150.9 MHz, $CDCl_3$) 13.6 [CH_3, $C(4')H_3$], 14.0 (CH_3, $OCH_2\underline{C}H_3$), 19.9 [CH_2, $C(3')H_2$], 31.0 [CH_2, $C(2')H_2$], 39.4 [CH_2, $C(1')H_2$], 61.3 (CH_2, $O\underline{C}H_2CH_3$), 108.5 [C,

C(4)], 126.5 (CH, CH_{Ar}), 126.8 (CH, CH_{Ar}), 129.2 (CH, CH_{Ar}), 135.0 (C, $C_{Ar(q)}$), 140.1 [C, C(3) or C(5)], 146.1 [C, C(3) or C(5)], 158.2 (C, C=O amide), 160.7 (C, C=O ester) ppm; HRMS (ES+): Exact mass calculated for $C_{17}H_{21}N_3O_3S$ $[M+H]^+$ 348.1376. Found 348.1377; m/z (ES+) 348.3 {[($C_{17}H_{21}N_3O_3S$)+H^+], 84%}, 714.7 (100%).

Ethyl 4-(benzylthio)-3-carbamoyl-1*H*-pyrazole-5-carboxylate (major tautomer) and **ethyl 4-(benzylthio)-5-carbamoyl-1*H*-pyrazole-3-carboxylate** (minor tautomer) **177**

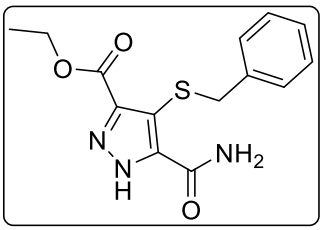

The title compound was prepared following the procedure described for **71** using ethyl diazoacetate (0.97 ml, 8 mmol, 87% in dichloromethane) and *Z*-3-chloro-2-(benzylthio)propenamide **45** (213 mg, 1 mmol)) in toluene (5 ml). A precipitate formed as the reaction progressed. After 24 h the reaction mixture was concentrated to dryness under reduced pressure and diethyl ether (10 ml) was added. The product was collected by filtration through a sintered glass funnel (grade 4), was washed thoroughly with cold diethyl ether, to give the pure pyrazole **177** as a white solid (208 mg, 71 %); mp 197-200 °C; Found C, 54.75; H, 4.92; N, 13.31. $C_{14}H_{15}N_3O_3S$ requires C, 55.07; H, 4.95; N, 13.76; ν_{max}/cm^{-1} (ATR) 3358 (NH stretch), 3149 (NH), 2975 (CH), 1728 (C=O ester), 1688 (C=O amide), 1233, 700; δ_H (300 MHz, DMSO-d_6) 1.31 (3H, t, *J* 7.1 Hz, $OCH_2C\underline{H}_3$), 4.11 (2H, s, SCH_2), 4.30 (2H, q, *J* 7.1 Hz, $OC\underline{H}_2CH_3$), 6.95-7.38 (5H, m, ArH), 7.52 (1H, br s, NH amide), 7.70 (1H, br s, NH amide), 14.28 (1H, br s, NH pyrazole) ppm; δ_H (600 MHz, DMSO-d_6) 1.31 (3H, br t, unresolved coupling, $OCH_2C\underline{H}_3$), 4.11 (2H, br s, SCH_2), 4.30 (2H, br s, $OC\underline{H}_2CH_3$), 6.97-8.06 (7H, m, 5 x ArH and 2 x NH amide; major and minor tautomers of NH amide), 14.31 (1H, br s, NH pyrazole) ppm; δ_C (150.9 MHz, DMSO-d_6)14.1 (CH_3, $OCH_2\underline{C}H_3$), approx. 39.5 [CH_2, SCH_2 (overlapping with DMSO-d_6 residual solvent signal)], 60.6 (CH_2, major tautomer, $O\underline{C}H_2CH_3$), 61.0 (CH_2, minor tautomer, $O\underline{C}H_2CH_3$), 110.0 [C, br, major tautomer, C(4)], 114.3 [C, br, minor tautomer, C(4)], 127.1 (CH, br, overlapping tautomers, CH_{Ar}), 128.2 (CH, br, CH_{Ar}), 128.8 (CH, CH_{Ar}), 135.4 (C, br, minor tautomer, $C_{Ar(q)}$), 137.2 (C, br, major tautomer, $C_{Ar(q)}$), 137.8 [C, br, minor tautomer, one of C(3), or C(5)], 139.9 [C, br, major tautomer, one of C(3) or C(5)], 145.0 [C, br, major tautomer, one of C(3) or C(5)], 148.2 [C, br, minor tautomer, one of C(3) or C(5)], 158.2 (C, br, minor tautomer, C=O amide), 159.1 (C, br, major tautomer, C=O amide), 161.2 (C, br, major tautomer, C=O ester), 163.0 (C, br, minor tautomer, C=O ester) ppm; HRMS (ES+): Exact mass calculated for m/z $C_{14}H_{15}N_3O_3S$ $[M+H]^+$ 306.0912. Found 306.0907; (ES+) 306.2 {[($C_{14}H_{15}N_3O_3S$)+H^+], 56%}, 630.5 (100%).

Ethyl 4-(benzylthio)-5-(butylcarbamoyl)-1*H*-pyrazole-3-carboxylate 178

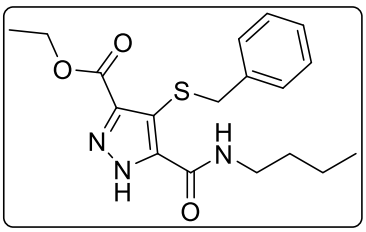

The title compound was prepared following the procedure described for **71** using ethyl diazoacetate (0.97 ml, 8 mmol, 87% in dichloromethane) and *N-n*-butyl-*Z*-3-chloro-2-(benzylthio)-propenamide **46** (283 mg, 1 mmol) in toluene (5 ml). Purification by flash column chromatography using hexane: ethyl acetate (65:35) as eluent afforded the pyrazole **178** with minor impurities. Further purification by column chromatography on silica gel using dichloromethane-ethyl acetate (gradient elution 10-20% ethyl acetate) gave the pure pyrazole **178** a clear oil (189 mg, 52 %); ν_{max}/cm^{-1} (ATR) 3158 (NH stretch), 2936 (CH), 1721 (C=O ester), 1628 (C=O amide), 1568, 1228; δ_H (300 MHz, $CDCl_3$) 0.95 [3H, t, *J* 7.2 Hz, C(4')H_3], 1.21-1.52 [4H, m, C(2')H_2 and C(3')H_2 overlapping with 3H, t, *J* = 7.1 Hz, $OCH_2C\underline{H}_3$], 3.25 [2H, m, C(1')H_2], 4.11 (2H, s, SCH_2), 4.47 (2H, q, *J* 7.1 Hz, $OC\underline{H}_2CH_3$), 6.96-7.06 (2H, m, ArH), 7.15-7.26 (3H, m, ArH), 7.92 (1H, br t, unresolved coupling, NH amide), 13.13 (1H, br s, NH pyrazole) ppm; δ_C (75.5 MHz, $CDCl_3$) 13.6 [CH_3, C(4')H_3], 14.2 (CH_3, $OCH_2\underline{C}H_3$), 20.1 [CH_2, C(3')H_2], 31.0 [CH_2, C(2')H_2], 39.1 [CH_2, C(1')H_2], 41.1 (CH_2, SCH_2), 61.3 (CH_2,

$OC\underline{H}_2CH_3$), 110.4 [C, one of C(4)], 127.6 (CH, CH_{Ar}), 128.5 (CH, CH_{Ar}), 128.6 (CH, CH_{Ar}), 137.2 (C, $C_{Ar(q)}$), 139.7 [C, br, one of C(3) or C(5)], 145.8 [C, br, one of C(3) or C(5)], 158.2 (C, C=O amide), 161.3 (C, C=O ester) ppm; HRMS (ES+): Exact mass calculated for $C_{18}H_{23}N_3O_3S$ $[M+H]^+$ 362.1533. Found 362.1527; m/z (ES+) 362.2 {[($C_{18}H_{23}N_3O_3S$)+H^+], 40%}.

Ethyl 4-(benzylthio)-5-(phenylcarbamoyl)-1*H*-pyrazole-3-carboxylate 179

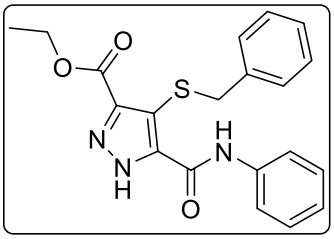

The title compound was prepared following the procedure described for **71** using ethyl diazoacetate (0.97 ml, 8 mmol, 87% in dichloromethane) and *N*-phenyl-*Z*-3-chloro-2-(benzylthio)-propenamide **179** (303 mg, 1 mmol) in toluene (5 ml). Purification by flash column chromatography on silica gel using hexane: ethyl acetate (80:20) as eluent followed by trituration with diethyl ether gave a 91:9 mixture of pyrazole **179** and pyrazoline **190** as a white solid. Further purification by flash column chromatography using dichloromethane: ethyl acetate (gradient elution 5-20% ethyl acetate) gave the pyrazole **179** as a white solid (108 mg, 28 %); mp 159-162°C; Found C, 62.74; H, 5.07; N, 10.57; $C_{20}H_{19}N_3O_3S$ requires C, 62.98; H, 5.02; N, 11.02 %; ν_{max}/cm^{-1} (ATR) 3258 (NH stretch), 3063 (CH), 1724 (C=O ester), 1684 (C=O amide), 1555, 1235, 749, 688; δ_H (600 MHz, $CDCl_3$) 1.48 (3H, t, *J* 7.1 Hz, $OCH_2C\underline{H}_3$), 4.17 (2H, s, SCH_2), 4.50 (2H, q, *J* 7.1 Hz, $O\underline{C}H_2CH_3$), 6.98-7.19 (6H, m, ArH), 7.34 (2H, t, unresolved coupling, ArH), 7.50 (2H, d, *J* 7.9 Hz, ArH), 9.85 (1H, br s, NH amide), 12.77 (1H, br s, NH pyrazole) ppm; δ_C (150.9 MHz, $CDCl_3$) 14.2 (CH_3, $OCH_2\underline{C}H_3$), 41.4 (CH_2, SCH_2), 61.6 (CH_2, $O\underline{C}H_2CH_3$), 110.7 [C, br, C(4)] , 120.2 (CH, CH_{Ar}), 125.0 (CH, CH_{Ar}), 127.7 (CH, CH_{Ar}), 128.5 (CH, CH_{Ar}), 128.6 (CH, CH_{Ar}), 129.0 (CH, CH_{Ar}), 136.7 (C, $C_{Ar(q)}$), 136.8 (C, $C_{Ar(q)}$), 140.0 [C, br, one of C(3) or C(5)], 145.8 [C, br, one of C(3) or C(5)], 155.9 (C, C=O amide), 161.1 (C, C=O ester) ppm; HRMS (ES+): Exact mass calculated for m/z $C_{20}H_{19}N_3O_3S$ $[M+H]^+$ 382.1208. Found 382.1212; m/z (ES+) 382.2 {[($C_{20}H_{19}N_3O_3S$)+H^+], 34%}.

Ethyl 5-(benzylcarbamoyl)-4-(benzylthio)-1*H*-pyrazole-3-carboxylate 180

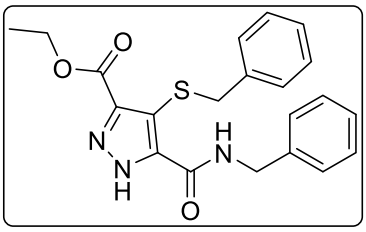

The title compound was prepared following the procedure described for **71** using ethyl diazoacetate (0.97 ml, 8 mmol, 87% in dichloromethane) and *N*-benzyl-*Z*-3-chloro-2-(phenylthio)-propenamide **48** (317 mg, 1 mmol) in toluene (5 ml). Purification by flash column chromatography using hexane: ethyl acetate (gradient elution 25-30% ethyl acetate), followed by trituration with diethyl ether gave the pyrazole **180** as a white solid (237 mg, 60 %); mp 105-107˚C; ν_{max}/cm^{-1} (ATR) 3159 (NH stretch), 3028 (CH), 1727 (C=O ester), 1627 (C=O amide), 1567, 1226, 692; Found C, 63.49; H, 5.38; N, 10.44; $C_{21}H_{21}N_3O_3S$ requires C, 63.78; H, 5.35; N, 10.44; δ_H (600 MHz, $CDCl_3$) 1.46 (3H, t, *J* 7.1 Hz, $OCH_2C\underline{H}_3$), 4.06 (2H, s, SCH_2), 4.41-4.53 [4H, m, overlapping 2H quartet (*J* 7.1 Hz) and 2H doublet (*J* 6.5 Hz), $OC\underline{H}_2CH_3$ and $C\underline{H}_2NH$ respectively], 6.87 (2H, d, *J* 7.3 Hz, ArH), 7.06-7.19 (3H, m, ArH), 7.22-7.43 (5H, m, ArH), 8.31 (1H, br s, NH amide), 13.06 (1H, br s, NH pyrazole) ppm; δ_C (150.9 MHz, $CDCl_3$) 14.2 (CH_3, $OCH_2\underline{C}H_3$), 41.0 (CH_2, SCH_2), 43.5 (CH_2, CH_2NH), 61.4 (CH_2, $O\underline{C}H_2CH_3$), 110.8 (C, C(4)], 127.5 (CH, CH_{Ar}), 127.7 (CH, CH_{Ar}), 127.9 (CH, CH_{Ar}), 128.5 (CH, br, 2 overlapping CH_{Ar} environments), 128.8 (CH, CH_{Ar}), 136.9 (C, 2 overlapping $C_{Ar(q)}$), 139.4 [C, C(3) or C(5)], 145.8 [C, C(3) or C(5)], 158.2 (C, C=O amide), 161.3 (C, C=O ester) ppm; HRMS (ES+): Exact mass calculated for $C_{21}H_{21}N_3O_3S$ $[M+H]^+$ 396.1376. Found 396.1381; m/z (ES+) 396.2 {[($C_{21}H_{21}N_3O_3S$)+H^+], 92%}.

Ethyl 4-(benzylthio)-5-((4′-fluorophenyl)carbamoyl)-1*H*-pyrazole-3-carboxylate 181

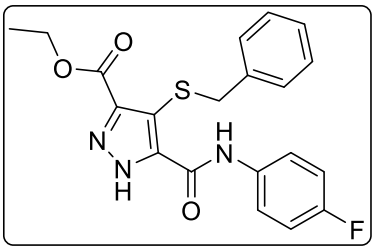

The title compound was prepared following the procedure described for **71** using ethyl diazoacetate (0.97 ml, 8 mmol, 87% in dichloromethane) and *N*-(4′-flurophenyl)-*Z*-3-chloro-2-(benzylthio)-propenamide **49** (321 mg, 1 mmol) in toluene (5 ml). Purification firstly by flash column chromatography on silica gel using hexane: ethyl acetate (70:30) as eluent, followed secondly by flash column chromatography on silica gel using dichloromethane: ethyl acetate (90:10) as eluent, followed by trituration with diethyl ether gave the pure pyrazole **181** as a white solid (75 mg, 19 %); mp 166-168˚C; ν_{max}/cm^{-1} (ATR) 3216 (NH stretch), 3158, 1725 (C=O ester), 1683 (C=O amide), 1561, 1510, 1213; δ_H (600 MHz, $CDCl_3$) 1.48 (3H, t, *J* 7.1 Hz, $OCH_2C\underline{H}_3$), 4.17 (2H, s, SCH_2), 4.50 (2H, q, *J* 7.1 Hz, $OC\underline{H}_2CH_3$), 6.95-7.18 (7H, m, ArH), 7.37-7.51 (2H, m, ArH), 9.79 (1H, br s, NH amide), 12.61 (1H, br s, NH pyrazole) ppm; δ_C (150.9 MHz, $CDCl_3$) 14.2 (CH_3, $OCH_2\underline{C}H_3$), 41.4 (CH_2, SCH_2), 61.7 (CH_2, $O\underline{C}H_2CH_3$), 110.8 [C, br, C(4)], 115.7 [CH, d, $^2J_{CF}$ 22.4 Hz, C(3′)H], 121.9 [CH, d, $^3J_{CF}$ 8.1 Hz, C(2′)H], 127.8 (CH, CH_{Ar}), 128.4 (CH, CH_{Ar}), 128.7 (CH, CH_{Ar}), 132.6 [C, d, $^4J_{CF}$ 2.9 Hz, C_{Ar}(1′)NH], 136.9 (C, $C_{Ar(q)}$), 139.8 [C, br, C(3) or C(5)], 146.0 [C, br, C(3) or C(5)], 155.9 (C, C=O amide), 159.7 [C, d, $^1J_{CF}$ 244.3 Hz, C_{Ar}(4′)F], 161.1 (C, C=O ester) ppm; HRMS (ES+): Exact mass calculated for $C_{20}H_{18}FN_3O_3S$ $[M+H]^+$ 400.1126. Found 400.1127; m/z (ES-) 398.2 {[($C_{20}H_{18}FN_3O_3S$)-H^+], 90%}.

Ethyl 4-(benzylthio)-5-(2′,2′-dimethylpropylcarbamoyl)-1*H*-pyrazole-3-carboxylate 182

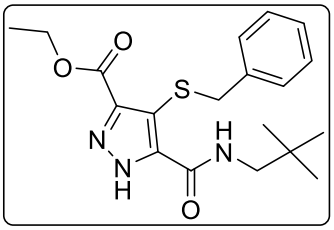

The title compound was prepared following the procedure described for **71** using ethyl diazoacetate (0.97 ml, 8 mmol, 87% in dichloromethane) and *N*-(2′,2′-dimethylpropyl)-*Z*-3-chloro-2-(phenylthio)propenamide **50** (297 mg, 1 mmol) in toluene (5 ml). Purification by flash column chromatography on silica gel using hexane: ethyl acetate (gradient elution 20-30% ethyl acetate) gave a 61:39 mixture of pyrazole **182** and pyrazoline **190** as a yellow oil. Further purification by flash column chromatography on silica gel using dichloromethane: ethyl acetate (gradient elution 10-20% ethyl acetate) gave the pyrazole **182** as a clear oil (223 mg, 59 %); ν_{max}/cm^{-1} (ATR) 3136 (NH stretch), 2956 (CH), 1721 (C=O ester), 1650 (C=O amide), 1557, 1222, 699; δ_H (600 MHz, $CDCl_3$) 0.93 [9H, s, $C(CH_3)_3$], 1.46 (3H, t, *J* 7.1 Hz, $OCH_2C\underline{H}_3$), 3.09 (2H, s, *J* 6.2 Hz, $C\underline{H}_2NH$), 4.14 (2H, s, SCH_2), 4.47 (2H, q, *J* 7.1 Hz, $OC\underline{H}_2CH_3$), 6.96-7.08 (2H, m, ArH), 7.13-7.25 (3H, m, ArH), 8.07 (1H, br t, unresolved splitting, NH amide), 13.15 (1H, br s, NH pyrazole) ppm; δ_C (150.9 MHz, $CDCl_3$) 14.2 (CH_3, $OCH_2\underline{C}H_3$), 27.3 [CH_3, $C(\underline{C}H_3)$], 31.6 (CH_2, SCH_2), 41.2 [C, $\underline{C}(CH_3)_3$], 50.7 (CH_2, CH_2NH), 61.4 (CH_2, $O\underline{C}H_2CH_3$), 110.5 [C, C(4)], 127.6 (CH, CH_{Ar}), 128.55 (CH, CH_{Ar}), 128.57 (CH, CH_{Ar}), 137.0 (C, $C_{Ar(q)}$), 139.6 [C, C(3) or C(5)], 145.7 [C, C(3) or C(5)], 158.4 (C, C=O amide), 161.3 (C, C=O ester) ppm; HRMS (ES+): Exact mass calculated for $C_{19}H_{25}N_3O_3S$ $[M+H]^+$ 376.1689. Found 376.1690; m/z (ES+) 376.3 {[($C_{19}H_{25}N_3O_3S$)+H^+], 40%}.

Ethyl 4-(benzylthio)-5-((4′-methoxyphenyl)carbamoyl)-1*H*-pyrazole-3-carboxylate 183

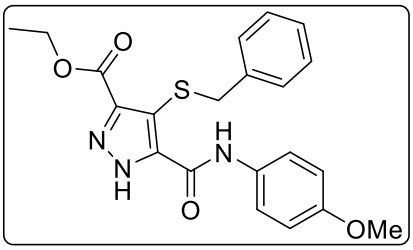

The title compound was prepared following the procedure described for **71** using ethyl diazoacetate (0.97 ml, 8 mmol, 87% in dichloromethane) and *N*-(4′-methoxyphenyl)-*Z*-3-chloro-2-(benzylthio)propenamide **51** (333 mg, 1 mmol) in toluene (5 ml). Purification by flash column chromatography using hexane-ethyl acetate (gradient elution 25-30% ethyl acetate), followed by trituration with diethyl ether gave the pyrazole **183** as a white

solid (227 mg, 55 %); mp 142-145°C; Found C, 60.78; H, 5.14; N, 9.70; $C_{21}H_{21}N_3O_4S$ requires C, 61.30; H, 5,14; N, 10.21; ν_{max}/cm^{-1} (ATR) 3263 (NH), 3202, 3147, 1722 (C=O ester), 1678 (C=O amide), 1509, 1232, 1172, 819; δ_H (600 MHz, $CDCl_3$) 1.47 (3H, t, *J* 7.2 Hz, $OCH_2C\underline{H}_3$), 3.81 (3H, s, OCH_3), 4.16 (2H, s, SCH_2), 4.49 (2H, q, *J* 7.2 Hz, $OC\underline{H}_2CH_3$), 6.83-6.92 (2H, m, ArH), 6.98-7.07 (2H, m, ArH), 7.09-7.17 (3H, m, ArH), 7.36-7.44 (2H, m, ArH), 9.75 (1H, br s, NH amide), 13.03 (1H, br s, NH pyrazole) ppm; δ_C (150.9 MHz, $CDCl_3$) 14.2 (CH_3, $OCH_2\underline{C}H_3$), 41.3 (CH_2, SCH_2), 55.4 (CH_3, $ArOCH_3$), 61.5 (CH_2, $O\underline{C}H_2CH_3$), 110.4 [C, br, C(4)], 114.0 (CH, CH_{Ar}), 121.7 (CH, CH_{Ar}), 127.6 (CH, CH_{Ar}), 128.4 (CH, CH_{Ar}), 128.6 (CH, CH_{Ar}), 129.7 (C, $C_{Ar(q)}$), 136.8 (C, $C_{Ar(q)}$), 139.9 [C, br, one of C(3) or C(5)], 145.7, [C, br, one of C(3) or C(5)], 155.7 (C, C=O amide), 156.7 (C, $C_{Ar(q)}$), 161.1 (C, C=O ester) ppm; HRMS (ES+): Exact mass calculated for $C_{21}H_{21}N_3O_4S$ $[M+H]^+$ 412.1307. Found 412.1318; m/z (ES+) 412.2 {[($C_{21}H_{21}N_3O_4S$)+H^+], 76%}, 842.8 (100%).

Ethyl 5-(benzylcarbamoyl)-4-(butylthio)-1*H*-pyrazole-3-carboxylate 184

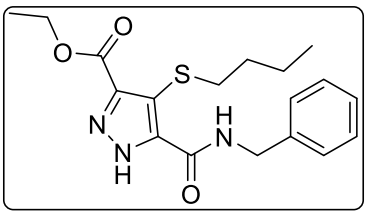

The title compound was prepared following the procedure described for **71** using ethyl diazoacetate (0.97 ml, 8 mmol, 87% in dichloromethane) and *N*-benzyl-*Z*-3-chloro-2-(*n*-butylthio)-propenamide **52** (269 mg, 1 mmol) in toluene (5 ml). Purification by flash column chromatography on silica gel using hexane-ethyl acetate (70: 30) as eluent gave a 40:60 mixture of pyrazole **184** and pyrazoline **190**. Further purification by flash column chromatography on silica gel using dichloromethane: ethyl acetate (gradient elution 10-20% ethyl acetate) as eluent gave the pure pyrazole **184** as a clear oil (159 mg, 44 %); ν_{max}/cm^{-1} (ATR) 3160 (NH stretch), 2959 (CH), 1721 (C=O ester), 1643 (C=O amide), 1562, 1224, 698; δ_H (300 MHz, $CDCl_3$) 0.80 [3H, t, *J* 7.3 Hz, C(4′)H_3], 1.26 [2H, sextet, *J* 7.3 Hz, C(3′)H_2], 1.33-1.46 [5H, m, overlapping 3H, t (*J* 7.1 Hz), and 2H, m, $OCH_2C\underline{H}_3$ and C(2′)H_2 respectively], 2.87 [2H, t, unresolved coupling, C(1′)H_2], 4.44 (2H, q, *J* 7.1 Hz, $OC\underline{H}_2CH_3$], 4.73 (2H, d, *J* 5.7 Hz, NCH_2), 7.19-7.45 (5H, m, ArH), 8.97 (1H, br s, NH amide), 13.37 (1H, br s, NH pyrazole) ppm; δ_C (75.5 MHz, $CDCl_3$) 13.5 [CH_3, C(4′)H_3], 14.1 [CH_3, $OCH_2C\underline{H}_3$], 21.7 [CH_2, C(3′)H_2], 31.3 [CH_2, C(2′)H_2], 36.6 [CH_2, SC(1′)H_2], 43.5 (CH_2, NCH_2), 61.3 (CH_2, $OC\underline{H}_2CH_3$), 112.2 [C, br, C(4)], 127.76 (CH, CH_{Ar}), 127.83 (CH, CH_{Ar}), 128.7 (CH, CH_{Ar}), 137.0 (C, $C_{Ar(q)}$), 139.0 [C, C(3) or C(5)], 145.7 [C, C(3) or C(5)], 158.7 (C, C=O amide), 161.1 (C, C=O ester) ppm; HRMS (ES+): Exact mass calculated for $C_{18}H_{23}N_3O_3S$ $\{M+H\}^+$ 362.1533. Found 362.1529; m/z (ES+) 362.2 {[($C_{18}H_{23}N_3O_3S$)+H^+], 20%}.

Ethyl 4-(*n*-butylthio)-5-(4′-methylphenylcarbamoyl)-1*H*-pyrazole-3-carboxylate 185

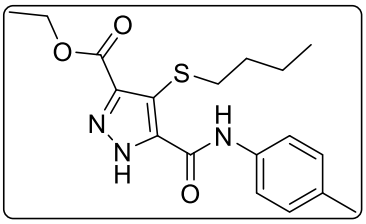

The title compound was prepared following the procedure described for **71** using ethyl diazoacetate (0.97 ml, 8 mmol, 87% in dichloromethane) and *N*-(4′-methylphenyl)-*Z*-3-chloro-2-(*n*-butylthio)propenamide **53** (269 mg, 1 mmol) in toluene (5 ml). Purification by flash column chromatography on silica gel using hexane: ethyl acetate (70: 30) as eluent, followed by trituration with diethyl ether gave the pure pyrazole **185** as a white solid (128 mg, 35 %); mp 139-140˚C; ν_{max}/cm^{-1} (ATR) 3258 (NH stretch), 2923 (CH), 1725 (C=O ester), 1684 (C=O amide), 1551, 1236, 807; δ_H (600 MHz, $CDCl_3$) 0.87 [3H, t, *J* 7.3 Hz, C(4′)H_3], 1.35-1.48 [5H, overlapping 3H, t (*J* 7.1 Hz) and 2H, m, $OCH_2C\underline{H}_3$ and C(3′)H_2 respectively], 1.54-1.62 [2H, m, C(2′)H_2], 2.35 (3H, s, $ArCH_3$), 3.00 [2H, t, unresolved coupling, C(1′)H_2], 4.47 (2H, q, *J* 7.1 Hz, $OC\underline{H}_2CH_3$), 7.20 (2H, d, *J* 8.3 Hz, ArH), 7.60 (2H, d, *J* 8.4 Hz, ArH), 10.49 (1H, br s, NH amide), 12.90 (1H, br s, NH pyrazole) ppm; δ_C (150.9 MHz, $CDCl_3$) 13.5 [CH_3, $ArCH_3$], 14.2 (CH_3, $OCH_2\underline{C}H_3$), 20.9 (CH_3, $ArCH_3$), 21.9 [CH_2, C(3′)H_2], 31.5 [CH_2, C(2′)H_2], 36.8 [CH_2, C(1′)H_2], 61.4 (CH_2, $OC\underline{H}_2CH_3$), 111.8 [C, C(4)], 120.1 (CH, CH_{Ar}), 129.7 (CH, CH_{Ar}), 134.4 (C, $C_{Ar(q)}$), 134.9

(C, $C_{Ar(q)}$), 139.2 [C, C(3) or C(5)], 146.0 [C, C(3) or C(5)], 156.3 (C, C=O amide), 161.1 (C, C=O ester) ppm; HRMS (ES+): Exact mass calculated for $C_{18}H_{23}N_3O_3S$ $[M+H]^+$ 362.1533. Found 362.1532; m/z (ES+) 362.2 {[($C_{18}H_{23}N_3O_3S$)+H^+], 84%}.

3-Ethyl 5-methyl 4-(phenylthio)-1*H*-pyrazole-3,5-dicarboxylate 186

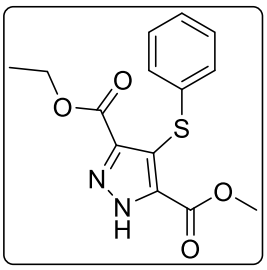

The title compound was prepared following the procedure described for **71** using ethyl diazoacetate (0.97 ml, 8 mmol, 87% in dichloromethane) and methyl-*Z*-3-chloro-2-(phenylthio)propenoate **69** (228 mg, 1 mmol) in toluene (5 ml). Purification by flash column chromatography on silica gel using hexane: ethyl acetate (70:30) as eluent gave the pyrazole **186** as a yellow oil with minor impurities. Further purification by column chromatography on silica gel using dichloromethane: ethyl acetate (90:10) as eluent gave the pure pyrazole **186** as a clear oil which solidified overnight to give a white solid (150 mg, 49 %); mp 84-86˚C; ν_{max}/cm^{-1} (ATR) 3236 (NH stretch), 1723 (C=O ester), 1681 (C=O ester), 1224, 734; δ_H (600 MHz, $CDCl_3$) 1.22 (3H, t, *J* 7.1 Hz, $OCH_2C\underline{H}_3$), 3.83 (3H, s, OCH_3), 4.30 (2H, q, *J* 7.1 Hz, $OC\underline{H}_2CH_3$), 7.04-7.26 (5H, m, ArH), 12.90 (1H, br s, NH) ppm; δ_C (150.9 MHz, $CDCl_3$) 13.8 (CH_3, $OCH_2\underline{C}H_3$), 52.3 (CH_3, OCH_3), 61.8 (CH_2, OCH_2CH_3), 116.2 [C, C(4)], 125.9 (CH, CH_{Ar}), 127.7 (CH, CH_{Ar}), 128.7 (CH, CH_{Ar}), 136.9 (C, $C_{Ar(q)}$), 141.0 [C, br, overlapping C(3) and C(5)], 159.6 (C, br, C=O ethyl ester), 160.2 (C, br, C=O methyl ester) ppm; HRMS (ES+): Exact mass calculated for $C_{14}H_{14}N_2O_4S$ $[M+H]^+$ 307.0747. Found 307.0746; m/z (ES+) 307.2 {[($C_{14}H_{14}N_2O_4S$)+H^+], 60%}.

Benzyl 4-(phenylthio)-3-(4′-methylphenylcarbamoyl)-1*H*-pyrazole-5-carboxylate (major tautomer) and **benzyl 4-(phenylthio)-5-(4′-methylphenylcarbamoyl)-1*H*-pyrazole-3-carboxylate** (minor tautomer) **187**

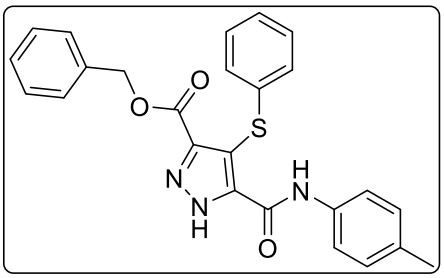

The title compound was prepared following the procedure described for **71** using benzyl diazoacetate (1.34 ml, 8 mmol, 90% in dichloromethane) and *N*-(4′-methylphenyl)-*Z*-3-chloro-2-(phenylthio)propenamide **9** (304 mg, 1 mmol) in toluene (5 ml). Purification by flash column chromatography using hexane: ethyl acetate (gradient elution 20-40% ethyl acetate) as eluent, followed by trituration with diethyl ether gave the pure pyrazole **187** as a white solid (279 mg, 63 %); mp 158-160˚C; Found C, 67.24; H, 4.79; N, 9.62; $C_{25}H_{21}N_3O_3S$ requires C, 67.70; H, 4.77; N, 9.47; ν_{max}/cm^{-1} (ATR) 3281 (NH stretch), 3169 (NH), 3048 (CH), 1724 (C=O ester), 1654 (C=O amide), 1554, 1232; δ_H (300 MHz, DMSO-d_6) 2.26 (3H, s, $ArCH_3$), 5.29 (2H, s, OCH_2Ph), 6.98-7.68 (14H, m, ArH), 10.25 (1H, br s, NH amide), 14.85 (1H, br s, NH pyrazole) ppm; δ_H (600 MHz, DMSO-d_6) 2.26 (3H, s, $ArCH_3$), 5.25 and 5.30 (1H, overlapping broad singlets, minor and major tautomers respectively, OCH_2], 6.98-7.67 [14H, m, broadness observed, CH_{Ar}], 10.26 and 10.31 (1H, overlapping broad singlets, major and minor tautomers respectively, NH amide), 14.83 and 14.91 (1H, overlapping broad singlets, minor and major tautomers respectively) ppm; δ_C (150.9 MHz, DMSO-d_6) 20.5 (CH_3, $ArCH_3$), 66.0 (CH_2, br, minor tautomer, OCH_2), 66.6 (CH_2, br, major tautomer, OCH_2), 108.7 [C, br, minor tautomer, C(4)], 111.3 [C, br, major tautomer, C(4)], 119.7 and 119.9 [CH, overlapping broad singlets, minor and major tautomers respectively, CH_{Ar}], 125.5 (CH, br, major tautomer, CH_{Ar}), 125.9 (CH, br, minor tautomer), 126.8 (CH, CH_{Ar}), 127.9 (CH, CH_{Ar}), 128.1 (CH, CH_{Ar}), 128.4 (CH, CH_{Ar}), 128.7-129.5 (CH, m, complex overlap of broad signals, multiple overlapping major and minor tautomers, CH_{Ar}), 132.7 (C, br, major tautomer, $C_{Ar(q)}$), 133.6 (C, br, minor tautomer, $C_{Ar(q)}$), 135.3 (C, br, major tautomer, $C_{Ar(q)}$), 135.8 (C, br, minor tautomer, $C_{Ar(q)}$), 136.1 (C, br, major tautomer, $C_{Ar(q)}$), 136.6 (C, br, minor tautomer, $C_{Ar(q)}$), 137.3

[C, br, major tautomer, one of C(3) or C(5)], 142.3 [C, br, minor tautomer, one of C(3) or C(5)], 144.4 [C, br, minor tautomer, one of C(3) or C(5)], 150.1 [C, br, major tautomer, one of C(3) or C(5)], 156.1 (C, br, minor tautomer, C=O amide), 157.9 (C, br, major tautomer, C=O amide), 159.2 [C, br, major tautomer, C=O ester], 160.6 [C, br, minor tautomer, C=O ester] ppm; HRMS (ES+): Exact mass calculated for $C_{25}H_{21}N_3O_3S$ $[M+H]^+$ 444.1376. Found 444.1383; m/z (ES+) 444.2 {[($C_{25}H_{21}N_3O_3S$)+H^+], 4%}.

3,4,5-Triethyl-4,5-dihydro-1*H*-pyrazole-3,4,5-tricarboxylate 190[110]

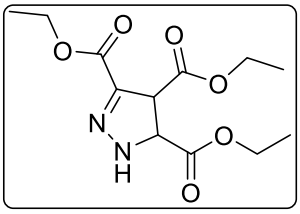

The pyrazoline by-product **190** co-eluted with pyrazoles **174**, **178**, **179**, **182** and **184** during chromatography on silica gel using hexane: ethyl acetate as eluent. Further purification by flash column chromatography on silica gel using dichloromethane: ethyl acetate (90:10 or 80:20) as eluent gave 3,4,5-triethyl-4,5-dihydro-1*H*-pyrazole-3,4,5-tricarboxylate **190** as a white solid (least polar spot by TLC in all instances); mp 88-91°C (lit.[139] 98-99°C); ν_{max}/cm^{-1} (ATR) 3296 (NH stretch), 2959 (CH stretch), 1724 (C=O ester), 1696, 1638, 1547 (NH bend), 1212; δ_H (400 MHz, $CDCl_3$) 1.21-1.44 (9H, m, overlapping triplets, 3 x $OCH_2C\underline{H}_3$), 4.19-4.37 (6H, m, overlapping quartets, 3 x $OC\underline{H}_2CH_3$), 4.42 [1H, d, *J* 5.4 Hz, C(4)H or C(5)H], 4.76 [1H, d, *J* 5.4 Hz, C(4)H or C(5)H], 6.82 (1H, br s, NH) ppm; δ_C (100 MHz, $CDCl_3$) 13.96 (CH_3, one of $OCH_2\underline{C}H_3$), 14.02 (CH_3, one of $OCH_2\underline{C}H_3$), 14.1 (CH_3, one of $OCH_2\underline{C}H_3$), 52.4 [CH, C(4)H or C(5)H], 61.5 (CH_2, one of $O\underline{C}H_2CH_3$), 62.2 (CH_2, one of $O\underline{C}H_2CH_3$), 62.6 (CH_2, one of $O\underline{C}H_2CH_3$), 66.1 [CH, C(4)H or C(5)H], 140.1 [C, C(3)], 161.2 (C, C=O), 169.0 (C, C=O), 169.8 (C, C=O) ppm; HRMS (ES+): Exact mass calculated for $C_{12}H_{18}N_2O_6$ $[M+H]^+$ 287.1238. Found 287.1241.

2.9.10.3. [3+2] Dipolar Cycloadditions of α-Diazoacetates and α-Sulfinyl-β-chloroacrylamides

Ethyl 5-(4′-methylphenylcarbamoyl)-1*H*-pyrazole-3-carboxylate 191

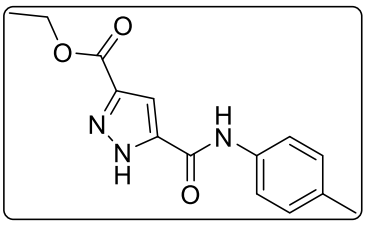

Ethyl diazoacetate (0.97 ml, >87% in dichloromethane, 8 mmol) was added in one portion to a stirring solution of *N*-(4′-methylphenyl)-Z-3-chloro-2-(benzenesulfinyl)propenamide **54** (319 mg, 1 mmol) in toluene (2 ml) at room temperature. The reaction mixture was heated gradually to 100˚C and was stirred at this temperature under nitrogen for 48 h. Upon completion, the reaction mixture was cooled to room temperature during which a precipitate formed. The reaction mixture was further cooled in an ice bath for 1 h. The precipitate was collected by filtration through a sintered glass funnel (grade 4), and was washed thoroughly with diethyl ether until all the yellow impurity had been removed to give the pyrazole **191** as a white solid (128 mg, 47%); mp 216-218°C; ν_{max}/cm^{-1} (ATR) 3341 (NH stretch), 3213 (NH) 3000 (CH), 1692 (C=O ester), 1667 (C=O amide), 1509, 826; δ_H (300 MHz, $CDCl_3$) 1.41 (3H, t, *J* 7.1 Hz, $OCH_2C\underline{H}_3$), 2.34 (3H, s, 3H, $ArCH_3$), 4.43 (2H, q, *J* 7.1 Hz, $OC\underline{H}_2CH_3$), 7.17 (2H, d, *J* 8.2 Hz, ArH), 7.42 [1H, s, C(4)H], 7.56 (2H, d, *J* 8.3 Hz, ArH), 8.61 (1H, br s, NH amide), 11.33 (1H, br s, NH pyrazole) ppm; δ_H (600 MHz, DMSO-d_6) 1.32 (3H, t, *J* 7.1 Hz, $OCH_2C\underline{H}_3$), 2.27 (3H, s, $ArCH_3$), 4.32 (2H, q, J 7.1 Hz, $OC\underline{H}_2CH_3$), 7.15 (2H, d, *J* 8.2 Hz, ArH), 7.48 [1H, br s, C(4)H], 7.65 (2H, d, *J* 8.3 Hz, ArH), 10.18 (1H, br s, NH amide), 14.47 (1H, br s, NH pyrazole) ppm; δ_C (150.9 MHz, DMSO-d_6) 14.2 (CH_3, $ArCH_3$), 20.5 (CH_3, $OCH_2\underline{C}H_3$), 60.7 (CH_2, $O\underline{C}H_2CH_3$), 108.6 [CH, C(4)H], 120.3 (CH, CH_{Ar}), 129.1 (CH, CH_{Ar}), 133.0 (C, $C_{Ar(q)}$), 135.9 (C, $C_{Ar(q)}$), 157.6 (C, br, C=O amide), 160.3 (C, br, C=O ester) ppm; HRMS (ES+): Exact mass calculated for $C_{14}H_{15}N_3O_3$ $[M+H]^+$ 274.1196. Found 274.1196.

Note: *In the ^{13}C NMR spectrum of pyrazole **191** at 150.9 MHz the C(3) and C(5) carbons were not readily observed (using a 10s delay time). Signals for the minor tautomer, ethyl 3-(4′-methylphenylcarbamoyl)-1H-pyrazole-5-carboxylate were not observed.*

Ethyl 5-(benzylcarbamoyl)-1*H*-pyrazole-3-carboxylate (major tautomer) and **ethyl 3-(benzylcarbamoyl)-1*H*-pyrazole-5-carboxylate** (minor tautomer) **192**

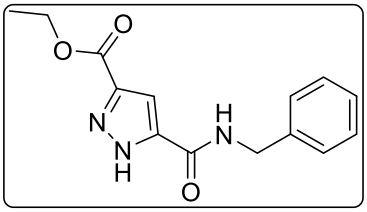

The title compound was prepared following the procedure described for **191** using ethyl diazoacetate (0.97 ml, 8 mmol, 87% in dichloromethane) and *N*-benzyl-Z-3-chloro-2-(benzenesulfinyl)-propenamide **55** (319 mg, 1 mmol) in toluene (2 ml). Upon completion, the reaction mixture was cooled to room temperature during which a precipitate formed. The reaction mixture was further cooled in an ice bath for 1 h. The precipitate was collected by filtration through a sintered glass funnel (grade 4), and was washed thoroughly with diethyl ether until all the yellow impurity had been removed to give the pyrazole **192** as a white solid (84 mg, 31 %); mp 185-187°C; ν_{max}/cm^{-1} (ATR) 3378 (NH stretch), 3201 (NH), 3135 (CH), 1699 (C=O ester), 1650 (C=O amide), 1538, 1277, 697; δ_H (300 MHz, DMSO-d_6) 1.31 (3H, t, *J* 7.1 Hz, $OCH_2C\underline{H}_3$), 4.31 (2H, q, *J* 7.1 Hz, $OC\underline{H}_2CH_3$), 4.46 (2H, d, *J* 6.1 Hz, CH_2NH), 7.13-7.46 [6H, m, overlapping 5 x ArH and C(4)H], 9.05 (1H, br s, NH amide), 14.32 (1H, br s, NH pyrazole) ppm; δ_H (600 MHz, DMSO-d_6) 1.32 (3H, app. t, unresolved coupling, $OCH_2C\underline{H}_3$), 4.29 (2H, br s, $OC\underline{H}_2CH_3$), 4.51 (2H, br s, $C\underline{H}_2NH$), 6.99-7.55 [6H, m, overlapping 5 x ArH and C(4)H], 8.94 and 9.16 (1H, broad singlets, minor and major tautomers respectively, NH amide), 14.3 (1H, broad singlets, major and minor tautomers respectively, NH pyrazole) ppm; δ_C (150.9 MHz, DMSO-d_6) 14.1 (CH_3, $OCH_2\underline{C}H_3$), 42.0 (CH_2, CH_2NH), 60.3 (CH_2, major tautomer $O\underline{C}H_2CH_3$), 61.1 (CH_2, minor tautomer $O\underline{C}H_2CH_3$), 107.6 [CH, major tautomer, C(4)H], 108.6 [CH, minor tautomer, C(4)H], 126.9 (CH, br, major and minor tautomers, CH_{Ar}), 127.3 (CH, major and minor tautomers, CH_{Ar}), 128.3 (CH, br, major and minor tautomers, CH_{Ar}), 134.8 [C, br, minor tautomer, one of C(3) or C(5)], 138.2 [C, br, major tautomer, one of C(3) or C(5)], 138.9 (C, br, major tautomer, $C_{Ar(q)}$), 139.7 (C, br, minor tautomer, $C_{Ar(q)}$), 143.4 [C, br, major tautomer, one of C(3) or C(5)], 147.5 [C, br, minor tautomer, one of C(3) or C(5)], 158.1 (C, br, major tautomer, C=O amide), 158.7 (C, br, minor tautomer, C=O amide), 160.8 (C, br, minor tautomer, C=O ester), 161.6 (C, br, major tautomer, C=O ester) ppm; HRMS (ES+): Exact mass calculated for $C_{14}H_{15}N_3O_3$ $[M+H]^+$ 274.1186. Found 274.1189; m/z (ES-) 272.3 {$[(C_{14}H_{15}N_3O_3)-H^+]$, 100%}.

Ethyl 5-((4′-fluorophenyl)carbamoyl)-1*H*-pyrazole-3-carboxylate (major tautomer) and **Ethyl 3-((4′-fluorophenyl)carbamoyl)-1*H*-pyrazole-5-carboxylate** (minor tautomer) **193**

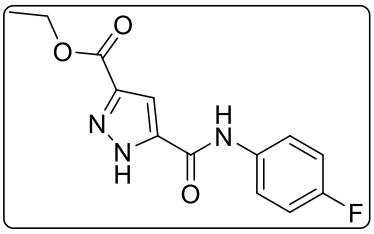

The title compound was prepared following the procedure described for **191** using ethyl diazoacetate (0.97 ml, 8 mmol, 87% in dichloromethane) and *N*-(4′-fluorophenyl)-Z-3-chloro-2-(benzenesulfinyl)propenamide **56** (323 mg, 1 mmol) in toluene (2 ml). Upon completion, the reaction mixture was cooled to room temperature during which time a precipitate formed. The reaction mixture was further cooled in an ice bath for 1 h. The precipitate was collected by filtration through a sintered glass funnel (grade 4), and was washed thoroughly with diethyl ether until all the yellow impurity had been removed to give the pyrazole **193** as a white solid (76 mg, 27 %); mp 184-187°C; ν_{max}/cm^{-1} (ATR) 3349 (NH stretch), 3262 (NH), 3142 (CH), 2989 (CH), 1703 (C=O ester), 1666 (C=O amide), 1530, 1301, 1261; δ_H (300 MHz, DMSO-d_6) 1.33 (3H, t, *J* 7.1 Hz, $OCH_2C\underline{H}_3$), 4.34 (2H, d, *J* 7.1 Hz, $OC\underline{H}_2CH_3$), 7.20 (2H, t, *J* 8.9 Hz, ArH), 7.46 [1H, br s, C(4)H], 7.74-7.88 (2H, m, ArH), 10.32 (1H, s, NH amide), 14.50 (1H, br s, NH pyrazole) ppm; δ_H (600 MHz, DMSO-d_6) 1.32

(3H, t, *J* 7.1 Hz, $OCH_2C\underline{H}_3$), 4.32 (2H, d, *J* 7.1 Hz, $OC\underline{H}_2CH_3$), 7.19 (2H, t, *J* 8.7 Hz, ArH), 7.46 [1H, br s, C(4)H], 7.74-7.85 (2H, m, ArH), 10.34 (1H, s, NH amide), 14.51 (1H, br s, NH pyrazole) ppm; δ_C (150.9 MHz, DMSO-d_6) 14.2 (CH_3, $OCH_2\underline{C}H_3$), 60.8 (CH_2, $O\underline{C}H_2CH_3$), 108.7 [CH, C(4)H], 115.3 [CH, d, $^2J_{CF}$ = 22.2 Hz, C(3′)H], 122.2 [CH, d, $^3J_{CF}$ = 7.8 Hz, C(2′)H], 134.8 [C, C(1′)NH, no $^4J_{CF}$ coupling observed], 138.2, 134.4, 147.4 [C, br, major and minor tautomers, C(3) or C(5)], 157.0 (C, C=O amide), 161.4 (C, C=O ester), 158.4 [C, d, $^1J_{CF}$ = 239.8 Hz, C(4′)F] ppm; HRMS (ES+): Exact mass calculated for $C_{13}H_{12}N_3O_3F$ $[M+H]^+$ 278.0935. Found 278.0935.

Ethyl 5-(2′,2′-dimethylpropylcarbamoyl)-1*H*-pyrazole-3-carboxylate (major tautomer) and **ethyl 5-(2′,2′-dimethylpropylcarbamoyl)-1*H*-pyrazole-3-carboxylate** (minor tautomer) **194**

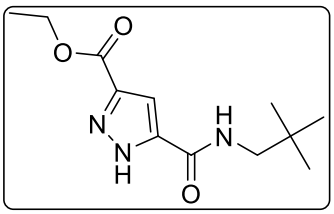

The title compound was prepared following the procedure described for **191** using ethyl diazoacetate (0.97 ml, 8 mmol, 87% in dichloromethane) and *N*-(2′,2′-dimethypropyl)-*Z*-3-chloro-2-(benzenesulfinyl)propenamide **57** (299 mg, 1 mmol) in toluene (2 ml). Upon completion, the reaction mixture was cooled to room temperature, before further being cooled in an ice bath for 1 h. Minimal precipitation was observed in this instance. Purification by flash column chromatography on silica gel using hexane: ethyl acetate (60:40) as eluent, followed by trituration with diethyl ether gave the pure pyrazole **194** as a white solid (48 mg, 19 %); mp 156-158°C; ν_{max}/cm^{-1} (ATR) 3389 (NH stretch), 3134 (NH), 2962 (CH), 1721 (C=O ester), 1634 (C=O amide), 1552, 1266; δ_H (300 MHz, DMSO-d_6) 0.88 [9H, s, $C(C\underline{H}_3)_3$], 1.30 (3H, t, *J* 7.1 Hz, $OCH_2C\underline{H}_3$), 3.08 (2H, d, *J* 6.4 Hz, NCH_2), 4.30 (2H, q, *J* 7.1 Hz, $OC\underline{H}_2CH_3$), 7.37 [1H, br s, C(4)H], 8.32 (1H, br s, NH amide), 14.23 (1H, br s, NH pyrazole) ppm; δ_H (600 MHz, DMSO-d_6) 0.88 [9H, s, $C(C\underline{H}_3)_3$], 1.30 (3H, t, *J* 7.1 Hz, $OCH_2C\underline{H}_3$), 3.07 (2H, d, *J* 6.4 Hz, NCH_2), 4.29 (2H, br q, unresolved coupling, $OC\underline{H}_2CH_3$), 7.16 and 7.47 [1H, overlapping broad singlets, minor and major tautomers respectively, C(4)H], 8.13 and 8.45 [1H, overlapping broad singlets, minor and major tautomers respectively, NH amide], 13.99-14.55 (1H, overlapping broad singlets, major and minor tautomers, NH pyrazole) ppm; δ_C (150.9 MHz, DMSO-d_6) 14.2 (CH_3, $OCH_2\underline{C}H_3$), 27.4 [CH_3, $C(\underline{C}H_3)_3$], 32.5 [C, $\underline{C}(CH_3)_3$], 49.5 (CH_2, CH_2NH), 60.3 and 60.9 (CH_2, overlapping broad signals, major and minor tautomers respectively, $O\underline{C}H_2CH_3$), 107.7 and 108.3 [C, overlapping broad singlets, major and minor tautomers respectively, C(4)H], 134.5 [C, br, minor tautomer, one of C(3) or C(5)], 138.4 [C, br, major tautomer, one of C(3) or C(5)], 143.2 [C, br, minor tautomer, one of C(3) or C(5)], 147.6 [C, br, minor tautomer, one of C(3) or C(5)], 158.4 (C, br, C=O amide), 161.7 (C, br, C=O ester) ppm; HRMS (ES+): Exact mass calculated for m/z $C_{12}H_{19}N_3O_3$ $[M+H]^+$ 254.1499. Found 254.1490; m/z (ES-) 252.4 {$[(C_{12}H_{19}N_3O_3)-H^+]$, 78%}.

Ethyl 5-((4′-methoxyphenyl)carbamoyl)-1*H*-pyrazole-3-carboxylate (major tautomer) and **Ethyl 3-((4′-methoxyphenyl)carbamoyl)-1*H*-pyrazole-5-carboxylate** (minor tautomer) **195**

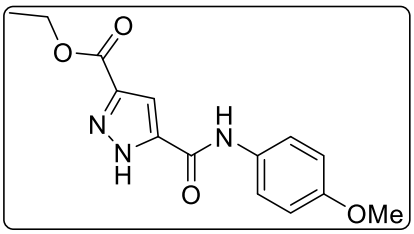

The title compound was prepared following the procedure described for **191** using ethyl diazoacetate (0.97 ml, 8 mmol, 87% in dichloromethane) and *N*-(4′-methoxyphenyl)-*Z*-3-chloro-2-(phenylthio)propenamide **58** (335 mg, 1 mmol) in toluene (2 ml). Upon completion, the reaction mixture was cooled to room temperature during which a precipitate formed. The reaction mixture was further cooled in an ice bath for 1 h. The precipitate was collected by filtration through a sintered glass funnel (grade 4), and was washed thoroughly with diethyl ether until all the yellow impurity had been removed to give the pyrazole **195** as a white solid (49 mg, 17 %); mp 204-207°C; ν_{max}/cm^{-1} (ATR) 3342 (NH stretch), 3229 (NH), 3141 (CH), 1699 (C=O

ester), 1655 (C=O amide), 1514, 814; δ_H (300 MHz, DMSO-d_6) 1.32 (3H, t, *J* 7.1 Hz, $OCH_2C\underline{H}_3$), 3.74 (3H, s, $ArOCH_3$), 4.33 (2H, q, *J* 7.1 Hz, $OC\underline{H}_2CH_3$), 6.93 (2H, d, *J* 9.0 Hz, ArH), 7.46 [1H, br s, C(4)H], 7.68 (2H, d, *J* 9.0 Hz, ArH), 10.13 (1H, s, NH amide), 14.42 (1H, br s, NH pyrazole) ppm; δ_H (600 MHz, DMSO-d_6) 1.33 (3H, t, *J* 7.1 Hz, $OCH_2C\underline{H}_3$), 3.74 (3H, s, $ArOCH_3$), 4.33 (2H, br s, $OC\underline{H}_2CH_3$), 6.93 (2H, br s, ArH), 7.28 [1H, br s, major tautomer, C(4)H], 7.62 [1H, br s, minor tautomer, C(4)H], 7.68 (2H, br s, ArH), 10.19 (1H, br s, overlapping major and minor tautomers, NH amide), 14.40 and 14.55 (1H, 2 overlapping broad singlets, major and minor tautomers respectively, NH pyrazole) ppm; δ_C (150.9 MHz, DMSO-d_6) 14.2 (CH_3, $OCH_2\underline{C}H_3$), 55.2 (CH_3, $ArOCH_3$), 60.3 (CH_2, major tautomer, $O\underline{C}H_2CH_3$), 61.1 (CH_2, minor tautomer, $O\underline{C}H_2CH_3$), 108.0 [CH, major tautomer, C(4)H], 109.0 [CH, minor tautomer, C(4)H], 113.7 (CH, minor tautomer, CH_{Ar}), 113.9 (CH, major tautomer, CH_{Ar}), 121.9 (CH, CH_{Ar}), 131.2 (C, major tautomer, $C_{Ar(q)}$), 131.7 (C, minor tautomer, $C_{Ar(q)}$), 134.9 [C, minor tautomer, one of C(3) or C(5)], 138.4 [C, major tautomer, one of C(3) or C(5)], 143.4 [C, major tautomer, one of C(3) or C(5)], 147.7 [C, minor tautomer, one of C(3) or C(5)], 155.5 (C, minor tautomer, $C_{Ar(q)}$), 155.9 (C, major tautomer, $C_{Ar(q)}$), 156.3 (C, major tautomer, C=O amide), 158.7 (C, minor tautomer, C=O amide), 159.1 (C, minor tautomer, C=O ester), 161.6 (C, major tautomer, C=O ester) ppm; HRMS (ES+): Exact mass calculated for $C_{14}H_{15}N_3O_4$ $[M+H]^+$ 290.1135. Found 290.1135; m/z (ES+) 290.3 {$[(C_{14}H_{15}N_3O_4)+H^+]$, 64%}.

Ethyl 3-(*n*-butylcarbamoyl)-1*H*-pyrazole-5-carboxylate 196

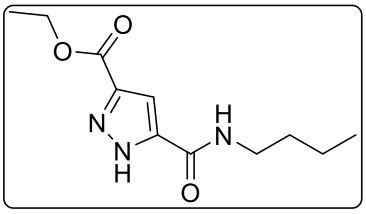

The title compound was prepared following the procedure described for **191** using ethyl diazoacetate (0.97 ml, 8 mmol, 87% in dichloromethane) and *N*-*n*-butyl-Z-3-chloro-2-(benzenesulfinyl)-propenamide **59** (285 mg, 1 mmol) in toluene (2 ml). Upon completion, the reaction mixture was cooled to room temperature, however in this instance no precipitation of product was observed. The crude reaction mixture in toluene was applied directly onto a silica gel column. Purification by repeated flash column chromatography on silica gel using hexane: ethyl acetate (60:40) as eluent followed by dichloromethane: ethyl acetate (gradient elution 10-20% ethyl acetate) gave the pure pyrazole **196** as a white solid (31 mg, 13 %); mp 151-154°C; ν_{max}/cm^{-1} (ATR) 3400 (NH stretch), 3130 (NH), 2932 (CH), 1716 (C=O ester), 1634 (C=O amide), 1555, 1275; δ_H (600 MHz, $CDCl_3$) 0.95 [3H, t, *J* 7.4 Hz, C(4′)H_3], 1.33-1.46 [5H, overlapping 3H, t, *J* 7.1 Hz, $OCH_2C\underline{H}_3$, and 2H, m, C(3′)H_2], 1.53-1.68 [2H, m, C(2′)H_2], 3.46 [2H, app. q, *J* 7.0 Hz, C(1′)H_2], 4.40 (2H, q, *J* 7.1 Hz, $O\underline{C}H_2CH_3$), 6.51-7.16 (1H, overlapping broad singlets, major and minor tautomers, NH amide), 7.36 (1H, br s, C(4)H], 11.97 (0.85H, br s, major tautomer, NH pyrazole), 12.62 (0.15H, br s, minor tautomer, NH pyrazole) ppm; δ_C (150.9 MHz, $CDCl_3$) 13.7 [CH_3, C(4′)H_3], 14.2 (CH_3, $OCH_2\underline{C}H_3$), 20.1 [CH_2, C(3′)H_2], 31.6 [CH_2, C(2′)H_2], 39.1 [CH_2, C(1′)H_2], 61.8 (CH_2, $O\underline{C}H_2CH_3$), 109.3 [CH, C(4)H], 135.4 [C, C(3) or C(5)], 148.3 [C, C(3) or C(5)], 159.3 (C, C=O amide), 161.2 (C, C=O ester) ppm; HRMS (ES+): Exact mass calculated for $C_{11}H_{17}N_3O_3$ $[M+H]^+$ 262.1162. Found 262.1150; m/z (ES-) 238.3 {$[(C_{11}H_{17}N_3O_3)-H^+]$, 42%}.

Benzyl 5-(4′-methylphenylcarbamoyl)-1*H*-pyrazole-3-carboxylate (major tautomer) and **benzyl 3-(4′-methylphenylcarbamoyl)-1*H*-pyrazole-5-carboxylate** (minor tautomer) **197**

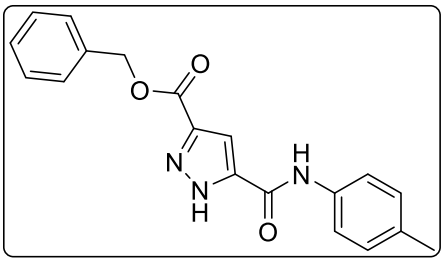

The title compound was prepared following the procedure described for **191** using benzyl diazoacetate (8.8 ml, 10% in toluene, 5 mmol) and *N*-(4′-methylphenyl)-Z-3-chloro-2-(benzenesulfinyl)propenamide **54** (319 mg, 1 mmol) in toluene (2 ml). The cooled reaction mixture was concentrated under reduced pressure and diethyl ether (10 ml) was added. The reaction mixture was cooled in an ice bath overnight

during which time a precipitate formed. The precipitate was collected by filtration through a sintered glass funnel (grade 4), and was washed thoroughly with cold diethyl ether until all the yellow coloured impurity had been removed to give the pyrazole **197** as a white solid (60 mg, 18 %); mp 204-206˚C; ν_{max}/cm^{-1} (ATR) 3378 (NH stretch), 3128 (NH), 2990 (CH), 1718 (C=O ester), 1650 (C=O amide), 1538, 1253, 879; δ_H (300 MHz, DMSO-*d*$_6$) 2.27 (3H, s, ArCH$_3$), 5.40 (2H, s, OCH$_2$), 7.16 (2H, d, *J* 8.3 Hz, ArH), 7.31-7.53 [6H, m, overlapping C(4)H and 5 x ArH], 7.64 (2H, d, *J* 8.2 Hz, ArH), 10.16 (1H, br s, NH amide), 14.48 (1H, br s, NH pyrazole) ppm; δ_H (600 MHz, DMSO-*d*$_6$) 2.27 (3H, s, ArCH$_3$), 5.34 and 5.39 (2H, overlapping broad singlets, major and minor tautomers respectively, OCH$_2$), 7.02-7.78 (10H, m, overlapping C(4)H and 9 x ArH), 10.12 and 10.22 (1H, overlapping broad singlets, minor and major tautomers respectively, NH amide), 14.45 and 14.63 (1H, overlapping broad singlets, minor and major tautomers respectively, NH pyrazole) ppm; δ_C (150.9 MHz, DMSO-*d*$_6$) 20.5 (CH$_3$, ArCH$_3$), 65.9 (CH$_2$, major tautomer, OCH$_2$), 66.4 (CH$_2$, minor tautomer, OCH$_2$), 108.2 [C, major tautomer, C(4)], 109.4 [C, minor tautomer, C(4)], 120.3 (CH, CH$_{Ar}$), 128.0-128.4 (CH, overlapping broad signals, indistinguishable major and minor tautomers, CH$_{Ar}$), 128.6 (CH, CH$_{Ar}$), 129.0 (CH, br, CH$_{Ar}$), 129.2 (CH, CH$_{Ar}$), 132.6 (C, br, minor tautomer, C$_{Ar(q)}$), 133.2 (C, br, major tautomer, C$_{Ar(q)}$), 134.7 (C, br, minor tautomer, C$_{Ar(q)}$), 135.6 (C, br, minor tautomer, C$_{Ar(q)}$), 135.7 (C, br, major tautomer, C$_{Ar(q)}$), 136.0 (C, br, major tautomer, C$_{Ar(q)}$), 136.1 [C, br, minor tautomer, one of C(3) or C(5)], 138.4 [C, br, major tautomer, one of C(3) or C(5)], 143.1 [C, br, major tautomer, one of C(3) or C(5)], 147.7 [C, br, minor tautomer, one of C(3) or C(5)], 156.4 (C, major tautomer, C=O amide), 158.5 (C, minor tautomer, C=O amide), 159.2 (C, major tautomer, C=O ester), 161.4 (C, minor tautomer, C=O ester) ppm; HRMS (ES+): Exact mass calculated for $C_{19}H_{17}N_3O_3$ [M+H]$^+$ 336.1343. Found 336.1339; m/z (ES-) 334.3 {[($C_{19}H_{17}N_3O_3$)-H$^+$], 64%}.

Benzyl 5-(benzylcarbamoyl)-1*H*-pyrazole-3-carboxylate (major tautomer) and **benzyl 5-(benzylcarbamoyl)-1*H*-pyrazole-3-carboxylate** (minor tautomer) **198**

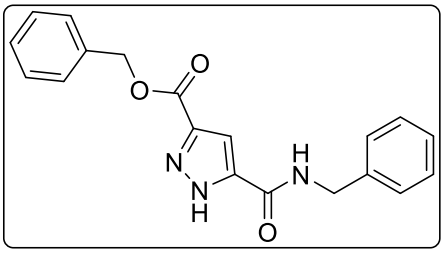

The title compound was prepared following the procedure described for **191** using benzyl diazoacetate (8.8 ml, 10% in toluene, 5 mmol) and *N*-benzyl-Z-3-chloro-2-(benzenesulfinyl)propenamide **55** (319 mg, 1 mmol) in toluene (2 ml). Upon completion, the reaction mixture was cooled to room temperature during which a precipitate formed. The reaction mixture was further cooled in an ice bath for 1 h. The precipitate was collected by filtration through a sintered glass funnel (grade 4), and was washed thoroughly with diethyl ether until all the yellow coloured impurity had been removed to give the pyrazole **198** as a white solid (89 mg, 27 %); mp 198-200˚C; ν_{max}/cm^{-1} (ATR) 3394 (NH stretch), 3130 (NH), 2998 (CH), 1716 (C=O ester), 1636 (C=O amide), 1548, 1274; δ_H (300 MHz, DMSO-*d*$_6$) 4.46 (2H, d, *J* 5.7 Hz, C<u>H</u>$_2$NH), 5.34 (2H, s, OCH$_2$), 7.04-7.68 (11H, m, overlapping C(4)H and 10 x CH$_{Ar}$), 9.12 (1H, br s, NH amide), 14.36 (1H, br s, NH pyrazole) ppm; δ_H (600 MHz, DMSO-*d*$_6$) 4.46 (2H, s, C<u>H</u>$_2$NH), 5.32 and 5.36 (1H, overlapping broad singlets, major and minor tautomers respectively, OCH$_2$), 7.06-7.60 (11H, m, broadness observed, overlapping C(4)H and 10 x CH$_{Ar}$), 8.94 and 9.17 (1H, overlapping broad singlets, minor and major tautomers respectively, NH amide), 14.35 and 14.51 (1H, overlapping broad singlets, major and minor tautomers respectively, NH pyrazole) ppm; δ_C (150.9 MHz, DMSO-*d*$_6$) 42.1 (CH$_2$, CH$_2$NH), 65.8 (CH$_2$, br, major tautomer, O<u>C</u>H$_2$), 66.3 (CH$_2$, br, minor tautomer, O<u>C</u>H$_2$), 107.7 (C, br, major tautomer, C(4)H], 108.9 [C, br, minor tautomer, C(4)H], 126.8 and 127.0 (CH, overlapping broad signals, indistinguishable major and minor tautomers, CH$_{Ar}$), 127.3 (CH, CH$_{Ar}$), 128.16, 128.21, 128.3 (CH, overlapping broad signals, indistinguishable major and minor tautomers, CH$_{Ar}$), 128.5 (CH, CH$_{Ar}$), 134.5 [C, br, minor tautomer, C(3)], 135.6 (C, br, minor tautomer, C$_{Ar(q)}$), 136.0 [C, br, major tautomer, C(3)], 138.3 [C, br, major tautomer, C$_{Ar(q)}$), 138.9 [C, br, major tautomer, C$_{Ar(q)}$), 139.7 [C, br, minor tautomer, C$_{Ar(q)}$), 143.1 [C, br, major tautomer, C(5)], 147.5 [C, br, minor tautomer, C(5)], 158.1

(C, br, major tautomer, C=O amide), 158.5 (C, br, minor tautomer, C=O amide), 160.8 (C, br, minor tautomer, C=O ester), 161.4 (C, br, major tautomer, C=O ester) ppm; HRMS (ES+): Exact mass calculated for $C_{19}H_{17}N_3O_3$ $[M+H]^+$ 336.1343. Found 336.1335; m/z (ES-) 334.3 {$[(C_{19}H_{17}N_3O_3)-H^+]$, 100%}.

Benzyl 3-(4′-fluorophenylcarbamoyl)-1*H*-pyrazole-5-carboxylate (major tautomer) and **benzyl 5-(4′-fluorophenylcarbamoyl)-1*H*-pyrazole-3-carboxylate** (minor tautomer) **199**

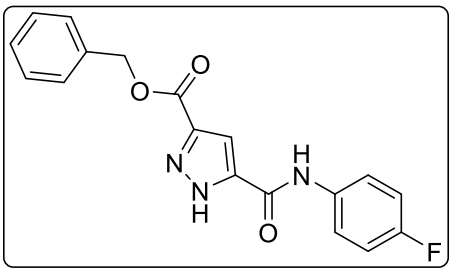

The title compound was prepared following the procedure described for **191** using benzyl diazoacetate (8.8 ml, 10% in toluene, 5 mmol) and *N*-(4′-fluorophenyl)-Z-3-chloro-2-(benzenesulfinyl)propenamide **56** (323 mg, 1 mmol) in toluene (2 ml). Upon completion, the reaction mixture was cooled to room temperature during which a precipitate formed. The reaction mixture was further cooled in an ice bath for 1 h. The precipitate was collected by filtration through a sintered glass funnel (grade 4), and was washed thoroughly with diethyl ether until all the yellow coloured impurity had been removed to give the pyrazole **199** as a white solid (167 mg, 49 %); mp 211-213˚C; ν_{max}/cm^{-1} (ATR) 3308 (NH stretch), 3133, 2982 (CH), 1726 (C=O ester), 1644 (C=O amide), 1549 , 1210, 834; δ_H (300 MHz, DMSO-d_6) 5.37 (1.7H, s, major tautomer, OCH_2), 5.42 (0.3H, s, minor tautomer, OCH_2), 7.11-7.26 (2H, m, ArH), 7.30-7.60 [6H, m, overlapping C(4)H and 5 x ArH], 7.71-7.89 (2H, m, ArH), 10.33 and 10.38 (1H, overlapping singlets, major and minor tautomers, NH amide), 14.56 (1H, br s, NH pyrazole) ppm; δ_H (600 MHz, DMSO-d_6) 5.36 (1.75H, s, major tautomer, OCH_2), 5.42 (0.25H, s, minor tautomer, OCH_2), 7.14-7.24 (2H, m, ArH), 7.31-7.62 [6H, m, overlapping C(4)H and 5 x ArH], 7.72-7.87 (2H, m, ArH), 10.35 (0.86H, br s, NH amide), 10.41 (0.14H, br s, NH amide), 14.58 (1H, br s, NH pyrazole) ppm; δ_C (600 MHz, DMSO-d_6) 66.1 (CH_2, major tautomer, OCH_2), 66.5 (CH_2, minor tautomer, OCH_2), 108.8 [C, C(4)H], 115.2 [CH, d, $^2J_{CF}$ 22.0 Hz, minor tautomer, C(3′)H], 115.3 [CH, d, $^2J_{CF}$ 22.0 Hz, major tautomer, C(3′)H], 122.1 [CH, d, $^3J_{CF}$ 7.8 Hz, minor tautomer, C(2′)H], 122.2 1 [CH, d, $^3J_{CF}$ 7.9 Hz, major tautomer, C(2′)H], 128.0 [CH, minor tautomer, CH_{Ar}), 128.20 (CH, CH_{Ar}), 128.22 [CH, minor tautomer, CH_{Ar}), 128.5 [CH, sharp with underlying broad peak, major and minor tautomers, CH_{Ar}], 134.7 [C, d, $^4J_{CF}$ 2.6 Hz, $C(1')_{Ar(q)}NH$], 135.5 (C, minor tautomer, $C_{Ar(q)}$), 135.8 (C, major tautomer, $C_{Ar(q)}$), 158.4 [C, d, $^1J_{CF}$ 241.2 Hz, $C(1')_{Ar(q)}F$] ppm; HRMS (ES+): Exact mass calculated for $C_{18}H_{14}N_3O_3F$ $[M+H]^+$ 340.1092. Found 340.1087; m/z (ES-) 338.2 {$[(C_{18}H_{14}N_3O_3F)-H^+]$, 84%}.

Note: *In the ^{13}C NMR spectrum of pyrazole **199** at 600 MHz the C(3), C(5) and the two carbonyl signals for the ester and amide respectively were not observed, even with a delay time of 10s. This is attributed to the combination of the dynamic equilibrium between the tautomers in DMSO-d_6 and the coupling effects due to the presence of fluorine in the structure.*

2.9.10.4. [3+2] Dipolar Cycloadditions of α-Diazoacetates and α-Sulfonyl-β-chloroacrylamides

Purification of commercial *m*CPBA[140]

In a 1L volumetric flask sodium hydroxide (0.1 M, 410 ml) and potassium phosphate monobasic (0.2 M, 250 ml) were mixed. The flask was filled up to 1 L with deionised water and the solution was stirred vigorously for 2 min to generate the buffer solution (pH 7.5). Commercial *m*CPBA (10 g, 65-77 %) was dissolved in diethyl ether (150 ml), and washed three times with buffer solution (pH 7.5, 150 ml). The ether layer was dried with $MgSO_4$, filtered and carefully evaporated under reduced pressure to give 6.88 g pure *m*CPBA as a white solid. The peracid was transferred to a plastic container and stored in

the refrigerator for 3 months without decomposition. The purity was determined by ^{1}H NMR spectroscopy.

Caution: *It has been determined that 95-100% mCPBA can be detonated by shock or sparks, whereas commercial 70-85 % mCPBA is not shock sensitive. It should be stored in a refrigerator in tightly closed containers.*

Ethyl 4-(phenylsulfonyl)-5-(4′-methylphenylcarbamoyl)-1*H*-pyrazole-3-carboxylate 204

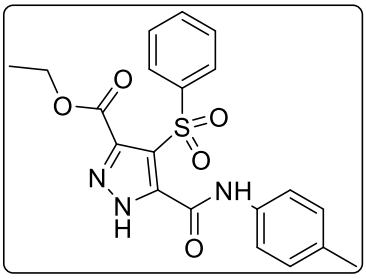

*m*CPBA (77%, 448 mg, 2 mmol) in dichloromethane (15 ml) was added dropwise over 2 minutes to a stirring solution of *N*-(4′-methylphenyl)-Z-3-chloro-2-(benzenesulfinyl)propenamide **54** (319 mg, 1 mmol) in dichloromethane (5 ml) at room temperature. The reaction progress was monitored by ^{1}H NMR spectroscopy. Once the impurity profile of the reaction was observed to increase relative to the increase in sulfoxide **54** to sulfone **200** oxidation the reaction mixture was concentrated under reduced pressure to an approximate volume of 10 ml in dichloromethane. Ethyl diazoacetate (0.49 ml, 4 mmol, >87% in dichloromethane) was added in one portion to the crude sulfone and the reaction mixture was stirred overnight at room temperature under nitrogen. Repeated purification by flash column chromatography on silica gel using hexane: ethyl acetate (60:40) as eluent, followed by dichloromethane: ethyl acetate (80:20) gave the pure pyrazole **204** as a white solid (67 mg, 16 % over 2 steps); mp 179-181˚C; ν_{max}/cm^{-1} (ATR) 3193 (NH), 1736 (C=O ester), 1659 (C=O amide), 1311 (asymmetric SO_2), 1241, 1148 (symmetric SO_2); δ_H (600 MHz, $CDCl_3$) 1.37 (3H, t, *J* 7.1 Hz, $OCH_2C\underline{H}_3$), 2.35 (3H, s, $ArCH_3$), 4.41 (2H, q, *J* 7.1 Hz, $OC\underline{H}_2CH_3$), 7.20 (2H, d, *J* 8.1 Hz, ArH), 7.53 (2H, d, *J* 7.8 Hz, ArH), 7.59-7.70 (3H, m, ArH), 8.07 (2H, d, *J* 7.8 Hz, ArH), 11.20 (1H, br s, NH amide) ppm; δ_C (150.9 MHz, $CDCl_3$) 14.0 (CH_3, $OCH_2C\underline{H}_3$), 21.0 (CH_3, $ArCH_3$), 62.5 (CH_2, $O\underline{C}H_2CH_3$), 120.0 [C, C(4)], 120.3 (CH, CH_{Ar}), 127.5 (CH, CH_{Ar}), 129.2 (CH, CH_{Ar}), 129.8 (CH, CH_{Ar}), 134.0 (CH, CH_{Ar}), 134.3 (C, $C_{Ar(q)}$), 135.5 (C, $C_{Ar(q)}$), 138.6 [C, one of C(3) or C(5)], 140.7 (C, $C_{Ar(q)}$), 145.2 [C, one of C(3) or C(5)], 154.0 (C, C=O amide), 160.3 (C, C=O ester) ppm; HRMS (ES+): Exact mass calculated for $C_{20}H_{19}N_3O_5S$ $[M+H]^+$ 414.1118. Found 414.1123; m/z (ES-) 412.2 {[($C_{20}H_{19}N_3O_5S$)-H^+], 100%}. The regiochemistry was determined by single X-ray diffraction on a crystalline sample of **204** recrystallised from dichloromethane. Crystals of **204** are triclinic, space group *P*, formula $C_{20}H_{19}N_3O_3S$, MW = 413.44 g mol^{-1}, a = 7.6015(5) Å, b = 8.4522(6) Å, c = 15.5976(11) Å, α = 81.209(2)°, β = 81.359(2)°, γ = 70.921(2)°, U = 930.55(11) Å3 , F(000) = 432, μ(Mo Kα) = 0.214 mm^{-1} , R_1(F) = 0.0560 and S = 1.019 for 4588 observed reflections with I > 2σ(I), $wR_2(F^2)$ = 0.1698 for all 7982 unique reflections.

CCDC 1906490 contains the supplementary crystallographic data for the pyrazole **204**. This data can be obtained free of charge from The Cambridge Crystallographic Data Centre.

The title compound **204** was also prepared by addition of *m*CPBA (113 mg, 0.655 mmol, 100%) to a stirring solution of 4-(phenylthio)-5-(4′-methylphenylcarbamoyl)-1*H*-pyrazole-3-carboxylate **71** (100 mg, 0.262 mmol) in dichloromethane (5 ml) at room temperature. The reaction solution was heated to reflux and stirred overnight. Sodium thiosulfate (10 ml, 10% w/v) was added to the cooled reaction mixture and the layers were separated. The organic layer was washed with sodium thiosulfate (2 x 10 ml, 10% w/v), sat. sodium bicarbonate (3 x 10 ml), brine (10 ml), dried, filtered and concentrated under reduced pressure to give the pure pyrazole **204** as a white solid (89 mg, 82%). Spectroscopic characteristics were consistent with those outlined previously.

Ethyl 5-(benzylcarbamoyl)-4-(phenylsulfonyl)-1*H*-pyrazole-3-carboxylate 210

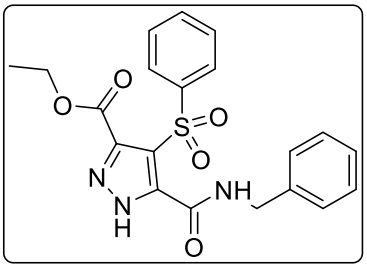

*m*CPBA (77%, 448 mg, 2 mmol) in dichloromethane (15 ml) was added dropwise over 2 minutes to a stirring solution of *N*-benzyl-*Z*-3-chloro-2-(benzenesulfinyl)propenamide **40** (319 mg, 1 mmol) in dichloromethane (5 ml) at room temperature. The reaction mixture was heated to gentle reflux and was stirred at this temperature under nitrogen. The reaction progress was monitored by ^{1}H NMR spectroscopy. Once the impurity profile of the reaction was observed to increase relative to the increase in sulfoxide **40** to sulfone **205** oxidation the reaction mixture was concentrated under reduced pressure to an approximate volume of 10 ml in dichloromethane. Ethyl diazoacetate (0.49 ml, 4 mmol, >87% in dichloromethane) was added in one portion to the crude sulfone and the reaction mixture was stirred overnight at room temperature under nitrogen. Repeated purification by flash column chromatography on silica gel using hexane: ethyl acetate (60:40) as eluent, followed by dichloromethane: ethyl acetate (90:10) gave the pure pyrazole **210** as a white solid (75 mg, 18 % over 2 steps); mp 153-155˚C; Found C, 57.72; H, 4.35; N, 10.00. $C_{20}H_{19}N_3O_5S$ requires C, 58.10; H, 4.35; N, 10.16; ν_{max}/cm^{-1} (ATR) 3297 (NH), 3132 (NH), 1740 (C=O ester), 1652 (C=O amide), 1328 (asymmetric SO_2), 1230, 1150 (symmetric SO_2) 681, 604; δ_H (600 MHz, $CDCl_3$) 1.35 (3H, t, *J* 7.1 Hz, $OCH_2C\underline{H}_3$), 4.39 (2H, q, *J* 7.1 Hz, $OC\underline{H}_2CH_3$), 4.70 (2H, d, *J* 5.6 Hz, $C\underline{H}_2NH$), 7.28-7.48 (5H, m, ArH), 7.57 (1H, t, *J* 7.4 Hz, ArH), 7.90 (2H, d, *J* 7.8 Hz, ArH), 9.64 (1H, br s, NH amide), 13.40 (1H, br s, NH pyrazole) ppm; δ_C (150.9 MHz, $CDCl_3$) 13.9 (CH_3, $OCH_2\underline{C}H_3$), 44.3 (CH_2, CH_2NH), 62.4 (CH_2, $O\underline{C}H_2CH_3$), 120.2 [C, br, C(4)], 127.4 (CH, CH_{Ar}), 127.9 (CH, CH_{Ar}), 128.1 (CH, CH_{Ar}), 128.9 (CH, CH_{Ar}), 129.0 (CH, CH_{Ar}), 133.8 (CH, CH_{Ar}), 136.6 (C, $C_{Ar(q)}$), 137.9 [C, br, one of C(3) or C(5)], 140.6 (C, $C_{Ar(q)}$), 145.0 [C, br, one of C(3) or C(5)], 156.6 (C, C=O amide), 160.5 (C, C=O pyrazole) ppm; HRMS (ES+): Exact mass calculated for $C_{20}H_{19}N_3O_5S$ $[M+H]^+$ 414.1118. Found 414.1100; m/z (ES+) 414.2 {$[(C_{20}H_{19}N_3O_5S)+H^+]$, 100%}.

Ethyl 5-(4′-fluorophenylcarbamoyl)-4-(phenylsulfonyl)-1*H*-pyrazole-3-carboxylate 211

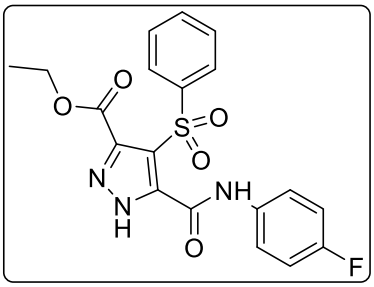

The title compound was prepared following the procedure described for **210** using *m*CPBA (77%, 448 mg, 2 mmol), *N*-(4′-fluorophenyl)-Z-3-chloro-2-(benzenesulfinyl)propenamide **41** (319 mg, 1 mmol) and ethyl diazoacetate (0.49 ml, 4 mmol, >87% in dichloromethane) in dichloromethane (20 ml). Repeated purification by flash column chromatography on silica gel using hexane: ethyl acetate (60:40) as eluent, followed by dichloromethane: ethyl acetate (90:10) gave the pure pyrazole **211** as a white solid (57 mg, 14 % over 2 steps); mp 166-168°C; Found C, 54.38; H, 3.65; N, 9.69; $C_{19}H_{16}FN_3O_5S$ requires C, 54.67; H, 3.86; N, 10.07; ν_{max}/cm^{-1} (ATR) 3152 (NH), 1732 (C=O ester), 1650 (C=O amide), 1508, 1306 (asymmetric SO_2), 1218, 1151 (symmetric SO_2), 836, 728; δ_H (300 MHz, $CDCl_3$) 1.36 (3H, t, *J* 7.1 Hz, $OCH_2C\underline{H}_3$), 4.40 (2H, q, *J* 7.1 Hz, $OC\underline{H}_2CH_3$), 7.10 [2H, t, *J* 8.5 Hz, ArH), 7.46-7.84 (5H, m, ArH), 8.07 (2H, d, *J* 7.5 Hz, ArH), 11.24 (1H, br s, NH amide), 12.79 (1H, br s, NH pyrazole) ppm; δ_C (300 MHz, $CDCl_3$) 13.0 (CH_3, $OCH_2\underline{C}H_3$), 62.5 (CH_2, OCH_2CH_3), 116.1 [CH, d, $^2J_{CF}$ 22.7 Hz, C(3′)H], 120.4 [C, br, C(4)], 122.2 [CH, d, $^3J_{CF}$ 8.2 Hz, C(2′)H], 127.5 (CH, CH_{Ar}), 129.2 (CH, CH_{Ar}), 133.0 [C, d, $^4J_{CF}$ 2.5 Hz, C_{Ar}(1′)NH], 134.1 (C, $C_{Ar(q)}$), 138.5 [C, br, C(3) or C(5)], 140.7 (C, $C_{Ar(q)}$), 145.1 [C, br, C(3) or C(5)], 154.2 (C, C=O amide), 160.08 (C, C=O ester), 160.11 [C, d, $^1J_{CF}$ 245.6 Hz, C_{Ar}(4′)F] ppm.

Ethyl 5-((4′-methoxyphenyl)carbamoyl)-4-(phenylsulfonyl)-1*H*-pyrazole-3-carboxylate 212

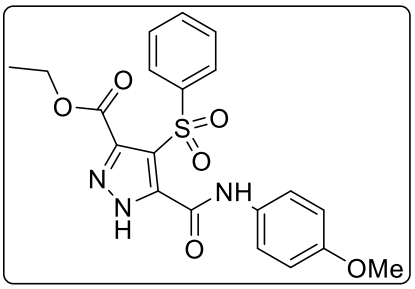

The title compound was prepared following the procedure described for **210** using *m*CPBA (100%, 345 mg, 2 mmol), *N*-(4′-methoxyphenyl)-*Z*-3-chloro-2-(phenylthio)propenamide **43** (335 mg, 1 mmol) and ethyl diazoacetate (0.49 ml, 4 mmol, >87% in dichloromethane) in dichloromethane (20 ml). Repeated purification by flash column chromatography on silica gel using hexane: ethyl acetate (60:40) as eluent, dichloromethane: ethyl acetate (90:10) followed by recrystallisation using ethyl acetate: heptane gave the pure pyrazole **212** as a white solid (67 mg, 16 % over 2 steps); mp 185-187°C; Found C, 55.76; H, 4.37; N, 9.31; $C_{20}H_{19}N_3O_6S$ requires C, 55.94; H, 4.46, N, 9.78; ν_{max}/cm^{-1} (ATR) 3147 (NH), 1736 (C=O ester), 1663 (C=O amide), 1310 (asymmetric SO_2), 1246, 1156 (symmetric SO_2), 721, 615; δ_H (300 MHz, $CDCl_3$) 1.37 (3H, t, *J* 7.1 Hz, $OCH_2C\underline{H}_3$), 3.82 (3H, s, $ArOCH_3$), 4.40 (2H, q, *J* 7.1 Hz, $OC\underline{H}_2CH_3$), 6.94 (2H, d, *J* 8.9 Hz, ArH), 7.44-7.84 (5H, m, ArH), 8.07 (2H, d, *J* 7.5 Hz, ArH), 11.19 (1H, br s, NH amide), 12.81 (1H, br s, NH pyrazole) ppm; δ_C (75.5 MHz, $CDCl_3$) 14.0 (CH_3, $OCH_2\underline{C}H_3$), 55.5 (CH_3, $ArOCH_3$), 62.4 (CH_2, $O\underline{C}H_2CH_3$), 114.4 (CH, CH_{Ar}), 120.0 [C, br, C(4)], 121.9 (CH, CH_{Ar}), 127.5 (CH, CH_{Ar}), 129.1 (CH, CH_{Ar}), 130.1 (C, $C_{Ar(q)}$), 134.0 (CH, CH_{Ar}), 140.8 (C, $C_{Ar(q)}$), 153.8 (C, C=O amide), 157.3 (C, $C_{Ar(q)}$), 160.3 (C, C=O ester) ppm; HRMS (ES+): Exact mass calculated for $C_{20}H_{19}N_3O_6S$ $[M+H]^+$ 430.1067. Found 430.1060.

Ethyl 5-(*n*-butylcarbamoyl)-4-(phenylsulfonyl)-1*H*-pyrazole-3-carboxylate 213

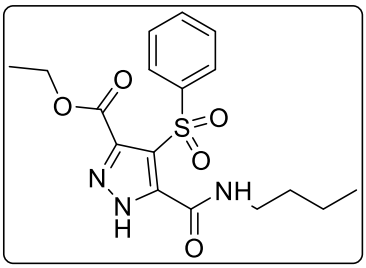

The title compound was prepared following the procedure described for **210** using *m*CPBA (100%, 345 mg, 2 mmol), *N*-*n*-butyl-Z-3-chloro-2-(benzenesulfinyl)propenamide **44** (285 mg, 1 mmol) and ethyl diazoacetate (0.49 ml, 4 mmol, >87% in dichloromethane) in dichloromethane (20 ml). Purification by repeated flash column chromatography on silica gel using hexane: ethyl acetate (60:40), dichloromethane: ethyl acetate (90:10) and diethyl ether: methanol (150:1) as eluents gave the pure pyrazole **213** as a white solid (61 mg, 16 % over 2 steps); mp 131-133˚C; ν_{max}/cm^{-1} (ATR) 3310 (NH stretch), 3133, 2932 (CH), 1737 (C=O ester), 1652 (C=O amide), 1331 (asymmetric SO_2); 1231, 1152 (symmetric SO_2); δ_H (600 MHz, $CDCl_3$) 0.98 [3H, t, *J* 7.3 Hz, C(4′)H_3], 1.36 (3H, t, *J* 7.1 Hz, $OCH_2C\underline{H}_3$), 1.46 [2H, sextet, *J* 7.4 Hz, C(3′)H_2], 1.67 [2H, app. quintet, unresolved coupling, C(2′)H_2], 3.53 [2H, app. q, unresolved coupling, C(1′)H_2], 4.39 (2H, q, *J* 7.1 Hz, $OC\underline{H}_2CH_3$), 7.54 (2H, app. t, unresolved coupling, ArH), 7.60-7.66 (1H, m, ArH), 8.03 (2H, d, *J* 7.7 Hz, ArH), 9.32 (1H, br s, NH amide), 12.84 (1H, br s, NH pyrazole) ppm; δ_C (150.9 MHz, $CDCl_3$) 13.7 [CH_3, C(4′)H_3], 14.0 (CH_3, $OCH_2\underline{C}H_3$), 20.1 [CH_2, C(3′)H_3], 30.9 [CH_2, C(2′)H_2], 40.2 [CH_2, C(1′)H_2], 62.4 (CH_2, $O\underline{C}H_2CH_3$), 120.0 [C, C(4)], 127.4 (CH, CH_{Ar}), 129.1 (CH, CH_{Ar}), 133.9 (CH, CH_{Ar}), 138.2 [C, C(3)] 141.0 (C, $C_{Ar(q)}$), 145.3 [C, C(5)], 156.5 (C, C=O amide), 160.4 (C, C=O ester) ppm; HRMS (ES+): Exact mass calculated for $C_{17}H_{21}N_3O_5S$ $[M+H]^+$ 380.1275. Found 380.1270; m/z (ES+) 380.2 {[($C_{17}H_{21}N_3O_5S$)+H^+], 92%}.

The title compound **213** was also prepared by addition of *m*-CPBA (100%, 85 mg, 0.49 mmol) to a stirring solution of ethyl 5-(butylcarbamoyl)-4-(phenylthio)-1*H*-pyrazole-3-carboxylate **176** (68 mg, 0.196 mmol) in dichloromethane (5 ml) at room temperature. The reaction solution was heated to reflux and stirred overnight. After the reaction solution returned to room temperature sodium thiosulfate (10 ml, 10% w/v) was added and the layers separated. The organic layer was washed with sodium thiosulfate (2 x 10 ml, 10% w/v), sat. sodium bicarbonate (3 x 10 ml), brine (10 ml), dried,

filtered and concentrated under reduced pressure to give the pure pyrazole **213** as a white solid (58 mg, 78 %). Spectroscopic characteristics were consistent with those outlined previously.

Ethyl 4-(benzylsulfonyl)-3-((4′-fluorophenyl)carbamoyl)-1*H*-pyrazole-5-carboxylate 214

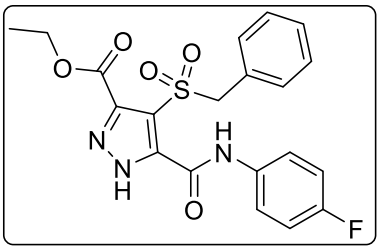

The title compound was prepared following the procedure described for **210** using *m*CPBA (100%, 345 mg, 2 mmol), *N*-(4′-fluorophenyl)-Z-3-chloro-2-(benzylsulfinyl)propenamide **60** (337 mg, 1 mmol)and ethyl diazoacetate (0.49 ml, 4 mmol, >87% in dichloromethane) in dichloromethane (20 ml). Repeated purification by flash column chromatography on silica gel using hexane: ethyl acetate (60: 40) as eluent, followed by dichloromethane: ethyl acetate (90:10) gave the pure pyrazole **214** as a white solid (39 mg, 9 % yield over 2 steps); mp 206-209˚C; ν_{max}/cm^{-1} (ATR) 3231 (NH stretch), 3170, 3120, 1733 (C=O ester), 1674 (C=O amide), 1509, 1301 (asymmetric SO_2), 1216, 1152 (symmetric SO_2), 831, 697; δ_H (300 MHz, DMSO-d_6) 1.32 (3H, t, *J* 7.0 Hz, $OCH_2C\underline{H}_3$), 4.35 (2H, q, unresolved coupling, $OC\underline{H}_2CH_3$), 4.90 (2H, s, CH_2SO_2), 7.09-7.47 (7H, m, ArH), 7.55-7.83 (2H, br m, ArH), 10.70 (1H, s, NH amide), 15.00 (1H, br s, NH pyrazole) ppm; δ_H (600 MHz, DMSO-d_6) 1.31 (3H, t, *J* 7.0 Hz, $OCH_2C\underline{H}_3$), 4.34 (2H, q, *J* 7.1 Hz, $OC\underline{H}_2CH_3$), 4.90 (2H, s, CH_2SO_2), 7.23 (2H, t, *J* 8.9 Hz, ArH), 7.25-7.38 (5H, m, ArH), 7.63 (2H, br s, ArH), 10.72 (1H, s, NH amide), 15.02 (1H, br s, NH pyrazole) ppm; δ_C (150.9 MHz, DMSO-d_6) 13.9 (CH_3, $OCH_2C\underline{H}_3$), 61.5 (CH_2, SO_2CH_2), 62.2 (CH_2, $OC\underline{H}_2CH_3$), 115.6 [CH, d, $^2J_{CF}$ 22.5 Hz, C(3′)H], 118.7 [C, C(4)], 121.8 [CH, d, $^2J_{CF}$ 7.9 Hz, C(3′)H], 127.7 (C, $C_{Ar(q)}$), 128.6 (CH, CH_{Ar}), 128.7 (CH, CH_{Ar}), 131.1 (CH, CH_{Ar}), 134.6 [C, C(1′)NH], 158.7 [C, d, $^1J_{CF}$ 241.7 Hz, C(4′)$_{Ar(q)}$F] ppm; HRMS (ES+): Exact mass calculated for $C_{20}H_{18}FN_3O_5S$ $[M+H]^+$ 432.1024. Found 432.1021; m/z (ES-) 430.2 {[($C_{20}H_{18}FN_3O_5S$)-H^+], 100%}.

Note: *In the ^{13}C NMR spectrum of pyrazole **214** at 600 MHz the C(3), C(5) and the two carbonyl signals for the ester and amide respetively were not observed, even with a delay time of 10s. This is attributed to the combination of the dynamic equilibrium between the tautomers in DMSO-d_6 and the coupling effects due to the presence of fluorine in the structure.*

Ethyl 4-(benzylsulfonyl)-5-((4′-methoxyphenyl)carbamoyl)-1*H*-pyrazole-3-carboxylate 215

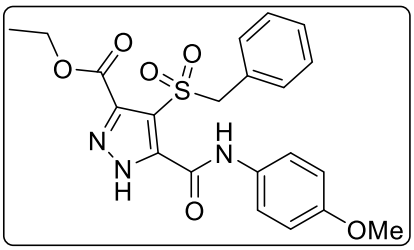

The title compound was prepared following the procedure described for **210** using *m*CPBA (100%, 345 mg, 2 mmol), *N*-(4′-methoxyphenyl)-*Z*-3-chloro-2-(benzylthio)propenamide **61** (349 mg, 1 mmol) and ethyl diazoacetate (0.49 ml, 4 mmol, >87% in dichloromethane) in dichloromethane (20 ml). Purification by repeated flash column chromatography on silica gel using hexane: ethyl acetate (60:40), dichloromethane: ethyl acetate (90:10) as eluents, followed by trituration using diethyl ether gave the pure pyrazole **215** as a white solid (59 mg, 13 % over 2 steps); mp 188-191˚C; ν_{max}/cm^{-1} (ATR) 3215 (NH stretch), 3154, 1730 (C=O ester), 1671 (C=O amide), 1513, 1302 (asymmetric SO_2), 1230, 1142 (symmetric SO_2), 697; δ_H (600 MHz, $CDCl_3$) 1.50 (3H, t, *J* 7.2 Hz, $OCH_2C\underline{H}_3$), 3.82 (3H, s, $ArCH_3$), 4.55 (2H, q, *J* 7.2 Hz, $OC\underline{H}_2CH_3$), 4.92 (2H, s, CH_2SO_2), 6.88 (2H, d, *J* 8.8 Hz, ArH), 7.10-7.24 (5H, m, ArH), 7.40 (2H, d, *J* 8.8 Hz, ArH), 10.30 (1H, br s, NH amide), 11.97 (1H, br s, NH pyrazole) ppm; δ_C (150.9 MHz, $CDCl_3$) 14.1 (CH_3, $OCH_2C\underline{H}_3$), 55.4 (CH_3, $ArOCH_3$), 62.8 (CH_2,CH_2SO_2), 62.9 (CH_2, $O\underline{C}H_2CH_3$), 114.1 (CH, CH_{Ar}), 116.6 [C, C(4)], 121.9 (CH, CH_{Ar}), 127.2 (C, $C_{Ar(q)}$), 128.9 (CH, CH_{Ar}), 129.5 (CH, CH_{Ar}), 129.7 (C, $C_{Ar(q)}$), 130.8 (CH, CH_{Ar}), 139.7 [C, one of C(3) or C(5)], 145.9 [C, one of C(3) or C(5)], 152.5 (C, C=O amide), 157.1 (C, $\underline{C}_{Ar(q)}OCH_3$), 161.0 (C, C=O ester) ppm; HRMS (ES+): Exact mass calculated for $C_{21}H_{21}N_3O_6S$ $[M+H]^+$ 444.1224. Found 444.1220; m/z (ES+) 444.1 {[($C_{21}H_{21}N_3O_6S$)+H^+], 82%}.

2.9.10.5. [3+2] Dipolar Cycloadditions of *N*-Benzyl-α-diazoacetamide with α-Thio-β-Chloroacrylamides

N^3-benzyl-1-(2-(benzylamino)-2-oxoethyl)-N^5-phenyl-4-(phenylthio)-1*H*-pyrazole-3,5-dicarboxamide 232 and **N^5-Benzyl-1-(2-(benzylamino)-2-oxoethyl)-4-(phenylthio)-N^3-(*p*-tolyl)-1*H*-pyrazole-3,5-dicarboxamide 233**

N-Benzyl-α-diazoacetamide **39** (700 mg, 4 mmol) was added in one portion to a solution of *N*-(4′-methylphenyl)-*Z*-3-chloro-2-(phenylthio)propenamide **9** (303 mg, 1 mmol) in toluene (5 ml) at room temperature under nitrogen. The reaction mixture was then heated under reflux for 24 h. On cooling to room temperature, a precipitate formed, which was collected by suction filtration, and subsequently washed with hexane and diethyl ether. ^{1}H NMR spectroscopy of the crude product indicated a 45:55 ratio of N–H insertion products **232** and **233**. Purification by flash column chromatography on silica gel using dichloromethane: ethyl acetate (gradient elution 4-20% ethyl acetate) afforded the pure N–H insertion products **232** and **233** as white solids.

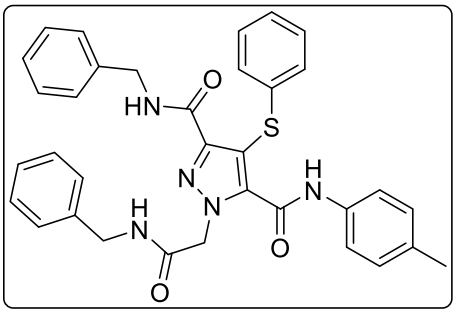

Pyrazole **232** (53 mg, 9%); less polar; ν_{max}/cm^{-1} (ATR) 3057 (CH stretch), 1682 (C=O), 1663 (C=O), 1546, 1477, 1076, 742; δ_H (300 MHz, DMSO) 2.27 (3H, s, ArCH$_3$), 4.31 [2H, d, *J* 5.7 Hz, N(1)CH$_2$COC<u>H</u>$_2$], 4.39 [2H, d, *J* 6.1 Hz, C(3)COC<u>H</u>$_2$], 5.24 [2H, s, N(1)CH$_2$], 6.91-7.43 (17H, m, ArH), 7.52 (2H, d, *J* 8.4 Hz, ArH), 8.78 [2H, t, unresolved coupling, overlapping C(3)CONH and N(1)CH$_2$CON<u>H</u>], 10.57 [1H, br s, C(5)CONH] ppm; δ_C (75.5 MHz, DMSO-d_6) 20.5 (CH$_3$, ArCH$_3$), 42.0 [CH$_2$, C(3)CONH<u>C</u>H$_2$], 42.3 [CH$_2$, N(1)CH$_2$CONH<u>C</u>H$_2$], 54.0 [CH$_2$, N(1)CH$_2$], 108.0 [C, C(4)], 119.8 (CH, CH$_{Ar}$), 125.7 (CH, CH$_{Ar}$), 126.6 (CH, CH$_{Ar}$), 126.7 (CH, CH$_{Ar}$), 126.9 (CH, CH$_{Ar}$), 127.0 (CH, CH$_{Ar}$), 127.2 (CH, CH$_{Ar}$), 128.1 (CH, CH$_{Ar}$), 128.2 (CH, CH$_{Ar}$), 128.9 (CH, CH$_{Ar}$), 129.1 (CH, CH$_{Ar}$), 133.4 (C, C$_{Ar(q)}$), 135.6 (C, C$_{Ar(q)}$), 137.3 (C, C$_{Ar(q)}$), 138.6 (C, C$_{Ar(q)}$), 139.4 (C, C$_{Ar(q)}$), 142.8 [C, C(5)], 146.7 [C, C(3)], 156.6 [C, C(5)C=O], 160.3 [C, C(3)C=O], 165.7 [C, N(1)CH$_2$<u>C</u>=O]; HRMS (ES+): Exact mass calculated for $C_{33}H_{29}N_5O_3S$ [M+H]$^+$ 576.2069. Found 576.2066.

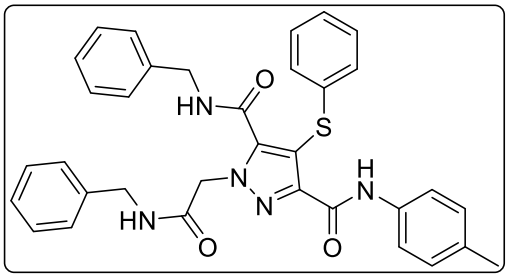

Pyrazole **233** (94 mg, 16%); more polar; mp 230-232°C; ν_{max}/cm^{-1} (ATR) 3297 (NH stretch), 1665 (C=O amide), 1644 (C=O amide), 1551, 1525 (NH bend), 1250; δ_H (300 MHz, DMSO) 2.25 (3H, s, ArCH$_3$), 4.33 [2H, d, *J* 5.8 Hz, CH$_2$CONHC<u>H</u>$_2$], 4.43 [2H, d, *J* 6.0 Hz, C(5)CONHC<u>H</u>$_2$], 5.27 [2H, s, N(1)CH$_2$], 7.00-7.40 (17H, m, ArH), 7.58 (2H, d, *J* 8.4 Hz, ArH), 8.74 (1H, t, *J* 5.8 Hz, CH$_2$CON<u>H</u>), 9.06 [1H, t, *J* 6.0, N(5)CON<u>H</u>], 10.17 [1H, br s, C(3)CON<u>H</u>] ppm; δ_C (75.5 MHz, DMSO-d_6) 20.4 (CH$_3$, ArCH$_3$), 42.3 [CH$_2$, N(1)CH$_2$CONH<u>C</u>H$_2$], 42.4 [CH$_2$, C(5)CONHCH$_2$], 54.3 [CH$_2$, N(1)CH$_2$], 107.2 [C, C(4)], 119.7 (CH, CH$_{Ar}$), 125.4 (CH, CH$_{Ar}$), 126.2 (CH, CH$_{Ar}$), 126.5 (CH, CH$_{Ar}$), 126.6 (CH, CH$_{Ar}$), 126.7 (CH, CH$_{Ar}$), 127.1 (CH, CH$_{Ar}$), 127.9 (CH, CH$_{Ar}$), 128.1 (CH, CH$_{Ar}$), 128.71 (CH, CH$_{Ar}$), 128.74 (CH, CH$_{Ar}$), 132.7 (C, C$_{Ar(q)}$), 136.0 (C, C$_{Ar(q)}$), 137.1 (C, C$_{Ar(q)}$), 138.3 (C, C$_{Ar(q)}$), 138.8 (C, C$_{Ar(q)}$), 142.2 [C, C(5)], 147.4 [C, C(3)], 158.3 [C, C(5)C=O], 158.7 [C, C(3)<u>C</u>=O], 165.7 [C, N(1)CH$_2$<u>C</u>=O] ppm; HRMS (ES+): Exact mass calculated for $C_{33}H_{29}N_5O_3S$ [M+H]$^+$ 576.2069. Found 576.2068.

2.9.11. Synthesis of the α-Sulfonyl-β-chloroacrylamide of the Weinreb Amide

***N*-Methoxy-*N*-methyl-2-chloropropanamide 224**[16, 52]

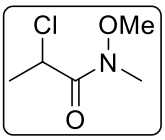

The title compound was prepared following the procedure described for **72** from 2-chloropropionyl chloride **94** (10.05 ml, 103.55 mmol), *N*,*O*-dimethylhydroxylamine hydrochloride **223** (10 g, 102.52 mmol) and triethylamine (20.85 g, 206.07 mmol) in dichloromethane (120 ml) to give the α-chloroamide **224** as an orange oil (14.28 g, 92%) which required no further purification; δ_H (300 MHz, $CDCl_3$) 1.65 [3H, d, *J* 6.7 Hz, C(3)H_3], 3.24 (3H, s, NCH_3), 3.79 (3H, s, OCH_3), 4.89 [1H, br q, unresolved coupling, C(2)H] ppm; δ_C (75.5 MHz, $CDCl_3$) 20.7 [CH_3, C(3)H_3], 32.5 (CH_2, br, NCH_3), 48.6 [CH, C(2)H], 61.7 (CH_3, OCH_3) ppm.

Note: *The carbonyl carbon was not observed in the reported ^{13}C NMR spectrum consistent with Lynch's earlier work.*[16]

***N*-Methoxy-*N*-methyl-2-phenylthiopropanamide 225**[16, 52]

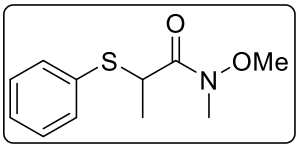

The title compound was prepared following the procedure described for **6** using *N*-methoxy-*N*-methyl-2-chloropropanamide **224** (7.79 g, 51.55 mmol), thiophenol (6.32 ml, 61.86 mmol), and sodium (1.42 g, 61.86 mmol) in dry ethanol (80 ml). The reaction mixture was stirred for 16 h before work up as described for **6** afforded the sulfide (10.31 g, 89 %) as a yellow oil which required no further purification; ν_{max}/cm^{-1} (ATR) 2971 (CH), 2933 (CH), 1657 (C=O), 1439, 1381, 985; δ_H (400 MHz, $CDCl_3$) 1.46 [3H, d, *J* 7.0 Hz, C(3)H_3], 3.19 (3H, s NCH_3), 3.64 (3H, s, OCH_3), 4.23-4.36 [1H, br q, unresolved coupling, C[2)H], 7.27-7.38 (3H, m, ArH), 7.45-7.54 (2H, m, ArH) ppm; δ_C (100 MHz, $CDCl_3$) 17.7 [CH_3, C(3)H_3], 32.5 (CH_2, br, NCH_3), 41.7 [CH, C(2)H], 61.4 (CH_3, OCH_3), 127.9 (CH, CH_{Ar}), 128.5 (CH, CH_{Ar}), 133.1 (C, $C_{Ar(q)}$), 133.5 (CH, CH_{Ar}), 173.0 (C, C=O) ppm.

***N*-Methoxy-*N*-methyl-Z-3-chloro-2-phenylthiopropenamide 226**[16, 52]

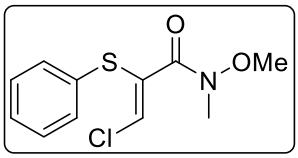

The title compound was prepared following the procedure described for **9** using *N*-methoxy-*N*-methyl-2-phenylthiopropanamide **225** (10.16 g, 45.16 mmol), *N*-chlorosuccinimide (11.76 g, 88.06 mmol), and toluene (100 ml). The reaction mixture was heated at 90 °C for 3 h. Following filtration and evaporation of the solvent at reduced pressure, the crude products were obtained in a 2:1 ratio of *Z*-**226** to *E*-**227**. The crude product mixture was purified by flash column chromatography on silica gel using hexane: ethyl acetate (gradient elution5-20% ethyl acetate) as eluent to give the more polar pure product *Z*-**226** (4.33 g, 37 %) as a clear oil; ν_{max}/cm^{-1} (ATR) 3060 (CH), 2936 (CH), 1653 (C=O), 1439, 1381, 966, 740, 690.

Note: *The ^{1}H and ^{13}C NMR spectra of Z-**226** at 300 MHz (in $CDCl_3$) were very complex due to restricted rotation about the amide C–N bond. Lynch established that this complexity is due to presence of three rotameric species Z-**226a**, Z-**226b** and Z-**226c**. Accordingly, Lynch carried out comprehensive variable temperature NMR studies on this derivative to enable full spectroscopic characterisation.*[16] *This work was not repeated as part of this work, however, despite not being assigned above, both the ^{1}H and ^{13}C NMR spectra of Z-**226** obtained in this work are included in Appendix **2** for reference.*

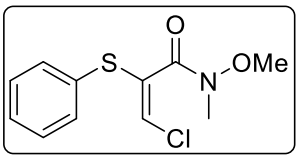

The less polar minor *E*-isomer, *N*-methoxy-*N*-methyl-*E*-3-chloro-2-phenylthiopropenamide **227**,[16, 52] was also isolated as clear oil (1.34 g, 15%); ν_{max}/cm^{-1} (ATR) 3060 (CH), 2974 (CH), 1652 (C=O), 1440, 970, 747, 691; δ_H (300 MHz, $CDCl_3$) 2.98 (3H, br s, NCH_3), 3.46 (3H, br s, OCH_3), 6.59 [1H, s, ClC(3)H=], 7.27-7.36 (3H, m, ArH), 7.46-7.55 (2H, m, ArH) ppm; δ_C

(75.5 MHz, $CDCl_3$) 34.0 (CH_3, br, NCH_3), 61.1 (CH_3, OCH_3), 120.4 [CH, ClC(3)H=], 128.7 (CH, CH_{Ar}), 129.0 (CH, CH_{Ar}), 133.4 (CH, CH_{Ar}), 135.1 [C, C(2)S] ppm.

Note: *Neither the carbonyl carbon nor the quaternary aromatic carbon was observed in the ^{13}C NMR spectrum.*

(*Z*)-3-Chloro-*N*-methoxy-*N*-methyl-2-(phenylsulfonyl)acrylamide 228[16]

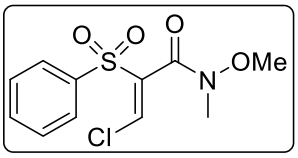

The title compound was prepared following the procedure described for **54** using *N*-methoxy-*N*-methyl-Z-3-chloro-2-phenylthiopropenamide **227** (3.80 g, 14.78 mmol) in acetone (160 ml) and Oxone® (18.17 g, 29.56 mmol) in water (10 ml). Following stirring at room temperature for 16 h and aqueous work up the crude sulfone **228** was obtained as a yellow oil. Purification by flash column chromatography on silica gel using hexane: ethyl acetate (80:20) as eluent gave the pure sulfone **228** (2.29 g, 54%) as a white solid; mp 79-81°C; ν_{max}/cm^{-1} (ATR) 3084 (CH), 2924 (CH), 1647 (C=O), 1309 (asymmetric SO_2), 1145 (symmetric SO_2), 960, 728; δ_H (300 MHz, $CDCl_3$) 3.27 and 3.31 (3H, s and br s, overlapping major and minor rotamers respectively, NCH_3), 3.76 (3H, s, OCH_3), 7.48-7.71 [4H, m, overlapping ArH and ClC(3)H=], 7.85-7.96 (2H, m, ArH) ppm; δ_C (75.5 MHz, $CDCl_3$) 32.2 (CH_3, major rotamer, NCH_3), 35.8 (CH_3, br, minor rotamer, NCH_3), 60.7 (CH_3, br, minor rotamer, OCH_3), 62.2 (CH_3, major rotamer, OCH_3), 128.4 (CH, major rotamer, CH_{Ar}), 128.6 (CH, br, minor rotamer, CH_{Ar}), 129.1 [CH, major rotamer, CH_{Ar} or C(3)H=], 129.2 [CH, br, minor rotamer, CH_{Ar} or C(3)H=], 134.0 (CH, major rotamer, CH_{Ar}), 134.2 (CH, minor rotamer, CH_{Ar}), 134.4 [CH, CH_{Ar} or C(3)H=], 139.5 [C, $C_{Ar(q)}$ or $C(2)SO_2$], 141.1 [C, $C_{Ar(q)}$ or $C(2)SO_2$], 160.2 (C, C=O) ppm.

2.9.12. Synthesis of 3-Ethyl 4,5-Dimethyl 1*H*-Pyrazole-3,4-5-Tricarboxylate

3-Ethyl 4,5-dimethyl 1*H*-pyrazole-3,4-5-tricarboxylate 230[141]

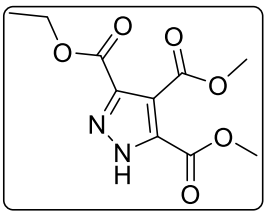

Ethyl diazoacetate (0.137 ml, 1 mmol, >13% dichloromethane) was added dropwise to a stirring solution of dimethyl acetylenedicarboxylate **156** (0.148 ml, 1.2 mmol) in dichloromethane (2 ml) under nitrogen at 0°C. The reaction mixture was stirred at 0°C for 1 h at which point the ice-bath was removed and the reaction mixture was heated gradually to reflux. After 1 h the reaction mixture was cooled to room temperature and was concentrated under reduced pressure to give the crude product as a yellow solid. Purification by flash column chromatography on silica gel using hexane: ethyl acetate (70:30) as eluent gave the pure pyrazole **230** (259 mg, quant.) as a white solid; mp 97-99°C (lit.[141] 93-96°C); ν_{max}/cm^{-1} (ATR) 3237 (CH stretch), 1754 (C=O), 1718 (C=O), 1259; δ_H (300 MHz, $CDCl_3$) 1.36 (3H, t, *J* 7.1 Hz, $OCH_2C\underline{H}_3$), 3.93 (3H, s, OCH_3), 3.96 (3H, s, OCH_3), 4.39 (2H, q, *J* 7.1 Hz, $OC\underline{H}_2CH_3$), 12.36 (1H, br s, NH pyrazole) ppm; δ_C (75.5 MHz, $CDCl_3$) 13.9 (CH_3, $OCH_2\underline{C}H_3$), 52.8 (CH_3, OCH_3), 53.0 (CH_3, OCH_3), 62.1 (CH_2, $O\underline{C}H_2CH_3$), 119.3 [C, C(4)], 158.9 (C, C=O ethyl ester), 159.7 (C, C=O methyl ester), 163.4 (C, C=O methyl ester) ppm.

Note: *Signals for C(3) and C(5) not observed in the ^{13}C NMR spectrum due to signal broadening*.

2.9.13. Derivatisation of the Pyrazole Scaffold

Ethyl 4-(phenylsulfinyl)-5-(4′-methylphenylcarbamoyl)-1*H*-pyrazole-3-carboxylate 234

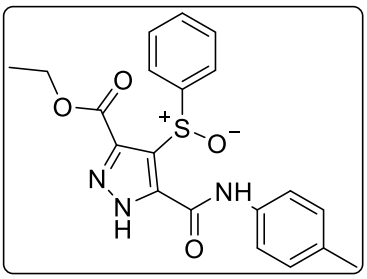

*m*CPBA (35 mg, 0.2 mmol, 100%) was added in one portion to a stirring solution of 4-(phenylthio)-5-(4′-methylphenylcarbamoyl)-1*H*-pyrazole-3-carboxylate **71** (40 mg, 0.1 mmol) in dichloromethane (10 ml) at room temperature. After stirring overnight sodium thiosulfate (10 ml, 10% w/v) was added and the layers were separated. The organic layer was washed with sodium thiosulfate (2 x 10 ml, 10% w/v), sat. sodium bicarbonate (3 x 10 ml) and brine, dried with magnesium sulfate and concentrated under reduced pressure to give the crude product as a white solid. ^{1}H NMR analysis of the crude product indicated complete consumption of the starting material with evidence for both the sulfoxide **234** and sulfone **204** present (approx. 85:15). Purification by flash column chromatography using hexane: ethyl acetate as eluent (gradient elution 20-30% ethyl acetate) gave sulfoxide **234** as a white solid (26 mg, 66 %); mp 187-189°C; ν_{max}/cm^{-1} (ATR) 3096 (NH stretch), 2994 (CH), 2918 (CH), 1699 (C=O ester), 1669 (C=O amide), 1235, 1029 (S=O), 980; δ_H (300 MHz, $CDCl_3$) 1.43 (3H, t, *J* 7.1 Hz, $OCH_2C\underline{H}_3$), 2.34 (3H, s, $ArCH_3$), 4.36-4.57 (2H, m, $OC\underline{H}_2CH_3$), 7.18 (2H, d, *J* 8.1 Hz, ArH), 7.37-7.51 (3H, m, ArH), 7.63-7.83 (4H, m, ArH), 12.36 (1H, br s, NH amide), 12.79 (1H, br s, NH pyrazole) ppm; δ_C (75.5 MHz, $CDCl_3$) 14.2 (CH_3, $OCH_2\underline{C}H_3$), 21.0 (CH_3, $ArCH_3$), 62.3 (CH_2, $O\underline{C}H_2CH_3$), 120.3 (CH, CH_{Ar}), 124.1 [C, C(4)], 125.1 (CH, CH_{Ar}), 129.6 (CH, 2 overlapping CH_{Ar} signals), 131.7 (CH, CH_{Ar}), 134.8 (C, $C_{Ar(q)}$) 135.1 (C, $C_{Ar(q)}$), 139.6 [C, one of C(3) or C(5)], 142.8 [C, one of C(3) or C(5)], 143.4 (C, $C_{Ar(q)}$), 154.8 (C, C=O amide), 161.2 (C, C=O ester) ppm; HRMS (ES+): Exact mass calculated for $C_{20}H_{19}N_3O_4S$ $[M+H]^+$ 398.1169. Found 398.1183.

Ethyl 5-((4′-methoxyphenyl)carbamoyl)-4-(phenylsulfinyl)-1*H*-pyrazole-3-carboxylate 235

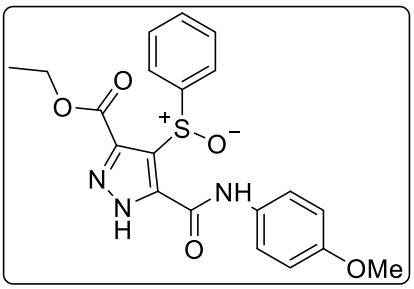

The title compound was prepared following the procedure for **234** using *m*CPBA (87 mg, 0.50 mmol, 100%) and ethyl 5-((4′-methoxyphenyl)carbamoyl)-4-(phenylthio)-1*H*-pyrazole-3-carboxylate **175** (200 mg, 0.50 mmol) in dichloromethane (5 ml). Following work up the pure pyrazole **235** was obtained (196 mg, 94 %); mp 194-197°C; ν_{max}/cm^{-1} (ATR) 2997 (NH stretch), 2904 (CH), 1703 (C=O ester), 1662 (C=O amide), 1508, 1238, 1032 (S=O); δ_H (300 MHz, $CDCl_3$) 1.43 (3H, t, *J* 7.1 Hz, $OCH_2C\underline{H}_3$), 3.81 (3H, s, $ArCH_3$), 4.37-4.54 (2H, m, $OC\underline{H}_2CH_3$), 6.86-6.95 (2H, m, ArH), 7.38-7.50 (3H, m, ArH), 7.66-7.83 (4H, m, ArH), 12.35 (1H, s, NH amide), 12.91 (1H, br s, NH pyrazole) ppm; δ_C (75.5 MHz, $CDCl_3$) 14.2 (CH_3, $O\underline{C}H_2CH_3$), 55.4 (CH_3, $ArOCH_3$), 62.3 (CH_2, $O\underline{C}H_2CH_3$), 114.3 (CH, CH_{Ar}), 121.7 (CH, CH_{Ar}), 124.0 [C, C(4)], 125.1 (CH, CH_{Ar}), 129.6 (CH, CH_{Ar}), 130.9 (C, $C_{Ar(q)}$), 131.7 (CH, CH_{Ar}), 139.7 [C, C(3) or C(5)], 142.8 [C, C(3) or C(5)], 143.4 (C, $C_{Ar(q)}$), 154.6 (C, C=O amide), 156.9 (C, $C_{Ar(q)}$), 161.2 (C, C=O ester) ppm; HRMS (ES+): Exact mass calculated for $C_{20}H_{19}N_3O_5S$ $[M+H]^+$ 414.1118 Found 414.1110.

Ethyl 1-(2-ethoxy-2-oxoethyl)-4-(phenylthio)-3-(*4′*-methylphenylcarbamoyl)-1*H*-pyrazole-5-carboxylate 169 and **ethyl 1-(2-ethoxy-2-oxoethyl)-4-(phenylthio)-5-(*4′*-methylphenylcarbamoyl)-1*H*-pyrazole-3-carboxylate 170**

Ethyl 4-(phenylthio)-5-(4′-methylphenylcarbamoyl)-1*H*-pyrazole-3-carboxylate **71** (150 mg, 0.393 mmol), potassium carbonate (71 mg, 0.512 mmol) and a stirrer bar were placed in a vial. Anhydrous dimethyl sulfoxide (3 ml) was added and the resultant mixture was stirred at room temperature under nitrogen. Ethyl bromoacetate (0.06 ml, 0.472 mmol) was added and the resulting mixture was stirred at room temperature for 24 h. The reaction mixture was quenched with iced water (10 ml). The resulting mixture was extracted with ethyl acetate (2 x 15 ml). The combined organic layers were washed with brine (20 ml), dried over magnesium sulfate, and concentrated under reduced pressure to give the crude product as a yellow oil which contained a mixture of *N*-alkylated pyrazoles **169**:**170** in a ratio of 72:28. Purification by column chromatography on silica gel using hexane: ethyl acetate (80:20) as eluent gave pure pyrazole **169** as a clear oil which solidified overnight to give a white solid (112 mg, 61 %), pure pyrazole **170** as a white solid (46 mg, 25 %), and a mixed fraction of **169** and **170** as a clear oil which solidified overnight to give a white solid (11 mg, 6 %) to give a combined yield of 92 %.

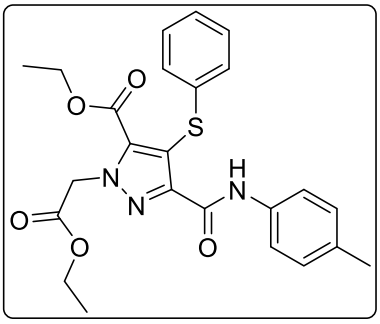

Pyrazole **169**; more polar; mp 107-109°C; ν_{max}/cm^{-1} (ATR) 3340 (NH stretch), 2993 (CH stretch), 1736 (C=O ester), 1708 (C=O ester), 1682 (C=O amide), 1531 (NH bend), 1270; δ_H (600 MHz, $CDCl_3$) 1.15 [3H, t, *J* 7.1 Hz, one of C(5)$CO_2CH_2C\underline{H}_3$ or $NCH_2CO_2CH_2C\underline{H}_3$], 1.28 [3H, t, *J* 7.2 Hz, one of C(5)$CO_2CH_2C\underline{H}_3$ or $NCH_2CO_2CH_2C\underline{H}_3$], 2.29 (3H, s, $ArCH_3$), 4.21 and 4.24 [4H, overlapping quartets, *J* 7.1 Hz, C(5)$CO_2C\underline{H}_2$ or $NCH_2CO_2C\underline{H}_2$], 5.38 (2H, s, NCH_2CO), 7.03-7.26 (7H, m, ArH), 7.49 (2H, d, *J* 8.5 Hz, ArH), 9.09 (1H, s, NH amide) ppm; δ_C (150.9 MHz, $CDCl_3$) 13.6 [CH_3, one of C(5)$CO_2CH_2\underline{C}H_3$ or $NCH_2CO_2CH_2\underline{C}H_3$], 13.9 [$CH_3$, one of C(5)$CO_2CH_2\underline{C}H_3$ or $NCH_2CO_2CH_2\underline{C}H_3$], 20.7 ($CH_3$, $ArCH_3$), 55.0 (CH_2, $N\underline{C}H_2CO$], 62.0 (CH_2, overlapping C(5)$CO_2\underline{C}H_2$ or $NCH_2CO_2\underline{C}H_2$], 113.7 [C, C(4)], 119.8 (CH, CH_{Ar}), 125.9 (CH, CH_{Ar}), 126.8 (CH, CH_{Ar}), 128.9 (CH, CH_{Ar}), 129.3 (CH, CH_{Ar}), 133.9 (C, $C_{Ar(q)}$), 134.9 (C, $C_{Ar(q)}$), 136.4 (C, $C_{Ar(q)}$), 137.1 [C, C(5)], 146.6 [C, C(3)], 157.6 (C, C=O amide), 158.8 [C, C(5)$\underline{C}$=O], 166.7 [C, $NCH_2\underline{C}$=O] ppm; δ_H (600 MHz, DMSO-d_6) 1.06 [3H, t, *J* 7.1 Hz, C(5)$CO_2CH_2C\underline{H}_3$], 1.21 [3H, t, *J* 7.1 Hz, $NCH_2CO_2CH_2C\underline{H}_3$], 2.25 (3H, s, $ArCH_3$), 4.14 [2H, q, *J* 7.1 Hz, C(5)$CO_2C\underline{H}_2$], 4.19 [2H, q, *J* 7.1 Hz, $NCH_2CO_2C\underline{H}_2$], 5.44 (2H, s, NCH_2CO), 7.06-7.15 (5H, m, ArH), 7.21-7.28 (2H, m, ArH), 7.56 (2H, d, *J* 8.5 Hz, ArH), 10.34 (1H, s, NH amide) ppm; δ_C (150.9 MHz, DMSO-d_6) 13.5 [CH_3, C(5)$CO_2CH_2\underline{C}H_3$], 14.0 [CH_3, $NCH_2CO_2CH_2\underline{C}H_3$], 20.5 ($CH_3$, $ArCH_3$), 54.8 (CH_2, $N\underline{C}H_2CO$), 61.5 [CH_2, C(5)$CO_2\underline{C}H_2$], 61.7 [$NCH_2CO_2\underline{C}H_2$], 111.3 [C, C(4)], 119.9 (CH, CH_{Ar}), 125.7 (CH, CH_{Ar}), 126.6 (CH, CH_{Ar}), 128.9 (CH, CH_{Ar}), 129.0 (CH, CH_{Ar}), 132.9 (C, $C_{Ar(q)}$), 135.9 (C, $C_{Ar(q)}$), 136.1 (C, $C_{Ar(q)}$), 137.0 [C, C(5)], 148.6 [C, C(3)], 158.1 [C, C(5)$\underline{C}$=O], 158.6 (C, C=O amide), 167.3 [C, $NCH_2\underline{C}$=O] ppm; δ_H (600 MHz, Toluene-d_8) 0.83 [3H, t, *J* 7.1 Hz, 3H, one of C(5)$CO_2CH_2C\underline{H}_3$ or $NCH_2CO_2CH_2C\underline{H}_3$], 0.89 [3H, t, *J* 7.1 Hz, one of C(5)$CO_2CH_2C\underline{H}_3$ or $NCH_2CO_2CH_2C\underline{H}_3$], 2.06 (3H, s, $ArCH_3$), 3.86 [2H, q, *J* 7.1 Hz, C(5)$CO_2C\underline{H}_2$], 3.88 [2H, q, *J* 7.1 Hz, $NCH_2CO_2C\underline{H}_2$], 5.03 (2H, s, NCH_2CO), 6.80 (1H, t, unresolved coupling, ArH), 6.87 (2H, d, *J* 8.3 Hz, ArH), 6.92 (2H, t, *J* 7.8 Hz, ArH), 7.27 (2H, d, *J* 7.5 Hz, ArH), 7.49 (2H, d, *J* 8.3 Hz, ArH), 8.60 (1H, s, NH amide) ppm; δ_C (150.9 MHz, Toluene-d_8) δ13.6 [CH_3, one of C(5)$CO_2CH_2\underline{C}H_3$] or $NCH_2CO_2CH_2\underline{C}H_3$], 13.9 [$CH_3$, one of C(5)$CO_2CH_2\underline{C}H_3$ or $NCH_2CO_2CH_2\underline{C}H_3$], 20.7 ($CH_3$, overlapping with residual toluene-d_8 signal, $ArCH_3$), 54.9 (CH_2, $N\underline{C}H_2CO$), 61.7 [CH_2, C(5)$CO_2\underline{C}H_2$], 61.8 [$NCH_2CO_2\underline{C}H_2$], 115.9 [C, C(4)], 119.7 (CH, CH_{Ar})*, 125.8 (CH, CH_{Ar}), 127.8 (CH, CH_{Ar}), 129.6 (CH, CH_{Ar}), 133.2 (C, $C_{Ar(q)}$), 136.3 (C, $C_{Ar(q)}$), 137.2 (C, $C_{Ar(q)}$), 138.3 [C, C(5)], 147.5 [C, C(3)], 157.4 (C, C=O amide), 159.5 [C, C(5)$\underline{C}$=O], 166.8 [C, $NCH_2\underline{C}$=O] ppm; * 1 x CH_{Ar} signal in toluene-d_8 spectrum overlapping with residual solvent signal; HRMS (ES+): Exact mass calculated for

$C_{24}H_{25}N_3O_5S$ $[M+H]^+$ 468.1588. Found 468.1587; m/z (ES+) 468.2 {[($C_{24}H_{25}N_3O_5S$)+H^+], 100%}. The regiochemistry was determined by single X-ray diffraction on a crystalline sample of **169** recrystallised from dichloromethane. Crystals of pyrazole **169** are triclinic, space group $P\bar{1}$, formula $C_{24}H_{25}N_3O_5S$, MW = 467.53 g mol^{-1}, a = 9.456(2) Å, b = 11.142(3) Å, c = 12.695(3) Å, α = 70.288(8)°, β = 81.753(8)°, γ = 70.999(8)°, U = 1189.7(5) $Å^3$, F(000) = 492, m(Mo Ka) = 0.176 mm^{-1}, R_1(F) = 0.0546 and S = 1.031 for 2701 observed reflections with I > 2σ(I), $wR_2(F^2)$ = 0.1564 for all 4552 unique reflections.

CCDC 1906489 contains the supplementary crystallographic data for pyrazole **169**. This data can be obtained free of charge from The Cambridge Crystallographic Data Centre.

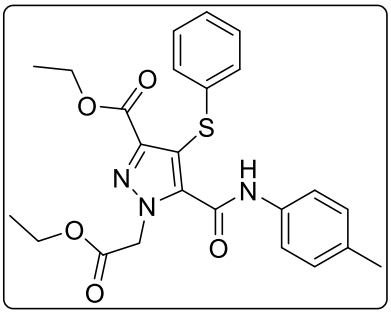

Pyrazole **170**; less polar; mp 124-127°C; ν_{max}/cm^{-1} (ATR) 3301 (NH stretch), 1741 (C=O ester), 1732 (C=O ester), 1650 (C=O amide), 1539 (NH bend), 1216, 1057; δ_H (600 MHz, $CDCl_3$) 1.27 [3H, t, J 7.2 Hz, $NCH_2CO_2CH_2C\underline{H}_3$], 1.29 [3H, t, J 7.2 Hz, $C(3)CO_2CH_2C\underline{H}_3$], 2.31 (3H, s, $ArCH_3$), 4.24 [2H, q, J 7.1 Hz, $NCH_2CO_2C\underline{H}_2$], 4.36 [2H, q, J 7.1 Hz, $C(3)CO_2C\underline{H}_2$], 5.58 (2H, s, NCH_2CO), 7.11 (2H, d, J 8.4 Hz, ArH), 7.16-7.23 (3H, m, ArH), 7.24-7.30 (2H, m, ArH), 7.35 (2H, d, J 8.4 Hz, ArH), 10.04 (1H, br s, NH amide) ppm; δ_C (150.9 MHz, $CDCl_3$) 14.0 (CH_3, one of $C(3)CO_2CH_2\underline{C}H_3$ or $NCH_2CO_2CH_2\underline{C}H_3$), 14.1 ($CH_3$, one of $C(3)CO_2CH_2\underline{C}H_3$ or $NCH_2CO_2CH_2\underline{C}H_3$), 20.8 ($CH_3$, $ArCH_3$), 55.8 (CH_2, $N\underline{C}H_2CO$), 61.5 [CH_2, $C(3)CO_2\underline{C}H_2$], 61.9 [CH_2, $NCH_2CO_2C\underline{H}_2$], 110.3 [C, C(4)], 120.5 (CH, CH_{Ar}), 126.8 (CH, CH_{Ar}), 127.0 (CH, CH_{Ar}), 129.4 (CH, CH_{Ar}), 129.5 (CH, CH_{Ar}), 134.2 (C, $C_{Ar(q)}$), 134.6 (C, $C_{Ar(q)}$), 134.9 (C, $C_{Ar(q)}$), 138.8 [C, C(5)], 144.6 [C, C(3)], 155.9 (C, C=O amide), 160.4 [C, C(3)$\underline{C}$=O], 167.0 [C, $NCH_2\underline{C}$=O] ppm; δ_H (600 MHz, DMSO-d_6) 1.14 [3H, t, J 7.1 Hz, $NCH_2CO_2CH_2C\underline{H}_3$], 1.17 [3H, t, J 7.1 Hz, $C(3)CO_2CH_2C\underline{H}_3$], 2.26 (3H, s, $ArCH_3$), 4.15 [2H, q, J 7.1 Hz, $NCH_2CO_2C\underline{H}_2$], 4.19 [2H, q, J 7.1 Hz, $C(3)CO_2C\underline{H}_2$], 5.40 (2H, s, NCH_2CO), 6.96-7.27 (7H, m, ArH), 7.47-7.50 (2H, m, ArH), 10.56 (1H, s, NH amide) ppm; δ_C (150.9 MHz, DMSO-d_6) 13.88 [CH_3, $NCH_2CO_2CH_2\underline{C}H_3$], 13.90 [$CH_3$, $C(3)CO_2CH_2\underline{C}H_3$], 20.5 ($CH_3$, $ArCH_3$), 53.6 (CH_2, $N\underline{C}H_2CO$), 60.8 [CH_2, $C(3)CO_2\underline{C}H_2$], 61.5 [CH_2, $NCH_2CO_2\underline{C}H_2$], 110.7 [C, C(4)], 119.9 (CH, CH_{Ar}), 125.9 (CH, CH_{Ar}), 126.6 (CH, CH_{Ar}), 129.1 (CH, CH_{Ar}), 129.2 (CH, CH_{Ar}), 133.7 (C, $C_{Ar(q)}$), 135.3 (C, $C_{Ar(q)}$), 136.9 (C, $C_{Ar(q)}$), 142.4 [C, C(5)], 143.2 [C, C(3)], 156.1 (C, C=O amide), 160.2 [C, C(3)$\underline{C}$=O], 167.0 [C, $NCH_2\underline{C}$=O] ppm; δ_H (600 MHz, Toluene-d_8) 0.87 [3H, t, J 7.1 Hz, $NCH_2CO_2CH_2C\underline{H}_3$], 0.97 [3H, t, J 7.1 Hz, $C(3)CO_2CH_2C\underline{H}_3$], 2.02 (3H, s, $ArCH_3$), 3.86 [2H, q, J 7.1 Hz, $NCH_2CO_2C\underline{H}_2$], 4.05 [2H, q, J 7.1 Hz, $C(3)CO_2C\underline{H}_2$], 5.31 (2H, s, NCH_2CO), 6.72-6.77 (1H, m, ArH), 6.79-6.86 (4H, m, ArH), 7.15-7.19 (2H, m, ArH), 7.44-7.49 (2H, m, ArH), 10.09 (s, 1H, NH amide) ppm; δ_C (150.9 MHz, Toluene-d_8) 13.9 [CH_3, $NCH_2CO_2CH_2\underline{C}H_3$], 14.1 [$CH_3$, $C(3)CO_2CH_2\underline{C}H_3$], 20.7 ($CH_3$, overlapping with residual toluene-d_8 signal, $ArCH_3$), 55.9 (CH_2, $N\underline{C}H_2CO$), 60.9 [CH_2, $C(3)CO_2\underline{C}H_2$], 61.5 [CH_2, $NCH_2CO_2\underline{C}H_2$], 110.6 [C, C(4)], 120.2 (CH, CH_{Ar}), 126.8 (CH, CH_{Ar}), 127.6 (CH, CH_{Ar}), 129.5 (CH, CH_{Ar}), 129.8 (CH, CH_{Ar}), 134.3 (C, $C_{Ar(q)}$), 135.5 (C, $C_{Ar(q)}$), 135.7 (C, $C_{Ar(q)}$), 138.8 [C, C(5)], 145.2 [C, C(3)], 156.2 (C, C=O amide), 160.6 [C, C(3)$\underline{C}$=O], 167.0 [C, $NCH_2\underline{C}$=O] ppm; HRMS (ES+): Exact mass calculated for $C_{24}H_{25}N_3O_5S$ $[M+H]^+$ 468.1588. Found 468.1583; m/z (ES+) 468.2 {[($C_{24}H_{25}N_3O_5S$)+H^+], 68%}, 721.1 (100%).

Note: *The title compounds **169** and **170** were also isolated as by-products in the [3+2] dipolar cycloaddition of α-thio-β-chloroacrylamide **71** and ethyl diazoacetate, through competing N–H insertion. Spectroscopic data are consistent with that outlined above.*

Ethyl 1-benzyl-4-(phenylthio)-3-(4′-methylphenylcarbamoyl)-1*H*-pyrazole-5-carboxylate 236 and **ethyl 1-benzyl-4-(phenylthio)-5-(4′-methylphenylcarbamoyl)-1*H*-pyrazole-3-carboxylate 237**

The title compounds were prepared following the procedure described for **169**/**170** using ethyl 4-(phenylthio)-5-(4′-methylphenylcarbamoyl)-1*H*-pyrazole-3-carboxylate **71** (150 mg, 0.393 mmol), benzyl bromide (81 mg, 0.472 mmol) and potassium carbonate (71 mg, 0.512 mmol) in anhydrous dimethylsulfoxide (3ml). ^{1}H NMR analysis of the crude mixture indicated a 78:22 ratio of pyrazoles **236**:**237**. Purification by column chromatography (one spot by TLC) on silica gel using dichloromethane (100%) as eluent gave the pure pyrazole **236** as a clear oil (53 mg, 29 %), pyrazole **237** (in 87% purity by ^{1}H NMR spectroscopy) as a white solid (27 mg, 15 %), and a mixed fraction of **236** and **237** as a white solid (58 mg, 32 %) to give a combined yield of 76 %.

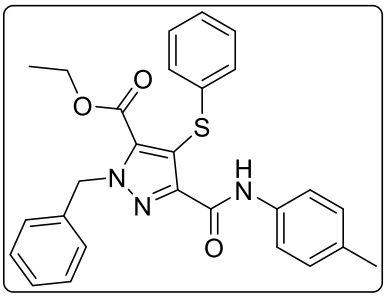

Pyrazole **236**; more polar; ν_{max}/cm^{-1} (ATR) 2982 (CH), 1716 (C=O ester), 1681 (C=O amide), 1525, 1259; δ_H (300 MHz, $CDCl_3$) 1.10 (3H, t, *J* 7.1 Hz, $OCH_2C\underline{H}_3$), 2.30 (3H, s, $ArCH_3$), 4.15 (2H, q, *J* 7.1 Hz, $OC\underline{H}_2CH_3$), 5.79 (2H, s, NCH_2CO), 7.02-7.40 (12H, m, ArH), 7.51 (2H, d, *J* 8.3 Hz, ArH), 9.07 (1H, s, NH amide) ppm; δ_C (75.5 MHz, $CDCl_3$) 13.7 (CH_3, $OCH_2C\underline{H}_3$), 20.8 (CH_3, $ArCH_3$), 56.6 (CH_2, NCH_2), 61.9 (CH_2, $OC\underline{H}_2CH_3$), 113.8 [C, C(4)], 119.8 (CH, CH_{Ar}), 125.9 (CH, CH_{Ar}), 127.1 (CH, CH_{Ar}), 127.5 (CH, CH_{Ar}),128.1 (C, $C_{Ar(q)}$), 128.7 (CH, CH_{Ar}), 128.9 (CH, CH_{Ar}), 129.4 (CH, CH_{Ar}), 133.8 (C, $C_{Ar(q)}$), 135.0 (C, $C_{Ar(q)}$), 135.6 (C, $C_{Ar(q)}$), 136.6 (C, $C_{Ar(q)}$), 136.9 [C, C(5)], 146.3 [C, C(3)], 157.9 (C, C=O amide), 158.9 (C, C=O ester) ppm; HRMS (ES+): Exact mass calculated for $C_{27}H_{25}N_3O_3S$ $[M+OH]^+$ 488.1639. Found 488.1641.

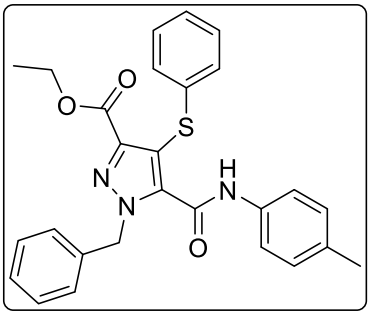

Pyrazole **237**; (87% pure by ^{1}H NMR spectroscopy – contains 13% pyrazole **236**); less polar; mp 127-133°C; ν_{max}/cm^{-1} (ATR) 3429 (NH stretch), 2989 (CH), 1724 (C=O ester), 1671 (C=O amide), 1543, 1219; δ_H (300 MHz, $CDCl_3$) 1.30 (3H, t, *J* 7.1 Hz, $OCH_2C\underline{H}_3$), 2.30 (3H, s, $ArCH_3$), 4.37 (2H, q, unresolved coupling, $OC\underline{H}_2CH_3$), 6.04 (2H, s, NCH_2CO), 7.01-7.41 (14H, m, ArH), 9.68 (1H, s, NH amide) ppm; δ_C (75.5 MHz, $CDCl_3$) 14.2 (CH_3, $OCH_2C\underline{H}_3$), 20.9 (CH_3, $ArCH_3$), 57.1 (CH_2, NCH_2), 61.5 (CH_2, $OC\underline{H}_2CH_3$), 110.4 [C, C(4)], 120.5 (CH, CH_{Ar}), 126.8 (CH, CH_{Ar}), 127.1 (CH, CH_{Ar}), 127.99 (CH, CH_{Ar}), 128.04 (CH, CH_{Ar}), 128.6 (CH, CH_{Ar}), 129.5 (CH, CH_{Ar}), 129.6 (CH, CH_{Ar}), 134.3 (C, $C_{Ar(q)}$), 134.91 (C, $C_{Ar(q)}$), 134.94 (C, $C_{Ar(q)}$), 136.0 (C, $C_{Ar(q)}$), 138.4 [C, C(3], 144.5 [C, C(5)], 155.9 (C, C=O amide), 160.9 (C, C=O ester) ppm; HRMS (ES+): Exact mass calculated for $C_{27}H_{25}N_3O_3S$ $[M+OH]^+$ 488.1639. Found 488.1640.

Ethyl 1-(2-oxo-2-phenylethyl)-4-(phenylthio)-3-(4′-methylphenylcarbamoyl)-1*H*-pyrazole-5-carboxylate 238 and **ethyl 1-(2-oxo-2-phenylethyl)-4-(phenylthio)-5-(4′-methylphenylcarbamoyl)-1*H*-pyrazole-3-carboxylate 239**

The title compounds were prepared following the procedure described for **169**/**170** using ethyl 4-(phenylthio)-5-(4′-methylphenylcarbamoyl)-1*H*-pyrazole-3-carboxylate **71** (150 mg, 0.393 mmol), 2-bromoacetophenone (94 mg, 0.472 mmol) and potassium carbonate (71 mg, 0.512 mmol) in anhydrous dimethyl sulfoxide (3ml). ^{1}H NMR analysis of the crude mixture indicated a 75:25 ratio of pyrazoles **238**:**239**. Purification by column chromatography on silica gel using hexane: ethyl acetate (80:20) as eluent gave the pure pyrazole **238** as a white solid (89 mg, 45 %), pure pyrazole **239** as a white solid (32 mg, 16 %), and a mixed fraction of **238** and **239** as a clear oil which solidified overnight to give a white solid (45 mg, 23 %) to give a combined yield of 84 %.

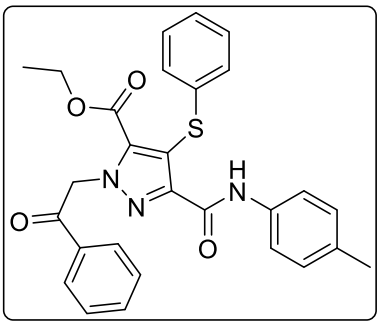

Pyrazole **238**; more polar; mp 138-141°C; ν_{max}/cm^{-1} (ATR) 3206 (NH stretch), 2995 (CH), 1730 (C=O ester), 1702 (C=O ketone), 1659 (C=O amide), 1245; δ_H (300 MHz, $CDCl_3$) 1.08 (3H, t, *J* 7.1 Hz, $OCH_2C\underline{H}_3$), 2.30 (3H, s, $ArCH_3$), 4.15 (2H, q, *J* 7.1 Hz, $OC\underline{H}_2CH_3$), 6.13 (2H, s, NCH_2CO), 7.04-7.31 (7H, m, ArH), 7.44-7.72 (5H, m, ArH), 7.93-8.03 (2H, m, ArH), 9.17 (1H, s, NH amide) ppm; δ_C (75.5 MHz, $CDCl_3$) 13.6 (CH_3, $OCH_2\underline{C}H_3$), 20.8 (CH_3, $ArCH_3$), 60.0 (CH_2, $N\underline{C}H_2CO$), 62.0 (CH_2, $O\underline{C}H_2CH_3$), 113.2 [C, C(4)], 119.9 (CH, CH_{Ar}), 125.9 (CH, CH_{Ar}), 126.8 (CH, CH_{Ar}), 127.9 (CH, CH_{Ar}), 129.0 (CH, CH_{Ar}), 129.1 (CH, CH_{Ar}), 129.4 (CH, CH_{Ar}), 133.9 (C, $C_{Ar(q)}$), 134.1 (C, $C_{Ar(q)}$), 134.3 (CH, CH_{Ar}), 135.0 (C, $C_{Ar(q)}$), 137.7 [C, C(5)], 146.9 [C, C(3)], 157.8 (C, C=O amide), 159.0 (C, C=O ester), 190.9 (C, C=O ketone) ppm; HRMS (ES+): Exact mass calculated for $C_{28}H_{25}N_3O_4S$ $[M+H]^+$ 500.1639. Found 500.1630.

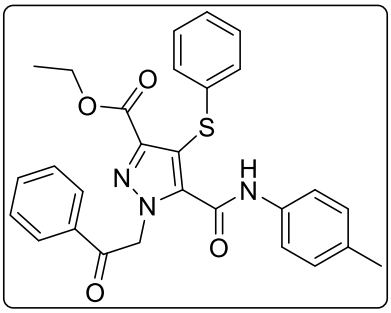

Pyrazole **239**; less polar; mp 163-166°C; ν_{max}/cm^{-1} (ATR) 3233 (NH stretch), 2946 (CH), 1731 (C=O ester), 1698 (C=O ketone), 1657 (C=O amide), 1219; δ_H (300 MHz, $CDCl_3$) 1.29 (3H, t, *J* 7.1 Hz, $OCH_2C\underline{H}_3$), 2.27 (3H, s, ArH), 4.37 (2H, q, *J* 7.1 Hz, $OC\underline{H}_2CH_3$), 6.35 (2H, s, NCH_2CO), 7.07 (2H, d, *J* 8.3 Hz, ArH), 7.15-7.37 (7H, m, ArH), 7.44-7.72 (3H, m, ArH), 7.92-8.05 (2H, m, ArH), 10.06 (1H, s, NH amide) ppm; δ_C (75.5 MHz, $CDCl_3$) 14.1 (CH_3, $OCH_2\underline{C}H_3$), 20.9 (CH_3, $ArCH_3$), 60.8 (CH_2, $N\underline{C}H_2CO$), 61.5 (CH_2, OCH_2CH_3), 110.2 [C, C(4)], 120.6 (CH, CH_{Ar}), 126.7 (CH, CH_{Ar}), 127.0 (CH, CH_{Ar}), 128.0 (CH, CH_{Ar}), 128.9 (CH, CH_{Ar}), 129.5 (CH, CH_{Ar}), 134.0 (CH, CH_{Ar}), 134.1 (C, $C_{Ar(q)}$), 134.3 (C, $C_{Ar(q)}$), 134.8 (C, $C_{Ar(q)}$), 134.9 (C, $C_{Ar(q)}$), 139.3 [C, C(5)], 144.7 [C, C(3)], 156.0 (C, C=O amide), 160.5 (C, C=O ester), 191.2 (C, C=O ketone) ppm; HRMS (ES+): Exact mass calculated for $C_{28}H_{25}N_3O_4S$ $[M+H]^+$ 500.1639. Found 500.1630.

Ethyl 1-ethyl-4-(phenylthio)-3-(4′-methylphenylcarbamoyl)-1*H*-pyrazole-5-carboxylate 240

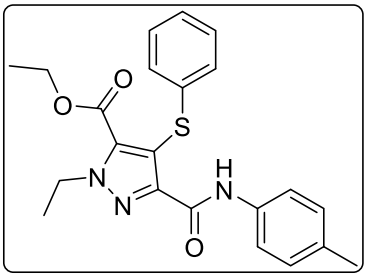

The title compound was prepared following the procedure described for **169/170** using ethyl 4-(phenylthio)-5-(4′-methylphenylcarbamoyl)-1*H*-pyrazole-3-carboxylate **71** (150 mg, 0.393 mmol), bromoethane (52 mg, 0.472 mmol) and potassium carbonate (71 mg, 0.512 mmol) in anhydrous dimethyl sulfoxide (3 ml). Purification by flash column chromatography on silica gel using hexane: ethyl acetate (75:25) as eluent, followed by recrystallisation from ethyl acetate: heptane gave the pure pyrazole **240** as a white solid (113 mg, 70 %); mp 94-96°C; ν_{max}/cm^{-1} (ATR) 3397 (NH stretch), 2981 (CH), 1726 (C=O ester), 1690 (C=O amide), 1520, 1251, 1048; δ_H (300 MHz, $CDCl_3$) 1.19 (3H, t, *J* 7.1 Hz, $OCH_2C\underline{H}_3$), 1.52 (3H, t, *J* 7.1 Hz, $NCH_2C\underline{H}_3$), 2.30 (3H, s, ArH), 4.25 (2H, q, *J* 7.1 Hz, $OC\underline{H}_2CH_3$), 4.63 (2H, q, *J* 7.1 Hz, $NC\underline{H}_2CH_3$), 7.03-7.30 (7H, m, ArH), 7.52 (2H, d, *J* 8.4 Hz, ArH), 9.13 (1H, s, NH amide) ppm; δ_C (75.5 MHz, $CDCl_3$) 13.8 (CH_3, $OCH_2\underline{C}H_3$), 15.6 (CH_3, $N\underline{C}H_2CH_3$), 20.8 (CH_3, $ArCH_3$), 48.9 (CH_2, $N\underline{C}H_2CH_3$), 62.0 (CH_2, OCH_2CH_3), 112.7 [C, C(4)], 119.8 (CH, CH_{Ar}), 125.9 (CH, CH_{Ar}), 127.0 (CH, CH_{Ar}), 129.0 (CH, CH_{Ar}), 129.4 (CH, CH_{Ar}), 129.6 (CH, CH_{Ar}), 133.8 (C, $C_{Ar(q)}$), 135.1 (C, $C_{Ar(q)}$), 136.4 [C, C(5)], 136.6 (C, $C_{Ar(q)}$), 146.0 [C, C(3)], 158.0 (C, C=O amide), 159.0 (C, C=O ester) ppm; HRMS (ES+): Exact mass calculated for $C_{22}H_{23}N_3O_3S$ $[M+H]^+$ 410.1533. Found 410.1534.

4-(Phenylthio)-5-(4-methylphenylcarbamoyl)-1*H*-pyrazole-3-carboxylic acid 241

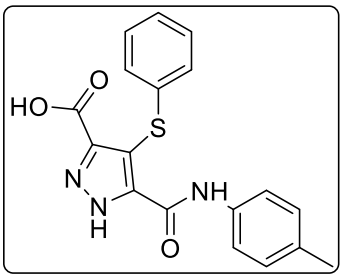

Sodium hydroxide (97 mg, 2.43 mmol) in water (15 ml) was added in one portion to a stirring solution of ethyl 4-(phenylthio)-5-(4'-methylphenylcarbamoyl)-1*H*-pyrazole-3-carboxylate **71** (232 mg, 0.61 mmol) in methanol (5 ml) at room temperature. The heterogenous reaction mixture was heated to reflux at which point the reaction mixture became homogenous, and was stirred at this temperature overnight. The reaction mixture was concentrated under reduced pressure to dryness. Water (15 ml) and ethyl acetate (15 ml) was added, and the layers separated. Concentrated HCl was added until a pH of 2 was achieved, which caused the carboxylic acid **241** to precipitate out of solution. Ethyl acetate (15 ml) was added and the layers separated. The aqueous layer was further extracted with ethyl acetate (2 x 15 ml). The combined organic layers were washed with brine (15 ml), dried, and concentrated under reduced pressure to give the pure pyrazole **241** (195 mg, 91 %) as a white solid; mp 226-229°C; ν_{max}/cm^{-1} (ATR) 3126 (OH stretch), 3025 (NH), 2953 (CH), 1690 (C=O carboxylic acid), 1648 (C=O amide), 1606, 1474, 1235; δ_H (600 MHz, DMSO-d_6) 2.26 (3H, s, ArCH$_3$), 3.40 (1H, br s, COOH), 7.04-7.30 (7H, m, ArH), 7.55 (2H, d, *J* 8.1 Hz, ArH), 10.18 (1H, s, NH amide), 14.64 (1H, br s, NH pyrazole) ppm; δ_H (600 MHz, DMSO-d_6) 2.25 (3H, s, ArCH$_3$), 3.38 (1H, br s, COOH), 7.02-7.28 (7H, m, ArH), 7.46-7.64 (2H, d, *J* 8.1 Hz, ArH), 10.20 (1H, s, NH amide), 14.67 (1H, br s, NH pyrazole) ppm; δ_C (150.9 MHz, DMSO-d_6) 20.9 (CH$_3$, ArCH$_3$), 110.8 [C, C(4)], 120.3 (CH, CH$_{Ar}$), 125.7 (CH, CH$_{Ar}$), 126.9 (CH, CH$_{Ar}$), 129.3 (CH, CH$_{Ar}$), 129.5 (CH, CH$_{Ar}$), 133.1 (C, C$_{Ar(q)}$), 136.5 (C, C$_{Ar(q)}$), 138.0 (C, C$_{Ar(q)}$), 150.2 (C, C=O carboxylic acid), 159.7 (C, C=O amide) ppm; HRMS (ES+): Exact mass calculated for $C_{18}H_{15}N_3O_3S$ $[M+H]^+$ 354.0907. Found 354.0901.

Note: *C(3) and C(5) not observed at 150.9 MHz*

***N*^{3}-(4′-Methoxyphenyl)-4-(phenylthio)-*N*^{5}-(4′-methylphenyl)-1*H*-pyrazole-3,5-dicarboxamide 242**

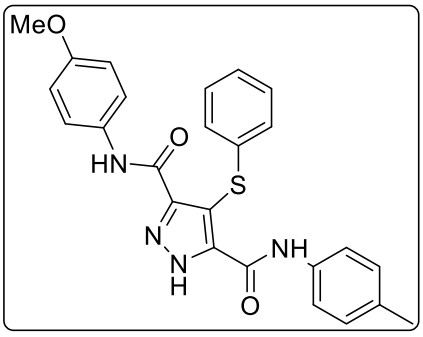

4-Dimethylaminopyridine (7 mg, 0.06 mmol) and *p*-anisidine (150 mg, 1.22 mmol) were added to a stirring solution of 4-(phenylthio)-5-(4-methylphenylcarbamoyl)-1*H*-pyrazole-3-carboxylic acid **241** (195 mg, 0.55 mmol) in dichloromethane (25 ml) at 0˚C. The solution was stirred at this temperature for 2 minutes at which point *N*′,*N*′-diisopropylcarbodiimide (105 mg, 0.83 mmol) was added in dichloromethane (5 ml). The reaction mixture was immediately heated to reflux and was stirred at this temperature for 12 h. The cooled reaction mixture was washed with water (30 ml) and the layers separated. The organic layer was washed with 2M hydrochloric acid (2 x 30 ml) and brine (30 ml), dried, and concentrated under reduced pressure to give the crude product as a grey/brown solid. Purification by recrystallisation using ethyl acetate: heptane gave the pure product **242** as a grey solid (162 mg, 64 %); mp 237-239°C; ν_{max}/cm^{-1} (ATR) 3211 (NH stretch), 2917 (CH), 1682, (C=O amide), 1666 (C=O amide), 1320, 1161; ^{1}H NMR (300 MHz, DMSO-d_6) δ = 2.26 (s, 3H, ArCH$_3$), 3.73 (s, 3H, ArOCH$_3$), 6.58-7.87 (m, 13H, ArH), 10.18 (s, 1H, NH amide), 10.22 (s, 1H, NH amide),14.67 (br s, NH pyrazole) ppm; δ_H (600 MHz, DMSO-d_6) 2.27 (3H, s, ArCH$_3$), 3.73 (3H, s, ArOCH$_3$), 6.62-7.90 (13H, m, ArH), 10.22 (1H, s, NH amide), 10.26 (1H, s, NH amide), 14.70 (1H, br s, NH pyrazole) ppm; δ_C (150.9 MHz, DMSO-d_6) 20.5 (CH$_3$, ArCH$_3$), 55.2 (CH$_3$, ArOCH$_3$), 106.5 [C, C(4)], 113.9 (CH, CH$_{Ar}$), 119.9 (CH, CH$_{Ar}$), 121.4 (CH, CH$_{Ar}$), 125.8 (CH, CH$_{Ar}$), 126.7 (CH, CH$_{Ar}$), 129.1 (CH, CH$_{Ar}$), 129.2 (CH, CH$_{Ar}$), 131.3 (C, br, C$_{Ar(q)}$), 133.1 (C, br, C$_{Ar(q)}$), 135.7 (C, br, C$_{Ar(q)}$), 136.9 (C, C$_{Ar(q)}$), 142.2 [C, br, one of C(3) or C(5)], 148.0 [C, br, one of C(3) or C(5)], 155.8 (C, C$_{Ar(q)}$OMe), 157.6 (C, br, overlapping

C=O amides) ppm; HRMS (ES+): Exact mass calculated for $C_{25}H_{22}N_4O_3S$ $[M+H]^+$ 459.1485. Found 459.1486.

Bibliography

1. M. M. Schaeffer and A. R. Maguire, unpublished results, University College Cork, **1993**.
2. M. Kennedy, A. R. Maguire and M. A. McKervey, *Tetrahedron Lett.*, **1986**, 27, 761-764.
3. M. Kennedy, M. A. McKervey, A. R. Maguire and S. Naughton, *J. Chem. Soc. Perkin 1*, **1990**, 1041-1045.
4. B. M. Dilworth and M. A. McKervey, *Tetrahedron*, **1986**, 42, 3731-3752.
5. N. W. A. Geraghty, *Comprehensive Organic Functional Group Transformations;* Eds. A. R. Katritzky; O. Meth-Cohn; C. W. Rees*;* Permagon Press, Oxford, **1995**, Vol. 4, pg 63.
6. A. R. Maguire, M. E. Murphy, M. Schaeffer and G. Ferguson, *Tetrahedron Lett.*, **1995**, 36, 467-470.
7. M. Murphy, D. Lynch, M. Schaeffer, M. Kissane, J. Chopra, E. O'Brien, A. Ford, G. Ferguson and A. R. Maguire, *Org. Biomol. Chem.*, **2007**, 5, 1228-1241.
8. M. Kissane, D. Lynch, J. Chopra, S. E. Lawrence and A. R. Maguire, *Org. Biomol. Chem.*, **2010**, 8, 5602-5613.
9. M. Kissane, S. E. Lawrence and A. R. Maguire, *Org. Biomol. Chem.*, **2010**, 8, 2735-2748.
10. M. Kissane, S. E. Lawrence and A. R. Maguire, *Tetrahedron*, **2010**, 66, 4564-4572.
11. M. Kissane, S. E. Lawrence and A. R. Maguire, *Tetrahedron: Asymmetry.*, **2010**, 21, 871-884.
12. M. Kissane, D. Lynch, J. Chopra, S. E. Lawrence and A. R. Maguire, *Tetrahedron: Asymmetry.*, **2008**, 19, 1256-1273.
13. M. Kissane, M. Murphy, S. E. Lawrence and A. R. Maguire, *Tetrahedron: Asymmetry.*, **2010**, 21, 2550-2558.
14. M. Kissane, M. Murphy, E. O'Brien, J. Chopra, L. Murphy, S. G. Collins, S. E. Lawrence and A. R. Maguire, *Org. Biomol. Chem.*, **2011**, 9, 2452-2472.
15. M. Murphy, *Ph. D. Thesis*, University College Cork, **1998**.
16. D. Lynch, *Ph. D. Thesis*, University College Cork, **2000**.
17. D. A. Foley, C. W. Doecke, J. Y. Buser, J. M. Merritt, L. Murphy, M. Kissane, S. G. Collins, A. R. Maguire and A. Kaerner, *J. Org. Chem.*, **2011**, 76, 9630-9640.
18. V. M. Y. Cacheux, *Ph. D. Thesis*, University College Cork, **2018**.
19. O. C. Dennehy, V. M. Y. Cacheux, B. J. Deadman, D. Lynch, S. G. Collins, H. A. Moynihan and A. R. Maguire, *Beilstein J. Org. Chem.*, **2016**, 12, 2511-2522.
20. J. Chopra, *Ph. D. Thesis*, University College Cork, **2007**.
21. M. Kissane, *Ph. D. Thesis*, University College Cork, **2009**.
22. M. Kissane and A. R. Maguire, *Synlett*, **2011**, 1212-1232.
23. J. A. Joule and K. Mills, *Heterocyclic Chemistry*, John Wiley & Sons, **2010**.
24. T. L. Gilchrist and G. W. Gribble, in *Progress in Heterocyclic Chemistry*, Elsevier, **1985**.
25. T. Eicher, S. Hauptmann and A. Speicher, in *The Chemistry of Heterocycles*, Wiley-VCH, **1995**.
26. V. J. Ram, A. Sethi, M. Nath and R. Pratap, in *The Chemistry of Heterocycles: Chemistry of Six to Eight Membered N, O, S, P and Se Heterocycles* Elsevier.
27. A. F. Pozharskii, A. T. Soldatenkov and A. R. Katritzky, in *Heterocycles in Life and Society: An Introduction to Heterocyclic Chemistry, Biochemistry and Applications*, Wiley, **2011**.
28. J. Alvarez-Builla; J. J. Vaquero; J. Barluenga; *Modern Heterocyclic Chemistry*, **2011**.
29. *Heterocycles in Natural Product Synthesis* Wiley, **2011**.
30. A. Ansari, A. Ali, M. Asif and Shamsuzzaman, *New J. Chem.*, **2017**, 41, 16-41.
31. M. J. Naim, O. Alam, F. Nawaz, M. J. Alam and P. Alam, *J. Pharm. Bioallied Sci.*, **2016**, 8, 2-17.
32. S. Andreas and D. Andrij, *Curr. Org. Chem.*, **2011**, 15, 1423-1463.
33. V. Kumar, K. Kaur, G. K. Gupta and A. K. Sharma, *Eur. J. Med. Chem.*, **2013**, 69, 735-753.
34. T. D. Penning, J. J. Talley, S. R. Bertenshaw, J. S. Carter, P. W. Collins, S. Docter, M. J. Graneto, L. F. Lee, J. W. Malecha, J. M. Miyashiro, R. S. Rogers, D. J. Rogier, S. S. Yu, G. D. Anderson, E. G. Burton, J. N. Cogburn, S. A. Gregory, C. M. Koboldt, W. E. Perkins, K. Seibert, A. W. Veenhuizen, Y. Y. Zhang and P. C. Isakson, *J. Med. Chem.*, **1997**, 40, 1347-1365.
35. P. Krishnappa, E. Fernandez-Pascual, J. Carballido and J. I. Martinez-Salamanca, *Int. J. Impot. Res.*, **2019**, 31, 65-70.
36. M. Rinaldi-Carmona, F. Barth, M. Héaulme, D. Shire, B. Calandra, C. Congy, S. Martinez, J. Maruani, G. Néliat, D. Caput, P. Ferrara, P. Soubrié, J. C. Brelière and G. Le Fur, *FEBS Letters*, **1994**, 350, 240-244.
37. M. E. Y. Francisco, H. H. Seltzman, A. F. Gilliam, R. A. Mitchell, S. L. Rider, R. G. Pertwee, L. A. Stevenson and B. F. Thomas, *J. Med. Chem.*, **2002**, 45, 2708-2719.
38. R. König, *Colour Additives for Food and Beverages* Woodhead Publishing, Oxford, **2015**.
39. A. Aajoud, P. Ravanel and M. Tissut, *J. Agric. Food Chem.*, **2003**, 51, 1347-1352.

40. S. Fustero, A. Simón-Fuentes and J. F. Sanz-Cervera, *Org. Prep. Proced. Int.*, **2009**, 41, 253-290.
41. Y. H. Kao, C. H. Chong, W. T. Ng and D. Lim, *Occup. Med.*, **2007**, 57, 535-537.
42. K. Martina, S. Tagliapietra, V. V. Veselov and G. Cravotto, *Front. Chem.*, **2019**, 7.
43. T. L. Gilchrist and R. C. Storr, in *Organic Reactions and Orbital Symmetry*, Cambridge University Press **1972**.
44. S. D. Andrews, A. C. Day and A. N. McDonald, *J. Chem. Soc. C: Org.*, **1969**, 787-790.
45. M. Kissane and A. R. Maguire, *Chem. Soc. Rev.,* **2010**, 39, 845-883.
46. J. Gracia-Vitoria, I. Osante, C. Cativiela, P. Merino and T. Tejero, *J. Org. Chem.*, **2018**, 83, 3960-3972.
47. J. Britton and T. F. Jamison, *Angew. Chem. Int. Ed.*, **2017**, 56, 8823-8827.
48. H. Jangra, Q. Chen, E. Fuks, I. Zenz, P. Mayer, A. R. Ofial, H. Zipse and H. Mayr, *J. Am. Chem. Soc*, **2018**, 140, 16758-16772.
49. M. Breugst, R. Huisgen and H.-U. Reissig, *Eur. J. Org. Chem*, **2018**, 2477-2485.
50. M. Flipo, N. Willand, N. Lecat-Guillet, C. Hounsou, M. Desroses, F. Leroux, Z. Lens, V. Villeret, A. Wohlkönig, R. Wintjens, T. Christophe, H. Kyoung Jeon, C. Locht, P. Brodin, A. R. Baulard and B. Déprez, *J. Med. Chem.*, **2012**, 55, 6391-6402.
51. F. G. Bordwell and D. L. Hughes, *J. Org. Chem.*, **1982**, 47, 3224-3232.
52. M. Kissane, M. Murphy, D. Lynch, A. Ford and A. R. Maguire, *Tetrahedron*, **2008**, 64, 7639-7649.
53. C. Murphy, *Ph. D Thesis*, University College Cork, **2020**.
54. L. E. Murphy, *Ph. D Thesis*, University College Cork, **2013**.
55. H. G. Viehe, Z. Janousek, R. Merenyi and L. Stella, *Acc. Chem. Res.*, **1985**, 18, 148-154.
56. F. Pietrocola, L. Galluzzi, José M. Bravo-San Pedro, F. Madeo and G. Kroemer, *Cell Metab.*, **2015**, 21, 805-821.
57. J. Staunton and K. J. Weissman, *Nat. Prod. Rep.*, **2001**, 18, 380-416.
58. E. Erba, D. Bergamaschi, S. Ronzoni, M. Faretta, S. Taverna, M. Bonfanti, C. V. Catapano, G. Faircloth, J. Jimeno and M. D'Incalci, *Br. J. Cancer*, **1999**, 80, 971-980.
59. Y. Kanda, T. Ashizawa, S. Kakita, Y. Takahashi, M. Kono, M. Yoshida, Y. Saitoh and M. Okabe, *J. Med. Chem.*, **1999**, 42, 1330-1332.
60. R. J. Kennedy and A. M. Stock, *J. Org. Chem.*, **1960**, 25, 1901-1906.
61. W. Adam, R. Curci and J. O. Edwards, *Accounts of Chemical Research*, **1989**, 22, 205-211.
62. R. W. Murray, *Chem. Rev.*, **1989**, 89, 1187-1201.
63. R. W. Murray and R. Jeyaraman, *J. Org. Chem.*, **1985**, 50, 2847-2853.
64. R. W. Murray, R. Jeyaraman and M. K. Pillay, *J. Org. Chem.*, **1987**, 52, 746-748.
65. P. Hanson, R. A. A. J. Hendrickx and J. R. Lindsay Smith, *Org. Biomol. Chem.*, **2008**, 6, 762-771.
66. P. Hanson, R. A. A. J. Hendrickx and J. R. Lindsay Smith, *New J. Chem.*, **2010**, 34, 65-84.
67. P. Hanson, R. A. A. J. Hendrickx and J. R. L. Smith, *Org. Biomol. Chem.*, **2008**, 6, 745-761.
68. S. Korneev and C. Richter, *Synthesis*, **1995**, 1995, 1248-1250.
69. S. Zhu, J. V. Ruppel, H. Lu, L. Wojtas and X. P. Zhang, *J. Am. Chem. Soc*, **2008**, 130, 5042-5043.
70. A. M. van Leusen and J. Strating, *Recl. Trav. Chim. Pays-Bas*, **1965**, 84, 151-164.
71. A. M. v. Leusen and J. Strating, *Org. Synth.*, **1977**, 57.
72. R. A. Weatherhead-Kloster, Corey, E. J., *Org. Lett.*, **2005**, 8, 171-174.
73. C. Plessis, D. Uguen, A. De Cian and J. Fischer, *Tetrahedron Lett.*, **2000**, 41, 5489-5493.
74. Y. Yan, G. Ma, W. Wei and J. Zhao, *Aust. J. Chemistry*, **2016**, 69, 239-242.
75. R. Seshadri, W. J. Pegg and M. Israel, *J. Org. Chem.*, **1981**, 46, 2596-2598.
76. H. Loghmani-Khouzani, M. R. Poorheravi, M. M. M. Sadeghi, L. Caggiano and R. F. W. Jackson, *Tetrahedron*, **2008**, 64, 7419-7425.
77. R. P. Wurz, W. Lin and A. B. Charette, *Tetrahedron Lett.*, **2003**, 44, 8845-8848.
78. D. Marcovici-Mizrahi, H. E. Gottlieb, V. Marks and A. Nudelman, *J. Org. Chem.*, **1996**, 61, 8402-8406.
79. D. Kost and N. Kornberg, *Tetrahedron Lett.*, **1978**, 19, 3275-3276.
80. M. Regitz, *Angew. Chem. Int. Ed.*, **1967**, 6, 733-749.
81. J. S. Baum, D. A. Shook, H. M. L. Davies and H. D. Smith, *Synth. Commun.*, **1987**, 17, 1709-1716.
82. T. Curtius, *Berichte der deutschen chemischen Gesellschaft*, **1883**, 16, 2230-2231.
83. *Organic Syntheses, Col Vol 3*, Wiley, New York, **1955**.
84. W. R. Bamford and T. S. Stevens, *J. Chem. Soc.*, **1952**, 4735-4740.
85. J. R. Fulton, V. K. Aggarwal and J. de Vicente, *Eur. J. Org. Chem*, **2005**, 1479-1492.
86. T. L. Holton and H. Schechter, *J. Org. Chem.*, **1995**, 60, 4725-4729.
87. M. E. Furrow and A. G. Myers, *J. Am. Chem. Soc.*, **2004**, 126, 12222-12223.
88. R. J. Baumgarten, *J. Org. Chem.*, **1967**, 32, 484-485.

89. M. Schroen and S. Bräse, *Tetrahedron*, **2005**, 61, 12186-12192.
90. T. J. D. Boer and H. J. Backer, *Org. Synth., Coll. Vol. 4,* Wiley New York, **1963**.
91. E. L. Myers and R. T. Raines, *Angew. Chem. Int. Ed.*, **2009**, 48, 2359-2363.
92. W. Ando, *Acc. Chem. Res.*, **1977**, 10, 179-185.
93. A. Padwa and S. F. Hornbuckle, *Chem. Rev.*, **1991**, 91, 263-309.
94. R. A. Weatherhead-Kloster and E. J. Corey, *Org. Lett.*, **2006**, 8, 171-174.
95. O. De Lucchi, V. Lucchini, L. Pasquato and G. Modena, *J. Org. Chem.*, **1984**, 49, 596-604.
96. M. Regitz and G. Maas, in *Diazo Compounds. Properties and Synthesis*, Academic Press: London, **1986**.
97. N. S. Goulioukina, N. N. Makukhin, E. D. Shinkarev, Y. K. Grishin, V. A. Roznyatovsky and I. P. Beletskaya, *Org. Biomol. Chem.*, **2016**, 14, 10000-10010.
98. D. Vuluga, J. Legros, B. Crousse and D. Bonnet-Delpon, *Green. Chem.*, **2009**, 11, 156-159.
99. E. Keller, B. de Lange, M. T. Rispens and B. L. Feringa, *Tetrahedron*, **1993**, 49, 8899-8910.
100. B. de Lange and B. L. Feringa, *Tetrahedron Lett.*, **1988**, 29, 5317-5320.
101. S. He, L. Chen, Y.-N. Niu, L.-Y. Wu and Y.-M. Liang, *Tetrahedron Lett.*, **2009**, 50, 2443-2445.
102. A. Kamal, K. N. V. Sastry, D. Chandrasekhar, G. S. Mani, P. R. Adiyala, J. B. Nanubolu, K. K. Singarapu and R. A. Maurya, *J. Org. Chem.*, **2015**, 80, 4325-4335.
103. K. M. J. Cheung, J. Reynisson and E. McDonald, *Tetrahedron Lett.*, **2010**, 51, 5915-5918.
104. M. Di and K. S. Rein, *Tetrahedron Lett.*, **2004**, 45, 4703-4705.
105. M. P. Sibi, L. M. Stanley and T. Soeta, *Org. Lett.*, **2007**, 9, 1553-1556.
106. J. Huang, M. Wu, L. Hu, H. Guo and S. Sun, *Asian. J. Org. Chem.*, **2016**, 5, 462-465.
107. M.-A. Plancquaert, M. Redon, Z. Janousek and H. G. Viehe, *Tetrahedron*, **1996**, 52, 4383-4396.
108. T. L. Gilchrist and R. C. Storr, in *Organic Reactions and Orbital Symmetry* Cambridge University Press **1972**.
109. I. Fleming, in *Frontier Orbitals and Organic Chemical Reactions* Wiley Interscience London, **1976**.
110. B. Abeykoon, T. Devic, J.-M. Grenèche, A. Fateeva and A. B. Sorokin, *Chem. Comm.*, **2018**, 54, 10308-10311.
111. M. Basato, C. Tubaro, A. Biffis, M. Bonato, G. Buscemi, F. Lighezzolo, P. Lunardi, C. Vianini, F. Benetollo and A. Del Zotto, *Chem. Eur. J*, **2009**, 15, 1516-1526.
112. *X-ray struture determination was conducted by Dr. S.R. Lawrence, School of Chemistry, Univerisity College Cork*.
113. K. Nikitin, K. V. Rajendran, H. Müller-Bunz and D. G. Gilheany, *Angew. Chem. Int. Ed.*, **2014**, 53, 1906-1909.
114. D. Sahu, S. Dey, T. Pathak and B. Ganguly, *Org. Lett.*, **2014**, 16, 2100-2103.
115. R. Kumar, D. Nair and I. N. N. Namboothiri, *Tetrahedron*, **2014**, 70, 1794-1799.
116. T. V. Baiju and I. N. N. Namboothiri, *Chem. Rec.*, **2017**, 17, 939-955.
117. *X-ray struture determination was conducted by Dr. U. B. Rao. Khandavilli, School of Chemistry, Univerisity College Cork*.
118. P. L. Fuchs and T. F. Braish, *Chem. Rev.*, **1986**, 86, 903-917.
119. M. C. Pérez-Aguilar and C. Valdés, *Angew. Chem. Int. Ed.*, **2015**, 54, 13729-13733.
120. A. C. Cope, D. E. Morrison and L. Field, *J. Am. Chem. Soc*, **1950**, 72, 59-67.
121. Y. Shao, J. Tong, Y. Zhao, H. Zheng, L. Ma, M. Ma and X. Wan, *Org. Biomol. Chem.*, **2016**, 14, 8486-8492.
122. D. Pinto, C. Santos and A. Silva, in *8 Advanced NMR techniques for structural characterisation of heterocyclic structures* **2007**.
123. A. Huang, K. Wo, S. Y. C. Lee, N. Kneitschel, J. Chang, K. Zhu, T. Mello, L. Bancroft, N. J. Norman and S.-L. Zheng, *J. Org. Chem.*, **2017**, 82, 8864-8872.
124. B. A. Trofimov, *Sulf. Rep.*, **1992**, 11, 207-227.
125. N. M. Vitkovskaya, E. Y. Larionova, A. D. Skitnevskaya, V. B. Kobychev and B. A. Trofimov, *Russ. Chem. Bull.*, **2013**, 62, 26-32.
126. *APEX2 v2009.3-0; Bruker AXS, Inc.; Madison, WI, **2009**.*
127. G. M. Sheldrick, *Acta Crystalogr., Sect. C: Struct. Chem*, **2015**, 71, 3-8.
128. I. J. B. C. F. Macrae, J. A. Chisholm, P. R. Edgington, P. McCabe, E. Pidcock, L. Rodriguez-Monge, R. Taylor, J. van de Streek and P. A. Wood, *J. Appl. Crystallogr.*, **2008**, 41, 466-470.
129. L. X., W. D., W. J. and X. W., *Heterocycles*, 2005, 65, 2741-2751.
130. A. Monge, I. Aldana, H. Cerecetto and A. Rivero, *J. Heterocycl. Chem.*, **1995**, 32, 1429-1439.
131. S. Kushner, R. I. Cassell, J. Morton and J. H. Williams, *J. Org. Chem.*, **1951**, 16, 1283-1288.
132. D. J. C. Prasad and G. Sekar, *Org. Lett.*, **2011**, 13, 1008-1011.
133. Y.-S. Xiong, J. Weng and G. Lu, *Adv. Synth. Catal.*, **2018**, 360, 1611-1616.

134. M. M. D. Pramanik and N. Rastogi, *Org. Biomol. Chem.*, **2016**, 14, 1239-1243.
135. L. K. Liu, Y. Chi and K.-Y. Jen, *J. Org. Chem.*, **1980**, 45, 406-410.
136. João D. G. Correia, Â. Domingos and I. Santos, *Eur. J. Inorg. Chem.*, **2000**, 1523-1529.
137. B. L. Nilsson, L. L. Kiessling and R. T. Raines, *Org. Lett.*, **2000**, 2, 1939-1941.
138. A. K. Gupta, X. Yin, M. Mukherjee, A. A. Desai, A. Mohammadlou, K. Jurewicz and W. D. Wulff, *Angew. Chem. Int. Ed.*, **2019**, 58, 3361-3367.
139. E. Buchner and C. von der Heide, *Berichte der deutschen chemischen Gesellschaft*, **1901**, 34, 345-348.
140. V. K. Aggarwal, Z. Gültekin, R. S. Grainger, H. Adams and P. L. Spargo, *J. Chem. Soc., Perk. Trans. 1*, **1998**, 2771-2782.
141. M. E. Hermes and F. D. Marsh, *J. Am. Chem. Soc*, **1967**, 89, 4760-4764.

University College Cork, Ireland
Coláiste na hOllscoile Corcaigh

Cork Open Research Archive
Cartlann Taighde Oscailte Chorcaí

Flynn, A. J. 2020. Development and application of synthetic methodologies based on organosulfur and organophosphorus chemistry. PhD Thesis, University College Cork.

Please note that Chapters 3&4 (pp. 250-403) are unavailable due to a restriction requested by the author.

CORA Cork Open Research Archive http://cora.ucc.ie

Appendices

Appendix 1: *Crystallographic data*

Single-crystal X-ray analysis was performed on a Bruker APEX II DUO diffractometer at room temperature using graphite monochromatic Mo K_α (λ = 0.7107 Å) radiation. All calculations and refinement were made using the APEX software, containing the SHELX suite of programs and diagrams prepared with Mercury 3.10. All non-hydrogen atoms were located and refined with anisotropic thermal parameters. Hydrogen atoms were included in calculated positions or were located and refined with isotropic thermal parameters.

Ethyl 4-(phenylsulfonyl)-5-(4′-methylphenylcarbamoyl)-1*H*-pyrazole-3-carboxylate 204

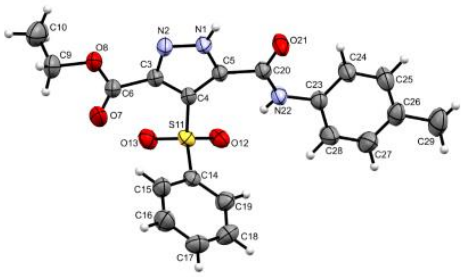

Crystals of **204** are triclinic, space group *P*, formula $C_{20}H_{19}N_3O_3S$, MW = 413.44 g mol^{-1}, a = 7.6015(5) Å, b = 8.4522(6) Å, c = 15.5976(11) Å, α = 81.209(2)°, β = 81.359(2)°, γ = 70.921(2)°, U = 930.55(11) Å3 , F(000) = 432, μ(Mo Kα) = 0.214 mm^{-1} , R_1(F) = 0.0560 and S = 1.019 for 4588 observed reflections with I > 2σ(I), $wR_2(F^2)$ = 0.1698 for all 7982 unique reflections.

CCDC 1906490 contains the supplementary crystallographic data for the pyrazole **204**. This data can be obtained free of charge from The Cambridge Crystallographic Data Centre.

Ethyl 1-(2-ethoxy-2-oxoethyl)-4-(phenylthio)-3-(*4*′-methylphenylcarbamoyl)-1*H*-pyrazole-5-carboxylate 169

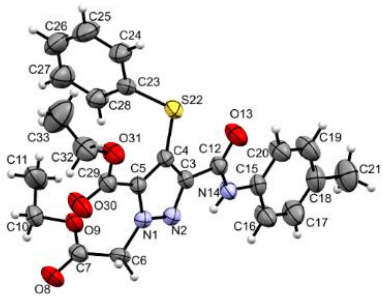

Crystals of pyrazole **169** are triclinic, space group $P\bar{1}$, formula $C_{24}H_{25}N_3O_5S$, MW = 467.53 g mol^{-1}, a = 9.456(2) Å, b = 11.142(3) Å, c = 12.695(3) Å, α = 70.288(8)°, β = 81.753(8)°, γ = 70.999(8)°, U = 1189.7(5) Å^3, F(000) = 492, m(Mo Ka) = 0.176 mm^{-1}, R_1(F) = 0.0546 and S = 1.031 for 2701 observed reflections with I > 2σ(I), $wR_2(F^2)$ = 0.1564 for all 4552 unique reflections.

CCDC 1906489 contains the supplementary crystallographic data for pyrazole **169**. This data can be obtained free of charge from The Cambridge Crystallographic Data Centre.

Appendix 2: *^{1}H and ^{13}C NMR spectroscopic data for Weinreb amide Z-**226***

The ^{1}H and ^{13}C NMR spectra of Z-**226** at 300 MHz (in $CDCl_3$) were very complex due to restricted rotation about the amide C–N bond. Lynch established that this complexity is due to presence of three rotameric species Z-**226a**, Z-**226b** and Z-**226c**. Accordingly, Lynch carried out comprehensive variable temperature NMR studies on this derivative to enable full spectroscopic characterisation. This work was not repeated as part of this research, however, despite not being assigned above, both the ^{1}H and ^{13}C NMR spectra of Z-**226** obtained in this work are included below for reference.

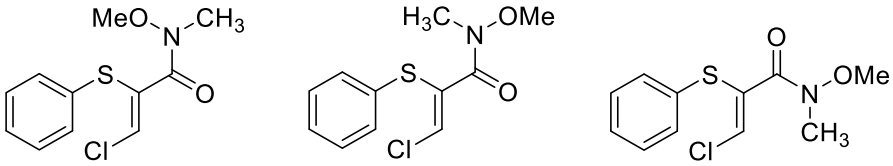

Z-**226a** Z-**226b** Z-**226c**

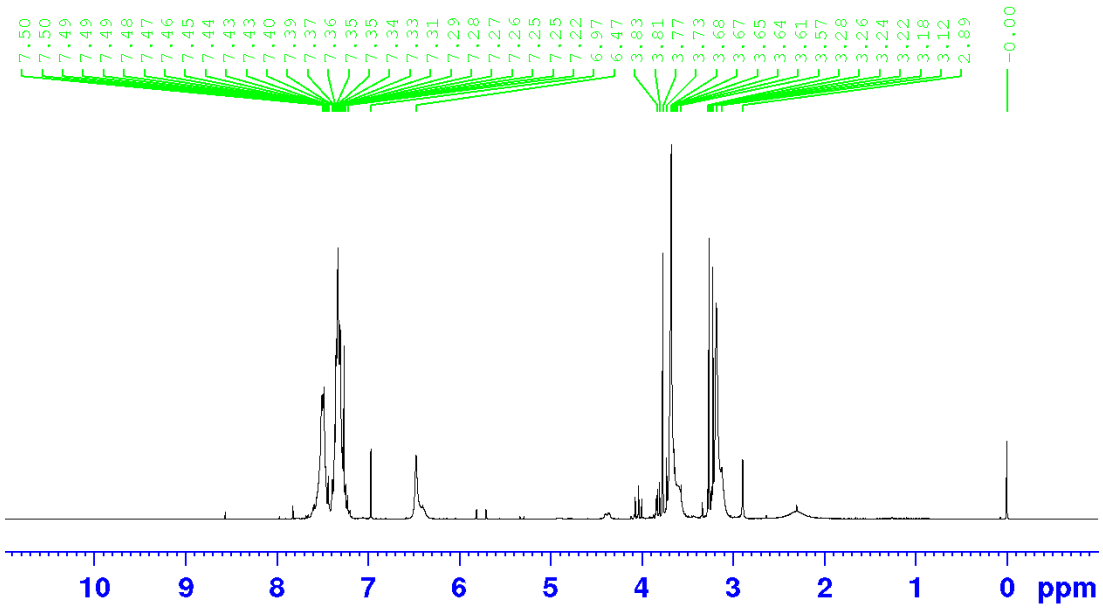

Figure A.1.: ^{1}H NMR spectrum of Z-**226** (300 MHz, $CDCl_3$)

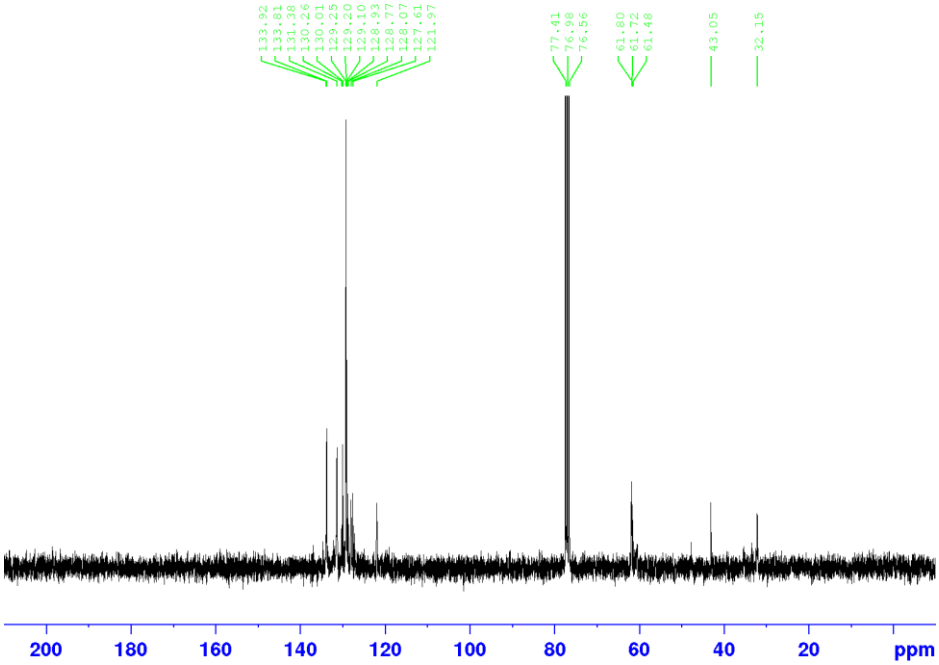

Figure A.2: ^{13}C NMR spectrum of Z-**226** (75.5 MHz, $CDCl_3$)

Appendix 3: *HPLC conditions for determination of enantiopurity (% ee) of sulfoxides*

Sulfoxide	Wavelength (nm)	Flow rate (ml min^{-1})	Temp (°C)	Mobile phase Hexane: IPA	T_{ret} (min)	Column
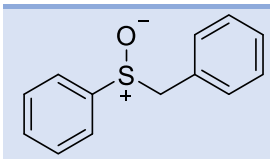	254	1.0	40	95:5	t_R (*R*) = 18.6, t_R (*S*) = 22.5	Chiracel OD-H
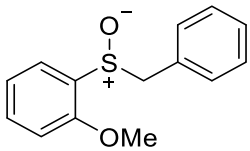	254	0.5	20	90:10	t_R (*R*) = 41.4, t_R (*S*) = 45.2	Lux Amylose-1
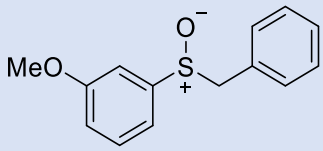	254	0.5	20	90:10	t_R (*R*) = 40.2, t_R (*S*) = 45.7	Lux Amylose-1
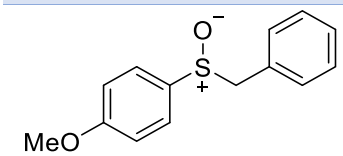	254	0.5	20	90:10	t_R (*R*) = 49.7, t_R (*S*) = 54.4	Lux Amylose-1
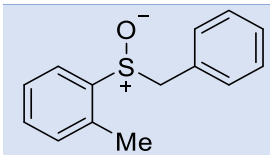	254	0.5	20	90:10	t_R (*R*) = 24.3, t_R (*S*) = 26.9	Lux Amylose-1
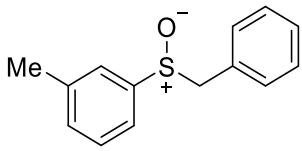	254	0.5	20	90:10	t_R (*R*) = 23.1, t_R (*S*) = 25.6	CHIRALPAK IB
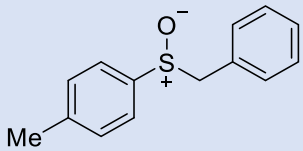	254	0.5	20	90:10	t_R (*R*) = 29.4, t_R (*S*) = 33.0	Lux Amylose-1
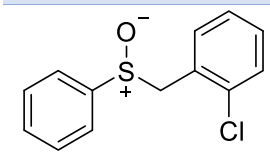	254	0.5	20	90:10	t_R (*R*) = 26.5, t_R (*S*) = 36.6	Lux Amylose-1
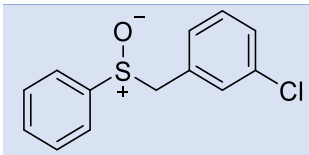	254	1.0	20	80:20	t_R (*R*) = 29.6, t_R (*S*) = 32.2	Lux Amylose-2
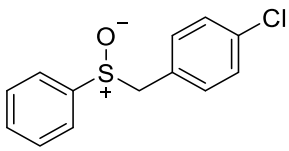	254	0.5	20	95:5	t_R (*S*) = 68.4, t_R (*R*) = 70.9	Lux Amylose-1

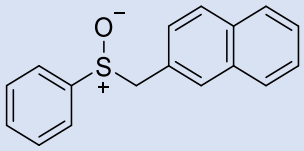	254	1.0	40	90:10	t_R (*R*) = 27.7, t_R (*S*) = 33.2	Chiralcel-OD-H
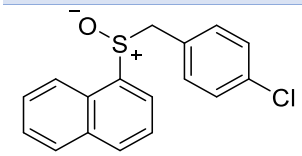	254	0.5	20	90:10	t_R (*S*) = 38.4, t_R (*R*) = 52.1	Lux Amylose-1
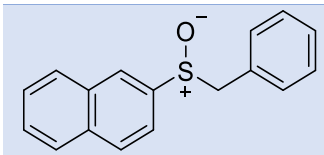	254	0.5	20	90:10	t_R (*R*) = 46.7, t_R (*S*) = 53.3	Lux Amylose-1
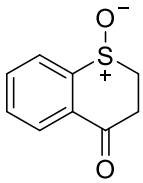	254	1.0	25	90:10	t_R (*R*) = 47.8, t_R (*S*) = 67.2	Lux Cellulose-4

Appendix 4:

Representative examples of HPLC chromatograms for enantioenriched sulfoxides **399**, **416**–**427** and **397**

(*R*)-(+)-Benzyl phenyl sulfoxide **399 (Table 4.20, Entry 1a)**

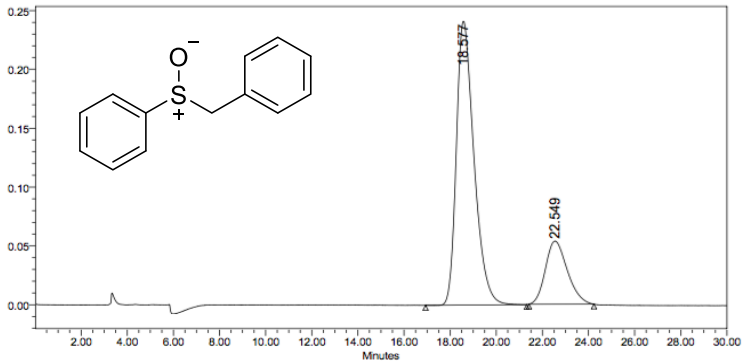

	RT	Area	% Area	Height
1	18.577	12801902	78.34	241356
2	22.549	3538993	21.66	53646

(*R*)-(+)-Benzyl 2-methoxyphenyl sulfoxide **416 (Table 4.20, Entry 2a)**

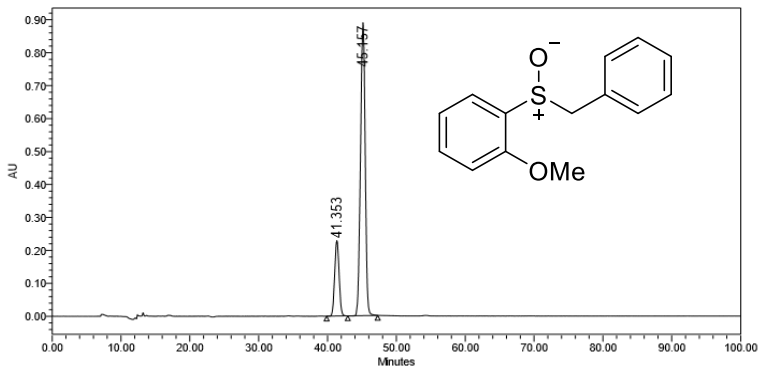

	RT	Area	% Area	Height
1	41.353	10189198	19.51	228943
2	45.157	42047141	80.49	888244

(*R*)-(+)-Benzyl 3-methoxyphenyl sulfoxide **417 (Table 4.20, Entry 3a)**

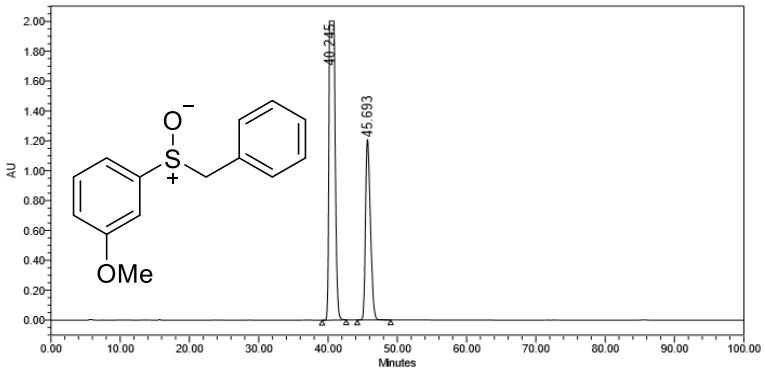

	RT	Area	% Area	Height
1	40.245	123767916	67.73	2004275
2	45.693	58955834	32.27	1208556

(*R*)-(+)-Benzyl 4-methoxyphenyl sulfoxide **418 (Table 4.20, Entry 4a)**

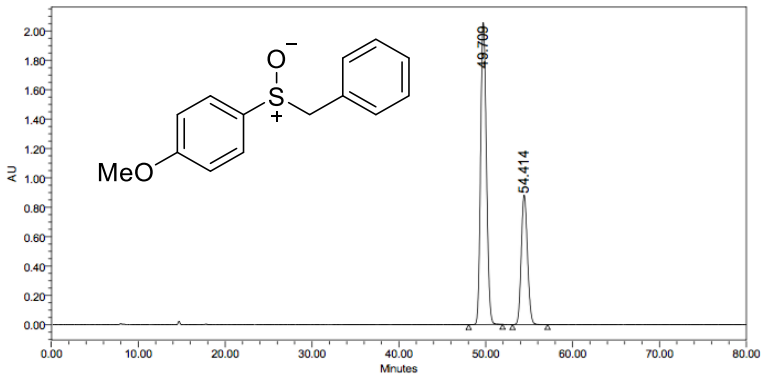

	RT	Area	% Area	Height
1	49.709	95515261	68.57	2056810
2	54.414	43774366	31.43	881888

(*R*)-(+)-Benzyl *o*-tolyl sulfoxide **419 (Table 4.20, Entry 5a)**

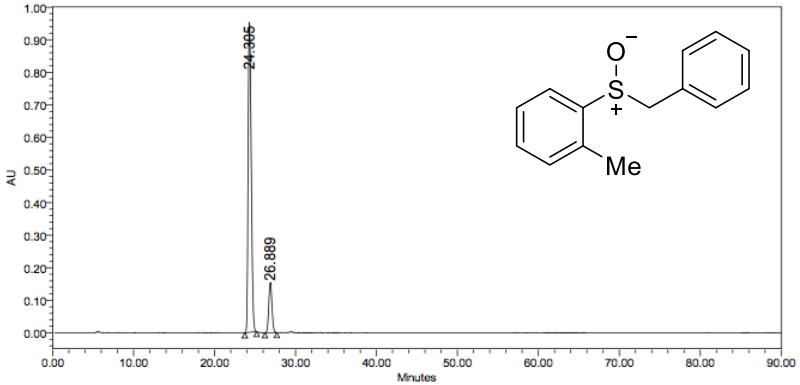

	RT	Area	% Area	Height
1	24.305	25103434	85.62	951905
2	26.889	4217411	14.38	152967

(*R*)-(+)-Benzyl *m*-tolyl sulfoxide **420 (Table 4.20, Entry 6a)**

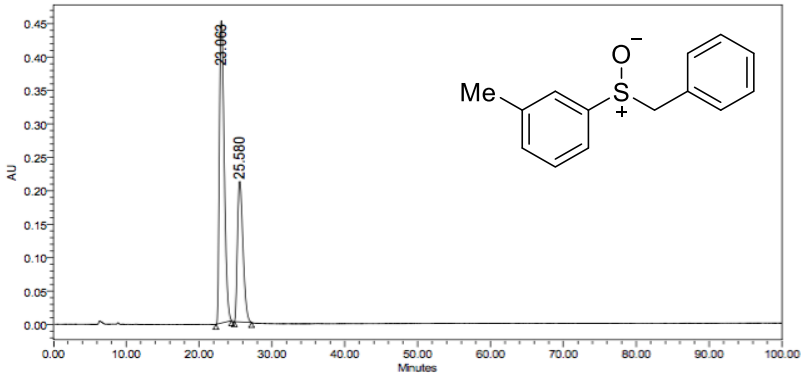

	RT	Area	% Area	Height
1	23.063	20915462	65.27	452870
2	25.580	11128891	34.73	210073

(*R*)-(+)-Benzyl *p*-tolyl sulfoxide **421 (Table 4.20, Entry 7a)**

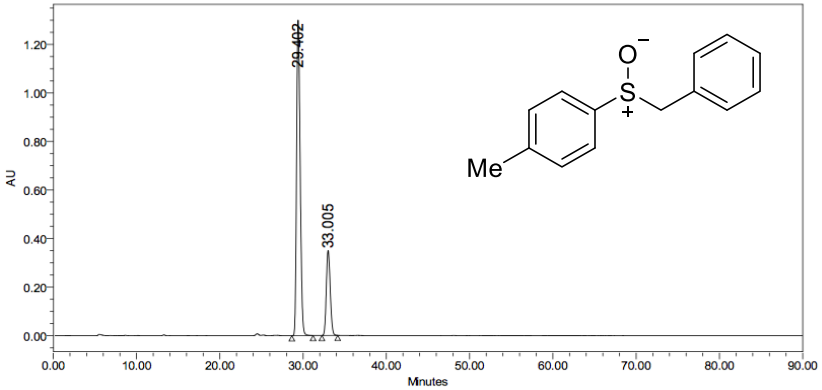

	RT	Area	% Area	Height
1	29.402	38832123	77.33	1298718
2	33.005	11381806	22.67	350564

(*R*)-(+)-2-chlorobenzyl phenyl sulfoxide **422 (Table 4.20, Entry 8a)**

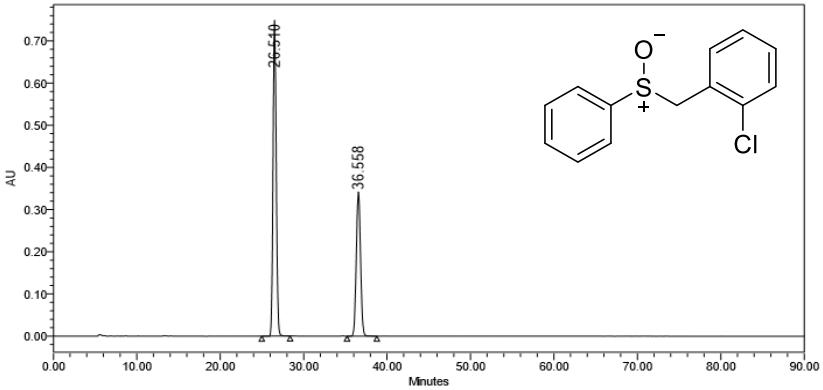

	RT	Area	% Area	Height
1	26.510	20111143	62.59	748905
2	36.558	12022407	37.41	342175

(*R*)-(+)-3-chlorobenzyl phenyl sulfoxide **423 (Table 4.20, Entry 9a)**

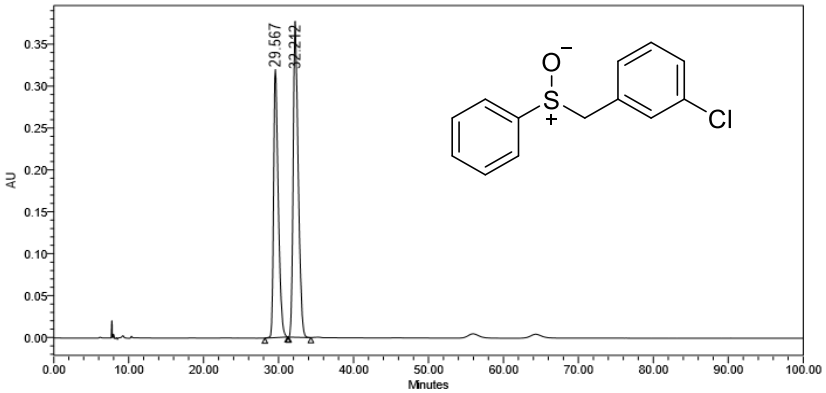

	RT	Area	% Area	Height
1	29.567	13878389	44.26	319849
2	32.212	17474815	55.74	376910

(*R*)-(+)-4-chlorobenzyl phenyl sulfoxide **424 (Table 4.20, Entry 10a)**

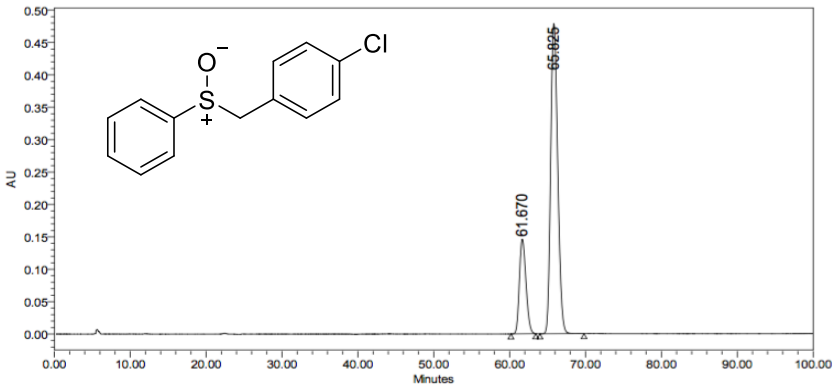

	RT	Area	% Area	Height
1	61.670	8793540	22.20	145899
2	65.825	30822044	77.80	478670

(*R*)-(+)-2-Naphthylmethyl phenyl sulfoxide **425 (Table 4.21, Entry 1a)**

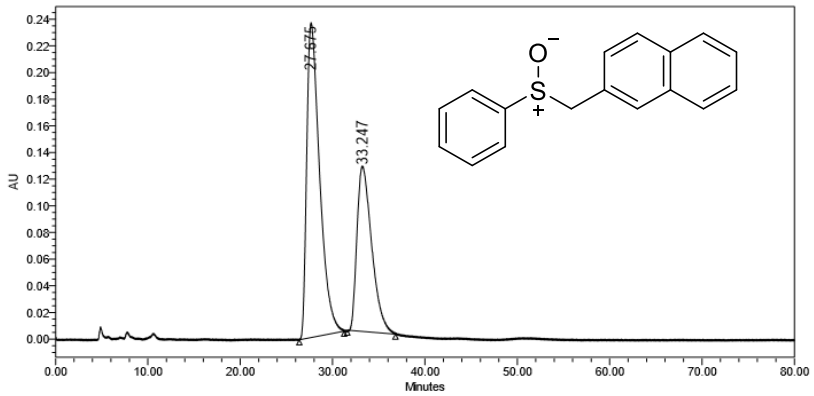

	RT	Area	% Area	Height
1	27.675	22890305	62.42	235670
2	33.247	13783778	37.58	123765

(*R*)-(+)-1-Naphthyl 4-chlorobenzyl sulfoxide **426 (Table 4.21, Entry 2a)**

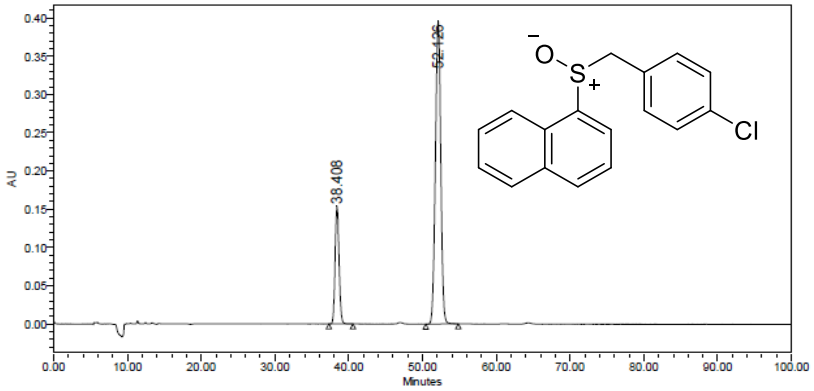

	RT	Area	% Area	Height
1	38.408	5751214	22.26	153995
2	52.126	20086483	77.74	396018

(*R*)-(+)-2-Naphthyl benzyl sulfoxide **427 (Table 4.21, Entry 3a)**

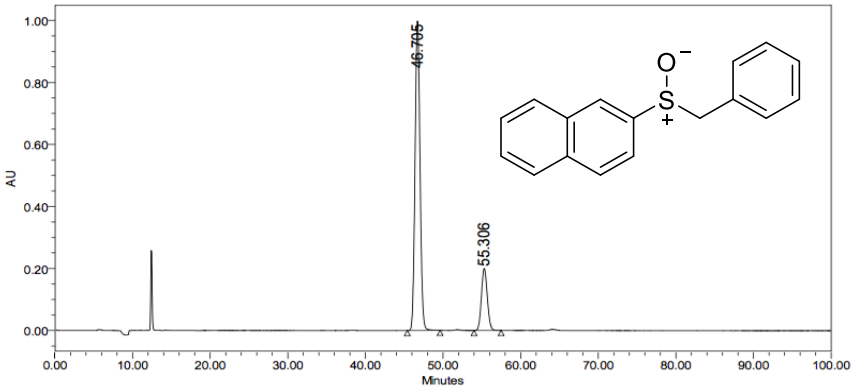

	RT	Area	% Area	Height
1	46.705	44411090	80.93	997687
2	55.306	10463565	19.07	200241

(*R*)-(−)-Thiochroman-4-one *S*-oxide **397 (Table 4.26, Entry 9)**

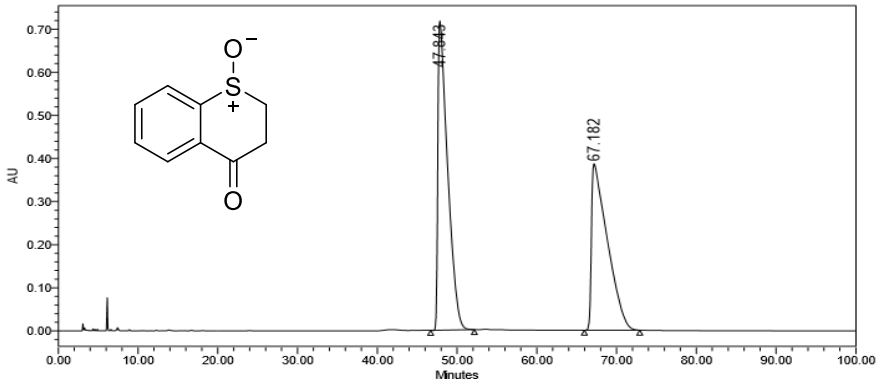

	RT	Area	% Area	Height
1	47.843	60798941	53.26	717027
2	67.182	53348165	46.74	385699

Appendix 5: *Abbreviations*

%	percent
$[\alpha]_D^T$	specific rotation
3TC	lamivudine
A	adenine
Å	angstrom
ABC	abacavir
p-ABSA	*p*-acetamidobenzenesulfonyl azide
Ac	acetyl
ADP	adenosine diphosphate
AIBN	azobisisobutyronitrile
AMP	adenosine monophosphate
Ar	aryl
ATR	attenuated total reflectance
Aux	auxiliary
AZT	azidothymidine
ATP	adenosine triphosphate
B	base
BHT	dibutylhydroxytoluene
BINOL	1,1′-bi-2-naphthol
Bn	benzyl
Boc	*tert*-butyloxycarbonyl
BP	biphenyl
BQ	1,4-benzoquinone
br s	broad singlet
BTAC	behentrimonium chloride
*i*Bu	*iso*-butyl
busalcx	2,4-di-*tert*-butyl-6-[[2-[(3,5-di-*tert*-butyl-2-hydroxyphenyl)methylideneamino]cyclohexyl]-iminomethyl]phenol
busalen	2,4-di*tert*-butyl-6-[2-[(3,5-di*tert*-butyl-2-hydroxyphenyl)methylideneamino]-ethylimino-methyl]phenol
*n*Bu	*n*-butyl
*t*Bu	*tert*-butyl
Bz	benzoyl
c	concentration
C	cytosine
°C	degrees Celsius
CB1	cannabinoid receptor 1
CD	cyclodextrin
CD4	cluster of differentiation 4
CD39	cluster of differentiation 39
CD73	cluster of differentiation 73
α-CNP	α-carboxy nucleoside phosphonate
COSY	correlation spectroscopy
COX-2	cyclooxygenase-2
*m*CPBA	*meta*-chloroperoxybenzoic acid
CTL	cytotoxic T-lymphocyte
CTLA-4	cytotoxic T-lymphocyte-associated protein 4
Cy	cyclohexyl
d	doublet
d	days
de	diastereomeric excess
d4T	stavudine
DBU	1,8-diazabicyclo[5.4.0]undec-7-ene
DCC	*N,N*′-dicyclohexylcarbodiimide
DCE	dichloroethane

dd	doublet of doublets
ddC	2′-,3′-dideoxycytidine
ddd	doublet of doublet of doublets
ddI	didanosine
DEAD	diethyl azodicarboxylate
DEPT	distortionless enhancement by polarisation transfer
DFT	density functional theory
DIAD	diisopropyl azodicarboxylate
DIC	*N,N*′-diisopropylcarbodiimide
DIPA	diisopropylamine
DMAD	dimethyl acetyledicarboxylate
DMAP	4-dimethylaminopyridine
DMEAD	di-2-methoxyethyl azodicarboxylate
DMF	dimethylformamide
DMSO	dimethyl sulfoxide
DNA	deoxyribose nucleic acid
dNTP	deoxynucleoside triphosphate
DPBIF	1,3-diphenylisobenzofuran
DPE	1,1-diphenylethylene
dr	diastereomeric ratio
dt	doublet of triplets
DTBP	di-*tert*-butylhydroperoxide
$E_{1C}B$	elimination unimolecular conjugate base
ECR	electrocyclic ring-closure
EDG	electron-donating group
ee	enantiomeric excess
equiv	equivalents
EPR	electron paramagnetic resonance
ESI-MS	electrospray ionisation-mass spectrometry
Et	ethyl
EWG	electron withdrawing group
FABMS	fast atom bombardment mass spectrometry
5-FU	5-fluorouracil
FTIR	fourier-transform infrared
g	grams
G	guanine
ΔG	change in Gibbs free energy
GABA	*gamma*-aminobutyric acid
GC	gas chromatography
h	hours
HCMV-1 DNA pol	human cytomegalovirus-1 DNA polymerase
HIV	human immunodeficiency virus
HIV-1 RT	human immunodeficiency virus-1 reverse transcriptase
HMBC	heteronuclear multiple bond correlation
HOMO	highest occupied molecular orbital
HPLC	high performance liquid chromatography
HRMS	high resolution mass spectrometry
HSQC	heteronuclear single quantum coherence
HSV-1 DNA pol	herpes simplex virus type 1 DNA polymerase
hv	photochemical energy
Hz	hertz
IM	intermediate
IR	infrared
kcal/mol	kilocalorie per mole
KHMDS	potassium bis(trimethylsilyl)amide

KIE	kinetic isotope effect
kJ mol^{-1}	kilojoule per mole
LC-MS	liquid chromatography-mass spectrometry
LDA	lithium diisopropylamine
LED	light emitting diode
LFP	laser flash photolysis
LiHMDS	lithium hexamethyldisilazide
lit.	literature
LiTMP	lithium tetramethylpiperidine
LUMO	lowest occupied molecular orbital
m	multiplet
M	moles per litre
MCM-41	mobil composition of matter no. 41
MDSC	myeloid-derived suppressor cell
Me	methyl
MeCN	acetonitrile
Mes	mesityl
MHz	megahertz
min	minutes
mL	millilitre
mmol	millimole
MMPP	magnesium monoperoxyphthalate
MOF	metal organic framework
mol %	mole percent
mp	melting point
Ms	mesyl
MS	molecular sieves
NBS	*N*-bromosuccinimide
NCS	*N*-chlorosuccinimide
NHC	*N*-heterocyclic carbene
NHPI	*N*-hydroxyphthalimide
NHS	*N*-hydroxysuccinimide
NK	natural killer
nm	nanometer
NMO	*N*-methylmorpholine *N*-oxide
NMR	nuclear magnetic resonance
NRTI	nucleoside reverse transcriptase inhibitor
Ns	nitrobenzenesulfonyl
N(t)RTI	nucleotide reverse transcriptase inhibitor
Oxone®	potassium peroxymonosulfate
PAA	phosphonacetic acid
PC	photocatalyst
PC*	excited photocatalyst
PCC	pyridinium chlorochromate
PD-1	programmed cell death protein-1
PES	potential energy surface
PFA	phosphonoformic acid
Ph	phenyl
phen	1,10-phenanthroline
Phth	phthaloyl
Piv	pivaloyl
PMB	*p*-methoxybenzyl
ppm	parts per million
*i*Pr	isopropyl
*n*Pr	propyl
P.T.	proton transfer
PTSA	*p*-toluenesulfonic acid

PXRD	powder x-ray diffraction
pyr	pyridine
q	quartet
RDS	rate-determining step
ref.	reference
RNA	ribonucleic acid
r.t.	room temperature
s	singlet
salen	*N,N'*-ethylenebis(salicylimine)
salpn	*N,N'*-bis(salicylidene)-1,2-propanediamine
SAR	structure-activity relationship
SDE	self-disproportionation of enantiomers
SET	single-electon transfer
Su	succinimide
t	triplet
T	thymine
TBAB	tetra-*n*-butylammonium bromide
TBAF	tetra-*n*-butylammonium fluoride
TBDMS	*tert*-butyldimethylsilyl
TBDPS	*tert*-butyldiphenylsilyl
td	triplet of doublets
temp	temperature
TEMPO	(2,2,6,6-tetramethylpiperidin-1-yl)oxyl
Tf	triflyl
TFA	trifluoroacetic acid
THF	tetrahydrofuran
TIPS	triisopropylsilyl
TLC	thin layer chromatography
TMS	trimethylsilyl
Tol	tolyl
TS	transition state
Ts	tosyl
U	uracil
UATR	universal attenuated total reflectance
UV	ultraviolet
µW	micromolar
µW	microwave
VZV DNA pol	varicella-zoster virus DNA polymerase

Publications

Organic & Biomolecular Chemistry

ROYAL SOCIETY OF CHEMISTRY

REVIEW

Check for updates

Cite this: *Org. Biomol. Chem.*, 2020, **18**, 2549

Synthetic and mechanistic aspects of sulfonyl migrations

Aaran J. Flynn, [a] Alan Ford [b] and Anita R. Maguire *[c]

Over the past 20 years reports of sulfonyl migrations have appeared, frequently described as 'unusual' and 'unexpected'. This comprehensive review compiles, for the first time, sulfonyl migrations reported over the last 20 years including formal 1,2-, 1,3-, 1,4-, 1,5-, 1,6- and 1,7-sulfonyl shifts, occurring through either radical or polar processes, either inter- or intramolecularly. Discussion of the sulfonyl migrations is structured according to reaction type, *i.e.* nitrogen–carbon, nitrogen–oxygen, nitrogen–nitrogen, oxygen–carbon (including anionic and non-anionic thia-Fries rearrangements), oxygen–oxygen and carbon–carbon migrations. Discussion of the underlying mechanisms for the migrations is included, with particular attention afforded to the principal techniques utilised for their elucidation, namely isotopic-labelling, crossover experiments, density functional theory calculations and electron paramagnetic resonance spectroscopy amongst others.

Received 4th December 2019,
Accepted 3rd February 2020

DOI: 10.1039/c9ob02587a

rsc.li/obc

[a]*School of Chemistry, Analytical and Biological Research Facility, Synthesis and Solid State Pharmaceutical Centre, University College Cork, Cork, Ireland*
[b]*School of Chemistry, Analytical and Biological Research Facility, University College Cork, Cork, Ireland*
[c]*School of Chemistry and School of Pharmacy, Analytical and Biological Research Facility, Synthesis and Solid State Pharmaceutical Centre, University College Cork, Cork, Ireland. E-mail: a.maguire@ucc.ie*

1. Introduction

Retrosynthetic analysis, formalised by E. J. Corey in the 1989 book *The Logic of Chemical Synthesis* revolutionised the art of total synthesis of complex organic molecules,[1] and coupled with an ever increasing number of efficient and selective synthetic methodologies with predictable outcomes across a diverse substrate range, has delivered elegant total syntheses. Critical to success is the ability to accurately anticipate the

This journal is © The Royal Society of Chemistry 2020

ChemPubSoc Europe
DOI: 10.1002/ejoc.201900494
EurJOC European Journal of Organic Chemistry
Full Paper

SPECIAL ISSUE

Sulfonyl Shift

Regioselective Thermal [3+2]-Dipolar Cycloadditions of α-Diazoacetates with α-Sulfenyl/Sulfinyl/Sulfonyl-β-Chloroacrylamide Derivatives to Form Densely Functionalised Pyrazoles

Aaran J. Flynn,[a] Alan Ford,[b] U. B. Rao Khandavilli,[a] Simon E. Lawrence,[a] and Anita R. Maguire*[c]

Abstract: Highly regioselective synthetic methodology leading to densely functionalised C(3), C(4) and C(5) substituted pyrazoles **10a–q, 14a-i and 16a–g** via thermal [3+2]-dipolar cycloaddition, of α-diazoacetates and α-thio-β-chloroacrylamides, at the sulfide, sulfoxide and sulfone levels of oxidation, is described. This method allows access to C(4)-sulfenyl or sulfonyl pyrazoles, through migration of the sulfur substituent at the sulfide and sulfone oxidation levels, while elimination of the sulfinyl group leading to 3,5-disubstituted pyrazoles, is observed. While the sulfide migration is readily rationalised, the carbon to carbon 1,2-sulfonyl migration is unprecedented and mechanistically intriguing. The synthetically versatile generation of densely functionalised pyrazoles containing substituents amenable to further modification offers advantages over alternative synthetic routes. Isolation of the *N*-alkylated pyrazoles **11a** and **12a** as by-products from the cycloaddition through further reaction of the pyrazoles **10** with excess α-diazoacetate, proved useful in rationalising the tautomeric behaviour evident in the NMR spectra of the pyrazoles, with the position of tautomeric equilibrium influenced by solvent and substituents.

Introduction

Heterocycles are an indispensable and ubiquitous class of compounds; notably they make up more than half of all known organic compounds and have a broad range of biological, chemical and physical properties spanning an expansive spectrum of reactivity and stability.[1] Among heterocycles, the pyrazole moiety and its derivatives are an important class of nitrogen containing five-membered heterocyclic compounds that have garnered significant interest in recent times predominantly due to their usefulness as targets in drug discovery.[2] Notably, several commercialised synthetic pyrazoles have come to prominence in recent decades highlighting the diverse biological effects associated with this critical scaffold. Celecoxib **(1)**, a COX-2 inhibitor is widely used as a non-steroidal anti-inflammatory drug,[3] rimonabant **(2)** was used in the treatment of obesity by acting as an inverse agonist of the cannabinoid receptor CB1 prior to its withdrawal from market,[4] fipronil **(3)** is a broad spectrum insecticide that acts on GABA-gated and glutamate-gated chloride channels in the insect nervous system,[5] sildenafil **(4)** is used for the treatment of erectile dysfunction and pulmonary hypertension,[6] and tartrazine **(5)** is a synthetic lemon azo dye primarily used as a food colouring (Figure 1).[7] Of significant interest is the presence of highly

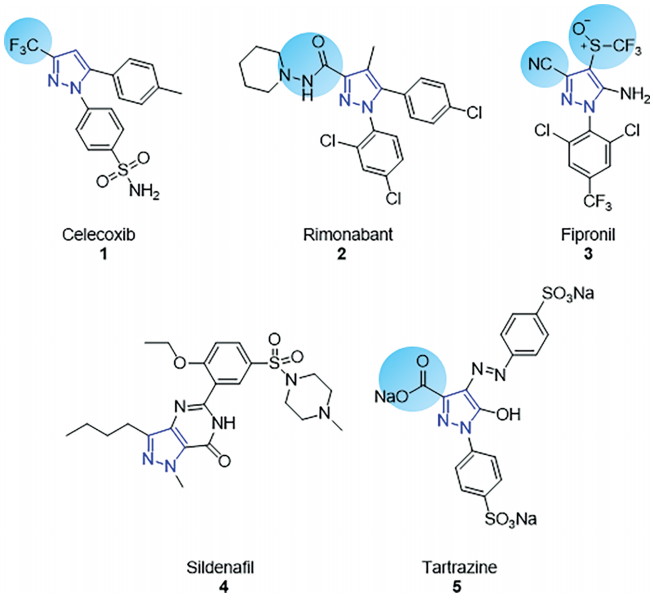

Figure 1. Commercialised substances containing the pyrazole moiety.

[a] School of Chemistry, Analytical and Biological Chemistry Research Facility, Synthesis and Solid State Pharmaceutical Centre, University College Cork, Cork, Ireland
[b] School of Chemistry, Analytical and Biological Chemistry Research Facility, University College Cork, Cork, Ireland
[c] School of Chemistry and School of Pharmacy, Analytical and Biological Chemistry Research Facility, Synthesis and Solid State Pharmaceutical Centre, University College Cork, Cork, Ireland
E-mail: a.maguire.ucc.ie
http://publish.ucc.ie/researchprofiles/V001/amaguire
Supporting information and ORCID(s) from the author(s) for this article are available on the WWW under https://doi.org/10.1002/ejoc.201900494.

© 2019 Wiley-VCH Verlag GmbH & Co. KGaA, Weinheim

functionalised diversified substituents bonded to the pyrzazole nucleus, many of which are electron withdrawing groups, that are critical to the compound's activity.

Markedly, the condensation of 1,3-dicarbonyl compounds with hydrazine derivatives remains the prevailing synthetic route towards formation of the pyrazole scaffold despite its associated limitations, namely the multistep sequences (in many instances) required to generate the desired starting materials, limited functional group tolerance, harsh reaction conditions and poor regioselectivities (Scheme 1A).[2e,8] The safety aspects of using hydrazines and its derivatives must also be considered.[9]

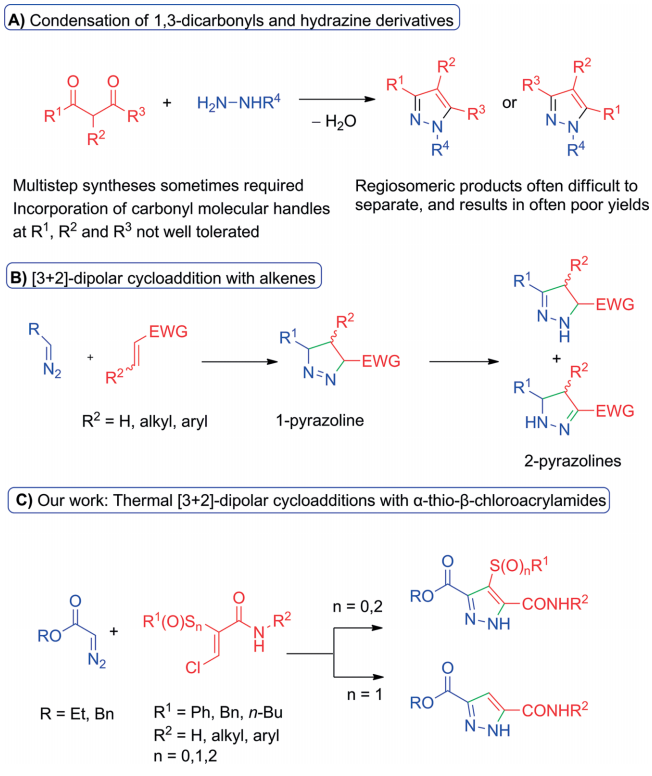

Scheme 1. Synthetic routes toward functionalised 3,4,5-substituted pyrazoles.

The [3+2]-dipolar cycloaddition offers a unique atom-economical solution to many of the aforementioned problems with excellent regioselectivities and tolerance of functional group diversity characteristic of the reaction.[10] The [3+2]-dipolar cycloaddition of alkenes with diazoalkanes is well-documented generally forming the 1-pyrazoline that readily isomerises to the more thermodynamically stable 2-pyrazoline, however a further oxidative step is usually required to form the pyrazole (Scheme 1B).[11]

This problem can be circumvented by employing diazo compounds with an in-built synthetic handle that is retained through the cycloaddition, that can much more readily undergo further synthetic transformations. While the use of inexpensive commercially available ethyl diazoacetate as a 1,3-dipole is well-known, and the ester moiety is an excellent synthetic handle, its use is not without challenges. High temperatures,[12] Lewis acid catalysis,[13] prolonged reaction times[14] and structurally simple dipolarophiles are typical in its use in [3+2]-dipolar cycloadditions, several of which actively contribute to its known degradation pathways and side reactions.

A major advantage of the [3+2]-dipolar cycloaddition is that the dipolarophile can be tuned to incorporate a comprehensive range of functionality that would otherwise be a difficult task using other methods. We have previously reported comprehensively on the synthesis and reactivity of α-thio-β-chloroacrylamides,[15] a family of sulfur-containing compounds that undergo a large range of reactions such as oxidation,[16] addition-substitution,[17] Diels-Alder cycloaddition[18] and [3+2] dipolar cycloaddition.[19] Significantly, while the [3+2] dipolar cycloaddition of ethyl diazoacetate with a diverse range of functionalised dipolarophiles is well explored, dipolarophiles bearing halides capable of acting as a leaving group and as a potential source of functional group migrations remains substantially less studied. In this work, we present the use of α-thio-β-chloroacrylamides as a unique dipolarophile scaffold at each of the sulfide, sulfoxide and sulfone level of oxidation with the electron deficient α-diazoacetates to generate a series of novel highly functionalised pyrazoles at the C(3), C(4) and C(5) positions (Scheme 1C).

Results and Discussion

Fifteen α-thio-β-chloroacrylamides **8a–o** were chosen for investigation in this study, some of which were described in our earlier work and others which are novel **(8d, 8e, 8l, 8m)**. Each of the known substrates were synthesised following our optimised procedures as summarised in Scheme 2, affording multigram quantities of these compounds, the majority of which were amenable to storage at room temperature for several months without any appreciable degradation. An exception to

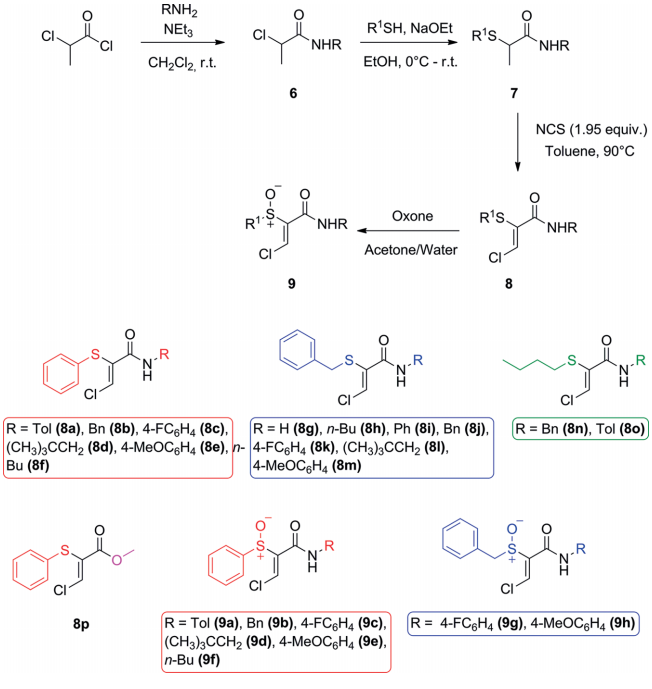

Scheme 2. Synthetic route towards dipolarophile precursors (See Supporting Information for more details).

© 2019 Wiley-VCH Verlag GmbH & Co. KGaA, Weinheim

Table 1. Synthesis of novel dipolarophile precursors **8** and **9**.

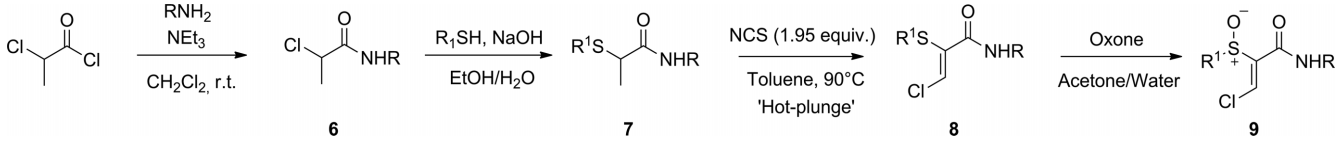

Entry	R	α-Chloroamide	Yield[a] [%]	R^1	α-Thioamide	Yield[a,b] [%]	α-Thio-β-chloroacrylamide	Yield[c] [%]	α-Sulfinyl-β-chloroacrylamide	Yield[c,d] [%]
		6	**6**		**7**	**8**	**8**	**8**	**9**	**9**
1	$(CH_3)_3CCH_2$	**6d**	98	Ph	**7d**	98[b]	**8d**	77	**9d**	96[d]
2				Bn	**7l**	86[a]	**8l**	65	–	–
3	4-MeOC_6H_4	**6e**	97	Ph	**7e**	89[b]	**8e**[e]	34	**9e**	79[c]
4				Bn	**7m**	94[b]	**8m**[e]	40	**9h**	92[c]

[a] Isolated % yield post basic work up; column chromatography not required. [b] Isolated % yield post filtration; column chromatography not required. [c] Isolated % yield after chromatography on silica gel. [d] Isolated % yield post aqueous work up; column chromatography not required. [e] Low yields of α-thio-β-chloroacrylamide **8e** and **8m** due to the solubility issues encountered during chromatography.

this included the *N*-alkyl amide **8f** and alkyl sulfides **8h–o** used in this study which required storage in the freezer to avoid degradation.

The α-chloroamides were generated in almost quantitative yields from commercially available 2-chloropropionyl chloride and the requisite aromatic or aliphatic amine source and were sufficiently pure to not require further purification. While previously described α-thioamides were generated using either thiophenol, benzyl mercaptan or 1-butanethiol in the presence of freshly prepared sodium ethoxide, each of the novel α-thioamides **7d, 7e, 7l, 7m** were generated using aqueous sodium hydroxide as base, obviating the requirement for chromatographic purification. While the generation of α-thio-β-chloroacrylamides in continuous flow is amenable to scale up,[20] all substrates used in this study were formed using optimised batch conditions described previously.[21] The novel α-thio-β-chloroacrylamides **8d, 8e, 8l, 8m** are fully characterised in this work. Notably, the signal for the β-H is very distinctive, and as a result, all novel α-thio-β-chloroacrylamides generated in this work were assigned as the Z-stereoisomer, in line with our earlier work. The α-thio-β-chloroacrylamides underwent oxidation to their sulfoxide derivatives by treatment with Oxone® overnight, without evidence for over oxidation to the sulfone. The sulfoxides in most instances were much more labile than the sulfide derivatives and required storage in the freezer to avoid degradation. In order to investigate the effect of replacing the amide functionality with an ester moiety, with greater synthetic potential, the α-thio-β-chloroacrylate **8p** was also generated.[15] The synthesis of the novel precursors is summarised in Table 1.

[3+2]-Dipolar Cycloadditions of α-Thio-β-chloroacrylamides with Ethyl Diazoacetate

The dipolarophilic reactivity of the α-thio-β-chloroacrylamides towards ethyl diazoacetate (EDA) as the 1,3-dipole was first explored as shown in Table 2. An excess (8 equivalents) of ethyl diazoacetate was added in one portion to a stirring solution of the α-thio-β-chloroacrylamide in toluene (0.2 M) at room temperature. The reaction solution was heated gradually to 100 °C and the temperature was maintained at this temperature for 24 h. After 24 h the reaction mixture was cooled to room temperature and an aliquot was concentrated under reduced pressure and analysed by ^{1}H NMR spectroscopy. The ^{1}H NMR spectra indicated incomplete consumption of α-thio-β-chloroacrylamide in all instances except for pyrazole **10c**, however characteristic methylene NCH_2 signals for the two regioisomeric N–H insertion **11** and **12** was observed in most instances. As a result, despite evidence for residual α-thio-β-chloroacrylamide **8** remaining after 24 hours, further ethyl diazoacetate was not added to avoid increased formation of the N–H insertion byproducts **11** and **12**.

The pyrazoles **10a–q** were isolated in moderate to good yields across the α-thio-β-chloroacrylamides **8a–o** substrate range, predominantly as solids that proved stable on storage. Interestingly, variation of the steric and electronic properties on either the sulfur or amide substituent did not have a noticeable impact on the outcome of the cycloaddition, highlighting the generality of the method. In some instances (entries 2, 4 and 11, Table 2) the formation of the N–H insertion products **11** and **12**, through further reaction of the rearranged pyrazoles with ethyl diazoacetate was significant; extensive optimization of the reaction conditions was not attempted. In addition to variation of the amide and sulfide substituents across **10a–o**, the [3+2]-dipolar cycloaddition between benzyl diazoacetate and α-thio-β-chloroacrylamide **8a** afforded the pyrazole **10q** in 63 % yield, while the α-thio-β-chloroacrylate ester **8p** also underwent cycloaddition with ethyl diazoactetate to give the C(3) and C(5) substituted dicarboxylate **10p** in 49 % yield.

In line with the [3+2]-dipolar cycloadditions of α-diazoalkanes with α-thio-β-chloroacrylamides,[19] the reactions of **8a–o** and α-thio-β-chloroacrylate **8p** were found to proceed with complete regiocontrol, the carbon atom of ethyl diazoacetate adding to the electrophilic β-carbon of the α-thio-β-chloroacrylamide, followed by rearrangement to form pyrazoles **10a–q**. From literature precedent, [3+2]-dipolar cycloadditions of α-diazoacetates to alkenes bearing electron withdrawing groups in direct conjugation with the dipolarophilic component are generally dipole-HOMO controlled, hence the predominant in-

© 2019 Wiley-VCH Verlag GmbH & Co. KGaA, Weinheim

Table 2. [3+2]-dipolar cycloaddition using α-thio-β-chloroacrylamides **8a–p**.

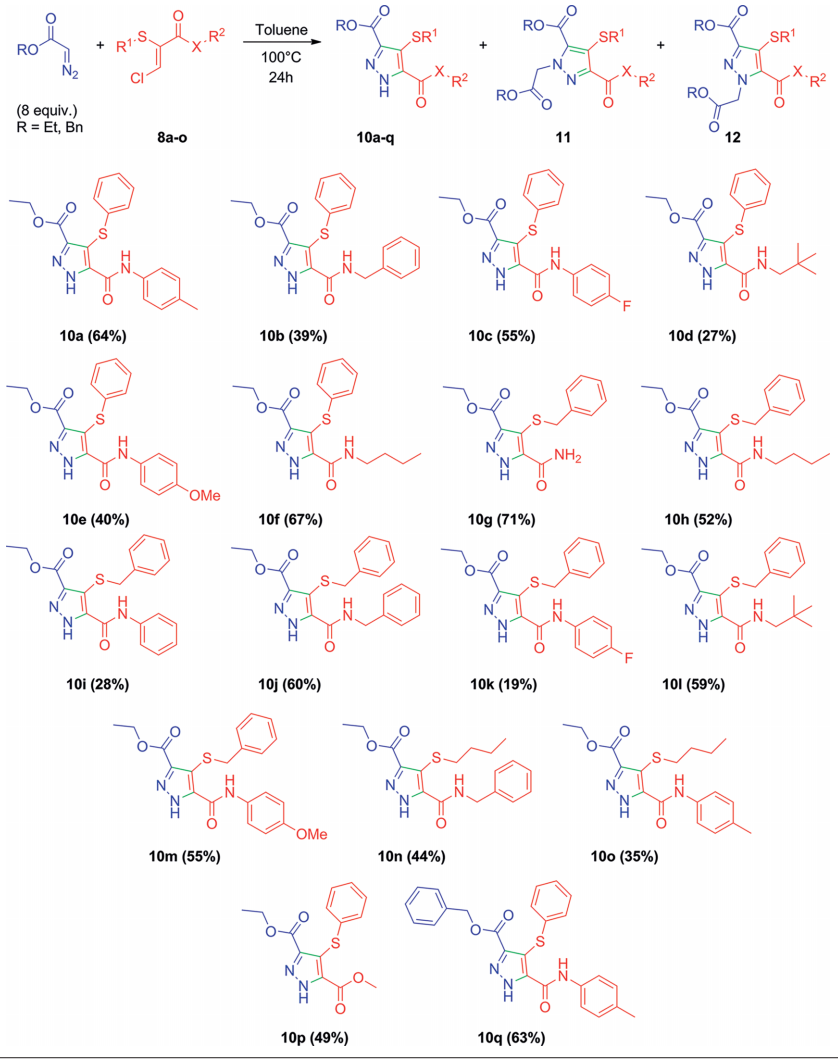

Entry	R	α-thio-β-chloro-acrylamide **8**	R^1	X	R^2	Conversion[a,b,c,d] **8** : **10**: **11**+**12**	Pyrazole **10**	Yield[e,f,g,h] **10** [%]	Pyrazole Recovery[i] **10** [%]
1	Et	**8a**	Ph	NH	Tol	[b]	**10a**	64[e]	–
2	Et	**8b**	Ph	NH	Bn	2:66:32	**10b**	39[e]	60
3	Et	**8c**	Ph	NH	4-FC_6H_4	0:82:18	**10c**	55[e]	67
4	Et	**8d**	Ph	NH	$(CH_3)_3CCH_2$	6:44:50	**10d**	27[f]	62
5	Et	**8e**	Ph	NH	4-$MeOC_6H_4$	12:66:22	**10e**	40[e]	60
6	Et	**8f**	Ph	NH	*n*Bu	7:78:15	**10f**	67[f]	85
7	Et	**8g**	Bn	NH_2	–	8:86:5	**10g**	71[g,h]	83
8	Et	**8h**	Bn	NH	*n*Bu	17:70:13	**10h**	52[f]	74
9	Et	**8i**	Bn	NH	Ph	5:74:21	**10i**	28[f]	38
10	Et	**8j**	Bn	NH	Bn	12:79:9	**10j**	60[e]	76
11	Et	**8k**	Bn	NH	4-FC_6H_4	3:38:58	**10k**	19[f]	49
12	Et	**8l**	Bn	NH	$(CH_3)_3CCH_2$	24:68:8	**10l**	59[f]	87
13	Et	**8m**	Bn	NH	4-$MeOC_6H_4$	39:61:0	**10m**	55[e]	90
14	Et	**8n**	*n*Bu	NH	Bn	9:77:14	**10n**	44[f]	57
15	Et	**8o**	*n*Bu	NH	Tol	2:84:14	**10o**	35[e]	42
16	Et	**8p**	Ph	O	Me	15:77:8	**10p**	49[f]	64
17	Bn	**8a**	Ph	NH	Tol	[d]	**10q**	63[e,h]	–

[a] Estimated % conversion of α-thio-β-chloroacrylamide **8** to pyrazole **10** and combined N–H insertion products **11**+**12** were calculated from the ^{1}H NMR spectra of the crude product in $CDCl_3$ taken after 24 h. Estimated by integration of the β-H signal of **8,** the pyrazole **10** NH signal, and the 2H, methylene NCH_2CO signals of the N–H insertion products **11** and **12**. [b] ^{1}H NMR analysis of the crude reaction mixture for the generation of pyrazole **10a** was not recorded. [c] N–H Insertion products **11** and **12** not isolated except for **11a** and **11b**; assignment of the N–H insertion products **11** and **12** in the crude ^{1}H NMR was made tentatively by analogy using the methylene NCH_2CO signals. [d] Estimated % conversion for [3+2]-dipolar cycloaddition of α-thio-β-chloroacrylamide **8a** with benzyl diazoacetate not recorded as N–H insertion products **11p and 12p** (not isolated) could not readily be identified from the ^{1}H NMR of the crude reaction mixture. [e] Isolated % yield after column chromatography on silica gel using hexane/ethyl acetate as eluent followed by trituration using diethyl ether. [f] Isolated % yield after column chromatography (twice) on silica gel, first using hexane/ethyl acetate as eluent then dichloromethane/ethyl acetate. [g] Isolated % yield by filtration of the reaction mixture. [h] As the NMR spectra of pyrazoles **10g** and **10q** were recorded in DMSO-d_6 both the 3-, and 5-carboxylate tautomers were observed (see Supplementary Information for more details). [i] Calculated % recovery of pyrazole **10** based on ratio of pyrazole **10** in the ^{1}H NMR spectrum of the crude product mixture.

© 2019 Wiley-VCH Verlag GmbH & Co. KGaA, Weinheim

teraction involves the two atoms with the largest orbital coefficients in the dipole and dipolarophile respectively, which accounts for the regiocontrol observed (Scheme 3).[11a,22]

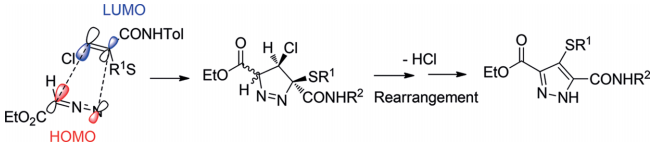

Scheme 3. Regiochemistry of the [3+2]-dipolar cycloaddition of ethyl diazoacetate with α-thio-β-chloroacrylamide.

The lower yields of pyrazoles **10d**, **10i**, **10k**, **10l** and **10n** are attributable in part to their co-elution during column chromatography with the pyrazoline by-product **13** derived from the thermal decomposition of ethyl diazoacetate (Scheme 4).[23]

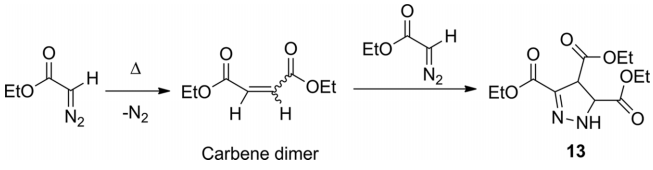

Scheme 4. Thermal decomposition of ethyl diazoacetate and subsequent formation of pyrazoline **13**.

The N–H insertion by-products **11a** and **12a** were isolated to facilitate structural assignment, however, the other derivatives **11b–q** and **12b–q** were not isolated and characterised (Scheme 5). In all instances the pyrazole **11** is observed in the ^{1}H NMR spectrum of the crude product in greater amounts than **12** indicating that N–H insertion preferentially occurs to give the 5-carboxylate **11**.

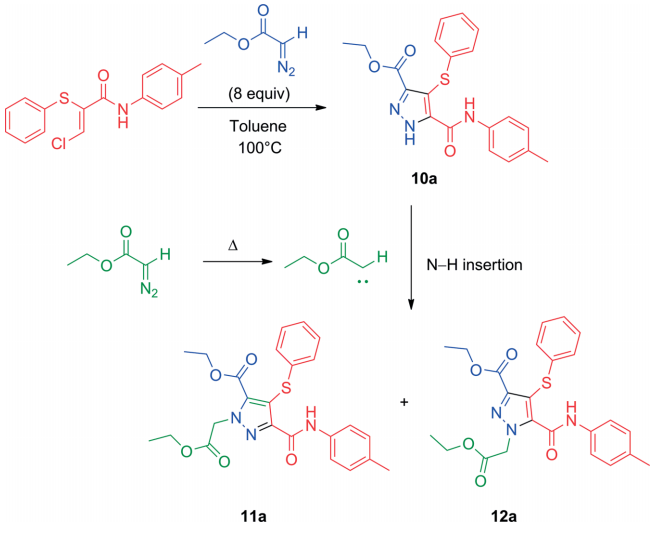

Scheme 5. Formation of the 5-carboxylate **11a** and 3-carboxylate **12a** by N–H insertion.

^{1}H-^{13}C Heteronuclear multiple bond correlation spectroscopy (HMBC) was used to determine the regiochemistry of the two N–H insertion products **11a** and **12a**. The NMR experiment revealed that the methylene protons at 5.58 ppm and the amide NH at 10.01 ppm in pyrazole **12a** both correlated to the same C(5) ring carbon at 138.8 ppm. In pyrazole **11a** the methylene protons at 5.38 ppm correlated to the C(5) ring carbon at 137.2 ppm, however there was no correlation between the amide NH at 9.07 ppm and C(5). Therefore, the pyrazole **12a** was assigned as the 3-carboxylate and pyrazole **11a** as the 5-carboxylate (Figure 2). As illustrated in Figure 2, the ^{13}C NMR chemical shifts of the C(3), C(4) and C(5) carbons of the pyrazole ring are predominantly influenced by the regiochemistry of the pyrazole, with limited impact of alteration of the substituent. Finally, X-ray crystallography of pyrazole **11a** following recrystallisation from dichloromethane unambiguously confirmed the assignment of pyrazole **11a** as the 5-carboxylate (Figure 3).

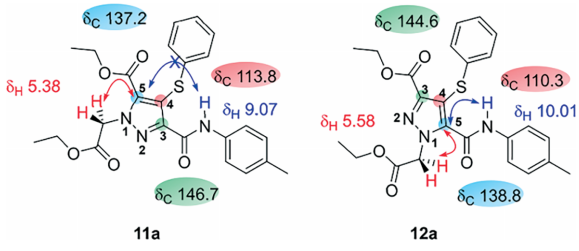

Figure 2. ^{1}H-^{13}C HMBC 3 bond correlations indicating the assignments of NH-insertion products **11a** and **12a** including relevant ^{1}H and ^{13}C NMR chemical shifts (in ppm).

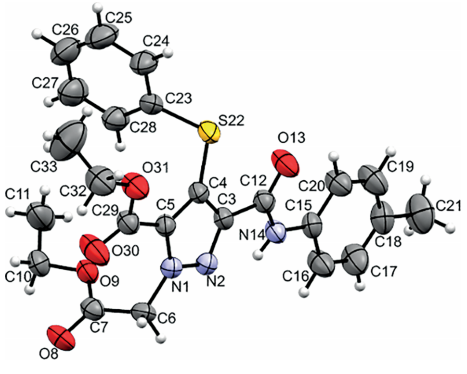

Figure 3. X-ray structure of pyrazole **11a** (anisotropic displacement parameters drawn at the 50 % probability level).

Two potential mechanisms can be envisaged for the formation of the rearranged pyrazoles **10a–q**. Firstly, thermally induced regiospecific [3+2]-dipolar cycloaddition of ethyl diazoacetate with the α-thio-β-chloroacrylamides leads to the initial pyrazoline cycloadduct **(i)**. In the first instance an E_1 elimination can be considered, with loss of chloride to form a sulfur stabilised carbocation [Scheme 6, Mechanism A, **(ii)**]. Subsequent generation of an episulfonium ion intermediate **(iii)**, followed by deprotonation of the acidic α-carbon leads to ring opening of the episulfonium ion and completes the sulfur migration to form **(iv)**. Finally, tautomerisation leads to aromatisation and the rearranged pyrazoles.

Alternatively, the following $E_{1C}B$-like mechanism is postulated to be more likely (Scheme 7, Mechanism B). Deprotonation of the acidic α-carbon, adjacent to the ester moiety, in the initial pyrazoline cycloadduct **(i)** generates an enolate **(ii)** that is stabilised through extended conjugation. Subsequent elimination of chloride generates the anti-aromatic pyrazole **(iii)**. The sulfur migration can be envisaged to occur through an intra-

© 2019 Wiley-VCH Verlag GmbH & Co. KGaA, Weinheim

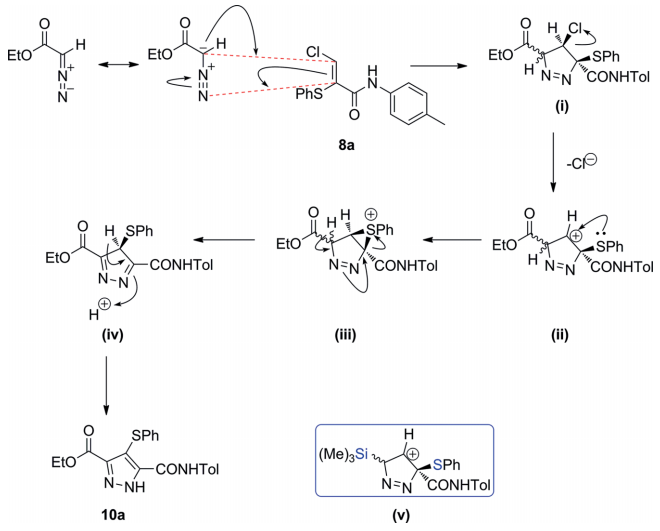

Scheme 6. **(Mechanism A).** E_1 elimination.

molecular conjugate addition to generate the episulfonium ion intermediate **(iv)**, that subsequently ring opens to complete the sulfur migration to form **(v)**. Tautomerisation affords the aromatic pyrazole **10a**. It is believed that the driving force for the sulfur migration in both mechanistic pathways is the restoration of the pyrazole aromaticity. In our earlier work with trimethylsilyldiazomethane, formation of the carbocation **(v)** analogous to **(ii)** (Scheme 6) was readily envisaged due to the β-silicon effect, however in the ester derivative the formation of the carbocation **(ii)** is less likely and as a result, the mechanistic details may be altered by the different substituents on the 1,3-dipole.[19] Studies into the nature of the mechanistic pathway are currently underway.

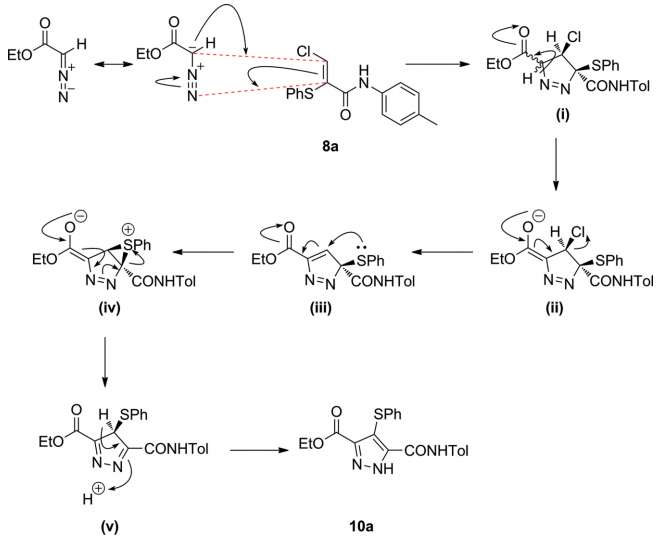

Scheme 7. **(Mechanism B).** $E_{1C}B$-like elimination.

[3+2]-Dipolar Cycloadditions of α-Sulfinyl-β-chloroacrylamides

Initial attempts to achieve [3+2]-dipolar cycloaddition of ethyl diazoacetate (8 equivalents) and α-sulfinyl-β-chloroacrylamide **9a** at room temperature or at reflux in dichloromethane did not result in cycloaddition. Reverting to toluene at 100 °C resulted in full consumption of the sulfoxide dipolarophile after 48 h. The ^{1}H NMR spectra of the crude product mixtures were complex, hindering accurate determination of product ratios. Under these conditions a series of α-benzenesulfinyl-β-chloroacrylamides were treated with ethyl diazoacetate and benzyl diazoacetate to afford the novel pyrazoles **14a-i** in yields of 13–47 % (Table 3). However, in most instances the 3,5-substituted pyrazoles generated proved to be insoluble in toluene allowing isolation by filtration from the reaction mixture on cooling (Table 3). Analysis of the mother liquors demonstrated some loss of product through the filtration process. In cases in which no precipitate formed the pyrazoles were purified by column chromatography **(14d**, **14f)**. The low yields of the desulfinylated pyrazoles may be attributable to the generation of benzenesulfinyl chlor-

Table 3. [3+2]-Dipolar cycloadditions using α-sulfinyl-β-chloroacrylamides **9a–f**.

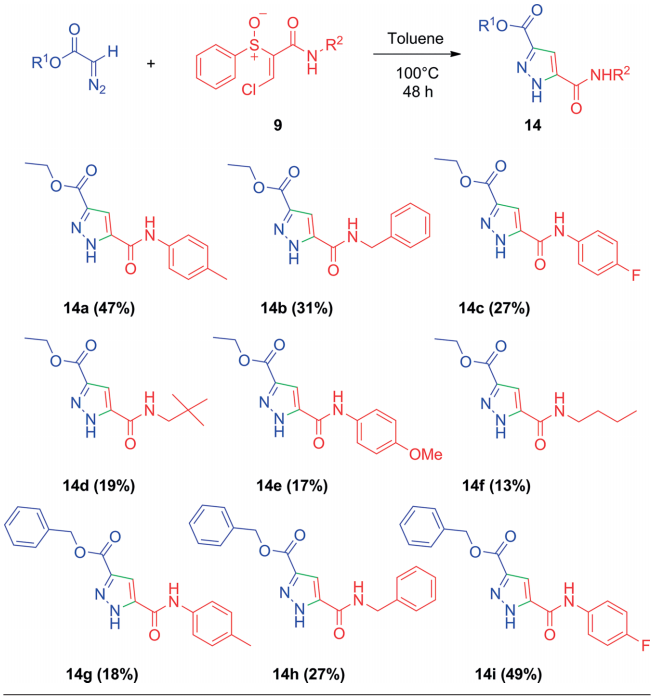

Entry	R^1	α-Sulfinyl-β-chloro-acryl-amide **9**	R^2	Pyrazole **14**	Yield[a,b,c,d] [%] **14**
1	Et	**9a**	Tol	**14a**	47
2	Et	**9b**	Bn	**14b**	31
3	Et	**9c**	4-FC_6H_4	**14c**	27
4	Et	**9d**	$(CH_3)_3CCH_2$	**14d**	19[b]
5	Et	**9e**	4-$MeOC_6H_4$	**14e**	17
6	Et	**9f**	*n*Bu	**14f**	13[b,d]
7	Bn	**9a**	Tol	**14g**	18
8	Bn	**9b**	Bn	**14h**	27
9	Bn	**9c**	4-FC_6H_4	**14i**	49

[a] Isolated % yield collected by filtration of the reaction mixture unless otherwise stated. [b] Isolated % yield after column chromatography. [c] As the NMR spectra were recorded in DMSO-d_6 (unless otherwise stated) the 3-, and 5-carboxylate tautomers were observed (see Supplementary Information for more details).

© 2019 Wiley-VCH Verlag GmbH & Co. KGaA, Weinheim

ide which could result in side reactions, or to the enhanced reactivity of the α-sulfinyl-β-chloroacrylamides relative to the α-thio-β-chloroacrylamides.

In all instances complete regiocontrol was observed, with the α-carbon of the α-diazoacetate adding to the β-carbon of the dipolarophile, with concomitant desulfinylation and aromatisation to the 3,5-disubstituted pyrazoles observed. The regiochemistry of the pyrazoles **14a-i** was assigned by comparison of the characteristic C(4) ring carbon of the ^{13}C NMR spectra to literature values for related compounds.[19] For these reactions, the outcome was comparable to our group's earlier work using trimethylsilyldiazomethane, both in terms of yield and desulfinylation, albeit the α-diazoacetates requiring more forcing conditions.

[3+2]-Dipolar cycloaddition to form the initial pyrazoline cycloadduct **(i)** is envisaged, followed by spontaneous *syn*-elimination of benzenesulfinyl chloride from the pyrazoline intermediate, leading to the desulfinylated cycloadduct **(ii)**. Subsequent tautomerisation affords the aromatic pyrazole **14** (Scheme 8).

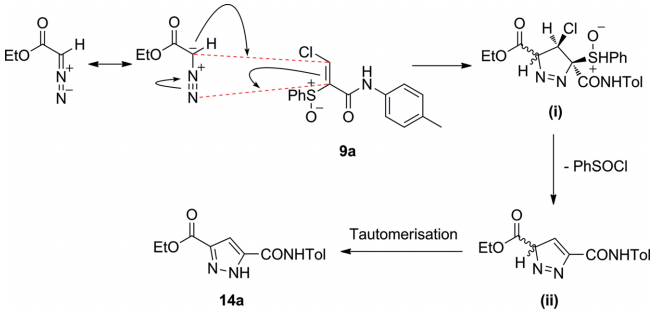

Scheme 8. Mechanistic route toward desulfinylated 3,5-substituted pyrazoles through 1,2-elimination of benzenesulfinyl chloride.

[3+2]-Dipolar Cycloadditions of α-Sulfonyl-β-chloroacrylamides

Vinyl sulfones are among the most reactive and versatile dipolarophiles,[24] owing to the strongly electron withdrawing character of the sulfone moiety. Namboothiri et al. have reported extensively on the base-mediated [3+2]-dipolar cycloaddition of phosphorylated and sulfonylated dipoles with various dipolarophiles, including vinyl sulfones, to generate functionalised C(3)-substituted sulfonylpyrazoles.[25] However, in light of our methodology forming the C(4)-substituted sulfenylpyrazoles (Table 2) we were keen to explore whether α-sulfonyl-β-chloroacrylamides would undergo cycloaddition with α-diazoacetates, and if so, would sulfur migration be observed at this level of oxidation.

Previous work in our group demonstrated that the α-sulfonyl-β-chloroacrylamides are extremely labile compounds, for example as potent Michael acceptors, that can be generated and used directly without isolation, for example in the successful Diels–Alder cycloaddition between cyclopentadiene and sulfone **15a** (Scheme 9).[18] Notably, an extensive oxidant screen including H_2O_2, peracetic acid, $KMnO_4$, Oxone®, and MMPP determined that *m*CPBA was the only oxidant that could actuate oxidation.

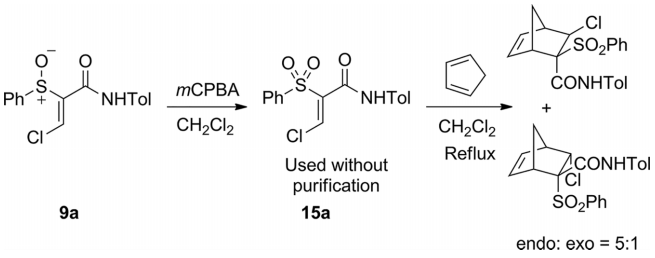

Scheme 9. Diels–Alder cycloaddition with crude α-sulfonyl-β-chloroacrylamides **15a** and cyclopentadiene.

With this is mind, the sulfoxide **9a** was treated with *m*-CPBA (2 equiv.) in dichloromethane at room temperature for 43 h. Reaction monitoring by ^{1}H NMR spectroscopy over several time increments indicated that the oxidation did not go to completion, and that over time the impurity profile deteriorated. For this reason, addition of ethyl diazoacetate was made once the level of impurities was observed to significantly increase relative to the increase of sulfone **15a**. After the addition the reaction mixture was stirred overnight at room temperature. The loading of ethyl diazoacetate was decreased to 4 equivalents relative to the 8 equivalents used at the sulfide and sulfoxide levels of cycloaddition due to the anticipated increased reactivity of the dipolarophile. The ^{1}H NMR spectrum of the crude reaction mixture was very complex, however no evidence for residual sulfone **15a** was apparent. Repeated column chromatography afforded the pure rearranged 4-sulfonylpyrazole **16a** in 16 % yield over two steps.

As the oxidation to form the sulfone is a limiting factor in the overall transformation, optimisation was undertaken including variation of time and/or increasing the reaction temperature to reflux in dichloromethane. While it is clear that the sulfone is sensitive to prolonged heating at reflux in dichloromethane, with close monitoring of the reaction mixture by ^{1}H NMR spectroscopy, optimal conversions can be achieved within 10–14 hours, leading to comparable results to when the oxidation was conducted for 48 hours at room temperature.

Due to the unusual nature of the observed sulfone migration, extension of this methodology to a range of α-sulfonyl-β-chloroacrylamides with varying electronic and steric properties at both the sulfone and amide was undertaken leading to a series of 4-sulfonylpyrazoles **16a–g**, albeit in low yields of 14–18 %, confirming that the sulfone migration was consistent across a series of compounds (Table 4).

The regiochemistry of the [3+2]-dipolar cycloaddition and subsequent rearrangement of pyrazole **16a** was determined by single X-ray crystallography following recrystallisation from dichloromethane (Figure 4). Furthermore, the X-ray crystal structure confirms that migration of the sulfone moiety has occurred, with the sulfone at the C(4) position analogous to that of the sulfide migration. The regiochemistry of the 4-sulfenylpyrazole **10a** was further confirmed by independently oxidising **10a** to the 4-sulfonylpyrazole **16a** using *m*CPBA in refluxing dichloromethane (see Table S2, supplementary information).

Comparison of the ^{1}H, ^{13}C and IR spectroscopic data confirmed that the regiochemistry of the 4-sulfenylpyrazole **10a** and 4-sulfonylpyrazole **16a** cycloadducts were identical.

© 2019 Wiley-VCH Verlag GmbH & Co. KGaA, Weinheim

Table 4. [3+2]-Dipolar cycloadditions with α-sulfonyl-β-chloroacrylamides **15**.

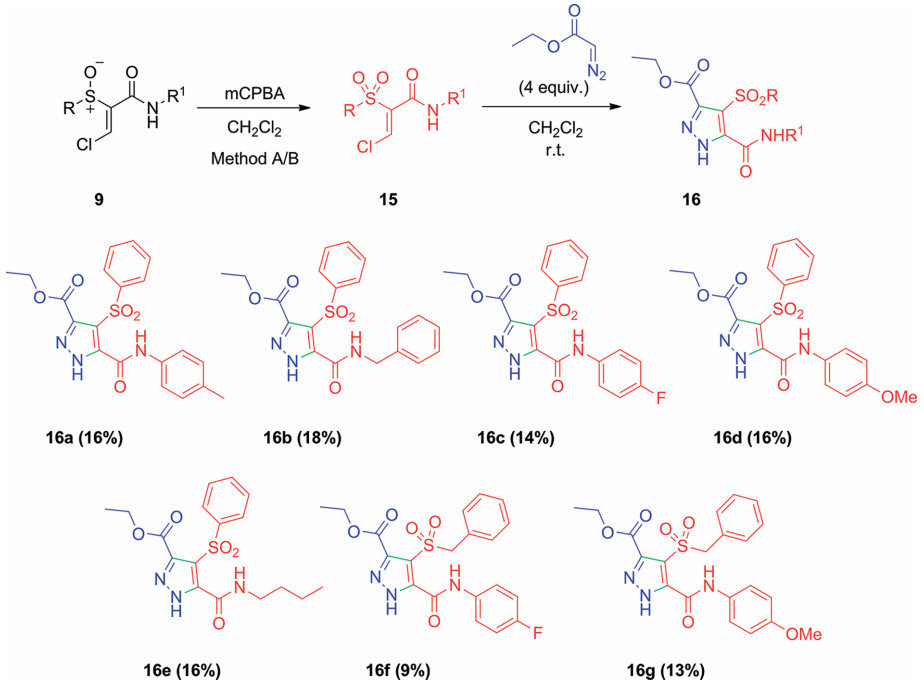

Entry	R	R^1	α-sulfinyl-β-chloroacrylamide **9**	Method[a]	% α-sulfonyl-β-chloroacrylamide[b] **15**	Pyrazole **16**	Yield[c] **16** [%]
1	Ph	Tol	**9a**	A	78	**16a**	16
2	Ph	Bn	**9b**	A	71	**16b**	18
3	Ph	4-FC_6H_4	**9c**	B	63	**16c**	14
4	Ph	4-$MeOC_6H_4$	**9e**	B	30	**16d**	16
5	Ph	*n*Bu	**9f**	B	[d]	**16e**	16
6	Bn	4-FC_6H_4	**9g**	B	[d]	**16f**	9
7	Bn	4-$MeOC_6H_4$	**9h**	B	[d]	**16g**	13

[a] Method A: 2 equiv. *m*CPBA in dichloromethane (15 mL) was added dropwise to a stirring solution of α-sulfinyl-β-chloroacrylamide **9** in dichloromethane (5 mL) at room temperature under nitrogen. The reaction mixture was stirred at room temperature for up to 48 h. Method B: 2 equiv. *m*CPBA in dichloromethane (15 mL) was added dropwise to a stirring solution of α-sulfinyl-β-chloroacrylamide **9** in dichloromethane (5 mL) at room temperature under nitrogen. The reaction mixture was heated to gentle efflux and stirred at this temperature for 10–14 h. Both methods were monitored by ^{1}H NMR spectroscopy at regular time intervals. [b] Estimated % of α-sulfonyl-β-chloroacrylamide **15** present in the reaction mixture prior to the addition of ethyl diazoacetate. Determined from the ^{1}H NMR spectra of the crude reaction mixture. [c] Isolated % yield calculated over two steps after purification by repeated column chromatography. [d] % conversion could not be accurately determined due to complexity of the ^{1}H NMR spectrum of the crude reaction mixture.

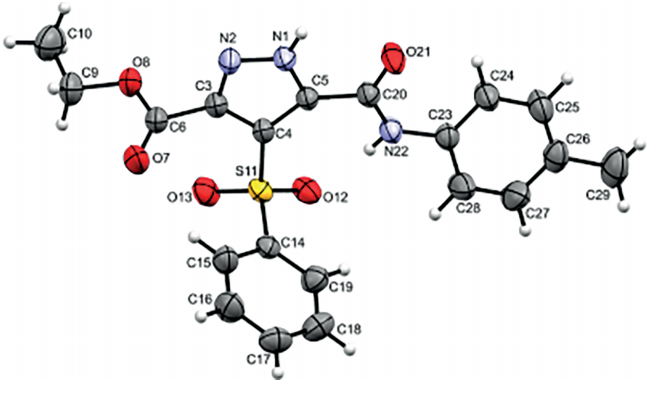

Figure 4. X-ray structure of pyrazole **16a** (anisotropic displacement parameters drawn at the 50 % probability level).

To the best of our knowledge, at the time of writing, carbon to carbon 1,2-sulfonyl migration is unprecedented, thus the rearrangement leading to **16** involving a 1,2-sulfonyl shift is highly unusual. The mechanism for the formation of the rearranged 4-sulfonylpyrazoles **16a–g** is not well understood, but several mechanistic routes can be considered based on the confirmed regiochemistry of the products. In all instances, regioselective [3+2]-dipolar cycloaddition of the crude α-sulfonyl-β-chloroacrylamide leads to the initial pyrazoline cycloadduct **(i)**, which readily undergoes elimination of HCl to give the intermediate cycloadduct **(ii)** (Scheme 10). While the sulfur migration at the sulfide level can be readily understood due to the nucleophilic character of the sulfide, extending this to rationalise the unprecedented 1,2-sulfonyl shift is not feasible.

In light of the following two reports a [1,5]-sigmatropic shift can be considered to rationalise the sulfonyl migration. Fuchs et al. reported the thermally induced rearrangement of a γ-sulfonyl enone to the rearranged sulfone in almost quantitative yields (Scheme 11, A).[26] The authors rationalised the transformation through the formation of the enol intermediate which

© 2019 Wiley-VCH Verlag GmbH & Co. KGaA, Weinheim

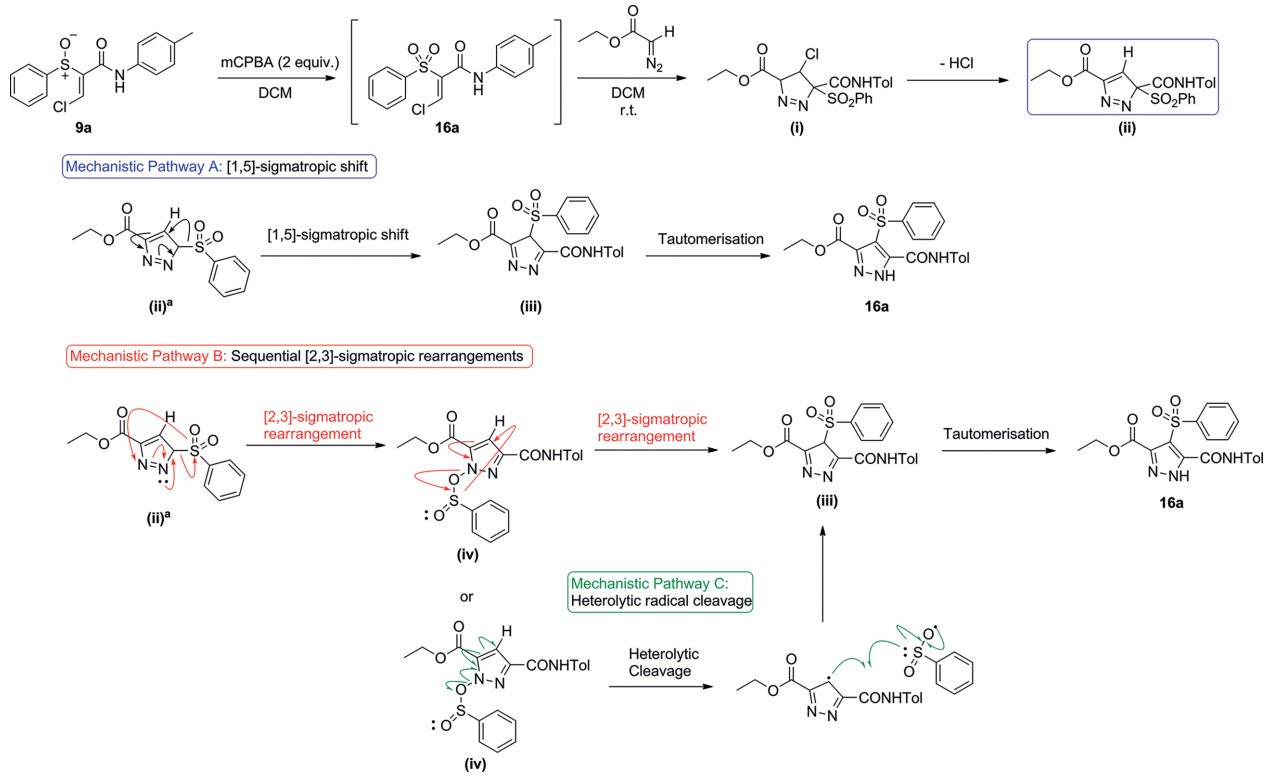

Scheme 10. Proposed mechanistic routes for sulfone migration [**(a)** CONHTol substituent not shown in intermediate **(ii)**].

undergoes a [1,5]-sigmatropic rearrangement. Notably, however this reaction was carried out in toluene at 145 °C in a sealed tube. Recently, Valdés et al. reported the synthesis of chiral pyrazoles through the [3+2]-dipolar cycloaddition of α-chiral tosylhydrazones with alkynes (Scheme 11, B).[27] Interestingly, they observed that the initial cycloadduct underwent [1,5]-sigmatropic rearrangement with migration of the alkyl group. Significantly in their study, they observed that the [1,5]-sigmatropic rearrangement, which has two regioisomeric outcomes, preferentially, but not exclusively, migrates to nitrogen rather than

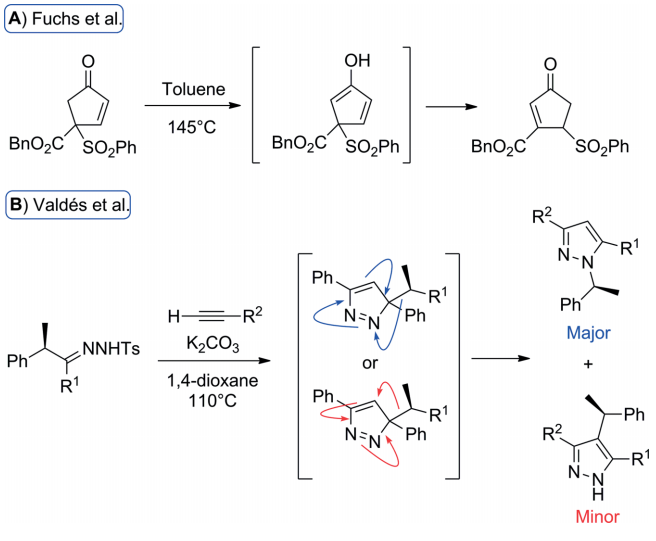

Scheme 11. Literature examples of **1)** [1,5]-sigmatropic shift of sulfone moiety; **2)** [1,5]-sigmatropic shift of alkyl group in pyrazole system.

the C(4) carbon. Forcing reaction conditions (110 °C in 1,4-dioxane) were also required in this instance. Considering these reports, we note that the pyrazoles **16** could be generated through a [1,5]-sigmatropic shift of the sulfonyl moiety (Scheme 10, Mechanistic Pathway A). However, the [3+2]-dipolar cycloadditions in this work were carried out at room temperature, while [1,5]-sigmatropic shifts generally require much higher temperatures as can be seen above. While the *N*(1)-substituted sulfone was not isolated or observed, since the recoveries were very low it is impossible to exclude its formation.

An alternative mechanistic pathway can be envisaged with two sequential [2,3]-sigmatropic rearrangements of the sulfonyl moiety as illustrated in Scheme 10 (Mechanistic Pathway B) followed by re-aromatisation via tautomerisation at the end of the sequence to afford the C(3) carboxylate pyrazole **17a**. The second [2,3]-sigmatropic rearrangement is somewhat akin to an allylic sulfinate-sulfone rearrangement.[28] Alternatively, from the intermediate **(iv)**, homolytic cleavage of the weak N–O bond could be envisaged generating a radical pair which on recombination forms the more stable C–S bond (Scheme 10, Mechanistic Pathway C).

Spectroscopic Determination of the Tautomeric Composition of 3,4,5-Substituted Pyrazoles

Definitive spectroscopic analysis of unsubstituted NH pyrazole scaffolds is complicated by the dynamic tautomeric nature of these compounds. For this reason, significant attention has been paid in the literature to the spectroscopic analysis of these compounds particularly using ^{1}H-^{13}C HMBC and NOE experi-

© 2019 Wiley-VCH Verlag GmbH & Co. KGaA, Weinheim

ments, often in conjunction with each other.[29] Unambiguous assignment of the ^{13}C NMR signals for the C(3), C(4) and C(5) carbons is particularly challenging, especially in the absence of an adjoining proton (Figure 5). In order to conclusively characterise our novel pyrazoles an in-depth ^{13}C NMR study was performed.

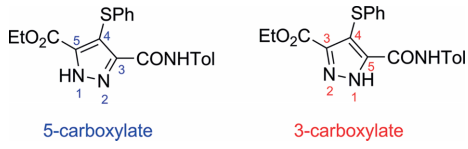

Figure 5. Tautomeric forms of pyrazole **10a** in solution.

The elucidation of the C(3), C(4) and C(5) pyrazole ring carbon chemical shifts by ^{13}C NMR at 75.5 MHz for pyrazoles **10** in $CDCl_3$ proved to be challenging, with the C(3) and C(5) carbons not observed at this field strength, believed to be due to dynamic tautomerism in conjunction with the absence of either direct or indirect coupling to hydrogen. In most instances, however, a weak signal was observed for the C(4) carbon as the chemical shift of this carbon remains largely unaffected by tautomerism. In contrast, at 150.9 MHz broad signals were observed for C(3), C(4) and C(5). Interestingly when the spectra of the pyrazoles **10a–f** and **10h–p** were recorded at 150.9 MHz in the noninteracting solvent $CDCl_3$ only a single set of carbon signals are seen indicating one of the following possibilities:

A) one exclusive tautomer in solution, *or*

B) tautomers rapidly interconverting on the NMR timescale, *or*

C) two tautomers in dynamic equilibrium with the equilibrium highly favouring one tautomer with the concentration of the minor tautomer so negligible that it is not detectable by ^{13}C NMR.

Due to the broadening of the signals for the C(3), C(4) and C(5), it is unlikely that one tautomer exists exclusively in solution, although the signal broadening could be due in part to the quadrupolar moment of ^{14}N rather than tautomerism only. Furthermore, the ^{13}C NMR spectra of the pyrazoles **11a** and **12a** could readily be obtained at 75.5 MHz with each of the C(3), C(4) and C(5) ring carbons observed as sharp signals, consistent with the pyrazoles **11a** and **12a** being unable to undergo prototropic tautomerism due to the alkylation of the respective N(1) positions (Figure 2). This strongly suggests that the signal broadening observed in pyrazole **10a** is not due to the ^{14}N quadrupolar moment. Direct comparison of the sp^2 region of the ^{13}C NMR spectra of the pyrazole **10a** and the two N–H insertion products **11a** and **12a** demonstrated that the chemical shifts in pyrazole **10a** and **12a** were remarkably similar, and substantially different to those of pyrazole **11a** (Figure 6). This observation allowed assignment of the major tautomer of **10a** in $CDCl_3$ to be identified as the 3-carboxylate, however, it is not the exclusive tautomer as both *N*-alkylated pyrazoles **11a** and **12a** are formed through the N–H insertion reaction. This allows us to conclude that for pyrazoles of the type **10** in the noninteracting solvent $CDCl_3$ that the tautomers exist in dynamic equilibrium albeit with the 5-carboxylate form present in undetectable concentrations. An alternative possible explanation for the signal broadening could be due to the presence of amide rotamers; comparison of the ^{13}C NMR spectra of pyrazole **10a** with the two NH insertion products **11a** and **12a**, however, highlights that the signal broadening is due to tautomers, with no dynamic effects observed in the ^{13}C NMR spectra of **11a** and **12a**.

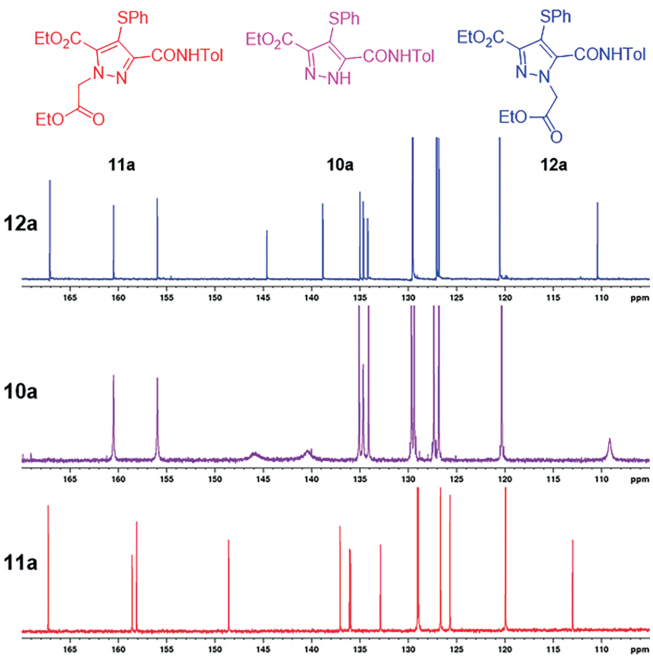

Figure 6. ^{13}C NMR (150.9 MHz) spectra of pyrazole **10a** and N–H insertion products **11a** and **12a** illustrating that the major and minor tautomer of pyrazole **10a** in $CDCl_3$ is the 3-carboxylate.

While it appears that the dynamic equilibrium in $CDCl_3$ favours the 3-carboxylate tautomeric form it is interesting that it is, in fact, the minor tautomer that undergoes N–H insertion more readily to give the pyrazole **11a** as the major regioisomer. To test whether this was due to the minor tautomer being more reactive or whether the dynamic equilibrium tended towards the 5-carboxylate in the reaction solution, ^{13}C NMR spectra for the pyrazole **10a** and the N–H insertion products **11a** and **12a** were recorded in toluene-d_8, the solvent used for the cycloaddition, at 150.9 MHz (see Figure S16, supplementary information). As was observed in $CDCl_3$, substantial overlap of the signals was observed with those for N–H insertion product **12a**, indicating that the major tautomer present in toluene-d_8, and presumably the reaction medium, is the 3-carboxylate. Therefore, despite the observation that the equilibrium between the 3-carboxylate and 5-carboxylate tautomers in non-interacting solvents strongly favours the 3-carboxylate tautomer, isolation of the 5-carboxylate as the major N–H insertion product **11a** suggests that the minor tautomer is significantly more reactive.

As pyrazoles **10g** and **10q** were insoluble in $CDCl_3$ their NMR spectra were recorded in DMSO-d_6 with broad signals for both tautomers observed in each instance. Considering this, the solvent dependency on the position of equilibrium was studied by comparing the ^{13}C NMR spectra for pyrazoles **10a**, **11a** and **12a** in DMSO-d_6 with those in $CDCl_3$. Notably in DMSO-d_6, two distinct sets of broad signals were observed for pyrazole **10a** at

© 2019 Wiley-VCH Verlag GmbH & Co. KGaA, Weinheim

150.9 MHz (see Figure S17, supplementary information), characteristic of both the 3-carboxylate and 5-carboxylate tautomer, with the 5-carboxylate predominating as the major tautomer in solution as evidenced by comparison of carbon signals with that of pyrazole **11a**. For tautomer assignment one of the characteristic features is that the C(4) chemical shift for the 5-carboxylate tautomer is always more deshielded than that for the 3-carboxylate. Accordingly, in the experimental section, the pyrazoles **10g** and **10q** are characterised as a mixture of the 3-, and 5-carboxylate tautomers while pyrazoles **10a–f** and **10h–p** were characterised as the major 3-carboxylate tautomer as their spectra were recorded in $CDCl_3$ (Figure 7). The impact of solvent on the dynamic equilibrium between the 3- and 5-carboxylate tautomers for pyrazole **10a** is summarised in Scheme 12.

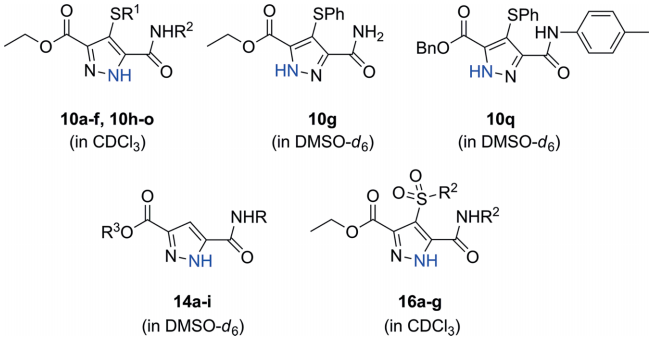

Figure 7. Principal tautomers of 3,4,5 substituted pyrazoles **10a–q** and **16a–g**, and 3,5-substituted pyrazoles **14a-i** illustrating the importance of solvent on the dynamic equilibrium. Structures are named and numbered accordingly in the experimental section/supplementary information.

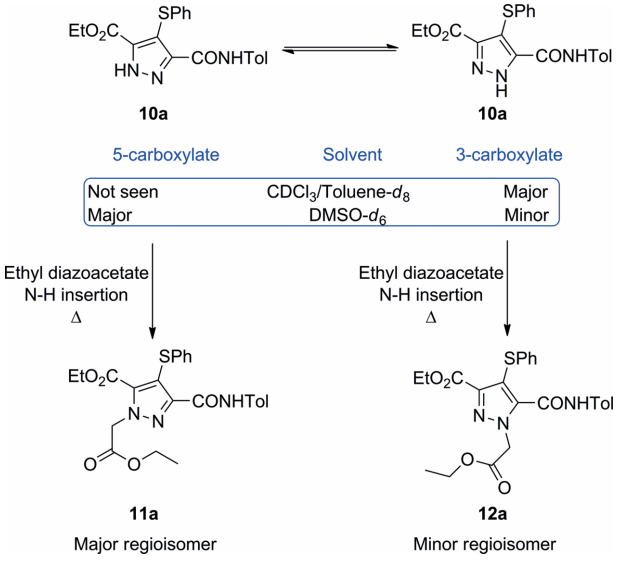

Scheme 12. Summary of solvent effects on the dynamic equilibrium between the 3, and 5-carboxylate tautomers for pyrazole **10a**.

Pyrazoles **14a-i** were significantly less soluble than their 3,4,5-substituted counterparts, and DMSO-d_6 was required to solubilise these compounds for NMR spectroscopy. The NMR spectra of **14f** could be recorded in $CDCl_3$. Pyrazole **14f** exhibited one set of broad signals in the ^{13}C NMR spectrum at 150.9 MHz in $CDCl_3$, while splitting of both the NH pyrazole and NH amide signals, into major and minor components, was observed in the ^{1}H NMR spectrum at 600 MHz. Two sets of broad signals were observed in the ^{13}C NMR spectra for pyrazoles **14a-e** and **14g–i** recorded in DMSO-d_6, indicative of the 3-carboxylate and 5-carboxylate, however, comparison of the ^{13}C NMR spectra of pyrazoles **10** and **14** in DMSO-d_6 strongly suggests that the dynamic equilibrium shifts towards the 3-carboxylate on removal of the sulfur moiety at the C(4) position (see supplementary information for further details). Therefore, similar solvent effects on the dynamic equilibrium are observed for both the 3,5-substituted and 3,4,5-substituted pyrazoles **10** and **14** respectively, however, with the 5-carboxylate predominating for the 3,4,5-substuted pyrazoles **10** and the 3-carboxylate predominating for the 3,5-substituted pyrazoles **14** in DMSO-d_6. Accordingly, the pyrazoles **14a-i** are characterised as the 3-carboxylate in this work (Figure 7).

In the solid state, the 4-sulfonylpyrazole **16a** exists as the tautomer with the carboxylate at the C(3) position (Figure 4). As is the case for the pyrazoles formed at sulfide oxidation level, one set of ^{13}C NMR signals is observed for the 4-sulfonylpyrazoles **16** in the non-interacting solvent $CDCl_3$, however the C(4) carbon is considerably sharper and more deshielded for this set of compounds than for the sulfide analogues. The C(3) and C(5) carbons remain very broad, suggesting that the pyrazoles **17** are also in dynamic equilibrium, with the 3-carboxylate the favoured tautomer, and the 5-carboxylate tautomer undetectable in the ^{13}C NMR spectra as seen at the sulfide level of cycloaddition. The 4-sulfonylpyrazoles **17** are assigned as the major 3-carboxylate tautomer in this work (Figure 7).

Further Derivatisation of the Pyrazole Scaffold

The [3+2]-dipolar cycloaddition of α-diazoacetates is a powerful synthetic methodology that has the advantage that it allows incorporation of highly functionalised substituents at each the C(3), C(4) and C(5) positions of the pyrazole core. As there are very few examples of 3,4,5-trisubstituted pyrazoles (particularly bearing a sulfur moiety), with each substituent bearing functionalisable groups investigation of the synthetic potential of these compounds was briefly undertaken utilising pyrazole **10a** as a standard substrate.

Notably, selective oxidation of sulfides **10** to either sulfoxides **19** or sulfones **16** can readily be achieved in high yields using *m*CPBA. Therefore, despite the limitations associated with the [3+2]-dipolar cycloadditions at both the sulfoxide and sulfone levels, C(4) substituted sulfoxide and sulfone pyrazole derivatives can be accessed readily in synthetically useful quantities in the same overall number of synthetic steps. Regioselective *N*-alkylation using alkyl bromides and K_2CO_3 in DMSO[30] afforded the alkylated products in high combined yields, with the 5-carboxylate formed preferentially in all instances, consistent with selective alkylation of the major tautomer present in DMSO (Scheme 12). Hydrolysis of the ester moiety to the carboxylic acid **20** and subsequent amide coupling gave pyrazole **21** illustrating that the use of α-diazoacetates as dipoles and α-sulfenyl-β-chloroacrylamides as dipolarophiles allows access

© 2019 Wiley-VCH Verlag GmbH & Co. KGaA, Weinheim

not only to the generation of highly functionalised pyrazoles but importantly functionalised pyrazoles amenable to significant further synthetic transformations. An overview of these synthetic transformations is outlined in Scheme 13, with the tabulated results included in the supplementary information (Table S1–S2 and Scheme S1).

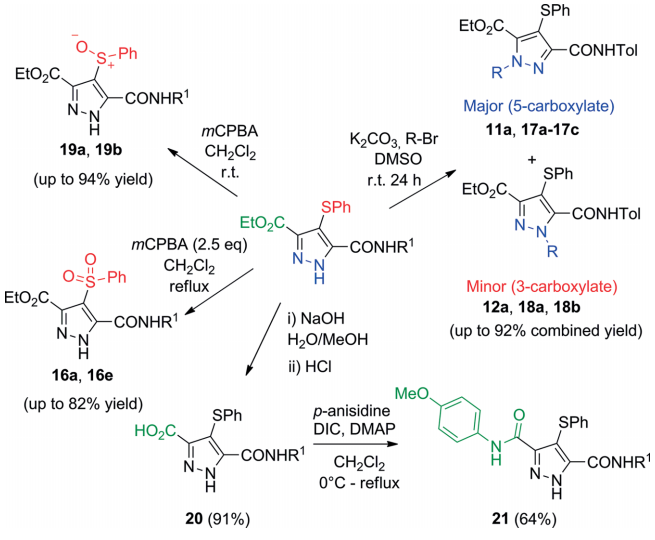

Scheme 13. Overview of the synthetic potential of the densely functionalised 3,4,5-substituted pyrazoles **10**; facile selective sulfur oxidation, regioselective *N*-alkylation, ester hydrolysis and sequential amide coupling.

Conclusions

In summary, we have presented herein highly regioselective synthetic methodology leading to densely functionalised C(3), C(4) and C(5) substituted pyrazoles **10a–q** and **16a–g** via thermal [3+2]-dipolar cycloaddition, of α-diazoacetates and α-thio-β-chloroacrylamides, at the sulfide, sulfoxide and sulfone levels of oxidation. Significantly, this work allows access to C(4)-sulfenyl or sulfonyl pyrazoles, through migration of the sulfur substituent at the sulfide and sulfone oxidation levels, while elimination of the sulfinyl group is observed, leading to 3,5-disubstituted pyrazoles **14a-i**. Notably, use of highly functionalised dipolarophiles, and in particular a chlorine which can act as a leaving group, enables the key rearrangement following cycloaddition to provide the synthetically versatile pyrazoles, where each of the three substituents has the potential for orthogonal functional group interconversion. While the sulfide migration to the electron deficient carbon is readily rationalised, the analogous carbon–carbon 1,2-sulfonyl migration is unprecedented and mechanistically intriguing. Notably, we have found that the [3+2]-dipolar cycloaddition is remarkably insensitive to the nature of the substituent present on both the amide and sulfide, with extension to esters also possible. While moderate to good yields are obtained using the dipolarophiles at the sulfide level of oxidation, efficiencies are decreased when conducted using the sulfoxide or sulfone, reflecting the labile nature of the reactants and products under the reaction conditions.

In contrast to alternative synthetic methods leading to pyrazoles, such as hydrazine condensation, this methodology offers distinct synthetic advantage enabling access to highly substituted and structurally diverse pyrazoles with functionality amenable to further selective synthetic transformations.

Isolation of the *N*-alkylated pyrazoles **11a** and **12a** as byproducts from the cycloaddition through further reaction of the pyrazoles **10** with excess α-diazoacetate, proved useful in rationalising the tautomeric behaviour evident in the NMR spectra of the pyrazoles, with the position of tautomeric equilibrium influenced by solvent and substituents.

Experimental Section

General Procedures: Solvents were distilled prior to use as follows: Dichloromethane was distilled from phosphorus pentoxide, ethyl acetate was distilled from potassium carbonate; and hexane was distilled prior to use. For [3+2]-dipolar cycloadditions HPLC grade toluene was used. All commercial reagents were used without further purification unless otherwise stated.

^{1}H NMR spectra were run at either 300, 400 or 600 MHz and ^{13}C NMR spectra were recorded at either 75.5, 100 or 150.9 MHz. All spectra were recorded at room temperature (300K) in deuterated chloroform ($CDCl_3$), unless otherwise stated using tetramethylsilane (TMS) as an internal standard. Chemical shifts (δ_H and δ_C) are reported in parts per million (ppm) relative to TMS, and coupling constants are expressed in Hertz (Hz). Splitting patterns in ^{1}H NMR spectra are designated as s (singlet), br s (broad singlet), d (doublet), t (triplet), q (quartet), dd (doublet of doublets) and m (multiplet). ^{13}C NMR spectra were calibrated using the solvent signal, i.e., $CDCl_3$ δ_C 77.0 ppm, [D_6]DMSO 39.5 ppm, [D_8]toluene 20.4 ppm. Assignments were made with the aid of DEPT experiments and 2D NMR experiments including COSY, HSQC and HMBC.

Infrared spectra were measured using a FTIR UATR2 spectrometer or were recorded as films on sodium chloride plates on a PerkinElmer Paragon 1000 FT-IR spectrometer. Flash column chromatography was carried out using Kieselgel silica gel 60, 0.035–0.075 mm (Merck).

Thin-layer chromatography (TLC) was carried out on precoated silica gel plates (Merck 60 PF254). Visualization was achieved by UV (254 nm) light absorption.

The Microanalysis Laboratory, National University of Ireland, Cork, performed elemental analysis using a PerkinElmer 240 and Exeter Analytical CE440 elemental analyser. Low-resolution mass spectra (LRMS) was recorded on a Waters Quattro Micro triple quadrupole instrument in electrospray ionization (ESI) mode using 50 % acetonitrile/water containing 0.1 % formic acid as eluent. High resolution (precise) mass spectra (HRMS) were recorded on a Waters LCT Premier Tof LC–MS instrument in electrospray ionization (ESI) mode using 50 % acetonitrile/water containing 0.1 % formic acid as eluent. High-resolution (precise) mass spectra (HRMS) were also recorded on an Agilent 6530B Accurate Mass Q-TOF LC/MS instrument in electrosprayionisation mode using 50 % acetonitrile/water containing 0.1 % formic acid as eluent. Samples were prepared for either LRMS or HRMS by employing acetonitrile as solvent.

Melting points were obtained using a Unimelt Thomas–Hoover capillary melting point apparatus and are uncorrected.

Single-crystal X-ray analysis was performed on a Bruker APEX II DUO diffractometer at room temperature using graphite monochromatic Mo K_α (λ = 0.7107 Å) radiation. All calculations and refinement were made using the APEX software,[31] containing the SHELX suite of

© 2019 Wiley-VCH Verlag GmbH & Co. KGaA, Weinheim

programs[32] and diagrams prepared with Mercury 3.10.[33] All non-hydrogen atoms were located and refined with anisotropic thermal parameters. Hydrogen atoms were included in calculated positions or were located and refined with isotropic thermal parameters.

General Procedure for the Preparation for the Formation of α-Chloroamides

2-Chloro-*N*-(2′,2′-dimethylpropyl)propanamide (6d): 2-Chloropropionyl chloride (7.61 g, 59.94 mmol) in dichloromethane (50 mL) was added dropwise over 20 min to a solution of 2,2-dimethylpropylamine (5.17 g, 59.35 mmol) and triethylamine (6.07 g, 59.94 mmol) in dichloromethane (100 mL) at 0 °C, while stirring under nitrogen. On completion of the addition, the reaction solution was removed from the ice bath and stirred at room temperature for 4 h. Water (200 mL) was added and the layers separated. The organic layer was washed with a saturated solution of sodium bicarbonate (2 × 150 mL), water (200 mL), and brine (200 mL), dried, filtered and concentrated under reduced pressure to give the α-chloroamide **6d** as a white solid (15.38 g, 97 %) which required no further purification; m.p. 79–81 °C; ν_{max}/cm^{-1} (ATR) 3255 (NH), 3093 (CH), 2957 (CH), 1652 (CO), 1574, 1374 (CN stretch); ^{1}H NMR (300 MHz, $CDCl_3$) δ = 0.94 [s, 9H, $C(CH_3)_3$], 1.75 [d, *J* = 7.1 Hz, 3H, $C(3)H_3$], 3.06 [dd, A of ABX system, J_{AB} = 13.3 Hz, J_{AX} = 6.3 Hz, 1H, one of CH_2NH], 3.13 [dd, B of ABX system, J_{BA} = 13.3 Hz, J_{BX} = 6.4 Hz, 1H, one of CH_2NH], 4.45 [q, *J* = 7.1 Hz, 1H, C(2)H], 6.70 (br s, 1H, NH) ppm; ^{13}C NMR (75.5 MHz, $CDCl_3$) δ = 22.8 [CH_3, $C(3)H_3$], 27.0 [$C(CH_3)_3$], 31.9 [C, $C(CH_3)_3$], 50.8 (CH_2NH), 56.3 [CH, C(2)H], 169.4 (C=O) ppm; HRMS (ES$^+$): Exact mass calculated for $C_8H_{16}NO^{35}Cl$ [M + H]$^+$ 178.0993, found 178.0995; m/z (ES$^+$) 180.3 {[($C_8H_{16}NO^{37}Cl$)$^+$H$^+$], 30 %}, 178.3 {[($C_8H_{16}NO^{35}Cl$) + H$^+$], 100 %}.

General Procedure for the Preparation for the Formation of α-Thioamides

***N*-(2′,2′-Dimethylpropyl)-2-(phenylthio)propanamide (7d):** Thiophenol (2.89 mL, 28.2 mmol) in ethanol (22 mL) was added to a solution of aqueous sodium hydroxide (0.8 M, 78 mL, 54.20 mmol). Immediately, a solution of 2-chloro-*N*-(2′,2′-dimethylpropyl)propenamide **6d** (4.80 g, 27.10 mmol) in ethanol (60 mL) was added gradually over 15 minutes to the reaction mixture. Following heating under reflux for 1 h, the reaction was cooled in an ice bath and was quenched by the addition of water (70 mL). The solid precipitate was isolated by suction filtration to give pure *N*-(2′,2′-dimethylpropyl)-2-(phenylthio)propenamide **7d** as a white solid (6.67 g, 98 %); m.p. 87–89 °C; ν_{max}/cm^{-1} (ATR) 3272 (NH), 2964 (CH), 2953 (CH), 1640 (C=O amide), 1564, 1203; ^{1}H NMR (300 MHz, $CDCl_3$) δ = 0.78 [s, 9H, $C(CH_3)_3$], 1.56 [d, *J* = 7.3 Hz, 3H, $C(2)H_3$], 2.95 [dd, A of ABX system, J_{AB} = 13.3 Hz, J_{AX} = 6.0 Hz, 1H, one of CH_2NH], 3.06 [dd, B of ABX system, J_{BA} = 13.3 Hz, J_{BX} = 6.7, 1H, one of CH_2NH], 3.91 [q, *J* = 7.4 Hz, 1H, C(2)H], 6.79 (br s, 1H, NH), 7.15–7.36 (m, 5H, ArH) ppm; ^{13}C NMR (75.5 MHz, $CDCl_3$) δ = 18.3 [CH_3, $C(3)H_3$], 26.9 [CH_3, $C(CH_3)_3$] 31.6 [C, $C(CH_3)_3$], 46.6 [CH, C(2)H], 50.6 (CH_2, CH_2NH), 126.7 (CH, CH_{Ar}), 129.0 (CH, CH_{Ar}), 129.1 (CH, CH_{Ar}), 134.1 [C, $C_{Ar(q)}$], 171.5 (C=O) ppm; HRMS (ES$^+$): Exact mass calculated for $C_{14}H_{21}NOS$ [M + H]$^+$ 252.1422, found 252.1428; m/z (ES$^+$) 252.4 {[($C_{14}H_{21}NOS$) + H$^+$], 100 %}.

Novel compounds **7e** and **7l–m** were similarly prepared, see supplementary information for characterisation data.

General procedure for the preparation for the formation of α-thio-β-chloroacrylamides.

***N*-(2′,2′-Dimethylpropyl)-*Z*-3-chloro-2-(phenylthio)propenamide (8d):** Unrecrystallised *N*-chlorosuccinimide (5.19 g, 38.90 mmol) was added in one portion to a solution of *N*-(2′,2′-dimethylpropyl)-2-(phenylthio)propenamide **7d** (5.01 g, 19.95 mmol) in toluene (110 mL). The flask was immediately immersed in an oil bath at 90 °C and heating was maintained with stirring for 3 h. The reaction mixture was cooled to 0 °C and the succinimide by-product was removed by filtration. The solvent was removed at reduced pressure to give the crude product as a brown solid. This was purified by column chromatography on silica gel using hexane/ethyl acetate (95:5) as eluent to give the pure α-thio-β-chloroacrylamide **8d** as a white solid (4.13 g, 77 %); m.p. 79–82 °C; Found C, 59.39; H, 6.35; N, 4.96. $C_{14}H_{18}NOSCl$ requires C, 59.25; H, 6.39; N, 4.94; ν_{max}/cm^{-1} (ATR) 3382 NH), 2955 (CH), 1646 (C=O amide), 1519, 1232; ^{1}H NMR (300 MHz, $CDCl_3$) δ = 0.68 [s, 9H, $C(CH_3)_3$], 3.02 (d, *J* = 6.4 Hz, 2H, CH_2NH), 6.92 (br s, 1H, NH), 7.16–7.33 (m, 5H, ArH), 7.97 [s, 1H, ClHC(3)=] ppm; ^{13}C NMR (75.5 MHz, $CDCl_3$) δ = 26.8 [CH_3, $C(CH_3)_3$], 31.7 [C, $C(CH_3)_3$], 51.1 (CH_2, CH_2NH), 127.0 (CH, CH_{Ar}), 127.8 (CH, CH_{Ar}), 129.5 (CH, CH_{Ar}), 130.4 [C, SC(2)=], 133.0 (C, $C_{Ar(q)}$), 139.7 [CH, C(3)HCl=], 162.1 (C=O) ppm; HRMS (ES$^+$): Exact mass calculated for $C_{14}H_{18}NOS^{35}Cl$ [M + H]$^+$ 284.0858, found 284.0866; m/z (ES$^+$) 286.3 {[($C_{14}H_{18}NOS^{37}Cl$) + H$^+$], 40 %}, 284.3 {[($C_{14}H_{18}NOS^{35}Cl$) + H$^+$], 100 %}.

Novel compounds **8e** and **7l–m** were similarly prepared, see supplementary information for characterisation data.

General Procedure for the Preparation for the Formation of α-Sulfinyl-β-chloroacrylamides

***N*-(2′,2′-Dimethylpropyl)-*Z*-3-chloro-2-(benzenesulfinyl)propenamide (9d):** A solution of Oxone® (6.69 g, 21.76 mmol) in water (40 mL) was added dropwise to a stirring solution of *N*-(2′,2′-dimethylpropyl)-*Z*-3-chloro-2-(phenylthio)propenamide **8d** (3.08 g, 10.88 mmol) in acetone (120 mL) at room temperature. A colourless precipitate formed immediately. The reaction mixture was stirred overnight at which point water (200 mL) was added. The layers were separated and the aqueous layer was extracted with dichloromethane (3 × 70 mL). The combined organic extracts were washed with water (2 × 100 mL) and brine (100 mL), dried, filtered and concentrated to give the pure sulfoxide **9d** as a clear oil (3.13 g, 96 %); ν_{max}/cm^{-1} (ATR) 3267 (NH stretch), 3059 (CH stretch), 2957 (CH), 1668 (C=O amide), 1556 (NH bend), 1030 (SO); ^{1}H NMR (300 MHz, $CDCl_3$) δ = 0.82 [s, 9H, $C(CH_3)_3$], 2.91–3.00 [dd, A of ABX system, J_{AB} = 13.3 Hz, J_{AX} = 5.5 Hz, 1H one of CH_2NH], 3.10–3.19 [dd, B of ABX system, J_{BA} = 13.3 Hz, J_{BX} = 6.5 Hz, 1H, one of CH_2NH], 7.47–7.70 (m, 5H, ArH), 7.80 (s, 1H, ClHC(3)=), 8.34 (C=O) ppm; ^{13}C NMR (75.5 MHz, $CDCl_3$) δ = 27.2 [CH_3, $C(CH_3)_3$], 31.7 [C, $C(CH_3)_3$], 50.8 (CH_2, CH_2NH), 124.2 (CH, CH_{Ar}), 129.6 (CH, CH_{Ar}), 131.6 (CH, CH_{Ar}), 137.5 [CH, C(3)HCl=], 138.7 [C, SC(2)=], 141.2 (C, $C_{Ar(q)}$), 160.8 (C=O) ppm; HRMS (ES$^+$): Exact mass calculated $C_{14}H_{18}NO_2S^{35}Cl$ [M + H]$^+$ 300.0820, found 300.0827; m/z (ES$^+$) 302.2 {[($C_{14}H_{18}NO_2S^{37}Cl$) + H$^+$], 40 %} 300.2 {[($C_{14}H_{18}NO_2S^{35}Cl$) + H$^+$], 100 %}.

Novel compounds **9e** and **9h** were similarly prepared, see supplementary information for characterisation data.

General Procedure for the [3+2]-Dipolar Cycloaddition of α-Diazoacetetes and α-Sulfenyl-β-chloroacrylamides

Ethyl 4-(Phenylthio)-5-(4′-methylphenylcarbamoyl)-1*H*-pyrazole-3-carboxylate (Major Tautomer) and Ethyl 4-(Phenylthio)-3-(4′-methylphenylcarbamoyl)-1*H*-pyrazole-5-carboxylate (Minor Tautomer) (10a): Ethyl diazoacetate (0.97 mL, 8 mmol, 87 % in dichloromethane) was added in one portion to a solution of *N*-(4′-methylphenyl)-*Z*-3-chloro-2-(phenylthio)propenamide **8a** (303 mg, 1 mmol) in toluene (5 mL) at room temperature. The solution was heated gradually to 100 °C and stirred under nitrogen for 24 h. The cooled reaction mixture in toluene was transferred directly onto a silica gel column to prevent any potential degradation of unreacted EDA if concentrated. Purification by column chromatography using

© 2019 Wiley-VCH Verlag GmbH & Co. KGaA, Weinheim

hexane/ethyl acetate (gradient elution 20–30 % ethyl acetate) as eluent, followed by trituration with diethyl ether gave the pyrazole **10a** as a white solid (245 mg, 64 %); m.p. 155–158 °C; ν_{max}/cm^{-1} (ATR) 3188 (NH), 1717 (C=O ester), 1661 (C=O amide), 1235, 817, 737; ^{1}H NMR (600 MHz, $CDCl_3$) δ = 1.28 (t, *J* = 7.1 Hz, 3H, OCH_2CH_3), 2.32 (s, 3H, $ArCH_3$), 4.35 (q, *J* = 7.1 Hz, 2H, OCH_2CH_3), 7.15 (d, *J* = 8.3 Hz, 2H, ArH), 7.17–7.30 (m, 5H, ArH), 7.49 (d, *J* = 8.3 Hz, 2H, ArH), 9.95 (br s, 1H, NH amide), 13.08 (br s, 1H, NH pyrazole) ppm; ^{1}H NMR (600 MHz, DMSO-d_6) δ = 1.13 (t, *J* = 7.1 Hz, 3H, OCH_2CH_3), 2.25 (s, 3H, $ArCH_3$), 4.20 (q, *J* = 7.0 Hz, 2H, OCH_2CH_3), 7.11 (app. t, unresolved coupling, 5H, ArH), 7.23 (app. t, unresolved coupling, 2H, ArH), 7.51–7.61 (m, 2H, ArH), 10.27 (br s, 1H, NH amide), 14.80 (br s, 1H, NH pyrazole) ppm; ^{1}H NMR (600 MHz, toluene-d_8) δ = 1.01 (t, *J* = 7.1 Hz, 3H, OCH_2CH_3), 2.04 (s, 3H, $ArCH_3$), 4.07 (q, *J* = 7.1 Hz, 2H, OCH_2CH_3), 6.74–6.92 (m, 5H, ArH), 7.12–7.17 (m, 2H, ArH), 7.55–7.60 (m, 2H, ArH), 9.83 (s, 1H, NH amide), 12.63 (br s, 1H, NH pyrazole) ppm; ^{13}C NMR (150.9 MHz, $CDCl_3$) δ = 14.0 (CH_3, OCH_2CH_3), 20.9 (CH_3, $ArCH_3$), 61.5 (CH_2, OCH_2CH_3), 109.1 [C, br, C(4)], 120.3 (CH, CH_{Ar}), 126.8 (CH, CH_{Ar}), 127.4 (CH, CH_{Ar}), 129.3 (CH, CH_{Ar}), 129.6 (CH, CH_{Ar}), 134.1 (C, $C_{Ar(q)}$), 134.7 (C, $C_{Ar(q)}$), 135.0 (C, $C_{Ar(q)}$), 140.4 [C, br, one of C(3) or C(5)], 145.8 [C, br, one of C(3) or C(5)], 156.0 (C, C=O amide), 160.5 (C, C=O ester) ppm; ^{13}C NMR (150.9 MHz, DMSO-d_6) δ = 13.8 (CH_3, OCH_2CH_3), 20.5 (CH_3, $ArCH_3$), 60.5 (CH_2, minor tautomer, OCH_2CH_3), 61.3 (CH_2, major tautomer, OCH_2CH_3), 108.5 [C, minor tautomer, C(4)], 111.4 [C, major tautomer, C(4)], 120.0 (CH, CH_{Ar}), 125.5 (CH, CH_{Ar}), 125.9 (CH, CH_{Ar}), 126.7 (CH, CH_{Ar}), 128.9, 129.0 129.3 (CH, overlapping broad signals, major and minor tautomers, CH_{Ar}), 132.7 (C, major tautomer, $C_{Ar(q)}$), 133.6 (C, minor tautomer, $C_{Ar(q)}$), 135.3 (C, minor tautomer, $C_{Ar(q)}$), 136.2 (C, major tautomer, $C_{Ar(q)}$),136.3 (C, major tautomer, $C_{Ar(q)}$), 136.8 (C, minor tautomer, $C_{Ar(q)}$), 137.5 [C, major tautomer, one of C(3) or C(5)],142.1 [C, minor tautomer, one of C(3) or C(5)], 144.8 [C, minor tautomer, one of C(3) or C(5)], 149.9 [C, major tautomer, one of C(3) or C(5)], 156.2 (C, minor tautomer, C=O amide), 158.0 (C, major tautomer, C=O amide), 159.2 (C, major tautomer, C=O ester), 160.8 (C, minor tautomer, C=O ester) ppm; ^{13}C NMR (150.9 MHz, toluene-d_8) δ = 14.1 (CH_3, OCH_2CH_3), 20.8 (CH_3, $ArCH_3$), 61.0 (CH_2, OCH_2CH_3), 109.6 [C, br, C(4)], 120.2 (CH, CH_{Ar}), 126.8 (CH, CH_{Ar}), 129.4 (CH, CH_{Ar}), 129.9 (CH, CH_{Ar}), 134.4 (C, $C_{Ar(q)}$), 135.4 (C, $C_{Ar(q)}$), 135.8 (C, $C_{Ar(q)}$), 140.9 [C, br, one of C(3) or C(5)], 146.0 [C, br, one of C(3) or C(5)], 156.0 (C, C=O amide), 160.5 (C, C=O ester) ppm; HRMS (ES$^+$): Exact mass calculated for $C_{20}H_{19}N_3O_3S$ [M + H]$^+$ 382.1208, found 382.1215; m/z (ES$^+$) 382.2 {[($C_{20}H_{19}N_3O_3S$) + H$^+$], 48 %}, 782.7 (100 %).

Note: 4 × CH_{Ar} signals observed for 5 × CH_{Ar} signals in ^{13}C NMR spectrum of pyrazole **10a** in [D_8]toluene. 1 CH_{Ar} signal overlapping with toluene-d_8 residual solvent peaks.

Compounds **10b–q** were similarly prepared, see supplementary information for characterisation data.

General Procedure for the [3+2]-Dipolar Cycloaddition of α-Diazoacetetes and α-Sulfinyl-β-chloroacrylamides

Ethyl 5-(4′-Methylphenylcarbamoyl)-1*H*-pyrazole-3-carboxylate (14a): Ethyl diazoacetate (0.97 mL, >87 % in dichloromethane, 8 mmol) was added in one portion to a stirring solution of *N*-(4′-methylphenyl)-Z-3-chloro-2-(benzenesulfinyl)propenamide **9a** (319 mg, 1 mmol) in toluene (2 mL) at room temperature. The reaction mixture was heated gradually to 100 °C and was stirred at this temperature under nitrogen for 48 h. Upon completion, the reaction mixture was cooled to room temperature during which a precipitate formed. The reaction mixture was further cooled in an ice bath for 1 h. The precipitate was collected by filtration through a sintered glass funnel (grade 4), and was washed thoroughly with diethyl ether until all the yellow impurity had been removed to give the pyrazole **14a** as a white solid (128 mg, 47 %); m.p. 216–218 °C; ν_{max}/cm^{-1} (ATR) 3341 (NH stretch), 3213 (NH) 3000 (CH), 1692 (C=O ester), 1667 (C=O amide), 1509, 826; ^{1}H NMR (300 MHz, $CDCl_3$) δ = 1.41 (t, *J* = 7.1 Hz, 3H, OCH_2CH_3), 2.34 (s, 3H, ArH), 4.43 (q, *J* = 7.1 Hz, 2H, OCH_2CH_3), 7.17 (d, *J* = 8.2 Hz, 2H, ArH), 7.42 [s, 1H, C(4)H], 7.56 (d, *J* = 8.3 Hz, 2H, ArH), 8.61 (br s, 1H, NH amide), 11.33 (br s, 1H, NH pyrazole) ppm; ^{1}H NMR (600 MHz, DMSO-d_6) δ = 1.32 (t, *J* = 7.1 Hz, 3H, OCH_2CH_3), 2.27 (s, 3H, $ArCH_3$), 4.32 (q, J = 7.1 Hz, 2H, OCH_2CH_3), 7.15 (d, *J* = 8.2 Hz, 2H, ArH), 7.48 [br s, 1H, C(4)H], 7.65 (d, *J* = 8.3 Hz, 2H ArH), 10.18 (br s, 1H, NH amide), 14.47 (br s, 1H, NH pyrazole) ppm; ^{13}C NMR (150.9 MHz, DMSO-d_6) 14.2 (CH_3, $ArCH_3$), 20.5 (CH_3, OCH_2CH_3), 60.7 (CH_2, OCH_2CH_3), 108.6 [CH, C(3)H], 120.3 (CH, CH_{Ar}), 129.1 (CH, CH_{Ar}), 133.0 (C, $C_{Ar(q)}$), 135.9 (C, $C_{Ar(q)}$), 157.6 (C, br, C=O amide), 160.3 (C, br, C=O ester) ppm; HRMS (ES$^+$): Exact mass calculated for $C_{14}H_{15}N_3O_3$ [M + H]$^+$ 274.1196, found 274.1196.

Note: In the ^{13}C NMR spectrum of pyrazole **14a** at 150.9 MHz the C(3) and C(5) carbons were not readily observed (10 s delay time). Signals for the minor tautomer, ethyl 3-(4′-methylphenylcarbamoyl)-1H-pyrazole-5-carboxylate were not observed.

Compounds **14b–i** were similarly prepared, see supplementary information for characterisation data.

Purification of Commercial *m*CPBA:[34] In a 1 L volumetric flask sodium hydroxide (0.1 M, 410 mL) and potassium phosphate monobasic (0.2 M, 250 mL) were mixed. The flask was filled up to 1 L with deionised water and the solution was stirred vigorously for 2 min to generate the buffer solution (pH 7.5). Commercial *m*CPBA (10 g, 65–77 %) was dissolved in diethyl ether (150 mL), and washed three times with buffer solution (pH 7.5, 150 mL). The ether layer was dried with $MgSO_4$, filtered and carefully evaporated under reduced pressure to give 6.88 g pure *m*CPBA as a white solid. The peracid was transferred to a plastic container and stored in the refridgerator for 3 months without decomposition. The purity was determined by ^{1}H NMR spectroscopy.

Caution: It has been determined that 95–100 % mCPBA can be detonated by shock or sparks, whereas commercial 70–85 % mCPBA is not shock sensitive. It should be stored in a refridgerator in tightly closed containers.

General Procedure for the [3+2]-Dipolar Cycloaddition of α-Diazoacetetes and α-Sulfonyl-β-chloroacrylamides

Ethyl 4-(Phenylsulfonyl)-5-(4′-methylphenylcarbamoyl)-1H-pyrazole-3-carboxylate (16a): *m*-CPBA (77 %, 448 mg, 2 mmol) in dichloromethane (15 mL) was added dropwise over 2 minutes to a stirring solution of *N*-(4′-methylphenyl)-Z-3-chloro-2-(benzenesulfinyl)propenamide **9a** (319 mg, 1 mmol) in dichloromethane (5 mL) at room temperature. The reaction progress was monitored by ^{1}H NMR spectroscopy. Once the impurity profile of the reaction was observed to increase relative to the increase in sulfoxide **9a** to sulfone **15a** oxidation the reaction mixture was concentrated under reduced pressure to an approximate volume of 10 mL in dichloromethane. Ethyl diazoacetate (0.49 mL, 4 mmol, >87 % in dichloromethane) was added in one portion to the crude sulfone and the reaction mixture was stirred overnight at room temperature under nitrogen. Repeated purification by column chromatography on silica gel using hexane/ethyl acetate (60:40) as eluent, followed by dichloromethane/ethyl acetate (80:20) gave the pure pyrazole **16a** as a white solid (67 mg, 16 % over 2 steps); m.p. 179–181 °C; ν_{max}/cm^{-1} (ATR) 3193 (NH), 1736 (C=O ester), 1659 (C=O amide), 1311 (asymmetric SO_2), 1241, 1148 (symmetric SO_2); ^{1}H NMR (600 MHz, $CDCl_3$) δ = 1.37 (t, *J* = 7.1 Hz, 3H, OCH_2CH_3), 2.35 (s, 3H, $ArCH_3$),

© 2019 Wiley-VCH Verlag GmbH & Co. KGaA, Weinheim

4.41 (q, J = 7.1 Hz, 2H OCH_2CH_3), 7.20 (d, J = 8.1 Hz, 2H, ArH), 7.53 (d, J = 7.8 Hz, 2H, ArH), 7.59–7.70 (m, 3H, ArH), 8.07 (d, J = 7.8 Hz, 2H, ArH), 11.20 (br s, 1H, NH amide) ppm; ^{13}C NMR (150.9 MHz, $CDCl_3$) δ = 14.0 (CH_3, OCH_2CH_3), 21.0 (CH_3, $ArCH_3$), 62.5 (CH_2, OCH_2CH_3), 120.0 [C, C(4)], 120.3 (CH, CH_{Ar}), 127.5 (CH, CH_{Ar}), 129.2 (CH, CH_{Ar}), 129.8 (CH, CH_{Ar}), 134.0 (CH, CH_{Ar}), 134.3 (C, $C_{Ar(q)}$), 135.5 (C, $C_{Ar(q)}$), 138.6 [C, one of C(3) or C(5)], 140.7 (C, $C_{Ar(q)}$), 145.2 [C, one of C(3) or C(5)], 154.0 (C, C=O amide), 160.3 (C, C=O ester) ppm; HRMS (ES$^+$): Exact mass calculated for $C_{20}H_{19}N_3O_5S$ [M + H]$^+$ 414.1118, found 414.1123; m/z (ES-) 412.2 {[($C_{20}H_{19}N_3O_5S$)-H$^+$], 100 %}. The regiochemistry was determined by single X-ray diffraction on a crystalline sample of **16a** recrystallised from dichloromethane. Crystals of **16a** are triclinic, space group P, formula $C_{20}H_{19}N_3O_3S$, MW = 413.44 g mol^{-1}, a = 7.6015(5) Å, b = 8.4522(6) Å, c = 15.5976(11) Å, α = 81.209(2)°, β = 81.359(2)°, γ = 70.921(2)°, U = 930.55(11) Å3, F(000) = 432, μ(Mo K_α) = 0.214 mm-1, R_1(F) = 0.0560 and S = 1.019 for 4588 observed reflections with $I > 2\sigma(I)$, $wR_2(F^2)$ = 0.1698 for all 7982 unique reflections.

Compounds **16b–g** were similarly prepared, see supplementary information for characterisation data.

The title compound **16a** was also prepared by addition of *m*-CPBA (113 mg, 0.655 mmol, 100 %) to a stirring solution of 4-(phenylthio)-5-(4′-methylphenylcarbamoyl)-1*H*-pyrazole-3-carboxylate **10a** (100 mg, 0.262 mmol) in dichloromethane (5 mL) at room temperature. The reaction solution was heated to reflux and stirred overnight. Sodium thiosulfate (10 mL, 10 % w/v) was added to the cooled reaction mixture and the layers were separated. The organic layer was washed with sodium thiosulfate (2 × 10 mL, 10 % w/v), sat. sodium bicarbonate (3 × 10 mL), brine (10 mL), dried, filtered and concentrated under reduced pressure to give the pure pyrazole **16a** as a white solid (89 mg, 82 %). Spectroscopic characteristics were consistent with those outlined previously.

General Procedure for the *N*-Alkylation of Pyrazole 10a

Ethyl 1-(2-Ethoxy-2-oxoethyl)-4-(phenylthio)-3-(4′-methylphenylcarbamoyl)-1*H*-pyrazole-5-carboxylate (11a) and Ethyl 1-(2-Ethoxy-2-oxoethyl)-4-(phenylthio)-5-(4′-methylphenylcarbamoyl)-1*H*-pyrazole-3-carboxylate (12a): Ethyl 4-(phenylthio)-5-(4′-methylphenylcarbamoyl)-1*H*-pyrazole-3-carboxylate **10a** (150 mg, 0.393 mmol), potassium carbonate (71 mg, 0.512 mmol) and a stirrer bar were placed in a vial. Anhydrous dimethyl sulfoxide (3 mL) was added and the resultant mixture was stirred at room temperature under nitrogen. Ethyl bromoacetate (0.06 mL, 0.472 mmol) was added and the resulting mixture was stirred at room temperature for 24 h. The reaction mixture was quenched with iced water (10 mL). The resulting mixture was extracted with ethyl acetate (2 × 15 mL). The combined organic layers were washed with brine (20 mL), dried with magnesium sulfate, and concentrated under reduced pressure to give the crude product as a yellow oil which contained a mixture of *N*-alkylated pyrazoles **11a**:**12a** in a ratio of 72:28. Purification by column chromatography on silica gel using hexane/ethyl acetate (80:20) as eluent gave pure pyrazole **11a** as a clear oil which solidified overnight to give a white solid (112 mg, 61 %), pure pyrazole **12a** as a white solid (46 mg, 25 %), and a mixed fraction of **11a** and **12a** as a clear oil which solidified overnight to give a white solid (11 mg, 6 %) to give a combined yield of 92 %.

Pyrazole **11a**; more polar; m.p. 107–109 °C; ν_{max}/cm^{-1} (ATR) 3340 (NH stretch), 2993 (CH stretch), 1736 (C=O ester), 1708 (C=O ester), 1682 (C=O amide), 1531 (NH bend), 1270; ^{1}H NMR (600 MHz, $CDCl_3$) δ = 1.15 [t, J = 7.1 Hz, 3H, one of $C(5)CO_2CH_2CH_3$ or $NCH_2CO_2CH_2CH_3$], 1.28 [t, J = 7.2 Hz, 3H, one of $C(5)CO_2CH_2CH_3$ or $NCH_2CO_2CH_2CH_3$], 2.29 (s, 3H, $ArCH_3$), 4.21 and 4.24 [overlapping quartets, 4H, J = 7.1 Hz, $C(5)CO_2CH_2$ or $NCH_2CO_2CH_2$], 5.38 (s, 2H, NCH_2CO), 7.03–7.26 (m, 7H, ArH), 7.49 (d, J = 8.5 Hz, 2H, ArH), 9.09 (s, 1H, NH amide) ppm; ^{13}C NMR (150.9 MHz, $CDCl_3$) δ = 13.6 [CH_3, one of $C(5)CO_2CH_2CH_3$ or $NCH_2CO_2CH_2CH_3$], 13.9 [CH_3, one of $C(5)CO_2CH_2CH_3$ or $NCH_2CO_2CH_2CH_3$], 20.7 (CH_3, $ArCH_3$), 55.0 (CH_2, NCH_2CO], 62.0 (CH_2, overlapping $C(5)CO_2CH_2$ or $NCH_2CO_2CH_2$], 113.7 [C, C(4)], 119.8 (CH, CH_{Ar}), 125.9 (CH, CH_{Ar}), 126.8 (CH, CH_{Ar}), 128.9 (CH, CH_{Ar}), 129.3 (CH, CH_{Ar}), 133.9 (C, $C_{Ar(q)}$), 134.9 (C, $C_{Ar(q)}$), 136.4 (C, $C_{Ar(q)}$), 137.1 [C, C(5)], 146.6 [C, C(3)], 157.6 (C, C=O amide), 158.8 [C, C(5)C=O], 166.7 [C, NCH_2C=O] ppm; ^{1}H NMR (600 MHz, DMSO-d_6) δ = 1.06 [t, J = 7.1 Hz, 3H, $C(5)CO_2CH_2CH_3$], 1.21 [t, J = 7.1 Hz, 3H, $NCH_2CO_2CH_2CH_3$], 2.25 (s, 3H, $ArCH_3$), 4.14 [q, J = 7.1 Hz, 2H, $C(5)CO_2CH_2$], 4.19 [q, J = 7.1 Hz, 2H, $NCH_2CO_2CH_2$], 5.44 (s, 2H, NCH_2CO), 7.06–7.15 (m, 5H, ArH), 7.21–7.28 (m, 2H, ArH), 7.56 (d, J = 8.5 Hz, 2H, ArH), 10.34 (s, 1H, NH amide) ppm; ^{13}C NMR (150.9 MHz, DMSO-d_6) δ = 13.5 [CH_3, $C(5)CO_2CH_2CH_3$], 14.0 [CH_3, $NCH_2CO_2CH_2CH_3$], 20.5 (CH_3, $ArCH_3$), 54.8 (CH_2, NCH_2CO), 61.5 [CH_2, $C(5)CO_2CH_2$], 61.7 [$NCH_2CO_2CH_2$], 111.3 [C, C(4)], 119.9 (CH, CH_{Ar}), 125.7 (CH, CH_{Ar}), 126.6 (CH, CH_{Ar}), 128.9 (CH, CH_{Ar}), 129.0 (CH, CH_{Ar}), 132.9 (C, $C_{Ar(q)}$), 135.9 (C, $C_{Ar(q)}$), 136.1 (C, $C_{Ar(q)}$), 137.0 [C, C(5)], 148.6 [C, C(3)], 158.1 [C, C(5)C=O], 158.6 (C, C=O amide), 167.3 [C, NCH_2C=O] ppm; ^{1}H NMR (600 MHz, toluene-d_8) δ = 0.83 [t, J = 7.1 Hz, 3H, one of $C(5)CO_2CH_2CH_3$ or $NCH_2CO_2CH_2CH_3$], 0.89 [t, J = 7.1 Hz, 3H, one of $C(5)CO_2CH_2CH_3$ or $NCH_2CO_2CH_2CH_3$], 2.06 (s, 3H, $ArCH_3$), 3.86 [q, J = 7.1 Hz, 2H, $C(5)CO_2CH_2$], 3.88 [q, J = 7.1 Hz, 2H, $NCH_2CO_2CH_2$], 5.03 (s, 2H, NCH_2CO), 6.80 (t, unresolved coupling, 1H, ArH), 6.87 (d, J = 8.3 Hz, 2H, ArH), 6.92 (t, J = 7.8 Hz, 2H, ArH), 7.27 (d, J = 7.5 Hz, 2H, ArH), 7.49 (d, J = 8.3 Hz, 2H, ArH), 8.60 (s, 1H, NH amide) ppm; ^{13}C NMR (150.9 MHz, toluene-d_8) δ = 13.6 [CH_3, one of $C(5)CO_2CH_2CH_3$] or $NCH_2CO_2CH_2CH_3$], 13.9 [CH_3, one of $C(5)CO_2CH_2CH_3$ or $NCH_2CO_2CH_2CH_3$], 20.7 (CH_3, overlapping with residual toluene-d_8 signal, $ArCH_3$), 54.9 (CH_2, NCH_2CO), 61.7 [CH_2, $C(5)CO_2CH_2$], 61.8 [$NCH_2CO_2CH_2$], 115.9 [C, C(4)], 119.7 (CH, CH_{Ar})*, 125.8 (CH, CH_{Ar}), 127.8 (CH, CH_{Ar}), 129.6 (CH, CH_{Ar}), 133.2 (C, $C_{Ar(q)}$), 136.3 (C, $C_{Ar(q)}$), 137.2 (C, $C_{Ar(q)}$), 138.3 [C, C(5)], 147.5 [C, C(3)], 157.4 (C, C=O amide), 159.5 [C, C(5)C=O], 166.8 [C, NCH_2C=O] ppm; * 1 × CH_{Ar} signal in toluene-d_8 spectrum overlapping with residual solvent signal; HRMS (ES$^+$): Exact mass calculated for $C_{24}H_{25}N_3O_5S$ [M + H]$^+$ 468.1588, found 468.1587; m/z (ES$^+$) 468.2 {[($C_{24}H_{25}N_3O_5S$) + H$^+$], 100 %}. The regiochemistry was determined by single X-ray diffraction on a crystalline sample of **11a** recrystallised from dichloromethane. Crystals of pyrazole **11a** are triclinic, space group P, formula $C_{24}H_{25}N_3O_5S$, MW = 467.53 g mol^{-1}, a = 9.456(2) Å, b = 11.142(3) Å, c = 12.695(3) Å, α = 70.288(8)°, β = 81.753(8)°, γ = 70.999(8)°, U = 1189.7(5) Å^3, F(000) = 492, m(Mo-K_α) = 0.176 mm^{-1}, R_1(F) = 0.0546 and S = 1.031 for 2701 observed reflections with $I > 2\sigma(I)$, $wR_2(F^2)$ = 0.1564 for all 4552 unique reflections.

Pyrazole **12a**; less polar; m.p. 124–127 °C; ν_{max}/cm^{-1} (ATR) 3301 (NH stretch), 1741 (C=O ester), 1732 (C=O ester), 1650 (C=O amide), 1539 (NH bend), 1216, 1057; ^{1}H NMR (600 MHz, $CDCl_3$) δ = 1.27 [t, J = 7.2 Hz, 3H, $NCH_2CO_2CH_2CH_3$], 1.29 [t, J = 7.2 Hz, 3H, $C(3)CO_2CH_2CH_3$], 2.31 (s, 3H, $ArCH_3$), 4.24 [q, J = 7.1 Hz, 2H, $NCH_2CO_2CH_2$], 4.36 [q, J = 7.1 Hz, 2H, $C(3)CO_2CH_2$], 5.58 (s, 2H, NCH_2CO), 7.11 (d. J = 8.4 Hz, 2H, ArH), 7.16–7.23 (m, 3H, ArH), 7.24–7.30 (m, 2H, ArH), 7.35 (d, J = 8.4 Hz, ArH), 10.04 (br s, 1H, NH amide) ppm; ^{13}C NMR (150.9 MHz, $CDCl_3$) δ = 14.0 (CH_3, one of $C(3)CO_2CH_2CH_3$ or $NCH_2CO_2CH_2CH_3$), 14.1 (CH_3, one of $C(3)CO_2CH_2CH_3$ or $NCH_2CO_2CH_2CH_3$), 20.8 (CH_3, $ArCH_3$), 55.8 (CH_2, NCH_2CO), 61.5 [CH_2, $C(3)CO_2CH_2$], 61.9 [CH_2, $NCH_2CO_2CH_2$], 110.3 [C, C(4)], 120.5 (CH, CH_{Ar}), 126.8 (CH, CH_{Ar}), 127.0 (CH, CH_{Ar}), 129.4 (CH, CH_{Ar}), 129.5 (CH, CH_{Ar}), 134.2 (C, $C_{Ar(q)}$), 134.6 (C, $C_{Ar(q)}$), 134.9 (C, $C_{Ar(q)}$), 138.8 [C, C(5)], 144.6 [C, C(3)], 155.9 (C, C=O amide), 160.4

© 2019 Wiley-VCH Verlag GmbH & Co. KGaA, Weinheim

[C, C(3)*C*=O], 167.0 [C, NCH_2*C*=O] ppm; ^{1}H NMR (600 MHz, DMSO-d_6) δ = 1.14 [t, *J* = 7.1 Hz, 3H, $NCH_2CO_2CH_2CH_3$], 1.17 [t, *J* = 7.1 Hz, 3H, $C(3)CO_2CH_2CH_3$], 2.26 (s, 3H, $ArCH_3$), 4.15 [q, *J* = 7.1 Hz, 2H, $NCH_2CO_2CH_2$], 4.19 [q, *J* = 7.1 Hz, 2H, $C(3)CO_2CH_2$], 5.40 (s, 2H, NCH_2CO), 6.96–7.27 (m, 7H, ArH), 7.47–7.50 (m, 2H, ArH), 10.56 (s, 1H, NH amide) ppm; ^{13}C NMR (150.9 MHz, DMSO-d_6) δ = 13.88 [CH_3, $NCH_2CO_2CH_2CH_3$], 13.90 [t, *J* = 7.1 Hz, 3H, $C(3)CO_2CH_2CH_3$], 20.5 (CH_3, $ArCH_3$), 53.6 (CH_2, NCH_2CO), 60.8 [CH_2, $C(3)CO_2CH_2$], 61.5 [CH_2, $NCH_2CO_2CH_2$], 110.7 [C, C(4)], 119.9 (CH, CH_{Ar}), 125.9 (CH, CH_{Ar}), 126.6 (CH, CH_{Ar}), 129.1 (CH, CH_{Ar}), 129.2 (CH, CH_{Ar}), 133.7 (C, $C_{Ar(q)}$), 135.3 (C, $C_{Ar(q)}$), 136.9 (C, $C_{Ar(q)}$), 142.4 (C, C(5)], 143.2 (C, C(3)], 156.1 (C, C=O amide), 160.2 [C, C(3)*C*=O], 167.0 [C, NCH_2*C*=O] ppm; ^{1}H NMR (600 MHz, toluene-d_8) δ = 0.87 [t, *J* = 7.1 Hz, 3H, $NCH_2CO_2CH_2CH_3$], 0.97 [t, *J* = 7.1 Hz, 3H, $C(3)CO_2CH_2CH_3$], 2.02 (s, 3H, $ArCH_3$), 3.86 [q, *J* = 7.1 Hz, 2H, $NCH_2CO_2CH_2$], 4.05 [q, *J* = 7.1 Hz, 2H, $C(3)CO_2CH_2$], 5.31 (s, 2H, NCH_2CO), 6.72–6.77 (m, 1H, ArH), 6.79–6.86 (m, 4H, ArH), 7.15–7.19 (m, 2H, ArH), 7.44–7.49 (m, 2H, ArH), 10.09 (s, 1H, NH amide) ppm; ^{13}C NMR (150.9 MHz, toluene-d_8) δ = 13.9 [CH_3, $NCH_2CO_2CH_2CH_3$], 14.1 [CH_3, $C(3)CO_2CH_2CH_3$], 20.7 (CH_3, overlapping with residual toluene-d_8 signal, $ArCH_3$), 55.9 (CH_2, NCH_2CO), 60.9 [CH_2, $C(3)CO_2CH_2$], 61.5 [CH_2, $NCH_2CO_2CH_2$], 110.6 [C, C(4)], 120.2 (CH, CH_{Ar}), 126.8 (CH, CH_{Ar}), 127.6 (CH, CH_{Ar}), 129.5 (CH, CH_{Ar}), 129.8 (CH, CH_{Ar}), 134.3 (C, $C_{Ar(q)}$), 135.5 (C, $C_{Ar(q)}$), 135.7 (C, $C_{Ar(q)}$), 138.8 [C, C(5)], 145.2 [C, C(3)], 156.2 (C, C=O amide), 160.6 [C, C(3)*C*=O], 167.0 [C, NCH_2*C*=O] ppm; HRMS (ES$^+$): Exact mass calculated for $C_{24}H_{25}N_3O_5S$ [M + H]$^+$ 468.1588, found 468.1583; m/z (ES$^+$) 468.2 {[($C_{24}H_{25}N_3O_5S$) + H$^+$], 68 %}, 721.1 (100 %).

Note: The title compounds **11a** and **12a** were also isolated as by-products in the [3+2]-dipolar cycloaddition of α-thio-β-chloroacrylamide **8a** and ethyl diazoacetate, through competing N–H insertion. Spectroscopic data are consistent with that outlined previously.

Compounds **17a–c and 18a–b** were similarly prepared, see supplementary information for characterisation data.

General Procedure for the Selective Oxidation of Pyrazoles 10

Ethyl 4-(Phenylsulfinyl)-5-(4′-methylphenylcarbamoyl)-1*H*-pyrazole-3-carboxylate (19a): *m*CPBA (35 mg, 0.2 mmol, 100 %) was added in one portion to a stirring solution of 4-(phenylthio)-5-(4′-methylphenylcarbamoyl)-1*H*-pyrazole-3-carboxylate **10a** (40 mg, 0.1 mmol) in dichloromethane (10 mL) at room temperature. After stirring overnight sodium thiosulfate (10 mL, 10 % w/v) was added and the layers were separated. The organic layer was washed with sodium thiosulfate (2 x 10 mL, 10 % w/v), sat. sodium bicarbonate (3 × 10 mL) and brine, dried with magnesium sulfate and concentrated under reduced pressure to give the crude product as a white solid. ^{1}H NMR analysis of the crude product indicated complete consumption of the starting material with evidence for both the sulfoxide **19a** and sulfone **16a** present (approx. 85:15). Purification by column chromatography using hexane/ethyl acetate as eluent (gradient elution 20–30 % ethyl acetate) gave sulfoxide **19a** as a white solid (26 mg, 66 %); m.p. 187–189 °C; ν_{max}/cm^{-1} (ATR) 3096 (NH stretch), 2994 (CH), 2918 (CH), 1699 (C=O ester), 1669 (C=O amide), 1235, 1029 (S=O), 980; ^{1}H NMR (300 MHz, $CDCl_3$) δ = 1.43 (t, *J* = 7.1 Hz, 3H, OCH_2CH_3), 2.34 (s, 3H, $ArCH_3$), 4.36–4.57 (m, 2H, OCH_2CH_3), 7.18 (d, *J* = 8.1 Hz, 2H, ArH), 7.37–7.51 (m, 3H, ArH), 7.63–7.83 (m, 4H, ArH), 12.36 (br s, 1H, NH amide), 12.79 (br s, 1H, NH pyrazole) ppm; ^{13}C NMR (75.5 MHz, $CDCl_3$) δ = 14.2 (CH_3, OCH_2CH_3), 21.0 (CH_3, $ArCH_3$), 62.3 (CH_2, OCH_2CH_3), 120.3 (CH, CH_{Ar}), 124.1 [C, C(4)], 125.1 (CH, CH_{Ar}), 129.6 (CH, 2 overlapping CH_{Ar} signals), 131.7 (CH, CH_{Ar}), 134.8 (C, $C_{Ar(q)}$) 135.1 (C, $C_{Ar(q)}$), 139.6 [C, one of C(3) or C(5)], 142.8 [C, one of C(3) or C(5)], 143.4 (C, $C_{Ar(q)}$), 154.8 (C, C=O amide), 161.2 (C, C=O ester) ppm; HRMS (ES$^+$): Exact mass calculated for $C_{20}H_{19}N_3O_4S$ [M + H]$^+$ 398.1169, found 398.1183.

Compounds **16a**, **16e** and **19b** were similarly prepared, see supplementary information for characterisation data.

4-(Phenylthio)-5-(4-methylphenylcarbamoyl)-1*H*-pyrazole-3-carboxylic Acid (20): Sodium hydroxide (97 mg, 2.43 mmol) in water (15 mL) was added in one portion to a stirring solution of ethyl 4-(phenylthio)-5-(4′-methylphenylcarbamoyl)-1*H*-pyrazole-3-carboxylate **10a** (232 mg, 0.61 mmol) in methanol (5 mL) at room temperature. The heterogeneous reaction mixture was heated to reflux at which point the reaction mixture became homogeneous, and was stirred at this temperature overnight. The reaction mixture was concentrated under reduced pressure to dryness. Water (15 mL) and ethyl acetate (15 mL) was added, and the layers separated. Concentrated HCl was added until a pH of 2 was achieved, which caused the carboxylic acid **20** to precipitate out of solution. Ethyl acetate (15 mL) was added and the layers separated. The aqueous layer was further extracted with ethyl acetate (2 × 15 mL). The combined organic layers were washed with brine (15 mL), dried, and concentrated under reduced pressure to give the pure pyrazole **20** (195 mg, 91 %) as a white solid; m.p. 226–229 °C; ν_{max}/cm^{-1} (ATR) 3126 (OH stretch), 3025 (NH), 2953 (CH), 1690 (C=O carboxylic acid), 1648 (C=O amide), 1606, 1474, 1235; ^{1}H NMR (300 MHz, DMSO-d_6) δ = 2.26 (s, 3H, $ArCH_3$), 3.40 (br s, 1H, COOH), 7.04–7.30 (m, 7H, ArH), 7.55 (d, *J* = 8.1 Hz, 2H, ArH), 10.18 (s, 1H, NH amide), 14.64 (br s, 1H, NH pyrazole) ppm; ^{1}H NMR (600 MHz, DMSO-d_6) δ = 2.25 (s, 3H, $ArCH_3$), 3.38 (br s, 1H, COOH), 7.02–7.28 (m, 7H, ArH), 7.46–7.64 (d, *J* = 8.1 Hz, 2H, ArH), 10.20 (s, 1H, NH amide), 14.67 (br s, 1H, NH pyrazole) ppm; ^{13}C NMR (600 MHz, DMSO-d_6) δ = 20.9 (CH_3, $ArCH_3$), 110.8 [C, C(4)], 120.3 (CH, CH_{Ar}), 125.7 (CH, CH_{Ar}), 126.9 (CH, CH_{Ar}), 129.3 (CH, CH_{Ar}), 129.5 (CH, CH_{Ar}), 133.1 (C, $C_{Ar(q)}$), 136.5 (C, $C_{Ar(q)}$), 138.0 (C, $C_{Ar(q)}$), 150.2 (C, C=O carboxylic acid), 159.7 (C, C=O amide) ppm; HRMS (ES$^+$): Exact mass calculated for $C_{18}H_{15}N_3O_3S$ [M + H]$^+$ 354.0907, found 354.0901.

Note: C(3) and C(5) not observed at 600 MHz

***N*^{3}-(4′-Methoxyphenyl)-4-(phenylthio)-*N*^{5}-(4′-methylphenyl)-1*H*-pyrazole-3,5-dicarboxamide (21):** 4-Dimethylaminopyridine (7 mg, 0.06 mmol) and *p*-anisidine (150 mg, 1.22 mmol) were added to a stirring solution of 4-(phenylthio)-5-(4-methylphenylcarbamoyl)-1*H*-pyrazole-3-carboxylic acid **20** (195 mg, 0.55 mmol) in dichloromethane (25 mL) at 0 °C. The solution was stirred at this temperature for 2 minutes at which point *N*′,*N*′-diisopropylcarbodiimide (105 mg, 0.83 mmol) was added in dichloromethane (5 mL). The reaction mixture was immediately heated to reflux and was stirred at this temperature for 12 h. The cooled reaction mixture was washed with water (30 mL) and the layers separated. The organic layer was washed with 2 M hydrochloric acid (2 × 30 mL) and brine (30 mL), dried, and concentrated under reduced pressure to give the crude product as a grey/brown solid. Purification by recrystallistation using ethyl acetate/heptane gave the pure product as a grey solid (162 mg, 64 %); m.p. 237–239 °C; ν_{max}/cm^{-1} (ATR) 3211 (NH stretch), 2917 (CH), 1682, (C=O amide), 1666 (C=O amide), 1320, 1161; ^{1}H NMR (300 MHz, DMSO-d_6) δ = 2.26 (s, 3H, $ArCH_3$), 3.73 (s, 3H, $ArOCH_3$), 6.58–7.87 (m, 13H, ArH), 10.18 (s, 1H, NH amide), 10.22 (s, 1H, NH amide),14.67 (br s, NH pyrazole) ppm; ^{1}H NMR (600 MHz, [D$_6$]DMSO) δ = 2.27 (s, 3H, $ArCH_3$), 3.73 (s, 3H, $ArOCH_3$), 6.62–7.90 (m, 13H, ArH), 10.22 (s, 1H, NH amide), 10.26 (s, 1H, NH amide), 14.70 (br s, 1H, NH pyrazole) ppm; ^{13}C NMR (150.9 MHz, DMSO-d_6) δ = 20.5 (CH_3, $ArCH_3$), 55.2 (CH_3, $ArOCH_3$), 106.5 [C, C(4)], 113.9 (CH, CH_{Ar}), 119.9 (CH, CH_{Ar}), 121.4 (CH, CH_{Ar}), 125.8 (CH, CH_{Ar}), 126.7 (CH, CH_{Ar}), 129.1 (CH, CH_{Ar}), 129.2 (CH, CH_{Ar}), 131.3 (C, br, $C_{Ar(q)}$), 133.1 (C, br, $C_{Ar(q)}$), 135.7 (C, br, $C_{Ar(q)}$), 136.9 (C, $C_{Ar(q)}$), 142.2 [C, br, one of C(3) or C(5)], 148.0 [C, br, one of C(3) or C(5)], 155.8 (C, $C_{Ar(q)}$OMe), 157.6 (C, br, overlapping C=O amides) ppm; HRMS (ES$^+$): Exact mass calculated for $C_{25}H_{22}N_4O_3S$ [M + H]$^+$ 459.1485, found 459.1486.

© 2019 Wiley-VCH Verlag GmbH & Co. KGaA, Weinheim

CCDC 1906490 (for pyrazole **16a**), 1906489 (for **11a**) contain the supplementary crystallographic data for this paper. These data can be obtained free of charge from The Cambridge Crystallographic Data Centre.

Acknowledgments

Financial support from the Synthesis and Solid State Pharmaceutical Centre supported by Science Foundation Ireland, co-funded under the European Regional Development Fund (grant number: 12/RC/2275) and with use of equipment provided by Science Foundation Ireland through a research infrastructure award for process flow spectroscopy (Prospect) (grant number: SFI 15/RI/3221) are gratefully acknowledged. The authors would like to acknowledge Dr. Denis Lynch for enabling access to ProSpect.

Keywords: [3+2]-Dipolar cycloaddition · Sulfonyl migration · Pyrazole · Tautomers · α-Thio-β-chloroacrylamide

[1] a) J. A. Joule, K. Mills in *Heterocyclic Chemistry*, John Wiley & Sons, **2010**; b) Z. Časar in *Synthesis of Heterocycles in Contemporary Medicinal Chemistry*, Springer International Publishing, **2016**.
[2] a) A. Ansari, A. Ali, M. Asif, Shamsuzzaman, *New J. Chem.* **2017**, *41*, 16–41; b) M. J. Naim, O. Alam, F. Nawaz, M. J. Alam, P. Alam, *J. Pharm. Bioallied Sci.* **2016**, *8*, 2–17; c) S. Andreas, D. Andrij, *Curr. Org. Chem.* **2011**, *15*, 1423–1463; d) V. Kumar, K. Kaur, G. K. Gupta, A. K. Sharma, *Eur. J. Med. Chem.* **2013**, *69*, 735–753; e) L. Yet, in *Comprehensive Heterocyclic Chemsitry* III (Eds.: A. R. Katritzky, C. A. Ramsden, E. F. V. Scriven, R. J. K. Taylor), Elsevier, Oxford, **2008**, pp. 1–141.
[3] T. D. Penning, J. J. Talley, S. R. Bertenshaw, J. S. Carter, P. W. Collins, S. Doctor, M. J. Graneto, L. F. Lee, J. W. Malecha, J. M. Miyashiro, R. S. Rogers, D. J. Rogier, S. S. Yu, G. D. Anderson, E. G. Burton, J. N. Cogburn, S. A. Gregory, C. M. Koboldt, W. E. Perkins, K. Seibert, A. W. Veenhuizen, Y. Y. Zhang, P. C. Isakson, *J. Med. Chem.* **1997**, *40*, 1347–1365.
[4] a) M. E. Y. Francisco, H. H. Seltzman, A. F. Gilliam, R. A. Mitchell, S. L. Rider, R. G. Petwee, L. A. Stevenso, B. F. Thomas, *J. Med. Chem.* **2002**, *45*, 2708–2719; b) M. Rinaldi-Carmona, *FEBS Lett.* **1994**, *350*, 240–244.
[5] A. Aajoud, P. Ravanel, M. Tissut, *J. Agric. Food Chem.* **2003**, *51*, 1347–1352.
[6] P. Krishnappa, E. Fernandez-Pascual, J. Carballido, J. I. Martinez-Salamanca, *Int. J. Impotence Res.* **2019**, *31*, 65–70.
[7] J. König, in *Colour Additives for Foods and Beverages* (Ed.: M. J. Scotter), Woodhead Publishing, Oxford, **2015**, pp. 35–60.
[8] S. Fustero, A. Simón-Fuentes, J. F. Sanz-Cervera, *Org. Prep. Proced. Int.* **2009**, *41*, 253–290.
[9] Y. H. Kao, C. H. Chong, W. T. Ng, D. Lim, *Occup. Med.* **2007**, *57*, 535–537.
[10] R. Huisgen, in *1,3-Dipolar cycloaddition chemistry* (Ed.: A. Padwa), John Wiley and Sons, New York, **1984**.
[11] a) T. L. Gilchrist, R. C. Storr, *Organic Reactions and Orbital Symmetry*, Cambridge University Press, **1972**; b) S. D. Andrews, A. C. Day, A. N. McDonald, *J. Chem. Soc., C* **1969**, 787–790; c) M. Kissane, A. R. Maguire, *Chem. Soc. Rev.* **2010**, *39*, 845–883.
[12] a) N. S. Goulioukina, N. N. Makukhin, E. D. Shinkarev, Y. K. Grishin, V. A. Roznyatovsky, I. P. Beletskaya, *Org. Biomol. Chem.* **2016**, *14*, 10000–10010; b) K. M. J. Cheung, J. Reynisson, E. McDonald, *Tetrahedron Lett.* **2010**, *51*, 5915–5918.
[13] a) S. He, L. Chen, Y.-N. Niu, L.-Y. Wu, Y.-M. Liang, *Tetrahedron Lett.* **2009**, *50*, 2443–2445; b) T. Kano, T. Hashimoto, K. Maruoka, *J. Am. Chem. Soc.* **2006**, *128*, 2174–2175; c) P. Radha Krishna, E. Raja Sekhar, *Tetrahedron Lett.* **2008**, *49*, 6733–6936.
[14] J.-W. Xie, Z. Wang, W.-J. Yang, L.-C. Kong, D.-C. Xu, *Org. Biomol. Chem.* **2009**, *7*, 4352–4354.
[15] M. Kissane, M. Murphy, D. Lynch, A. Ford, A. R. Maguire, *Tetrahedron* **2008**, *64*, 7639–7649.
[16] M. Kissane, D. Lynch, J. Chopra, S. E. Lawrence, A. R. Maguire, *Tetrahedron: Asymmetry* **2008**, *19*, 1256–1273.
[17] M. Kissane, M. Murphy, E. O'Brien, J. Chopra, L. Murphy, S. G. Collins, S. E. Lawrence, A. R. Maguire, *Org. Biomol. Chem.* **2011**, *9*, 2452–2472.
[18] M. Kissane, D. Lynch, J. Chopra, S. E. Lawrence, A. R. Maguire, *Org. Biomol. Chem.* **2010**, *8*, 5602–5613.
[19] M. Kissane, S. E. Lawrence, A. R. Maguire, *Org. Biomol. Chem.* **2010**, *8*, 2735–2748.
[20] O. C. Dennehy, V. M. Y. Cacheux, B. J. Deadman, D. Lynch, S. G. Collins, H. A. Moynihan, A. R. Maguire, *Beilstein J. Org. Chem.* **2016**, *12*, 2511–2522.
[21] M. Murphy, D. Lynch, M. Schaeffer, M. Kissane, J. Chopra, E. O'Brien, A. Ford, G. Ferguson, A. R. Maguire, *Org. Biomol. Chem.* **2007**, *5*, 1228–1241.
[22] I. Fleming, *Frontier Orbitals and Organic Chemical Reactions*, Wiley-Interscience, London, **1976**.
[23] B. Abeykoon, T. Devic, J.-M. Grenèche, A. Fateeva, A. B. Sorokin, *Chem. Commun.* **2018**, *54*, 10308–10311.
[24] D. Sahu, S. Dey, T. Pathak, B. Ganguly, *Org. Lett.* **2014**, *16*, 2100–2103.
[25] a) R. Kumar, D. Nair, I. N. N. Namboothiri, *Tetrahedron* **2014**, *70*, 1794–1799; b) T. V. Baiju, *Chem. Rec.* **2017**, *17*, 939–955.
[26] M. H. Nantz, P. L. Fuchs, *J. Org. Chem.* **1987**, *52*, 5298–5299.
[27] M. C. Pérez-Aguilar, *Angew. Chem. Int. Ed.* **2015**, *54*, 13729–13733; *Angew. Chem.* **2015**, *127*, 13933.
[28] A. C. Cope, D. E. Morrison, L. Field, *J. Am. Chem. Soc.* **1950**, *72*, 59–67.
[29] D. Pinto, C. Santos, A. Silva, *8 Advanced NMR techniques for structural characterization of heterocyclic structures*, Vol. 37661, **2007**.
[30] a) A. Huang, K. Wo, S. Y. C. Lee, N. Kneitschel, J. Chang, K. Zhu, T. Mello, L. Bancroft, N. J. Norman, S.-L. Zheng, *J. Org. Chem.* **2017**, *82*, 8864–8872; b) B. A. Trofimov, *Sulf. Rep.* **1992**, *11*, 207–227; c) N. M. Vitkovskaya, E. Y. Larionova, A. D. Skitnevskaya, V. B. Kobychev, B. A. Trofimov, *Russ. Chem. Bull.* **2013**, *62*, 26–32.
[31] *APEX2 v2009.3–0*; Bruker AXS, Inc.: Madison, WI, **2009**.
[32] G. M. Sheldrick, *Acta Crystallogr., Sect. C: Struct. Chem.* **2015**, *71*, 3–8.
[33] C. F. Macrae, I. J. Bruno, J. A. Chisholm, P. R. Edgington, P. McCabe, E. Pidcock, L. Rodriguez-Monge, R. Taylor, J. van de Streek, P. A. Wood, *J. Appl. Crystallogr.* **2008**, *41*, 466–470.
[34] V. K. Aggarwal, Z. Gültekin, R. S. Grainger, H. Adams, P. L. Spargo, *J. Chem. Soc., Perkin Trans. 1* **1998**, 2771–2782.

Received: April 1, 2019

 © 2019 Wiley-VCH Verlag GmbH & Co. KGaA, Weinheim

JOC The Journal of Organic Chemistry

pubs.acs.org/joc Note

Localized Partitioning of Enantiomers in Solid Samples of Sulfoxides: Importance of Sampling Method in Determination of Enantiopurity

Aaran J. Flynn, Alan Ford, and Anita R. Maguire*

Cite This: J. Org. Chem. 2020, 85, 10216−10221 Read Online

ACCESS | Metrics & More | Article Recommendations | Supporting Information

ABSTRACT: Localized partitioning of amorphous enantioenriched aryl benzyl sulfoxides in the solid state can lead to substantial variation in enantiopurities, even for sulfoxides which do not show detectable levels of self-disproportionation of enantiomers (SDE) during chromatography on an achiral stationary phase. The importance of preparation of representative samples of enantioenriched sulfoxides for chiral HPLC to enable reproducible results is clear.

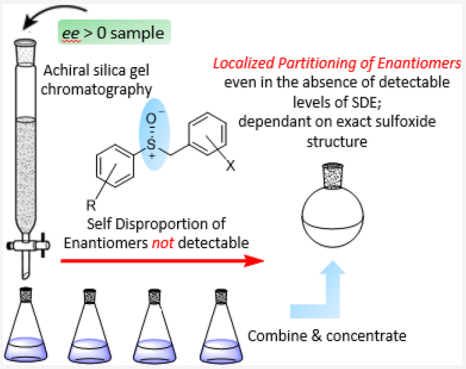

Downloaded via UNIV COLG CORK on January 24, 2021 at 18:55:13 (UTC).
See https://pubs.acs.org/sharingguidelines for options on how to legitimately share published articles.

Enantioenriched sulfoxides have attracted considerable interest in the field of asymmetric synthesis largely due to their importance as chiral auxiliaries or as synthetic intermediates with wide ranging applications. The sulfoxide moiety has been demonstrated to be an efficient chiral auxiliary in carbon−carbon and carbon−oxygen bond forming reactions, in asymmetric catalysis, in radical addition reactions, in Michael reactions, and in cycloaddition reactions.[1−8] The ability of the sulfoxide moiety to promote such reactions is explained in terms of the structural features inherent to the sulfinyl group. Not only does the sulfinyl group possess a high configurational stability, but there can be significant steric and stereoelectronic differences between the inequivalent organic substituents at the sulfur atom.

In addition to uses in synthetic methodology, enantiopure sulfoxides have also gained significance in the pharmaceutical industry due to their important biological activity. One of the most successful sulfoxide-containing APIs is Astra Zeneca's esomeprazole, a gastric acid secretion inhibitor, commercialized as Nexium. Esomeprazole is the (S)-enantiomer of omeprazole, its racemic predecessor.

Synthesis of enantioenriched sulfoxides is undertaken primarily employing two principal strategies, nucleophilic displacement from sulfinate precursors[9] and asymmetric sulfoxidation of prochiral sulfides mediated by transition metal catalysts.[1,10−13] Extensive reports of asymmetric sulfur oxidation have appeared over the past 30 years since the seminal reports from Kagan[14,15] and Modena[16] utilizing titanium mediated oxidation.

Central to these reports are the methods exploited for the determination of enantiopurity of the resulting sulfoxides. Chiral HPLC, whereby a chiral stationary phase is used to generate diasteromeric interactions between the analyte and the stationary phase, is the method of choice since its emergence as a more accurate and reproducible descriptor of enantiopurity when compared with other analytical techniques such as ^{1}H NMR analysis using a chiral shift reagent or measurement of optical rotation.

Of particular interest were the seminal reports of the self-disproportionation of enantiomers (SDE) for enantioenriched sulfoxides by chromatography on an achiral phase as reported by Kagan and co-workers in 1994.[17,18] Self-disproportionation of enantiomers in fractional crystallization of solids is well-known, leading to formation of racemates and/or conglomerates, depending on the structure of a compound.[19] Indeed our reports on the solid state properties of sulfoxides highlight that for benzyl *p*-tolyl sulfoxide spontaneous resolution occurs to form enantiopure crystals of the conglomerate even when a racemic synthesis is undertaken, a property not seen with other aryl benzyl sulfoxides.[20] Observation of this spontaneous

Received: May 5, 2020
Published: July 2, 2020

ACS Publications © 2020 American Chemical Society

Table 1. Investigation of Peroxide Loading and HPLC Sampling Method

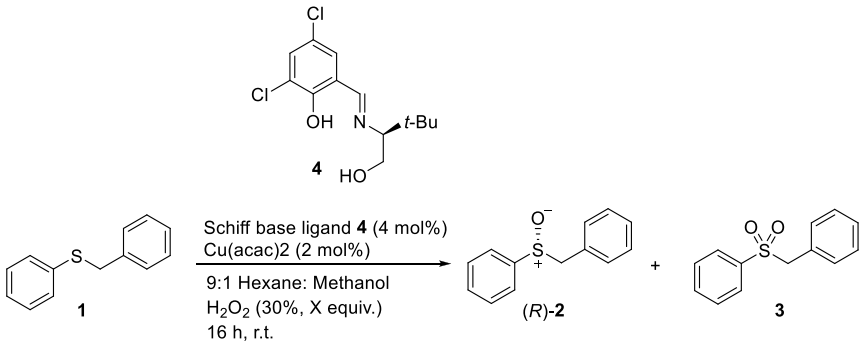

entry	X equiv of 30% H_2O_2	1:2:3[a]	% ee (R)-[2][b] solid sample 1[c]	solid sample 2[c]	solid sample 3[c]	representative sample[d]	% yield [2][e]
1	1.1	56:44:0	N/A	N/A	N/A	52	29
2	1.3	6:93:1	62	62	67	56	74
3	1.5	1:98:1	79	73	60	57	75
4	1.7	4:95:1	65	61	63	56	75
5	1.9	3:96:1	70	66	64	56	70
6	2.1	10:89:1	61	60	60	58	57

[a]Ratio of **1**:**2**:**3** determined from the ^{1}H NMR spectrum of the crude product. [b]Determined by HPLC analysis on chiral column (Chiralcel OD-H); absolute configuration determined by comparison of HPLC elution order to literature values. [c]Solid sample obtained by taking a random 3 mg of amorphous sulfoxide product and dissolving in 3 mL of HPLC grade methanol. [d]Representative sample obtained by dissolving the entirety of recovered sulfoxide post chromatography. [e]After purification by column chromatography.

resolution is notable, as it is believed that at most only 5−10% of crystalline racemates form conglomerates.

Our group has previously reported on the copper mediated asymmetric oxidation of aryl benzyl sulfides to the corresponding sulfoxides, with enantioselectivities of up to 97% ee achieved through ligand and substrate optimization.[21,22] During investigation of the further scope of this transformation, challenges were encountered in relation to the reproducibility of the enantioselectivities with variable outcomes in the oxidation of certain substrates. Furthermore, it is evident that the efficiency of the oxidation is very sensitive to variation in the reaction temperature.

One of our initial aims was to optimize the peroxide loading in order to maximize sulfide consumption while keeping the overoxidation product, the sulfone, to a minimum. Therefore, the oxidation of benzyl phenyl sulfide **1** was examined using varying equivalents of hydrogen peroxide (30%) using our previously reported optimized conditions (Table 1). Previous work in the group demonstrated that the optimized conditions required Schiff base ligand **4** in conjunction with copper(II) acetylacetonate and a heterogeneous solvent system of hexane and methanol.

We found that the use of 1.5 equiv of H_2O_2 was necessary to ensure complete consumption of the sulfide (entry **3**), and while the use of more oxidant did not lead to any increase in sulfone formation, the conversion to sulfoxide was hampered, presumably due to degradation of the catalyst (entries **4**−**6**).

During optimization studies exploring the impact of the number of equivalents of H_2O_2, we encountered some challenges in reproducibility of enantioselectivities for certain sulfur oxidations; therefore, we looked in more detail at the HPLC sampling method used in conjunction with this work. Irrespective of peroxide loading, the enantioselectivity of the copper Schiff base catalyzed sulfoxidation was reproducibly in the range of 52−58%, so long as the entirety of the recovered enantioenriched sulfoxide post chromatography was dissolved prior to dilution for chiral HPLC analysis; however, if instead of dissolving the complete sample recovered from chromatography, a portion of the noncrystalline solid material is extracted from the collection flask then the ee determined by chiral HPLC varies from the representative value.

It is well established that the self-disproportionation of enantiomers (SDE) of sulfoxides is frequently observed during achiral chromatography,[10,23−28] and accordingly it is essential that representative samples are utilized for determination of enantiopurity to avoid errors in determination of % ee in individual samples. However, investigation of the enantiopurity of fractions of enantioenriched benzyl phenyl sulfoxide **2** recovered from chromatography did not display any evidence of SDE with this compound (Table 2).

It is clear that with sulfoxides, in addition to the possibility of SDE occurring during column chromatography, sampling of apparently amorphous solid samples of enantioenriched sulfoxides can produce samples with varying enantiopurity, and accordingly extreme care must be taken when sampling solid sulfoxides even in cases where apparently homogeneous noncrystalline samples are recovered through evaporation of solutions. Thus, it would seem that we are seeing an example of localized partitioning in the solid state of amorphous solids, even in the absence of (1) crystallization and (2) detectable levels of self-disproportionation of enantiomers via achiral chromatography.

Having identified the variation in ee values for enantioenriched (*R*)-benzyl phenyl sulfoxide as summarized in Table 1, it was initially thought that the variation may be consistent across a range of enantioenriched substituted aryl benzyl sulfoxides exhibiting amorphous morphology following evaporation of eluent after chromatography. To gain a better understanding of the extent of this phenomenon, a further five

https://dx.doi.org/10.1021/acs.joc.0c01094
J. Org. Chem. 2020, 85, 10216−10221

Table 2. Investigation of Self-Disproportionation of Enantiomers for Enantioenriched (*R*)-Benzyl Phenyl Sulfoxide

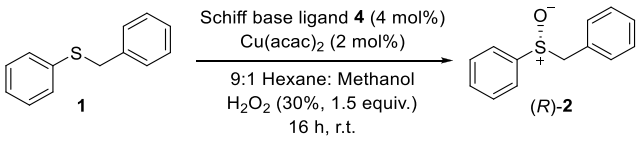

fraction number post column chromatography[a]	% product 2 recovered[b]	% ee (*R*)-2[c]
1	7	58
2	26	57
3	30	58
4	17	58
5	6	59
6	2	59
7	1	57

[a]Fraction obtained post purification by flash column chromatography on silica gel using hexane−ethyl acetate (60:40) as the eluent. At the 1 mmol scale, each fraction was collected in a 40 mL test tube. [b]Each fraction was concentrated under reduced pressure prior to being dissolved in HPLC grade methanol and diluted to give a HPLC sample with a concentration of 1 mg/mL. [c]Determined by HPLC analysis (Daicel Chiracel OD-H); absolute configuration determined by comparison of HPLC elution order to literature values.

enantioenriched sulfoxides were generated using our copper Schiff base methodology.

For each of the five substrates, the representative ee was measured by combining all fractions containing the recovered enantioenriched sulfoxide following chromatography, concentrating them to dryness under reduced pressure to give an amorphous solid and dissolving the entirety of the sample in HPLC grade methanol. Once dissolved, the representative sample was diluted accordingly to give a 1 mg/mL sample for chiral HPLC analysis. After analysis, the representative sample was restored to the original sample, which was again concentrated under reduced pressure to give the amorphous solid. From this reconcentrated residue, five individual 3 mg solid samples were randomly selected and each dissolved in 3 mL of HPLC grade methanol.

As can be seen in Table 3, the significant variation in enantioselectivity that was observed for enantioenriched benzyl phenyl sulfoxide **2** was not seen consistently across the series of aryl benzyl sulfoxides studied, and rather it would appear that the variation is strongly dependent on the exact substitution pattern and therefore the structure of the selected aryl benzyl sulfoxide. In the cases of sulfoxides **5** and **7**, the representative samples and solid samples withdrawn from the amorphous sulfoxide product provided essentially similar % ee data (entries 1 and 3). Sulfoxide **8** demonstrated a very minor increase in % ee when a solid sample was taken (entry 4). Sulfoxide **9** however demonstrated a somewhat variable decrease in enantiopurity when analyzing the solid samples (entry 5). Sulfoxide **6** gave essentially reproducible solid sample data; however, this ee value was approximately 10% greater than the representative enantiomeric excess of 37% (entry 2).

Thus, far, all HPLC sampling of the solid amorphous material had been carried out in a random manner, so that no indication could be made as to whether the partitioning of the solid state was occurring in an ordered predictable manner while evaporated under reduced pressure. Thus, enantioenriched 2-naphthyl benzyl sulfoxide **11** was generated using our copper Schiff base methodology to give a sample with 62% ee (entry 1, Table 4). As in previous instances, the representative sample was restored to the bulk sample, dissolved, and concentrated under reduced pressure in a 100 mL round-bottom flask. Solid amorphous material was collected from both the upper and lower parts of the flask to give a % ee of 59% and 73%, respectively (entries 2 and 3), indicating localized partitioning of the enantiomers of the sulfoxide throughout the evaporation process. Thus, the degree of partitioning is dependent on several factors which may include size of collection vessel post chromatography, choice of eluent system for chromatography, and relative rate of evaporation of solvents during solid acquisition post chromatography, in addition to the exact sulfoxide structure.

In conclusion, observation of localized partitioning of enantiomers in amorphous noncrystalline samples of sulfoxides even in the absence of detectable levels of self-disproportionation of enantiomers via chromatography on an achiral phase can be rationalized on the basis of the strong intermolecular noncovalent interactions in the solid state between R and S enantiomers of sulfoxides. Observation of this behavior with highly polar compounds such as sulfoxides, and moreover

Table 3. Comparison of Sampling Methods for Substituted Aryl Benzyl Sulfoxides

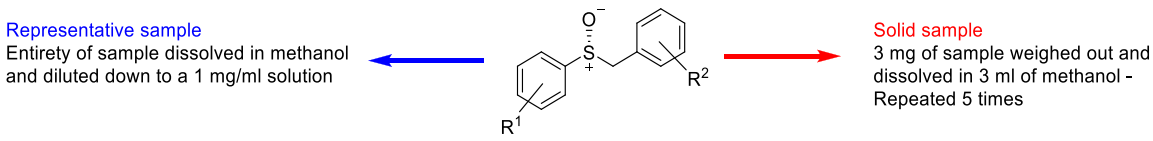

					solid sample[b]				
entry	sulfoxide[a]	R^1	R^2	representative % ee (*R*)[b]	% ee (*R*) sample **1**	% ee (*R*) sample **2**	% ee (*R*) sample **3**	% ee (*R*) sample **4**	% ee (*R*) sample **5**
1	**5**	3-Me		31	30	28	32	30	32
2	**6**	4-MeO		37	48	48	47	47	47
3	**7**	2-Me		71	72	71	72	71	70
4	**8**	4-Me		55	60	58	56	57	55
5	**9**		4-Cl	55	51	42	56	39	50

[a]Sulfoxides **5**−**9** were generated as per "Experimental Procedure for Asymmetric Sulfide Oxidation". [b]Determined by HPLC analysis (Chiralpak IB for sulfoxide **5**, Phenomenex Lux Amylose-1 for sulfoxides **6**−**9**). Absolute configuration determined by comparison of HPLC elution order to literature values.

https://dx.doi.org/10.1021/acs.joc.0c01094
J. Org. Chem. 2020, 85, 10216−10221

Table 4. HPLC Sampling of Enantioenriched (*R*)-2-Naphthyl Benzyl Sulfoxide

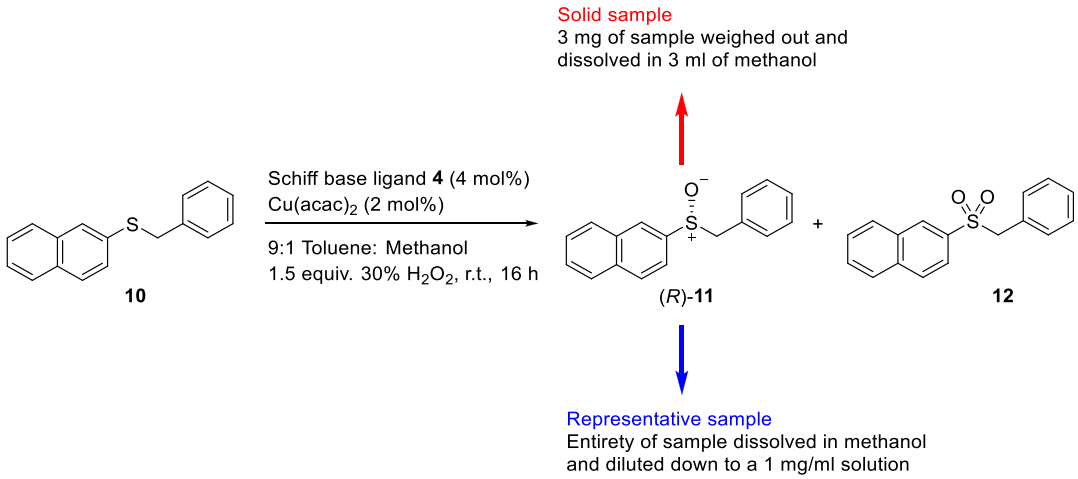

entry	HPLC sampling method used	part of 100 mL round-bottom flask sample taken from	% ee (*R*) **11**
1	representative sample	entirety	62
2	3 mg/mL solid sample	bottom	73
3	3 mg/mL solid sample	top	59

[a]Determined by HPLC analysis (Phenomenex Lux Amylose-1); absolute configuration determined by comparison of HPLC elution order to literature values.

considering the significant variation in the nature of the substituents on sulfur as opposed to stereogenic carbon, is arguably not surprising. According to Hunter's hydrogen-bond parameter table, sulfoxides are among the most potent hydrogen bond acceptors leading to strong intermolecular interactions in the solid state.[29] Accordingly, when conducting studies in asymmetric sulfoxidation, additional care should be taken to eliminate potential errors in the determination of enantiomeric excess not only via self-disproportionation of enantiomers in sulfoxide samples through chromatography but also through localized partitioning in the solid state, even in the absence of crystallization.

■ EXPERIMENTAL SECTION

General Procedures. All solvents were distilled prior to use by the following methods: methanol was distilled from magnesium methoxide and stored over 3 Å molecular sieves; toluene was distilled from sodium benzophenone ketyl; ethyl acetate was distilled from potassium carbonate; and hexane was distilled prior to use. All commercial reagents were used without further purification unless otherwise stated. Hydrogen peroxide was standardized by titration using potassium permanganate.

^{1}H (300 MHz) NMR spectra were recorded on a Bruker Avance 300 NMR spectrometer. All spectra were recorded at 300 K in deuterated chloroform ($CDCl_3$) using tetramethylsilane (TMS) as an internal standard. Chemical shifts (δ_H) are reported in parts per million (ppm) relative to TMS, and coupling constants are expressed in hertz (Hz). Splitting patterns in ^{1}H NMR spectra are designated as s (singlet), d (doublet), dd (doublet of doublets), and m (multiplet).

Flash column chromatography was carried out using Kieselgel silica gel 60, 0.035−0.075 mm (Merck). Thin-layer chromatography (TLC) was carried out on precoated silica gel plates (Merck 60 PF254). Visualization was achieved by UV (254 nm).

The enantiopurity of chiral compounds was measured using chiral stationary phase high-performance liquid chromatography (HPLC), carried out on either a Chiralcel OD-H, Phenomenex Lux Amylose-1, or a Chiralpak IB column. Details of the column conditions and mobile phase employed are included in the Experimental Section; data for the plots were extracted at 254 nm, at which wavelength all of the compounds exhibited good absorption. In all instances baseline resolution was obtained, and injection of racemic reference samples for each run confirmed the accuracy of the integration of the chromatograms, regardless of retention time.

HPLC analysis was performed on a Waters alliance 2695 separations module with a Waters alliance 2996 photodiode array detector. High-temperature chiral HPLC analysis was obtained using an Igloo column heater/cooler.

Experimental Procedure for Asymmetric Sulfide Oxidation. Copper(II) acetylacetonate (5.2 mg, 2.0 mol %) was added to a 25 mL round-bottom flask containing Schiff base ligand **4** (11.6 mg, 4.0 mol %) and 9:1 hexane (or toluene)/methanol (1 mL). The resulting mixture was stirred at r.t. for 5 min, and then a solution of sulfide (1 mmol) in 9:1 hexane (or toluene)/methanol (1 mL) was added. After a further 5 min of stirring at r.t., hydrogen peroxide (0.170 mL, 30%, 1.5 mmol) was added dropwise to the mixture. The reaction mixture was stirred at r.t. for a further 16 h. Water (10 mL) and dichloromethane (10 mL) were then added and the phases separated; the organic layer was washed with water (2 × 10 mL) and brine (10 mL), dried with $MgSO_4$, filtered, and concentrated under reduced pressure to give the crude product. The product was purified by flash column chromatography on silica gel (60:40 hexane:ethyl acetate) to afford the enantioenriched sulfoxide as an amorphous white solid. Each of sulfoxides **2**, **5**−**9**, and **11** were prepared and purified using these conditions.

(R)-(+)-Benzyl Phenyl Sulfoxide ***2*** *(Table 1, Entry 3).*[21,30] White solid (162 mg, 75%, 57% ee); ^{1}H NMR ($CDCl_3$, 300 MHz) 7.51−7.34 (m, 5H), 7.33−7.20 (m, 3H), 7.03−6.94 (m, 2H), 4.10 (d, 1H, J = 12.5 Hz), 3.99 (d, 1H, J = 12.5 Hz); HPLC: t_R (*R*) = 18.6 min, t_R (*S*) = 22.5 min [Chiralcel OD-H; flow rate 1 mL min^{-1}; hexane/2-PrOH (95:5); 40 °C].[31]

(R)-(+)-Benzyl m-Tolyl Sulfoxide ***5*** *(Table 3, Entry 1).*[21,32] White solid (199 mg, 86%, 31% ee); ^{1}H NMR ($CDCl_3$, 300 MHz) 7.33−7.11 (m, 7H), 7.04−6.94 (m, 2H), 4.05 (d, 1H, J = 12.5 Hz), 3.95 (d, 1H, J = 12.5 Hz), 2.32 (s, 3H); HPLC: t_R (*R*) = 23.1 min, t_R (*S*) = 25.6 min [Chiralpak IB; flow rate 0.5 mL min^{-1}; hexane/2-PrOH (90:10); 20 °C].

(R)-(+)-Benzyl p-Methoxy Sulfoxide ***6*** *(Table 3, Entry 2).*[22,33] White solid (143 mg, 58%, 37% ee); ^{1}H NMR ($CDCl_3$, 300 MHz) 7.35−7.18 (m, 5H), 7.03−6.86 (m, 4H), 4.10 (d, 1H, J = 12.4 Hz), 3.95 (d, 1H, J = 12.4 Hz), 3.82 (s, 3H); HPLC: t_R (*R*) = 49.7 min, t_R (*S*) = 54.4 min [Lux Amylose-1; flow rate 0.5 mL min^{-1}; hexane/2-PrOH (90:10); 20 °C].

https://dx.doi.org/10.1021/acs.joc.0c01094
J. Org. Chem. 2020, 85, 10216−10221

(R)-(+)-Benzyl o-Tolyl Sulfoxide ***7*** *(Table 3, Entry 3).*[21,34] White solid (174 mg, 76%, 71% ee); ^{1}H NMR ($CDCl_3$, 300 MHz) 7.74−7.66 (m, 1H), 7.37−7.16 (m, 5H), 7.13−7.06 (m, 1H), 7.00−6.92 (m, 2H), 4.07 (d, 1H, J = 12.6 Hz), 3.98 (d, 1H, J = 12.6 Hz), 2.06 (s, 3H); HPLC: t_R (R) = 24.3 min, t_R (S) = 26.9 min [Lux Amylose-1; flow rate 0.5 mL min^{-1}; hexane/2-PrOH (90:10); 20 °C].

(R)-(+)-Benzyl p-Tolyl Sulfoxide ***8*** *(Table 3, Entry 4).*[21,35] White solid (150 mg, 65%, 55% ee); ^{1}H NMR ($CDCl_3$, 300 MHz) 7.32−7.14 (m, 7H), 7.05−6.92 (m, 2H), 4.07 (d, 1H, J = 12.6 Hz), 3.96 (d, 1H, J = 12.6 Hz), 2.38 (s, 3H); HPLC: t_R (R) = 29.4 min, t_R (S) = 33.0 min [Lux Amylose-1; flow rate 0.5 mL min^{-1}; hexane/2-PrOH (90:10); 20 °C].

(R)-(+)-4-Chlorobenzyl Phenyl Sulfoxide ***9*** *(Table 3, Entry 5).*[22,33] White solid (88 mg, 35%, 55% ee); ^{1}H NMR ($CDCl_3$, 300 MHz) 7.52−7.32 (m, 5H), 7.25−7.18 (m, 2H), 6.94−6.84 (m, 2H), 4.02 (d, 1H, J = 12.8 Hz), 3.96 (d, 1H, J = 12.8 Hz); HPLC: t_R (S) = 68.4 min, t_R (R) = 70.9 min [Lux Amylose-1; flow rate 0.5 mL min^{-1}; hexane/2-PrOH (95:5); 20 °C].

(R)-(+)-2-Naphthyl Benzyl Sulfoxide ***11*** *(Table 4, Entry 1).*[22,33] White solid (186 mg, 70%, 62% ee); δ_H (300 MHz, $CDCl_3$) 7.93−7.78 (m, 4H), 7.62−7.51 (m, 2H), 7.41 (dd, 1H, J = 8.6, 1.8 Hz), 7.31−7.17 (m, 3H), 7.02−6.96 (m, 2H), 4.17 (d, 1H, J = 12.6 Hz), 4.08 (d, 1H, J = 12.6 Hz); HPLC: t_R (R) = 46.7 min, t_R (S) = 55.3 min [Lux Amylose-1; flow rate 0.5 mL min^{-1}; hexane/2-PrOH (90:10); 20 °C].

■ ASSOCIATED CONTENT

Supporting Information

The Supporting Information is available free of charge at https://pubs.acs.org/doi/10.1021/acs.joc.0c01094.

Copies of chiral-phase HPLC chromatographs for compounds **2**, **5**−**9**, and **11** (PDF)

■ AUTHOR INFORMATION

Corresponding Author

Anita R. Maguire − *School of Chemistry and School of Pharmacy, Analytical and Biological Chemistry Research Facility, Synthesis and Solid State Pharmaceutical Centre, University College Cork, Cork, Ireland;* orcid.org/0000-0001-8306-1893; Email: a.maguire@ucc.ie

Authors

Aaran J. Flynn − *School of Chemistry, Analytical and Biological Chemistry Research Facility, Synthesis and Solid State Pharmaceutical Centre, University College Cork, Cork, Ireland;* orcid.org/0000-0003-3115-9965

Alan Ford − *School of Chemistry, Analytical and Biological Chemistry Research Facility, University College Cork, Cork, Ireland;* orcid.org/0000-0002-4316-4350

Complete contact information is available at: https://pubs.acs.org/10.1021/acs.joc.0c01094

Notes

The authors declare no competing financial interest.

■ ACKNOWLEDGMENTS

Financial support from the Synthesis and Solid State Pharmaceutical Centre supported by Science Foundation Ireland, cofunded under the European Regional Development Fund (Grant Numbers 12/RC/2275 and 12/RC/2275_2), is gratefully acknowledged.

■ REFERENCES

(1) Fernández, I.; Khiar, N. Recent Developments in the Synthesis and Utilization of Chiral Sulfoxides. *Chem. Rev.* **2003**, *103* (9), 3651−3706.

(2) Otocka, S.; Kwiatkowska, M.; Madalińska, L.; Kiełbasiński, P. Chiral Organosulfur Ligands/Catalysts with a Stereogenic Sulfur Atom: Applications in Asymmetric Synthesis. *Chem. Rev.* **2017**, *117* (5), 4147−4181.

(3) Kaiser, D.; Klose, I.; Oost, R.; Neuhaus, J.; Maulide, N. Bond-Forming and -Breaking Reactions at Sulfur(IV): Sulfoxides, Sulfonium Salts, Sulfur Ylides, and Sulfinate Salts. *Chem. Rev.* **2019**, *119* (14), 8701−8780.

(4) Colomer, I.; Velado, M.; Fernández de la Pradilla, R.; Viso, A. From Allylic Sulfoxides to Allylic Sulfenates: Fifty Years of a Never-Ending [2,3]-Sigmatropic Rearrangement. *Chem. Rev.* **2017**, *117* (24), 14201−14243.

(5) Sipos, G.; Drinkel, E. E.; Dorta, R. The emergence of sulfoxides as efficient ligands in transition metal catalysis. *Chem. Soc. Rev.* **2015**, *44* (11), 3834−3860.

(6) Mellah, M.; Voituriez, A.; Schulz, E. Chiral Sulfur Ligands for Asymmetric Catalysis. *Chem. Rev.* **2007**, *107* (11), 5133−5209.

(7) Carmen Carreño, M.; Hernández-Torres, G.; Ribagorda, M.; Urbano, A. Enantiopure sulfoxides: recent applications in asymmetric synthesis. *Chem. Commun.* **2009**, No. 41, 6129−6144.

(8) Mikołajczyk, M.; Drabowicz, J.; Kiełbasiński, P. *Chiral Sulfur Reagents: Applications in Asymmetric and Stereoselective Synthesis*; CRC Press: Boca Raton, FL, 1997.

(9) Andersen, K. K.; Bujnicki, B.; Drabowicz, J.; Mikolajczyk, M.; O'Brien, J. B. Synthesis of enantiomerically pure alkyl and aryl methyl sulfoxides from cholesteryl methanesulfinates. *J. Org. Chem.* **1984**, *49* (21), 4070−4072.

(10) Han, J.; Soloshonok, V. A.; Klika, K. D.; Drabowicz, J.; Wzorek, A. Chiral sulfoxides: advances in asymmetric synthesis and problems with the accurate determination of the stereochemical outcome. *Chem. Soc. Rev.* **2018**, *47* (4), 1307−1350.

(11) Volcho, K. P.; Salakhutdinov, N. F. Asymmetric oxidation of sulfides catalyzed by titanium and vanadium complexes in the synthesis of biologically active sulfoxides. *Russ. Chem. Rev.* **2009**, *78* (5), 457−464.

(12) O'Mahony, G. E.; Ford, A.; Maguire, A. R. Asymmetric oxidation of sulfides. *J. Sulfur Chem.* **2013**, *34* (3), 301−341.

(13) Volcho, K. P. Recent Developments in the Catalytic Asymmetric Sulfoxidation Reactions. In *Frontiers of Green Catalytic Selective Oxidations. Green Chemistry and Sustainable Technology*; Bryliakov, K., Ed.; Springer: Singapore, 2019.

(14) Pitchen, P.; Dunach, E.; Deshmukh, M. N.; Kagan, H. B. An efficient asymmetric oxidation of sulfides to sulfoxides. *J. Am. Chem. Soc.* **1984**, *106* (26), 8188−8193.

(15) Pitchen, P.; Kagan, H. B. An efficient asymmetric oxidation of sulfides to sulfoxides. *Tetrahedron Lett.* **1984**, *25* (10), 1049−1052.

(16) Di Furia, F.; Modena, G.; Seraglia, R. Synthesis of Chiral Sulfoxides by Metal-Catalyzed Oxidation with t-Butyl Hydroperoxide. *Synthesis* **1984**, *1984* (04), 325−326.

(17) Diter, P.; Taudien, S.; Samuel, O.; Kagan, H. B. Enantiomeric enrichment of sulfoxides by preparative flash chromatography on an achiral phase. *J. Org. Chem.* **1994**, *59* (2), 370−373.

(18) For discussion regarding the origin of the term self-disproportionation of enantiomers (SDE) see Soloshonok, V. A.; Klika, K. D. Terminology Related to the Phenomenon 'Self-Disproportionation of Enantiomers' (SDE). *Helv. Chim. Acta* **2014**, *97* (11), 1583−1589.

(19) Faigl, F.; Fogassy, E.; Nógrádi, M.; Pálovics, E.; Schindler, J. Separation of non-racemic mixtures of enantiomers: an essential part of optical resolution. *Org. Biomol. Chem.* **2010**, *8* (5), 947−959.

(20) Brondel, N.; Moynihan, E. J. A.; Lehane, K. N.; Eccles, K. S.; Elcoate, C. J.; Coles, S. J.; Lawrence, S. E.; Maguire, A. R. Does intermolecular S = O···H−C−S=O hydrogen bonding in sulfoxides and sulfones provide a robust supramolecular synthon in the solid state? *CrystEngComm* **2010**, *12* (10), 2910−2927.

(21) O'Mahony, G. E.; Ford, A.; Maguire, A. R. Copper-Catalyzed Asymmetric Oxidation of Sulfides. *J. Org. Chem.* **2012**, *77* (7), 3288−3296.
(22) O'Mahony, G. E.; Eccles, K. S.; Morrison, R. E.; Ford, A.; Lawrence, S. E.; Maguire, A. R. Investigation of steric and electronic effects in the copper-catalysed asymmetric oxidation of sulfides. *Tetrahedron* **2013**, *69* (47), 10168−10184.
(23) Han, J.; Wzorek, A.; Soloshonok, V. A.; Klika, K. D. The self-disproportionation of enantiomers (SDE): The effect of scaling down, potential problems versus prospective applications, possible new occurrences, and unrealized opportunities? *Electrophoresis* **2019**, *40* (15), 1869−1880.
(24) Han, J.; Kitagawa, O.; Wzorek, A.; Klika, K. D.; Soloshonok, V. A. The self-disproportionation of enantiomers (SDE): a menace or an opportunity? *Chem. Sci.* **2018**, *9* (7), 1718−1739.
(25) Soloshonok, V. A.; Roussel, C.; Kitagawa, O.; Sorochinsky, A. E. Self-disproportionation of enantiomers via achiral chromatography: a warning and an extra dimension in optical purifications. *Chem. Soc. Rev.* **2012**, *41* (11), 4180−4188.
(26) Song, W.; Zhou, Y.; Fu, Y.; Xu, W. Self-disproportionation of enantiomers of prazoles via achiral, gravity-driven silica gel column chromatography. *Tetrahedron: Asymmetry* **2013**, *24* (15), 909−912.
(27) Drabowicz, J.; Jasiak, A.; Wzorek, A.; Sato, A.; Soloshonok, V. A. Self-disproportionation of enantiomers (SDE) of chiral sulfoxides, amides and thioamides via achiral chromatography. *ARKIVOC* **2017**, *2017*, 557−578.
(28) Wzorek, A.; Klika, K. D.; Drabowicz, J.; Sato, A.; Aceña, J. L.; Soloshonok, V. A. The self-disproportionation of the enantiomers (SDE) of methyl *n*-pentyl sulfoxide via achiral, gravity-driven column chromatography: a case study. *Org. Biomol. Chem.* **2014**, *12* (26), 4738−4746.
(29) Hunter, C. A. Quantifying Intermolecular Interactions: Guidelines for the Molecular Recognition Toolbox. *Angew. Chem., Int. Ed.* **2004**, *43* (40), 5310−5324.
(30) Legros, J.; Bolm, C. Investigations on the Iron-Catalyzed Asymmetric Sulfide Oxidation. *Chem. - Eur. J.* **2005**, *11* (4), 1086−1092.
(31) We would like to thank the reviewers for their input in the preparation of this manuscript and would like to clarify that the use of an elevated column temperature for the resolution of benzyl phenyl sulfoxide **2** was in order to reduce the run time as this compound was used for optimization studies.
(32) Dai, W.; Li, G.; Wang, L.; Chen, B.; Shang, S.; Lv, Y.; Gao, S. Enantioselective oxidation of sulfides with H2O2 catalyzed by a pre-formed manganese complex. *RSC Adv.* **2014**, *4* (87), 46545−46554.
(33) Samanta, R.; Antonchick, A. P. Palladium-Catalyzed Double C−H Activation Directed by Sulfoxides in the Synthesis of Dibenzothiophenes. *Angew. Chem., Int. Ed.* **2011**, *50* (22), 5217−5220.
(34) Kwart, H.; Omura, H. Intermediates in hydrochloric acid-catalyzed cleavage and stereomutation reactions of sulfoxides. *J. Am. Chem. Soc.* **1971**, *93* (26), 7250−7256.
(35) Davis, F. A.; Reddy, R. T.; Han, W.; Carroll, P. J. Chemistry of oxaziridines. 17. N-(Phenylsulfonyl)(3,3-dichlorocamphoryl)-oxaziridine: a highly efficient reagent for the asymmetric oxidation of sulfides to sulfoxides. *J. Am. Chem. Soc.* **1992**, *114* (4), 1428−1437.

https://dx.doi.org/10.1021/acs.joc.0c01094
J. Org. Chem. 2020, 85, 10216−10221